Synthetic Routes to Well-Defined Biodegradable Polymers using Organoboron Catalysts

by

Ekaterina Slavko

A thesis submitted in conformity with the requirements
for the degree of Doctor of Philosophy

Department of Chemistry
University of Toronto

Synthetic Routes to Well-Defined Biodegradable Polymers using Organoboron Catalysts

Ekaterina Slavko

Doctor of Philosophy

Department of Chemistry
University of Toronto

2019

Abstract

Borinic acid catalysis is used as a tool for the synthesis of carbohydrate-derived polymers of biomedical interest. Polyols possessing 3 or 4 hydroxyl groups are subjected to site-selective polymerization without protecting group manipulations. Chapter 1 serves as an introduction describing common biomedical polymers and our approach to their synthesis. In Chapter 2, the synthesis of well-defined linear polyesters derived from glycerol is described as a proof-of-concept for the translation of borinic acid-catalyzed polyol derivatizations to macromolecular synthesis. In Chapter 3, linear polyesters derived from anomerically protected pyranosides are described, highlighting the scope of the borinic acid-promoted polycondensation. In Chapter 4, structure–property relationships among polyesters derived from monomers with diverse anomeric side-chains are uncovered, demonstrating the versatility of this new monomer class in modulating thermal, physical and degradation behaviours. Finally, concluding remarks are made in Chapter 5, along with a summary of related research directions, including the implementation of borinic acids as a tool for methacrylate monomer synthesis as well as their use in promoting the synthesis of glycerol- and pyranoside-derived polyurethanes.

Acknowledgments

First and foremost, I would like to thank my supervisor Prof. Mark Taylor for his guidance, patience and encouragement throughout the years. Mark has been tremendously supportive of me in all my endeavours, always *led* by example, and most importantly, he persistently challenged me. Thank you for making my PhD a genuinely transformative rite of passage. I would also like to thank the other members of my advisory committee, Prof. Dwight Seferos and Prof. Mitch Winnik, who gave me lots of ideas for my projects. I also want to recognize them for being great teachers and, along with Prof. Eugenia Kumacheva, giving me an introduction to the world of materials. Speaking of initiations into new worlds, I sincerely thank Prof. Paul Santerre from the Faculty of Dentistry for serving on my comprehensive oral examination committee and for his generosity in letting me use his lab space for my biological assay. His student Eric Tawagi deserves a special thank you for training me. I should also give credit to my friend Penny Le from the Winnik group for a series of insightful biology discussions. Generally, when it comes to the Winnik group, a lot of gratitude must be expressed: thank you to Joey Zhou and Rachel Keunen for help with GPC, Dr. Pietro Paolo de Oliveira e Silva for DMA training and our wonderful conversations, Mitch himself for all his warmth, wisdom and guidance, and many others for being helpful along the way. Similarly, members of the Seferos lab get a shout-out for being great neighbours and letting me use their stuff, particularly things that spin. To Nimrat Obhi, ma vie serait plate sans toi. I am extremely grateful for the Lash Miller NMR staff, including Drs. Karl Demmans, Sergyi Nokhrin, Darcy Burns and Jack Sheng. I have had many fun and enlightening discussions with Darcy, and his contribution to my quantitative NMR studies is just one of the things for which I owe him a debt of gratitude. I would also like to gratefully acknowledge Harry Soor from the Yudin group for LC-MS help. Of course, my time here would have been meaningless without my fellow group members. I want to particularly emphasize how thankful I am for everyone who mentored me when I first joined the group, notably Drs. Graham Garrett and Alan Vanderkooy, but also the sugar specialists who made carbohydrate chemistry look easy when it was time for my trial by caramelization: Dr. Sanjay Manhas, Kyan D'Angelo and Dr. Ross Mancini. I would like to thank my very first undergraduate student Álvaro Briceno-Strocchia for trailblazing my second polymer project and for expanding my vocabulary. I also thank my friend and collaborator Pierre-Olivier Ferko for

his contribution to the glycopolymer project. Yvonne Zhou, I am grateful for all your hard work on the sugar-derived polyurethanes project. I cannot imagine my time here without Victoria Dimakos keeping me sane and Grace Wang keeping me insanely fit, and Daniel Gorelik always laughing at my jokes, even in the darkest times. My first year in Toronto, along with all the people I met during that period, will always hold a special place in my heart, and I will never forget the original Taylor crew of fall 2014: Harumi Takasaki, Vincent Song, Graham Garrett, Shaan Singh, Ross Mancini, Sanjay Manhas, Kashif Tanveer, Alan Vanderkooy, Kyan D'Angelo, John H. Y. Su and Victoria Dimakos. Your names remain forever inscribed on the out-of-date sign outside our office. Thank you to the Graduate Office, and thank you Anna Liza Villavelez for all your admin help and for organizing the mentorship program that introduced me to my awesome mentor Dr. Darren Anderson. Finally, I would like to dedicate this to my mother who sacrificed everything to make me who I am today, and even offered to help me write this thesis. I may not have taken you up on that offer, but I am forever grateful for all your love.

Table of Contents

List of Abbreviations

2-MeTHF	2-methyltetrahydrofuran
Δ	heat
Đ	dispersity
Ac	acetyl
AIBN	azobisisobutyronitrile
Amu	arbitrary mass units
Bz	benzoyl
d	day(s)
DCM	dichloromethane
DIC	*N*,*N*′-diisopropylcarbodiimide
DIPEA	*N*,*N*-diisopropylethylamine
DMA	dynamic mechanical analysis
DMAP	4-(dimethylamino)pyridine
DMEM	Dulbecco's modified Eagle's medium
DMF	*N*,*N*-dimethyl formamide
DMSO	dimethyl sulfoxide
DMSO-d_6	deuterated dimethyl sulfoxide
DPBS	Dulbecco's phosphate buffered saline

DSC	differential scanning calorimetry
E'	storage modulus
ESI	electrospray ionization
Et	ethyl
FTIR	Fourier-transform infrared spectroscopy
GPC	gel permeation chromatography
h	hour(s)
HDI	hexamethylene diisocyanate
IR	infrared
LC-MS	liquid chromatography/mass spectrometry
m/z	mass-over-charge ratio
M	moles per liter
M_c	relative molecular weight between cross-links
Me	methyl
M_n	number-average molecular weight
mp	melting point
MPa	megapascal
MTT	3-(4,5-dimethylthiazol-2-yl)-2,5-diphenyltetrazolium bromide
M_w	mass-average molecular weight

NAD(P)H	nicotinamide adenine dinucleotide phosphate
NMP	*N*-methyl-2-pyrrolidone
oct	octyl
P3HB	poly(3-hydroxybutyrate)
PBS	poly(butylene succinate)
PCL	polycaprolactone
PEG	poly(ethylene glycol)
PGA	poly(glycerol adipate)
Ph	phenyl
PHA	poly(hydroxyalkanoate); poly(hydroxyalkanoate)s
PGS	poly(glycerol sebacate)
PLA	poly(lactic acid)
PLGA	poly(lactic-*co*-glycolic acid)
PMMA	poly(methyl methacrylate)
PTFE	polytetrafluoroethylene
PVPBA	poly(4-vinylphenylboronic acid)
r.t.	room temperature
RAFT	reversible addition−fragmentation chain-transfer
ROP	ring-opening polymerization

S_N2	bi-molecular nucleophilic substitution
tan δ	tangent delta
TCPS	tissue culture polystyrene
T_g	glass transition temperature
THF	tetrahydrofuran
TLC	thin layer chromatography

List of Tables

List of Figures

List of Schemes

Chapter 1: Introduction

1 Background

1.1 Biocompatible Polymers

Synthetic polymers have had an immensurable impact on human life and are being produced on a massive industrial scale.[1] Since their first commercial introduction, polymers have had their properties continuously improved, both for broad consumer appeal and for advanced applications. Physical properties such as strength, elasticity, solubility, durability and thermal behaviour can be rationalized and adjusted based on the repeat units and microstructure of the polymer chains. For example, the first commercially successful synthetic thermoplastic polymer, nylon, owes its high tensile strength and crystallinity to its regular, symmetrical backbone and hydrogen bonding amide groups which made it a sought-after silk substitute in the 1940s.[2] Since then, a plethora of new polymers were developed as low-cost alternatives to natural materials, and ever-advancing synthetic methods have provided access to polymers of well-defined architectures (*e.g.*, linear, cross-linked, brush, dendritic) for various applications. Specifically, polymers engineered to interact with living systems — biomaterials — have become increasingly prevalent and specialized.[3]

The use of polymeric materials of biological origin for medical applications has been widespread for thousands of years, some examples being silk threads and animal intestine-derived collagen fibers employed as sutures in ancient India and Greece[4] before synthetic

---

[1] Thomas, R. W. *Polymers: Plastics, Fibres, Rubbers and Silicones*; Oxford Pergamon Press, 1969.

[2] Hoff, G. P. *Ind. Eng. Chem.* **1940**, *32*, 1560–1564.

[3] Vert, M.; Doi, Y.; Hellwich, K.-H.; Hess, M.; Hodge, P.; Kubisa, P.; Rinaudo, M.; Schué, F. *Pure Appl. Chem.* **2012**, *84*, 377–410.

[4] Privalova, L. G.; Zaikov, G. E. *Polym. Plast. Technol. Eng.* **1990**, *29*, 455–520.

biodegradable polymers began being used for that purpose in the 1970s.[5] Repurposed naturally occurring polymeric materials or biopolymers such as starch, cellulose, chitosan and collagen, have since been widely employed in biomedical science.[6] Some features of naturally occurring biopolymers are taken into consideration when designing synthetic biomaterials to ideally replicate their desirable characteristics while improving their processability and physical properties. Synthetic polymers made from biomass-derived and biocompatible monomers similar to the building blocks found in Nature can be a versatile and inexpensive alternative to biopolymers, and have virtually no design limitations, provided that viable methods to produce them can be realized.

The ideal biomedical polymer should integrate with its living host. It must not cause an adverse host reaction (*i.e.*, be biocompatible) and must break down and be absorbed into the host tissue *(i.e.*, be biodegradable and bioresorbable).[7] Biodegradability is possible *in vivo* or in a composting environment and is promoted by living organisms or their enzymes, but some polymers have other modes of degradation, which are possible in a broader range of environmental conditions *(e.g.*, non-enzymatic hydrolysis). The absence of toxic effects in the constituent elements or degradation products of a biomaterial is a necessary, but not sufficient condition for biocompatibility. Many definitively non-toxic materials such as polyethylene and silicone are not biocompatible or biodegradable, which can manifest in thrombus formation and collagenous fiber encapsulation at the site of biomaterial implantation.[5] One of the first successful polymeric biomaterials was poly(methyl methacrylate) (PMMA) or Plexiglas, which was used in intraocular implants following ophthalmic surgery. Non-immunogenicity, a key aspect of biocompatibility, was ascribed to PMMA after it was observed that World War II soldiers' eyes suffered little immune response to implanted shards of broken Plexiglas

---

[5] Ikada, Y.; Tsuji, H. *Macromol. Rapid Commun.* **2000**, *21*, 117–132.

[6] Yadav, P.; Yadav, H.; Shah, V. G.; Shah, G.; Dhaka, G. *J. Clin. Diagnostic Res.* **2015**, *9*, 21–25.

[7] Ulery, B. D.; Nair, L. S.; Laurencin, C. T. *J. Polym. Sci. B Polym. Phys.* **2012**, *49*, 832–864.

comparatively to ordinary broken glass.[8] Ideally, a minimal number of components should be incorporated into a biomaterial to mitigate the risk of eliciting an immune response and to avoid short- or long-term toxicity to the patient. For example, the phasing-out of poly(vinyl chloride) medical devices containing the plasticizer di(2-ethyl hexyl)phthalate reflects concerns about phthalate toxicity and its ability to leach into the human body.[9] The structural characteristics of the polymer itself must also be taken into consideration: polycarbonates derived from Bisphenol A have also fallen out of favour in recent years due to the possible leaching of an endocrine disruptor upon hydrolysis of the main chain.[10] Thus, there is a constant impetus for creating new high performance materials that are compatible with living tissues, can be used without toxic additives, and biodegrade to form benign by-products.

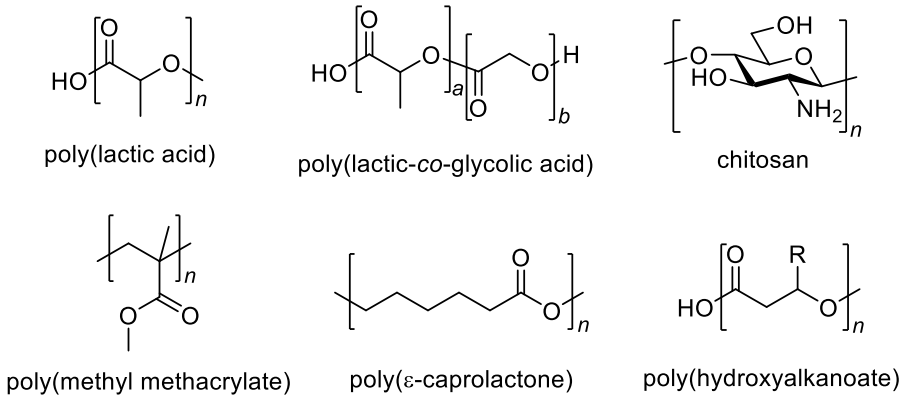

Figure 1.1 Common biodegradable polymers used in medicine.

1.2 Biomedically Significant Polyesters

Aliphatic polyesters represent a class of polymers that successfully realize the design outlined in Section 1.1: they contain hydrolyzable ester bonds and can be made from a structurally diverse selection of bio-sourced feedstocks. In fact, some polyesters are naturally occurring, notably the poly(hydroxyalkanoates) or PHA, granules of which were observed for the first time in 1888 in

---

[8] Ridley, H. *Lancet* **1952**, *1952*, 118–121.

[9] Stennett, D. J.; Egging, P. K.; Mazur, H. I. *J. Parenter. Enter. Nutr.* **1989**, *13*, 59–62.

[10] Howdeshell, K. L.; Peterman, P. H.; Judy, B. M.; Taylor, J. A.; Orazio, C. E.; Ruhlen, R. L.; vom Saal, F. S.; Welshons, W. V. *Environ. Health Perspect.* **2003**, *111*, 1180–1187.

the cytosol of some bacteria that use these polyesters as energy storage.[11] The physical properties of PHA vary a great deal depending on the nature of the side-chain, but most variants possess high strength, crystallinity, and hydrophobicity. The molecular weights of PHA can be manipulated through their biosynthetic pathway and can span orders of magnitude. Because of their biocompatibility and processability, PHA are being investigated as components of nanocarriers for targeted drug delivery, as well as surgical stents, tissue engineering scaffolds, and other applications. They face limitations due to their slow hydrolytic degradation rate and hydrophobicity which can be countered by their incorporation into blends with more hydrophilic polymers.[12] The use of PHA as bioplastics in the food packaging industry also involves incorporating them into a composite with a more elastic polymer and is currently too costly for widespread implementation as their production relies on a biosynthetic approach.[13]

An example of an almost ubiquitous medically useful biodegradable polyester is poly(lactic acid) (PLA) — a non-toxic, bio-sourced thermoplastic originally synthesized in 1932 through polycondensation of the naturally occurring metabolite lactic acid.[14] Unlike PHA, PLA can be hydrolyzed without the presence of any animal or microbial hydrolase enzymes. Today, PLA is synthesized by polycondensation of lactic acid or by ring-opening polymerization (ROP) of D- or L-lactide monomers as shown in Scheme 1.1a, and is used in a variety of biomedical devices, including as drug delivery implants, surgical sutures, tissue engineering scaffolds and bone fixation materials. PLA's properties depend strongly on its tacticity, and thus on its synthetic origins and the catalyst used to prepare it. Its use in the food packaging industry is common, albeit narrow in scope due to its thermal instability and permeability to water vapour

---

[11] Rathna, G. V. N.; Thorat Gadgil, B. S.; Killi, N. In *Biodegradable and Biobased Polymers for Environmental and Biomedical Applications*; Avérous, L.; Kalia, S., Eds.; Scrivener Publishing, 2016; pp. 25–54.

[12] Zhang, J.; Shishatskaya, E. I.; Volova, T. G.; da Silva, L. F.; Chen, G. Q. *Mater. Sci. Eng. C* **2018**, *86*, 144–150.

[13] Gülsah, K.; Gülnur, K.; Mikhael, B.; Céline, P.-B.; Mualla, Ö. *Pure Appl. Chem.* **2017**, *89*, 1841.

[14] Jamshidian, M.; Tehrany, E. A.; Imran, M.; Jacquot, M.; Desobry, S. *Compr. Rev. Food Sci. Food Saf.* **2010**, *9*, 552–571.

and oxygen.[15] Copolymers of lactic acid and glycolic acid (PLGA) are commonly used *in vivo*, affording higher biodegradation rates than pure PLA.[16] This class of polymers is characterized by glass transition temperatures (T_g) above 37 °C, and while they are brittle and thermally unstable, they possess relatively high tensile strength. Drawbacks to the *in vivo* use of lactic acid-containing degradable polymers stem from the inflammatory effects of lactic acid, which is often released at high rates once the structural integrity of the implant has been destroyed by bulk erosion.[17]

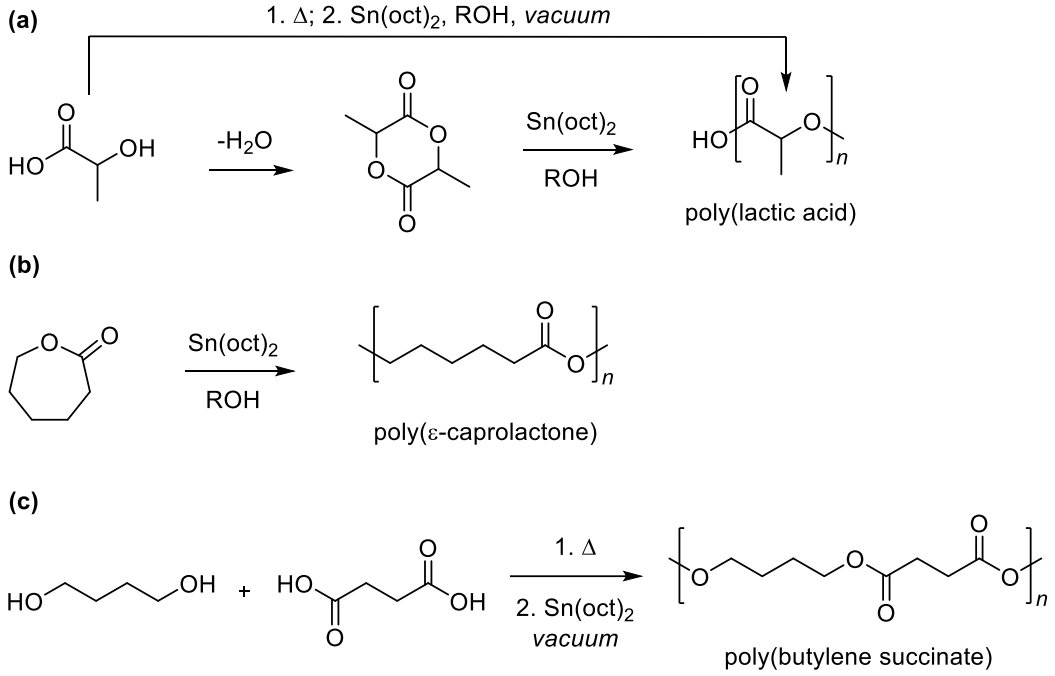

Scheme 1.1 Synthesis of common biodegradable polyesters of biological interest, showing (a) ROP and polycondensation to yield PLA, (b) ROP of ε-caprolactone, and (c) polycondensation of 1,4-butanediol with succinic acid to make PBS.

---

[15] Peelman, N.; Ragaert, P.; De Meulenaer, B.; Adons, D.; Peeters, R.; Cardon, L.; Van Impe, F.; Devlieghere, F. *Trends Food Sci. Technol.* **2013**, *32*, 128–141.

[16] Kalia, S.; Averous, L. *Biodegradable and Biobased Polymers for Environmental and Biomedical Applications*; Wiley, 2016.

[17] Athanasiou, K. A.; Niederauer, G. G.; Agrawal, C. M. *Biomaterials* **1996**, *17*, 93–102.

Poly(caprolactone) (PCL), on the other hand, is a slow degrading, low glass transition temperature (T_g) and low melting thermoplastic suitable for long-term implants and controlled drug delivery devices, or serving as the soft segment of polyurethanes. It is synthesized by ROP of a lactone monomer (Scheme 1.1b). Although it bears many similarities with PHA while costing much less, PCL is not sourced from renewable feedstocks and possesses limitations as a tissue engineering scaffold material due to its poor mechanical properties.[18] Commercially available poly(butylene succinate) (PBS), depicted in Scheme 1.1c, is made in part from potentially renewable succinic acid and has excellent processability and mechanical properties, combining a low T_g with relatively high tensile strength (Table 1.1). However, despite being used successfully in packaging, mulching films, and compost bags, PBS suffers from low biocompatibility and must be surface-modified in order to promote tissue regeneration when used as a tissue engineering scaffold.[19]

Table 1.1 Representative physical properties of common biodegradable polyesters.

	P3HB*	**PLA**	**PCL**	**PBS**
T_g (°C)	4	57–60	–60	–32
Tensile strength (MPa)	62	48–53	23	34
Young's modulus (MPa)	1100	3000–4000	400	700

* – refers to poly(3-hydroxybutyrate), the most commonly used PHA.

1.3 Functional Biomaterials from Functionalized Polymers

The continuous development of the biomaterials field over the course of the last century has led to a major paradigm shift with regards to the role that synthetic polymeric materials should serve in a patient's body under ideal conditions. While an appreciation for the relative innocence of certain materials when compared to others in eliciting adverse physiological reactions in the short term (*e.g.*, PMMA *vs.* glass) initially motivated the search for biologically inert materials, broader questions regarding the long-term fate of artificial implants in the body drove the development of materials that were biodegradable and bioresorbable rather than merely inert. In

[18] Mondal, D.; Griffith, M.; Venkatraman, S. S. *Int. J. Polym. Mater. Polym. Biomater.* **2016**, *65*, 255–265.

[19] Wang, H.; Ji, J.; Zhang, W.; Zhang, Y.; Jiang, J.; Wu, Z.; Pu, S.; Chu, P. K. *Acta Biomater.* **2009**, *5*, 279–287.

addition, tremendous efforts are being made in facilitating tissue regeneration and cell differentiation and proliferation at the biomaterial–host interface, including the manipulation of material microstructure using 3-D printing[20] and the development of bioactive composites.[21] Modern-day polymeric biomaterial designs strive to go even further, combining biocompatibility and degradability with bioactivity at the cellular level in response to the need for long-term implants that respond dynamically to changes in physiological conditions and biochemical stimuli, with the aim being to maximize the useful lifetime of implants minimize the need for repeat surgical procedures.[22]

The design of functional polymers allows for the integration of pharmacological components into physically and mechanically sound structures at the microscopic and macroscopic scales. Antimicrobial and anti-inflammatory agents can be incorporated into biodegradable polymers for their sustained release by blending or covalent attachment to promote tissue healing through the prevention of post-operative infections.[23] Attachment of various signaling molecules to pendant functional groups on biocompatible polymers has been found to improve the cell adhesion and cytocompatibility characteristics of various materials, for instance by directing neurite proliferation and differentiation through the attachment of a neurotransmitter mimic to a biomaterial used for nerve regeneration[24] or by functionalizing a material with cell type-specific adhesion proteins, *e.g.*, a hydrogel functionalized with a peptide that specifically promotes fibroblast attachment.[25] Biomaterials can be engineered to display a plethora of biological signaling molecules, an enterprise facilitated by the chemical modification of polymer structures with reactive functional groups such as OH, NH_2 and COOH. It should be

---

[20] Stratton, S.; Shelke, N. B.; Hoshino, K.; Rudraiah, S.; Kumbar, S. G. *Bioact. Mater.* **2016**, *1*, 93–108.

[21] Hench, L. L.; Jones, J. R. *Front. Bioeng. Biotechnol.* **2015**, *3*, 1–12.

[22] Hench, L. L.; Polak, J. M. *Science* **2002**, *295*, 1014–1017.

[23] Watson, E.; Tatara, A. M.; Kontoyiannis, D. P.; Mikos, A. G. *ACS Biomater. Sci. Eng.* **2017**, *3*, 1207–1220.

[24] Wang, S.; Jeffries, E.; Gao, J.; Sun, L.; You, Z.; Wang, Y. *ACS Appl. Mater. Interfaces* **2016**, *8*, 9590–9599.

[25] Schmedlen, R. H.; Masters, K. S.; West, J. L. *Biomaterials* **2002**, *23*, 4325–4332.

noted that free functional groups present at the cell interface themselves can have a strong impact on cell behaviour, such as the promotion of bone mineralization in osteoblasts by pendant OH groups[26] or the functional group-dependent direction of differentiation of stem cells.[27] In short, functional group incorporation is a major driving force behind the improvement of biologically active polymeric materials.

Pendant reactive groups can be introduced into biodegradable polymers using several methods. Surface modification is a highly researched field and includes creation of functional groups at the surface of materials to improve wettability, adhesion, and anti-fouling properties.[28] These methods only impact the surface of the material and present limitations for biomaterials that degrade by both bulk degradation and surface erosion, as well as restricting polymer processing options. Synthetic routes to intrinsically functionalized macromolecules are an attractive alternative. Most commonly, monomers bearing protected functionalities are polymerized or copolymerized, after which the protecting groups are removed (Scheme 1.2).[29] This protection/deprotection tactic is not atom economical and hinges on the assumption that the final deprotection step can be carried out quantitatively without chemically transforming the backbone, which is not always the case.[30] Alternatively, if the desired pendant functional group is orthogonal to that of the polymerizable groups of the monomer(s), functionalized polymers can be obtained in one step without the need for post-polymerization reactions, although this does not take into account the number of steps required to synthesize the bi- or trifunctional monomers compatible with such an approach. Functionalized polyesters have thus been prepared

---

[26] Bi, X.; You, Z.; Gao, J.; Fan, X.; Wang, Y. *Acta Biomater.* **2014**, *10*, 2814–2823.

[27] Benoit, D. S. W.; Schwartz, M. P.; Durney, A. R.; Anseth, K. S. *Nat. Mater.* **2008**, *7*, 816–823.

[28] Zhou, T.; Zhu, Y.; Li, X.; Liu, X.; Yeung, K. W. K.; Wu, S.; Wang, X.; Cui, Z.; Yang, X.; Chu, P. K. *Prog. Mater. Sci.* **2016**, *83*, 191–235.

[29] Noga, D. E.; Petrie, T. A.; Kumar, A.; Weck, M.; García, J.; Collard, D. M. *Biomacromolecules* **2008**, *9*, 2056–2062.

[30] Yokoe, M.; Aoi, K.; Okada, M. *J. Polym. Sci. Part A Polym. Chem.* **2005**, *43*, 3909–3919.

via an esterification that does not involve OH groups[31] and by conventional polycondensation of a monomer bearing an alkyne functionality for subsequent "click" derivatization.[32]

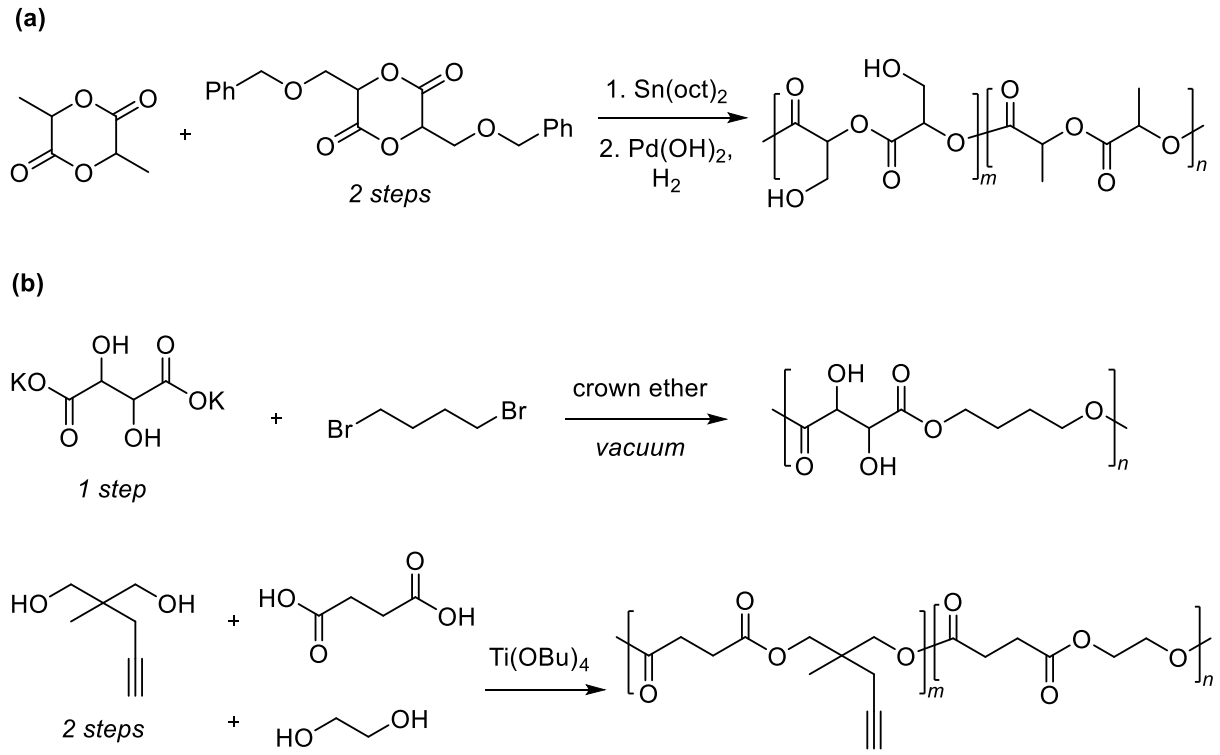

Scheme 1.2 Synthesis of some biocompatible polymers bearing pendant functional groups, illustrating (a) the protecting group approach and (b) the orthogonal reactivity approach.

2 Scope of Thesis

2.1 Catalyst-controlled Polycondensation

The second, third and fifth chapters of this thesis center on a catalysis-driven strategy toward the synthesis of functional polyesters derived from natural sources. Rather than employing protected monomers or "spectator" pendant functional groups to achieve a one-step polymerization, an inherently site-selective process was sought. A series of borinic acid catalysts was used to

---

[31] Sepulchre, M.-O.; El Idrissi, H.; Sepulchre, M.; Spassky, N. *Makromol. Chem.* **1993**, *194*, 677–687.

[32] Billiet, L.; Fournier, D.; Du Prez, F. *J. Polym. Sci. Part A Polym. Chem.* **2008**, *46*, 6552–6564.

activate specifically configured OH groups at rates significantly exceeding those of the background OH reactivity at other reactive sites. This approach can be compared to the one-step synthesis of polyol-derived polyesters enabled by the intrinsic specificity of an enzyme,[33] examples of which will be discussed in more detail in Chapter 2.

The synthesis of linear, OH-functionalized polyesters with precise microstructures prepared from glycerol (3 OH groups) and pyranoside derivatives (4 OH groups) is described along with illustrations of the synthetic utility of their pendant functional groups. Chapter 4 is an exploration of some of the physical, mechanical and biological properties of the new pyranoside-derived polyesters and comments on their potential applications in the biomaterials field. Parts of Chapter 5 report on the use of borinic acids to carry out site-selective polymerizations of glycerol and pyranoside derivatives to afford new polyurethanes by the same mechanism.

2.2 Catalyst-controlled Monomer Synthesis

Chapter 5 describes investigations into the synthesis of biocompatible macromolecules beyond polyesters. Specifically, a facile monomer synthesis is described wherein anomerically protected pyranoside derivatives are functionalized in one step using borinic acid catalysis to afford methacrylated sugar-derived monomers with 3 pendant OH groups. The controlled radical polymerization of these compounds leads to unprecedented polymers with pendant, partially protected carbohydrate residues whose hydrogel-forming ability is explored.

---

[33] Kline, B. J.; Beckman, E. J.; Russell, A. J. *J. Am. Chem. Soc.* **1998**, *120*, 9475–9480.

Chapter 2: Synthesis of Poly(glycerol ester)s

1 Statement of Contribution

Information in this chapter has been peer-reviewed and adapted from the published source material.[34] Synthesis and characterization of all compounds in Chapter 2 were done by Ekaterina Slavko and the manuscript for the source material was drafted and edited by Ekaterina Slavko and Mark S. Taylor.

2 Introduction

2.1 Glycerol-derived Polyesters

During the 1990s, research interest in biodegradable network polyesters based on glycerol and dicarboxylic acids started to ignite.[35] In 2002, the group of Langer introduced poly(glycerol sebacate) (PGS),[36] a degradable polyester obtained by bulk polycondensation of a 1:1 mixture of glycerol and sebacic acid followed by a thermal curing step, revealing a tough and elastic rubber-like network that showed great biocompatibility and desirable physical properties (Scheme 2.1).[37]

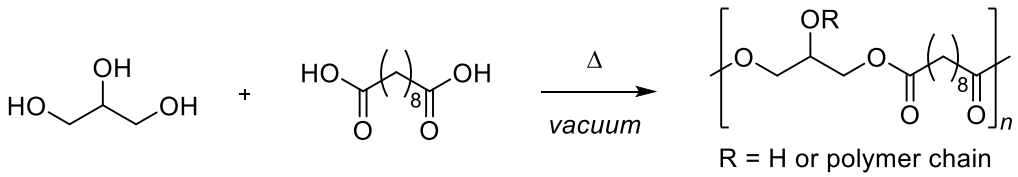

Scheme 2.1 Conventional polycondensation of glycerol and sebacic acid producing PGS.

The trifunctional nature of the comonomer glycerol provided the possibility for hydrogen bonding between chains and allowed for network formation *via* cross-linking during the curing

---

[34] Slavko, E.; Taylor, M. S. *Chem. Sci.* **2017**, *8*, 7106–7111.

[35] Kiyotsukuri, T.; Kanaboshi, M.; Tsutsumi, N. *Polym. Int.* **1994**, *33*, 1–8.

[36] Wang, Y.; Ameer, G. A.; Sheppard, B. J.; Langer, R. *Nat. Biotechnol.* **2002**, *20*, 602–606.

[37] Loh, X. J.; Karim, A. A.; Owh, C. *J. Mater. Chem. B* **2015**, *3*, 7641–7652.

step.[38] A new class of aliphatic polyesters of biomedical significance was born. Glycerol is a naturally occurring metabolite and its known biocompatibility underlies its widespread use in food, cosmetic, pharmaceutical and personal care products (*e.g.*, as a humectant, plasticizer, thickener, lubricant, sweetener). In addition, it is inexpensive due to the rising global production of biodiesel, which generates glycerol as a by-product of transesterification.[39] In this process, spent cooking oils are subjected to transesterification with base and methanol to produce methyl esters of their constituent fatty acids, thus yielding a bio-sourced fuel (Scheme 2.2). Over the last two decades, polyesters based on glycerol and the equally harmless aliphatic diacids have found applications as tissue engineering scaffolds,[40] surgical adhesives,[41] nanoparticles for drug delivery,[42,43] and drug carrier implants.[44]

---

[38] Rai, R.; Tallawi, M.; Grigore, A.; Boccaccini, A. R. *Prog. Polym. Sci.* **2012**, *37*, 1051–1078.

[39] Ayoub, M.; Abdullah, A. Z. *Renew. Sustain. Energy Rev.* **2012**, *16*, 2671–2686.

[40] Zaky, S. H.; Lee, K.; Gao, J.; Jensen, A.; Close, J.; Wang, Y.; Almarza, A. J.; Sfeir, C. *Tissue Eng. Part A* **2014**, *20*, 45–53.

[41] Lang, N.; Pereira, M. J.; Lee, Y.; Ingeborg, F.; Vasilyev, N. V; Feins, E. N.; Ablasser, K.; O'Cearbhaill, E. D.; Xu, C.; Fabozzo, A.; Padera, R.; Wasserman, S.; Freudenthal, F.; Ferreira, L. S.; Langer, R.; Karp, J. M.; del Nido, P. J. *Sci Transl Med.* **2015**, *6*, 1–19.

[42] Kallinteri, P.; Higgins, S.; Hutcheon, G. A.; Pourc, C. B. S.; Garnett, M. C. *Biomacromolecules* **2005**, *6*, 1885–1894.

[43] Weiss, V. M.; Naolou, T.; Hause, G.; Kuntsche, J.; Kressler, J.; Mäder, K. *J. Control. Release* **2012**, *158*, 156–164.

[44] Sun, Z.; Chen, C.; Sun, M.; Ai, C.; Lu, X.; Zheng, Y.-F.; Yang, B.-F.; Dong, D.-L. *Biomaterials* **2009**, *30*, 5209–5214.

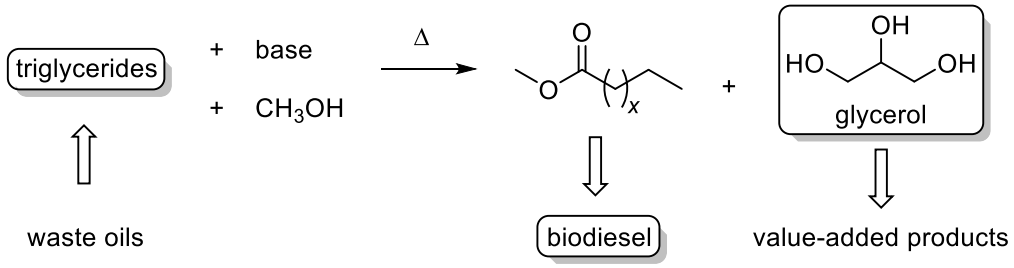

Scheme 2.2 Biodiesel production yielding glycerol as a by-product.

The mechanical and physiochemical properties of poly(glycerol ester)s synthesized through traditional polycondensation techniques are sensitive to reaction conditions.[45] The rather forcing, heat-intensive bulk polymerization procedures reported in the literature are subject to reproducibility challenges[46] due in part to the evaporation of glycerol under reduced pressure,[47] the rate of which is unpredictable and capable of significantly altering copolymer composition. Curing temperature, reaction time, and monomer feed ratio can be manipulated to influence the molecular weight, degree of crosslinking, degradation rate, toughness, strength, and other characteristics of the resulting elastomer. It is difficult, however, to tune each target property without affecting another property as an unintended "side effect". Molar ratios of sebacic acid and glycerol, for instance, have profound effects on the physical properties and biodegradability of the resulting PGS.[48,49] Using a molar excess of diacid during preparation of the polymer induces higher degrees of crosslinking and increases its tensile strength and elastic modulus;[50] however, the degree of polymerization of a step-growth polymer is significantly depressed when

---

[45] Li, Y.; Cook, W. D.; Moorhoff, C.; Huang, W.-C.; Chen, Q.-Z. *Polym. Int.* **2012**, *62*, 534–547.

[46] Li, X.; Hong, A. T.; Naskar, N.; Chung, H. *Biomacromolecules* **2015**, *16*, 1525–1533.

[47] Glycerine Producers' Association, *Physical Properties of Glycerine and Its Solutions*, Glycerine Producers' Association, New York, 1963.

[48] Liu, Q.; Tian, M.; Ding, T.; Shi, R.; Zhang, L. *J. Appl. Polym. Sci.* **2005**, *98*, 2033–2041.

[49] Liu, Q.; Tian, M.; Ding, T.; Shi, R.; Feng, Y.; Zhang, L.; Chen, D.; Tian, W. *J. Appl. Polym. Sci.* **2007**, *103*, 1412–1419.

[50] Kemppainen, J. M.; Hollister, S. J. *J Biomed Mater Res A* **2010**, *94*, 5–18.

monomer feed ratio deviates from 1:1,[51] resulting in lower number-average molecular weights (M_n), elevated dispersities (Đ) and reduced hydrolytic stability.[48] Such highly crosslinked, poorly defined macromolecular structures are also marked by low relative molecular weights between crosslinks (M_c). High M_c, however, can be desirable as it positively affects retention of the network structure *in vivo* and retards biodegradation.[52] A high cross-link density can also be attained through longer curing times, but at the expense of polymer elasticity.[53] These assiduous considerations and laborious protocols for tailoring mechanical and biological properties could be obviated through the synthesis and controlled post-polymerization transformation of well-defined poly(glycerol ester)s.

Glycerol is a trifunctional monomer possessing two reactive primary hydroxyl (OH) groups and one less reactive secondary OH group. This presents a challenge in synthesizing polyesters of well-defined architectures, as esterification events producing branch points compete significantly with those contributing to chain growth, and need to be suppressed *via* protecting group manipulation.[54] The uncontrolled and unpredictable polymerization behaviour of glycerol, particularly under heat-intensive conditions, makes the one-step synthesis of linear, regioregular and high-M_n polymers difficult to carry out. Several examples of lightly branched and hyperbranched poly(glycerol ester)s have been reported in the literature and are summarized in Scheme 2.3. Tin oxide catalysts were effective in the synthesis of hyperbranched polymers by

---

[51] Flory, P. J. *Chem. Rev.* **1946**, *39*, 137–197.

[52] Chen, Q.; Bismarck, A.; Hansen, U.; Junaid, S.; Tran, M. Q.; Harding, S. E.; Ali, N. N.; Boccaccini, A. R. *Biomaterials* **2008**, *29*, 47–57.

[53] Pomerantseva, I.; Krebs, N.; Hart, A.; Neville, C. M.; Huang, A. Y.; Sundback, C. A. *J. Biomed. Mater. Res. Part A* **2008**, 1038–1047.

[54] Tian, D.; Dubois, P.; Grandfils, C.; Jérôme, R. *Macromolecules* **1997**, *30*, 406–409.

the groups of Bruchmann,[55] Strahan[56] and Smith,[57] while the groups of Kobayashi[58] and Gross[59] used an immobilized lipase from *Candida antarctica* to prepare lightly branched polyesters of moderate M_n using divinyl sebacate and sebacic acid, respectively. Enzymatic stability to shear forces under the reaction conditions was identified as a major issue upon scale-up of Gross's method.[60] Russell *et al.* synthesized lightly branched poly(glycerol adipate) (PGA) by means of a lipase-catalyzed reaction with divinyl adipate, which resulted in a low-M_n polymer with a high dispersity.[33] The group of Baldessari[61] has been successful at preparing monodisperse PGA from glycerol and adipic acid using lipases, though the degree of polymerization was low and the exact architecture was never reported. Another report from Kobayashi spectroscopically confirmed the formation of regioregular, fully linear PGS from glycerol and divinyl sebacate catalyzed by *Candida antarctica* lipase,[62] albeit in moderate yields and with a high dispersity.

---

[55] Stumbé, J.-F.; Bruchmann, B. *Macromol. Rapid Commun.* **2004**, *25*, 921–924.

[56] Wyatt, V. T.; Strahan, G. D. *Polymers (Basel).* **2012**, *4*, 396–407.

[57] Zhang, T.; Howell, B. A.; Dumitrascu, A.; Martin, S. J.; Smith, P. B. *Polymer (Guildf).* **2014**, *55*, 5065–5072.

[58] Kobayashi, S.; Uyama, H.; Inada, K. *Macromol. Rapid Commun.* **1999**, *20*, 171–174.

[59] Kumar, A.; Kulshrestha, A. S.; Gao, W.; Gross, R. A. *Macromolecules* **2003**, *36*, 8219–8221.

[60] Korupp, C.; Weberskirch, R.; Müller, J. J.; Liese, A.; Hilterhaus, L. *Org. Proc. Res. Dev.* **2010**, *14*, 1118–1124.

[61] Iglesias, L. E.; Fukuyama, Y.; Nonami, H.; Erra-Balsells, R.; Baldessari, A. *Biotechnol. Tech.* **1999**, *13*, 923–926.

[62] Uyama, H.; Inada, K.; Kobayashi, S. *Macromol. Biosci.* **2001**, *1*, 40–44.

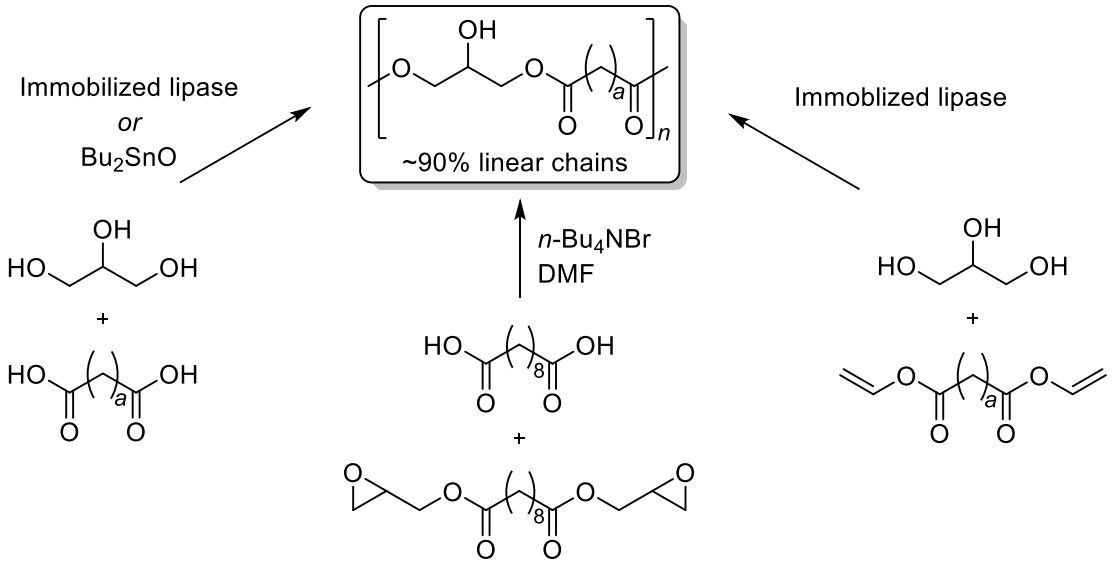

Scheme 2.3 Past synthetic routes to better-defined, solution-processable poly(glycerol ester)s.

A compelling illustration of the advantage of preparing a biomaterial from a well-defined functional polyester comes from the group of Wang.[63] By synthesizing a diglycidyl ester monomer and subjecting it to an epoxide ROP with sebacic acid, Wang was able to obtain a predominantly linear analog of PGS with good M_n (Scheme 2.3). This method necessitates multi-day, heat-intensive conditions and inevitably yields a degree of branching of approximately 10%, a fact that is reflected in the substantial Đ values of the product, as both Đ and apparent M_n increase with increasing branching of polymer chains. Nonetheless, the PGS analog was obtained in high yield and was shown to be soluble and amenable to facile post-polymerization reactions. Subsequent cross-linking of the linear polyester with only 1.1% sebacic acid resulted in a material five times tougher and more elastomeric than conventional PGS prepared by direct bulk polycondensation. This demonstrates that high crosslink densities attained through changes in monomer feed ratio or curing time are not necessary when targeting properties such as toughness or slow degradation profiles, which were previously attainable only *via* extensive network formation.[49] Furthermore, these findings reveal an improvement in biomaterial toughness and elasticity resulting from higher M_c values which in turn stem from high M_n in the native, solution-processable polymer.

---

[63] You, Z.; Cao, H.; Gao, J.; Shin, P. H.; Day, B. W.; Wang, Y. *Biomaterials* **2010**, *31*, 3129–3138.

2.2 Hypothesis

In light of the findings by Wang *et al.*, it would seem that a simple, inexpensive protocol for the preparation of high M_n, linear poly(glycerol ester)s would be a useful tool for the synthesis of biomaterials with tunable physical and biological properties. Controlled addition of hexamethylene diisocynate (HDI), a flexible cross-linking agent, has previously been shown to impart favourable physical properties to lightly branched solution-processable PGS prepolymers,[64] and such a treatment could be easily implemented for longer, fully linear PGS chains in solution. An additional advantage of linear functionalized polyesters would be the ability to quantitatively substitute the backbone OH groups. This could facilitate the attachment and controlled release of a therapeutic agent[65] as well as the introduction of functional groups for the purpose of downstream photo curing or cross-linking[66] or construction of higher-order structures such as molecular brushes.[67] An operationally simple and inherently site-selective polycondensation of glycerol would effectively underpin this strategy by allowing access to the native linear polyesters. We will demonstrate that borinic acids can be used to easily attain biopolymer precursor polymers with precise architectures.

2.3 Borinic Acids Induce Regiocontrol

To avoid having recourse to a multistep synthesis of poly(glycerol ester)s, we hoped to use catalysis to selectively activate the primary OH groups of glycerol to effect a regioregular polymerization. Luckily, sugar alcohols such as glycerol possess 1,2 and 1,3-diol motifs that have the potential to be protected or activated through formation of cyclic adducts. For instance,

---

[64] Pereira, M. J. N.; Ouyang, B.; Sundback, C. A.; Lang, N.; Friehs, I.; Mureli, S.; Pomerantseva, I.; McFadden, J.; Mochel, M. C.; Mwizerwa, O.; del Nido, P.; Sarkar, D.; Masiakos, P. T.; Langer, R.; Ferreira, L. S.; Karp, J. M. *Adv. Mater.* **2013**, *25*, 1209–1215.

[65] Oledzka, E.; Sobczak, M.; Nalecz-Jawecki, G.; Skrzypczak, A.; Kolodziejski, W. *Molecules* **2014**, *19*, 7543–7556.

[66] Nijst, C. L. E.; Bruggeman, J. P.; Karp, J. M.; Ferreira, L.; Zumbuehl, A.; Bettinger, C. J.; Langer, R. *Biomacromolecules* **2007**, *8*, 3067–3073.

[67] Ye, H.; Owh, C.; Jiang, S.; Ng, C. Z. Q.; Wirawan, D.; Loh, X. J. *Polymers (Basel).* **2016**, *8*.

cis diols have been routinely masked as acetals or ketals through diol condensation with carbonyl compounds or their synthetic equivalents (Scheme 2.4).[68] Organoboron compounds such as boronic acids ($RB(OH)_2$) are also well-known for readily forming tri- or tetracoordinate complexes with *cis*-1,2 and 1,3-diols, a property that allowed them to serve as carbohydrate sensors in aqueous solutions[69] as well as transient protecting groups for diol motifs.[70] The discovery that complexation of a Lewis base with a tricoordinate boronic acid-diol complex could site-selectively activate the diol toward alkylation through the formation of a tetracoordinate complex[71] shed light on the possibility of using organoboron compounds for catalytic activation of diols and polyols, rather than as labile protecting groups. One can imagine attaining higher step- and atom-economy if a catalytic amount of organoboron and base could selectively enhance the nucleophilic character of OH groups properly configured to form electron-rich tetracoordinate adducts (Scheme 2.4).

---

[68] Karmee, S. K. *Synth. Commun.* **2013**, *43*, 450–455.

[69] Nishiyabu, R.; Kubo, Y.; James, T. D.; Fossey, J. S. *Chem. Commun.* **2011**, *47*, 1106.

[70] Bhaskar K, V.; Duggan, P. J.; Humphrey, D. G.; Krippner, G. Y.; McCarl, V.; Offermann, D. A. *J. Chem. Soc. Perkin Trans. 1* **2001**, *0*, 1098–1102.

[71] Oshima, K.; Kitazono, E. I.; Aoyama, Y. *Tetrahedron Lett.* **1997**, *38*, 5001–5004.

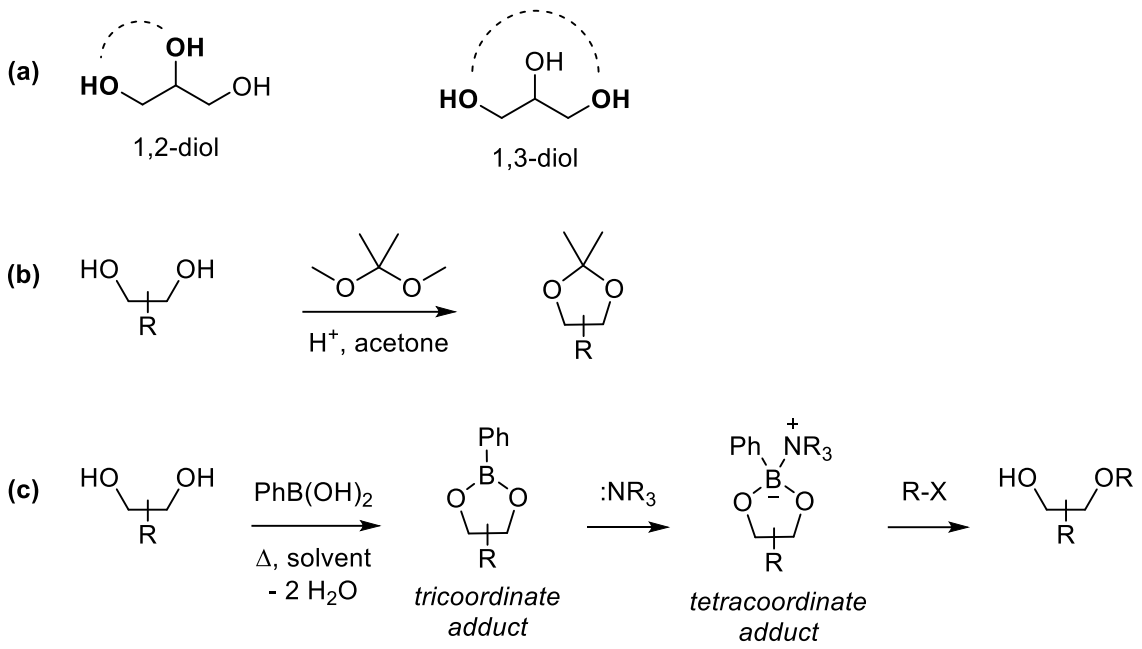

Scheme 2.4 (a) 1,2 and 1,3 binding motifs for glycerol. (b) 1,2-*cis*-diol protection *via* ketal formation. (c) Phenylboronic acid used to mask a 1,2-*cis*-diol as a tricoordinate adduct, followed by diol activation with Lewis base (tetracoordinate adduct).

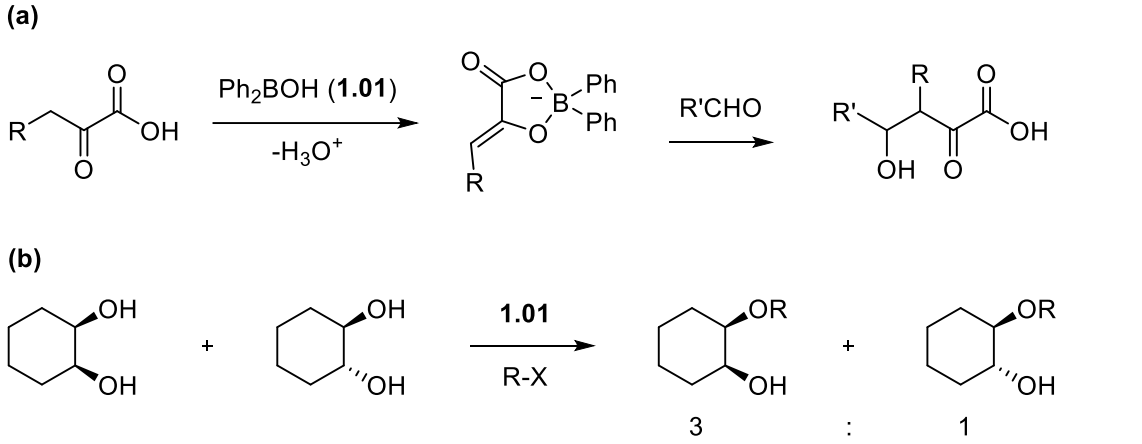

Scheme 2.5 Examples of the use of borinic acids for site-selective functionalizations of (a) pyruvic acids and (b) *cis*-configured diols.

Early work from the Taylor group exploited tetracoordinate boronate adducts for catalytic site-selective organic transformations. The starting point for this research was the catalytic aldol condensation of pyruvic acids with aldehydes in aqueous media, in which the pyruvic acid, in its

enol form, was activated *via* two-point binding to an organoboron species (Scheme 2.5).[72] In this study, a borinic acid (R_2BOH) capable of forming a tetracoordinate complex with *cis*-diols emerged as the most active catalyst, and subsequent studies demonstrated the effectiveness of diphenyl borinic acid **1.01** (see Scheme 2.5) in activating carbohydrate motifs to nucleophilic attack, specifically to acylation,[73] alkylation,[74] glycosylation,[75] and sulfonylation[76] reactions, all with high levels of selectivity. Site-selectivity of diol binding and of OH substitution are governed by the nature of the diol motif (*cis*-1,2-diols bind stronger than 1,3-diols) and by steric and electronic arguments (primary and equatorial OH groups are activated preferentially), respectively. We envisioned that the selective reactivity of primary or unencumbered OH groups in 1,2-diol motifs under borinic acid catalysis was a promising starting point for developing a site-selective *bis*-functionalization of glycerol.

2.4 Employing Borinic Acids as Polymerization Catalysts

The proposed polycondensation mechanism for glycerol *via* borinic acid-controlled acylation is shown in Scheme 2.6. Because both glycerol and 1-monoacyl glycerol possess a *cis*-1,2-diol motif while diacyl glycerol does not, and because borinic acids functionalize 1,2-diols approximately 30 times faster than isolated OH groups, we envisioned effectively converting glycerol, a trifunctional monomer prone to branching side-reactions, to a difunctional monomer, as the *bis*-acylated monomer would not react at an appreciable rate under the reaction conditions. In addition, we hypothesized that "second-generation" arylborinic acids **1.02** and **1.03** would prove more effective than their commercially available parent borinic acid **1.04** and its

---

[72] Lee, D.; Newman, S. G.; Taylor, M. S. *Org. Lett.* **2009**, *11*, 5486–5489.

[73] Lee, D.; Taylor, M. S. *J. Am. Chem. Soc.* **2011**, *133*, 3724–3727.

[74] Chan, L.; Taylor, M. S. *Org. Lett.* **2011**, *13*, 3090–3093.

[75] Gouliaras, C.; Lee, D.; Chan, L.; Taylor, M. S. *J. Am. Chem. Soc.* **2011**, *133*, 13926–13929.

[76] Lee, D.; Williamson, C. L.; Chan, L.; Taylor, M. S. *J. Am. Chem. Soc.* **2012**, *134*, 8260–8267.

deprotected analog **1.01** (Scheme 2.6). These boraanthracene-derived compounds[77] have been shown to promote site- and stereoselective glycosylations of carbohydrate derivatives at low catalyst loadings[78] and are good candidates for preparative polymerization due to their superior catalytic activity, thermal stability, and potential recoverability.

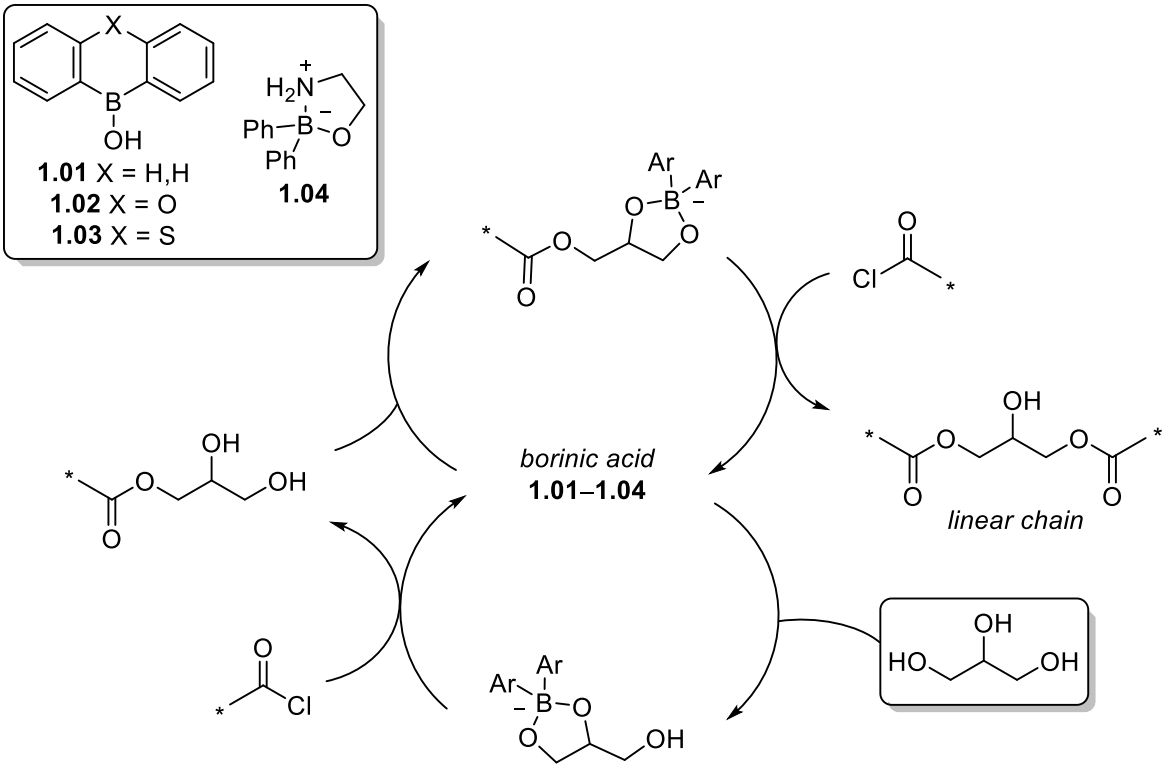

Scheme 2.6 Proposed catalytic cycle for a one-step site-selective polycondensation of glycerol showing first-generation (**1.01**, **1.04**) and second-generation (**1.02**, **1.03**) borinic acid catalysts.

3 Results and Discussion

3.1 Model Acylations

To assess the feasibility of using borinic acid catalysts in a preparative-scale polymerization of glycerol, we first attempted to simulate plausible polycondensation conditions by synthesizing small-molecule models of the polymer target. These exploratory "model reactions" were carried

---

[77] Dimitrijević, E.; Taylor, M. S. *Chem. Sci.* **2013**, *4*, 3298–3303.

[78] D'Angelo, K. A.; Taylor, M. S. *J. Am. Chem. Soc.* **2016**, *138*, 11058–11066.

out on 0.2 mmol scale and analyzed by quantitative ^{1}H NMR spectroscopy. Conditions that resulted in maximal conversion of glycerol to the 1,3-disubstituted glyceride model were used to predict optimal conditions for a regioregular copolymerization of glycerol with a diacyl chloride.

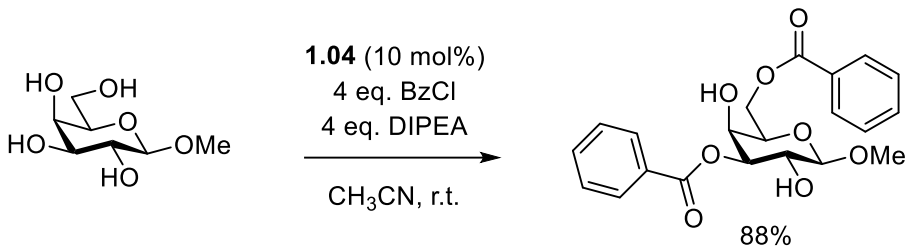

Scheme 2.7 Precedent for a high-yielding *bis*-functionalization of a polyol using a borinic acid catalyst.

To find potentially useful model reaction conditions, we drew inspiration from past work done by our group[73] in which the use of 10 mol% borinic acid catalyst promoted the *bis*-acylation of a galactopyranoside substrate in 88% yield in the presence of 4 equivalents of benzoyl chloride (BzCl) (Scheme 2.7). We sought to compare the free borinic acid **1.01** to its ligand-bound form **1.04** as well as select the optimal solvent for formation of 1,3-dibenzoylated glyceride. Table 2.1 summarizes the results of this optimization using 2 equivalents of BzCl, 3 equivalents of *N*,*N*-diisopropylethylamine (DIPEA), and 10 mol% of catalyst. In acetonitrile (CH_3CN) solvent, the unprotected borinic acid **1.01** showed dramatically higher conversion to the desired product than did **1.04** and was therefore explored further in a series of organic solvents. Tetrahydrofuran (THF) gave the best yield of 1,3 substituted diacylglycerol (Table 2.1, entry 6). Selecting THF as the solvent for preparative-scale polyester synthesis was also consistent with its widespread use in solubilizing PGS prepolymers.[45,79]

---

[79] Lee, K.; Wang, Y. *J. Vis. Exp.* **2011**, *50*, e2691.

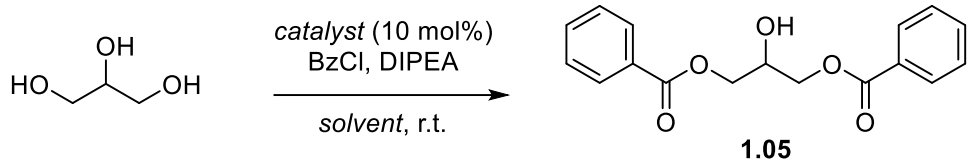

1.05

Table 2.1 Optimization of catalyst and solvent for model *bis*-benzoylation of glycerol.

Entry	Catalyst	Solvent	% Yield 1.05*
1	**1.04**	CH_3CN	56
2	**1.01**	CH_3CN	81
3	**1.01**	DCM	90
4	**1.01**	dichloroethane	94
5	**1.01**	acetone	92
6	**1.01**	THF	98

* – determined by ^{1}H NMR using mesitylene as internal standard.

3.2 Synthesis and Characterization of Linear PGS

When we subjected glycerol to a five-hour polycondensation with sebacoyl chloride using 5 mol% **1.01** and 3 equivalents of DIPEA in THF heated to 70 °C, we obtained PGS with a M_n of 37.7 kDa and a dispersity of 1.5, at 75% yield after precipitation from cold methanol. Relative molecular weights were obtained by gel permeation chromatography (GPC) in *N*-methyl-2-pyrrolidone (NMP) containing 1 g/L LiCl at 85 °C relative to PMMA standards. The product was a white powder and its high solubility in common organic solvents such as acetone, *N*,*N*-dimethylformamide (DMF), THF, dichloromethane, and chloroform ($CHCl_3$) was consistent with a linear structure free of significant cross-linking or network formation. In contrast, when glycerol was treated with sebacoyl chloride in the presence of the acylation catalyst 4-(dimethylamino)pyridine (DMAP), a gel-like material was obtained within minutes, reflecting extensive network formation under traditional catalytic conditions.

^{1}H NMR signals for PGS in deuterated dimethyl sulfoxide (DMSO-d_6) were sharp and well-resolved, suggesting a well-defined microstructure (see Figure 2.4, section 3.5). Despite overlapping significantly, proton signals in $CDCl_3$ were substantially sharper than those shown in existing literature reports. The presence of one major and one minor linkage type in the

polymer became apparent, but similarities in chemical shifts led to integrations that were lacking in dependability. To achieve reliable quantification of linear, terminal and branch polymer units, we turned to ^{13}C NMR for its higher sensitivity to small changes in chemical environment that result in more dramatic chemical shift differences between similarly bonded nuclei.[80] Luckily, ^{13}C NMR signals of the various PGS linkages were indeed baseline separated and presented diagnostic value (Figure 2.1). With the use of the relaxation agent tris(acetylacetonato) chromium(III), ^{13}C NMR spectra were used to determine the relative abundance of various linkage types by integrating their respective methine carbon signals.[81] The major signals identified in the product of the catalyzed polymerization were attributed to 1,3 (90–95%) and 1,2 (5–10%) diglyceride units. The level of branching of the PGS synthesized under these conditions was also lower than those reported for linear PGS prepared *via* ROP of diglycidyl ethers (<1 *vs.* approximately 10%).[63]

---

[80] Vlietinck, A. J.; Pieters, L. A. C. *J. Pharm. Biomed. Anal.* **1989**, *7*, 1405–1417.

[81] Otte, D. A. L.; Borchmann, D. E.; Lin, C.; Weck, M.; Woerpel, K. A. *Org. Lett.* **2014**, *16*, 1566–1569.

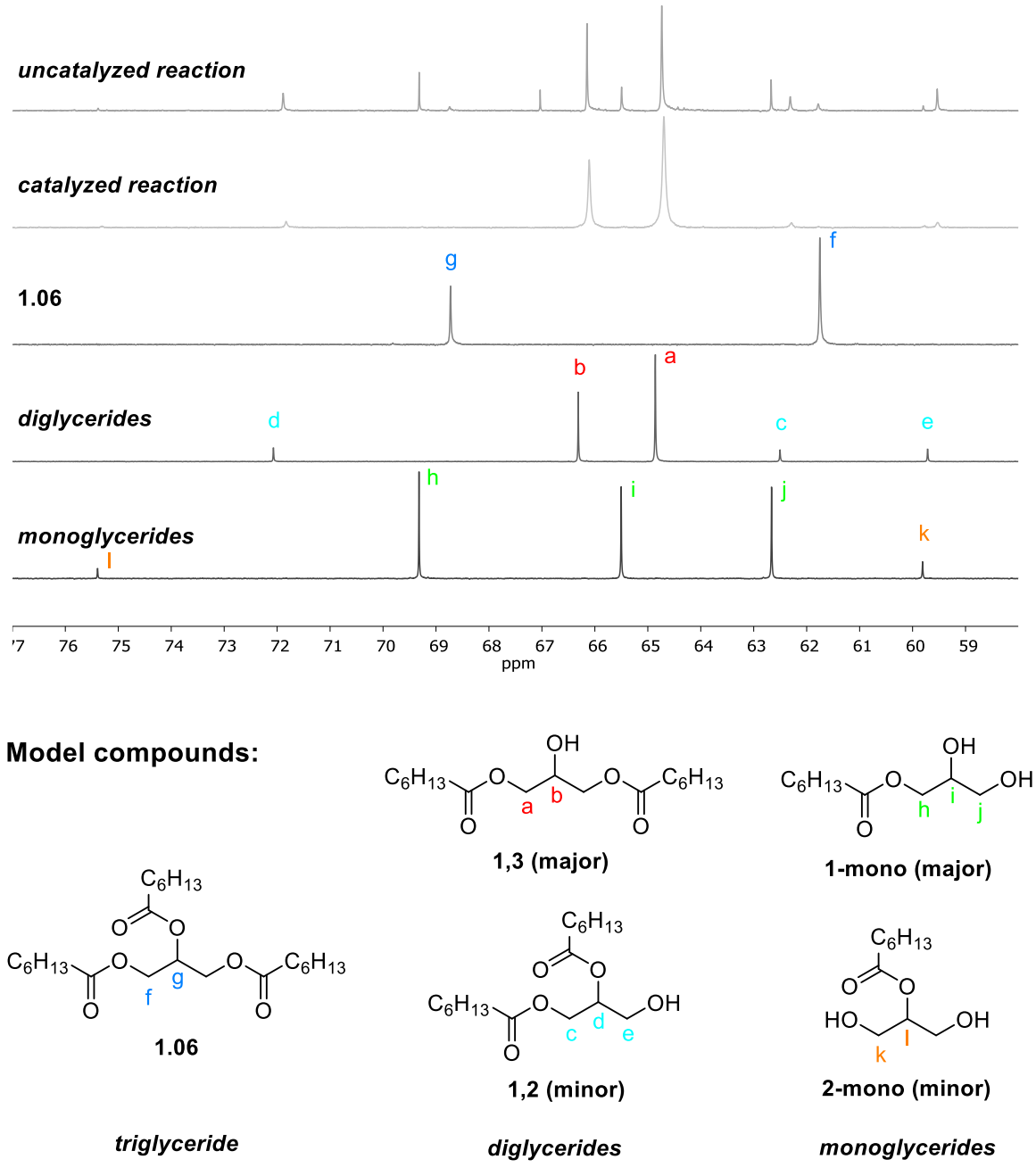

Figure 2.1 ^{13}C NMR spectra of PGS resulting from a catalyst-free control and a reaction catalyzed by **1.03**. The correspondence of PGS carbon signals to those of model glyceride compounds is shown. All spectra were taken in DMSO-d_6.

An uncatalyzed polycondensation was used as a control for the catalyst-controlled reaction, in addition to allowing for the characterization of a statistically determined distribution of linkages, which was found to be 20% mono-, 75% di- and 5% triglycerides. Signal

assignments in the glycerol region were consistent with previous reports.[56,57] Model compounds were also prepared to confirm ^{13}C NMR signal assignments: **1.06** was prepared by *tris*-functionalizing glycerol with a long-chain acyl chloride, and mixtures of mono- and diglyceride models were prepared using borinic acid catalysis (Figure 2.1). A complete analysis of the various linkage types produced from an uncontrolled polycondensation of glycerol with a diacyl chloride enabled us to further study the reaction and optimize conditions.

3.3 Optimization of Polymerization Conditions

To generate large quantities of a polymer, it is preferable to develop a process that uses a minimal amount of catalyst. For the purpose of this goal it is useful to evaluate the performance of the polymerization at lower catalyst loadings to establish the optimal catalyst for producing well-defined linear polyesters. Initial attempts to study the kinetics of the polycondensation by determining the rate of glycerol consumption by ^{1}H NMR spectroscopy were unsuccessful because a step-growth polymerization consumes monomers rapidly to form oligomers, rendering the ideal timescale of aliquot collection unfeasible. An alternate approach involved the monitoring of functional group disappearance by *in situ* infrared (IR) spectroscopy. We were able to observe the diminution of the acyl chloride C=O stretch for a short period of time, but the heterogeneous nature of the reaction due to the precipitation of hydrochloride salt impeded the collection of reliable data by this method. Attempts at studying a small-molecule model acylation using butyryl chloride ($CH_3CH_2CH_2COCl$) instead of sebacoyl chloride failed due to similar issues. Thus, we decided to compare the activity of various borinic acid catalysts indirectly.

Under catalytic reaction conditions, peracylation of glyceride motifs to yield a triglyceride unit can only result from acylation of isolated OH groups and therefore is predominantly reflective of background reactivity rather than catalyst-controlled reactivity. Therefore, we used the degree of linearity of a polymer as the figure of merit to identify the catalyst that would promote the formation of linear chains at minimal loading. The relative concentrations of undesirable branch points and 1,2 linkages were obtained from ^{13}C NMR spectra of polymers synthesized using catalysts **1.01**, **1.02**, **1.03**, or **1.04** and are shown in Table 2.2 along with the molecular weights of the polyesters. To avoid creating a bias for longer chains by precipitating the crude polymer mixture, molecular weight and linkage distributions are

shown for unfractionated polymers obtained after a mildly acidic aqueous wash in dichloromethane (DCM).

When **1.04** was used as catalyst, an insoluble precipitate quickly appeared in the reaction mixture and the resulting polyester was a dense solid with poor solubility relative to those obtained using unprotected catalysts. Performing quantitative NMR on this insoluble polymer was not feasible, and GPC analysis was probably limited to the soluble fraction that leached from the cross-linked network. This relatively uncontrolled process can be explained in part by the additional step required to remove the ethanolamine ligand to activate the borinic acid species, a process that could be consuming up to 1% of the acyl dichloride comonomer and limiting the amount of active catalyst present in the early stages of the reaction.[76] Despite leading to a successful polymerization at 5 mol%, **1.01** failed to fully suppress branching at 1 mol% loading, unlike **1.02** and **1.03**. We were not entirely surprised to find that the boraanthracene-derived catalysts were able to catalyze the formation of polyesters free of triacylglycerol repeat units more effectively, since these compounds are known to show higher activity with respect to the commercially available **1.01** due to the higher nucleophilicity of their corresponding tetracoordinate adducts.[77]

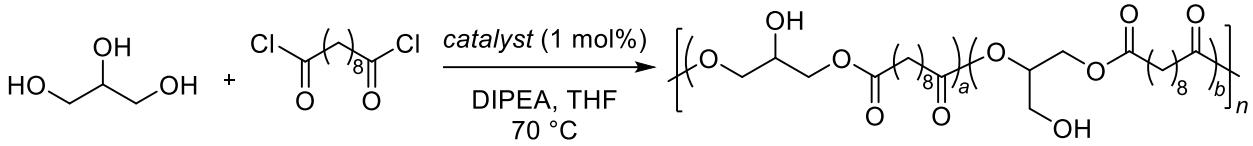

Table 2.2 Optimization of catalyst for the polycondensation of glycerol and a diacyl chloride.

Entry	Catalyst	M_n*	Đ*	% triacyl†	% 1,2†
1	-	8.7	1.7	5	11
2	**1.01**	12.5	1.3	<1	7
3	**1.02**	11.9	1.2	<1	6
4	**1.03**	19.2	1.2	<1	6
5	**1.04**	37.6	2.2	-	-

* – molecular weights are expressed in kDa relative to PMMA standards and determined by GPC, NMP, 85 °C. † – determined by quantitative ^{13}C NMR by comparing integrations at 66.2 (1,3), 71.9 (1,2) and 68.8 (triacyl) ppm.

Control of background reactivity appeared similar in both boraanthracene-derived catalysts at 1 mol% loading; therefore, a closer look at the outcome of their respective polymerizations was necessary. GPC indicated that polymers produced with **1.03** had considerably higher M_n values than those obtained with **1.02**, consistent with a more sluggish polymerization with **1.02**, which also resulted in a higher monoacyl end group content that pointed to a low degree of polymerization. The origins of the superior catalyst activity of **1.03** in a polycondensation is unclear. Despite resulting in M_n values lower than those obtained with **1.01**, **1.03** was selected as the optimal catalyst for the preparation of PGS, affording a good compromise between catalyst activity, average molecular weight, site-selectivity, yield and catalyst loading, giving a number-average degree of polymerization of roughly 74 (M_n = 19.2 kDa). We were able to scale up the polycondensation using **1.03** to 1 g, further improving all reaction parameters (see Table 2.3).

3.4 Scope

Several aliphatic and aromatic diacyl chloride comonomers were explored under standard conditions (Figure 2.2, Table 2.3), all affording polyesters which showed no significant branching by ^{13}C NMR spectroscopy. Polymerizations with acyl dichlorides of smaller size benefited from increased catalyst loadings in terms of M_n, dispersity index (Đ), definition of

peaks by ^{1}H NMR, and suppression of over-functionalization. To verify that all pendant OH groups in the polyesters were unreacted, we performed substitution experiments to show quantitative acetylation of all OH groups by ^{1}H NMR. Successful peracetylation of the products was consistent with a 1:1 monomer ratio (Figure 2.3).

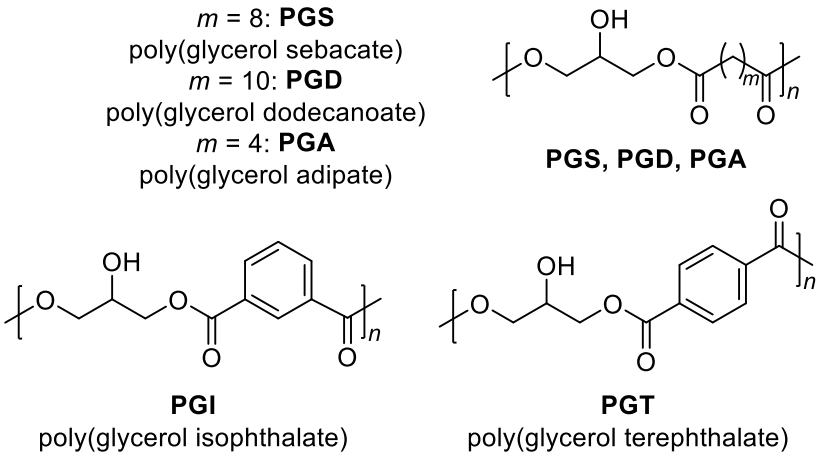

Figure 2.2 Scope of glycerol-derived polyesters explored in this chapter.

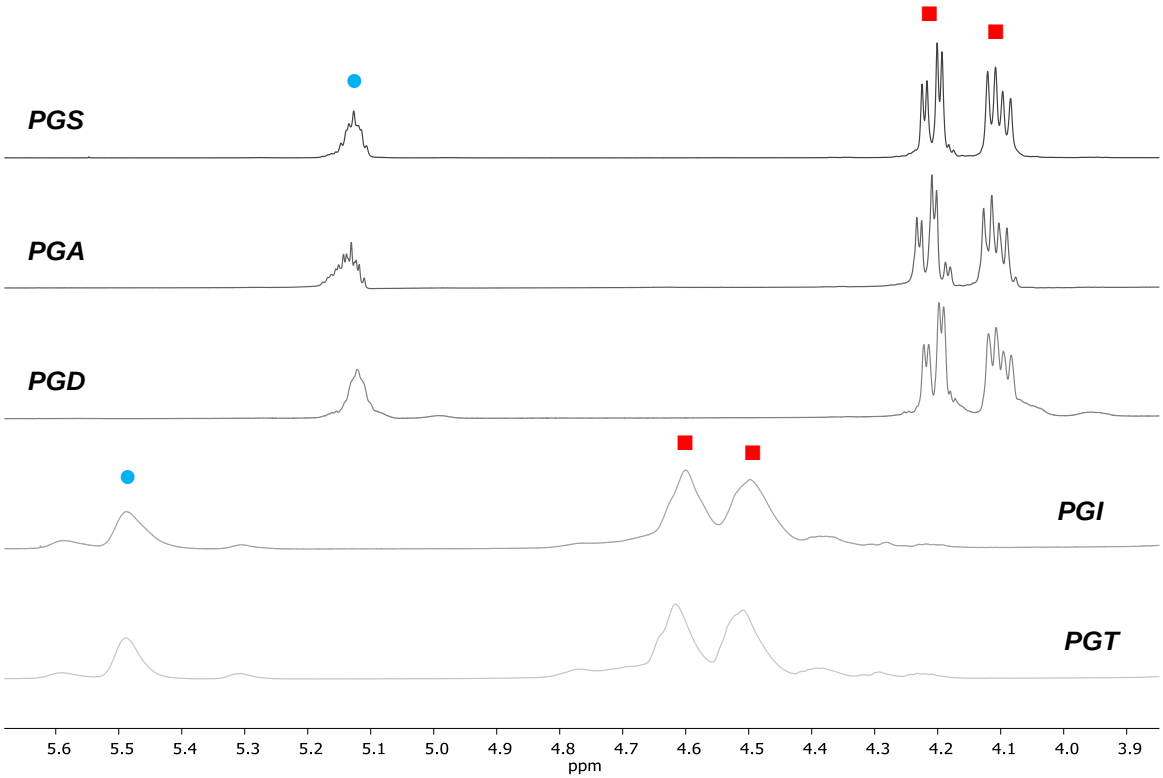

Figure 2.3 ^{1}H NMR spectra expansion of fully acetylated glycerol-derived polyesters showing methine (●) and methylene (■) groups of the triglyceride. Starting from the top: *O*-peracetylated PGS, PGA, PGD, PGI and PGT. All spectra were taken in DMSO-d_6.

Copolymerizations of short-chain aliphatic diacyl chlorides such as succinyl ($ClCOCH_2CH_2COCl$) and glutaryl ($ClCOCH_2CH_2CH_2COCl$) chlorides resulted in poorly isolable, insoluble black resins whose soluble fractions showed some level of branching by ^{13}C NMR. Similarly, in past reports in which succinic acid and glutaric acid were copolymerized in the bulk with glycerol, the resulting elastomers had a markedly higher degree of branching compared to longer-chain diacids.[56] The lower average-molecular weights of the aryl-derived copolymers and their higher branch rates at 1 mol% catalyst loading may be due to the low solubility of the polymer and a loss of catalyst control due to the higher reactivity of the electrophile, respectively. Typically, diacyl chlorides with more flexible chains were amenable to a more controlled polymerization, yielding a more homogenous microstructure, lower Đ, higher M_n, lower fraction of 1,2 linkages, as seen by the higher tolerance of dodecanedioyl chloride and sebacoyl chloride reactions for lower catalyst loadings. In the case of adipoyl chloride, reducing the equivalents of base from three to two was needed to maintain a high ratio of 1,3- to 1,2-

enchained units. This change of conditions reduces the rate of base-catalyzed acyl migration that results in equilibration between the two linkage types (see section 3.5).

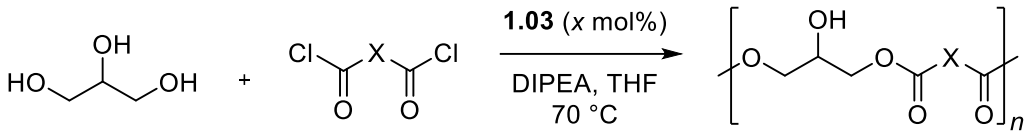

Table 2.3 Synthesis of glycerol-derived polyesters using **1.03** as catalyst.

Entry	Polymer	mol% 1.03	M_n*	Đ*	% 1,2†	% Yield
1‴	PGS	1	24.4	1.4	7	93
2	PGD	1	19.6	1.1	5	87
3‡	PGA	5	30.0	1.4	3	94
4	PGI	2	10.0	1.6	15	90
5	PGT	2	10.0	1.4	13	92

* – molecular weights are expressed in kDa relative to PMMA standards and determined by GPC, NMP, 85 °C. † – determined by quantitative ^{13}C NMR by comparing integrations at 66.2 (1,3) and 71.9 (1,2) ppm. ‴ – experiment was performed on 1 g scale. ‡ – 2 equivalents of DIPEA were used.

The physical and thermal properties of glycerol polyesters were strongly influenced by nature of the diacid component, with aromatic products behaving quite differently from their aliphatic counterparts. Poly(glycerol isophthalate), or PGI (Table 2.3, entry 4) and poly(glycerol terephthalate), or PGT (Table 2.3, Entry 5), were brittle, glassy and poorly soluble solids at room temperature. The T_g values for these materials, as measured by differential scanning calorimetry (DSC), were 58 and 66 °C respectively, indicating significant restrictions in chain mobility. The combined effects of hydrogen bonding arising from free OH groups and non-covalent interaction of the phenyl rings within the rigid backbone can be used to rationalize this effect. On the other hand, aliphatic copolymers PGS, poly(glycerol dodecanoate) (PGD) and poly(glycerol adipate) (PGA) (Table 2.3, entries 1–3) showed lower T_g values at –34, 18 and –36 °C, respectively, and were softer and more pliable (PGA was isolated as a highly soluble, viscous oil) compared to PGI and PGT. PGS and PGD, though structurally close, appeared to have vastly different T_g values, a trend noted in previous reports of their crosslinked analogs (*cf.* T_g below –80 °C for

PGS and 32 °C for PGD).[36,82] PGS and PGD also exhibited endotherms within the observed temperature range, likely stemming from the crystallization of their hydrocarbon domains. The long, flexible acyl chains contribute to the more rubbery characteristics of the aliphatic polymers, as well as to their superior solubility in a range of organic solvents.

3.5 Isomerization of Polymer Backbone

The predominance of 1,3-enchained units over 1,2-enchained units in polyesters produced by borinic acid catalysis appears to reflect kinetic rather than thermodynamic control, though the complete suppression of 1,2-enchained unit formation could not be achieved (Figure 2.4). To elucidate the origins of 1,2 linkages obtained under polymerization conditions, we subjected prepared polyesters to triethylamine (Et_3N, 3 equivalents per monomer unit) in THF at 70 °C to induce base-promoted acyl migration[83] in the backbone. As shown in Table 2.4, the proportion of 1,2 linkages as determined by quantitative ^{13}C NMR did increase until it reached equilibrium after about 12 hours. The increase in the fraction of 1,2-diacylglycerol motifs in polyester backbones was not accompanied by an increase in the degree of branching, indicating that the linear polymer architecture was maintained during the isomerization. In the case of PGS, a three-fold increase in 1,2 linkages was noted. PGD and PGA showed a similarly dramatic increase, while aromatic copolymers gave rise to almost no change in isomeric ratios.

---

[82] Migneco, F.; Huang, Y.; Birla, R. K.; Hollister, S. J. *Biomaterials* **2009**, *30*, 6479–6484.

[83] Roslund, M. U.; Aitio, O.; Wärna, J.; Maaheimo, H.; Murzin, D. Y.; Leino, R. *J. Am. Chem. Soc.* **2008**, *130*, 8769–8772.

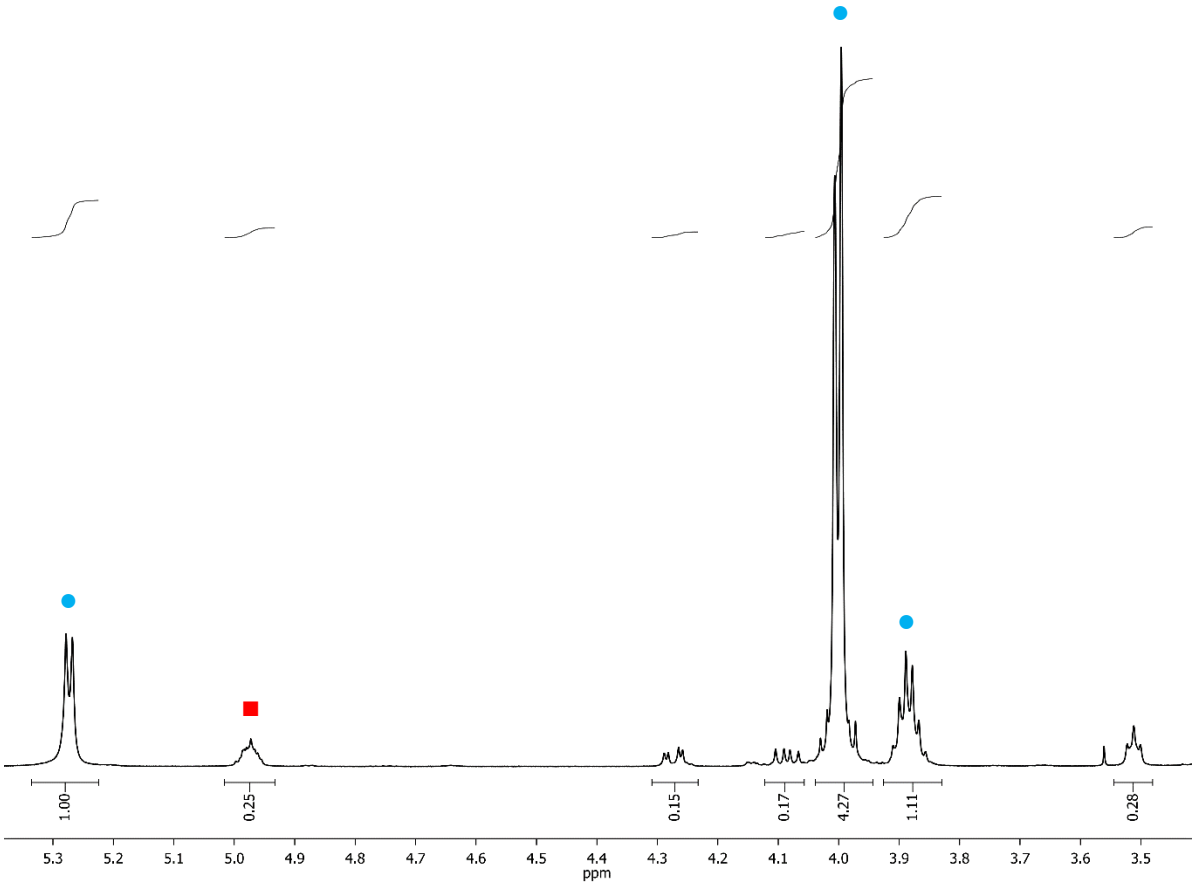

Figure 2.4 Expansion of the ^{1}H NMR spectrum of PGS in DMSO-d_6 obtained using 5 mol% **1.01** showing signals from 1,3- (●) and 1,2-enchained (■) units.

We speculate that the differences in 1,2-diacylglycerol content of the initially synthesized polymers most likely arise from varying extents of acyl migration under the polymerization conditions. In general, the levels of site-selectivity observed in the polymerizations were lower than those for simple acylations of primary versus secondary OH groups in diol substrates.[76] Presumably, acyl migration is more prevalent in the polymerizations because of the higher reaction temperatures employed: borinic acid-catalyzed acylations of diols were generally conducted at room temperature or below. In any case, this ability to use kinetic control to access polymers whose structures can be altered through a subsequent equilibration, while maintaining the linear architecture, is a noteworthy aspect of the catalyst-controlled polymerization.

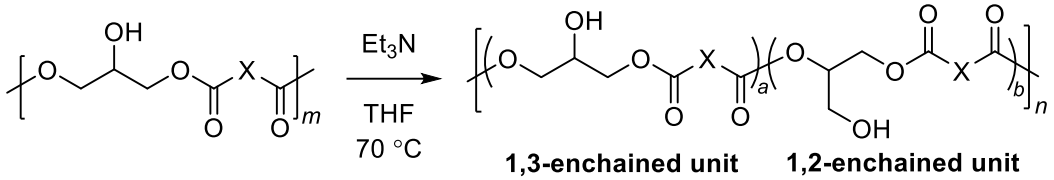

Table 2.4 Base-promoted isomerization of glycerol-derived polyesters.

Entry	Polymer	Initial % 1,2*	Final % 1,2*
1	**PGS**	7	20
2	**PGD**	5	22
3	**PGA**	3	32
4	**PGI**	15	21
5	**PGT**	13	21

* – determined by quantitative ^{13}C NMR by comparing integrations at 66.2 (1,3) and 71.9 (1,2) ppm.

3.6 Post-polymerization Reactions of Poly(glycerol sebacate)

A notable advantage of carrying out a site-selective polymerization of a monomer with three or more OH groups in one step is the establishment of a simple route toward linear polymers with multiple pendant functional groups. A high density of pendant OH groups would enable the attachment of a larger payload when the aim is to release a therapeutic agent locally, like in biodegradable polymeric wafers. Biologically active groups have also been attached to functionalized polyesters to facilitate cell adhesion.[29]

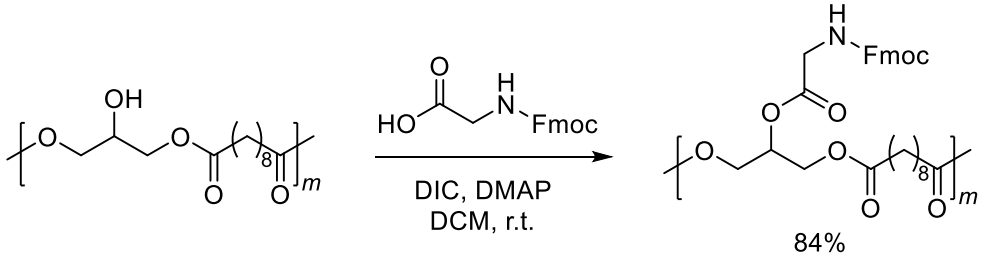

Scheme 2.8 Post-polymerization of PGS by installment of Fmoc–glycine.

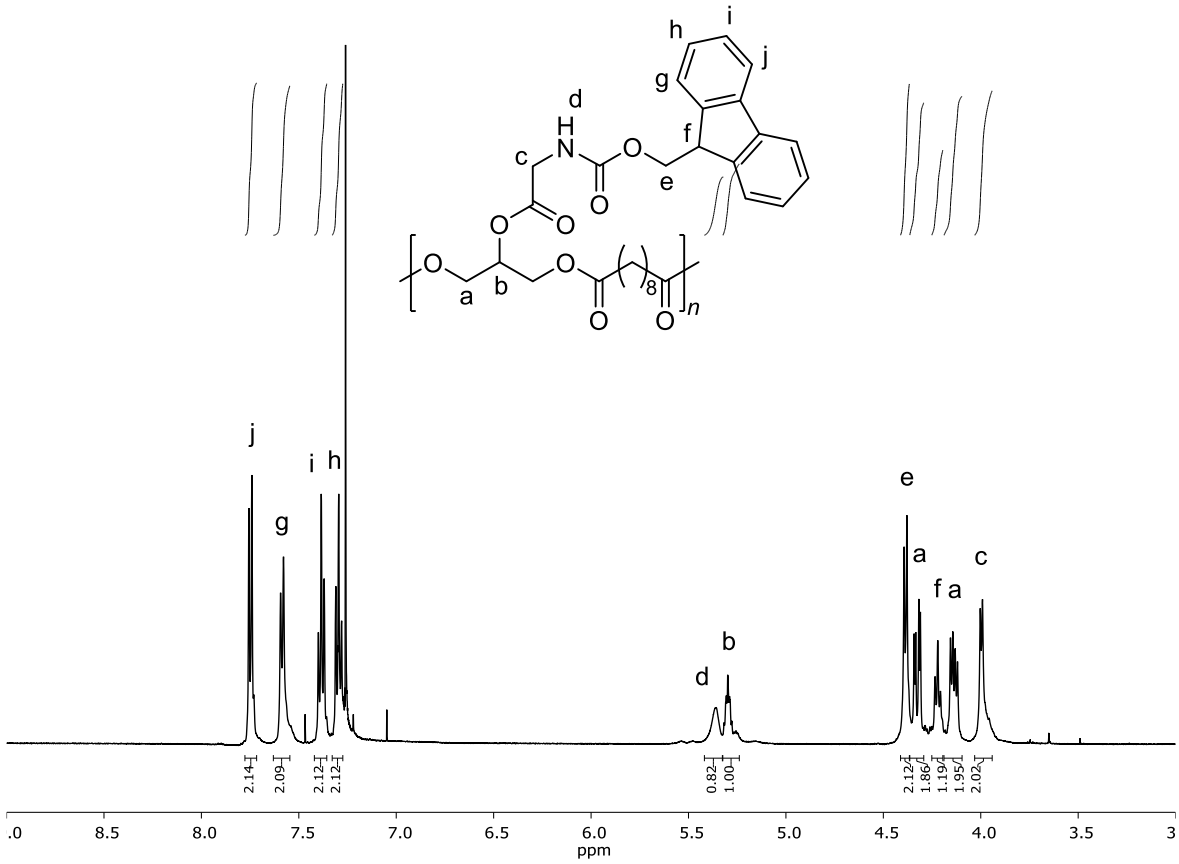

Figure 2.5 Expansion of the ^{1}H NMR spectrum of PGS glycinate in $CDCl_3$.

To confirm the utility of the free OH groups of linear PGS from a synthetic standpoint, we wanted to demonstrate that traditional, mild reaction conditions would allow for the quantitative installment of biologically relevant molecules onto the pendant functional groups. A successful implementation of this strategy would further illustrate the synthetic versatility of high M_n linear polyesters of this type for more advanced applications. To show this, a DMAP-catalyzed carboiimide-promoted amide coupling on a prepared PGS backbone was performed at room temperature using *N*,*N*′-diisopropylcarbodiimide as the coupling agent in DCM solvent. Quantitative attachment of the protected amino acid Fmoc–glycine was achieved (Scheme 2.8), with over 95% conversion to PGS glycinate shown by ^{1}H NMR spectroscopy (Figure 2.5).[63]

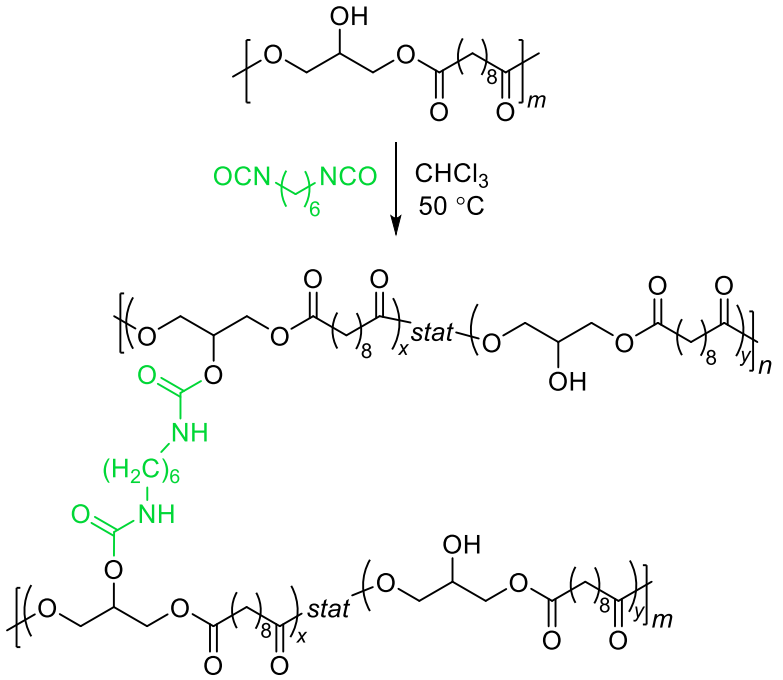

Scheme 2.9 Introduction of cross-links to linear PGS using HDI.

Finally, the establishment of a facile route to chemically cross-linked elastomeric materials derived from linear PGS was sought. Several attempts were made to introduce cross-links to the growing polymer *in situ* by introducing a small excess of sebacoyl chloride after 5 hours of standard borinic acid-promoted polycondensation at a 1:1 monomer feed ratio; however, final triacylglycerol content as judged by ^{13}C NMR was low and showed no correlation with the amount of extra chloride added, at least in the 1–5 mol% range. We feared that the addition of a larger excess of chloride would lead to network formation and impede isolation of the cross-linked material. Similar experiments involving *in situ* acylation with BzCl also failed to deliver a significant degree of functionalization of the pendant OH groups despite even the addition of catalytic amounts of DMAP, suggesting suppressed reactivity of isolated OH groups under the polymerization conditions. We cannot confidently pinpoint a cause for this, although it is possible that a relatively small hydrodynamic volume under these conditions is rendering the more centrally located backbone OH groups inaccessible to electrophilic approach. After a series of unsuccessful *in situ* cross-linking experiments, purified linear PGS was subjected to mild, catalyst-free cross-linking conditions at various cross-linker concentrations (Scheme 2.9). We selected the diisocyanate HDI as cross-linker to create urethane cross-links for the lack of by-

products generated during urethane formation and because we were aware of previous reports showing favourable elastomeric properties in polyurethane-doped polyesters.[84] By varying the HDI loading from 0.5 to 20 mol% per pendant OH group, a series of polymeric networks was generated. The incorporation of cross-links was quantified by attenuated total reflectance FTIR (Fourier-transform infrared) spectroscopy, and the peak height of the characteristic urethane C=O stretch at 1540 cm^{-1} was found to increase linearly as a function of mol% HDI added (Figure 2.6). From this data, it appears that urethane cross-links can be introduced with fine control.

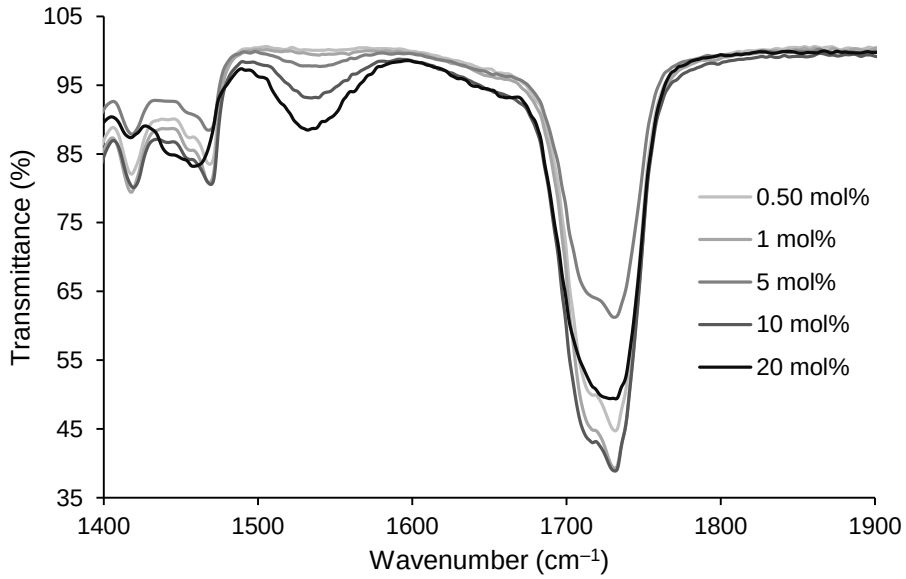

Figure 2.6 Representative IR spectra of cross-linked PGS at different HDI concentrations showing the carbonyl peak around 1730 cm^{-1} and the growing urethane peak around 1540 cm^{-1} used to estimate the rate of cross-link incorporation.

The physical properties of the cross-linked PGS products were quite different from native PGS, characterized by facile film formation, a marked reduction in solubility at 10 and 20 mol% HDI, as well as a slight increase in apparent M_n and Đ as judged by GPC analysis of the soluble networks (Table 2.5). The precise introduction of cross-links in such a post-polymerization step

[84] Dey, J.; Xu, H.; Shen, J.; Thevenot, P.; Gondi, S. R.; Nguyen, K. T.; Sumerlin, B. S.; Tang, L.; Yang, J. *Biomaterials* **2008**, *29*, 4637–4649.

is a potentially useful tool for the preparation of biomaterials with a specific set of physical, mechanical, and biodegradation characteristics required to suit diverse tissue engineering or drug delivery applications.

Table 2.5 GPC, IR and solubility data for urethane cross-linked PGS.

Entry	mol% HDI	Solubility	Urethane:ester ($\cdot 10^{-3}$)†	M_n*	Đ*
1	0	soluble	-	24.4	1.4
2	1	soluble	7.5	28.4	1.5
3	2	soluble	18	29.7	1.5
4	3	soluble	26	33.7	1.5
5	5	network	42	-	-
6	10	network	58	-	-
7	20	network	130	-	-

† – determined by FTIR by comparing peak heights at 1730 cm^{-1} (ester) and 1540 cm^{-1} (urethane). * – molecular weights are expressed in kDa relative to PMMA standards and determined by GPC, NMP, 85 °C.

4 Conclusions

The results outlined in this chapter are an illustration of the promise shown by organoboron catalysts in preparing polyol-derived polyesters with controlled microstructures. Specifically, this work showcases the ability of borinic acid catalysis to suppress the overfunctionalization of a trifunctional monomer and favour reactivity at more nucleophilic *cis*-1,2 or 1,3-diols over isolated secondary OH groups. Use of a boraanthracene-derived catalyst thus enables the synthesis of linear aliphatic and aromatic glycerol-based polyesters from readily available reagents and without recourse to protection/deprotection tactics. The development of this synthetic method is significant in light of the many applications of bio-derived macromolecules, particularly in the biomedical field. More broadly, this methodology can be extended to more complex polyols that currently face limitations as feedstocks for polymer chemistry due to their high degree of functionality, *e.g.*, carbohydrate derivatives. Later chapters will describe the exploration of these avenues.

5 Experimental

5.1 General Considerations

Reactions were carried out in oven-dried glassware without effort to exclude air, unless otherwise indicated. Stainless steel syringes were used to transfer air- and moisture-sensitive liquids. Flash chromatography was carried out using neutral silica gel from Silicycle. Analytical TLC was carried out using aluminum-backed silica gel 60 F_{254} plates (EMD).

5.1.1 Materials

HPLC grade THF and DCM were dried and purified using a solvent purification system equipped with columns of activated alumina, under nitrogen (Innovative Technology, Inc.). All other reagents and solvents were purchased from Sigma Aldrich and used without further purification.

5.1.2 Instrumentation

^{1}H and ^{13}C NMR spectra were recorded using an Agilent DD2-500 (500 MHz) spectrometer with XSens cryogenic probe. The spectra were processed using MestreNova. Chemical shifts are reported in parts per million (ppm) relative to tetramethylsilane with the solvent resonance resulting from incomplete deuteration as the internal standard. For ^{1}H NMR: $CDCl_3$ 7.26 ppm; DMSO-d_6 2.50 ppm, p; for ^{13}C NMR: $^{13}CDCl_3$ 77.0 ppm, t; DMSO-d_6 39.52 ppm, hept. Spectral features are tabulated in the following order: chemical shift (δ, ppm); multiplicity (s-singlet, d-doublet, t-triplet, q-quartet, m-complex multiplet, app-apparent); coupling constants (*J*); number of protons. For quantitative ^{13}C NMR, samples were dissolved in DMSO-d_6 containing 65 mM of relaxation agent $Cr(acac)_3$ with a concentration of 250 mg/mL. Acquisition parameters were set to a 10 second relaxation delay to allow for full relaxation of the ^{13}C nuclei. FTIR spectra were obtained on a Perkin-Elmer Spectrum 100 instrument equipped with a single-bounce diamond/ZnSe ATR accessory either in the solid state or as neat liquids, as indicated. The spectra were processed using Spectrum Express. GPC was conducted at 85 °C using a 1.0 g/L solution of LiCl in NMP as eluent, at a flow rate of 1.0 mL/min through two Agilent PLgel 5μm MIXED-C columns equipped with a guard column and a refractive index detector. PMMA

standards were used for calibration. Differential scanning calorimetry (DSC) was performed using a Thermal Advantage Q100 DSC under N_2, with a heating rate of 10 °C/min. Measurements were analyzed using TA Universal Analysis and the glass transition temperature (T_g) was taken as the midpoint of the inflection tangent on the second heating scan.

5.2 Synthesis and Characterization of Polymers

5.2.1 General Procedure for Polymer Synthesis

Glycerol (1 equivalent) and **1.03** (1–5 mol%) were weighed into a 100-mL round bottom flask equipped with a stir bar. THF (0.3 M) and DIPEA (3 equivalents, or 2.05 equivalents for PGA) were added *via* syringe and the resulting solution was stirred at 0 °C. Diacyl chloride (1 equivalent) was added dropwise (for isophthaloyl chloride, a solution in THF was made so that the final concentration of the reaction was 0.3 M; terephthaloyl chloride was added neat and allowed to dissolve slowly). A white precipitate appeared. The reaction was heated to 70 °C for 5 hours, cooled, and quenched by adding 5 mL methanol. The solution was concentrated by rotary evaporation, dissolved in a minimum amount of appropriate solvent, and precipitated by dropwise addition into a poor solvent or solvent mixture (see below for details).

5.2.1.1 Isolation of Unfractionated Polymers

Polymers were prepared according to the procedure outlined in section 5.2.1. After the reaction was stopped and concentrated, it was diluted with DCM and transferred to a 250-mL separatory funnel. The organic phase was washed twice with a saturated aqueous solution of ammonium chloride, dried over sodium sulfate, filtered, and concentrated by rotary evaporation. Crude samples were then dried under vacuum and analyzed by NMR and GPC as described above.

5.2.2 Polyester Synthesis and Characterization

Poly(glycerol sebacate) (PGS) Polymer was prepared from 12.3 mmol glycerol using 1 mol% **1.03** according to the general procedure. The resulting oil was dissolved in a minimum amount of THF and precipitated from 1 L of a 95:5 (v/v) mixture of methanol and water at 0 °C. Filtration followed by washing with methanol and drying under vacuum afforded 2.95 g of

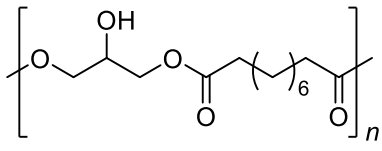

product as a beige powder (93%, M_n = 2.44 × 10^4; Đ = 1.40). Ratio of 1,2 to 1,3 linkages was 7:93 as calculated from the ratio of ^{13}C signals at 71.9 and 66.1 ppm, respectively. *Signals corresponding to 1,3-linkages (major):* ^{1}H NMR (500 MHz, DMSO-d_6) δ 5.24 (d, *J* = 5.2 Hz, 1H), 4.00–3.93 (m, 4H), 3.89–3.80 (m, 1H), 2.28 (t, *J* = 7.4 Hz, 4H), 1.72–1.40 (m, 4H), 1.31–1.13 (m, 8H) ppm. ^{13}C NMR (126 MHz, DMSO-d_6) δ 172.7, 66.1, 64.8, 33.4, 28.6, 28.4, 24.4 ppm. *Signals corresponding to 1,2-linkages (minor):* ^{1}H NMR (500 MHz, DMSO-d_6) δ 5.00–4.88 (m, 2H), 4.25 (dd, *J* = 11.9, 3.3 Hz, 1H), 4.09–4.04 (m, 1H), 3.48 (t, *J* = 5.8 Hz, 2H), 2.28 (t, *J* = 7.4 Hz, 4H), 1.72–1.40 (m, 4H), 1.31–1.13 (m, 8H) ppm. ^{13}C NMR (126 MHz, DMSO-d_6) δ 172.8, 71.9, 62.3, 59.6, 33.4, 28.6, 28.4, 24.4 ppm. IR (powder, cm^{-1}) 3464, 2924, 2851, 1732, 1716, 1217, 1167, 1136.

Poly(glycerol dodecanoate) (PGD) Polymer was prepared from 6.47 mmol glycerol using 1 mol% **1.03** according to the general procedure. The resulting oil was dissolved in a minimum amount of THF and precipitated from 800 mL of a 95:5 mixture of methanol and water at 0 °C. Filtration followed by washing with methanol and drying under vacuum afforded 1.61 g of product as a beige powder (87%, M_n = 1.96 × 10^4; Đ = 1.10). Ratio of 1,2 to 1,3 linkages was 5:95 as calculated from the ratio of ^{13}C signals at 71.9 and 66.1 ppm, respectively. *Signals corresponding to 1,3-linkages (major):* ^{1}H NMR (500 MHz, DMSO-d_6) δ 5.24 (m, 1H), 4.01–3.92 (m, 4H), 3.89–3.78 (m, 1H), 2.28 (t, *J* = 7.4 Hz, 4H), 1.57–1.43 (m, 4H), 1.28–1.17 (m, 12H) ppm. ^{13}C NMR (126 MHz, DMSO-d_6) δ 172.7, 66.1, 64.7, 33.4, 28.9, 28.7, 28.5, 24.4 ppm. *Signals corresponding to 1,2-linkages (minor):* ^{1}H NMR (500 MHz, DMSO-d_6) δ 4.97–4.87 (m, 1H), 4.79–4.61 (m, 1H), 4.23 (dd, *J* = 11.9, 3.2 Hz, 1H), 4.06–4.01 (m, 1H), 3.48–3.44 (m, 2H), 2.26 (t, *J* = 7.4 Hz, 4H), 1.56–1.39 (m, 4H), 1.26–0.99 (m, 12H) ppm. ^{13}C NMR (126 MHz, DMSO-d_6) δ 172.7, 71.9, 62.3, 59.5, 33.4, 28.9, 28.7, 28.4, 24.4 ppm. IR (powder, cm^{-1}) 3425, 2915, 2851, 1731, 1209, 1169, 1105.

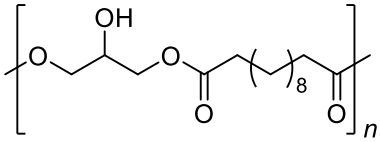

Poly(glycerol adipate) (PGA) Polymer was prepared from 6.08 mmol glycerol using 5 mol% **1.03** according to a modified variant of the general procedure using only 2 equivalents of DIPEA. The resulting oil was dissolved in a minimum amount of THF and precipitated from

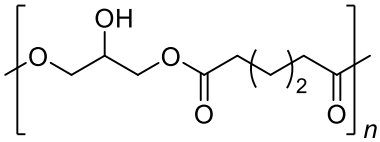

900 mL diethyl ether. The resulting amber oil was decanted, redissolved in THF, and precipitated from 800 mL water. Filtration followed by washing with water and toluene and drying under vacuum afforded 1.15 g of product as an amber oil (94%, M_n = 3.00 × 10^4; Đ = 1.42). Ratio of 1,2 to 1,3 linkages was 3:97 as calculated from the ratio of ^{13}C signals at 72.0 and 66.3 ppm, respectively. *Signals corresponding to 1,3-linkages (major):* ^{1}H NMR (500 MHz, DMSO-d_6) δ 5.25 (d, *J* = 5.3 Hz, 1H), 4.03–3.93 (m, 4H), 3.90–3.82 (m, 1H), 2.35–2.27 (m, 4H), 1.66–1.43 (m, 4H) ppm. ^{13}C NMR (126 MHz, DMSO-d_6) δ 172.7, 66.2, 64.9, 33.1, 23.8 ppm. *Signals corresponding to 1,2-linkages (minor):* ^{1}H NMR (500 MHz, DMSO-d_6) δ 5.05–4.89 (m, 2H), 4.24 (dd, *J* = 11.9, 3.5 Hz, 1H), 4.08 (dd, *J* = 5.6, 11.9 Hz, 1H), 3.49 (t, *J* = 5.6 Hz, 2H), 2.36–2.16 (m, 4H), 1.64–1.44 (m, 4H) ppm. ^{13}C NMR (126 MHz, DMSO-d_6) δ 172.7, 72.0, 62.3, 59.5, 33.1, 23.8 ppm. IR (thin film, cm^{-1}) 3458, 2954, 1727, 1134, 1069.

Poly(glycerol isophthalate) (PGI) Polymer was prepared from 6.42 mmol glycerol using 2 mol% **1.03** according to the general procedure. The resulting oil was dissolved in a minimum amount of THF and precipitated from 1 L isopropanol at 0 °C. Filtration followed by washing with isopropanol and drying under vacuum afforded 1.28 g of product as a brittle white solid (90%, M_n = 1.00 × 10^4; Đ = 1.55). Ratio of 1,2 to 1,3 linkages was 15:85 as calculated from the ratio of ^{13}C signals at 73.4 and 66.2 ppm, respectively. *Signals corresponding to 1,3-linkages (major):* ^{1}H NMR (500 MHz, DMSO-d_6) δ 8.66–8.33 (m, 1H), 8.29–7.97 (m, 2H), 7.78–7.46 (m, 1H), 4.60–4.32 (m, 4H), 4.28–4.11 (m, 1H) ppm. ^{13}C NMR (126 MHz, DMSO-d_6) δ 164.9, 133.8, 130.2, 129.9, 129.4, 66.3, 66.2 ppm. *Signals corresponding to 1,2-linkages (minor):* ^{13}C NMR (126 MHz, DMSO-d_6) δ 164.9, 133.8, 130.2, 129.9, 129.4, 73.5, 63.7, 59.6 ppm. IR (powder, cm^{-1}) 3449, 2960, 1713, 1608, 1223, 1074, 725.

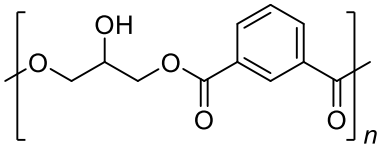

Poly(glycerol terephthalate) (PGT) Polymer was prepared from 6.59 mmol glycerol using 2 mol% **1.03** according to the general procedure. The resulting oil was dissolved in a minimum amount of DCM and methanol and precipitated from 1 L isopropanol. Filtration followed by washing with isopropanol and drying under vacuum afforded 1.35 g of product as a white solid (92%, M_n = 1.00 × 10^4; Đ = 1.44). Ratio of 1,2 to 1,3 linkages

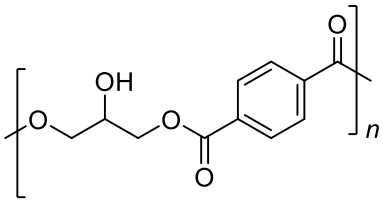

was 13:87 as calculated from the adjusted ratio of ^{13}C signals at 73.4 and 66.1 ppm, respectively. *Signals corresponding to 1,3-linkages (major):* ^{1}H NMR (500 MHz, DMSO-d_6) δ 8.13–7.96 (m, 4H), 4.44–4.33 (m, 4H), 4.25–4.18 (m, 1H) ppm. ^{13}C NMR (126 MHz, DMSO-d_6) δ 165.2, 133.8, 129.8, 66.1 ppm. *Signals corresponding to 1,2-linkages (minor):* ^{13}C NMR (126 MHz, DMSO-d_6) δ 165.2, 133.8, 129.8, 73.8, 63.5, 59.8 ppm. IR (powder, cm^{-1}) 3496, 2955, 1712, 1244, 1098, 873, 724.

5.2.3 Monomer Synthesis

Dodecanedioyl chloride Dodecanedioic acid (2.303 g, 10 mmol) was added to a 100-mL round

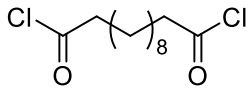

bottom flask equipped with a stir bar and dissolved in 20 mL anhydrous $CHCl_3$. One drop of DMF was then added by syringe at room temperature, followed by a dropwise addition of 1.8 mL (21 mmol) oxalyl chloride. The reaction was stirred at room temperature for 15 hours, then was heated to 60 °C for 1 hour, after which the solvent and excess oxalyl chloride were removed by rotary evaporation. The title compound was dried under vacuum and isolated as a clear oil (2.61 g, 98%) and used without further purification. Spectral data matched those reported in the literature.[85]

5.3 Synthesis and Characterization of Model Compounds

1-*O*-heptanoyl glycerol; 2-*O*-heptanoyl glycerol *(mixture)* Glycerol (154.2 mg, 1.68 mmol)

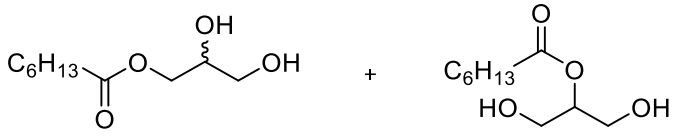

and **1.02** (16.4 mg, 0.083 mmol) were loaded into an oven-dried 25-mL round bottom flask equipped with a stir bar and dissolved in 10 mL acetonitrile. DIPEA (195 µL, 1.12 mmol) was added by syringe and the solution was cooled to 0 °C. Heptanoyl chloride (86 µL, 0.56 mmol) was added dropwise and the solution was warmed to room temperature and stirred for 4 hours. Upon completion, the reaction was diluted with DCM and washed with a solution of $NaHCO_3$, after which the aqueous layer was re-extracted twice with DCM. The combined organic layers were dried over $MgSO_4$, filtered, concentrated *in vacuo*, and the product was purified by flash column chromatography on

---

[85] K. Yamaguchi, Y. Tsuda, T. Shimakage and A. Kusumi, *Bull. Chem. Soc. Jpn*, 1998, **71**, 1923–1929.

silica gel to yield a clear oil containing 58.2 mg of a 3:1 mixture of the two title regioisomers (17% total yield). Spectral data were consistent with those reported in the literature.[86,87]

1,3-di-*O*-heptanoyl glycerol; 1,2-di-*O*-heptanoyl glycerol *(mixture)* Glycerol (94.6 mg, 1.03 mmol) and **1.02** (10.0 mg, 0.05 mmol) were loaded into an oven-dried 25-mL round bottom flask equipped with a stir bar and dissolved in 5 mL acetonitrile. DIPEA (537 µL, 3.09 mol) was added by syringe and the solution was cooled to 0 °C. Heptanoyl chloride (86 µL, 0.56 mmol) was added dropwise and the solution was warmed to room temperature and stirred for 4 hours. Upon completion, the reaction was diluted with DCM and washed with a solution of $NaHCO_3$, after which the aqueous layer was re-extracted twice with DCM. The combined organic layers were dried over $MgSO_4$, filtered, concentrated *in vacuo*, and the product mixture was purified by flash column chromatography on silica gel to yield a clear oil containing 146.5 mg of a 9:1 mixture of the title regioisomers (45% total yield). Spectral data were consistent with those reported in the literature.[88,89]

1,2,3-tri-*O*-heptanoyl glycerol (1.06) Glycerol (51.3 mg, 0.56 mmol) and DMAP (13.6 mg, 0.11 mmol) were loaded into a 25-mL round bottom flask equipped with a stir bar and dissolved in 3.5 mL DCM. Triethylamine (467 µL, 3.36 mmol), was added by syringe and the solution was cooled to 0 °C. Heptanoyl chloride (432 µL,

---

[86] Batovska, D. I.; Tsubota, S.; Kato, Y.; Asano, Y.; Ubukata, M. *Tetrahedron Asymmetry* **2004**, *15*, 3551–3559.

[87] T. Fukuoka, S. Ikeda, H. Habe, S. Sato, H. Sakai, M. Abe, D. Kitamoto and K. Sakaki, *J. Oleo Sci.*, 2012, **61**, 343–348.

[88] Da Rocha Ataide, T.; De Lima, M. R. F.; Valentim, I. B.; Pinheiro, D. M.; Sant'Ana, A. E. G. *Int. J. Food Sci. Technol.* **2007**, *42*, 1504–1508.

[89] Tateishi, H.; Anraku, K.; Koga, R.; Okamoto, Y.; Fujita, M.; Otsuka, M. *Org. Biomol. Chem.* **2014**, *12*, 5006–5022.

2.79 mmol) was added dropwise and the solution was warmed to room temperature and stirred overnight. Upon completion, the organic layer was washed with a solution of $NaHCO_3$, dried over $MgSO_4$, filtered, concentrated *in vacuo*, and the product was purified by flash column chromatography on silica gel to yield 201.8 mg of a light yellow solid (98%). Spectral data were consistent with those reported in the literature.[90] ^{1}H NMR (500 MHz, DMSO-d_6) δ 5.27–5.10 (m, 1H), 4.25 (dd, J = 12.0, 3.8 Hz, 2H), 4.12 (dd, J = 12.0, 6.5 Hz, 2H), 2.27 (q, J = 7.1 Hz, 6H), 1.50 (m, 6H), 1.35–1.14 (m, 18H), 0.85 (t, J = 6.8 Hz, 9H) ppm. ^{13}C NMR (126 MHz, DMSO-d_6) δ 68.73, 61.75, 30.91, 24.33, 21.93, 13.78 ppm.

1,2,3-tri-*O*-benzoyl glycerol Glycerol (46.0 mg, 0.5 mmol) and DMAP (18.0 mg, 0.15 mmol) were loaded into a scintillation vial equipped with a stir bar and dissolved in 2 mL DCM. Triethylamine (452 µL, 3.3 mmol), was added by syringe and the solution was cooled to 0 °C. Benzoyl chloride (350 µL, 3 mmol) was added dropwise and the solution was warmed to room temperature and stirred overnight. Upon completion of the reaction, the organic layer was washed with water, dried over $MgSO_4$, filtered, concentrated *in vacuo*, and the product was purified by column chromatography to yield 200.0 mg of a light yellow solid (99%). Spectral data were consistent with those reported in the literature.[91] ^{13}C NMR signals were used in assigning signals of PGI and PGT, with high similarity to assignments obtained from **1.06**. ^{1}H NMR (500 MHz, DMSO-d_6) δ 7.99–7.91 (m, 6H), 7.68–7.61 (m, 3H), 7.51 (td, J = 7.9, 1.9 Hz, 6H), 5.78 (m, 1H), 4.76 (dd, J = 12.0, 3.8 Hz, 2H), 4.68 (dd, J = 12.0, 6.4 Hz, 2H). ^{13}C NMR (126 MHz, DMSO-d_6) δ 165.40, 133.52, 129.25, 128.77, 69.94, 62.98 ppm.

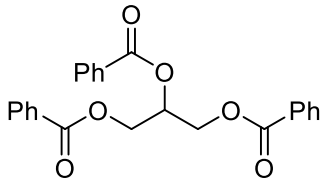

[90] Zhan, S.; Tao, X.; Cai, L.; Liu, X.; Liu, T. *Green Chem.* **2014**, *16*, 4649–4653.

[91] D'Accorso, N. B.; Thiel, I. M. E. *Carbohydr. Res.* **1987**, *167*, 19–27.

5.4 Post-polymerization Modifications

5.4.1 General Procedure for Polymer Peracetylation

0.3 mmol of polymer was placed in a 2-dram vial equipped with a stir bar and dissolved in 1 mL pyridine. 1 mL acetic anhydride was added dropwise. Then, the reaction was stirred for 21 hours. The solvent was removed by rotary evaporation and the residue was dissolved in toluene and evaporated four times before being dried under vacuum.

5.4.2 General Procedure for Polymer Isomerization

0.3 mmol of polymer was placed in a 2-dram vial equipped with a stir bar and dissolved in 1 mL THF. 3 equivalents of Et_3N were added *via* syringe and the solution was heated to 70 °C for 10 hours. The solvent was removed by rotary evaporation and the resulting polymer was dried under vacuum and analyzed by quantitative ^{13}C NMR.

5.4.3 General Procedure for Introduction of Cross-links

0.2–0.3 mmol of polymer was placed in a 2-dram vial equipped with a stir bar and dissolved in $CHCl_3$ (0.5 M). The solution was heated to 50 °C under argon and hexamethylene diisocyanate (0.5–20 mol%) was added dropwise *via* syringe. The reaction was allowed to stir overnight, stopped with methanol, and concentrated by rotary evaporation. The resulting cross-linked polymer was analyzed by FTIR.

5.4.4 Synthesis and Characterization of Modified PGS

Poly(glycerol sebacate) Fmoc glycinate PGS (50.7 mg, 0.2 mmol) and Fmoc–glycine (70.1 mg, 0.24 mmol) were placed in a 10-mL round bottom flask equipped with a stir bar and dissolved and sonicated in 3 mL DCM. The solution was cooled to 0 °C and *N*,*N*′-diisopropylcarbodiimide (46 µL, 0.3 mmol) was added dropwise and one fleck of DMAP was added. The reaction was stirred for 22 hours at room temperature under argon, filtered and precipitated from methanol at 0 °C to yield 90.2 mg of an off-white, brittle solid (84%). ^1H NMR (500 MHz, $CDCl_3$) δ 7.75 (d, *J* = 7.4 Hz, 2H), 7.59 (d, *J* = 7.5 Hz, 2H), 7.38 (t, *J* = 7.4 Hz, 2H), 7.30 (t, *J* = 7.5 Hz, 2H), 5.43–5.18 (m, 2H), 4.39 (d, *J* =

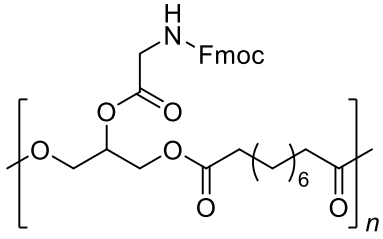

7.1 Hz, 2H), 4.33 (dd, *J* = 12.1, 4.1 Hz, 2H), 4.22 (t, *J* = 7.1 Hz, 1H), 4.14 (dd, *J* = 12.1, 6.0 Hz, 2H), 4.00 (d, *J* = 5.7 Hz, 2H), 2.28 (t, *J* = 7.7 Hz, 4H), 1.58 (m, 4H), 1.33–1.12 (m, 8H) ppm. ^{13}C NMR (126 MHz, $CDCl_3$) δ 173.37, 169.50, 156.35, 143.86, 141.37, 127.84, 127.18, 125.17, 120.11, 70.66, 67.35, 61.92, 47.18, 42.80, 34.00, 29.12, 24.83 ppm.

Chapter 3: Synthesis of Poly(pyranoside ester)s

1 Statement of Contribution

Monomer, polymer and model synthesis and characterization were carried out by Ekaterina Slavko.

2 Introduction

2.1 Carbohydrate-derived Polymers from Nature

The production of biomass-derived polymers in general, and the utilization of carbohydrate-derived feedstocks in particular, are research directions that have gained a great deal of impetus in recent years.[92,93,94] Aside from representing a move away from fossil-fuel derived monomers and all the environmental and political drawbacks of their continual use, sugars also offer an advantage because they can be remarkably inexpensive. For example, glucose costs $0.76 per kg and is produced at 5 metric tonnes a year, while methyl methacrylate costs $1.32 per kg and is produced at only 2.1 metric tonnes a year, making sugar feedstocks, at least in theory, economically feasible precursors for commodity polymers.[95] Major sugars such as glucose, galactose, and mannose are readily sourced from the agriculture, forestry and livestock industries; for instance, mannose is isolated from plants and spent coffee grounds,[96] while galactose can be isolated from plant biomass and red algae[97] as well as being a by-product of the

---

[92] Galbis, J. A.; de Gracia García-Martín, M.; Violante de Paz, M.; Galbis, E. *Chem. Rev.* **2016**, *116*, 1600–1636.

[93] Werpy, T.; Petersen, G. *Volume I - Results of Screening for Potential Candidates from Sugars and Synthesis Gas*; U.S. Department of Energy, 2004.

[94] Xiong, M.; Schneiderman, D. K.; Bates, F. S.; Hillmyer, M. A.; Zhang, K. *Proc. Natl. Acad. Sci.* **2014**, *111*, 8357–8362.

[95] Williams, C. K. *Chem. Soc. Rev.* **2007**, *36*, 1573–1580.

[96] Hu, X.; Shi, Y.; Zhang, P.; Miao, M.; Zhang, T.; Jiang, B. *Compr. Rev. Food Sci. Food Saf.* **2016**, *15*, 773–785.

[97] Yoon, J. J.; Kim, Y. J.; Kim, S. H.; Ryu, H. J.; Choi, J. Y.; Kim, G. S.; Shin, M. K. *Adv. Mater. Res.* **2010**, *93–94*, 463–466.

dairy industry.[98] Common naturally occurring monosaccharides are also unsurprisingly non-toxic and are metabolized in the body *via* the Krebs cycle, making them largely innocuous from an immunogenic perspective, much like the common metabolite glycerol which was explored in the previous chapter. In addition, the fact that they are decorated with multiple OH groups makes them more hydrophilic than most building blocks used commercially (*e.g.*, lactic acid), a property that can impart hypothetical synthetic sugar-derived polymers with advantages in the field of biomaterials by virtue of a potentially higher hydrolytic degradability, water solubility, and cell adhesion. The wide variation in constitutional and stereochemical isomerism inherent to this class of compounds also presents opportunities for varying the properties of polymers, as the spatial arrangement of functional groups of the building blocks can have a tremendous impact on material properties. Polymer chemists looking to fine-tune the mechanical or degradation properties of sugar-derived macromolecules have access to a wide array of similar carbohydrate compounds of formula $C_nH_{2n}O_n$ showing varying structural connectivity and orientation in space. For example, the hexoses glucose, galactose, mannose and allose represent the same constitutional isomer, but are all epimers of each other and would give rise to distinct chain orientations in space if incorporated into the backbone of a polymer.

The best-known class of macromolecules having sugars as part of the backbone are, of course, polysaccharides, which serve vitally important roles in plant and animal tissues, including energy storage and structural support. These biopolymers can be homo- or copolymers of monosaccharide repeat units and can be obtained from microbes, plants and animals. To overcome challenges associated with their processing and tailoring of physical properties, chemists routinely modify native polysaccharides through chemical or physical manipulation, *e.g.*, chitosan being the product of base-promoted de-acetylation of chitin (see Figure 1.1 from Chapter 1, section 1.1).[99] While modified versions of polysaccharides such as cellophane and hypromellose — both derived from cellulose — are commonly found in food packaging and

---

[98] Williams, C. A. Galactose. *Encyclopaedia of Food Science, Food Technology and Nutrition*, 1993, 2843–2846.

[99] Liu, J.; Willför, S.; Xu, C. *Bioact. Carbohydrates Diet. Fibre* **2015**, *5*, 31–61.

pharmaceutical applications due to their degradability and low toxicity, polysaccharides can also be employed in sophisticated applications that harness their unique physical properties and distinctive interactions with living systems.[100] The use of viscoelastic and anti-inflammatory hyaluronic acid in ophthalmic surgery, tissue engineering and drug delivery comes to mind,[101] as well as the utilization of the antimicrobial properties of chitosan in wound dressing and other applications,[102] the use of viscous, gelling, and pH-responsive alginate in the fields of dentistry, medicine, and regenerative medicine[103] and the investigations into the biomedical properties of hydrogels derived from a large variety of polysaccharides.[104] The breadth of applications of these bio-derived macromolecules, some representative structures of which are shown in Figure 3.1, is a reflection of both the complexity of the fundamental physiological interaction between cells and carbohydrates and the fine interplay between polymer microstructure and physical properties. Ongoing efforts are aimed at modifying polysaccharides in order to study their structure–activity relationships[105] and to create synthetic polysaccharides from sugar-based building blocks.[106] Animals do not intrinsically produce the enzyme responsible for cleaving the glycosidic linkages connecting the repeat units of a polysaccharide,[107] meaning that all polysaccharides are not biodegradable in the strict sense, even if they are biocompatible. Despite this, the demonstrable utility of this class of macromolecules as biomaterials points to opportunities for designing new, perhaps fully biodegradable polymers with biocompatible carbohydrate repeat units present in the backbone.

---

[100] Shoichet, M. S. *Macromolecules* **2010**, *43*, 581–591.

[101] Huang, G.; Huang, H. *J. Control. Release* **2018**, *278*, 122–126.

[102] Kong, M.; Chen, X. G.; Xing, K.; Park, H. J. *Int. J. Food Microbiol.* **2010**, *144*, 51–63.

[103] Szekalska, M.; Puciłowska, A.; Szymańska, E.; Ciosek, P.; Winnicka, K. *Int. J. Polym. Sci.* **2016**, *2016*, 1–17.

[104] Coviello, T.; Matricardi, P.; Marianecci, C.; Alhaique, F. *J. Control. Release* **2007**, *119*, 5–24.

[105] Caputo, H. E.; Straub, J. E.; Grinstaff, M. W. *Chem. Soc. Rev.* **2019**, *48*, 2338–2365.

[106] Bennett, C. S. *Org. Biomol. Chem.* **2014**, *12*, 1686–1698.

[107] Petersen, N.; Gatenholm, P. *Appl. Microbiol. Biotechnol.* **2011**, *91*, 1277–1286.

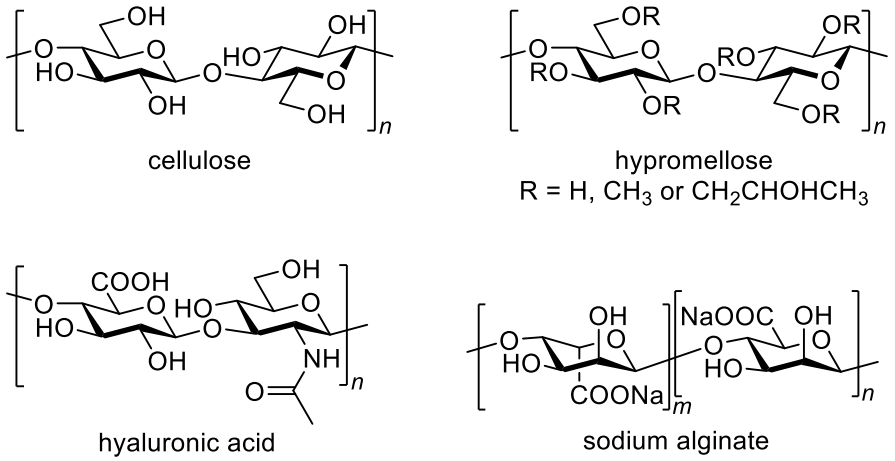

Figure 3.1 Examples of polysaccharides used in industry and medicine.

2.2 Synthetic Approaches to Carbohydrate-derived Polyesters

Biodegradable polymers that feature carbohydrates such as aldose or alditol derivatives as part of their backbone have been explored by several groups.[108] Sugar-derived polyesters are increasingly becoming a welcome addition to the family of existing biomedically relevant polymers as exemplified by a sorbitol-derived analog of poly(ethylene glycol) (PEG) synthesized by the group of Guan. This main-chain polyester is more resistant to non-specific protein binding and shows enhanced biodegradability due to its relatively labile ester-linked backbone.[109] To give another example, elastomeric polyester networks such as those derived from glycerol (see Chapter 2, section 2.1) have also been modified by replacing glycerol with higher sugar alcohols such as xylitol, sorbitol, mannitol and maltitol, affording a series of biodegradable biomaterials with an extended range of physical and degradation properties.[110] These polymers are prepared in the bulk similarly to cross-linked PGS and are the result of an uncontrolled pre-polymerization step followed by thermal curing (Figure 3.2).

---

[108] Wang, D.; Dordick, J. S.; Linhardt, R. J. *Chem. Mater.* **2002**, *14*, 3232–3244.

[109] Metzke, M.; Bai, J. Z.; Guan, Z. *J. Am. Chem. Soc.* **2003**, *125*, 7760–7761.

[110] Bruggeman, J. P.; de Bruin, B.; Bettinger, C. J.; Langer, R. *Biomaterials* **2008**, *29*, 4726–4735.

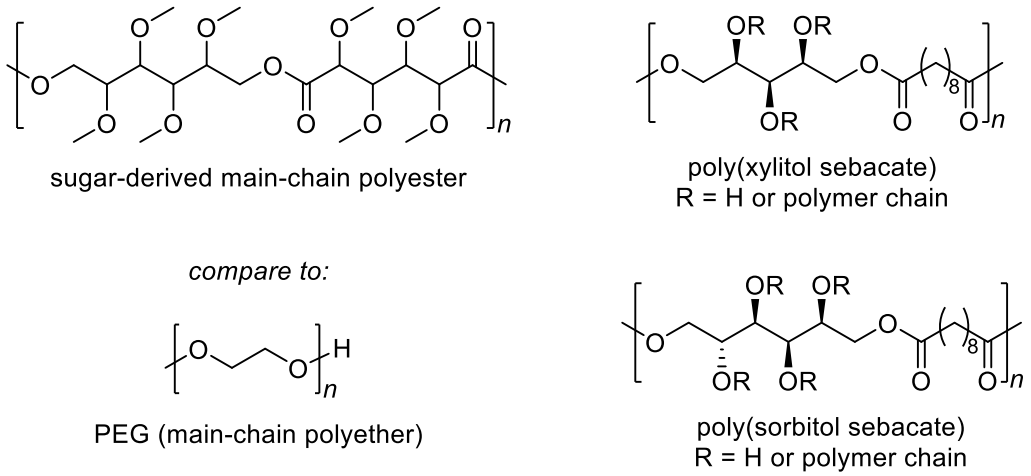

Figure 3.2 Examples of carbohydrate-derived biomedical polyesters.

The synthesis of carbohydrate-derived polyesters poses a unique challenge that is seldom remediated by the orthogonal reactivity approach outlined in section 1.3 of Chapter 1: because the formation of ester linkages usually involves OH groups and carbohydrates preponderantly possess OH functionality, partial protection of carbohydrate monomers is usually necessary to achieve linear polyesters. Some sugar-derived monomers are intrinsically difunctional, such as the isohexitols (*e.g.*, isosorbide, isomannide, isoidide), the products of dehydrative cyclization of sugar alcohols (Scheme 3.1). Polyesters prepared from these monomers are non-toxic and biodegradable, but the fact that these monomers only possess two secondary OH groups means that polymerization rates are generally modest and the final product does not contain pendant functional groups.[111]

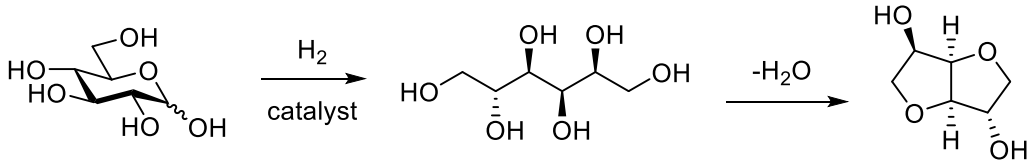

Scheme 3.1 Synthesis of isosorbide starting from D-glucose.

[111] Fenouillot, F.; Rousseau, A.; Colomines, G.; Saint-Loup, R.; Pascault, J. P. *Prog. Polym. Sci.* **2010**, *35*, 578–622.

Linear polymers with open-chain carbohydrate repeat units have been synthesized by installing protecting groups on sites of potential undesired reactivity (Scheme 3.2). Galbis and colleagues have performed polycondensations of difunctional, partially methylated arabitol and xylitol monomers possessing reactive OH groups[112] and COOH groups[113] with aromatic and aliphatic comonomers, yielding thermally stable copolymers with M_n values ranging from 20 to 40 kDa. The group of Williams employed a clever strategy involving the ROP of acetyl-protected glucorolactone to yield oligomers[114] and showed that the degree of polymerization could be enhanced by reducing the C-3 and C-4 positions of glucorolactone, obtaining macrocyclic polyester elastomers as the product.[115] While the above monomers were derived from the cyclic pyranoside forms of glucose, the resulting polyesters are composed of the open-chain sugar analog. ROP is an attractive way of preparing polymers because it generally allows for better control over degree of polymerization and lower dispersity, as well as being permissive of functional groups incorporated into the monomer (*e.g.*, azide[116] and alkyne[117] functionalities). Nevertheless, OH-functionalized polyesters cannot be prepared directly from lactones using such an approach because alcohols are initiators for the polymerization process and the presence of any unprotected OH groups could result in branching of the polymer. In contrast, there has been more success in preparing OH-functionalized polycarbonates derived from carbohydrates thanks to the greater stability of carbonate linkages compared to ester linkages. The group of Wooley used an organocatalytic ROP to synthesize polycarbonates containing a partially methylated

---

[112] Alla, A.; Hakkou, K.; Zamora, F.; De Ilarduya, A. M.; Galbis, J. A.; Muñoz-Guerra, S. *Macromolecules* **2006**, *39*, 1410–1416.

[113] García-Martín, M. D. G.; Pérez, R. R.; Hernández, E. B.; Galbis, J. A. *Macromolecules* **2006**, *39*, 7941–7949.

[114] Haider, A.; Williams, C. K. *J. Polym. Sci.: Part A: Polym. Chem*. **2008**, *46*, 2891–2896.

[115] Tang, M.; White, A. J. P.; Stevens, M. M.; Williams, C. K. *Chem. Commun.* **2009**, *3*, 941–943.

[116] Riva, R.; Schmeits, S.; Stoffelbach, F.; Jérôme, C.; Jérôme, R.; Lecomte, P. *Chem. Commun.* **2005**, 5334–5336.

[117] Parrish, B.; Breitenkamp, R. B.; Emrick, T. *J. Am. Chem. Soc.* **2005**, *127*, 7404–7410.

cyclic glucopyranoside repeat unit[118] and were able to employ a transient benzylidene protecting group that was removed post-polymerization without modifying the backbone (Scheme 3.3a).[119] A similar approach was used by Buchard with a mannopyranoside-derived carbonate monomer yielding after deprotection an insoluble, OH-functional polycarbonate.[120] Another group has carried out a polyaddition between a sugar-derived carbonate monomer and a diamine to yield linear, OH-functional polyurethanes in one step, a process made possible by the dramatic difference in reactivity between primary amines and secondary alcohols (Scheme 3.3b).[121] The OH groups are effectively orthogonal to the amine groups in this process, illustrating once again the persistent challenge of preparing functional carbohydrate-derived polyesters in one step.

---

[118] Mikami, K.; Lonnecker, A. T.; Gustafson, T. P.; Zinnel, N. F.; Pai, P. J.; Russell, D. H.; Wooley, K. L. *J. Am. Chem. Soc.* **2013**, *135*, 6826–6829.

[119] Felder, S. E.; Redding, M. J.; Noel, A.; Grayson, S. M.; Wooley, K. L. *Macromolecules* **2018**, *51*, 1787–1797.

[120] Gregory, G. L.; Jenisch, L. M.; Charles, B.; Kociok-Köhn, G.; Buchard, A. *Macromolecules* **2016**, *49*, 7165–7169.

[121] Schmidt, S.; Gatti, F. J.; Luitz, M.; Ritter, B. S.; Bruchmann, B.; Mülhaupt, R. *Macromolecules* **2017**, *50*, 2296–2303.

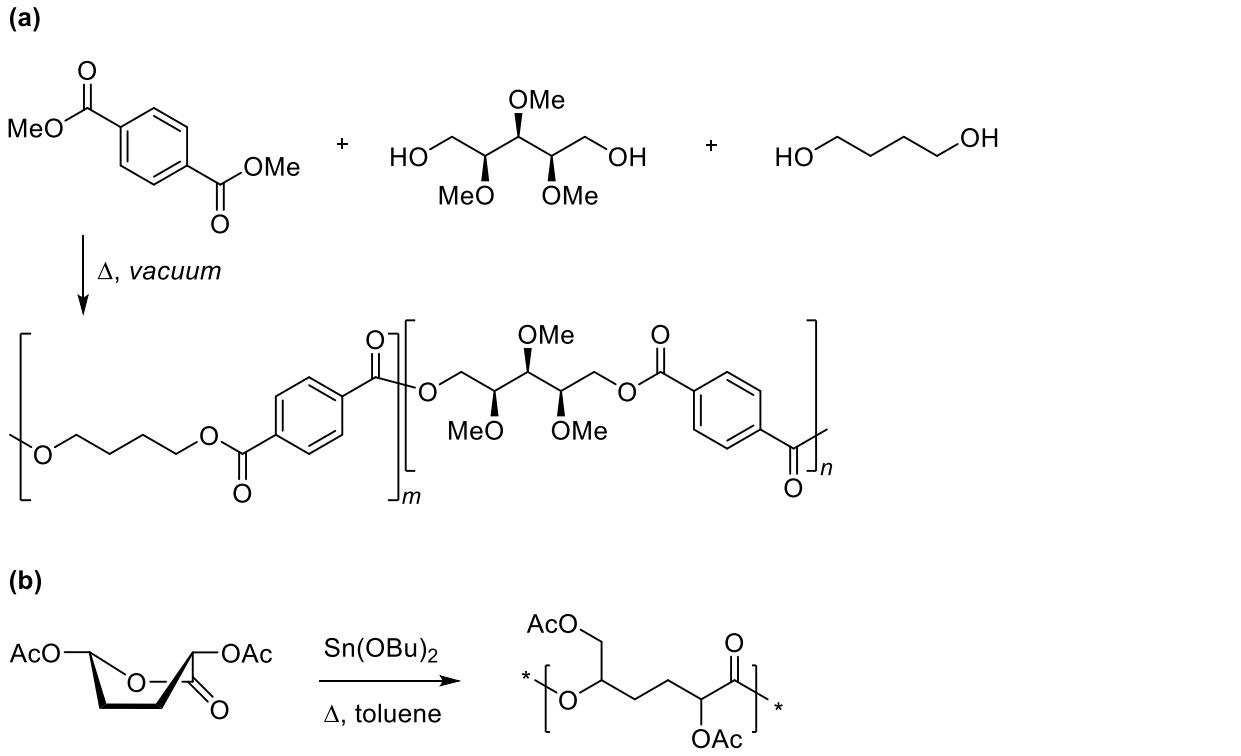

Scheme 3.2 Synthesis of unbranched carbohydrate-derived polyesters involving protecting groups.

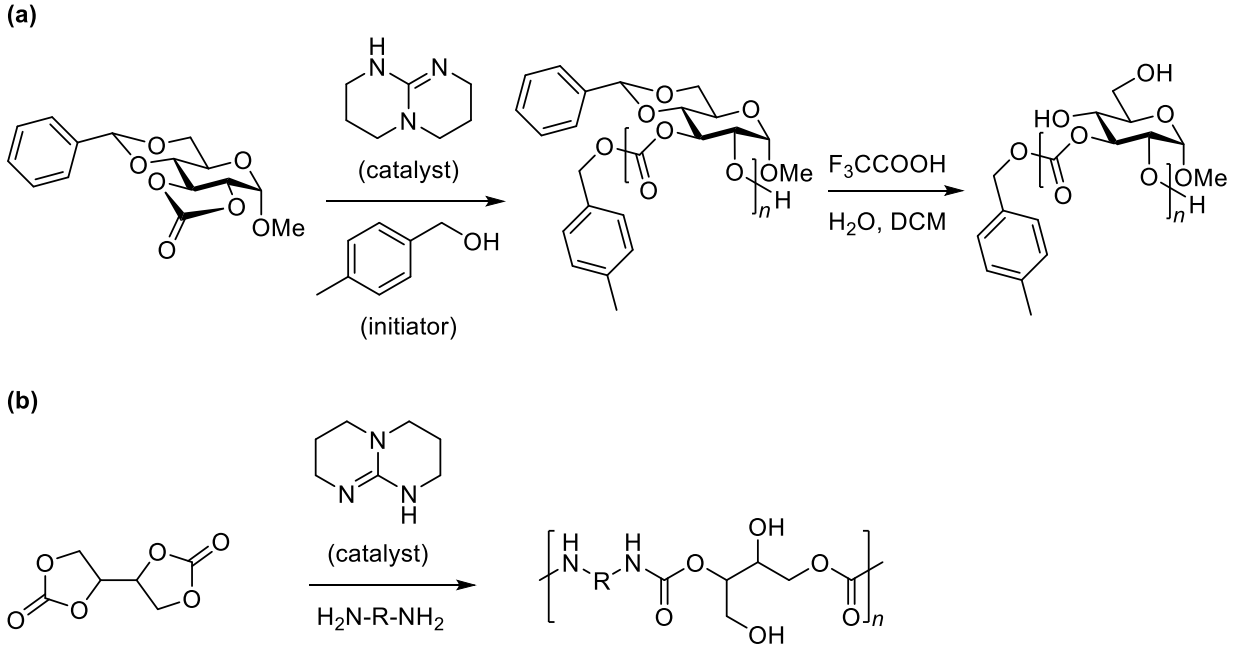

Scheme 3.3 Synthesis of functional carbohydrate-derived polycarbonates (a) and polyurethanes (b) showing post-polymerization deprotection and *in situ* unmasking of orthogonal OH groups, respectively.

The intrinsic differences in reactivity between primary and secondary OH groups of polyols have been successfully exploited using immobilized enzyme catalysis (see Chapter 2, section 2.1). This strategy can be implemented under mild conditions, albeit often under tight vacuum control, in part because volatile by-products must be removed from the reaction to overcome an animal lipase's natural propensity to cleave ester linkages rather than form them.[122] Extensive studies have been conducted on lipase-, esterase-, and protease-catalyzed polyester synthesis, uncovering an interesting dependence of polymerization control on polyol stereoconfiguration that is not well understood.[123] Cyclic saccharides are uncommon monomers in such polycondensation processes but examples by Dordick *et al.* have shown that sucrose can be copolymerized with bis(2,2,2-trifluoroethyl) adipate or divinyl adipate to give water-soluble sugar-derived polyesters (Scheme 3.4).[124] The molecular weights of these polymers are low but can be increased through copolymerization with a more reactive chain extension agent such as 1,8-octanediol.[125]

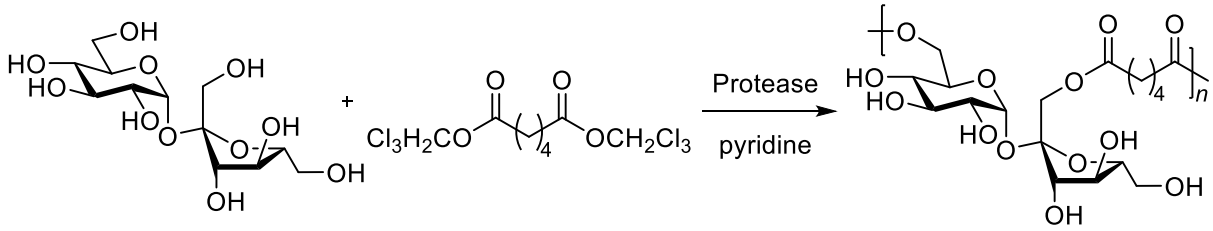

Scheme 3.4 Enzymatic synthesis of a sucrose-derived polyester.

2.3 Hypothesis

We proposed that borinic acids can promote site-selective polymerization of anomerically protected monosaccharides to yield well-defined linear polyesters. As described in Chapter 2,

---

[122] Gross, R. A.; Ganesh, M.; Lu, W. *Trends Biotechnol.* **2010**, *28*, 435–443.

[123] Hu, J.; Gao, W.; Kulshrestha, A.; Gross, R. A. *Macromolecules* **2006**, *39*, 6789–6792.

[124] Dordick, J. S. *Ann. N. Y. Acad. Sci.* **1992**, *672*, 352–362.

[125] Uyama, H.; Kobayashi, S. In *Enzyme-Catalyzed Synthesis of Polymers*; Kaplan, D.; Kobayashi, S.; Ritter, H., Eds.; Springer, 2006; pp. 133–158.

borinic acids bind to and enhance the nucleophilic character of *cis*-1,2 and 1,3-diols. The intrinsically more reactive of the two OH groups involved in two-point binding to the organoboron species is functionalized exclusively, with primary OH groups taking precedence over secondary OH groups and equatorial OH groups taking precedence over axial ones as illustrated in Scheme 3.5b.

Potential sugar-based substrates for a borinic acid-catalyzed polycondensation must therefore possess appropriately configured OH groups, preferably with two binding modes available. As shown in Scheme 3.5a, methyl D-rhamnopyranoside has only one *cis*-1,2-diol motif and would fail to be incorporated into a growing polymer chain because the O-3 monofunctionalized product does not have any binding sites for boron. Similarly, the glucose-derived tetraol in Scheme 3.5c is would also be limited to O-6 monofunctionalization and would not be able to undergo electrophilic substitution twice. Galacto- and manno-configured saccharides, however, both include both a *cis*-1,2 and a 1,3-diol motif, and can be seen as potentially viable difunctional monomers. Treatment of these compounds with a diacyl chloride would yield previously unexplored bio-sourced polyesters with potentially interesting properties. In addition, anomeric protecting groups present an opportunity for introducing structural variation into the resulting polymers to effect changes in physical properties. Many protocols for anomeric activation are described in the literature[126,127] and can be harnessed for specialized monomer synthesis.

---

[126] Toshima, K.; Tatsuta, K. *Chem. Rev.* **1993**, *93*, 1503–1531.

[127] Fischer, E. *Ber. Dtsch Chem Ges.* **1893**, *26*, 2400–2412.

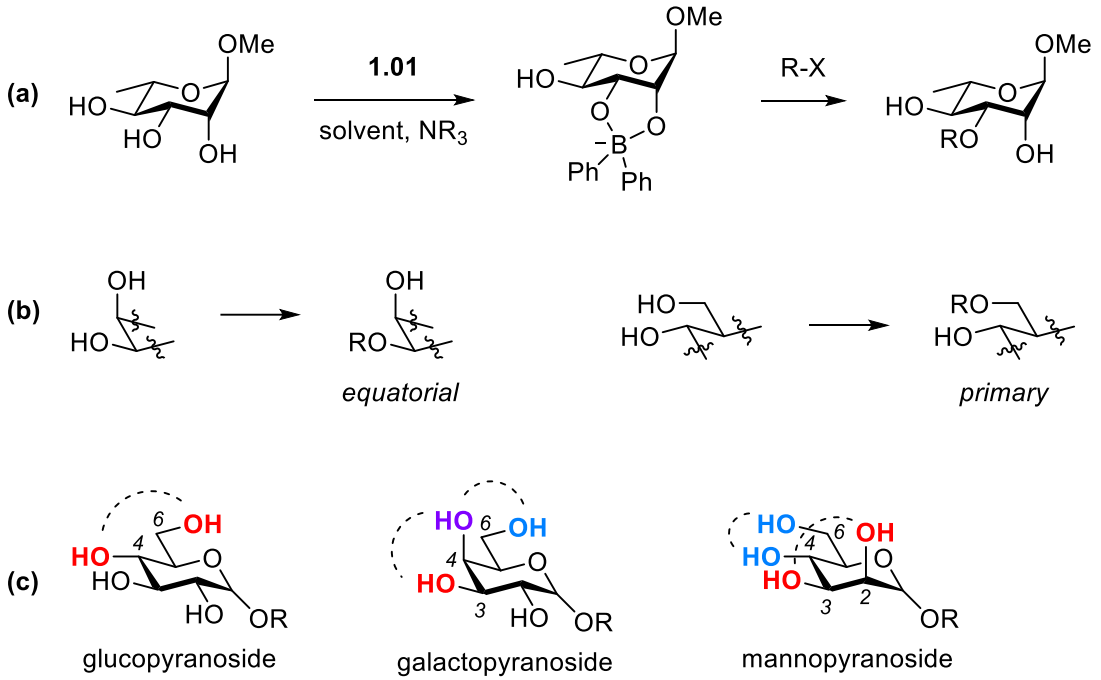

Scheme 3.5 (a) Borinic acid-promoted derivatization of a pyranoside. (b) "Rules" for 1,2 and 1,3-diol reactivity based on electronic and steric arguments. (c) 1,2 and 1,3 binding sites of common anomerically protected sugars.

3 Results and Discussion

3.1 Naming Convention

To improve readability, anomerically protected pyranosides will be named according to the following convention: the Greek letter shall refer to the anomeric configuration (α or β — defined by the configurational relationship between the anomeric and the anomeric reference atoms, the α anomer having C-1 and C-5 in the same configuration), followed by an abbreviated form of the alkyl protecting group at the anomeric position, followed by a three-letter abbreviation of the carbohydrate configuration (Gal = galactopyranoside, Man = mannopyranoside). For example, methyl β-D-galactopyranoside will be represented as βOMeGal.

3.2 Optimization of Reaction Conditions

We chose to explore the borinic acid-catalyzed polycondensation of commercially available methyl-protected pyranosides. As discussed in section 3.1 of Chapter 2, a previous report[73] had demonstrated the successful *bis*-acylation of βOMeGal using **1.04** as catalyst, which led us to use

this substrate as the starting point for the optimization of polymerization conditions. We drew inspiration for the reaction conditions from those used for the polymerization of glycerol described in Chapter 2 and attempted the polymerization in THF solvent using 3 equivalents of DIPEA at 70 °C for 4 hours using different catalysts. Recalling the poor performance of **1.04** in promoting the polycondensation of glycerol due to its disrupting the monomer feed ratio, we did not explore this catalyst and focussed on unprotected borinic acids.

To properly assess the chain length distributions obtained from each catalyst, a method for isolating unfractionated polymers was sought. Initially, the complete lack of aqueous solubility of the methyl glycoside-derived polyesters suggested a precipitation from distilled water could successfully remove side-products without significantly promoting the isolation of chains having a higher degree of polymerization. However, the presence of DIPEA in the crude reaction mixture was found to promote the isomerization of the polymer backbone at unpredictable rates (anywhere from 5 to 50%) through a previously reported acyl migration mechanism.[83] It was thus decided to isolate the unfractionated products obtained from the polycondensation by subjecting the crude mixture to an aqueous workup without further purification. Given that the polyesters were insoluble in ethyl acetate and DCM, 2-methyltetrahydrofuran (2-MeTHF) was selected as a polar, water-immiscible solvent for subjecting unfractionated polymers to a mildly acidic aqueous workup to remove DIPEA and its hydrochloride salt. The results of the catalyst screen are shown in Table 3.1; results obtained in the absence of catalyst yielded a mixture of isomers as judged by ^{1}H NMR spectroscopy and are omitted due to the exceedingly low apparent M_n of the oligomers leading to an undetectable refractive index signal. The optimal catalyst for preparing poly(βOMeGal sebacate) was determined to be **1.01**, successfully producing a brittle, glassy polymer of M_n = 5.8 kDa and Đ = 3.2 as determined by GPC against PMMA standards in NMP at 80 °C. The relatively low M_n of the polymer prompted us to explore alternative solvents, the reasoning being that the hydrophilic polyester could be exhibiting a small hydrodynamic radius in THF solution, limiting its own chain growth. The use of dioxane at 100 °C, however, led to similar results. Carrying out the polymerization in acetonitrile or DCM led to rapid network formation upon addition of the diacyl chloride. An increase in M_n was noted when the polymerization was scaled up from 3.6 mmol to 6.5 mmol (Table 3.1, entry 2), suggesting that a smaller error in monomer feed had been

achieved (Figure 3.3). The average degree of polymerization also increased slightly when the reaction was allowed to run for 72 hours, but this was offset by a multimodal GPC trace of the final product (Đ ≈ 27).

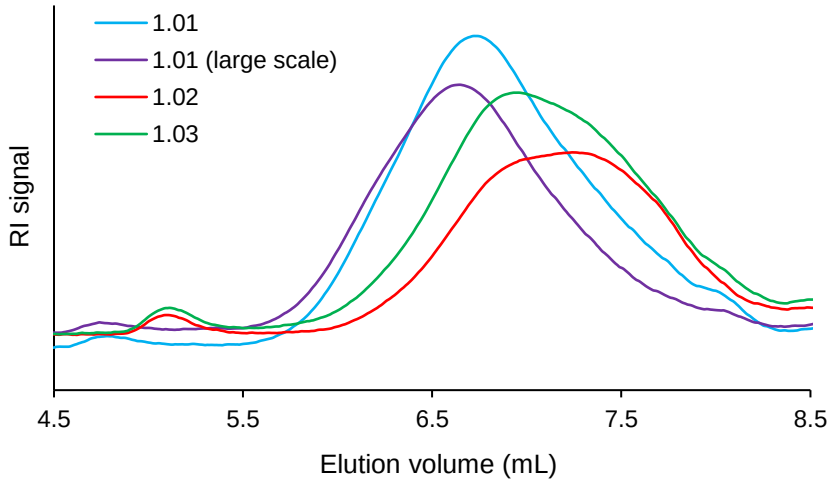

Figure 3.3 GPC traces of poly(βOMeGal sebacate)s obtained using 5 mol% **1.01**–**1.03**.

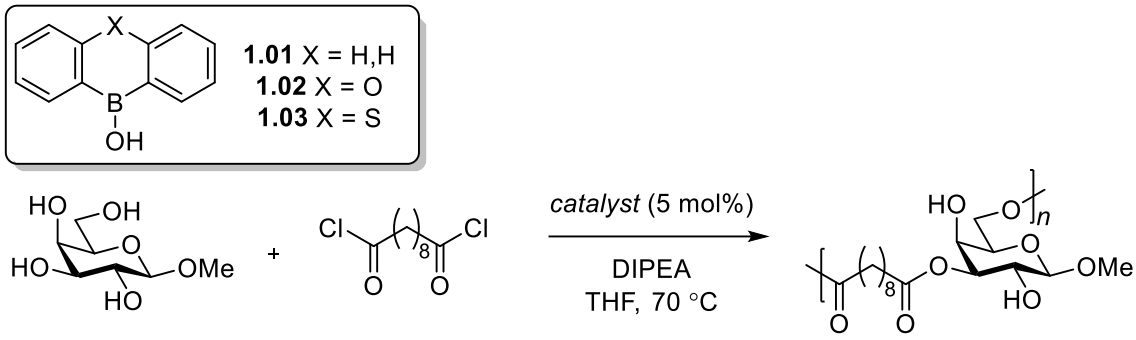

Table 3.1 Optimization of catalyst for the polycondensation of βOMeGal with sebacoyl chloride.

Entry	Catalyst	M_n*	Đ*
1	**1.01**	5.8	3.2
2†	**1.01**	8.1	2.6
3	**1.02**	3.1	3.0
4	**1.03**	3.2	3.2

* – molecular weights are expressed in kDa relative to PMMA standards and determined by GPC, NMP, 80 °C.
† – reaction was conducted on 6.5 mmol scale.

3.3 Spectroscopic Characterization of Polyesters

The structure of poly(βOMeGal sebacate) was confirmed by IR, ^{1}H NMR, and ^{13}C NMR spectroscopy, along with COSY analysis to assign the major linkages (Figure 3.4). Characteristic bands associated with the carbonyl C=O stretch were observed at approximately 1730 cm^{-1}, along with O-H stretches at approximately 3450 cm^{-1}, indicating the presence of pendant OH groups.

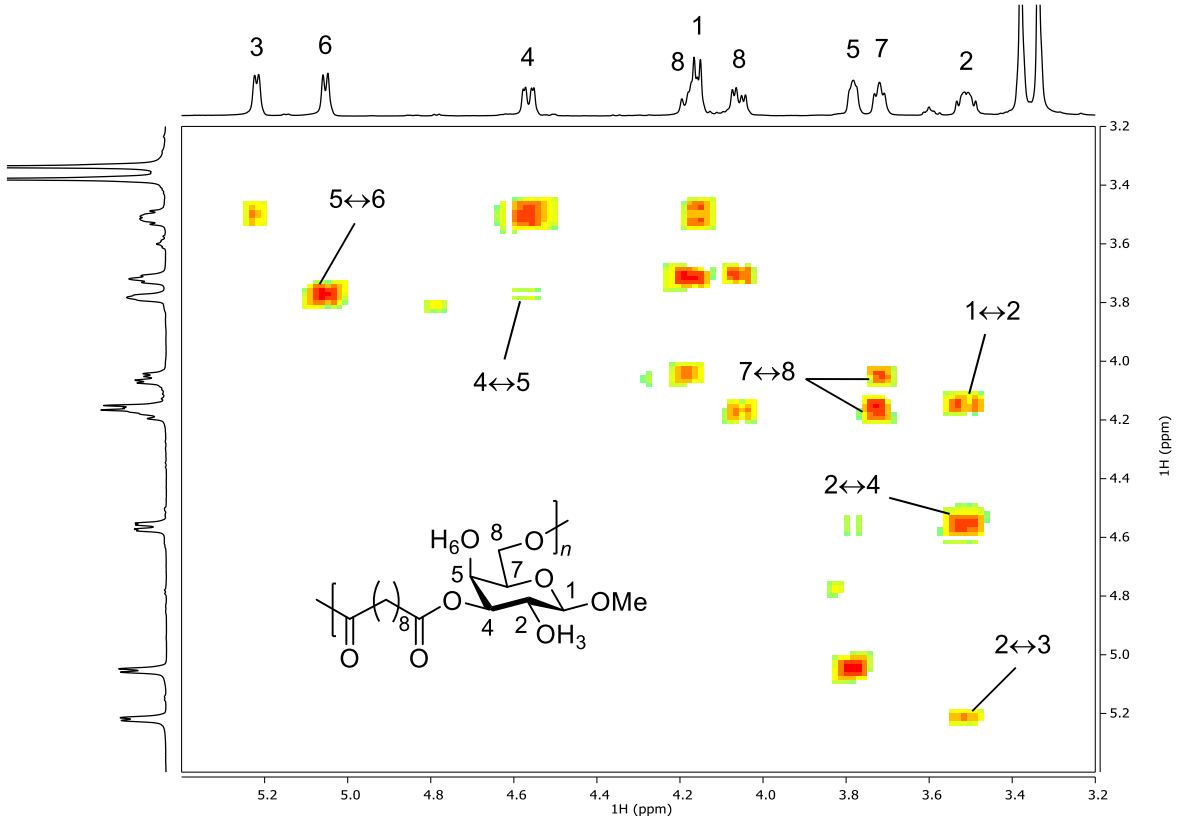

Figure 3.4 Carbohydrate region of the ^{1}H-^{1}H COSY NMR spectrum of poly(βOMeGal sebacate) in DMSO-d_6.

As was the case for the aliphatic poly(glycerol ester)s, NMR signals associated with poly(βOMeGal sebacate) were sharp and indicated that the polyester was predominantly linked at the O-3 and O-6 positions (3,6-linked). Interestingly, the only distinguishable end-group was the O-3 monofunctionalized galactoside unit, the identity of which was confirmed by comparing minor proton and carbon signals of the polyesters to model compound **3.01**. This observation suggests that the rate of functionalization at the secondary O-3 position is significantly higher than that at the primary O-6 position. Previous studies involving **1.02**-promoted sulfations of pyranosides[128] revealed high levels of selectivity for the O-3 position in manno- and galacto-configured carbohydrates and DMAP-catalyzed monoacylation of glucose derivatives can favour

[128] Gorelik, D.; Lin, Y. C.; Briceno-Strocchia, A. I.; Taylor, M. S. *J. Org. Chem.* **2019**, *84*, 900–908.

substitution at the O-3 position,[129] although this effect has not been observed when using **1.01** as catalyst. It is possible that the sluggish reaction at the O-6 position contributes to limiting the degree of polymerization observed for βOMeGal. Figure 3.5 shows ^{1}H NMR spectra of model **3.01** and two polymer batches possessing different M_n (Table 3.1, entries 2 *vs.* 3), which highlights the inverse relationship between degree of polymerization and end-group content, as the O-3 end-group content was 6% for the high-M_n polymer and 25% for the low-M_n polymer. Overall, spectroscopic analysis revealed that borinic acid-promoted polymerizations of a galactopyranoside resulted in a site-selective reaction with only one predominant linkage and one type of end-group linkage.

[129] Kattnig, E.; Albert, M. *Org. Lett.* **2004**, *6*, 945–946.

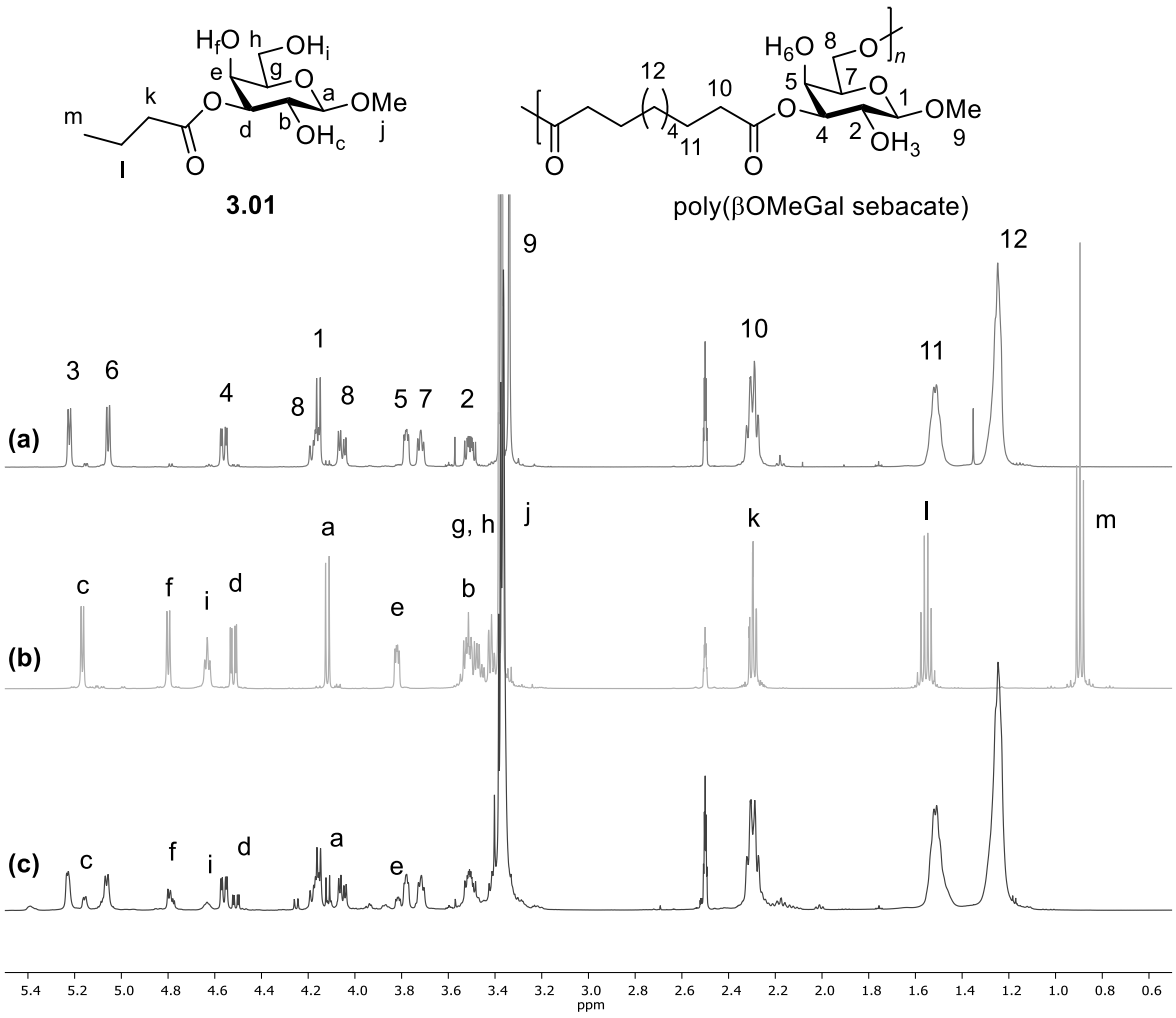

Figure 3.5 ^{1}H NMR spectra of poly(βOMeGal sebacate) resulting from reactions catalyzed by **1.01** (a) and **1.02** (c) compared to model compound **3.01** (b). Minor peaks in the bottom spectrum are labelled with the corresponding peaks arising from **3.01** but can be observed in the top spectrum as well. All spectra were taken in DMSO-d_6.

3.4 Synthesis of Monomers Bearing Diverse Anomeric Substituents

Evidently, commercially available βOMeGal underwent a controlled polymerization, suggesting that a series of similar monomers could potentially be used. The anomeric substituent of a carbohydrate derivative is not involved in the chain extension process and thus can be seen as a handle for structural diversification and potential expansion of the range of mechanical, thermal and biological properties of the corresponding polymers. The brittle and glassy nature of the originally synthesized polymers pointed to strong intermolecular forces and tight chain packing,

which inspired us to explore pendant groups which could increase free volume and result in softer, lower-T_g materials.[130] In addition, we were curious to examine whether the use of a more soluble monomer would lead to higher polymerization rates, as methyl glycosides display low solubility in most aprotic organic solvents. We selected *n*-octyl and *i*-octyl (2-ethylhexyl) flexible side chains to investigate their effect on physical properties and replaced the methyl protecting group with an ethyl protecting group to offset the potential toxicity concerns related to the generation of methanol upon polymer degradation in the body.[131] To explore any potential dependence of monomer reactivity or polymer properties on anomeric configuration, both the α- and β-configured galactose derivatives for each anomeric substituent were synthesized. We limited our scope to α-configured mannosides because the challenging synthesis of β-configured mannosides[126] makes them restrictively costly to prepare and unlikely candidates for preparative-scale polymerizations required for biomaterial synthesis.

3.4.1 Fischer Glycosidations

Traditional glycosidation reactions originally reported by Fischer[127] predominantly result in a mixture of glycosides. Due to the anomeric effect,[132] axially configured alkoxy groups are thermodynamically favoured over equatorially configured ones. This is attributed to the combined effects of dipole minimization and electron density transfer from the lone pair of the hemiacetal oxygen to the σ* orbital of the glycosidic bond. As a result, variable levels of axial pyranoside, equatorial pyranoside, axial furanoside and equatorial furanoside products are formed (Scheme 3.6). Heating D-galactose or D-mannose in ethanol with a proton source (in this case, HCl generated *in situ* from acetyl chloride ethanolysis) overnight yielded a mixture of glycosides, including the desired α-pyranosides. To facilitate chromatographic isolation of the target compound, the OH functionalities of the crude product mixture were masked through

---

[130] Song, Y.; Ji, X.; Dong, M.; Li, R.; Lin, Y. N.; Wang, H.; Wooley, K. L. *J. Am. Chem. Soc.* **2018**, *140*, 16053–16057.

[131] Dillingham, E. O.; Mast, R. W.; Bass, G. E.; Autian, J. *J. Pharm. Sci*. **1973**, *62*, 22–30.

[132] Cuevas, G.; Investigacih, C. De. *Tetrahedron* **1992**, *48*, 5019–5087.

peracetylation using acetic anhydride in pyridine overnight at room temperature. Despite significant β-galactoside formation under the reaction conditions as indicated by ^{1}H NMR spectroscopy, meticulous attempts at isolating 2,3,4,6-tetra-*O*-acetyl βOEtGal by flash column chromatography were unsuccessful due to its coelution with a by-product, presumably a furanoside. An alternative strategy was therefore chosen for preparing the β-anomer (see below). The peracetylated α-configured glycosides were isolated in 32% yield when starting from D-galactose and in 42% yield when starting from D-mannose, and were obtained on multigram scale. The modest yields are a reflection of the partial decomposition (caramelization) of the starting material under the harsh reaction conditions as well as the challenge in separating a mixture of compounds with similar retention factors as judged by TLC, with the latter condition being slightly ameliorated in the case of D-mannose due to negligible β-anomer formation. Deprotection of the peracetylated glycosides under Zemplén conditions using a methoxide base in methanol proceeded at high yields to afford the desired monomers which were further purified by recrystallization from hot ethanol (αOEtGal) or dried by lyophilisation (αOEtMan).

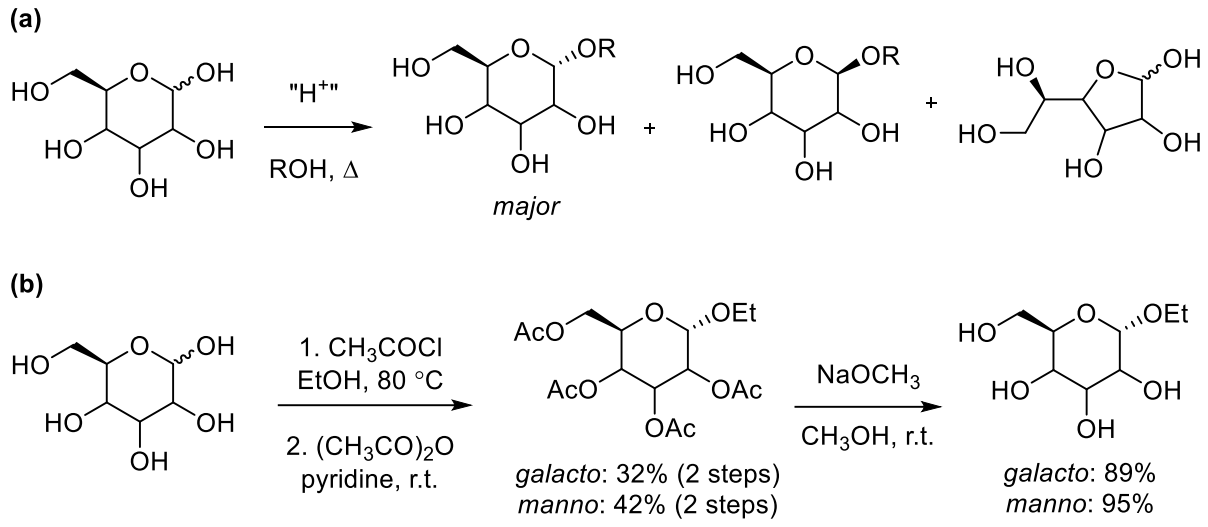

Scheme 3.6 (a) Typical Fischer glycosidation of a D-hexose showing the major α-pyranoside (six-membered ring) product along with the β-pyranoside and furanoside (five-membered ring) products. (b) Synthesis of α-configured galacto- and mannopyranosides.

Solubilisation of the hydrophilic starting material is a major issue in Fischer glycosidations. As a result, traditional reaction conditions are mostly applicable to the formation of glycosides with anomeric substituents derived from short-chain, low-boiling alcohols in which

free sugars are at least sparingly soluble and which are volatile enough to be used in excess and subsequently evaporated. To access monomers with long-chain anomeric substituents, we used a phase-transfer approach previously reported by our group.[133] This method allows for glycosidation of free sugars in non-polar organic solvents through the formation of a boronic ester which acts to solubilize the starting material and provide rate acceleration (Scheme 3.7). D-Galactose was subjected to a boronic acid-promoted condensation using phenylboronic acid as the phase-transfer agent, dichloroethane as the solvent, and camphorsulfonic acid as the catalyst to yield thermodynamic mixtures of substituted pyranosides and furanosides. *n*-Octyl and *i*-octyl alcohols were used as the glycosyl acceptors. Following cleavage of the boronic ester *via* transesterification with an alkaline D-sorbitol wash[134] originally reported by Hall *et al.*[135] the crude mixtures of free glycosides were peracetylated as described above and purified by flash column chromatography to afford the α-anomers in 60% and 37% yield for the *n*-octyl and *i*-octyl variants, respectively. A sizeable amount of β-configured pyranoside was observed in the crude reaction mixtures by ^{1}H NMR spectroscopy; however, the β-anomers were inseparable from furanoside by-products on silica, as was the case with the ethyl-substituted analogs. Attempts were made to increase the yield of the *i*-octyl-substituted galactoside (originally 30%) by changing the reaction time from 24 to 48 hours, which allowed for an increase in the proportion of thermodynamically favoured α-anomer from 1.7:1 to 2:1 α:β, resulting in a small increase in isolated yield.

The use of boronic acid to promote glycosidation of D-mannose thermodynamically favours the furanoside-selective pathway and is thus unsuitable for the formation of α-configured alkyl mannosides. A Lewis acid-promoted protocol was therefore selected (see below).

---

[133] Manhas, S.; Taylor, M. S. *J. Org. Chem.* **2017**, *82*, 11406–11417.

[134] Mancini, R. S.; Lee, J. B.; Taylor, M. S. *Org. Biomol. Chem.* **2017**, *15*, 132–143.

[135] Mothana, S.; Grassot, J.; Hall, D. G. *Angew. Chem. Int. Ed.* **2010**, *49*, 2883–2887.

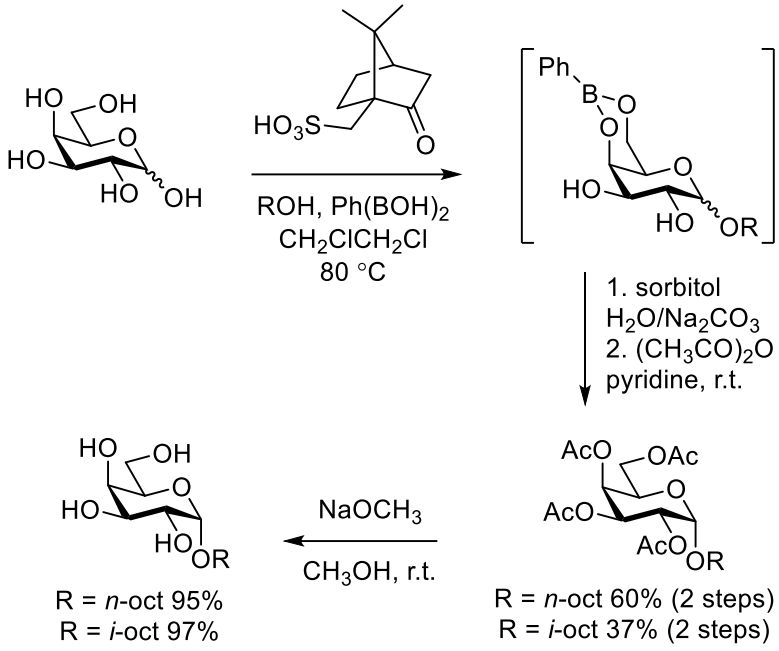

Scheme 3.7 Boronic acid-promoted Fischer glycosidation of D-galactose followed by boronic ester cleavage, protection, purification and deprotection. Only the pyranoside products are depicted.

3.4.2 Koenigs–Knorr Glycosidations

The Koenigs–Knorr glycosidation[136] was discovered in 1901 and involves silver-promoted selective formation of β-configured glycosides starting from protected glycosyl halide donors and a variety of glycosyl acceptors. A reversal of the typical trend favouring α glycoside formation is enforced by neighbouring group participation: a dioxolanium ion is formed upon abstraction of the halide leaving group by the silver salt, creating a *cis*-1,2 motif at C-1 and C-2, and high levels of β-selectivity subsequently arise from inversion of the C-1 stereocenter after S_N2-type nucleophilic attack by the glycosyl acceptor (Scheme 3.8).

[136] Koenigs, W.; Knorr, E. *Berichte der Dtsch. Chem. Gesellschaft banner* **1901**, *34*, 957–981.

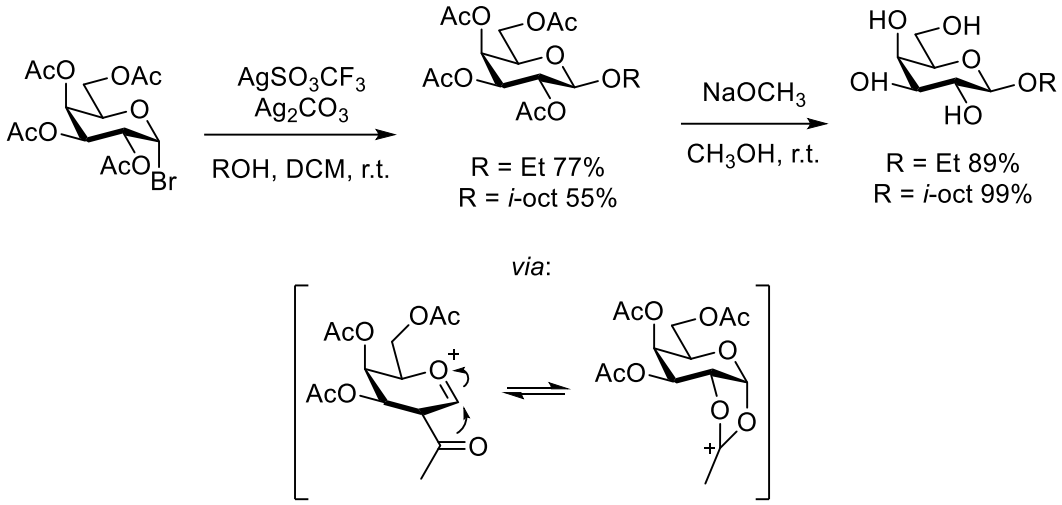

Scheme 3.8 Koenigs–Knorr glycosidation of galactopyranosyl bromide donor followed by deprotection to yield β-configured galactoside monomers. Origin of β-selectivity is rationalized by the formation of dioxolanium ion (right) from the oxocarbenium ion (left) shown in brackets.

Ethyl and isooctyl glycosides were successfully synthesized in good yields using silver trifluoromethanesulfonate and silver carbonate in DCM as previously reported,[137] yielding predominantly the β-anomer with some α-anomer formation. Flash column chromatography followed by ester hydrolysis afforded pure βOEtGal and βO*i*-OctGal. βOEtGal was additionally purified by recrystallization from hot ethanol. βO*n*-OctGal was acquired commercially.

3.4.3 Tin(IV) Chloride-promoted Mannoside Synthesis

An existing protocol[138] was employed to prepare manno-configured glycosides bearing long-chain alcohol-derived anomeric substituents. Tin(IV) chloride was used as a Lewis acid to activate mannosyl acetate toward attack by *n*-octyl and *i*-octyl alcohols through the intermediate of an oxocarbenium ion. Initially, a DCM solution of tin(IV) chloride was used with *n*-octyl alcohol, resulting in a 41% yield which increased to 50% when the Lewis acid was used neat. Flash column chromatography was used to purify the protected monomer precursors and the free

---

[137] Mancini, R. Selective Transformations of Unprotected Carbohydrates Using Organoboron Compounds to Modulate Hydroxyl Reactivity, 2017. University of Toronto, PhD thesis. [http://hdl.handle.net/1807/80829]

[138] Poláková, M.; Beláňová, M.; Petruš, L.; Mikušová, K. *Carbohydr. Res.* **2010**, *345,* 1339–1347.

glycosides were obtained at near-quantitative conversions after deprotection under Zemplén conditions.

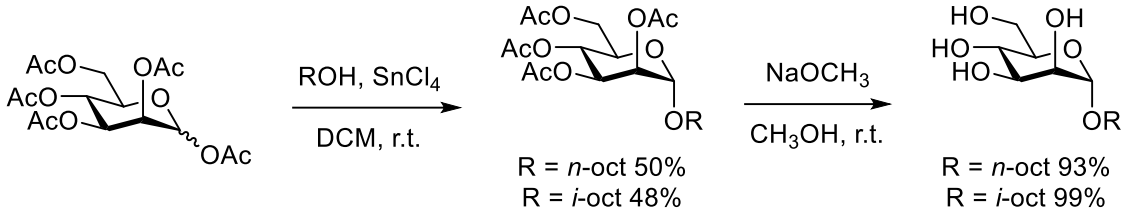

Scheme 3.9 Lewis acid-protomoted glycosidation to afford αO*n*-octMan and αO*i*-octMan.

3.5 Scope

The scope of polyesters synthesized in this study is shown in Table 3.2. The anomeric substituent was systematically varied among α- and β-galactopyranoside and α-mannopyranoside substrates to shed light onto any potential reactivity trends as well as to study the material properties as a function of the stereochemical configuration and anomeric substitution of the monomer (see Chapter 4). Additionally, βOMeGal was copolymerized with a series of acyl chlorides including sebacoyl chloride, dodecanedioyl chloride, adipoyl chloride, and isophthaloyl chloride to examine any differences in reactivity among acyl chlorides.

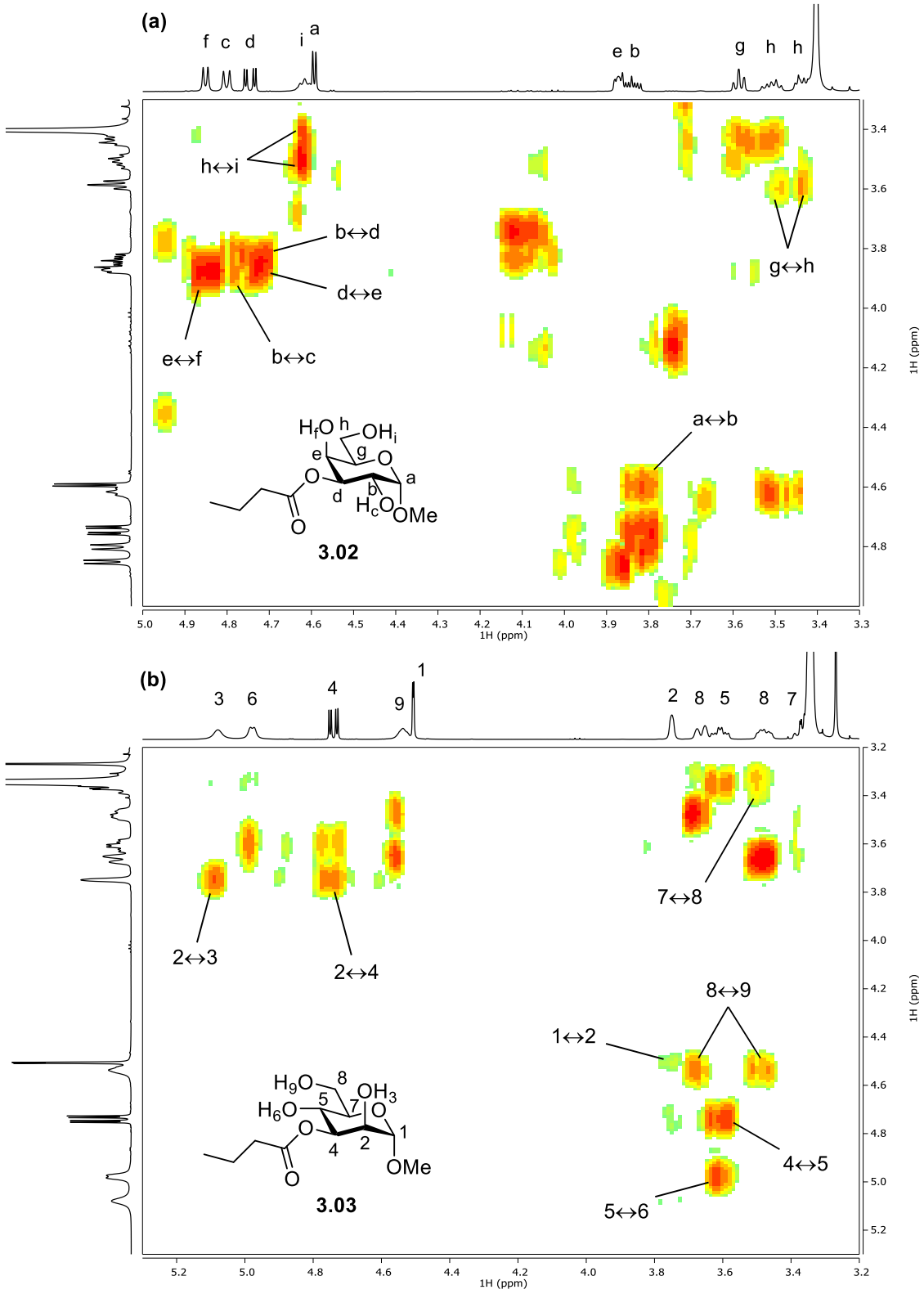

Figure 3.6 ^{1}H-^{1}H COSY NMR spectra of O-3 end-group models (a) **3.02** and (b) **3.03**.

Standard polymerizations were conducted on approximately 3.5 mmol scale under standard conditions and unfractionated polymer mixtures were isolated *via* a slightly acidic aqueous workup. Polyesters of methyl- and ethyl-substituted pyranosides were insoluble in water and non-polar organic solvents, but were soluble in polar protic and some aprotic solvents such as methanol, DMSO, pyridine, THF, acetonitrile and dioxane. Poly(βOMeGal adipate) and poly(βOMeGal isophthalate) had very low solubility in most solvents except highly polar solvents such as DMSO and hot dioxane, although unlike the previously reported poly(sucrose adipate)[139] they were water insoluble. *n*-Octyl-substituted substrates yielded softer solids with a wider solubility range including DCM, ethyl acetate, toluene and $CHCl_3$, while their *i*-octyl-substituted analogs were soft resins, with the α-galacto- and α-manno-substituted polymers being soluble, viscous liquids at room temperature.

^1H, ^{13}C and COSY NMR spectroscopy data indicated that the major linkage type across all pyranoside-derived polymers was 3,6. Subjecting αOMeGal and αOMeMan to monoacylation catalyzed by **1.02** produced O-3 end-group models **3.02** and **3.03** whose structures were confirmed by COSY NMR spectroscopy (Figure 3.6), and the ^{13}C NMR spectra of which were compared to crude polymer mixtures of galacto- and mannopyranoside-derived polyesters, respectively (Figures 3.7 and 3.8). Similarly to β-configured galactoside-derived polyesters, the presence of ^{13}C signals at similar chemical shifts in the α-configured pyranoside-derived polymers suggested that the O-3 monofunctionalized end-group was major in both galacto- and manno-configured sugar-derived polyesters, possibly because the 4,6-linked borinic acid adduct is disfavoured in both stereoisomers, or that its nucleophilic character is inferior to that of the 3,4 binding mode (in galactosides) or 2,3 binding mode (in mannosides) (see section 2.3, Scheme 3.5). Polymers that had lower M_n values as determined by GPC relative to PMMA standards concurrently exhibited higher O-3 end-group content (e.g., αO*i*-Oct substituted polymers of both stereoconfigurations).

---

[139] Patil, D. R.; Rethwisch, D. G.; Dordick, J. S. *Biotechnol. Bioeng.* **1991**, *37*, 639–646.

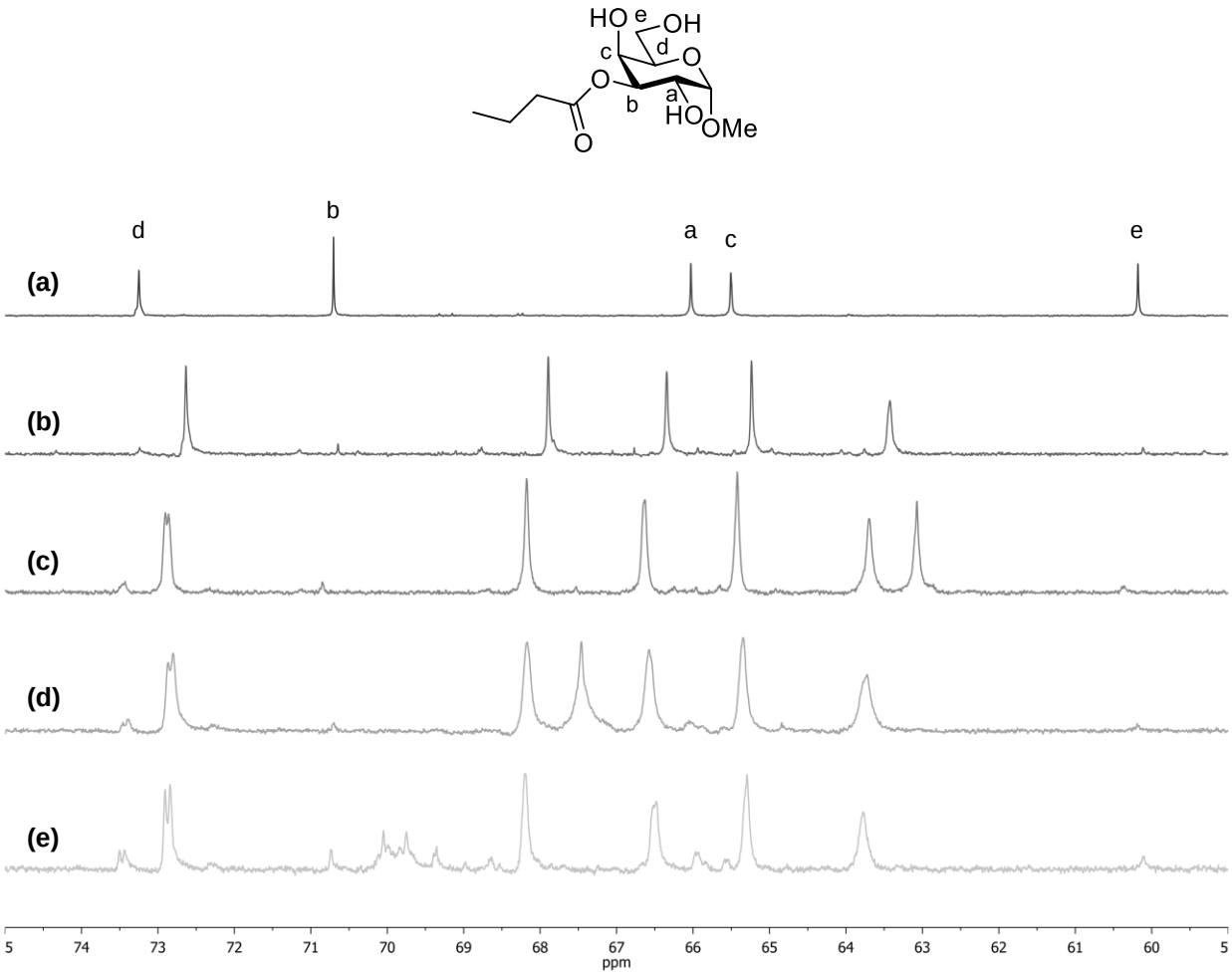

Figure 3.7 Carbohydrate region of ^{13}C NMR spectra of α-galactoside-derived polyesters compared to **3.02** (a). From the top: (b) αOMe, (c) αOEt, (d) αO*n*-oct, (e) O*i*-oct. Signals at 73, 71, 66, 65 and 60 ppm are consistent with the presence of O-3 monofunctionalized end-groups. All spectra were taken in DMSO-d_6.

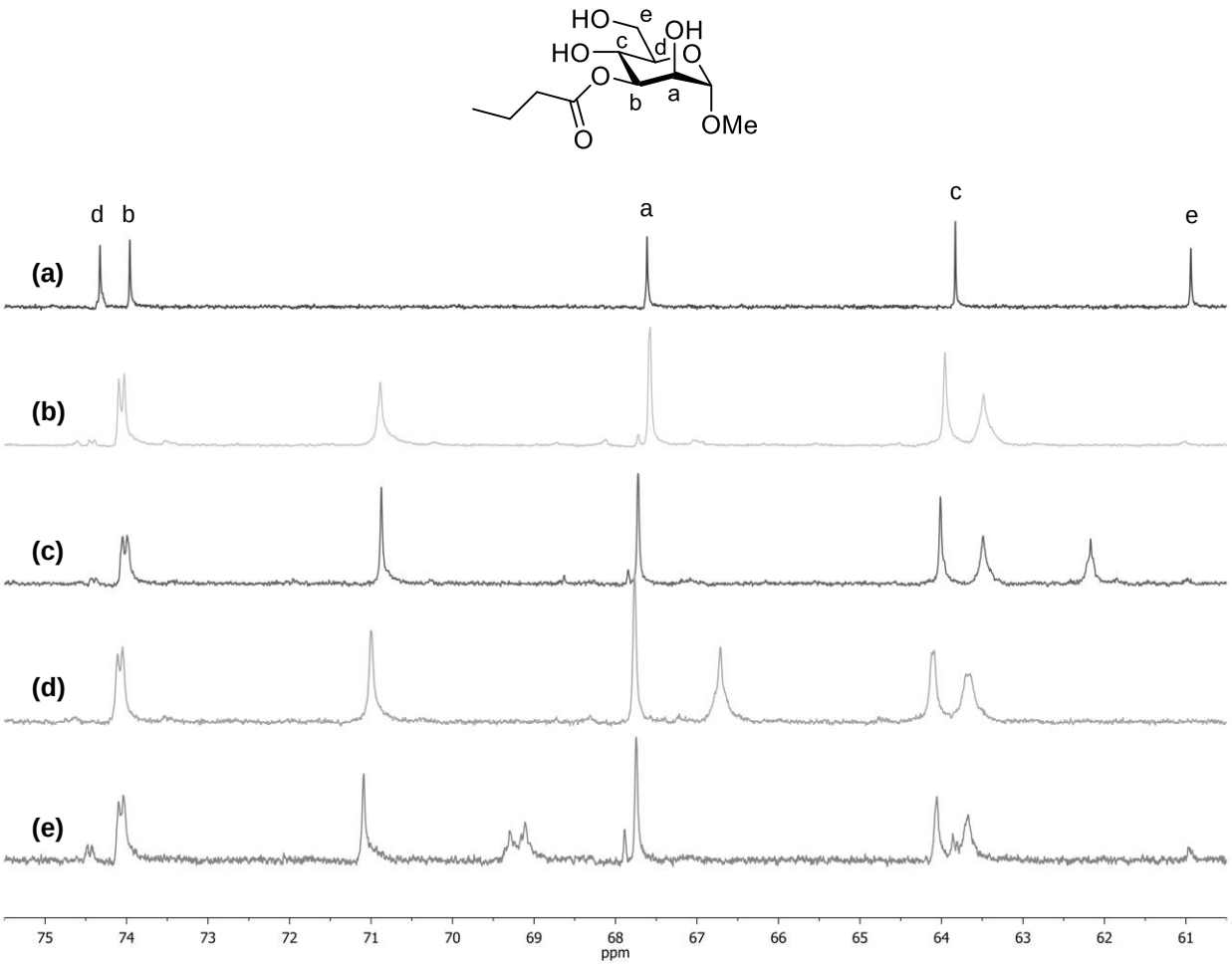

Figure 3.8 Carbohydrate region of ^{13}C NMR spectra of α-mannoside-derived polyesters compared to **3.03** (a). From the top: (b) αOMe, (c) αOEt, (d) αO*n*-oct, (e) αO*i*-oct. Signals at 74, 68 and 61 ppm are consistent with the presence of O-3 monofunctionalized end-groups. All spectra were taken in DMSO-d_6.

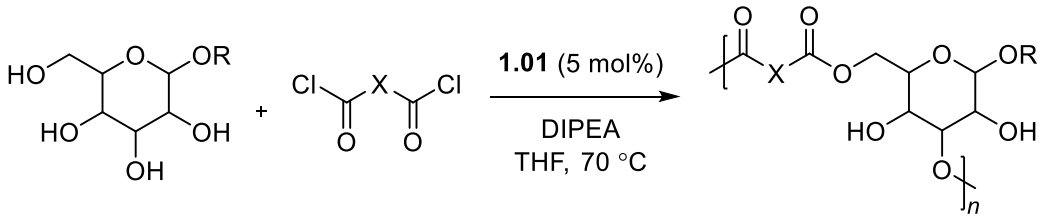

Table 3.2 Scope of pyranoside-derived polyesters.

Entry	Configuration	R =	X =	M_n*	Đ*
1	**α-*galacto*-**	Me	$(CH_2)_8$	2.5	2.0
2		Et	$(CH_2)_8$	5.8	2.9
3		*n*-oct	$(CH_2)_8$	4.0	2.9
4		*i*-oct	$(CH_2)_8$	3.5	2.3
5	**β-*galacto*-**	Me	$(CH_2)_8$	5.3	3.1
6		Me	$(CH_2)_{10}$	5.4	2.3
7		Me	$(CH_2)_4$	1.9	3.8
8		Me	*m*-C_6H_4	3.8	1.9
9		Et	$(CH_2)_8$	6.1	3.0
10		*n*-oct	$(CH_2)_8$	4.5	2.1
11		*i*-oct	$(CH_2)_8$	2.9	2.4
12†	**α-*manno*-**	Me	$(CH_2)_8$	5.0	6.3
13		Et	$(CH_2)_8$	5.1	2.5
14		*n*-oct	$(CH_2)_8$	15.1	3.3
15		*i*-oct	$(CH_2)_8$	3.9	2.3

* – molecular weights are expressed in kDa relative to PMMA standards and determined by GPC, NMP, 80 °C. † – 10 mol% **1.01** were used.

Degrees of polymerization as judged by GPC were typically modest and dispersities were consistent with a step-growth polymerization mechanism,[140] with some substrates suffering from particularly low polymerization rates, such as αOMeGal, all *i*-oct pyranosides, and adipoyl and isophthaloyl chlorides. Efforts were made to improve polycondensation conditions for

[140] Carothers, H. *Trans. Faraday Soc.* **1936**, *32*, 39–49.

commercially available monomer αOMeGal, including purifying the starting material by recrystallization to improve precision of stoichiometry. Exchanging the reaction solvent for acetonitrile (70 °C) or dioxane (100 °C) failed to significantly alter the degree of polymerization of poly(αOMeGal sebacate), as did increasing the catalyst loading to 10 mol%, increasing reaction time and scale, and employing a 1:1 mixture of **1.01** and **1.02**. The stark difference in polymerization rates between αOMeGal and βOMeGal is of unclear origin, as this effect is not observed for the ethyl analogs. The polymerization of αOMeMan led to the apparent formation of an insoluble polymer network in THF solvent, resulting in a high dispersity and partial loss of product due to insolubility. Reactions conducted in DCM or acetonitrile solvent became gel-like within minutes. The catalyst loading was increased to 10 mol% to better control chain growth and minimize heterogeneity (Table 3.2, entry 12). All other polymers remained mostly soluble under the reaction conditions. Poly(αO*n*-OctMan sebacate) had the highest M_n at 15.1 kDa, possibly by virtue of the monomer's high solubility in THF combined with the high reactivity of mannosides.

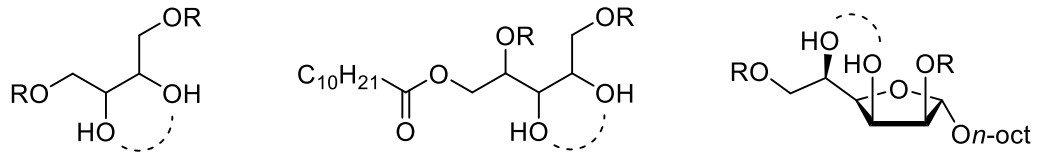

Figure 3.9 Likely outcomes of sugar alcohol and furanoside R-group substitution showing a potential organoboron binding site that could lead to further reactivity.

Tetraol substrates that did not feature a pyranoside ring structure were unsuccessful candidates for polymerization: model *bis*-acylations of these compounds yielded complex mixtures of regioisomers with various degrees of functionalization. Extensive efforts were made to optimize model *bis*-acylation conditions with the four-carbon sugar alcohols L-threitol and *meso*-erythritol ($HOCH_2(CH(OH))_2CH_2OH$), resulting in substantial triacyl side-product formation and a maximum diacyl tetraol yield of 46 and 32%, respectively, when 5 mol% **1.02** were used in THF at room temperature. Similarly, treating 1-*O*-decanoyl xylitol with two equivalents of butyryl chloride yielded a complex mixture as judged by ^{1}H NMR spectroscopy, and the same reaction conditions applied to *n*-octyl α-D-mannofuranoside resulted in a 62% yield of the 2,3,6-triacylated glycoside. The relative configuration of the remaining two OH groups after *bis*-acylation can be used to rationalize this effect, since in all the above substrates the

likely products of a *bis*-acylation still possess *cis*-1,2- or 1,3-diol motifs that are accessible to the borinic acid catalyst (Figure 3.9). This is exacerbated by the solubility differences among the various species present in the reaction, which follow the trend: starting material < monoacyl product < diacyl product. As a result of the lower solubility of species with more free OH groups, the solution phase of the reaction is enriched with species having higher degrees of acylation.

4 Conclusions

This chapter successfully demonstrates the application of a first-generation borinic acid catalyst for the controlled polymerization of anomerically protected galacto- and mannopyranosides. The catalyst was able to effect site-selective polymerization at rates superior to the catalyst-free control and allowed for the preparation of a series of sugar-derived polyesters with diverse anomeric pendant groups. Interestingly, the vast majority of end-groups identified by ^{1}H and ^{13}C NMR spectroscopy consisted of pyranosides acylated at the O-3 position, revealing a higher reactivity at the secondary OH than at the primary O-6 position. Future work may involve anomeric substitution of the carbohydrate-derived monomers with a pharmaceutical agent or reactive group (e.g., acetylene) for the synthesis of higher-order macromolecular structures. The next chapter describes studies into the properties of poly(pyranoside ester)s.

5 Experimental

5.1 General Considerations

Reactions were carried out in oven-dried glassware without effort to exclude air, unless otherwise indicated. Stainless steel syringes were used to transfer air- and moisture-sensitive liquids. Flash chromatography was carried out using neutral silica gel from Silicycle. Analytical TLC was carried out using aluminum-backed silica gel 60 F_{254} plates (EMD).

5.1.1 Materials

HPLC grade tetrahydrofuran (THF) and dichloromethane (DCM) were dried and purified using a solvent purification system equipped with columns of activated alumina, under nitrogen (Innovative Technology, Inc.). Catalysts were prepared according to previously reported

protocols.[141,77] Methyl glycosides and *n*-octyl β-D-galactopyranoside were purchased from Carbosynth and purified as specified. All other reagents and solvents were purchased from Sigma Aldrich and used without further purification.

5.1.2 Instrumentation

^{1}H, ^{13}C and ^{1}H-^{1}H COSY NMR experiments were performed using an Agilent DD2-500 (500 MHz) spectrometer with XSens cryogenic probe. ^{1}H-^{13}C HSQC and HMBC experiments were performed using an Agilent DD2-500 (500 MHz) spectrometer with OneNMR dual resonance probe. The spectra were processed using MestreNova. Chemical shifts are reported in parts per million (ppm) relative to tetramethylsilane with the solvent resonance resulting from incomplete deuteration as the internal standard. For ^{1}H NMR: $CDCl_3$ 7.26 ppm; DMSO-d_6 2.50 ppm, p; for ^{13}C NMR: $^{13}CDCl_3$ 77.0 ppm, t; DMSO-d_6 39.52 ppm, hept. Spectral features are tabulated in the following order: chemical shift (δ, ppm); multiplicity (s-singlet, d-doublet, t-triplet, q-quartet, m-complex multiplet, app-apparent); coupling constants (*J*); number of protons. Assignments were made on the basis of coupling constants and 2D NMR spectra. Infrared (IR) spectra were obtained on a Perkin-Elmer Spectrum 100 instrument equipped with a single-bounce diamond / ZnSe ATR accessory either in the solid state or as thin film liquids, as indicated. The spectra were processed using Spectrum Express. Spectral features are tabulated as follows: wavenumber (cm^{-1}); intensity (s-strong, m-medium, w-weak). High-resolution mass spectra (HRMS) were obtained on a JEOL AccuTOF JMST1000LC mass spectrometer equipped with a DART (direct analysis in real time) ion source. Specific rotations were measured with a Rudolph Autopol IV digital polarimeter equipped with a sodium lamp source (589 nm) and concentration (*c*) is reported in g/100 mL. Melting points (mp) were measured using a Fisher–Johns apparatus and are uncorrected. GPC was conducted at 80 °C using *N*-methylpyrrolidone (NMP) as eluent at a flow rate of 0.6 mL/min through an AM Gel Linear/5 exclusion column. A Waters 410 refractive index detector was used. Poly(methyl methacrylate) (PMMA) standards were used for calibration.

---

[141] Lee, D. Boron–Diol Interactions as the Basis for Novel Catalytic Transformations, 2014. University of Toronto, PhD thesis. [http://hdl.handle.net/1807/43646]

5.2 Synthesis and Characterization of Monomers

5.2.1 General Procedure for Monomer De-acetylation

2,3,4,6-Tetra-*O*-acetyl pyranoside was dissolved in methanol (0.05 M) in a round bottom flask of appropriate size equipped with a stir bar and the solution was cooled to 0 °C. Sodium methoxide (0.25 equivalents) was added and the reaction was allowed to warm to room temperature and stir until TLC showed complete disappearance of the protected starting material (typically 2–3 hours). Dowex® 50WX2 hydrogen form resin was added at 0 °C in small portions to the stirred solution until its pH became neutral as indicated by pH paper. The solution was then filtered through cotton, concentrated *in vacuo*, and purified further as indicated.

5.2.2 Monomer Synthesis and Characterization

Ethyl 2,3,4,6-tetra-*O*-acetyl α-D-galactopyranoside D-Galactose (9.12 g, 50.6 mmol) was loaded into a 250-mL round bottom flask equipped with a stir bar. Ethanol (100 mL) was added, followed by acetyl chloride (18 mL, 253 mmol). The mixture was heated to 70 °C and stirred for 6 hours under argon. After the reaction was cooled to 0 °C, Dowex® MARATHON basic resin was added in small portions until the pH of the solution became neutral as indicated by pH paper. The mixture was then filtered through cotton and concentrated *in vacuo* to yield a dark brown resin which was subjected to peracetylation without further purification. In a 250-mL round bottom flask equipped with a stir bar, the residue was dissolved in 30 mL of pyridine and cooled to 0 °C, after which acetic anhydride (30 mL) was added. The reaction was allowed to warm to room temperature and stirred for 20 hours. Toluene was added and the solution was concentrated *in vacuo*. Additional toluene was used for the azeotropic removal of residual pyridine and acetic anhydride, repeating the evaporation process three times. The resulting brown oil was purified by flash column chromatography on silica gel to yield 6.09 g of the title compound as a clear oil (32%). Spectral data were consistent with those reported in the literature.[142]

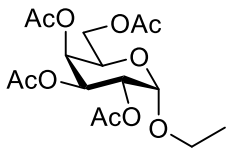

[142] Carmely, S.; Roll, M.; Loya, Y.; Kashman, Y. *J. Nat. Prod.* **1989**, *52*, 167–170.

Ethyl α-D-galactopyranoside (αOEtGal) Ethyl 2,3,4,6-tetra-*O*-acetyl α-D-galactopyranoside

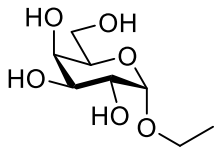

(4.54 g, 12.1 mmol) was deprotected according to the general procedure and the title compound was recrystallized from hot ethanol to yield 2.26 g of a white, crystalline powder (90%), mp 116–119 °C (lit. 139–140 °C).[143] Spectral data were consistent with those reported in the literature.[144]

Ethyl 2,3,4,6-tetra-*O*-acetyl β-D-galactopyranoside 2,3,4,6-Tetra-*O*-acetyl α-D-

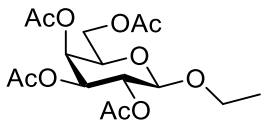

galactopyranosyl bromide (6.8 g, 16.5 mmol) and activated powdered 4Å molecular sieves (12 g) were loaded into a 250-mL round bottom flask equipped with a stir bar and placed under argon gas. 80 mL of ethanol were added. The solution was cooled to 0 °C and silver carbonate (4.55 g, 16.5 mmol) and silver triflate (4.24 g, 16.5 mmol) were added simultaneously. The suspension was allowed to warm to room temperature and left to stir for 20 hours, after which it was diluted with DCM and filtered through a pad of celite to remove the silver salts. The solution was concentrated and the yellow residue was purified by flash column chromatography on silica gel to yield 4.78 g of the title compound as a clear oil (77%). Spectral data were consistent with those reported in the literature.[145]

Ethyl β-D-galactopyranoside (βOEtGal) Ethyl 2,3,4,6-tetra-*O*-acetyl β-D-galactopyranoside

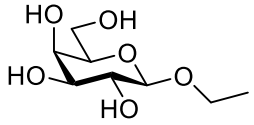

(4.51 g, 12 mmol) was deprotected according to the general procedure and the title compound was recrystallized from hot ethanol to yield 2.22 g of

---

[143] Jain, M. P.; Koul, S. K.; Dhar, K. L.; Atal, C. K. *Phytochemistry* **1980**, *19*, 1880–1882.

[144] Khan, K. M.; Perveen, S.; Ayattollahi, S. A. M.; Saba, N.; Rashid, A.; Firdous, S.; Haider, S. M.; Ullah, Z.; Rahat, S.; Khan, Z. *Nat. Prod. Lett.* **2002**, *16*, 283–290.

[145] Dahmén, J.; Frejd, T.; Gronberg, G.; Magnusson, G.; Noori, G. *Carbohydr. Res.* **1983**, *118*, 292–301.

clear needles (89%), mp 146–148 °C (lit. 160–161 °C).[146] Spectral data were consistent with those reported in the literature.[144]

Ethyl 2,3,4,6-tetra-*O*-acetyl α-D-mannopyranoside D-Mannose (4.97 g, 27.6 mmol) was

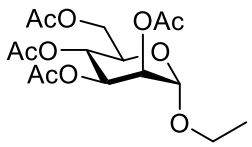

loaded into a 250-mL round bottom flask equipped with a stir bar. Ethanol (50 mL) was added, followed by acetyl chloride (7.8 mL, 110 mmol). The mixture was heated to 70 °C and stirred for 17 hours under argon. After the reaction was cooled to 0 °C, Dowex® MARATHON basic resin was added in small portions until the pH of the solution became neutral as indicated by pH paper. The mixture was then filtered through cotton and concentrated *in vacuo* to yield a dark brown resin which was subjected to peracetylation without further purification. In a 250-mL round bottom flask equipped with a stir bar, the residue was dissolved in 19 mL of pyridine and cooled to 0 °C, after which acetic anhydride (19 mL) was added. The reaction was allowed to warm to room temperature and stirred for 5 hours. Toluene was added and the solution was concentrated *in vacuo*. Additional toluene was used for the azeotropic removal of residual pyridine and acetic anhydride, repeating the evaporation process three times. The resulting brown oil was purified by flash column chromatography on silica gel to yield 4.36 g of the title compound as a clear oil (42%). ^{1}H NMR (500 MHz, $CDCl_3$) δ 5.36 (dd, *J* = 10.0, 3.5 Hz, 1H, H-3), 5.27 (m, 1H, H-4), 5.22 (dd, *J* = 3.5, 1.8 Hz, 1H, H-2), 4.81 (d, *J* = 1.8 Hz, 1H, H-1), 4.27 (dd, *J* = 12.2, 5.3 Hz, 1H, H-6), 4.10 (dd, *J* = 12.2, 2.5 Hz, 1H, H-6), 4.02–3.97 (m, 1H, H-5), 3.73 (dq, *J* = 9.8, 7.1 Hz, 1H, OCH_2), 3.53 (dq, *J* = 9.8, 7.1 Hz, 1H, OCH_2), 2.14 (s, 3H, CO-2 CH_3), 2.09 (s, 3H, CO-6 CH_3), 2.03 (s, 3H, CO-4 CH_3), 1.98 (s, 3H, CO-3 CH_3), 1.23 (t, *J* = 7.1 Hz, 3H, CH_3) ppm. ^{13}C NMR (126 MHz, $CDCl_3$) δ 170.78 (CO-6), 170.22 (CO-2), 170.02 (CO-3), 169.87 (CO-4), 97.50 (C-1), 69.92 (C-2), 69.24 (C-3), 68.49 (C-5), 66.45 (C-4), 64.09 (OCH_2CH_3), 62.67 (C-6), 21.05 (CO-2 CH_3), 20.87 ($COCH_3$), 20.84 ($COCH_3$), 20.83 ($COCH_3$), 15.03 (OCH_2CH_3) ppm. IR (thin film, cm^{-1}) 2956 (w), 1743 (s), 1370 (m), 1218 (s), 1135 (m), 1079 (m), 1041 (s), 977 (m).

---

[146] Mougne, G. *J. Pharm. Chim.* **1917**, 345–348.

HRMS (DART+, *m/z*): calcd for $C_{16}H_{28}NO_{10}$ $[M + NH_4]^+$ 394.17, found 394.17086. $[\alpha]_D^{20}$ = +73.9 (*c* = 0.165, CH_2Cl_2).

Ethyl α-D-mannopyranoside (αOEtMan) Ethyl 2,3,4,6-tetra-*O*-acetyl α-D-mannopyranoside

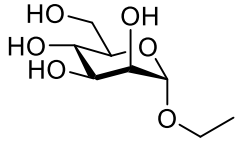

(4.4 g, 11.7 mmol) was deprotected according to the general procedure and the title compound was lyophilized from water to give 2.31 g of a clear glass (95%). ^{1}H NMR (500 MHz, DMSO-d_6) δ 4.71–4.65 (m, 2H, OH-2, OH-4), 4.60 (d, *J* = 1.7 Hz, 1H, H-1), 4.53 (d, *J* = 6.0 Hz, 1H, OH-3), 4.44 (t, *J* = 6.0 Hz, 1H, OH-6), 3.68–3.60 (m, 2H, H-5, H-6), 3.57 (ddd, *J* = 4.7, 3.4, 1.7 Hz, 1H, H-2), 3.47–3.41 (m, 2H, H-3, H-6), 3.39–3.26 (m, 3H, H-4, CH_2CH$_3$), 1.11 (t, *J* = 7.1 Hz, 3H, CH_3) ppm. ^{13}C NMR (126 MHz, DMSO-d_6) δ 99.54 (C-1), 73.92 (C-5), 71.02 (C-3), 70.42 (C-2), 67.10 (C-4), 61.66 (CH_2CH$_3$), 61.33 (C-6), 14.99 (CH_3) ppm. IR (thin film, cm^{-1}) 3340 (br), 2973 (m), 2911 (m), 1739 (m), 1380 (m), 1225 (w), 1131 (s), 1034 (s), 972 (2), 881 (m), 807 (m). HRMS (DART+, *m/z*): calcd for $C_8H_{20}NO_6$ $[M + NH_4]^+$ 226.12961, found 226.12945. $[\alpha]_D^{20}$ = +86.9 (*c* = 0.11, CH_3OH).

***n*-octyl 2,3,4,6-tetra-*O*-acetyl α-D-galactopyranoside** Compound was prepared according to an existing literature protocol.[133]

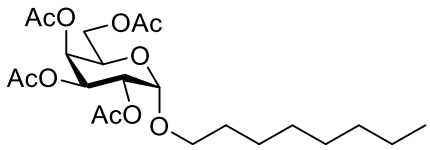

***n*-octyl α-D-galactopyranoside (αO*n*-OctGal)** *n*-octyl 2,3,4,6-tetra-*O*-acetyl α-D-galactopyranoside (1.97 g, 4.28 mmol) was deprotected according to the general procedure and the title compound was dried under high vacuum to yield 1.19 g of a white powder (95%). Spectral data were consistent with those reported in the literature.[147]

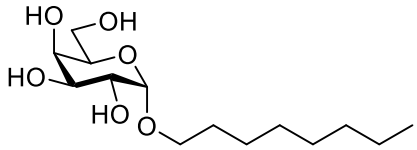

[147] Dimakos, V.; Garrett, G. E.; Taylor, M. S. *J. Am. Chem. Soc.* **2017**, *139*, 15515–15521.

***n*-octyl 2,3,4,6-tetra-*O*-acetyl α-D-mannopyranoside** Compound was prepared according to an existing literature protocol.[138]

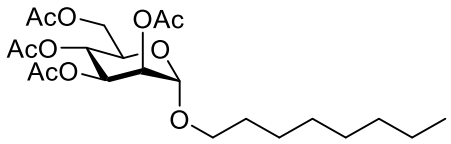

***n*-octyl α-D-mannopyranoside (αO*n*-OctMan)** *n*-octyl 2,3,4,6-tetra-*O*-acetyl α-D-mannopyranoside (2.07 g, 4.5 mmol) was deprotected according to the general procedure and the title compound was dried under high vacuum to yield 1.22 g of a white powder (93%). Spectral data were consistent with those reported in the literature.[148]

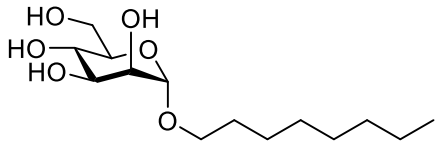

2-Ethylhexyl 2,3,5,6-tetra-*O*-acetyl α-D-galactopyranoside Procedure was adapted from an existing literature protocol.[133] Briefly, D-galactose (1.00 g, 5.59 mmol), (1*S*)-(+)-10-camphorsulfonic acid (324.6 mg, 1.40 mmol), and phenylboronic acid (681.4 mg, 5.59 mmol) were loaded into an oven-dried 50-mL round bottom flask equipped with a stir bar. The solids were purged with argon, after which anhydrous 1,2-dichloroethane was added to the vial (28 mL), followed by 2-ethyl-1-hexanol (4.3 mL, 28 mmol). The mixture was stirred at 80 °C under argon. After 28 h, the solvent was removed *in vacuo* and the resulting residue was dissolved in diethyl ether and washed twice for 5 min with an aqueous sorbitol solution (1 M Na_2CO_3 with 1 M D-sorbitol). The combined aqueous fractions were reextracted three times with diethyl ether and the combined organic extracts were dried over magnesium sulfate, filtered, and concentrated *in vacuo*. The resulting dark yellow oil was subjected to peracetylation without further purification. In a 100-mL round bottom flask equipped with a stir bar, the oil was dissolved in 10 mL of pyridine and cooled to 0 °C, after which acetic anhydride (10 mL) was added. The reaction was allowed to warm to room temperature and stirred for 15 hours. Toluene was added and the solution was concentrated *in vacuo*. Additional toluene was used for the azeotropic removal of residual pyridine and acetic anhydride, repeating the evaporation process three times. The

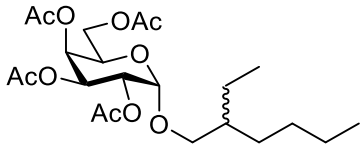

---

[148] Watt, J. A.; Williams, S. J. *Org. Biomol. Chem.* **2005**, *3*, 1982–1992.

resulting dark yellow oil was purified by flash column chromatography on silica gel to yield 952.5 mg of the title compound as a clear oil (37%). ^{1}H NMR (500 MHz, DMSO-d_6) δ 5.36 (d, J = 3.4 Hz, 1H, H-4), 5.18 (dd, J = 10.9, 3.4 Hz, 1H, H-3), 5.04 (d, J = 3.7 Hz, 1H, H-1), 4.94 (dd, J = 10.9, 3.7 Hz, 1H, H-2), 4.20–4.14 (m, 1H, H-5), 4.08–3.99 (m, 2H, H-6), 3.57 (ddd, J = 9.7, 7.2, 5.2 Hz, 1H, OCH_2CH(CH$_2$CH$_3$)), 3.28 (ddd, J = 9.8, 5.8, 4.2 Hz, 1H, OCH_2CH(CH$_2$CH$_3$)), 2.12 (s, 3H, CO-4 CH$_3$), 2.02 (s, 3H, COCH$_3$), 1.99 (s, 3H, COCH$_3$), 1.94 (s, 3H, CO-3 CH$_3$), 1.43–1.56 (m, 1H, OCH$_2$CH(CH$_2$CH$_3$)), 1.42–1.13 (m, 8H, CH$_2$), 0.97–0.77 (m, 6H, CH$_3$) ppm. ^{13}C NMR (126 MHz, DMSO-d_6) δ 169.96 (CO-4), 169.85 (CO-2, CO-6), 169.55 (CO-3), 95.49 (C-1), 95.42 (C-1), 69.97 (OCH$_2$), 69.94 (OCH$_2$), 67.93 (C-4), 67.69 (C-2), 67.06 (C-3), 66.08 (C-5), 61.78 (C-6), 61.77 (C-6), 38.70 (OCH$_2$$C$H), 38.61 (OCH$_2$$C$H), 30.07 ($CH_2CH_2CH_2CH_3$), 29.84 ($CH_2CH_2CH_2CH_3$), 28.44 (CH$_2$$CH_2CH_2CH_3$), 28.33 (CH$_2$$CH_2CH_2CH_3$), 23.55 (OCH$_2$CH($CH_2CH_3$)), 23.21 (OCH$_2$CH($CH_2CH_3$)), 22.51 (CH$_2CH_2$$CH_2CH_3$), 22.49 (CH$_2CH_2$$CH_2CH_3$), 20.44 (CO$CH_3$), 20.39 (CO$CH_3$), 20.36 (CO$CH_3$), 13.91 (CH$_2CH_2CH_2$$CH_3$), 13.89 (CH$_2CH_2CH_2$$CH_3$), 10.82 (OCH$_2$CH(CH$_2$$CH_3$)), 10.78 (OCH$_2$CH(CH$_2$$CH_3$)) ppm. IR (thin film, cm^{-1}) 2931 (m), 1744 (s), 1461 (w), 1370 (m), 1214 (s), 1160 (m), 1134 (m), 1036 (s), 954 (m). HRMS (DART+, *m/z*): calcd for $C_{22}H_{40}NO_{10}$ $[M + NH_4]^+$ 478.26577, found 478.26442.

2-Ethylhexyl α-D-galactopyranoside (αO*i*-OctGal) 2-Ethylhexyl 2,3,5,6-tetra-*O*-acetyl α-D-galactopyranoside (2.00 g, 4.35 mmol) was deprotected according to the general procedure and the title compound was dried under high vacuum to yield 1.23 g of a colorless resin (97%). ^{1}H NMR (500 MHz, DMSO-d_6) δ 4.68–4.50 (m, 3H, H-1, OH-3, OH-6), 4.38–4.34 (m, 2H, OH-2, OH-4), 3.70 (app s, 1H, H-4), 3.63–3.45 (m, 5H, H-2, H-3, H-5, H-6, OCH_2CH(CH$_2$CH$_3$)), 3.44–3.41 (m, 1H, H-6), 3.17 (ddd, J = 9.5, 7.1, 5.3 Hz, 1H, OCH_2CH(CH$_2$CH$_3$)), 1.53–1.18 (m, 9H, OCH$_2$CH(CH$_2$CH$_3$), CH$_2$), 0.90–0.78 (m, 6H, CH$_3$) ppm. ^{13}C NMR (126 MHz, DMSO-d_6) δ 99.20 (C-1), 99.07 (C-1), 71.27 (C-5), 69.65 (OCH$_2$), 69.59 (C-2), 69.48 (OCH$_2$), 68.85 (C-4), 68.41 (C-3), 60.54 (C-6), 39.08 (OCH$_2$$C$H), 38.91 (OCH$_2$$C$H), 30.03 ($CH_2CH_2CH_2CH_3$), 29.94 ($CH_2CH_2CH_2CH_3$), 28.58 (CH$_2$$CH_2CH_2CH_3$), 28.41 (CH$_2$$CH_2CH_2CH_3$), 23.43 (OCH$_2$CH($CH_2CH_3$)), 23.36 (OCH$_2$CH($CH_2CH_3$)), 22.56 (CH$_2CH_2$$CH_2CH_3$), 22.55 (CH$_2CH_2$$CH_2CH_3$), 14.01 (CH$_2CH_2CH_2$$CH_3$), 13.98 (CH$_2CH_2CH_2$$CH_3$), 11.12 (OCH$_2$CH(CH$_2$$CH_3$)), 10.82 (OCH$_2$CH(CH$_2$$CH_3$)) ppm. IR (thin film, cm^{-1}) 3372 (bs), 2927 (s),

1462 (w), 1153 (m), 1036 (s), 766 (m). HRMS (DART+, *m/z*): calcd for $C_{14}H_{32}NO_6$ $[M + NH_4]^+$ 310.22351, found 310.22387.

2-Ethylhexyl 2,3,5,6-tetra-*O*-acetyl β-D-galactopyranoside 2,3,4,6-Tetra-*O*-acetyl α-D-

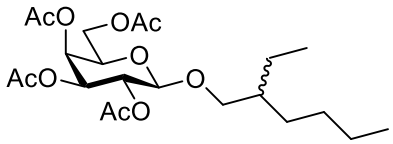

galactopyranosyl bromide (1.028 g, 2.5 mmol) and activated powdered 4Å molecular sieves (2.5 g) were loaded into a 100-mL Schlenk flask equipped with a stir bar and placed under argon gas. DCM (12.5 mL) was added, followed by 2-ethylhexanol (782 µL, 5 mmol). The solution was cooled to 0 °C and silver carbonate (689.5 mg, 2.5 mmol) and silver triflate (642.25 mg, 2.5 mmol) were added simultaneously under positive pressure of argon gas. The suspension was allowed to warm to room temperature and left to stir for 20 hours, after which it was diluted with DCM and filtered through a pad of celite to remove the silver salts. The solution was concentrated and the yellow residue was purified by flash column chromatography on silica gel to yield 633.2 mg of the title compound as a clear oil (55%). ^{1}H NMR (500 MHz, DMSO-d_6) δ 5.25 (dd, *J* = 3.6, 1.2 Hz, 1H, H-4), 5.16 (dd, *J* = 10.5, 3.6 Hz, 1H, H-3), 4.93 (dd, *J* = 10.5, 8.0 Hz, 1H, H-2), 4.65 (d, *J* = 8.0, 1H, H-1), 4.18 (td, *J* = 6.4, 1.2 Hz, 1H, H-5), 4.04 (qd, *J* = 11.2, 6.4 Hz, 2H, H-6), 3.68 (ddd, *J* = 9.7, 7.9, 5.0 Hz, 1H, OC*H*$_2$CH(CH$_2$CH$_3$)), 3.34–3.27 (m, 1H, OC*H*$_2$CH(CH$_2$CH$_3$)), 2.12 (s, 3H, CO-4 CH$_3$), 1.99 (s, 6H, CO-6, CO-2 CH$_3$), 1.91 (s, 3H, CO-3 CH$_3$), 1.48–1.36 (m, 1H, OCH$_2$C*H*(CH$_2$CH$_3$)), 1.36–1.13 (m, 8H, CH$_2$), 0.92–0.75 (m, 6H, CH$_3$) ppm. ^{13}C NMR (126 MHz, DMSO-d_6) δ 169.94 (C4-O), 169.83 (C6-O), 169.50 (C3-O), 168.94 (C2-O), 100.30 (C-1), 100.25 (C-1), 71.43 (OCH$_2$), 71.32 (OCH$_2$), 70.15 (C-3), 69.76 (C-5), 68.71 (C-2), 67.33 (C-4), 61.23 (C-6), 38.83 (OCH$_2$*C*H), 38.75 (OCH$_2$*C*H), 29.88 (*C*H$_2$CH$_2$CH$_2$CH$_3$), 29.58 (*C*H$_2$CH$_2$CH$_2$CH$_3$), 28.50 (CH$_2$*C*H$_2$CH$_2$CH$_3$), 28.28 (CH$_2$*C*H$_2$CH$_2$CH$_3$), 23.10 (OCH$_2$CH(*C*H$_2$CH$_3$)), 22.92 (OCH$_2$CH(*C*H$_2$CH$_3$)), 22.49 (CH$_2$CH$_2$*C*H$_2$CH$_3$), 20.47 (CO*C*H$_3$), 20.43 (CO*C*H$_3$), 20.39 (CO*C*H$_3$), 20.34 (CO*C*H$_3$), 13.93 (CH$_2$CH$_2$CH$_2$*C*H$_3$), 10.91 (OCH$_2$CH(CH$_2$*C*H$_3$)), 10.63 (OCH$_2$CH(CH$_2$*C*H$_3$)) ppm. IR (thin film, cm^{-1}) 2927 (w), 1746 (s), 1442 (w), 1369 (m), 1216 (s), 1174 (m), 1049 (s), 956 (m), 906 (m). HRMS (DART+, *m/z*): calcd for $C_{22}H_{40}NO_{10}$ $[M + NH_4]^+$ 478.26577, found 478.26502.

2-Ethylhexyl β-D-galactopyranoside (βO*i*-OctGal) 2-Ethylhexyl 2,3,5,6-tetra-*O*-acetyl β-D-galactopyranoside (2.40 g, 5.22 mmol) was deprotected according to the general procedure and the title compound was dried under high vacuum to afford 1.51 g of a white powder (99%). ^{1}H NMR (500 MHz, DMSO-d_6) δ 4.77–4.65 (m, 2H, OH-2, OH-4), 4.56 (t, *J* = 5.5 Hz, 1H, OH-6), 4.36 (d, *J* = 4.2 Hz, 1H, OH-3), 4.03 (d, *J* = 6.5 Hz, 1H, H-1), 3.68–3.59 (m, 2H, H-3, OC*H*$_2$CH(CH$_2$CH$_3$)), 3.57–3.49 (m, 1H, H-6), 3.48–3.40 (m, 1H, H-6), 3.31–3.22 (m, 4H, H-2, H-4, H-5, OC*H*$_2$CH(CH$_2$CH$_3$)), 1.50–1.16 (m, 9H, OCH$_2$C*H*(CH$_2$CH$_3$), CH$_2$), 0.95–0.75 (m, 6H, CH$_3$) ppm. ^{13}C NMR (126 MHz, DMSO-d_6) δ 103.92 (C-1), 103.82 (C-1), 75.10 (C-5), 73.58 (C-2), 71.27 (OCH$_2$), 71.15 (OCH$_2$), 70.62 (C-4), 68.07 (C-3), 60.33 (C-6), 39.08 (OCH$_2$*C*H), 29.81 (*C*H$_2$CH$_2$CH$_2$CH$_3$), 29.80 (*C*H$_2$CH$_2$CH$_2$CH$_3$), 28.54 (CH$_2$*C*H$_2$CH$_2$CH$_3$), 28.52 (CH$_2$*C*H$_2$CH$_2$CH$_3$), 23.13 (OCH$_2$CH(*C*H$_2$CH$_3$)), 23.07 (OCH$_2$CH(*C*H$_2$CH$_3$)), 22.60 (CH$_2$CH$_2$*C*H$_2$CH$_3$), 14.03 (CH$_2$CH$_2$CH$_2$*C*H$_3$), 10.89 (OCH$_2$CH(CH$_2$*C*H$_3$)), 10.82 (OCH$_2$CH(CH$_2$*C*H$_3$)) ppm. IR (thin film, cm^{-1}) 3377 (bs), 2928 (s), 1061 (s), 754 (m). HRMS (DART+, *m/z*): calcd for C$_{14}$H$_{32}$NO$_6$ [M + NH$_4$]$^+$ 310.22351, found 310.22319.

2-Ethylhexyl 2,3,5,6-tetra-*O*-acetyl α-D-mannopyranoside 1,2,3,4,6-Penta-*O*-acetyl α-D-mannopyranose (1.0964 g, 2.81 mmol) was loaded into a 100-mL Schlenk flask equipped with a stir bar and placed under argon gas. DCM (19 mL) was added and the resulting solution was cooled to 0 °C. Tin(IV) chloride (330 µL, 2.81 mmol) was added to the solution which was then stirred at 0 °C for 10 minutes, after which 2-ethylhexanol (530 µL, 3.41 mmol) was added dropwise. The reaction was allowed to warm to room temperature and left to stir for 24 hours. The mixture was diluted with DCM and washed twice with a cold saturated solution of NaHCO$_3$. The organic phase was dried over magnesium sulfate and concentrated *in vacuo*. The light amber residue was purified by flash column chromatography on silica gel to yield 621.1 mg of the title compound as a colorless resin (48%). ^{1}H NMR (500 MHz, CDCl$_3$) δ 5.34–5.18 (m, 3H, H-2, H-3, H-4), 4.75 (app s, 1H, H-1), 4.24 (dd, *J* = 12.2, 5.5 Hz, 1H, H-6), 4.08 (dd, *J* = 12.2, 2.3 Hz, 1H, H-6), 4.01–3.87 (m, 1H, H-5), 3.58 (ddd, *J* = 10.9, 9.6, 6.0 Hz, 1H, OC*H*$_2$CH(CH$_2$CH$_3$)), 3.37–3.20 (m, 1H, OC*H*$_2$CH(CH$_2$CH$_3$)), 2.13 (s, 3H, CO-2, CH$_3$), 2.07 (s, 3H, CO-6 CH$_3$), 2.02 (s, 3H, CO-4 CH$_3$), 1.96 (s, 3H, CO-3 CH$_3$), 1.51 (dq, *J* = 12.4, 6.1 Hz, 1H, OCH$_2$C*H*(CH$_2$CH$_3$)),

1.44–1.16 (m, 8H, CH_2), 0.96–0.77 (m, 6H, CH_3) ppm. ^{13}C NMR (126 MHz, $CDCl_3$) δ 170.75 (C6-O), 170.23 (C2-O), 170.00 (C3-O), 169.89 (C4-O), 97.96 (C-1), 97.88 (C-1), 71.27 (OCH_2), 71.20 (OCH_2), 69.84 (C-2), 69.33 (C-3), 68.65 (C-5), 66.39 (C-4), 62.71 (C-6), 39.52 (OCH_2CH), 39.36 (OCH_2CH), 30.51 ($CH_2CH_2CH_2CH_3$), 29.15 ($CH_2CH_2CH_2CH_3$), 23.97 ($OCH_2CH(CH_2CH_3)$), 23.84 ($OCH_2CH(CH_2CH_3)$), 23.10 ($CH_2CH_2CH_2CH_3$), 21.06 (CO-2 CH_3), 20.87 ($COCH_3$), 20.86 ($COCH_3$), 20.84 ($COCH_3$), 14.19 ($CH_2CH_2CH_2CH_3$), 11.24 ($OCH_2CH(CH_2CH_3)$), 11.07 ($OCH_2CH(CH_2CH_3)$) ppm. IR (thin film, cm^{-1}) 2940 (m), 1746 (s), 1444 (w), 1369 (m), 1219 (s), 1079 (s), 1045 (s), 977 (m), 906 (m) ppm. HRMS (DART+, *m/z*): calcd for $C_{22}H_{40}NO_{10}$ $[M + NH_4]^+$ 478.26577, found 478.26528.

2-Ethylhexyl-α-D-mannopyranoside (αO*i*-OctMan) 2-Ethylhexyl 2,3,5,6-tetra-*O*-acetyl α-D-mannopyranoside (1.80 g, 4.03 mmol) was deprotected according to the general procedure and the title compound was dried under high vacuum to yield 1.16 g of a white powder (99%). ^1H NMR (500 MHz, DMSO-d_6) δ 4.75 (d, *J* = 5.0 Hz, 1H, OH-4), 4.69 (d, *J* = 4.2 Hz, 1H, OH-2), 4.60 (d, *J* = 5.2 Hz, 1H, OH-3), 4.58–4.53 (m, 1H, H-1), 4.42 (t, *J* = 6.0 Hz, 1H, OH-6), 3.63 (dd, *J* = 11.6, 2.2 Hz, 1H, H-6), 3.60–3.56 (m, 1H, H-2), 3.52 (dt, *J* = 9.5, 6.2 Hz, 1H, $OCH_2CH(CH_2CH_3)$), 3.41–3.47 (m, 2H, H-3, H-6), 3.37 (td, *J* = 9.4, 3.2 Hz, 1H, H-4), 3.27 (ddd, *J* = 9.4, 6.2, 2.2 Hz, 1H, H-5), 3.18 (ddd, *J* = 9.6, 5.3, 3.1 Hz, 1H, $OCH_2CH(CH_2CH_3)$), 1.44 (pd, *J* = 6.2, 5.6, 2.6 Hz, 1H, $OCH_2CH(CH_2CH_3)$), 1.39–1.16 (m, 8H, CH_2), 0.93–0.80 (m, 6H, CH_3) ppm. ^{13}C NMR (126 MHz, DMSO-d_6) δ 100.03 (C-1), 99.96 (C-1), 74.04 (C-5), 71.05 (C-3), 70.43 (C-2), 68.84 (OCH_2), 68.78 (OCH_2), 66.90 (C-4), 61.25 (C-6), 38.93 (OCH_2CH), 38.84 (OCH_2CH), 30.11 ($CH_2CH_2CH_2CH_3$), 30.04 ($CH_2CH_2CH_2CH_3$), 28.57 ($CH_2CH_2CH_2CH_3$), 28.40 ($CH_2CH_2CH_2CH_3$), 23.52 ($OCH_2CH(CH_2CH_3)$), 23.49 ($OCH_2CH(CH_2CH_3)$), 22.52 ($CH_2CH_2CH_2CH_3$), 13.97 ($CH_2CH_2CH_2CH_3$), 13.95 ($CH_2CH_2CH_2CH_3$), 11.15 ($OCH_2CH(CH_2CH_3)$), 10.89 ($OCH_2CH(CH_2CH_3)$) ppm. IR (thin film, cm^{-1}) 3359 (bs), 2927 (s), 1597 (w), 1462 (w), 1064 (m). HRMS (DART+, *m/z*): calcd for $C_{14}H_{32}NO_6$ $[M + NH_4]^+$ 310.22351, found 310.22299.

5.3 Synthesis and Characterization of Polymers

5.3.1 General Procedure for Polymer Synthesis

3.5–4.0 mmol glycoside and 5 mol% **1.01** (unless otherwise specified) were loaded into a 50-mL round bottomed flask equipped with a stir bar and the flask was purged with argon gas. THF (0.3 M) and DIPEA (3 equivalents) were added by syringe before placing the flask in a 0 °C ice bath. Acyl dichloride (1 equivalent) was added dropwise by syringe over 10 minutes and the reaction was allowed to warm to room temperature and heated to 70 °C for 4 hours. Approximately 1 mL methanol was added to solubilize the hydrochloride salt precipitate and the reaction was diluted with 2-MeTHF, washed twice with a saturated aqueous solution of ammonium chloride, dried over sodium sulfate, filtered, and concentrated by rotary evaporation. Crude samples were then dried under vacuum and analyzed by NMR and GPC as described above. The entire distribution of oligomeric and polymeric chains were isolated in this manner along with non-volatile catalyst-derived impurities, leading to super-quantitative isolated yields in all cases. Aliquots of the unfractionated polymers were further purified by precipitation from diethyl ether or flash chromatography as indicated to remove catalyst-derived impurities. Purified polymers were used for DSC analysis, degradation experiments, cross-linking and subsequent mechanical testing, as well as *in vitro* experiments described in Chapter 4.

5.3.2 Polymer Synthesis and Characterization

Poly(methyl α-D-galactopyranoside sebacate) (poly(αOMeGal sebacate)) Starting material

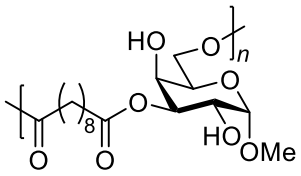

was recrystallized from hot isopropanol and polymerized according to the general procedure. The unfractionated polymer was isolated as a clear, brittle solid (M_n = 2.5 × 10^3 g/mol; Đ = 2.0). 120.3 mg of the unfractionated polymer was purified *via* precipitation from diethyl ether, yielding 113.3 mg (94%). ^{1}H NMR (500 MHz, DMSO-d_6) δ 5.10 (d, J = 5.6 Hz, 1H, OH-2), 4.90–4.83 (m, 1H, OH-4), 4.76 (dd, J = 10.6, 3.2 Hz, 1H, H-3), 4.63 (d, J = 3.7 Hz, 1H, H-1), 4.18–4.01 (m, 2H, H-6), 3.89–3.77 (m, 3H, H-2, H-4, H-5), 3.28 (s, 3H, OCH_3), 2.29–1.98 (m, 4H, $COCH_2$), 1.51 (p, J = 9.7, 8.9 Hz, 4H, $COCH_2CH_2$), 1.33–1.16 (m, 8H, CH_2) ppm. ^{13}C NMR (126 MHz, DMSO-d_6) δ 174.51 (CO), 174.35 (CO), 172.79 (CO), 99.88 (C-1), 72.65 (C-3), 72.60 (C-5), 67.88 (C-2), 66.33 (C-4), 65.22 (C-6), 63.42 (C-6), 54.53 (CH_3), 54.47 (CH_3)

(CO*C*H$_2$), 33.65 (CO*C*H$_2$), 33.47 (CO*C*H$_2$), 28.65 (COCH$_2$*C*H$_2$), 28.45 (COCH$_2$*C*H$_2$), 24.46 (CH$_2$), 24.36 (CH$_2$) ppm. IR (powder, cm^{-1}) 3458 (bm), 2930 (m), 2855 (w), 1731 (s), 1145 (s), 1047 (s), 772 (m).

Poly(methyl β-D-galactopyranoside sebacate) (poly(βOMeGal sebacate)) Starting material

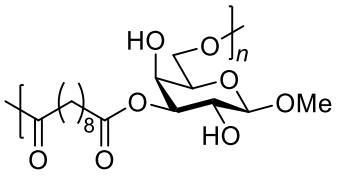

was recrystallized from hot ethanol and polymerized according to the general procedure. The unfractionated polymer was isolated as a light yellow, brittle solid (M_n = 8.1 × 10^3 g/mol; Đ = 2.6). 150.0 mg of the unfractionated polymer was purified *via* precipitation from diethyl ether to yield 146.8 mg (98%). ^{1}H NMR (500 MHz, DMSO-d_6) δ 5.23 (d, *J* = 5.2 Hz, 1H, OH-2), 5.07 (d, *J* = 5.9 Hz, 1H, OH-4), 4.56 (dd, *J* = 10.1, 3.2 Hz, 1H, H-3), 4.26–4.10 (m, 2H, H-1, H-6), 4.05 (dd, *J* = 11.2, 4.8 Hz, 1H, H-6), 3.83–3.76 (m, 1H, H-4), 3.71 (t, *J* = 6.3 Hz, 1H, H-5), 3.51 (ddd, *J* = 9.8, 7.7, 4.7 Hz, 1H, H-2), 3.38 (s, 3H, OCH$_3$), 2.29 (dt, *J* = 13.8, 7.3 Hz, 4H, COCH$_2$), 1.62–1.44 (m, 4H, COCH$_2$C*H$_2$*), 1.32–1.19 (m, 8H, CH$_2$) ppm. ^{13}C NMR (126 MHz, DMSO-d_6) δ 172.87 (CO), 172.85 (CO), 172.82 (CO), 104.06 (C-1), 75.62 (C-3), 71.84 (C-5), 67.50 (C-4), 67.45 (C-2), 65.78 (C-6), 63.10 (C-6), 55.89 (CH$_3$), 33.69 (CO*C*H$_2$), 33.53 (CO*C*H$_2$), 28.69 (COCH$_2$*C*H$_2$), 28.54 (COCH$_2$*C*H$_2$), 24.58 (CH$_2$), 24.43 (CH$_2$) ppm. IR (powder, cm^{-1}) 3457 (bm), 2923 (m), 1729 (s), 1129 (s), 1034 (s).

Poly(ethyl α-D-galactopyranoside sebacate) (poly(αOEtGal sebacate)) The unfractionated

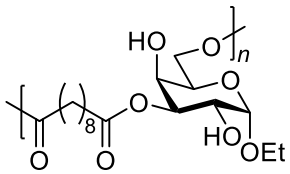

polymer was isolated as an off-white glass (M_n = 5.8 × 10^3 g/mol; Đ = 2.9). 200.0 mg of the unfractionated polymer was purified *via* precipitation from diethyl ether to yield 174.3 mg (87%). ^{1}H NMR (500 MHz, DMSO-d_6) δ 5.08 (d, *J* = 5.6 Hz, 1H, OH-2), 4.83–4.71 (m, 3H, H-1, H-3, OH-4), 4.16–4.03 (m, 2H, H-2, H-6), 3.91–3.79 (m, 3H, H-4, H-5, H-6), 3.68–3.57 (m, 1H, OC*H$_2$*CH$_3$), 3.50–3.41 (m, 1H, OC*H$_2$*CH$_3$)), 2.34–2.23 (m, 4H, COCH$_2$), 1.58–1.46 (m, 4H, COCH$_2$C*H$_2$*), 1.31–1.22 (m, 8H, CH$_2$), 1.16 (t, *J* = 7.0 Hz, 3H, CH$_3$) ppm. ^{13}C NMR (126 MHz, DMSO-d_6) δ 173.24 (CO), 173.11 (CO), 173.08 (CO), 98.96 (C-1), 98.92 (C-1), 72.90 (C-3), 72.87 (C-5), 68.18 (C-2), 66.64 (C-4), 65.42 (OCH$_2$), 63.70 (C-6), 63.07 (C-6), 33.86 (CO*C*H$_2$), 33.72 (CO*C*H$_2$), 28.77 (COCH$_2$*C*H$_2$), 28.66 (COCH$_2$*C*H$_2$), 24.66 (CH$_2$), 24.57 (CH$_2$), 15.23

(CH_3) ppm. IR (powder, cm^{-1}) 3458 (bw), 2931 (m), 1737 (s), 1366 (m), 1217 (m), 1147 (m), 1032 (m), 878 (w), 766 (w).

Poly(ethyl β-D-galactopyranoside sebacate) (poly(βOEtGal sebacate)) The unfractionated polymer was isolated as a clear glass (M_n = 6.1 × 10^3 g/mol; Đ = 3.0). 144.6 mg of the unfractionated polymer were purified *via* precipitation from diethyl ether to yield 136.6 mg (95%). ^{1}H NMR (500 MHz, DMSO-d_6) δ 5.18 (app dd, *J* = 5.4, 2.2 Hz, 1H, OH-2), 5.05 (d, *J* = 5.9, 1H, OH-4), 4.55 (dd, *J* = 10.1, 3.2 Hz, 1H, H-3), 4.23 (d, *J* = 7.7 Hz, 1H, H-1), 4.17 (dd, *J* = 11.3, 7.6 Hz, 1H, H-6), 4.04 (dd, *J* = 11.3, 4.7 Hz, 1H, H-6), 3.81–3.67 (m, 3H, H-4, H-5, OCH_2), 3.57–3.45 (m, 2H, H-2, OCH_2), 2.37–2.21 (m, 4H, $COCH_2$), 1.61–1.43 (m, 4H, $COCH_2CH_2$), 1.34–1.18 (m, 8H, CH_2), 1.14 (t, *J* = 7.0 Hz, 3H, CH_3) ppm. ^{13}C NMR (126 MHz, DMSO-d_6) δ 172.77 (CO), 102.87 (C-1), 75.68 (C-3), 71.75 (C-5), 67.46 (C-4), 65.76 (C-2), 64.10 (OCH_2), 63.11 (C-6), 33.65 ($COCH_2$), 33.49 ($COCH_2$), 28.66 ($COCH_2CH_2$), 28.47 ($COCH_2CH_2$), 24.53 (CH_2), 24.40 (CH_2), 15.22 (CH_3) ppm. IR (thin film, cm^{-1}) 3462 (bm), 2928 (m), 1730 (s), 1163 (m), 1128 (m), 1028 (s), 776 (w).

Poly(*n*-octyl α-D-galactopyranoside sebacate) (poly(αO*n*-OctGal sebacate)) The unfractionated polymer was isolated as a clear glass (M_n = 4.0 × 10^3 g/mol; Đ = 2.9). 102.5 mg of the unfractionated polymer were purified *via* precipitation from diethyl ether yielding 44.0 mg (43%). ^{1}H NMR (500 MHz, DMSO-d_6) δ 5.15–5.02 (m, 1H, OH-2), 4.81–4.67 (m, 3H, H-1, H-3, OH-4), 4.09 (qd, *J* = 11.3, 5.7 Hz, 2H, H-2, H-6), 3.92–3.78 (m, 3H, H-4, H-5, H-6), 3.62–3.50 (m, 1H, OCH_2), 3.41–3.31 (m, 1H, OCH_2), 2.37–2.20 (m, 4H, $COCH_2$), 1.63–1.41 (m, 6H, OCH_2CH_2, $COCH_2CH_2$), 1.39–1.11 (m, 18H, CH_2), 0.85 (t, *J* = 6.9 Hz, 3H, CH_3) ppm. ^{13}C NMR (126 MHz, DMSO-d_6) δ 172.81 (CO), 172.58 (CO), 98.83 (C-1), 72.69 (C-3), 68.05 (C-5), 67.31 (C-4), 66.42 (C-2), 65.20 (OCH_2), 63.65 (C-6), 33.65 ($COCH_2$), 33.56 ($COCH_2$), 31.33 ($OCH_2CH_2CH_2CH_2CH_2$), 29.14 (OCH_2CH_2), 28.86 ($OCH_2CH_2CH_2$), 28.81 ($OCH_2CH_2CH_2CH_2$), 28.69 ($COCH_2CH_2$), 28.52 ($COCH_2CH_2$), 25.83 ($COCH_2CH_2CH_2CH_2$), 24.50 ($COCH_2CH_2CH_2$),

24.37 ($COCH_2CH_2CH_2$), 22.16 (CH_2CH_3), 13.95 (CH_3) ppm. IR (thin film, cm^{-1}) 3440 (bw), 2924 (m), 2854 (w), 1730 (s), 1466 (w), 1353 (w), 1149 (s), 1032 (s), 879 (w), 779 (w), 723 (w).

Poly(*n*-octyl β-D-galactopyranoside sebacate) (poly(βO*n*-OctGal sebacate)) The

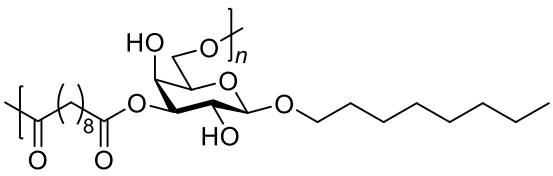

unfractionated polymer was isolated as a light yellow powder (M_n = 4.5 × 10^3 g/mol; Đ = 2.1). 203.1 mg of the unfractionated polymer were purified *via* precipitation from diethyl ether yielding 75.1 mg (37%). ^{1}H NMR (500 MHz, DMSO-d_6) δ 5.14 (app t, J = 4.8 Hz, 1H, OH-2), 5.04 (d, J = 6.0 Hz, 1H, OH-4), 4.55 (dd, J = 9.2, 2.1 Hz, 1H, H-3), 4.25–4.13 (m, 2H, H-1, H-6), 4.03 (dd, J = 11.2, 4.7 Hz, 1H, H-6), 3.82–3.73 (m, 1H, H-4), 3.73–3.65 (m, 2H, H-2, OCH_2), 3.54–3.41 (m, 2H, H-5, OCH_2), 2.39–1.98 (m, 4H, $COCH_2$), 1.65–1.43 (m, 6H, OCH_2CH_2, $COCH_2CH_2$), 1.36–1.15 (m, 18H, CH_2), 0.85 (t, J = 6.8 Hz, 3H, CH_3) ppm. ^{13}C NMR (126 MHz, DMSO-d_6) δ 172.69 (CO), 172.63 (CO), 103.08 (C-1), 75.65 (C-3), 71.75 (C-5), 68.75 (C-4), 67.43 (C-2), 65.76 (OCH_2), 63.13 (C-6), 33.62 ($COCH_2$), 33.50 ($COCH_2$), 31.30 ($CH_2CH_2CH_3$), 29.33 (OCH_2CH_2), 28.85 ($OCH_2CH_2CH_2$), 28.75 ($OCH_2CH_2CH_2CH_2$), 28.65 ($COCH_2CH_2$), 28.48 ($COCH_2CH_2$), 25.51 ($CH_2CH_2CH_2CH_3$), 24.52 ($COCH_2CH_2CH_2CH_2$), 24.37 ($COCH_2CH_2CH_2CH_2$), 22.14 (CH_2CH_3), 13.96 (CH_3) ppm. IR (powder, cm^{-1}) 3447 (bw), 2923 (m), 2853 (m), 1727 (s), 1366 (m), 1217 (s), 1164 (s), 1164 (s), 1129 (s), 1034 (s), 783 (w), 702 (w).

Poly(*i*-octyl α-D-galactopyranoside sebacate) (poly(αO*i*-OctGal sebacate)) The

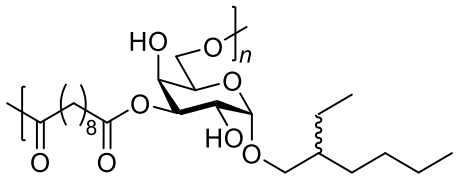

unfractionated polymer was isolated as an off-white resin (M_n = 3.5 × 10^3 g/mol; Đ = 2.3). 205.0 mg of the unfractionated polymer was purified *via* flash column chromatography to yield 100.5 mg (49%). ^{1}H NMR (500 MHz, DMSO-d_6) δ 5.15–5.01 (app t, J = 4.9 Hz, 1H, OH-2), 4.80–4.66 (m, 3H, H-1, H-3, OH-4), 4.19–4.02 (m, 2H, H-2, H-6), 3.93–3.77 (m, 3H, H-4, H-5, H-6), 3.54–3.43 (m, 1H, OCH_2), 3.22 (ddd, J = 17.5, 8.3, 4.8 Hz, 1H, OCH_2), 2.39–1.97 (m, 4H, $COCH_2$), 1.61–1.11 (m, 21H, CH_2), 0.85 (m, 6H, CH_3) ppm. ^{13}C NMR (126 MHz, DMSO-d_6) δ 172.87 (CO), 172.67 (CO), 172.61 (CO), 99.04 (C-1), 98.90 (C-1), 72.85 (C-3), 72.78 (C-5), 68.13 (C-2), 66.42 (C-4), 65.22

(OCH_2), 63.73 (C-6), 38.84 (OCH_2CH), 35.16 (OCH_2CH), 33.64 ($COCH_2$), 33.60 ($COCH_2$), 30.07 ($CH_2CH_2CH_2CH_3$), 29.93 ($CH_2CH_2CH_2CH_3$), 28.73 (OCH_2CH_2), 28.54 ($CH_2CH_2CH_2CH_3$), 25.15 ($COCH_2CH_2CH_2CH_2$), 24.53 ($COCH_2CH_2CH_2CH_2$), 24.36 ($COCH_2CH_2CH_2CH_2$), 23.44 ($OCH_2CH(CH_2CH_3)$), 23.32 ($OCH_2CH(CH_2CH_3)$), 22.64 ($CH_2CH_2CH_2CH_3$), 22.60 ($CH_2CH_2CH_2CH_3$), 13.97 ($CH_2CH_2CH_3$), 11.00 ($OCH_2CH(CH_2CH_3)$), 10.73 ($OCH_2CH(CH_2CH_3)$) ppm. IR (thin film, cm^{-1}) 3459 (bw), 2925 (m), 2857 (m), 1728 (s), 1461 (w), 1151 (s), 1041 (s), 777 (w), 702 (w).

Poly(*i*-octyl β-D-galactopyranoside sebacate) (poly(βO*i*-OctGal sebacate)) The

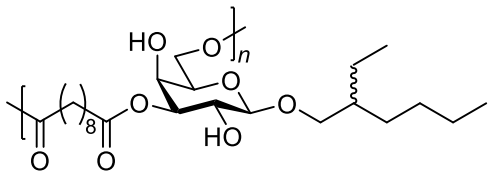

unfractionated polymer was isolated as an off-white resin (M_n = 2.9 × 10^3 g/mol; Đ = 2.4). 210.3 mg of the unfractionated polymer was purified *via* flash column chromatography to yield 85.7 mg (41%). ^{1}H NMR (500 MHz, DMSO-d_6) δ 5.13 (app t, J = 5.5 Hz, 1H, OH-2), 5.08–5.01 (m, 1H, OH-4), 4.55 (dd, J = 9.9, 3.1 Hz, 1H, H-3), 4.26–4.14 (m, 2H, H-1, H-6), 4.03 (dd, J = 11.4, 4.4 Hz, 1H, H-6), 3.77 (m, 1H, H-4), 3.69 (dt, J = 9.1, 4.4 Hz, 1H, H-2), 3.60 (dd, J = 10.3, 6.4 Hz, 1H, H-5), 3.55–3.47 (m, 1H, OCH_2), 3.34–3.25 (m, 1H, OCH_2), 2.39–1.97 (m, 4H, $COCH_2$), 1.63–1.12 (m, 21H, CH_2), 0.84 (t, J = 19.0 Hz, 6H, CH_3) ppm. ^{13}C NMR (126 MHz, DMSO-d_6) δ 172.71 (CO), 103.30 (C-1), 75.73 (C-3), 71.80 (C-5), 71.38 (C-2), 71.25 (C-2), 67.45 (OCH_2), 65.81 (OCH_2), 63.15 (C-6), 39.02 (OCH_2CH), 33.66 ($COCH_2$), 33.55 ($COCH_2$), 29.76 ($CH_2CH_2CH_2CH_3$), 28.68 (OCH_2CH_2), 28.50 ($CH_2CH_2CH_2CH_3$), 24.55 ($COCH_2CH_2CH_2CH_2$), 24.40 ($COCH_2CH_2CH_2CH_2$), 23.12 ($OCH_2CH(CH_2CH_3)$), 23.02 ($OCH_2CH(CH_2CH_3)$), 22.62 ($CH_2CH_2CH_2CH_3$), 14.02 ($CH_2CH_2CH_3$), 10.82 ($OCH_2CH(CH_2CH_3)$), 10.72 ($OCH_2CH(CH_2CH_3)$) ppm. IR (thin film, cm^{-1}) 3457 (bw), 2928 (m), 2857 (m), 1729 (s), 1463 (w), 1376 (m), 1164 (s), 1128 (s), 1072 (s), 1033 (s), 776 (w), 702 (w).

Poly(methyl β-D-galactopyranoside dodecanoate) (poly(βOMeGal dodecanoate)) Starting

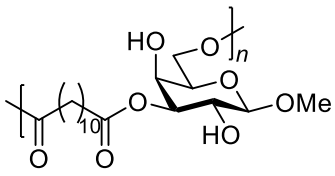

material was recrystallized from ethanol and polymerized according to the general procedure. The unfractionated polymer was isolated as an off-white powder (M_n = 5.4 × 10^3 g/mol; Đ = 2.3). 156.2 mg of the unfractionated polymer was purified *via* precipitation from

diethyl ether yielding 151.2 mg (97%). ^{1}H NMR (500 MHz, DMSO-d_6) δ 5.06 (d, J = 5.9 Hz, 1H, OH-2), 4.56 (d, J = 10.1 Hz, 1H, OH-4), 4.20–4.11 (m, 2H, H-3, H-1), 4.06 (dd, J = 11.2, 4.9 Hz, 1H, H-6), 3.78 (dd, J = 6.3, 3.5 Hz, 1H, H-6), 3.74–3.68 (m, 1H, H-4), 3.51 (ddd, J = 10.1, 7.7, 5.2 Hz, 1H, H-2), 3.38 (s, 3H, CH_3), 2.30 (dt, J = 11.7, 7.3 Hz, 4H, $COCH_2$), 1.51 (q, J = 7.0 Hz, 4H, $COCH_2C\mathit{H_2}$), 1.37–1.14 (m, 12H, CH_2) ppm. ^{13}C NMR (126 MHz, DMSO-d_6) δ 172.75 (CO), 104.03 (C-1), 75.57 (C-3), 71.78 (C-5), 67.43 (C-2), 67.38 (C-4), 63.03 (C-6), 55.91 (CH_3), 55.83 (CH_3), 33.63 ($CO\mathit{C}H_2$), 28.94 ($OCH_2\mathit{C}H_2$), 28.91 ($OCH_2\mathit{C}H_2$), 28.83 ($OCH_2CH_2\mathit{C}H_2$), 28.78 ($OCH_2CH_2\mathit{C}H_2$), 28.55 ($OCH_2CH_2CH_2\mathit{C}H_2$), 28.49 ($OCH_2CH_2CH_2\mathit{C}H_2$), 24.41 ($OCH_2CH_2CH_2CH_2\mathit{C}H_2$) ppm. IR (powder, cm^{-1}) 3465 (bw), 2924 (w), 1738 (s), 1366 (m), 1229 (m), 1217 (m), 1035 (w), 777 (w).

Poly(methyl β-D-galactopyranoside adipate) (poly(βOMeGal adipate)) Starting material was recrystallized from ethanol and polymerized according to the general procedure. The unfractionated polymer was isolated as a reddish powder (M_n = 1.9 × 10^3 g/mol; Đ = 3.8). 100.0 mg of the unfractionated polymer was purified *via* precipitation from diethyl ether yielding 98.5 mg (99%). ^{1}H NMR (500 MHz, DMSO-d_6) δ 5.31–5.17 (m, 1H, OH-2), 5.13–5.06 (m, 1H, OH-4), 4.56 (dd, J = 10.1, 3.3 Hz, 1H, H-3), 4.25–4.12 (m, 2H, H-1, H-6), 4.10–4.01 (m, 1H, H-6), 3.83–3.76 (m, 1H, H-4), 3.75–3.68 (m, 1H, H-5), 3.57–3.47 (m, 1H, H-2), 3.37 (s, 3H, CH_3), 2.41–2.23 (m, 4H, $COCH_2$), 1.70–1.44 (m, 4H, $COCH_2C\mathit{H_2}$) ppm. ^{13}C NMR (126 MHz, DMSO-d_6) δ 172.62 (CO), 103.93 (C-1), 75.64 (C-3), 71.79 (C-5), 67.40 (C-2), 65.72 (C-4), 63.20 (C-6), 55.92 (CH_3), 33.26 ($CO\mathit{C}H_2$), 33.09 ($CO\mathit{C}H_2$), 23.88 ($COCH_2\mathit{C}H_2$), 23.80 ($COCH_2\mathit{C}H_2$), 23.75 ($COCH_2\mathit{C}H_2$) ppm. IR (powder, cm^{-1}) 3469 (bw), 2971 (w), 1737 (s), 1366 (m), 1217 (s), 1130 (s), 1068 (s), 1032 (s), 767 (w), 704 (w).

Poly(methyl β-D-galactopyranoside isophthalate) (poly(βOMeGal isophthalate)) Starting material was recrystallized from ethanol and polymerized according to the general procedure. The unfractionated polymer was isolated as an off-white powder (M_n = 3.8 × 10^3 g/mol; Đ = 1.9). 102.0 mg of the unfractionated polymer was purified *via* precipitation from diethyl ether yielding 99.7 mg (98%). ^{1}H NMR (500 MHz, DMSO-d_6) δ 8.77–

8.45 (m, 1H, Ar*H*), 8.41–8.07 (m, 2H, Ar*H*), 7.70 (dt, *J* = 41.2, 7.8 Hz, 1H, Ar*H*), 5.47 (d, *J* = 40.3 Hz, 2H, OH-2, OH-4), 5.09–4.86 (m, 1H, H-3), 4.66–4.24 (m, 3H, H-1, H-6), 4.19–3.98 (m, 2H, H-4, H-5), 3.77 (m, 1H, H-2), 3.37 (s, 3H, CH_3) ppm. ^{13}C NMR (126 MHz, DMSO-d_6) δ 165.07 (CO), 164.89 (CO), 133.77 (CH), 130.79 (CH), 130.33 (CH), 130.18 (CH), 104.06 (C-1), 77.09 (C-5), 71.88 (C-3), 67.77 (C-2), 65.91 (C-4), 64.35 (C-6), 64.25 (C-6), 56.10 (CH_3) ppm. IR (powder, cm^{-1}) 3424 (bm), 1715 (s), 1230 (m), 1231 (s), 1132 (m), 1068 (s), 727 (m).

Poly(methyl α-D-mannopyranoside sebacate) (poly(αOMeMan sebacate)) Starting material

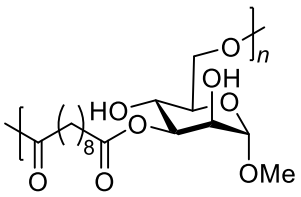

was recrystallized from hot ethanol and polymerized according to the general procedure using 10 mol% **1.01**. The unfractionated polymer had a highly heterogeneous texture and a portion of the product was lost due to insolubility, resulting in 1.07 g of a yellow, brittle glass (85%, M_n = 5.0 × 10^3 g/mol; Đ = 6.3). 231.7 mg of the crude polymer was purified *via* precipitation from diethyl ether yielding 205.6 mg (89%). ^{1}H NMR (500 MHz, DMSO-d_6) δ 5.21 (d, *J* = 6.4 Hz, 1H, OH-4), 5.16 (d, *J* = 5.2 Hz, 1H, OH-2), 4.73 (dd, *J* = 9.6, 3.2 Hz, 1H, H-3), 4.51 (d, *J* = 1.8 Hz, 1H, H-1), 4.31 (dd, *J* = 11.7, 1.9 Hz, 1H, H-6), 4.08 (dd, *J* = 11.7, 6.8 Hz, 1H, H-6), 3.76 (dt, *J* = 4.9, 2.7 Hz, 1H, H-2), 3.64 (td, *J* = 9.7, 6.1 Hz, 1H, H-4), 3.57 (ddd, *J* = 9.6, 6.8, 1.9 Hz, 1H, H-5), 3.26 (s, 3H, CH_3), 2.30 (t, *J* = 7.4 Hz, 4H, OCH_2), 1.52 (p, *J* = 7.0 Hz, 4H, $OCH_2C\mathit{H_2}$), 1.34–1.19 (m, 8H, CH_2). ^{13}C NMR (126 MHz, DMSO-d_6) δ 173.26 (CO), 173.11 (CO), 101.22 (C-1), 74.38 (C-3), 71.23 (C-5), 67.89 (C-2), 64.28 (C-4), 63.83 (C-6), 54.45 (CH_3), 34.10 ($COCH_2$), 33.93 ($COCH_2$), 29.07 ($COCH_2CH_2$), 28.88 ($COCH_2CH_2$), 24.90 (CH_2), 24.81 (CH_2) ppm. IR (powder, cm^{-1}) 3457 (bm), 2930 (m), 1737 (s), 1365 (m), 1130 (s), 1055 (s), 970 (m).

Poly(ethyl α-D-mannopyranoside sebacate) (poly(αOEtMan sebacate)) The unfractionated

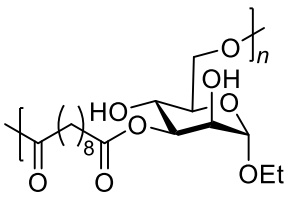

polymer was isolated as a clear, brittle glass (M_n = 5.1 × 10^3 g/mol; Đ = 2.5). 150.4 mg of the unfractionated polymer was purified *via* precipitation from diethyl ether yielding 136.0 mg (90%). ^{1}H NMR (500 MHz, DMSO-d_6) δ 5.20 (d, *J* = 4.9 Hz, 1H, OH-4), 5.14 (d, *J* = 5.1 Hz, 1H, OH-2), 4.83–4.72 (m, 1H, H-3), 4.62 (d, *J* = 1.7 Hz, 1H, H-1), 4.30 (app d, *J* = 11.6 Hz, 1H, H-6), 4.07 (dd, *J* = 11.7, 5.7 Hz, 1H, H-6), 3.80–3.72 (m, 1H, H-2), 3.69–3.57 (m, 3H, H-4, H-5,

OCH_2), 3.50–3.39 (m, 1H, OCH_2), 2.30 (q, *J* = 7.5 Hz, 4H, $COCH_2$), 1.52 (q, *J* = 6.4 Hz, 4H, $COCH_2CH_2$), 1.35–1.20 (m, 8H, CH_2), 1.15 (t, *J* = 7.0 Hz, 3H, CH_3) ppm. ^{13}C NMR (126 MHz, DMSO-d_6) δ 172.81 (CO), 172.72 (CO), 99.59 (C-1), 74.05 (C-3), 73.99 (C-5), 70.87 (C-2), 67.72 (C-4), 64.01 (OCH_2), 63.49 (C-6), 33.70 ($COCH_2$), 33.54 ($COCH_2$), 28.66 ($COCH_2CH_2$), 28.47 ($COCH_2CH_2$), 24.49 (CH_2), 24.42 (CH_2), 15.01 (CH_3), 14.95 (CH_3) ppm. IR (powder, cm^{-1}) 3443 (bw), 2929 (m), 2860 (w), 1714 (s), 1171 (m), 1136 (m), 1093 (m), 1052 (s), 975 (m), 890 (w), 800 (w).

Poly(*n*-octyl α-D-mannopyranoside sebacate) (poly(αO*n*-OctMan sebacate)) The

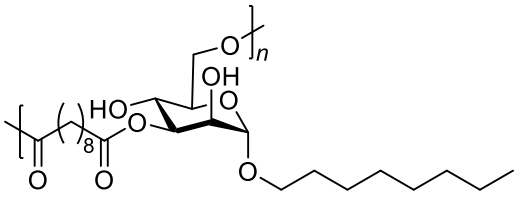

unfractionated polymer was isolated as a clear, rubbery solid (M_n = 1.5 × 10^4 g/mol; Đ = 3.3). 246.6 mg of the unfractionated polymer was purified *via* precipitation from cold diethyl ether yielding 219.7 mg (89%). ^{1}H NMR (500 MHz, DMSO-d_6) δ 5.22 (d, *J* = 4.7 Hz, 1H, OH-4), 5.13 (d, *J* = 4.4 Hz, 1H, OH-2), 4.78–4.71 (m, 1H, H-3), 4.59 (app s, 1H, H-1), 4.31 (d, *J* = 11.7 Hz, 1H, H-6), 4.06 (dd, *J* = 10.9, 5.4 Hz, 1H, H-6), 3.77–3.74 (m, 1H, H-2), 3.66–3.58 (m, 2H, H-4, H-5), 3.59–3.52 (m, 1H, OCH_2), 3.38–3.31 (m, 1H, OCH_2), 2.36–1.99 (m, 4H, $COCH_2$), 1.59–1.45 (m, 6H, CH_2), 1.34–1.17 (m, 18H, CH_2), 0.85 (t, *J* = 6.6 Hz, 3H, CH_3) ppm. ^{13}C NMR (126 MHz, DMSO-d_6) δ 172.61 (CO), 99.73 (C-1), 74.02 (C-3), 70.93 (C-5), 67.68 (C-2), 66.64 (C-4), 64.02 (OCH_2), 63.63 (C-6), 63.58 (C-6), 33.66 ($COCH_2$), 33.58 ($COCH_2$), 31.29 ($OCH_2CH_2CH_2CH_2CH_2$), 28.96 (OCH_2CH_2), 28.77 ($OCH_2CH_2CH_2$), 28.74 ($OCH_2CH_2CH_2$), 28.67 ($OCH_2CH_2CH_2CH_2$), 28.53 ($COCH_2CH_2$), 28.47 ($COCH_2CH_2$), 25.73 ($COCH_2CH_2CH_2$), 24.50 ($COCH_2CH_2CH_2$), 24.40 ($COCH_2CH_2CH_2$), 22.12 (CH_2CH_3), 13.94 (CH_3) ppm. IR (thin film, cm^{-1}) 3457 (bw), 2925 (m), 2855 (w), 1738 (s), 1457 (w), 1366 (m), 1217 (m), 1170 (s), 1129 (s), 1051 (s), 973 (m), 723 (w).

Poly(*i*-octyl α-D-mannopyranoside sebacate) (poly(αO*i*-OctMan sebacate)) The

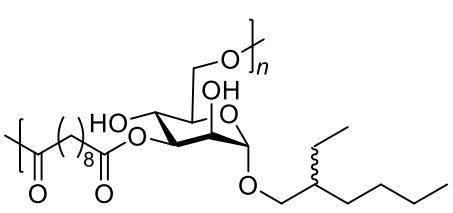

unfractionated polymer was isolated as a light yellow resin (M_n = 3.9 × 10^3 g/mol; Đ = 2.3). 100.0 mg of the unfractionated polymer was purified *via* flash column chromatography yielding 57.8 mg (58%). ^{1}H NMR (500

MHz, DMSO-d_6) δ 5.25 (d, J = 4.7 Hz, 1H, OH-4), 5.15 (d, J = 4.5 Hz, 1H, OH-2), 4.82–4.73 (m, 1H, H-3), 4.58 (app s, 1H, H-1), 4.36–4.27 (m, 1H, H-6), 4.12–4.01 (m, 1H, H-6), 3.82–3.73 (m, 1H, H-2), 3.68–3.56 (m, 2H, H-4, H-5), 3.55–3.45 (m, 1H, OCH_2), 3.28–3.16 (m, 1H, OCH_2), 2.38–1.95 (m, 4H, $COCH_2$), 1.64–1.17 (m, 21H, CH_2), 0.92–0.79 (m, 6H, CH_3) ppm. ^{13}C NMR (126 MHz, DMSO-d_6) δ 172.66 (CO), 100.01 (C-1), 99.87 (C-1), 74.09 (C-3), 74.04 (C-5), 71.09 (C-2), 69.29 ($OCH_2CH(CH_2CH_3)$), 69.11 ($OCH_2CH(CH_2CH_3)$), 67.74 (C-4), 64.06 (C-6), 63.68 (C-6), 38.84 (OCH_2CH), 38.67 (OCH_2CH), 33.65 ($COCH_2$), 33.61 ($COCH_2$), 30.03 ($OCH_2CH(CH_2CH_3)CH_2CH_2CH_2CH_3$), 29.95 ($CH_2CH_2CH_2CH_3$), 28.70, 28.63 ($OCH_2CH_2$), 28.51 ($CH_2CH_2CH_2CH_3$), 28.35 ($OCH_2CH(CH_2CH_3)CH_2CH_2CH_2CH_3$), 25.16 ($COCH_2CH_2CH_2CH_2$), 24.54 ($COCH_2CH_2CH_2CH_2$), 24.42 ($COCH_2CH_2CH_2CH_2$), 23.47 ($OCH_2CH(CH_2CH_3)$), 22.84 ($CH_2CH_2CH_2CH_3$), 13.96 ($CH_2CH_2CH_3$), 11.02 ($OCH_2CH(CH_2CH_3)$), 10.77 ($OCH_2CH(CH_2CH_3)$) ppm. IR (thin film, cm^{-1}) 3450 (bm), 2927 (s), 2858 (m), 1737 (s), 1459 (m), 1366 (m), 1170 (s), 1129 (s), 1053 (s), 976 (m), 645 (w).

5.4 Synthesis and Characterization of End-group Models

5.4.1 General Procedure for Model Synthesis

0.15 or 2 mmol glycoside and 10 mol% **1.02** were loaded into a 2-dram vial equipped with a stir bar and anhydrous solvent was added under argon (0.2 M) followed by 1.5 equivalents DIPEA. The suspension was cooled to 0 °C and 1.1 equivalents butyryl chloride were added dropwise. The reaction was allowed to warm to room temperature and starting material consumption was monitored by TLC. Upon completion, the mixture was quenched with methanol, concentrated *in vacuo*, dissolved in ethyl acetate and washed with distilled water. The aqueous phase was re-extracted twice with ethyl acetate and the combined organic phases were washed with brine. The organic phases were then concentrated and the resulting residue was purified by flash column chromatography on silica gel.

5.4.2 Model Synthesis and Characterization

3-*O*-butanoyl methyl α-D-galactopyranoside (3.02) Compound was prepared from 29.1 mg methyl α-D-galactopyranoside using THF as solvent, yielding 15.1 mg of a clear oil (38%). ^{1}H NMR (500 MHz, DMSO-d_6) δ 4.85 (d, J = 5.7 Hz, 1H, OH-4), 4.80 (d, J = 7.2 Hz, 1H, OH-2), 4.75 (dd, J = 10.6, 3.2 Hz, 1H, H-3), 4.65–4.60 (m, 1H, OH-6), 4.59 (d, J = 3.8 Hz, 1H, H-1), 3.90–3.81 (m, 2H, H-2, H-4), 3.59 (td, J = 6.3, 1.2 Hz, 1H, H-5), 3.55–3.47 (m, 1H, H-6), 3.46–3.42 (m, 1H, H-6), 3.28 (s, 3H, OCH_3), 2.29 (td, J = 7.3, 1.6 Hz, 2H, CO*C*$H_2CH_2CH_3$), 1.55 (h, J = 7.4 Hz, 2H, $COCH_2$*C*H_2CH_3), 0.89 (t, J = 7.4 Hz, 3H, $COCH_2CH_2$*C*H_3) ppm. ^{13}C NMR (126 MHz, DMSO-d_6) δ 172.87 (CO), 100.01 (C-1), 73.25 (C-5), 70.70 (C-3), 66.03 (C-2), 65.51 (C-4), 60.18 (C-6), 54.62 (OCH_3), 35.64 (CO*C*$H_2CH_2CH_3$), 17.96 ($COCH_2$*C*H_2CH_3), 13.56 ($COCH_2CH_2$*C*H_3) ppm. IR (thin film, cm^{-1}) 3440 (bs), 2921 (s), 2857 (m), 1740 (s), 1268 (m), 1196 (s), 1149 (m), 1059 (s), 766 (w). HRMS (DART+, *m/z*): calcd for $C_{11}H_{24}NO_7$ $[M + NH_4]^+$ 282.15583, found 282.15605. $[\alpha]_D^{20}$ = +6.67 (*c* = 0.12, CH_3OH).

3-*O*-butanoyl methyl β-D-galactopyranoside (3.01) Compound was prepared from 389.1 mg methyl α-D-galactopyranoside using CH_3CN as solvent, yielding 68.8 mg of a white solid (13%). ^{1}H NMR (500 MHz, DMSO-d_6) δ 5.17 (d, J = 5.4 Hz, 1H, OH-2), 4.80 (d, J = 5.9 Hz, 1H, OH-4), 4.68–4.60 (m, 1H, OH-6), 4.52 (dd, J = 10.1, 3.3 Hz, 1H, H-3), 4.12 (d, J = 7.7 Hz, 1H, H-1), 3.82 (ddd, J = 6.1, 3.3, 1.0 Hz, 1H, H-4), 3.57–3.38 (m, 4H, H-2, H-5, H-6), 3.37 (s, 3H, OCH_3), 2.30 (td, J = 7.3, 1.2 Hz, 2H, CO*C*$H_2CH_2CH_3$), 1.55 (h, J = 7.4 Hz, 2H, $COCH_2C$*H*$_2CH_3$), 0.89 (t, J = 7.5 Hz, 3H, $COCH_2CH_2C$*H*$_3$) ppm. ^{13}C NMR (126 MHz, DMSO-d_6) δ 172.70 (CO), 104.31 (C-1), 76.12 (C-5), 74.68 (C-3), 67.60 (C-2), 65.28 (C-4), 59.91 (C-6), 55.97 (OCH_3), 35.56 (CO*C*$H_2CH_2CH_3$), 17.94 ($COCH_2$*C*H_2CH_3), 13.52 ($COCH_2CH_2$*C*H_3) ppm. IR (thin film, cm^{-1}) 3402 (bm), 2938 (w), 1723 (m), 1375 (w), 1262 (w), 1189 (m), 1148 (m), 1051 (s), 977 (m), 893 (w), 734 (w). HRMS (DART+, *m/z*): calcd for $C_{11}H_{24}NO_7$ $[M + NH_4]^+$ 282.15583, found 282.15465. $[\alpha]_D^{20}$ = +38.8 (*c* = 0.175, CH_3OH).

3-*O*-butanoyl methyl α-D-mannopyranoside (3.03) Compound was prepared from 29.1 mg

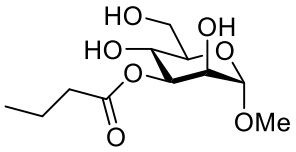

methyl α-D-mannopyranoside using THF as solvent, yielding 26.9 mg of a clear oil (68%). ^{1}H NMR (500 MHz, DMSO-d_6) δ 5.08 (s, 1H, OH-2), 4.98 (d, J = 6.2 Hz, 1H, OH-4), 4.74 (dd, J = 9.8, 3.3 Hz, 1H, H-3), 4.57–4.52 (m, 1H, OH-6), 4.51 (d, J = 1.7 Hz, 1H, H-1), 3.75 (d, J = 1.6 Hz, 1H, H-2), 3.69–3.64 (m, 1H, H-6), 3.61 (td, J = 9.8, 4.7 Hz, 1H, H-4), 3.48 (dt, J = 11.2, 4.8 Hz, 1H, H-6), 3.40–3.37 (m, 1H, H-5), 3.27 (s, 3H, OCH_3), 2.29 (t, J = 7.3 Hz, 2H, $COCH_2CH_2CH_3$), 1.55 (h, J = 7.4 Hz, 2H, $COCH_2CH_2CH_3$), 0.89 (t, J = 7.4 Hz, 3H, $COCH_2CH_2CH_3$) ppm. ^{13}C NMR (126 MHz, DMSO-d_6) δ 172.62 (CO), 100.78 (C-1), 74.33 (C-5), 73.96 (C-3), 67.61 (C-2), 63.83 (C-4), 60.94 (C-6), 54.00 (OCH_3), 35.60 ($COCH_2CH_2CH_3$), 17.92 ($COCH_2CH_2CH_3$), 13.49 ($COCH_2CH_2CH_3$) ppm. IR (thin film, cm^{-1}) 3376 (bm), 2935 (m), 1720 (m), 1454 (w), 1260 (w), 1186 (m), 1132 (s), 1090 (s), 1054 (s), 972 (s), 813 (w), 671 (w). HRMS (DART+, *m/z*): calcd for $C_{11}H_{24}NO_7$ $[M + NH_4]^+$ 282.15583, found 282.15580. $[\alpha]_D^{20}$ = +24.0 (c = 0.11, CH_3OH).

Chapter 4: Studies of the Physical and Biological Properties of Poly(pyranoside ester)s

1 Statement of Contribution

All experiments were carried out by Ekaterina Slavko.

2 Introduction

The practical applicability of bio-based polymers relies significantly on the ability to modulate the physical and biological properties of such macromolecules. Synthetic polymers derived from biomass are emerging as an alternative to naturally occurring biopolymers and embody the next generation of biomaterials, promising superior mechanical properties, processability, and degradability.[5] Exploring novel monomeric systems with diverse spatial configurations and functionalities is thus a key step in further improving the behaviour and performance of future biomaterials. As a monomer class, glycosides represent a particularly intriguing arena for the exploration of structure–property relationships of bio-based building blocks: the impact of variables such as their structural isomerism, stereoisomerism, linkage topology and substitution pattern can be systematically examined and channelled to design functional polymers meeting a desired set of thermal, mechanical, degradation and biocompatibility requirements. In the work described in this chapter, we hoped to outline the characteristics of the unprecedented poly(pyranoside ester)s synthesized in Chapter 3 and to establish how their properties vary with the carbohydrate configuration and the identity of the protecting group at the anomeric position. A brief review of the existing literature surrounding related macromolecules follows.

2.1 Physical Properties of Sugar-derived Polyesters

Tailoring the physical and mechanical properties of polymers to suit specific *in vivo* applications (e.g., orthopedic devices, drug delivery systems, surgical tools, components of micro- and nanoparticles) is a standing challenge.[149] While presenting advantages in terms of renewability

[149] Nair, L. S.; Laurencin, C. T. *Prog. Polym. Sci.* **2007**, *32*, 762–798.

and low toxicity, biodegradable polymers possess physical properties that often fail to replicate those of existing petrochemical commodity polymers. In striving to improve the properties of common biodegradable polymers such as poly(lactic acid) (PLA), many groups have had recourse to techniques such as blending with other polymers, incorporation into composite materials, and surface modification.[150] As mentioned earlier, diversifying the pool of available comonomers and establishing a way to modulate polymer properties based on the chemical composition of these new monomers would obviate the need for such modifications and drive the design of ever more specialized monomers. Anomerically substituted monosaccharides present the interesting quality of having a rigid ring structure with defined stereocenters in effectively immutable spatial orientations. The size of the backbone ring (furanoside or pyranoside) and the relative configurations of its substituents could potentially have a large impact on polymer properties: it is known from studies on oligosaccharides that monosaccharide stereochemistry, anomeric configuration and position and type of glycosidic linkage (topological composition) have profound influences on properties such as taste,[151] biological function,[152] hydrodynamic radius in solution[153] an glass transition temperature.[154]

The incorporation of cyclic sugar-based building blocks into degradable polyesters has been extensively studied from the standpoint of biomedical polymers as well as replacements for non-renewable commodity plastics, with furans and isohexides holding an especially prominent place in terms of their implementation.[155] Of particular interest here are the isohexides[111] briefly

---

[150] Rasal, R. M.; Janorkar, A. V.; Hirt, D. E. *Prog. Polym. Sci.* **2010**, *35*, 338–356.

[151] Birch, G. G.; Shallenberger, R. S. *Crit. Rev. Food Sci. Nutr.* **1976**, *8*, 57–95.

[152] Dwek, R. A. In *Molecular Recognition and Inclusion*; Coleman, A. W., Ed.; Springer, 1998; pp. 1–6.

[153] Boone, M. A.; Nymeyer, H.; Striegel, A. M. *Carbohydr. Res.* **2008**, *343*, 132–138.

[154] Furuki, T. *Carbohydr. Res.* **2002**, *337*, 441–450.

[155] Mahmood, K.; Noreen, A.; Zuber, M.; Tabasum, S. *Int. J. Biol. Macromol.* **2016**, *82*, 1028–1040.

discussed in Chapter 3, section 2.2, *bis*-acetals of sugar alcohols[156,157] and aldaric acids,[158] all bicyclic renewable monomers synthesized from readily available monosaccharides (Figure 4.1). Due to the rigid structure of these monomers, their corresponding polyesters display T_g values significantly higher than those derived from aliphatic diols and even the linear methylated analogs of the corresponding sugar alcohols,[159] consistent with theoretical calculations showing high energy barriers for rotation along the ester bond. This strong elevation in T_g has been harnessed by Muñoz-Guerra *et al.* to prepare isohexide- and *bis*-methylidene alditol-derived terephthalates to replace existing poly(alkylene terephthalate)s of petrochemical origin, with physical properties that matched or exceeded those of the original polyesters.[160] Literature precedent describing copolymers of poly(ethylene terephthalate) containing a range of mannitol-derived *bis*-acetyl comonomer admixtures reveals that the incorporation of cyclic carbohydrate-derived repeat units is responsible for increases in T_g, tensile strength, and elastic modulus.[161]

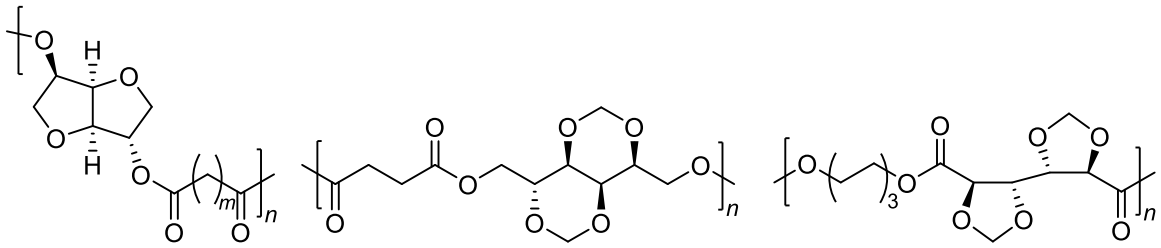

Figure 4.1 Examples of degradable polyesters derived from (a) isosorbide, (b) *bis*-acetyl glucitol and (c) *bis*-acetyl galactaric acid.

---

[156] Zakharova, E.; Alla, A.; Martínez De Ilarduya, A.; Muñoz-Guerra, S. *RSC Adv.* **2015**, *5*, 46395–46404.

[157] Lavilla, C.; Alla, A.; Martínez De Ilarduya, A.; Muñoz-Guerra, S. *Biomacromolecules* **2013**, *14*, 781–793.

[158] Lavilla, C.; Alla, A.; Ilarduya, A. M. De; Benito, E.; Galbis, J. A.; Muñoz-Guerra, S. *Biomacromolecules* **2011**, *12*, 2642–2652.

[159] Wu, J.; Eduard, P.; Thiyagarajan, S.; Jasinska-Walc, L.; Rozanski, A.; Guerra, C. F.; Noordover, B. A. J.; Van Haveren, J.; Van Es, D. S.; Koning, C. E. *Macromolecules* **2012**, *45*, 5069–5080.

[160] Muñoz-Guerra, S.; Lavilla, C.; Japu, C.; Martínez De Ilarduya, A. *Green Chem.* **2014**, *16*, 1716–1739.

[161] Lavilla, C.; Martínez De Ilarduya, A.; Alla, A.; Muñoz-Guerra, S. *Polym. Chem.* **2013**, *4*, 282–289.

Contrary to what one might expect, polyesters made from *bis*-acetyl galactaric acid (Figure 4.1c) exhibit higher T_g values and superior crystallinity than isohexide-derived polyesters that have two fused rings, despite the apparently greater flexibility of the former compared to the latter. Less surprisingly, monomer stereoconfiguration has a strong impact on T_g as it determines spatial orientation of the bicyclic structures in space: the increased strain of the *bis*-acetyl glucitol monomer when compared to the mannitol analog was thought to be implicated in raising the T_g by almost 40 °C.[156] Other factors affecting T_g are the length of the alkyl chain of the aliphatic comonomer, which is inversely proportional to T_g,[162] M_n, which correlates positively with T_g at lower molecular weights, and the topological composition of the monomeric unit.[163] The group of Coates has studied the conformational flexibility of renewable furan-derived polyesters using experimental and computational approaches,[164] revealing that the collective restriction in dihedral rotations along the ester backbone leading to chain stiffness is strongly influenced by the steric effect of methyl substituents on the backbone ring — this represents another source of variation in thermal properties resulting from subtle changes to monomeric structure. A decrease in the degree of crystallinity has been noted with the incorporation of bicyclic sugar-derived monomers,[165] which could be beneficial to the preparation of elastomeric materials from this type of building blocks.

Although significant literature precedent exists concerning bicyclic sugar-derived monomers and their corresponding polymers, it is unclear how this will translate into monocyclic, OH-functional repeat units, as a limited number of studies on the physical properties of such polymers exists. Polycarbonates derived from methylated glucopyranosides[118] and

---

[162] Okada, M.; Okada, Y.; Tao, A.; Aoi, K. *J. Appl. Polym. Sci.* **1996**, *62*, 2257–2265.

[163] Lonnecker, A. T.; Lim, Y. H.; Felder, S. E.; Besset, C. J.; Wooley, K. L. *Macromolecules* **2016**, *49*, 7857–7867.

[164] Yu, X.; Jia, J.; Xu, S.; Lao, K. U.; Sanford, M. J.; Ramakrishnan, R. K.; Nazarenko, S. I.; Hoye, T. R.; Coates, G. W.; DiStasio, R. A. *Nat. Commun.* **2018**, *9*.

[165] Japu, C.; Martínez De Ilarduya, A.; Alla, A.; García-Martín, M. G.; Galbis, J. A.; Muñoz-Guerra, S. *Polym. Chem.* **2014**, *5*, 3190–3202.

isopropylidene-protected xylofuranosides[166] have T_g values significantly higher than those reported for common aliphatic polycarbonates, suggesting that the restriction in chain mobility can be ascribed primarily to the rigid sugar ring structure as opposed to intermolecular attractive forces. In the presence of hydrogen bond-donating OH groups, however, intermolecular forces may start to make a greater contribution to the thermal properties of the resulting materials. Hydrogen bonding patterns of the hydrophilic sugar moiety influences the thermal transitions of liquid crystal mesogens of alkyl glycosides,[167] with axial OH groups raising the temperature at which the liquid crystal transitions to an anisotropic liquid (clearing point). Anomeric configuration also plays a role, with α-configured alkyl chains leading to higher clearing points, but the length and degree of branching of the hydrophobic group has the most dramatic effect on molecular packing and thus thermal transitions.[168] Long-chain alkyl glycosides such as those known to form liquid crystals were included in the scope of our polymerization; the effect, if any, of this type of thermal behaviour in the monomer on the thermal properties of the polymer remains to be seen.

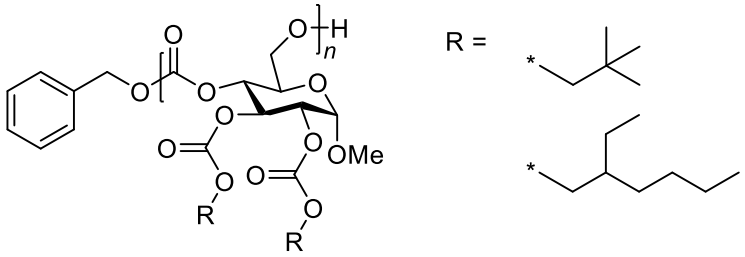

Figure 4.2 Glucopyranoside-derived polycarbonates bearing *tert*-butyl and *i*-octyl side-chains.

Investigations into glucopyranoside-derived polycarbonates have also revealed the effect of pendant alkyl chains on the thermal properties of the polymer. Polycarbonates possessing ester protecting groups with side-chains of varying steric bulk and conformational flexibility have

---

[166] Shen, Y.; Chen, X.; Gross, R. A. *Macromolecules* **1999**, *32*, 2799–2802.

[167] Vill, V.; Hashim, R. *Curr. Opin. Colloid Interface Sci.* **2002**, *7*, 395–409.

[168] Jeffrey, G. *Liq. Cryst.* **1992**, *12*, 179–202.

shown a relationship between their T_g and the nature of the side-chains, with bulky *tert*-butyl groups elevating the T_g (125 °C) and flexible side-chains such as *i*-oct depressing it (38 °C) (Figure 4.2).[130] We theorize that long, flexible anomeric substituents could act as intrinsic plasticizers in increasing free volume, lowering T_g and resulting in lower elastic and storage moduli compared to smaller anomeric groups.

2.2 Degradation Properties of Sugar-derived Polyesters

Degradation rate is an extremely important characteristic of biomedically relevant polymers when considering their target applications: for instance, the release profile of an embedded drug depends strongly on the rate and mechanism of polymeric implant degradation.[5] To give another example, the relatively rapid degradation of PGS has limited its application in regenerative medicine in cases where longer healing times are required (*e.g.*, in muscle tissue). The introduction of a denser network of cross-links would lead to a reduction in degradation rate,[169] but this comes with an undesirable increase in stiffness (see Chapter 2, section 2.1).[170] It is therefore desirable to effect changes in degradation rates through structural modification of the monomer.

Most polyesters degrade *via* surface erosion by virtue of the slow diffusivity of water into the polymer matrix as compared to the rate of ester linkage hydrolysis, meaning that the implant slowly shrinks in size over time. In some cases, bulk erosion accompanied by sudden structural collapse may occur when the rate of water diffusion is fast enough; often, an autocatalytic acceleration of chain cleavage by the degradation products is occurring concomitantly, as is the case with PLA under certain conditions.[171] Rates of polymer swelling in water may thus play a role in the degradation mechanism and behaviour of the polymeric matrix. It is also known that conformational flexibility relates positively to biodegradability, as seen in polymers possessing

---

[169] Bruggeman, J. P.; Bettinger, C. J.; Nijst, C. L. E.; Kohane, D. S.; Langer, R. *Adv. Mater.* **2008**, *20*, 1922–1927.

[170] Li, Y.; Huang, W.; Cook, W. D.; Chen, Q. *Biomed. Mater.* **2013**, *8*, 035006.

[171] von Burkersroda, F.; Schedl, L.; Göpferich, A. *Biomaterials* **2002**, *23*, 4221–4231.

shorter, inflexible linker chains and correspondingly slower biodegradation.[172] At low molecular weights, there is a dependence of degradation rate on M_n, with enzymatic chain cleavage of polymers such as poly(ε-caprolactone) and poly(hexamethylene adipate) becoming independent of molecular weight when $M_n > 4$ kDa.[173] Finally, parameters such as the monomeric composition can have a tremendous impact on biodegradability, with aromatic comonomers, for instance, reducing the rate of biodegradation in bio-derived polyesters.[174]

The literature describing the effect of sugar derivatives on the biodegradation of polymers is divergent. In a series of studies,[165] the group of Muñoz-Guerra demonstrated that the incorporation of ester-linked carbohydrate-derived building blocks to poly(terephthalate ester)s accelerates *in vitro* degradation of the resulting materials, a finding paralleled by the enhanced degradability of poly(butylene succinate) copolyesters doped with mannitol-derived monomers. The authors conjectured that increased lipase-mediated degradation with higher carbohydrate content was related to the lower degree of crystallinity resulting from carbohydrate monomer incorporation.[156] Okada *et al.* have conducted extensive studies into the hydrolytic and enzymatic degradation of isohexide-derived aliphatic and aromatic polyesters, uncovering the dependence of degradation on monomer stereoconfiguration, enzymatic bias toward 8-carbon aliphatic chains over 4- and 10-carbon chains, effects of M_n, and influence on substrate specificity depending on the enzyme used.[184,185]

It is unclear how the presence of pendant OH groups will influence the biodegradation of poly(pyranoside ester)s. Poly(xylitol sebacate) elastomers prepared from a higher-order sugar alcohol than glycerol and possessing a more hydrophilic polyol comonomer and higher OH group content than PGS, despite showing increased swelling under water vapor, degraded more

---

[172] Kopeček, J.; Ulbrich, K. *Prog. Polym. Sci.* **1983**, *9*, 1–58.

[173] Tokiwa, Y.; Suzuki, T.; Takeda, K. *Agric. Biol. Chem.* **1988**, *52*, 1937–1943.

[174] Zumstein, M. T.; Rechsteiner, D.; Roduner, N.; Perz, V.; Ribitsch, D.; Guebitz, G. M.; Kohler, H. P. E.; McNeill, K.; Sander, M. *Environ. Sci. Technol.* **2017**, *51*, 7476–7485.

slowly,[170] prompting the authors to suggest that steric hindrance from the pendant OH groups impeded enzyme approach. In contrast, Okada observed that polycarbonates derived from isohexide dicarbonate and erythritol-derived building blocks were more susceptible to enzymatic cleavage after the removal of the isopropylidene protecting group revealing the two pendant OH groups of the erythritol moiety.[30] Clearly, a complex interplay between hydrophilicity, chain flexibility, spatial orientation and enzyme specificity is responsible for observed polyester degradation rates.

3 Results and Discussion

3.1 Thermal Properties of Poly(pyranoside ester)s

Glass transition temperatures of poly(pyranoside ester)s as determined by DSC are shown in Table 4.1. As expected, T_g values were considerably higher than those found in Chapter 2 for glycerol-derived polyesters, as shown by the lowest T_g in the pyranoside series, –3 °C for poly(αO*i*-OctGal sebacate), which is still significantly higher than that of linear PGS (–34 °C). The rigidity of the backbone pyranoside ring is likely the largest factor contributing to the difference in chain stiffness, as noted in previous reports.[130] Another contribution to T_g elevation may originate from the additional hydrogen bonding capability arising from the two pendant OH groups in the macromolecule: as shown in entries 1 *vs.* 2, 6 *vs.* 7 and 14 *vs.* 15, *O*-peracetyl analogs of the methyl series had T_g values 11–26 °C lower than their native counterparts with unmasked OH groups. Exchanging the comonomer from sebacoyl chloride to adipoyl or isophthaloyl chloride resulted in a rise in T_g due to lower flexibility of the backbone (entries 9 and 10), and even switching to dodecanedioyl chloride slightly increased T_g (entry 8). Although the fact that the dodecanedioyl-derived polyester is glassier than the sebacoyl-derived one may appear counterintuitive as the former possesses a longer, more flexible hydrocarbon chain, this difference in T_g is actually minuscule compared to the 52-degree difference observed when comparing PGS and PGD (see Chapter 2, section 3.4). Comparable non-linear relationships between T_g and hydrocarbon chain length have been reported for isohexide-derived polyesters.[159] Poly(βOMeGal dodecanoate) also exhibited a melting temperature, unlike other polymers in the βOMeGal series, potentially pointing to stronger interactions between the alkyl

domains of the 10-carbon chain. Overall, methyl- and ethyl-substituted monomers gave rise to glassy polymers with T_g values higher than those previously reported for analogous isohexide-derived polyesters but lower than those of glucose-derived polycarbonates.

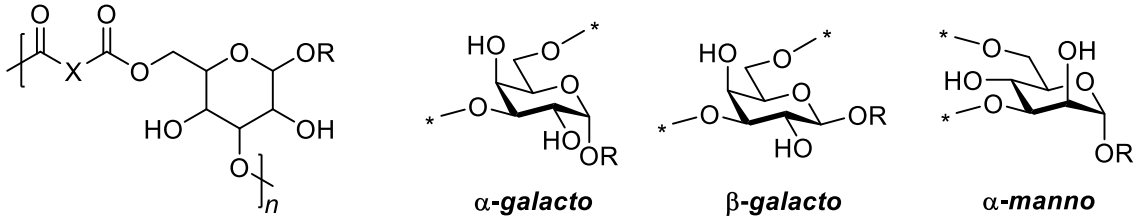

Table 4.1 Glass transition temperatures of carbohydrate-derived polyesters.

Entry	Configuration	R =	X =	M_n*	T_g† (°C)	T_m† (°C)
1	**α-*galacto*-**	Me	$(CH_2)_8$	2.5	37	-
2‡		Me	$(CH_2)_8$	-	14	-
3		Et	$(CH_2)_8$	5.8	45	-
4		*n*-oct	$(CH_2)_8$	4.0	11	-
5		*i*-oct	$(CH_2)_8$	3.5	–3	-
6	**β-*galacto*-**	Me	$(CH_2)_8$	5.3	50	-
7‡		Me	$(CH_2)_8$	-	39	-
8		Me	$(CH_2)_{10}$	5.4	56	78
9		Me	$(CH_2)_4$	1.9	80	-
10		Me	*m*-C_6H_4	3.8	164	-
11		Et	$(CH_2)_8$	6.1	53	-
12		*n*-oct	$(CH_2)_8$	4.5	25	46
13		*i*-oct	$(CH_2)_8$	2.9	17	-
14	**α-*manno*-**	Me	$(CH_2)_8$	5.0	46	-
15‡		Me	$(CH_2)_8$	-	20	-
16		Et	$(CH_2)_8$	5.1	46	-
17		*n*-oct	$(CH_2)_8$	15.1	24	-
18		*i*-oct	$(CH_2)_8$	3.9	16	-

* – molecular weights are expressed in kDa relative to PMMA standards and determined by GPC, NMP, 80 °C. † – determined by DSC using a 10 °C/min heating/cooling rate. ‡ – polymer was analyzed in its peracetylated form.

The softening effect brought about by the flexible anomeric alkyl chains was evident, as seen throughout the *n*-octyl and *i*-octyl series which all had their T_g values around or below room temperature, spanning –3–25 °C (entries 4, 5, 12, 13, 17 and 18). The relatively high-M_n poly(αO*n*-OctMan sebacate) was a soft, highly stretchable rubber when handled at room temperature (23 °C), and aside from poly(βO*n*-OctGal sebacate) which formed a brittle if somewhat waxy powder when dried under high vacuum, the octyl series were all either rubbery or resin-like (see Chapter 3, section 3.5).

β-Galactoside-derived polyesters showed the highest T_g values compared to the other two carbohydrate configurations. This result is not unexpected: compared to the α-galactosides which have axial anomeric groups, the equatorially configured anomeric group of β-galactosides may allow for more compact chain packing, leading to a higher energy barrier for long-chain segmental motion and consequently a lower free volume and higher T_g.[163] This is further supported by the observation that poly(βOMeGal sebacate) experienced the smallest drop in T_g upon peracetylation, presumably in part because hydrogen bonding contributes less to chain stiffness than does the spatial configuration of this monomer. Additionally, poly(βO*n*-OctGal sebacate) was the only semi-crystalline octyl glycoside-derived polyester (Table 4.1 entry 12), further suggesting that β-configured monomers allow for a more ordered polymer morphology. A relationship can thus be established between sugar conformation and T_g of its corresponding polymer (Figure 4.3). It must be noted that this trend is slightly exaggerated in the case of the methyl-substituted series due to the markedly lower M_n for poly(αOMeGal sebacate); the M_n of a polymer is known to strongly influence T_g below the $(T_g)_\infty$.

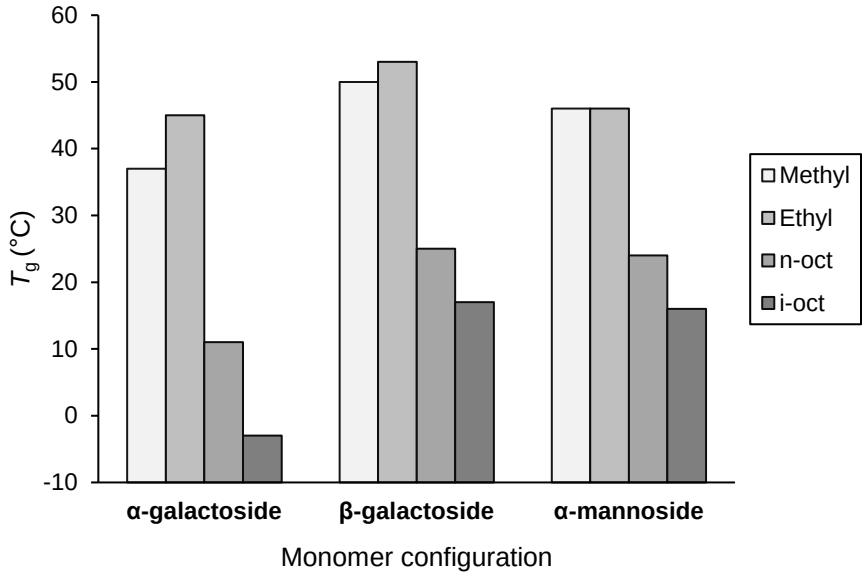

Figure 4.3 Observed T_g values of methyl-, ethyl-, *n*-octyl- and *i*-octyl-glycoside sebacate polyesters derived from monomers having different stereoconfigurations.

There was little difference in the thermal transitions of poly(αOMeMan sebacate) and poly(αOEtMan sebacate), which both showed similar M_n (approximately 5 kDa) and identical T_g values (46 °C), suggesting that the change from methyl to ethyl glycoside does not noticeably increase free volume. In fact, ethyl galactoside-derived polyesters showed slightly higher T_g values than their methyl counterparts (Table 4.1 entries 1 *vs.* 3 and 6 *vs.* 11), though in both cases the T_g gaps show some correspondence with the M_n gaps between the given polymers (the M_n for poly(αOMeGal sebacate) is 3.3 kDa lower than poly(αOEtGal sebacate) with a T_g that is 8 °C lower; the M_n for poly(βOMeGal sebacate) is 0.5 kDa lower than poly(βOEtGal sebacate) with a T_g that is 3 °C lower). Given this dependence on M_n and the small difference in size between the two anomeric substituents, it is unlikely that the slightly elevated T_g values of the ethyl series stem from steric hindrance limiting rotational flexibility of the polymer backbone.

T_g values were similar between polymers with α-manno-configured glycoside repeat units and those with β-galacto-configured repeat units. A rationalization for observing that backbone α-mannopyranosides restrict chain motion more than α-galactopyranosides is not immediately obvious. It may be that the spatial configurations of any these sugars' respective axial OH groups give rise to differing abilities to restrict segmental mobility of the polymer chains through steric

interactions. Performing a theoretical analysis of the conformational flexibility of these macromolecules as a function of monomer stereoconfiguration may shed more light on the origin of the observed T_g differences.[164] In addition, the finding that only two polymers in the series exhibited semicrystallinity in the long-chain carbohydrate domain warrants exploration into the relationship between polymer crystallization and the nature of the diacyl comonomer and anomeric group. It is possible that sebacate-based copolyemers may have displayed melting endotherms if a slower cooling ramp rate had been employed; the crystallization transition of poly(βOMeGal dodecanoate) is likely facilitated by the relatively high mobility of its hydrocarbon domains, and employing even longer-chain comonomers could increase the degree of crystallinity of this system. Structure–property relationships between the nature of the aglycon, anomeric configuration and diacyl length could be examined by comparing degrees of crystallinity in a series of polyesters using calorimetry, polarized microscopy and/or electron microscopy.

3.2 Mechanical Properties of Poly(pyranoside ester)s

3.2.1 Introduction of Urethane Cross-links and Solution Casting

Polyesters derived from methyl- and ethyl-substituted sugars were not ideal candidates for mechanical testing: in their native purified form, they underwent brittle fracture upon manipulation and could not be solution-cast into thin films. It is possible that the relatively low degree of polymerization contributes to this structural weakness, as poly(αO*n*-OctMan sebacate) had the highest M_n in the series and was the only polymer that could be cast into a manageable film in its native form. We surmised that comparing the mechanical properties of the various polymer series could be done after subjecting each polymer to identical cross-linking conditions in hopes of obtaining thermoset thin films amenable to physical manipulation.[175] By introducing similar cross-link densities to each polymer in the series, the effect of the monomer configuration and anomeric side-chain could be evaluated by tensile testing and dynamic mechanical analysis (DMA).

---

[175] Gustini, L.; Noordover, B. A. J.; Gehrels, C.; Dietz, C.; Koning, C. E. *Eur. Polym. J.* **2015**, *67*, 459–475.

To test this hypothesis, we first studied the cross-linking of poly(βOMeGal sebacate) by drawing inspiration from the cross-linking conditions described for PGS in Chapter 2, section 3.6 using 15 mol% HDI as the cross-linking agent and $CHCl_3$ as the solvent at a concentration of 0.5 M. Poly(βOMeGal sebacate) was partially soluble in $CHCl_3$ at room temperature as indicated by the turbidity of the solution phase, but heating the mixture to 80 °C produced a clear solution. After an hour of stirring, an increase in viscosity was noted, and the reaction was transferred to a Teflon mould. However, upon cooling to room temperature, the polymer underwent phase separation from the solvent, forming an uneven film. In addition, the high volatility of $CHCl_3$ caused the rapid evolution of bubbles when the mixture was air-dried, even in a closed system under positive vapour pressure of $CHCl_3$. Increasing the reaction concentration up to 1 M did not improve the outcomes of the solution-casting process. To address the miscibility issue, relatively hydrophilic solvents such as acetonitrile, DMF and 1,4-dioxane were tested under the same conditions. While the solubility of the starting material and evenness of film formation were ameliorated by this modification, the resulting dried films were not noticeably stronger and FTIR spectroscopy indicated little urethane bond formation (Table 4.2). This observation pointed to lower reaction rates in these alternative solvents, so a catalytic route using 1 mol% DMAP in 1,4-dioxane at 0.4 M and 100 °C was chosen.[176] This approach resulted in an even film that could be air-dried without bubble formation and subsequently cured in a vacuum oven to remove traces of residual solvent. Urethane C=O signal evolution as judged by FTIR was proportional to the number of equivalents of HDI used and films formed using 10, 15 and 25 mol% HDI were stiff, yet tougher plastics that could be handled without undergoing brittle fracture.

[176] Tian, D.; Dubois, P.; Jérôme, R. *J. Polym. Sci. Part A Polym. Chem.* **1997**, *35*, 2295–2309.

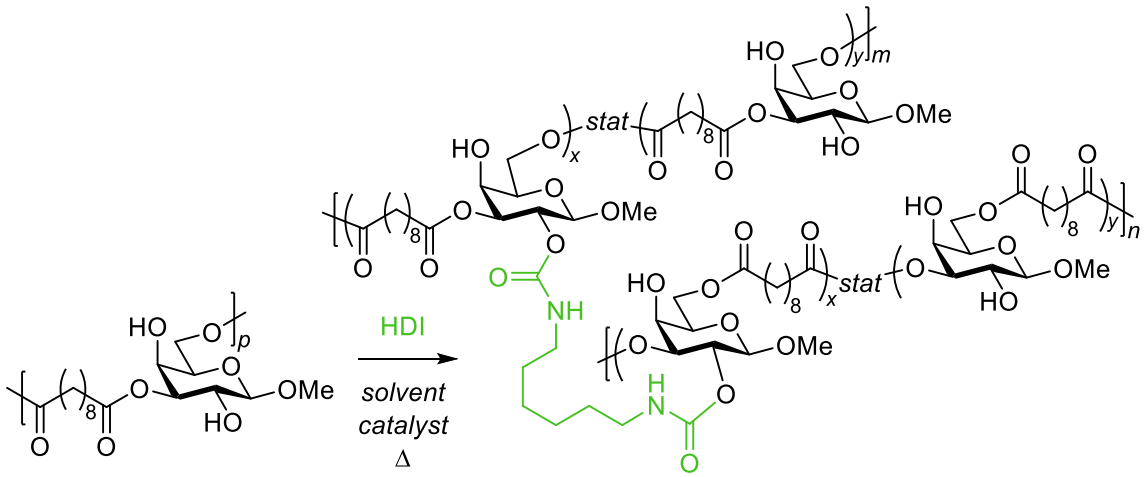

Table 4.2 Optimization of cross-link introduction in poly(βOMeGal sebacate).

Entry	mol% HDI	Concentration (M)	Solvent	Temperature (° C)	DMAP (mol%)	Urethane:ester (· 10^{-2})*
1	15	0.5	$CHCl_3$	80	-	5
2	15	1	$CHCl_3$	80	-	8
3	15	0.5	acetonitrile	80	-	3
4	15	0.5	DMF	100	-	2
5	15	0.4	1,4-dioxane	100	-	1
6	10	0.4	1,4-dioxane	100	1	4
7	15	0.4	1,4-dioxane	100	1	5
8	25	0.4	1,4-dioxane	100	1	9

* – determined by FTIR by comparing peak heights at 1730 cm^{-1} (ester) and 1540 cm^{-1} (urethane).

A number of polyesters were subjected to the above cross-linking conditions using 15 mol% HDI. High-T_g polyesters including poly(βOMeGal isophthalate), poly(βOMeGal adipate) and poly(βOMeGal dodecanoate) formed brittle films and their mechanical properties were not analyzed. FTIR analysis, used to obtain semi-quantitative information on the ratio of urethane to ester bonds based on the relative ratios of their IR signals, indicated a 0.04:1 to 0.07:1 ratio of urethane cross-links relative to ester linkages in these polymers, which was consistent with cross-linked poly(βOMeGal sebacate). The brittle nature of cross-linked poly(βOMeGal dodecanoate) could be attributed to its semi-crystallinity (poly(βO*n*-OctGal sebacate), the only other polymer showing a T_m by DSC, also formed a manageable but brittle film), but in the case of

poly(βOMeGal isophthalate) and poly(βOMeGal adipate), their low M_n partly explains their poor mechanical properties (M_n = 3.8 and 1.9 kDa, respectively). Poly(αOMeGal sebacate) had a M_n of 2.5 kDa and also failed to benefit from cross-link introduction, so poly(αOEtGal sebacate) (M_n = 5.8 kDa) was used in its place, as their T_g values were expected to be similar when controlling for molecular weight (see section 3.1). Cross-linked poly(αOMeGal sebacate) successfully formed an even thin film similarly to poly(βOMeGal sebacate). Due to their softness and low M_n, the *i*-oct series formed films that were too soft to handle and were thus excluded from the analysis. Table 4.3 shows the results of all successful cross-linking experiments.

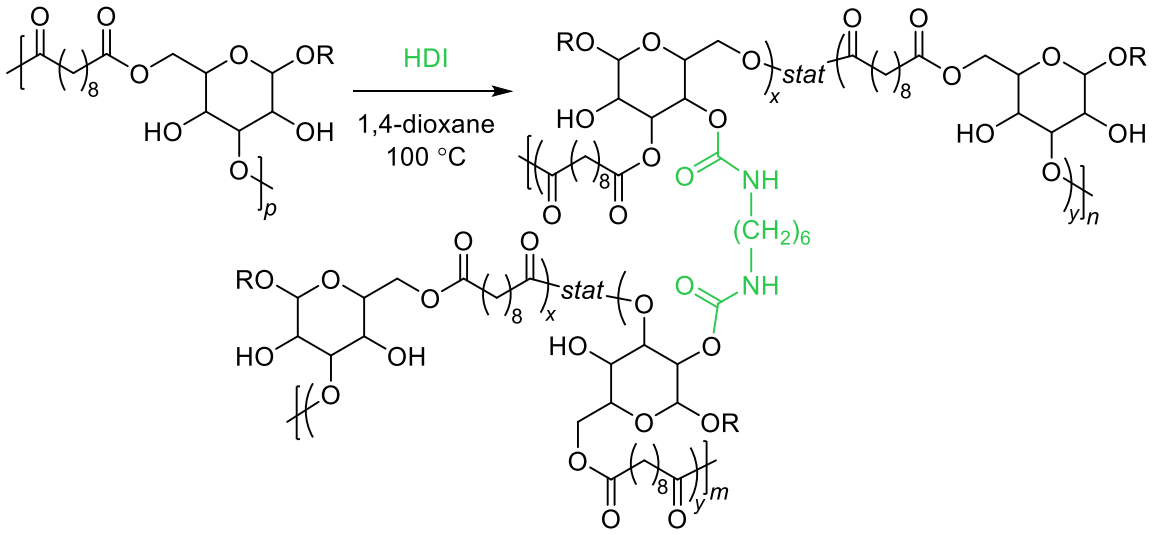

Table 4.3 Cross-link introduction in poly(pyranoside sebacate)s using 15 mol% HDI.

Entry	Comonomer	Reaction time (h)	Urethane:ester ($\cdot 10^{-2}$)*
1	αOEtGal	1	3
2	βOMeGal	3	3
3	αOMeMan	1.5	4
4	αO*n*-OctGal	4	5
5	βO*n*-OctGal	3	6
6	αO*n*-OctMan	2.5	7

* – determined by FTIR by comparing peak heights at 1730 cm^{-1} (ester) and 1540 cm^{-1} (urethane).

3.2.2 Viscoelastic Behaviour

DMA was used to establish the dynamic moduli of the urethane cross-linked polyesters. In these experiments, the temperature was varied while applying a constant sinusoidal strain, the value of which was determined by applying a series of strains to each sample and determining the linear viscoelastic region, defined as the range of strain values over which the storage and loss moduli are independent of applied deformation.[177] The strains within the linear viscoelastic regime were in the range 0.2–0.7 %.

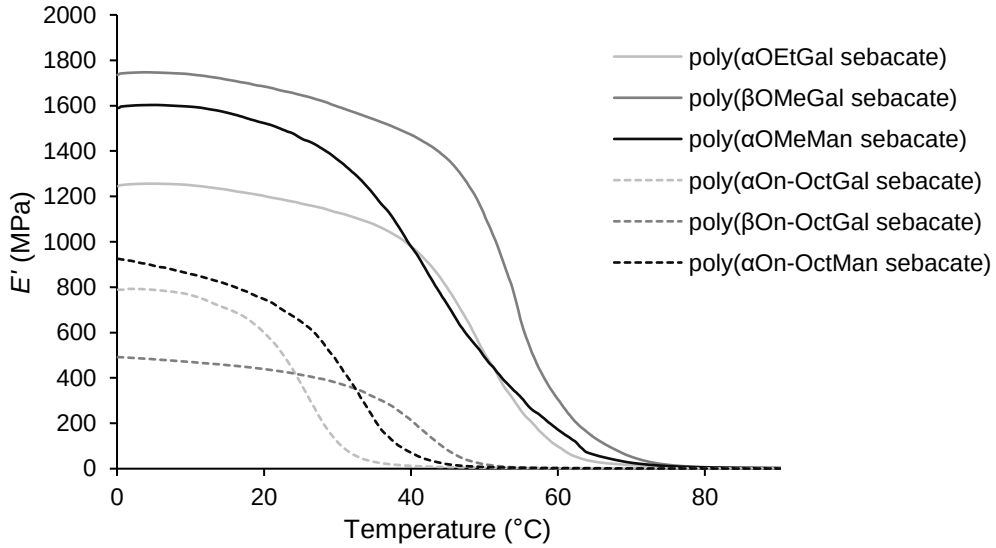

Figure 4.4 DMA traces of cross-linked polyesters showing storage modulus (*E′*) as a function of temperature.

Storage modulus as a function of temperature is shown in Figure 4.4 and tan δ (ratio of loss modulus to storage modulus) as a function of temperature is shown in Figure 4.5. T_g values of the cross-linked polyesters taken as the local maxima of the tan δ traces were 15–20 °C higher than those of their non-cross-linked precursors as judged by DSC, and varied with monomer configuration following the same general trends with both methods. The maxima of tan δ in the methyl (and ethyl) series for α-galacto-, β-galacto- and α-manno-derived polymers occurred at 64, 75 and 69 °C, respectively, and those of the *n*-octyl series for α-galacto-, β-galacto- and α-

[177] Schlesing, W.; Buhk, M.; Osterhold, M. *Prog. Org. Coatings* **2004**, *49*, 197–208.

manno-derived polymers were found at 37, 55 and 45 °C, respectively (*cf.* section 3.1). There was a sharp contrast between the moduli of the methyl and ethyl series and those of the *n*-octyl series, with the former showing higher storage modulus (*E′*) and lower damping (tan δ) close to T_g. This is consistent with softening of the polyester with flexible side-chain introduction, and better energy dissipation in the *n*-octyl series. In these materials, viscous behaviour is dominant (tan δ > 1) in the temperature range 30–60 °C, which makes this series potentially attractive for soft-tissue applications. The highest damping was observed for poly(αO*n*-OctGal sebacate), which showed the largest area under the tan δ curve.

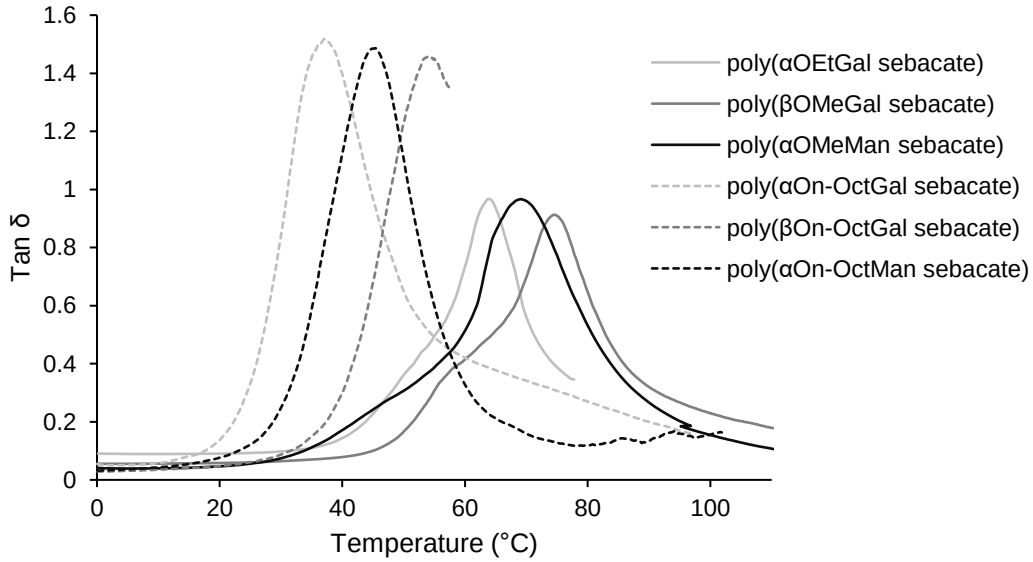

Figure 4.5 DMA traces of cross-linked polyesters showing tan δ as a function of temperature.

At high temperatures, two polymers exhibited irregular viscous behaviour resulting in rapid increase in tan δ by orders of magnitude followed by an erratic sinusoid curve (see DMA Traces in the Appendices), corresponding to the dominance of viscous flow as the polymer was melting or softening significantly. For poly(βO*n*-OctGal sebacate), this occurred around 57 °C, correlating to the observed T_m at 45 °C as determined by DSC. Poly(αOEtGal sebacate) consistently exhibited erratic loss modulus changes close to 80 °C and appeared to have softened dramatically upon retrieval from the DMA. The cause for the sudden oscillation of the loss modulus is unclear; a relatively low T_g reflecting weaker intermolecular forces combined with a relatively low elastic modulus could explain the failure of the material under stress at higher

temperatures. The cross-linked polymer with the highest *E′* was poly(βOMeGal sebacate), which also had the lowest damping and thus the highest degree of elastic behaviour. Poly(βO*n*-OctGal sebacate) had by far the lowest *E′* and showed a very gradual decrease in *E′* close to its T_g, a behaviour known to occur in semi-crystalline polymers.[178]

3.2.3 Tensile Properties

The physical properties of poly(αO*n*-OctGal sebacate) and poly(αO*n*-OctMan sebacate) treated with 15 mol% HDI suggested that these materials were elastomers. Informal inspection of their elastic and shape recovery properties showed that the samples returned to their original length after being extended by at least 60% for poly(αO*n*-OctGal sebacate) and at least 40% for poly(αO*n*-OctMan sebacate), as exemplified by the test depicted in Figure 4.6. These were encouraging results, as elasticity is a key characteristic of tissue engineering scaffolds, and soft tissues such as cardiac muscles typically experience strains of up to 15%.[179] In contrast, cross-linked poly(βO*n*-OctGal sebacate) needed to be handled cautiously due to its fragility and did not show much compliance. The semi-crystallinity of this polymer is consistent with this behaviour, as crystallinity is correlated with brittleness and low elasticity.[180] The cross-linked methyl and ethyl series, on the other hand, were stronger, stiff materials and were expected to exhibit plastic deformation.

---

[178] Ward, I. M.; Sweeney, J. *Mechanical Properties of Solid Polymers*; 3rd ed.; John Wiley & Sons, 2013.

[179] Gullberg, G. T.; Veress, A. I.; Weiss, J. A. *J. Biomech. Eng.* **2005**, *127*, 1195.

[180] Bessell, T. J.; Hull, D.; Shortall, J. B. *J. Mater. Sci.* **1975**, *10*, 1127–1136.

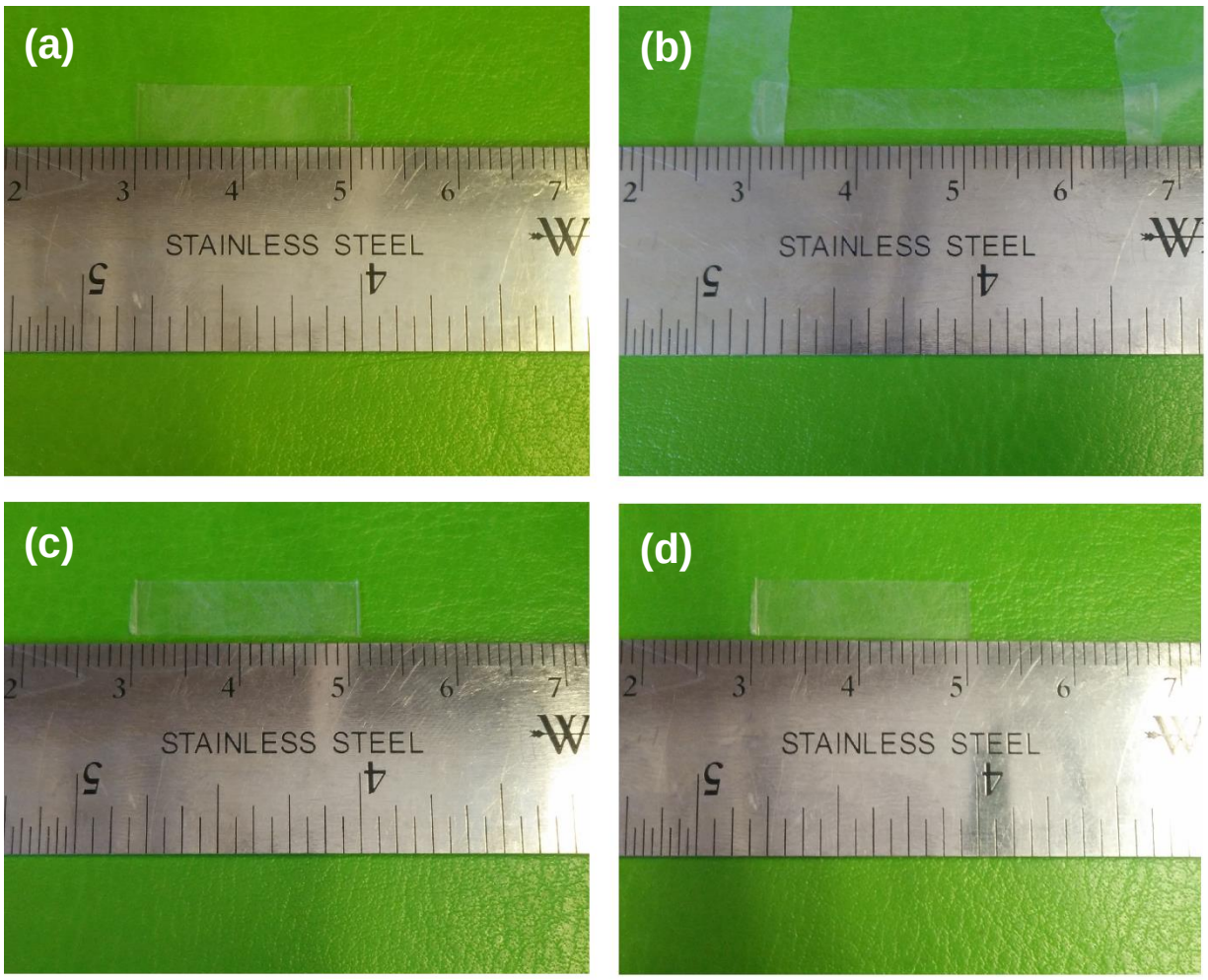

Figure 4.6 Shape recovery behaviour of poly(αO*n*-OctGal sebacate) cross-linked with 15 mol% HDI showing (a) initial conditions, (b) extension, (c) recovery after 1 min and (d) recovery after 1 h.

Films of cross-linked poly(ester urethanes) were subjected to uniaxial tensile testing and elongated to failure. The stress–strain curves of the ethyl/methyl and *n*-octyl series are shown in Figures 4.7 and 4.8, respectively, and their mechanical parameters are listed in Table 4.4. In both series, the behaviour of the β-galacto-derived polyesters is in sharp contrast to the other two stereoisomers, with higher elastic (Young's) modulus (*E*) and low elongation at failure, consistent with the brittle character of both their parent linear polyesters. The other two polymers in the ethyl/methyl series also behaved like plastics, having a low strain at yield but higher elongation at failure and much greater toughness than cross-linked poly(βOMeGal sebacate).

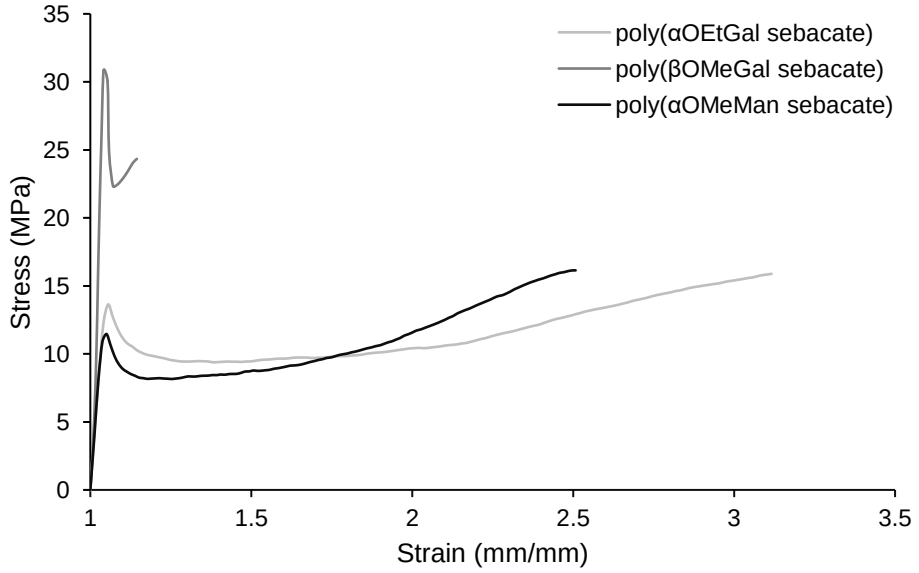

Figure 4.7 Stress–strain curves of the methyl/ethyl series polyesters cross-linked with 15 mol% HDI.

Cross-linked poly(βO*n*-OctGal sebacate) similarly underwent plastic deformation and fractured at a lower strain than the rest of the series: cross-linked poly(αO*n*-OctGal sebacate) and both linear and cross-linked poly(αO*n*-OctMan sebacate) exhibited elastomeric behaviour with high strains at failure and low *E*. Poly(αO*n*-OctMan sebacate)'s stiffness increased dramatically after curing, resulting in a tough material. Compared to cross-linked PGS as prepared by the group of Langer[36] which had a modulus of 0.28 MPa, tensile strength of 0.5 MPa and an elongation at break of 325%, these materials are stronger and stiffer while having comparable stretchability. The trends in *E* are generally in accordance with the relative T_g values of the corresponding linear analogs of the urethane cross-linked polyesters.

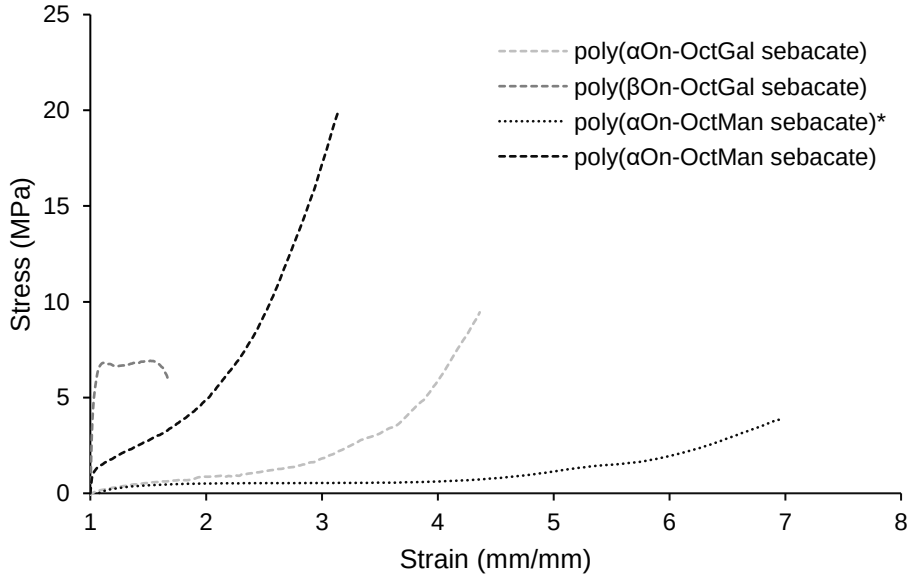

Figure 4.8 Stress–strain curves of the *n*-octyl series polyesters cross-linked with 15 mol% HDI. * represents untreated polymer.

Table 4.4 Tensile properties of poly(pyranoside sebacate)s cross-linked with 15 mol% HDI.

Entry	Comonomer	***E*** (MPa)	**Yield strength** (MPa)	**Strain at break** (%)
1	αOEtGal	255	14	212
2	βOMeGal	908	30	33
3	αOMeMan	238	12	150
4	αO*n*-OctGal	1.7	9.5	336
5	βO*n*-OctGal	36	5.8	67
6	αO*n*-OctMan	7.1	19.6	213
7*	αO*n*-OctMan	1.7	3.7	595

* – polymer was not subjected to cross-linking.

3.3 Degradability of Sugar-derived Polyesters

Degradation rates through hydrolysis and enzyme-mediated chain cleavage were compared across the entire series of sugar-derived polyesters. Porcine pancreatic lipase (EC 3.1.1.3) was selected for the enzymatic condition as it is inexpensive, frequently used in the literature and

known to digest a wide variety of bio-sourced polyesters.[181] Samples were incubated at body temperature for several days in phosphate buffer and their consequent mass losses were determined. Linear PGS synthesized according to the procedure described in Chapter 2 was used as a benchmark, since it is known to show rapid degradation *in vivo*. Deionized water behaved as an antisolvent for all the polyesters synthesized in Chapter 3, and the resin-like *i*-octyl series maintained a stable coating when submerged in the buffer solution without any noticeable delamination, enabling a reliable mass comparison between initial and final timepoints. Poly(βOMeGal adipate) exhibited swelling when incubated with shaking over multiple days, indicating that it had some level of water solubility despite forming a precipitate in water. The results of the degradation study are shown in Figure 4.9.

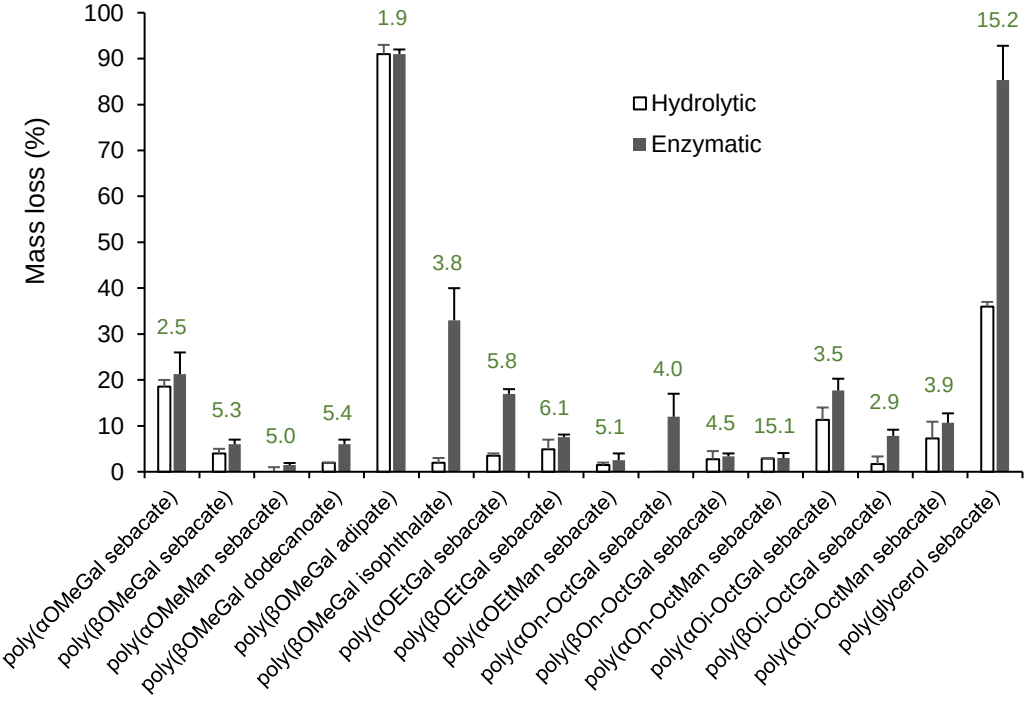

Figure 4.9 Hydrolytic and enzymatic degradation profiles of the poly(pyranoside ester) series and linear PGS as represented by mass loss over 6 days of incubation in phosphate buffer at 37 °C with shaking. Averages of two trials are shown. Data labels represent M_n values in kDa as judged by GPC.

[181] Kemme, M.; Prokesch, I.; Heinzel-Wieland, R. *Polym. Test.* **2011**, *30*, 743–748.

The rates of degradation of the pyranoside-derived polyester series were significantly lower than that of linear PGS, with all but poly(βOMeGal adipate) showing hydrolytic mass losses of up to 19% and enzymatic mass losses of up to 33%, in sharp contrast with PGS which showed a hydrolytic mass loss of 36% and enzymatic mass loss of 85%. Poly(βOMeGal adipate) was the only polymer in the series showing no susceptibility to cleavage by porcine pancreatic lipase as suggested by equivalent mass losses in the enzymatic and non-enzymatic conditions, both resulting in an approximate loss of 90%. It is well-known that the flexibility of the backbone has a large influence on enzymatic degradation[174] and that the relationship between degradability and diacid alkyl chain length can be non-linear;[182] in this case, the low rate of enzymatic cleavage is in agreement with reports on isohexide-derived aliphatic polyesters of different dicarboxylate chain lengths showing a low substrate specificity for poly(isohexide adipate)s by common esterases and lipases.[162] Studies on the soil degradation of polyesters comprising diacid comonomers of different lengths also uncovered an inverse relationship between comonomer chain flexibility (as related to its melting temperature) and biodegradation,[183] which leads us to believe that this effect may not be exclusive to the enzyme used in this study. The large difference in hydrolytic mass loss between poly(βOMeGal adipate) and the rest of the series can be rationalized by its swelling behaviour in water and low degree of polymerization (GPC showed an average chain length of approximately 6 pyranoside repeat units) that contributed to the partial solubility of this relatively hydrophilic polymer in phosphate buffer solution. Since it is unlikely that the rate of non-enzymatic ester bond hydrolysis is differs significantly across polymers, bulk erosion of poly(βOMeGal adipate) is probably occurring by virtue of its high water diffusion rate. Under the given conditions, all other polymers in the series seem to be undergoing surface erosion with a rate of hydrolysis lower than PGS owing to their low chain flexibility, high T_g values, and lack of aqueous solubility.

---

[182] Okada, M.; Tachikawa, K.; Aoi, K. *J. Appl. Polym. Sci.* **1999**, *74*, 3342–3350.

[183] Witt, U.; Müller, R. J.; Deckwer, W.-D. *J. Macromol. Sci. Part A* **1995**, *32*, 851–856.

Generally, the incorporation of pyranoside derivatives into the backbone did not increase the rate of hydrolytic or enzymatic degradation of these new polymers compared to the acyclic and more hydrophobic PGS, in contrast with prior reports where increasing the content of a gluctiol-derived comonomer was related to higher polymer degradation rates with and without enzyme.[156] The explanation for the low enzymatic degradability is likely a complex interplay of factors, as past reports have shown that sugar-based monomers can have a range of impacts on polymer biodegradation. Based on prior enzymatic degradation studies on isohexitol-derived polyesters, steric hindrance around the rigid cyclic structure within the backbone may be responsible for impeding the approach of enzymes, leading to dramatic differences in degradation rates among different stereoisomers.[184] The presence of two pendant OH groups and an anomeric substituent, both of which are made intransigent through their attachment to the pyranoside ring, is therefore a likely cause for the difference in enzymatic degradation between PGS and the poly(pyranoside ester) series. Interestingly, poly(βOMeGal isophthalate) showed the highest ratio of enzymatic *vs.* hydrolytic mass loss, which was unexpected based on the known low selectivity of most enzymes toward aromatic polyesters. The different spatial orientations of OH groups in the galacto- and manno-configured monomers also appears to have some effect on the relative rates of enzymatic degradation, as seen by a decrease in mass loss when switching from galacto- to manno-configured monomers in the methyl and ethyl series. α-Configured galactoside-based polymers showed degradation rates that were up to 15% higher than the other two isomers, in accordance with their T_g differences (poly(αOMeGal sebacate) had its T_g at 37 °C). Enhanced chain flexibility above T_g was previously found to increase the rate of degradation,[185] suggesting the possibility that the *n*-octyl and *i*-octyl series (T_g = –3–25 °C) would show increased mass loss rates. Such an effect was not found in the *n*-octyl series (in the case of poly(βO*n*-octylGal sebacate), crystallinity may be further depressing degradation rate), and increases in the degradabilities of the *i*-octyl series were modest and, considering the low degrees of polymerization among this series of polyesters, are likely strongly influenced by M_n.

---

[184] Okada, M.; Tsunoda, K.; Tachikawa, K.; Aoi, K. *J. Appl. Polym. Sci.* **2000**, *77*, 338–346.

[185] Okada, M.; Yokoe, M.; Aoi, K. *J. Appl. Polym. Sci.* **2002**, *86*, 872–880.

To gain more insights into the mechanism of enzymatic degradation and to validate the hypothesis that, unlike the rest of the series, the adipate-linked polyester lost mass due to partial solubilisation, we analyzed the evolution of degradation products in the phosphate buffer supernatants by liquid chromatography/mass spectrometry (LC-MS). Using electrospray ionization (ESI) and a quadrupole mass detector, we were able to observe ions with mass-to-charge ratios (*m/z*) of up to 1000 amu, as exemplified in Figure 4.10, which depicts ions obtained from lipase-mediated degradation of poly(βOMeGal sebacate). Resolving fragments in negative ionization mode enabled the detection of monomers and oligomers possessing carboxylate groups. This type of analysis is semi-quantitative owing to the presumably different ionization rates of each particular analyte and thus ion counts cannot be accurately compared between species and are used only to show trends in the evolution of individual degradation products. Furthermore, the low solubility of the dicarboxylic acids in phosphate buffer resulted in their partial precipitation from solution after 24 hours irrespective of the presence of lipase, presenting another caveat in the interpretation of the results. When analyzing the mass spectra, we did not find peaks with *m/z* equal to half of the exact mass of any of the detectable degradation products; therefore, we assumed that sebacic acid and oligomers having two carboxyl groups were deprotonated only once during ESI.

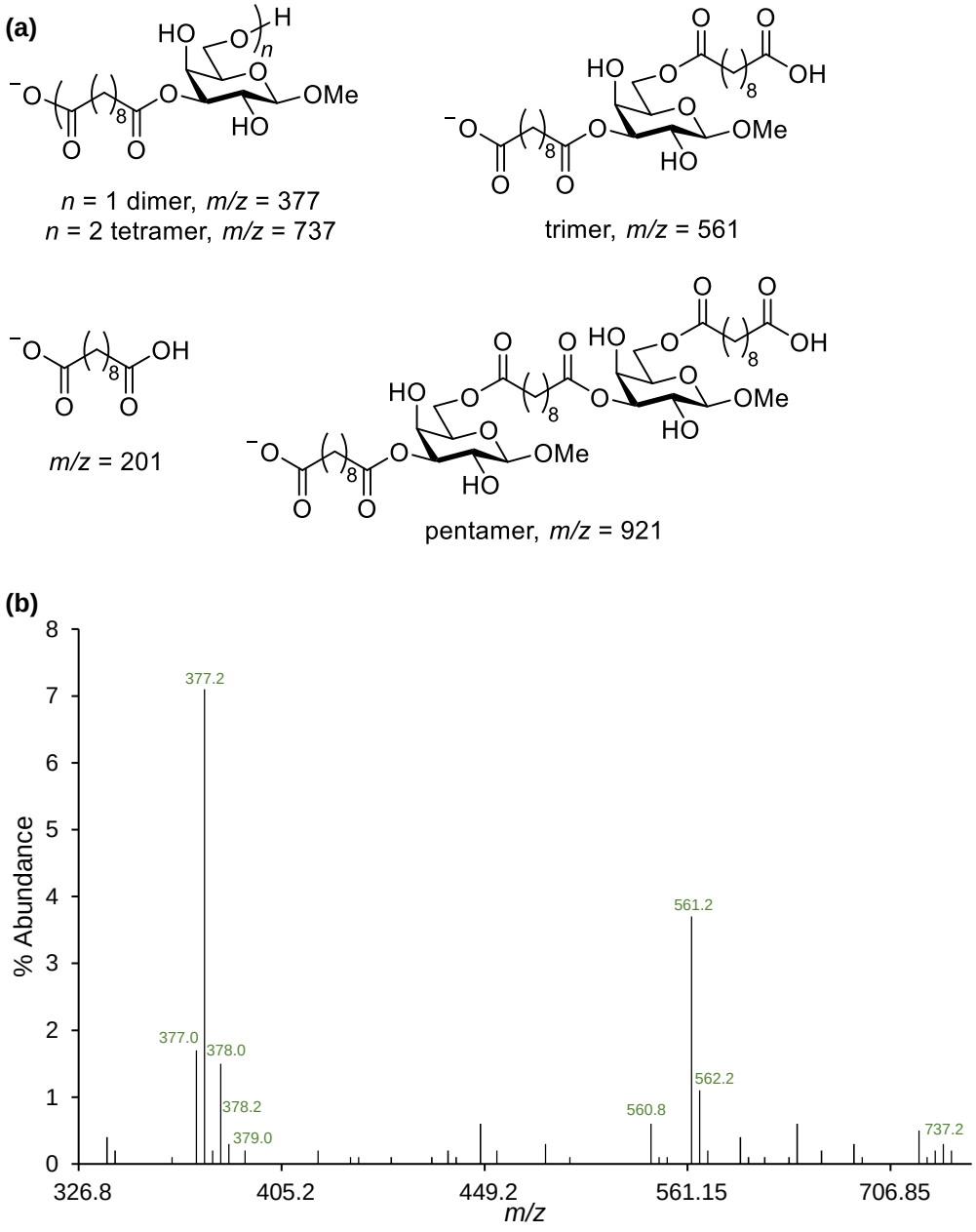

Figure 4.10 (a) Carboxylates obtained from ESI of degradation products from the digestion of poly(βOMeGal sebacate). Mass-to-charge ratios are approximate and do not reflect all possible isotope combinations. (b) Expansion of a low-resolution mass spectrum obtained after 6 days of enzymatic digestion showing dimer, trimer, and tetramer ion peaks.

A comparison between the degradation profiles of poly(βOMeGal sebacate) and poly(βOMeGal adipate) is shown in Figure 4.11. The close resemblance of the hydrolytic and enzymatic degradation graphs supports the hypothesis that poly(βOMeGal adipate) is a poor

substrate for porcine pancreatic lipase despite the partial solubilization of its oligomers. In contrast, significantly higher ion counts were observed under enzymatic conditions than under hydrolytic conditions in the case of poly(βOMeGal sebacate), and other polymers in the series exhibited a similar behaviour. The hydrolytic degradation profile of poly(βOMeGal sebacate) shows the upward evolution of all degradation products (except for the insoluble sebacic acid) while the enzymatic degradation profile suggests that longer oligomers are being digested in solution, seeing as their ion counts level off after an initial increase. The steady rise in dimer concentration is likely due to the combined effects of its high solubility compared to sebacic acid, cleavage from the polymer matrix and the solution-phase digestion of higher oligomers in solution. The trends in oligomer release also shed light on the mechanism of chain scission, specifically on whether the enzyme cleaves random ester bonds along the chain (*endo*-enzyme) or only cleaves chain ends (*exo*-enzyme).[186] It appears that porcine pancreatic lipase can behave as an *endo*-enzyme, as at 1 h under non-enzymatic conditions dimer, trimer, tetramer and pentamer ion counts were 0, 35, 11 and 23, respectively, while under enzymatic conditions 58, 127, 127 and 69 ions derived from the same oligomers were observed, while the sebacate ion counts were 94 without enzyme and 93 with enzyme. This suggests that the lipase is responsible for the removal of oligomers from the matrix to a greater extent than sebacate units, and thus that it can cleave the polymer randomly along the chain. It is unclear whether the lipase can also cleave chain ends: the persistence of dimers in solution may be an indication that it cannot, but an absolute quantification of the relative amounts of different oligomers would be needed to draw a definitive conclusion on this point.

---

[186] Wheatley, M. A.; Moo-Young, M. *Biotechnol. Bioeng.* **1977**, *19*, 219–233.

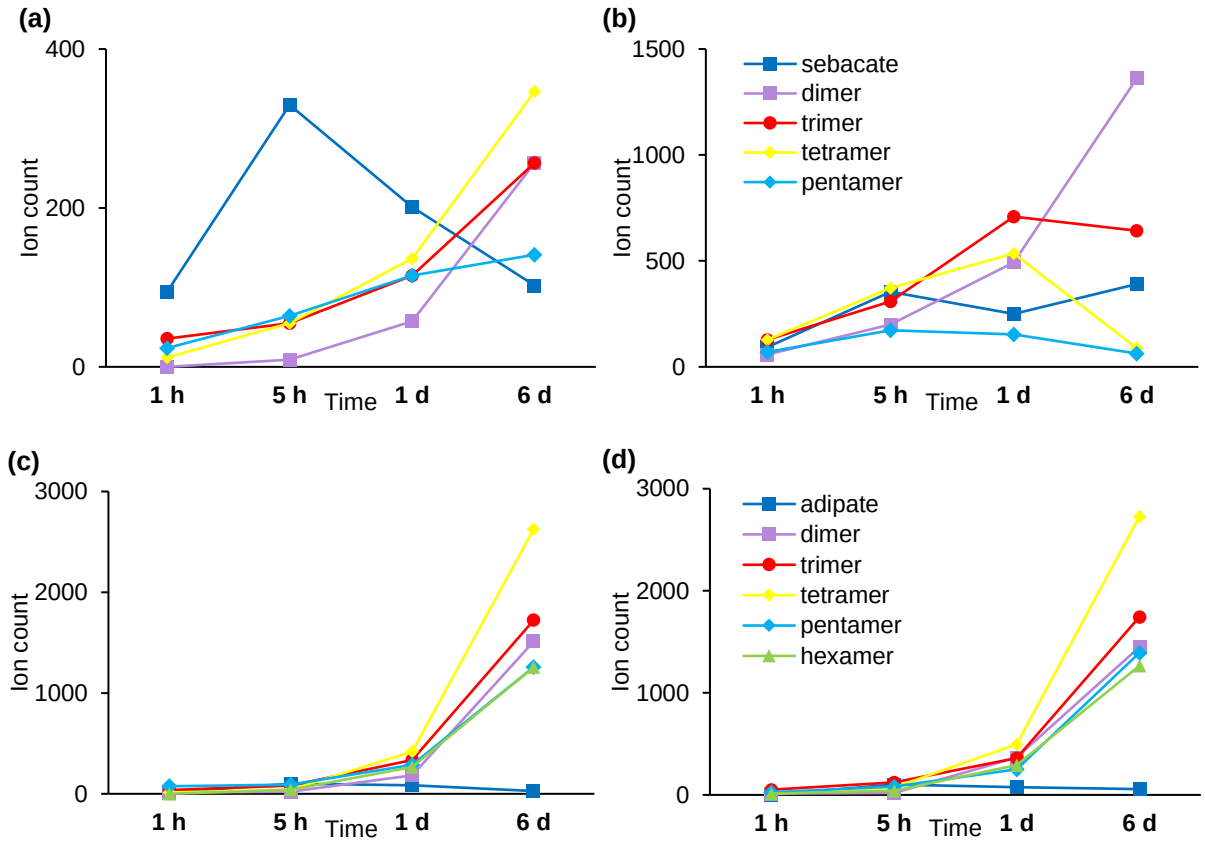

Figure 4.11 Ion counts of monomers and oligomers obtained by LC-MS at different timepoints of polymer degradation by incubation in phosphate buffer at 37 °C with shaking, showing (a) hydrolytic and (b) enzymatic degradation of poly(βOMeGal sebacate) and (c) hydrolytic and (d) enzymatic degradation of poly(βOMeGal adipate). Time axes are not to scale.

3.4 Cytocompatibility of Polymers

In vitro cytotoxicity was evaluated using a 3-(4,5-dimethylthiazol-2-yl)-2,5-diphenyltetrazolium bromide (MTT) assay by means of a direct-contact test.[187] The MTT assay is a colorimetric assay commonly used in the field of biomaterials[188] and provides information on the rate of proliferation of cells in the presence of a test compound, thus providing an indirect measure of cytotoxicity. The relative numbers of metabolically active cells in the experimental and control conditions are determined by quantifying the formation of formazan created through the

[187] ISO10993-5. Biological Evaluation of Medical Devices, Part 5: Tests for Cytotoxicity. *International Standard*, 2009, *5*, 2–9.

[188] You, Z.; Bi, X.; Fan, X.; Wang, Y. *Acta Biomater.* **2012**, *8*, 502–510.

reduction of MTT by NAD(P)H-dependent cellular oxidoreductase enzymes (Scheme 4.1). The reduction of tetrazolium to formazan occurs in active mitochondria, resulting in an accumulation of purple formazan crystals only in viable cells.[189] Upon cell lysis and solubilisation of the formazan crystals, the absorbance is measured at 500–600 nm using a spectrophotometer or plate reader, providing quantitative data on the relative metabolic activities of cells under different conditions.

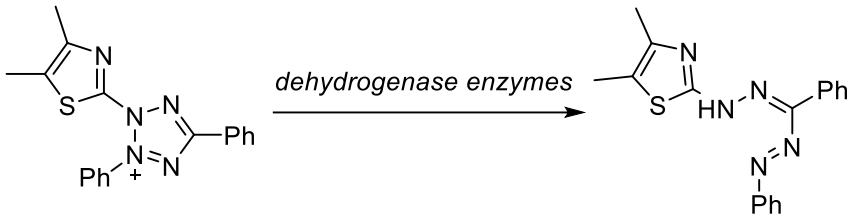

Scheme 4.1 Formation of formazan from the MTT tetrazolium salt inside metabolically active cells.

The ethyl series of polyesters was used to coat the bottom of tissue culture wells and tested against a murine fibroblast cell line (NIH 3T3) using pristine tissue culture polystyrene (TCPS) as a negative control and DMSO, a known cytotoxic agent, as a positive control. By using a series of polyesters with similar M_n values (5.1–6.1 kDa) and the same anomeric substituents, we hoped to establish any correlation between cytocompatibility and monomer stereoconfiguration. In addition, the ethyl series consisted of hard, water-insoluble polymers that formed smooth and even films when solution-cast from ethanol, indicating that they could easily coat common cell culture vessels. Coating the entire bottom surface of a cell culture environment before seeding the cells also allows one to determine whether the polymer is a suitable substrate for cell attachment.[190] The results of the assay are shown in Figure 4.12.

---

[189] Mosmann, T. *J. Immunol. Methods* **1983**, *65*, 55–63.

[190] American Type Culture Collection. ATCC Animal Cell Culture Guide: Tips and Techniques for Continuous Cell Lines, 2014.

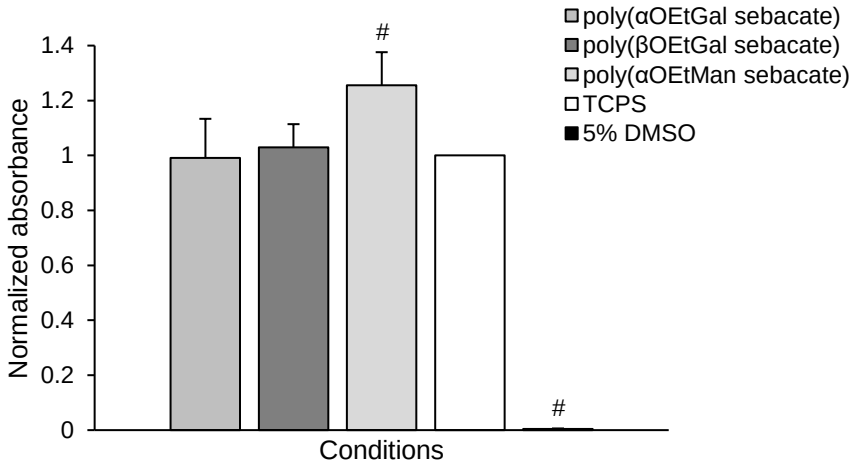

Figure 4.12 MTT assay of NIH 3T3 fibroblasts cultured for 24 hours on ethyl glycoside-derived polyesters. Experimental conditions are compared to an untreated negative control (TCPS) and a cytotoxic positive control (5% DMSO). The averages of four trials are normalized to TCPS. Statistically significant results ($p < 0.05$) are marked as # compared to TCPS.

Poly(ethyl glycoside ester)s did not inhibit cell proliferation when compared to untreated TCPS, with cells cultured on poly(αOEtMan sebacate) showing a small overall increase in metabolic activity. After proliferating for 24 hours, NIH 3T3 fibroblasts exhibited similar morphology in the experimental and control conditions when examined under the microscope. Based on the results of the enzymatic degradation experiments described in section 3.3, it is unlikely that the mannoside-derived polyester is promoting growth by providing additional nutrients *via* biodegradation, since among the ethyl series it showed the lowest degree of mass loss after 6 days. These results suggest that sugar-derived polyesters would promote cell attachment *in vivo*, possibly by virtue of their hydrophilicity and wettability, which is a promising characteristic for tissue engineering and other biomedical applications.

4 Conclusions

The physical, thermal and *in vitro* behaviours of poly(pyranoside ester)s were characterized and related to monomeric composition. Pendant OH groups present in the native polyesters were utilized to introduce urethane cross-links and improve material properties. Stereoconfiguration and substitution of the carbohydrate-derived monomer appeared to affect polyester chain

flexibility and/or interchain interactions, leading to differences in thermal behaviour and mechanical properties. Most notably, the impacts of α-configuration at the anomeric carbon within the galactoside series and the presence of a flexible anomeric side-chain included higher flexibility, lower complex modulus, improved damping ability and higher strains at failure in the corresponding urethane cross-linked elastomers and plastics. Future work could include conformational analysis of the polymer backbones of each series to elucidate the origin of these effects. The ethyl pyranoside-derived polyester series showed no detectable cytotoxic effects on a murine fibroblast cell line and the polymers exhibited enzymatic degradation rates lower than that of linear PGS, making them potentially attractive polymers for the fabrication of longer-term medical implants. The slower degradation among the sebacoyl-derived polyesters likely stems from a combination of backbone inflexibility and sufficient hydrophobicity impeding water diffusion into the polymer film. A detailed analysis of each polymer's degradation products would provide key insights into the mechanism of biodegradation.

5 Experimental

5.1 General Considerations

5.1.1 Materials

All chemical reagents, enzymes, growth media and biological-grade buffers were purchased from Sigma-Aldrich. Antibiotics and calf serum were purchased from Gibco. TrypLE Express was purchased from Invitrogen. Cell culture flasks and plates were purchased from Corning. NIH 3T3 fibroblasts were a generous gift from the group of Prof. Paul Santerre at the University of Toronto.

5.1.2 Instrumentation

IR spectra were obtained on a Perkin-Elmer Spectrum 100 instrument equipped with a single-bounce diamond / ZnSe ATR accessory in the solid state. The spectra were processed using Spectrum Express. Differential scanning calorimetry (DSC) was performed using a Thermal Advantage Q100 DSC under N_2, with a heating rate of 10 °C/min. Measurements were analyzed using TA Universal Analysis and the glass transition temperature (T_g) was taken as the local

maximum of the first derivative of the heat flow with respect to temperature. Dynamic mechanical analysis was performed on a Thermal Advantage Q800 DMA and the measurements were analyzed using TA Universal Analysis as described below. Tensile strength measurements were performed on an Instron 5543 tensiometer equipped with a 1 kN load cell and pneumatic grips. Absorbance readings were taken using a PerkinElmer EnVision 2104 multilabel microplate reader.

5.2 Cross-link Introduction and Curing

0.13 mmol (based on repeat units) purified polymer was loaded into a 2-dram vial equipped with a stir bar and purged with argon gas. 225 µL of a 0.88 mg/mL 1,4-dioxane solution of DMAP (0.2 mg, 0.0013 mmol) were added by syringe. The polymer was dissolved by stirring at 80 °C under argon and 100 µL of a 30 µL/mL 1,4-dioxane solution of HDI (3 µL, 15 mol%) were added dropwise. The reaction was heated to 100 °C and stirred for 1–3 hours before being transferred to a 2 × 2 cm Teflon mould using a Pasteur pipette when an increase in viscosity was noted. The film was air-dried overnight, dried under high vacuum, and cured at 100 °C in a –30 mmHg vacuum oven for 1 hour.

5.3 Dynamic Mechanical Analysis

Rectangular 5.5 × 20 × 1 mm samples were cut using a sample cutter and measured with a caliper before being analyzed using a TA Q800 DMA equipped with a film tension clamp. A strain sweep experiment was performed to determine the linear viscoelastic regime with an oscillatory rate of 1 Hz and amplitudes varying between 0.3 and 0.7% strain. Temperature ramps between either 0 and 120 °C or –10 and 100 °C were performed at a heating rate of 3 °C/min. T_g values were taken as the local maxima of the tan δ curves.

5.4 Tensile Tests

Uniaxial tensile tests were conducted on 5.5 × 20 × 1 mm polymer strips using an Instron 5543 mechanical tester equipped with a 1 kN load cell and pneumatic grips. The samples were elongated to failure at 10 mm/min. Young's modulus was calculated as the slope of the stress–strain curve at 10% strain for the *n*-octyl series and 5% strain for the methyl and ethyl series.

5.5 Enzymatic Degradation Experiments

Polymers (10–15 mg) were weighed into 15-mL Falcon tubes and dissolved in a minimum amount of methanol to coat the inner surface of the tube's conical segment. The tubes were dried under high vacuum for 10 hours and 5 mL of 0.1 M phosphate buffer (pH = 7.0) alone or containing 0.5 mg/mL porcine pancreatic lipase were added. The tubes were then incubated at 37 °C with shaking at 200 strokes/min for 6 days, after which they were centrifuged for 5 min at $2 \cdot 10^3$ rpm and the buffer solution was decanted. The polymer residues were washed three times with deionized water, redissolved in ethanol, and concentrated by rotary evaporation in pre-weighed 1-dram vials. Ethanol was added to the vials for a second evaporation to ensure azeotropic removal of residual water. The vials were dried under high vacuum for 12 hours and weighed to determine the polymer recovery.

5.5.1 Analysis of Degradation Products by Mass Spectrometry

100 µL aliquots of the buffer solution were removed from the incubating Falcon tubes at 1 hour, 5 hours, 1 day and 6 days. The aliquots were diluted with a 1:1 mixture of distilled water and acetonitrile to a total volume of 400 µL and filtered through a 0.2 µm polytetrafluoroethylene (PTFE) filter. Low-resolution mass spectra (ESI) were collected on an Agilent Technologies 1200 series HPLC paired to a 6130 Mass Spectrometer in negative ionization mode. Oligomers were resolved on Phenomenex's Kinetex 2.6u C18 50 × 4.6 mm column at room temperature at a flow rate of 1 mL/min. A linear gradient from 5 to 95% of 0.1% formic acid in acetonitrile in 0.1% formic acid in water over 7 minutes was used. Ion counts in the 2–5 minute region were tabulated using Agilent ChemStation to track carboxylate monomer and oligomer production. Ions of *m/z* within 1 amu of the predicted *m/z* all possible isotopes of the target compounds were included in the analysis.

5.6 *In vitro* Biocompatibility Assay

Poly(αOEtGal sebacate), poly(βOEtGal sebacate) and poly(αOEtMan sebacate) were purified by precipitation from diethyl ether and tested for cytotoxic effects by conducting an MTT assay.[191] Polymers were dissolved in ethanol (20 mg/mL), filtered through a 0.2 µm PTFE filter, and 5 µL of the solutions were added to 96-well tissue culture polystyrene (TCPS) plates, which were then air-dried overnight and triturated with 200 µL DPBS after solvent evaporation. NIH 3T3 mouse fibroblasts were cultured in Dulbecco's modified Eagle's medium (DMEM) supplemented with 10% inactivated bovine calf serum and 1% penicillin/streptomycin and kept in a humidified incubator (37 °C, 5% CO_2). As the culture approached confluency, it was washed with Dulbecco's phosphate buffered saline (DPBS) and incubated with TrypLE Express for 5 min. The detached cells were centrifuged for 5 min at $1.2 \cdot 10^3$ rpm, resuspended in DMEM and seeded onto the coated TCPS surfaces at $5 \cdot 10^4$ cells/well (6 replicates per condition). After 24 h of incubation, the culture medium was removed and the cells were washed with DPBS and incubated with 100 µL of a 5 mg/mL MTT solution in DPBS and 100 µL DMEM for 4 h. The MTT-containing medium was removed and the wells were washed gently with DPBS. The formazan crystals were solubilized by triturating with 100 µL DMSO and the absorbance of each solution was measured at 570 nm, including untreated TCPS controls and a positive control cultured in medium containing 5% DMSO. The assay was performed 4 times on cells of different passage numbers and average normalized absorbance values were used to quantify the relative rate of cell proliferation under each condition.

5.6.1 Statistical Analysis

All data are expressed as mean ± standard deviation. Statistical analysis was performed using a one-way ANOVA with *post-hoc* Bonferroni correction. A p value of < 0.05 was considered statistically significant.

---

[191] Hansen, M. B.; Nielsen, S. E.; Berg, K. *J. Immunol. Methods* **1989**, *119*, 203–210.

Chapter 5: Conclusion and New Directions

1 Statement of Contribution

This chapter summarizes some investigations carried out more recently as extensions of the work described in Chapters 2 and 3 on the role of borinic acid catalysis as a tool for macromolecular synthesis. The synthesis of carbohydrate-derived polyurethanes and their models was performed by Jingning Zhou.[192] Work on sugar-derived methacrylates and their corresponding glycopolymers was performed by Pierre-Olivier Ferko[193] and Ekaterina Slavko. Hydrogel preparation was done by Pierre-Olivier Ferko.

2 Linear Polyol-derived Polyurethanes

2.1 Introduction

Chapter 3 described the utility of borinic acids **1.01**–**1.03** in the site-selective synthesis of linear polyesters derived from anomerically protected pyranosides and aliphatic and aromatic diacyl chlorides. Building on this work, the basic concept was expanded to include the use of alternate electrophilic comonomers, namely isocyanates, resulting a series of novel linear polyurethanes.

Biomedical-grade polyurethanes were originally commercialized in the 1960s and comprise a diverse class of materials, often prepared as (block) copolymers containing "hard" segments connected with urethane to "soft" segments derived from polyether or polyester polyols.[194] Their physical properties vary greatly depending on factors such as cross-linking density and length of the soft segment, the latter of which is responsible for imparting flexibility to the materials. Carbohydrate derivatives are commonly incorporated into polyurethanes,

---

[192] Zhou, J. Unpublished undergraduate thesis, University of Toronto, 2019.

[193] Ferko, P. Galactose-derived Glycopolymers: Synthesis, characterization and applications, 2018. University of Toronto, MSc thesis. [http://hdl.handle.net/1807/91745]

[194] Guelcher, S. A. *Tissue Eng. Part B Rev.* **2008**, *14*, 3–17.

including isohexitols,[195] protected sugar alcohols,[196] and polysaccharides,[197] as efforts to make polyurethanes more biocompatible are driving a considerable research efforts into the exploration of non-toxic monomers. To attain polyurethanes with pendant functional groups,[198] isocyanate-free routes have been proposed, including ROP of cyclic carbonates by alkyl amines (see Chapter 3, section 2.2, Scheme 3.3b). The direct synthesis of functional sugar-derived polyurethanes faces challenges similar to those associated with synthesizing linear polyesters from multifunctional polyol monomers. We propose that a site-selective polycondensation using organoboron catalysis would enable a controlled polymerization resulting in a one-step synthesis of polyurethanes comprising pyranoside derivatives as the polyol segment (Scheme 5.1). Additionally, glycerol could be used as the soft segment, employing reactivity analogous to that outlined in Chapter 2.

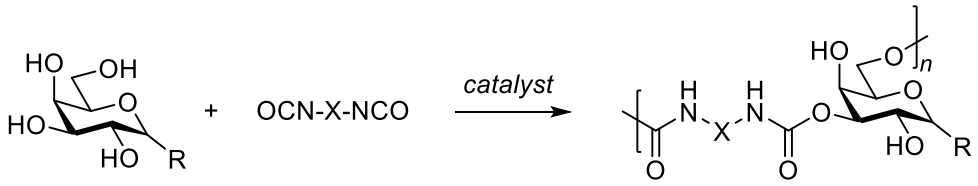

Scheme 5.1 Proposed catalytic approach for the preparation of galactopyranoside-derived polyurethanes.

2.2 Model Reactions

Model reactions were performed to assess the catalytic activity of borinic acids with respect to urethane formation, starting with methyl α-L-fucopyranoside, which was converted to **5.01** in quantitative yield using **1.04** as catalyst in THF (Scheme 5.2a). *Bis*-functionalization reactions using two equivalents of electrophile were carried out to determine possible polymerization

---

[195] Marín, R.; Alla, A.; de Ilarduya, A. M.; Muñoz-Guerra, S. *J. Appl. Polym. Sci.* **2012**, *123*, 986–994.

[196] Paz, M. V. de; Marín, R.; Zamora, F.; Hakkou, K.; Alla, A.; Galbis, J. A.; Muñoz-Guerra, S. *J. Polym. Sci. A Polym. Chem.* **2007**, *45*, 4109–4117.

[197] Barikani, M.; Zia, K. M.; Bhatti, I. A.; Zuber, M.; Bhatti, H. N. *Carbohydr. Polym.* **2008**, *74*, 621–626.

[198] Prömpers, G.; Keul, H.; Höcker, H. *Des. Monomers Polym.* **2005**, *8*, 547–569.

conditions using anomerically protected galactopyranosides such as αOMeGal (Scheme 5.2b) to form **5.02**, but yields were typically below 50% and the monofunctionalized product **5.03** was isolated in similar yields. The galactopyranoside series were converted to the difunctional product at a maximum yield of 62%, which was obtained when βS*i*-PrGal was used.

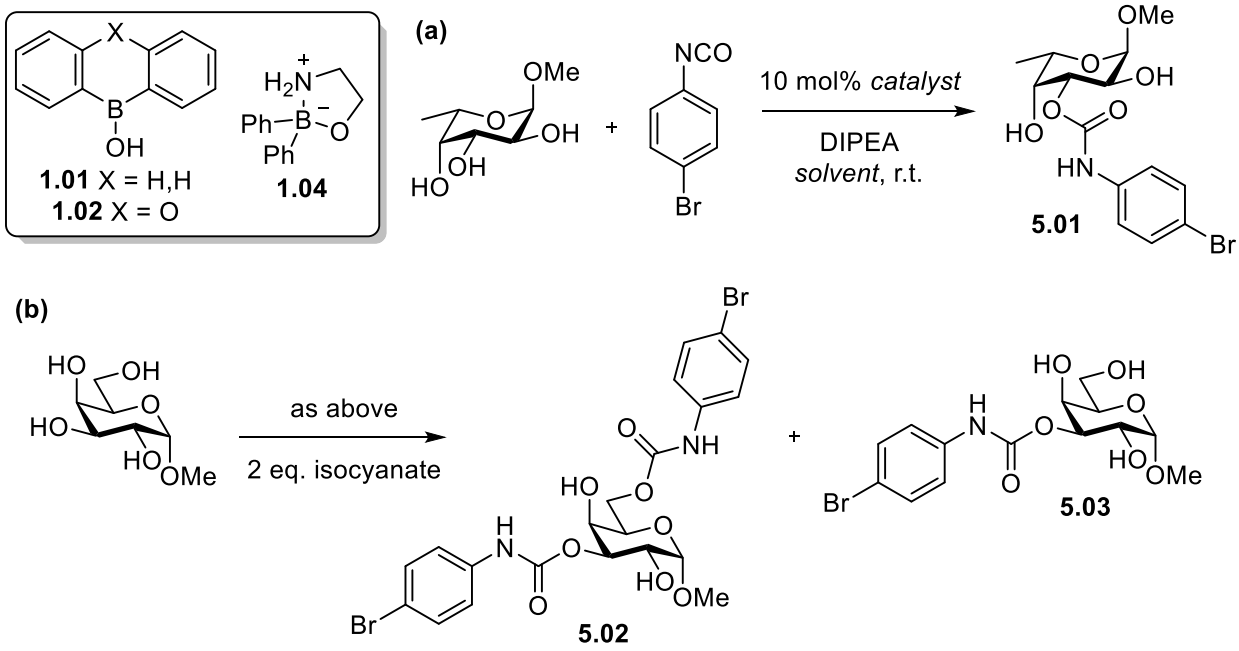

Scheme 5.2 Model functionalizations of pyranoside (a) triols and (b) teraols using borinic acid catalysts.

The use of 3 equivalents of isocyanate led to an increase in yield to 85% for βS*i*-PrGal, pointing to the possible low reactivity of the isocyanate. While this yield was more promising, the stoichiometric excess of isocyanate would not be ideal for step-growth polymerization conditions, in which a strict 1:1 monomer feed ratio is preferred for maximal M_n.[140] *Bis*-functionalizations of the more reactive substrate glycerol resulted in a yield of 91%, with optimal conditions involving heating to 80 °C.

2.3 Polymer Synthesis

Based on the best results from the model reaction optimization, βS*i*-PrGal and glycerol were polymerized using diisocyanate **5.04** to form polyurethanes (Scheme 5.3). As expected, low degrees of polymerization were obtained when an excess of isocyanate was used. Both polymers were isolated as poorly soluble solids owing to the rigid phenyl rings of the isocyanate moieties,

showing M_n = 5.8 kDa for βS*i*-PrGal and M_n = 7.1 kDa for glycerol as determined by GPC in NMP at 80 °C relative to PMMA standards. Dispersities for these polymers were quite high, at 26 and 53, respectively, suggesting solvent optimization might be needed, as some of the growing chains precipitated under the reaction conditions.

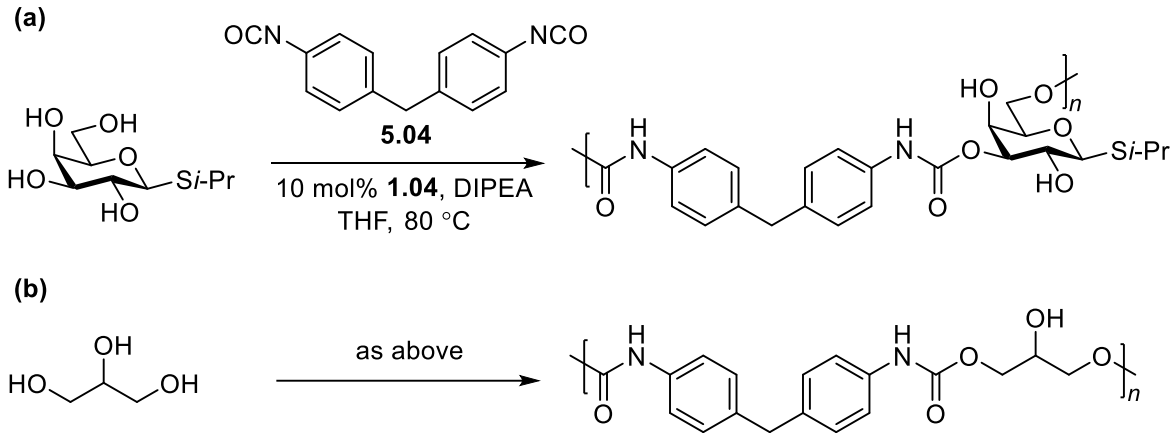

Scheme 5.3 Synthesis of (a) pyranoside- and (b) glycerol-derived polyurethanes.

2.4 Outlook

Preliminary results show moderate success in synthesizing well-defined polyurethanes from pyranosides and glycerol using borinic acid catalysis, with the poor reactivity of the isocyanate reagent identified as a major issue. Future work may involve the synthesis of a more soluble carbohydrate (polyol) segment, *e.g.*, through the incorporation of flexible anomeric side-chains or by using a sugar alcohol rather than a cyclic pyranoside, as the low solubility of the polymers was a limitation of the polymerization process.

3 Synthesis of Pyranoside-derived Glycopolymers

3.1 Introduction

Polymers with pendant carbohydrate residues, broadly referred to as glycopolymers, have garnered tremendous research interest over the past decades due to their ability to leverage the

biological signalling properties of carbohydrates.[199] Sugars have been incorporated into gold and polymeric nanoparticles to study carbohydrate interactions in the field of chemical glycobiology,[200] as well as utilized in targeted gene and drug delivery applications.[201] Galactose-containing glycopolymers specifically have been investigated for the treatment of cancer,[202] as liver cancer cells are known to overexpress asialoglycoprotein receptors that are competitively inhibited by galactose, motivating the group of Narain to explore the synthesis of sugar methacrylate polymers as well as their potential for drug or gene delivery and cell targeting.[203] An example of such a glycopolymer is shown in Figure 5.1. RAFT (reversible addition−fragmentation chain-transfer) polymerization[204] is commonly used to carry out controlled radical polymerizations to attain tailored M_n and low dispersities.

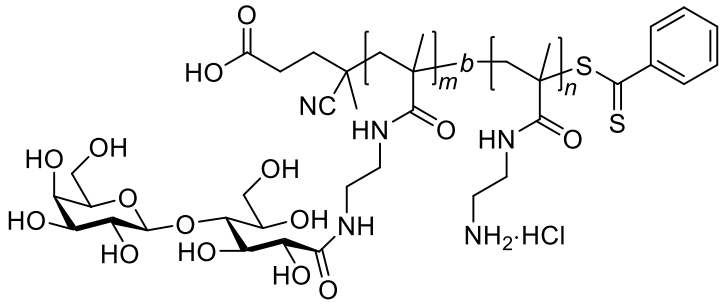

Figure 5.1 Glycopolymer-containing methacrylamide block copolymer designed for targeted gene delivery.

---

[199] Miura, Y.; Hoshino, Y.; Seto, H. *Chem. Rev.* **2016**, *116*, 1673–1692.

[200] Abeylath, S. C.; Turos, E.; Dickey, S.; Lim, D. V. *Bioorganic Med. Chem.* **2008**, *16*, 2412–2418.

[201] Ahmed, M.; Narain, R. *Biomaterials* **2011**, *32*, 5279–5290.

[202] Ahmed, M.; Mamba, S.; Yang, X.-H.; Darkwa, J.; Kumar, P.; Narain, R. *Bioconjugate Chem.* **2013**, *24*, 979–986.

[203] Quan, S.; Kumar, P.; Narain, R. *ACS Biomater. Sci. Eng.* **2016**, *2*, 853–859.

[204] Gody, G.; Maschmeyer, T.; Zetterlund, P. B.; Perrier, S. *Nat. Commun.* **2013**, 4, 2505.

A second interesting application of glycopolymers is the formation of hydrogels based on the interaction of polyols with organoboron species.[205] In such a setup, a polymer containing pendant oxophilic organoboron moieties forms cross-links with a polymer with pendant diol moieties (*e.g.*, catechol), resulting in a dynamic, pH-responsive network based on the aforementioned boron–diol interaction. Because this type of cross-linking is based on reversible covalent bond formation, hydrogels formed using this system often exhibit self-healing properties, meaning that they can recover from being torn by virtue of the dynamic intermolecular bonds maintaining their structure. This feature represents a highly promising avenue for the development of glycopolymer-based biomaterials, particularly for glycopolymers whose pendant carbohydrate residues have *cis*-1,2 or 1,3-diol motifs.

The synthesis of the open-chain carbohydrate-derived methacrylamide monomer depicted in its polymeric form in Figure 5.1 is facilitated by the difference in reactivity between the OH and hemiacetal groups of galactose and necessitates no protecting group manipulations. Access to pyranoside- or sugar alcohol-derived polymerizable monomers, however, must be achieved using protection/deprotection[206] or chemoenzymatic approaches.[207] We hoped to use borinic acids' capabilities in differentiating between OH groups to selectively monofunctionalize galactopyranoside derivatives to establish a simple synthetic route to OH-functional methacrylate monomers that could then be used to prepare a variety of glycopolymers *via* controlled chain growth polymerization. In addition, we wanted to carry out a proof-of-concept demonstration of the utility of these new glycopolymers with pendant triols capable of forming reversible covalent cross-links with boron species.

---

[205] Deng, C. C.; Brooks, W. L. A.; Abboud, K. A.; Sumerlin, B. S. *ACS Macro Lett.* **2015**, *4*, 220–224.

[206] Chiellini, E.; Solaro, R.; Bemporad, L.; Antone, S. D.; Giannasi, D.; Leonardi, G.; Solaro, R.; Bemporad, L.; Antone, S. D.; Giannasi, D.; Leonardi, G. *J. Biomater. Sci. Polym. Ed.* **2012**, *7*, 307–328.

[207] Martin, B. D.; Ampofo, S. A.; Linhardt, R. J.; Dordick, J. S. *Macromolecules* **1992**, *25*, 7081–7085.

3.2 Monomer Synthesis

The synthesis of monofunctionalized glycoside end-group models (see Chapter 3, section 3.3) as well as work on selective O-3 sulfations of galactopyranosides[128] served as entry points for the single-step preparation of **5.05** (Scheme 5.4). Using **1.02** as catalyst, the acrylation was carried out at room temperature using DIPEA as the base and acetonitrile as the solvent, producing monomers **5.06**–**5.08** in acceptable yields. Flash column chromatography was used to purify the monomers, with product decomposition being an issue.

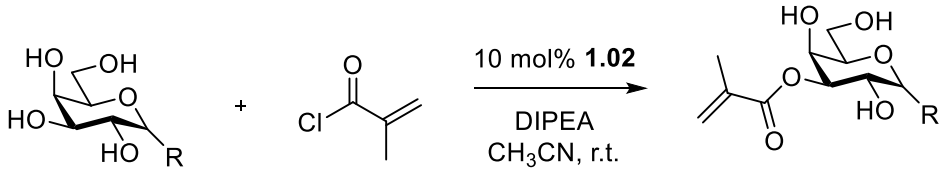

Scheme 5.4 Acrylation of galactose derivatives using a borinic acid catalyst.

3.3 RAFT Polymerization

5.07 was polymerized using azobisisobutyronitrile (AIBN) as an initiator, DMF as the solvent, and the RAFT chain-transfer agent depicted in Scheme 5.5, **5.09**. Poly(**5.07**) was obtained in 30–50% yield with M_n spanning 4.7–9.7 kDa depending on the monomer-to-initiator ratio, and a Đ of 1.3–1.6 as determined by GPC in NMP at 80 °C relative to PMMA standards. Some discrepancies between the degrees of polymerization obtained from ^{1}H NMR and GPC were noted; the use of more reliable NMR end-group analysis techniques would be a next step.

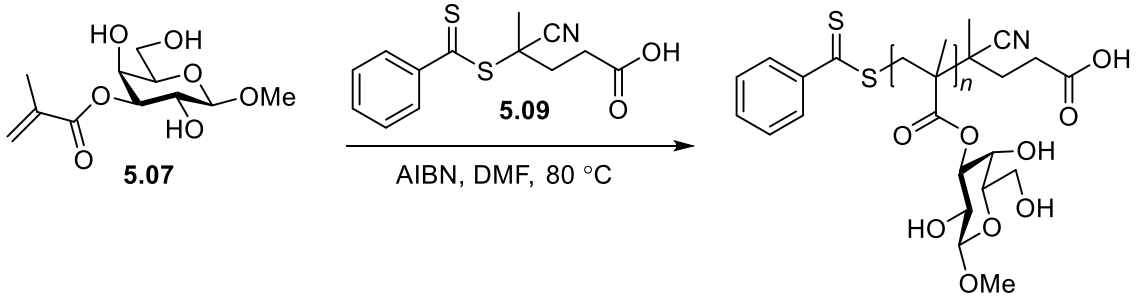

Scheme 5.5 RAFT polymerization of **5.07** to yield poly(**5.07**).

3.4 Hydrogel Formation

Attempts at introducing cross-links into the system by combining poly(**5.07**) with boric acid in an aqueous solution of pH 8–10.5 were not successful in producing a hydrogel. This was ascribed to the high strain at the boron center of the proposed cross-link as shown in Figure 5.2. Instead, a two-polymer system was used, with poly(4-vinylphenylboronic acid) (PVPBA) being used as the cross-linking agent. A successful gel inversion test indicated that poly(**5.07**) and PVPBA formed a cross-linked hydrogel when combined at a concentration of 6 mol% of each polymer in a 2M NaOH solution.

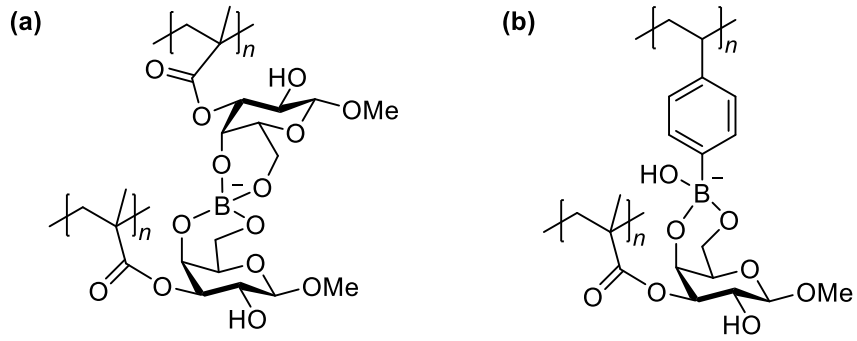

Figure 5.2 (a) Proposed boric acid-cross-linked hydrogel. (b) Hydrogel formed using poly(**5.07**) and PVPBA under basic conditions.

3.5 Outlook

Methacrylate monomers derived from galactose were obtained in one step using borinic acid catalysis, enabling the synthesis of novel glycopolymers with pendant boron-binding carbohydrate motifs. The formation of a hydrogel with a polyacrylate with pendant boronic acid groups in alkaline solution validated the functionality of the pendant sugar residues. An improved monitoring of the polymerization may be needed to obtain accurate degrees of polymerization. Carrying out a *bis*-methacrylation to provide tetrafunctional galactoside-derived cross-linking agents would in all likeliness be facile. Other further work could involve acylation of pyranosides with other polymerizable groups, including those that can undergo ring-opening

metathesis polymerization,[208,209] extending the range of possibilities of this class of polymers to nanoscale self-assembly.

4 Conclusion

We have shown that borinic acid catalysts grant access to a variety of new and interesting carbohydrate-derived macromolecules by (1) directly promoting the formation of linear polymers from triols and tetraols by effectively imparting them with diol-like reactivity and (2) enabling the synthesis of sugar-derived monomers without recourse to protecting group chemistry. Previously unknown poly(pyranoside ester)s obtained using route (1) were studied from the standpoint of their physical properties, degradability and biocompatibility, revealing that they show promise as biomaterials. Notably, the nature of the protecting group at the anomeric position was shown to influence polymer properties, suggesting their thermal and degradation behaviour can be modulated through structural variation at this position. Future work could include (1) expanding the scope of anomeric protecting groups and diacyl comonomers, (2) addressing the Flory–Huggins parameters likely responsible for the limited rate of polymerization for the pyranoside series, (3) characterizing the morphology of the polymers and establishing the structure–property relationships governing crystallinity, and (4) further exploring the interactions of these novel polymers with living systems.

---

[208] Debsharma, T.; Behrendt, F. N.; Laschewsky, A.; Schlaad, H. *Angew. Chemie Int. Ed.* **2019**, 1–5.

[209] Graham, B.; Fayter, A. E. R.; Houston, J. E.; Evans, R. C.; Gibson, M. I. *J. Am. Chem. Soc.* **2018**, *140*, 5682–5685.

Appendices

1 NMR Spectra for Title Compounds

1.1 Chapter 2

^{1}H NMR (500 MHz, DMSO-d_6) Poly(glycerol sebacate) (PGS)

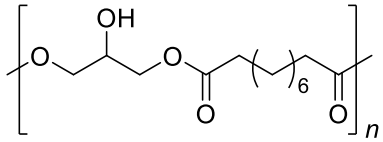

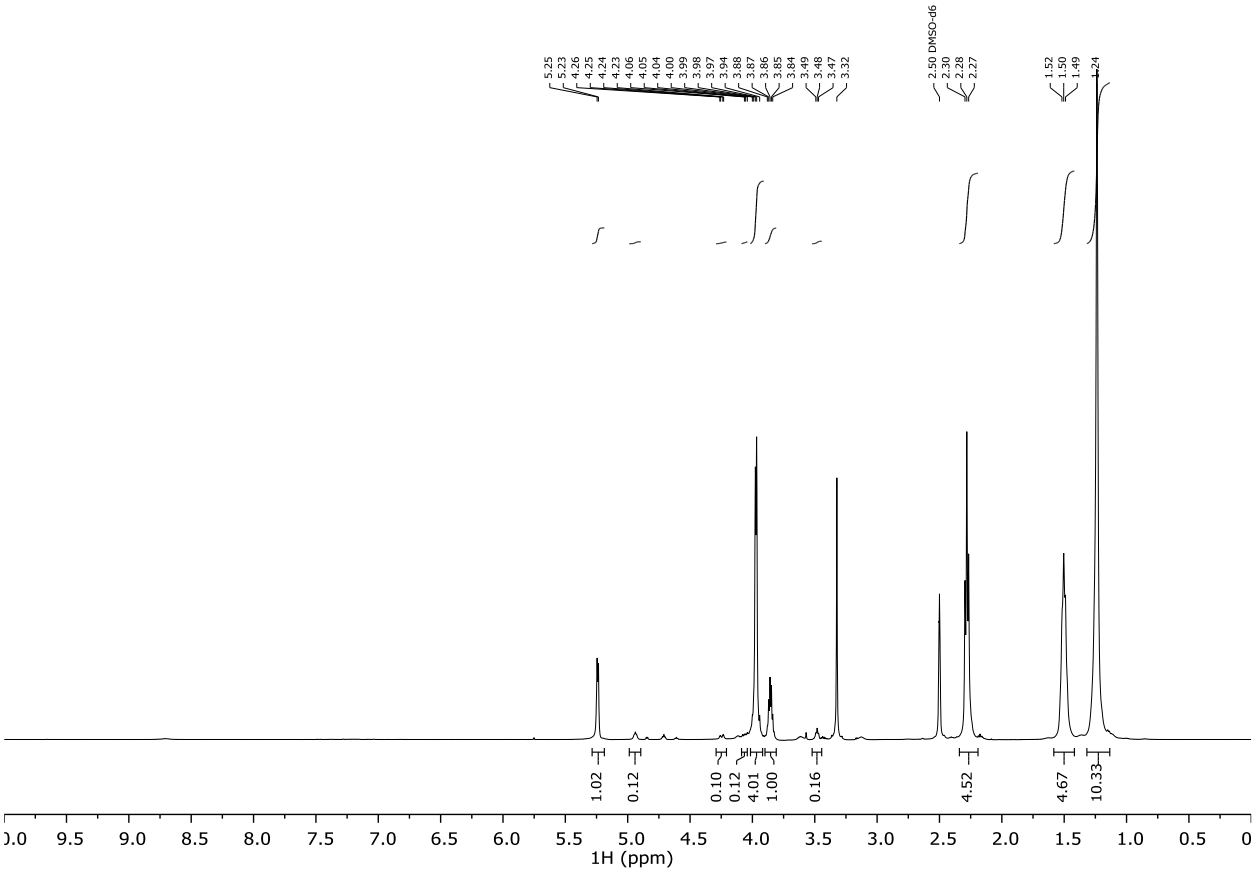

^{1}H NMR (500 MHz, DMSO-d_6) Poly(glycerol dodecanoate) (PGD)

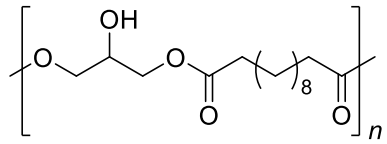

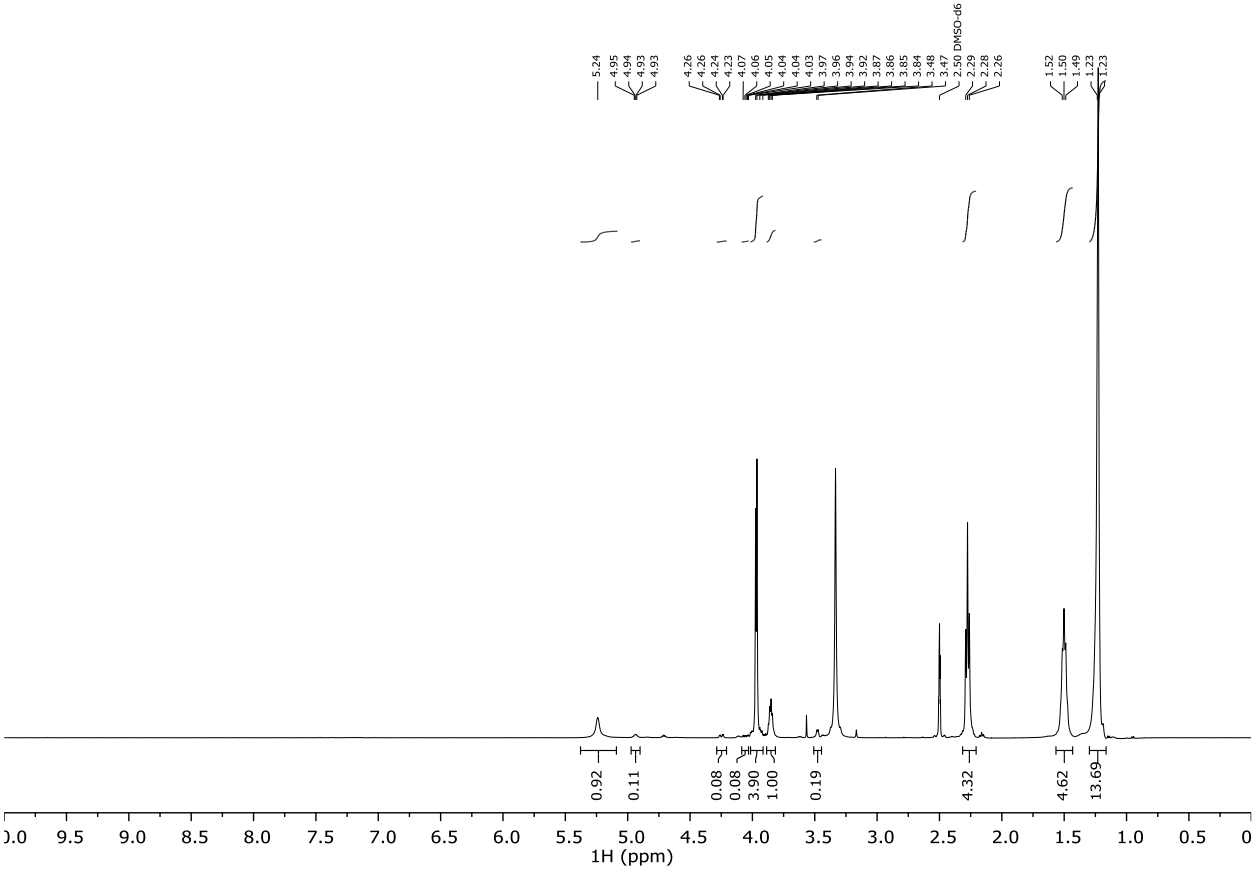

^{1}H NMR (500 MHz, DMSO-d_6) Poly(glycerol adipate) (PGA)

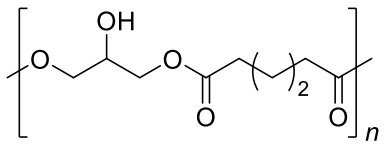

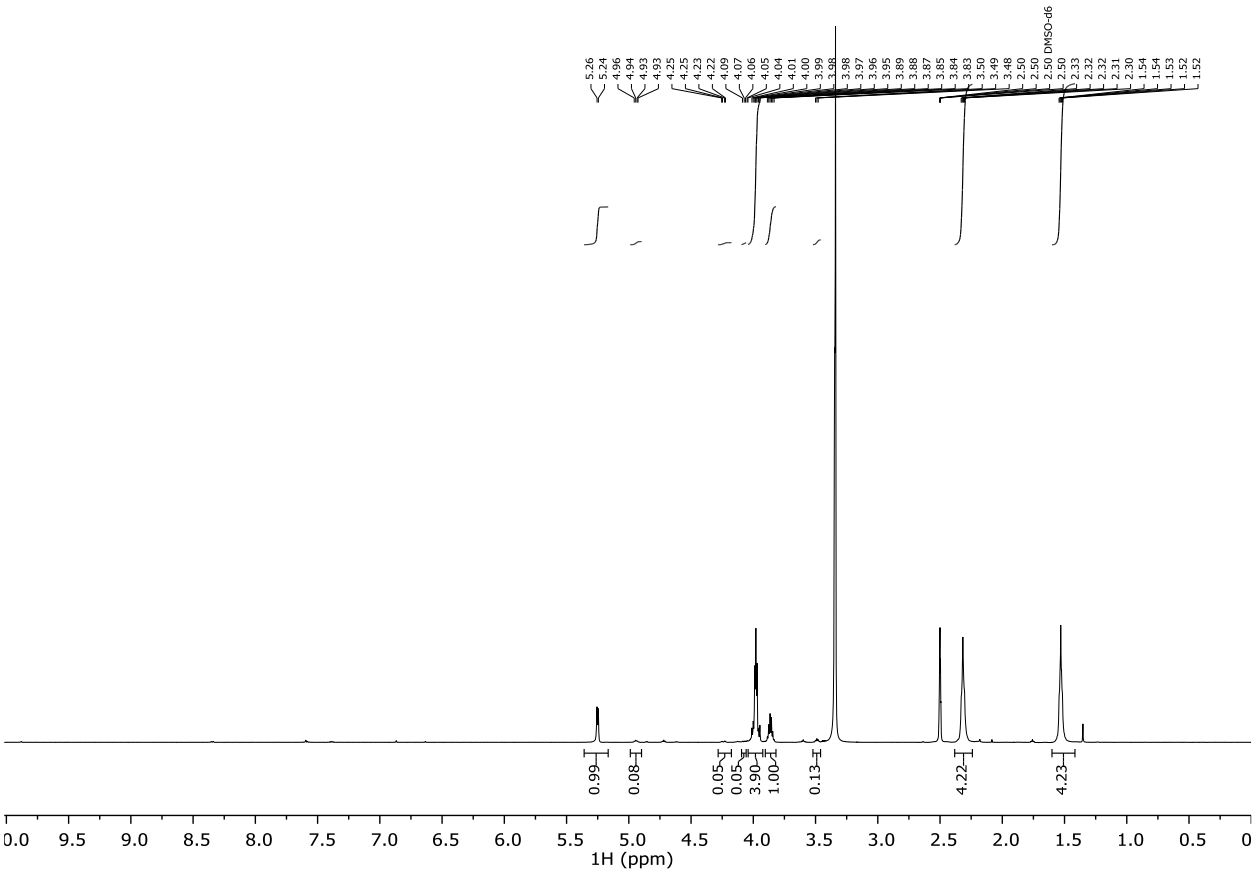

^{1}H NMR (500 MHz, DMSO-d_6) Poly(glycerol isophthalate) (PGI)

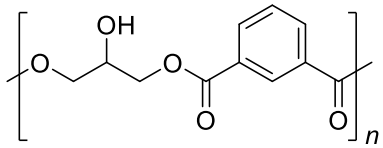

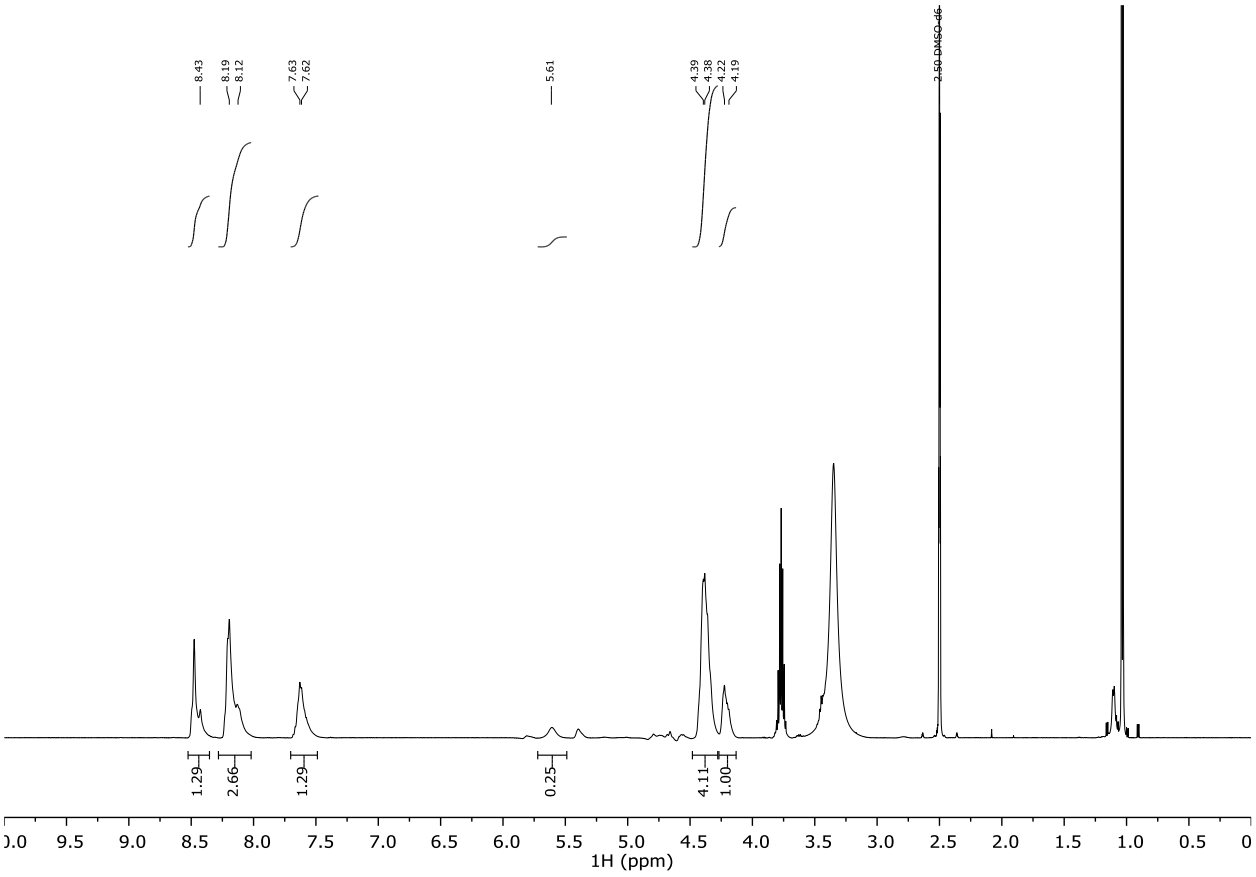

^{1}H NMR (500 MHz, DMSO-d_6) Poly(glycerol terephthalate) (PGT)

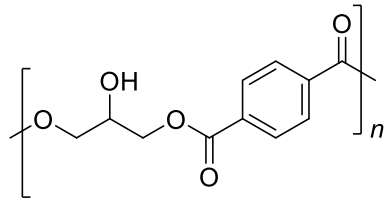

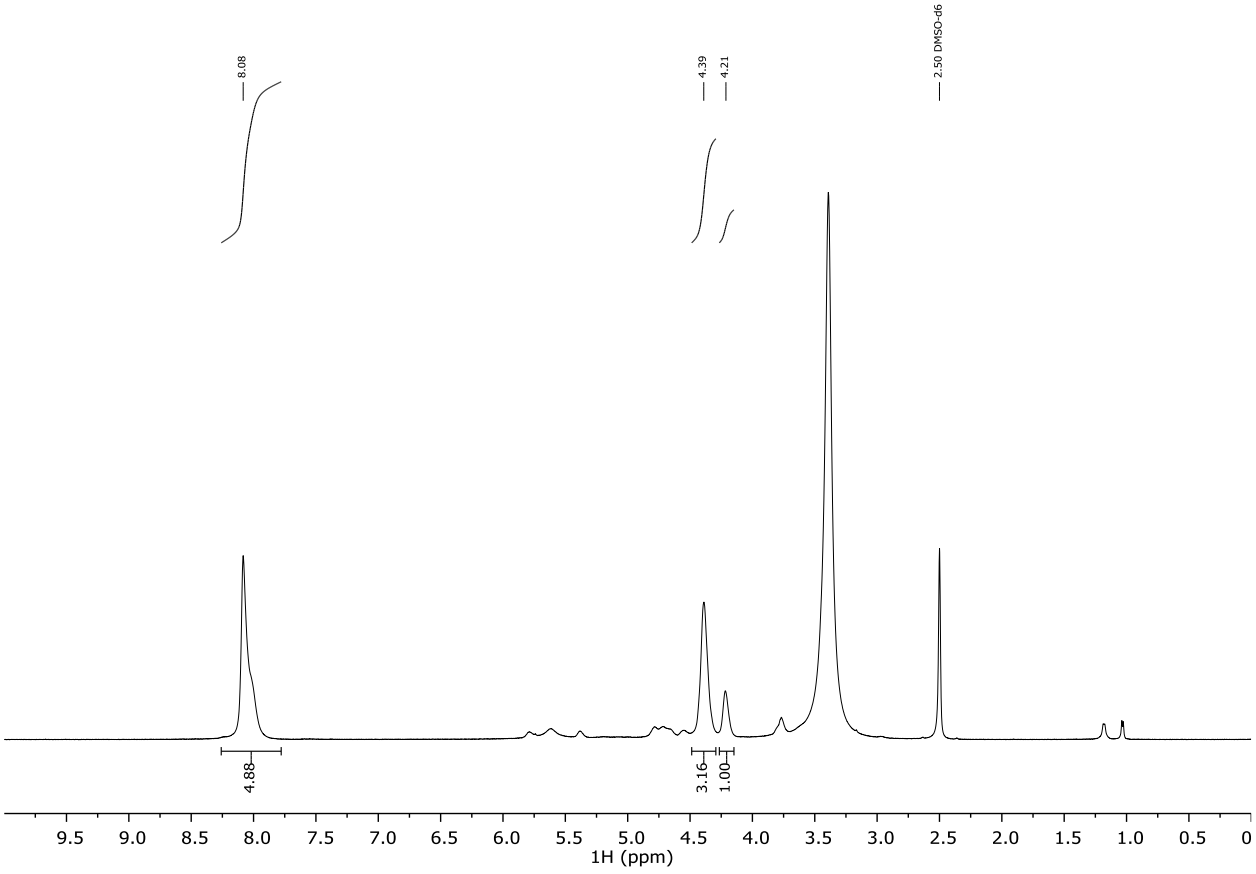

^{1}H NMR (500 MHz, DMSO-d_6) *O*-acetyl poly(glycerol sebacate)

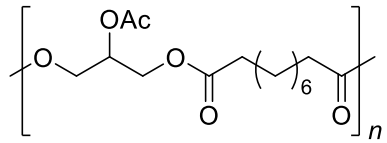

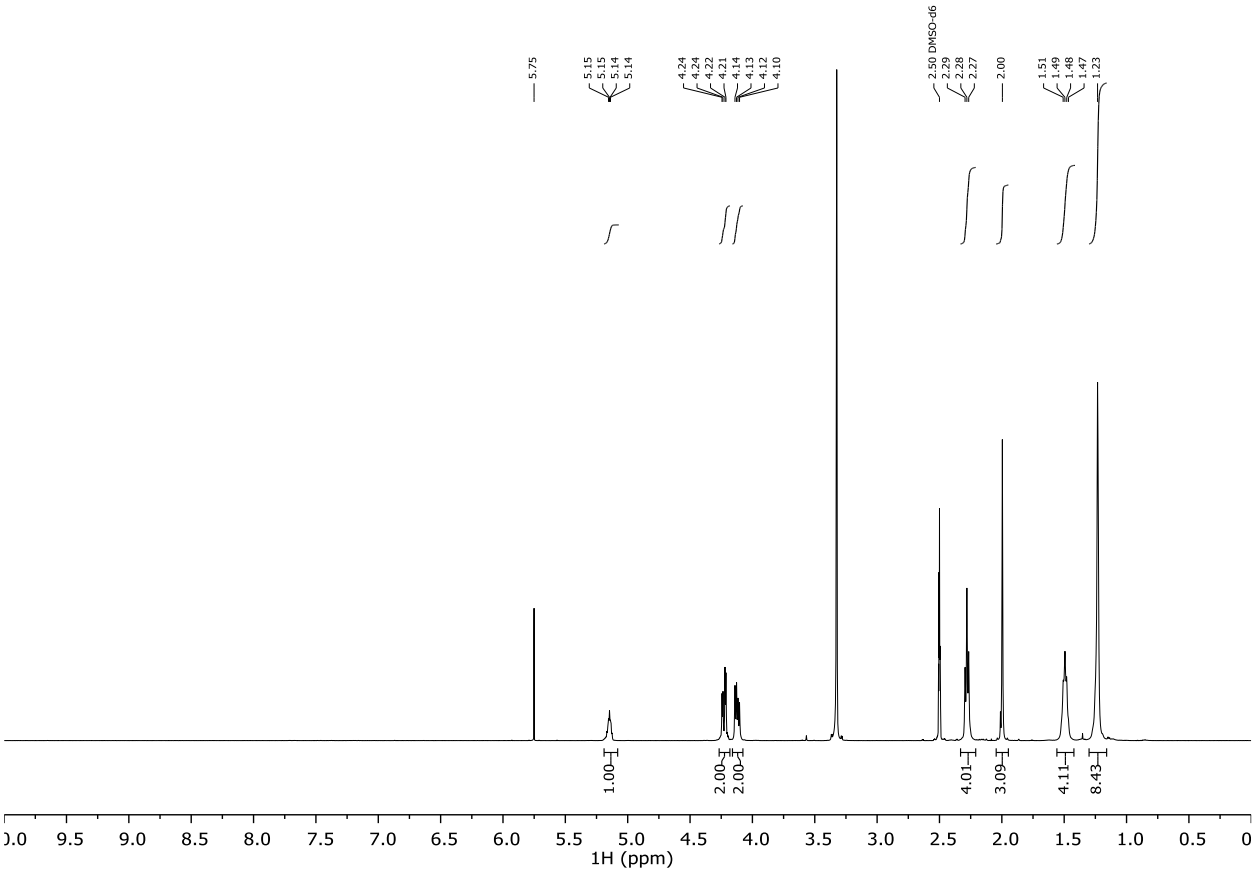

^{1}H NMR (500 MHz, DMSO-d_6) *O*-acetyl poly(glycerol dodecanoate)

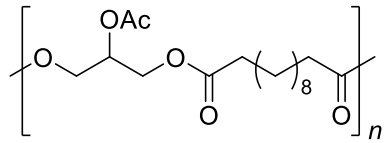

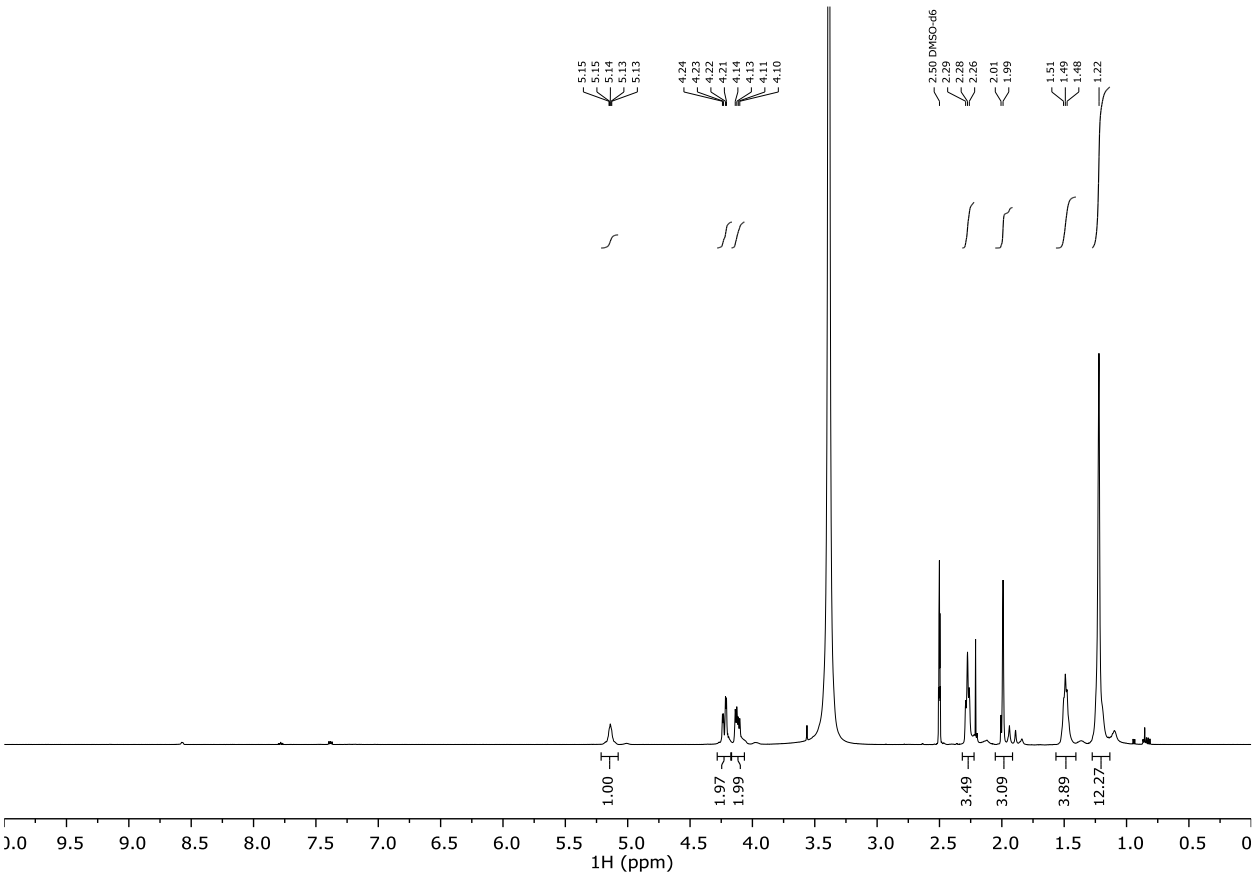

^{1}H NMR (500 MHz, DMSO-d_6) *O*-acetyl poly(glycerol adipate)

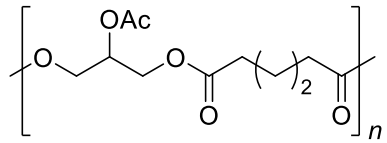

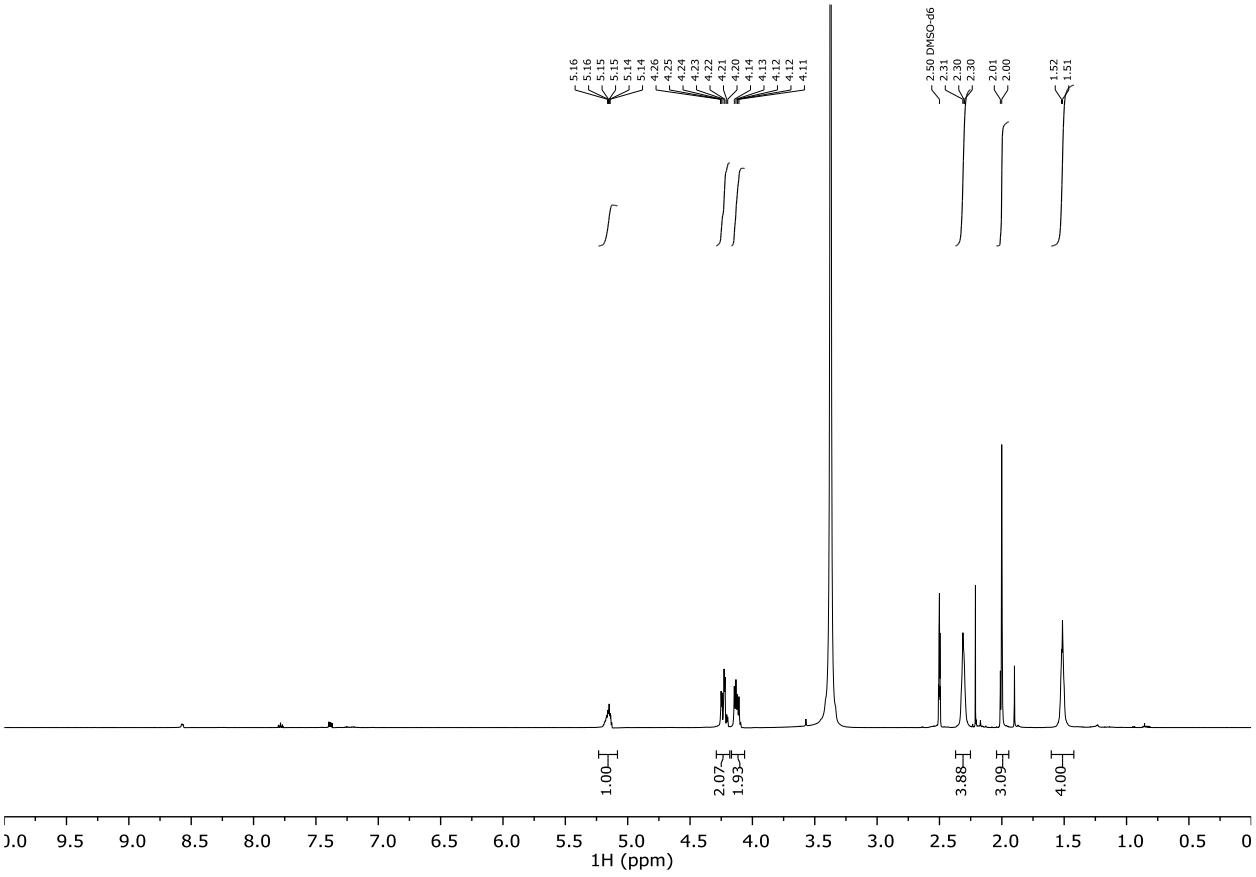

^{1}H NMR (500 MHz, DMSO-d_6) *O*-acetyl poly(glycerol isophthalate)

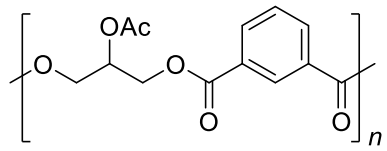

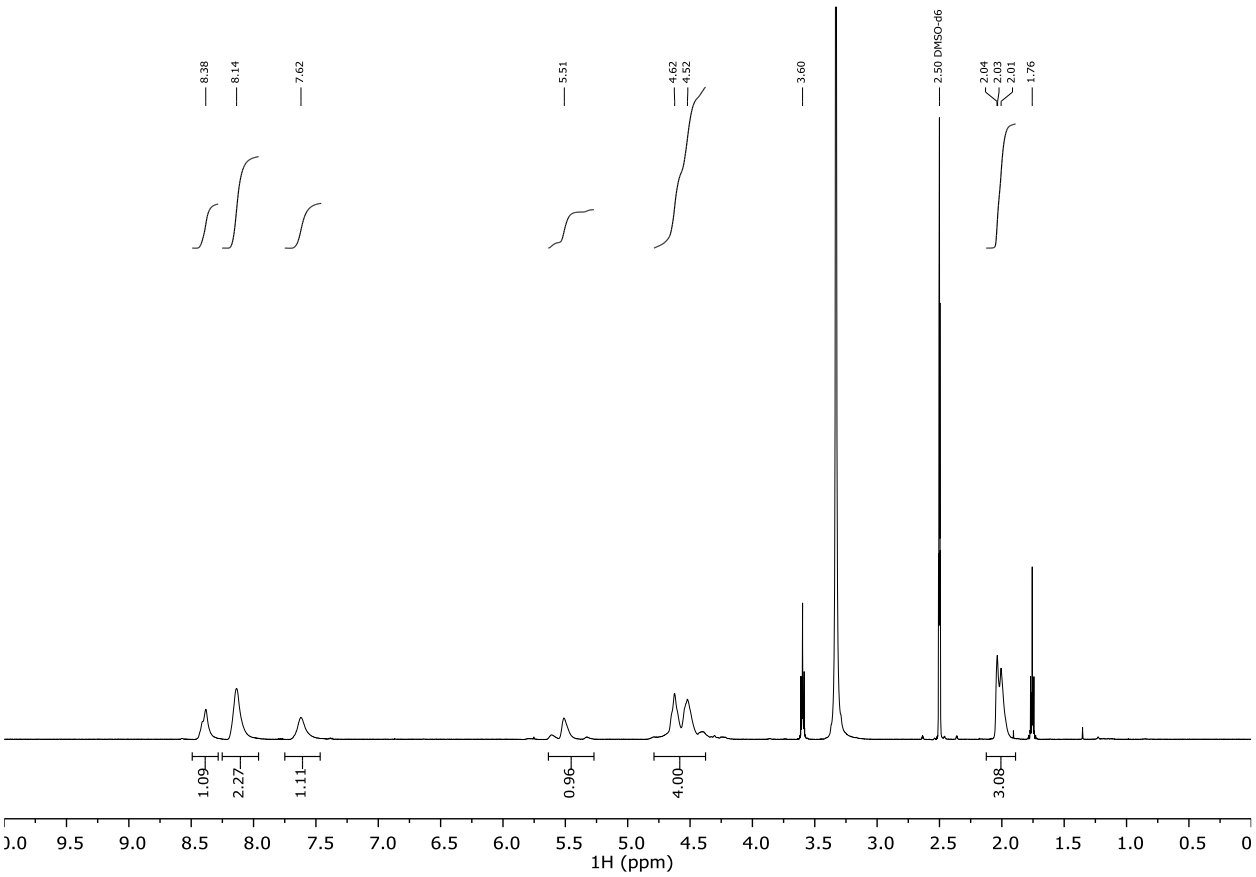

^{1}H NMR (500 MHz, DMSO-d_6) *O*-acetyl poly(glycerol terephthalate)

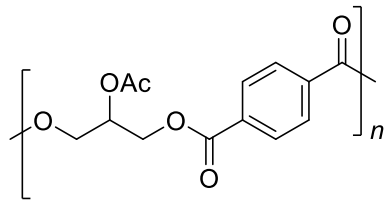

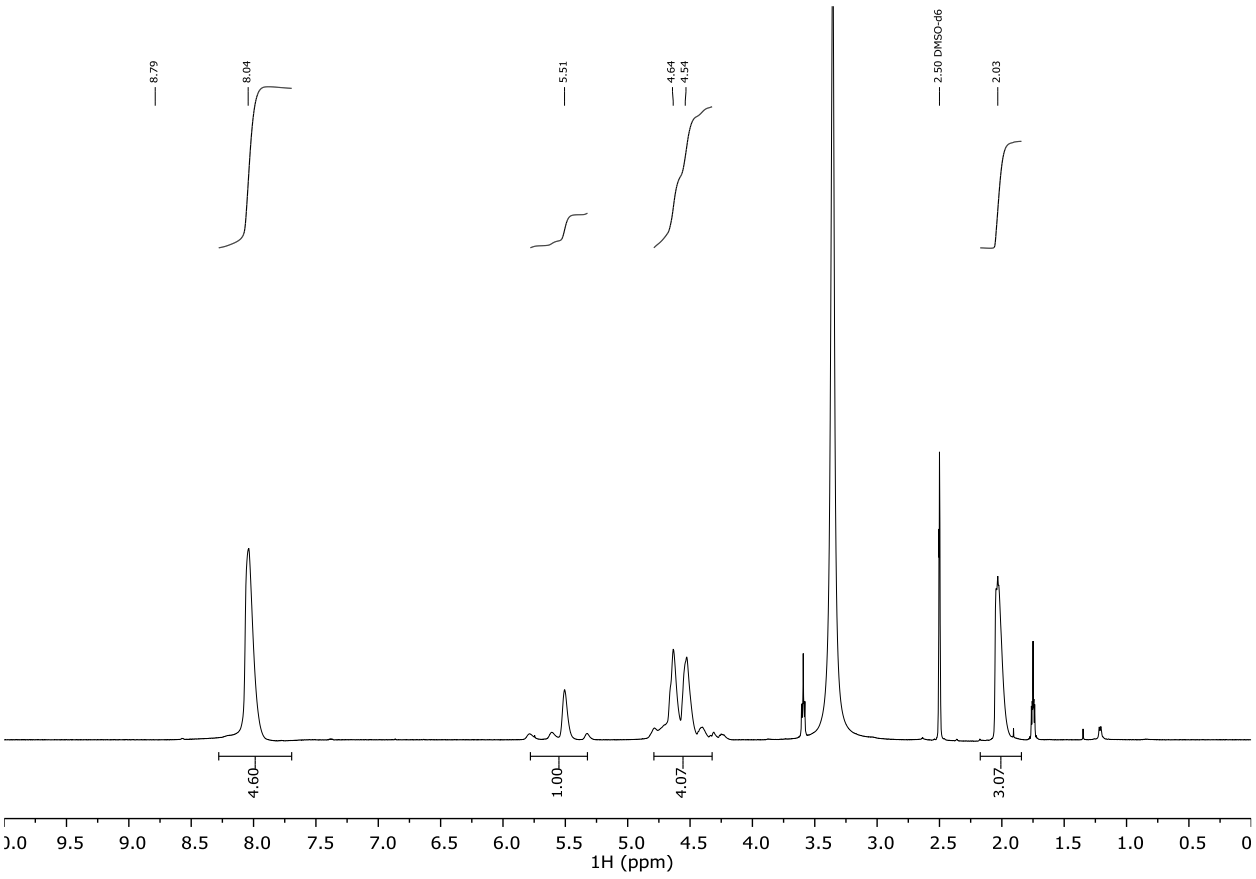

^{1}H NMR (500 MHz, $CDCl_3$) Poly(glycerol sebacate) Fmoc glycinate

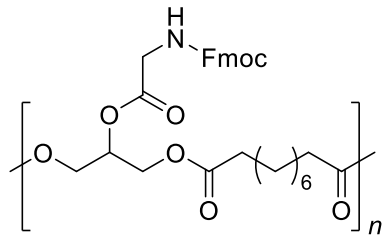

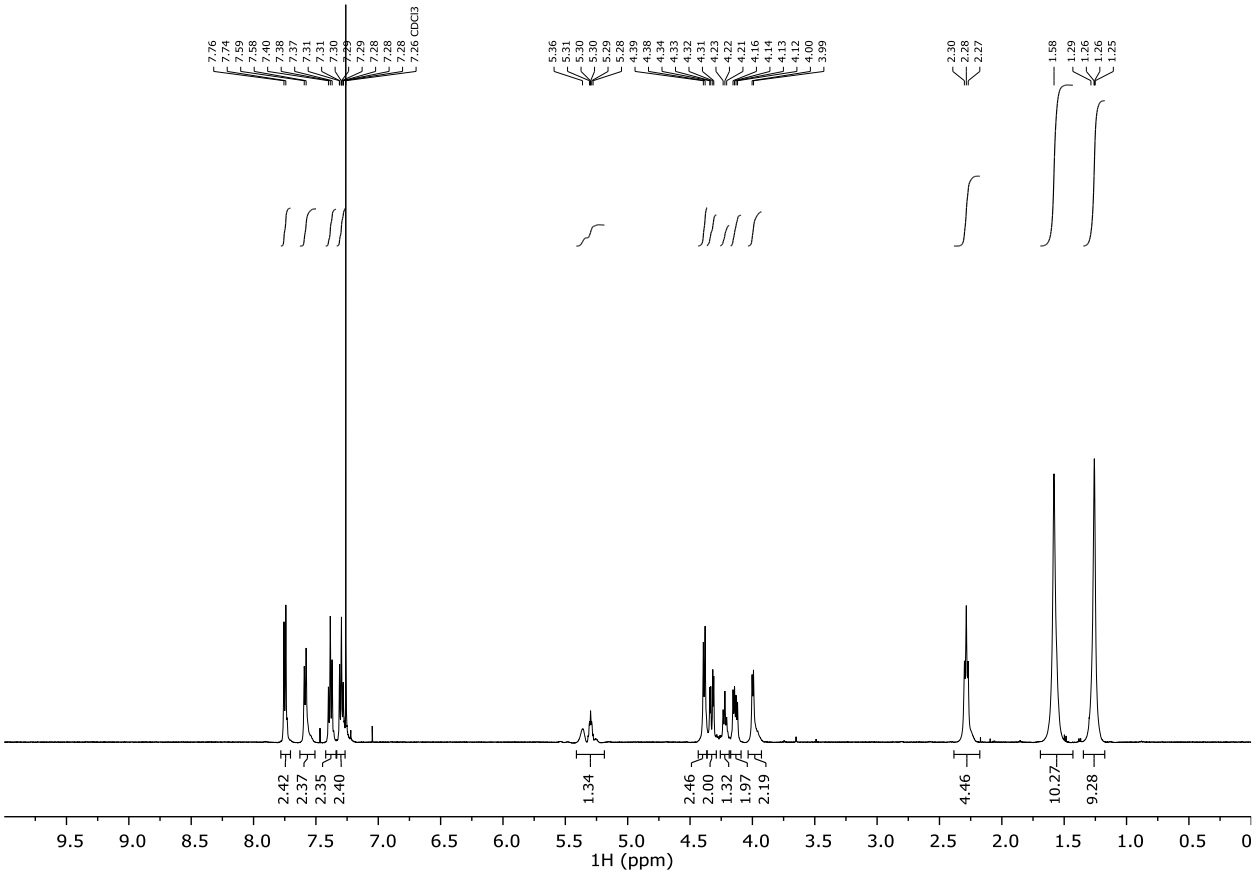

1.1.1 Quantitative ^{13}C NMR

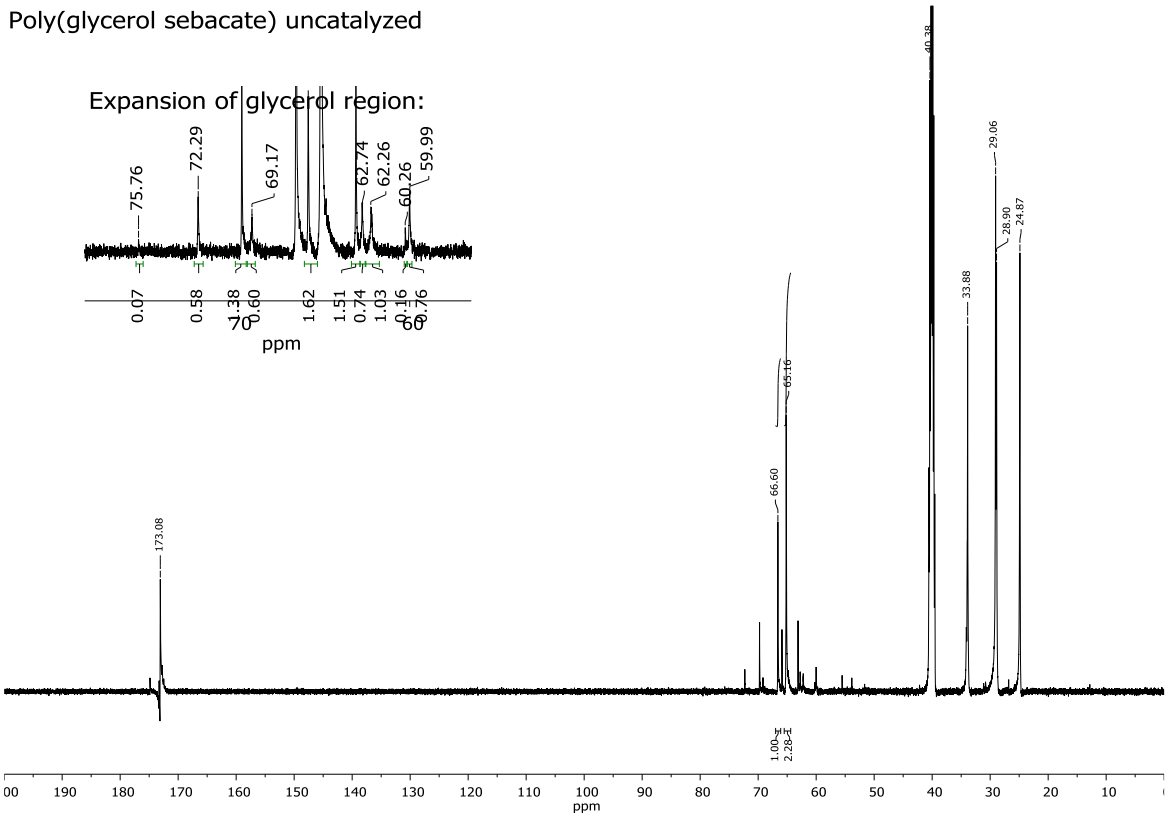

Poly(glycerol sebacate) 1 mol% 1.01

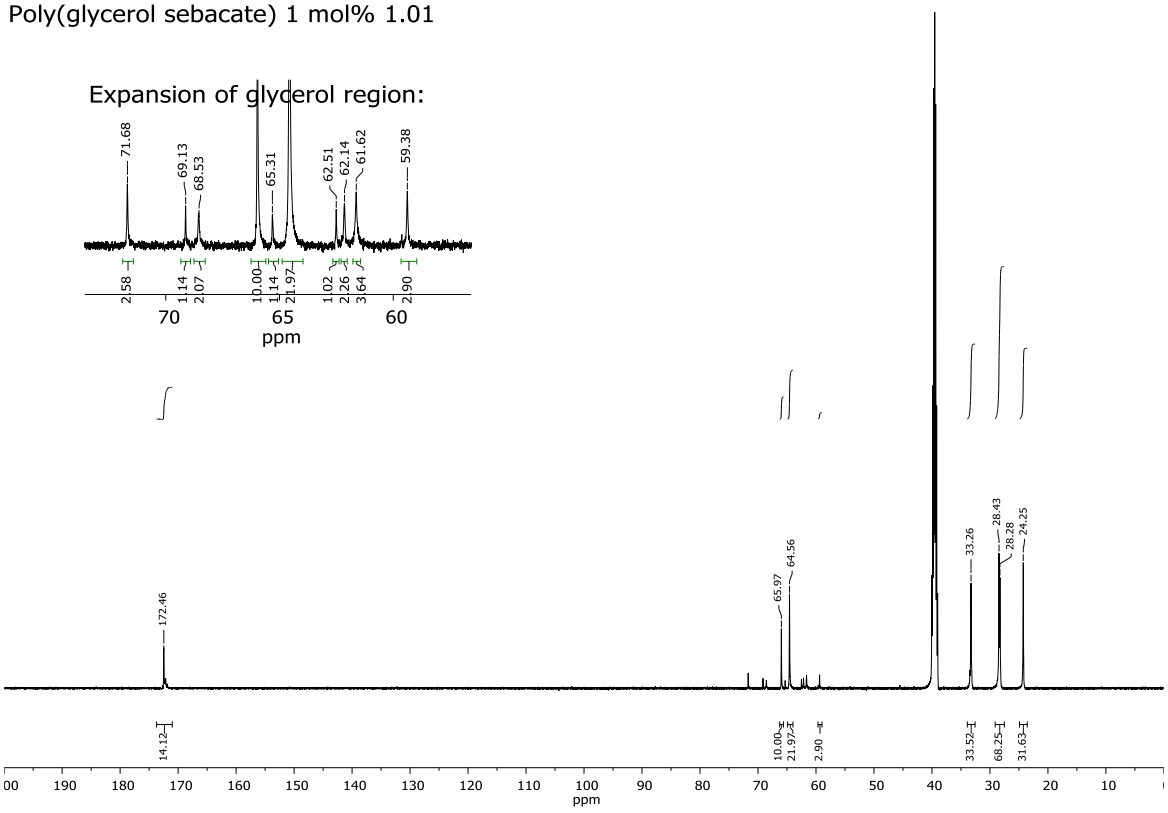

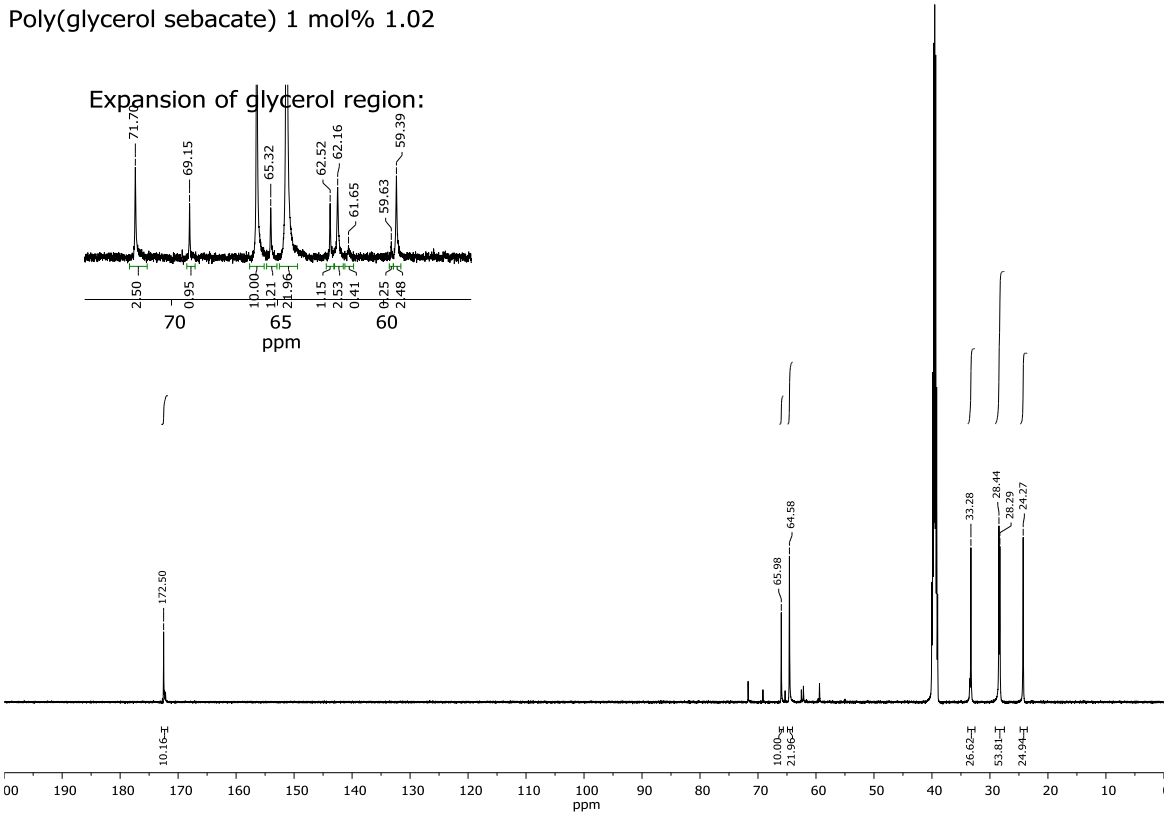
Poly(glycerol sebacate) 1 mol% 1.02
Expansion of glycerol region:
71.76
69.15
65.32
62.52
62.16
61.65
59.63
59.39
2.50
0.95
10.00
1.21
21.96
1.15
2.53
0.41
0.25
2.48
70
65
60
ppm
172.50
65.98
64.58
33.28
28.44
28.29
24.27
10.16
10.00
21.96
26.62
53.81
24.94
ppm

Poly(glycerol sebacate) 1 mol% 1.03

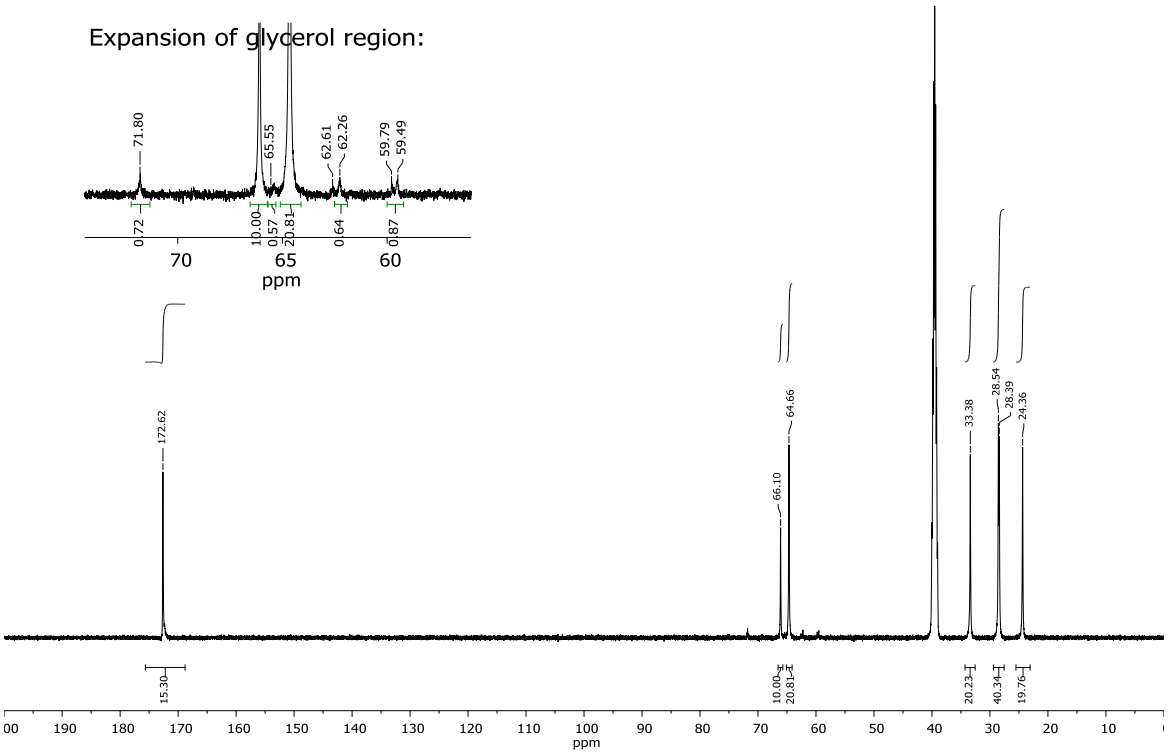

Poly(glycerol dodecanoate)

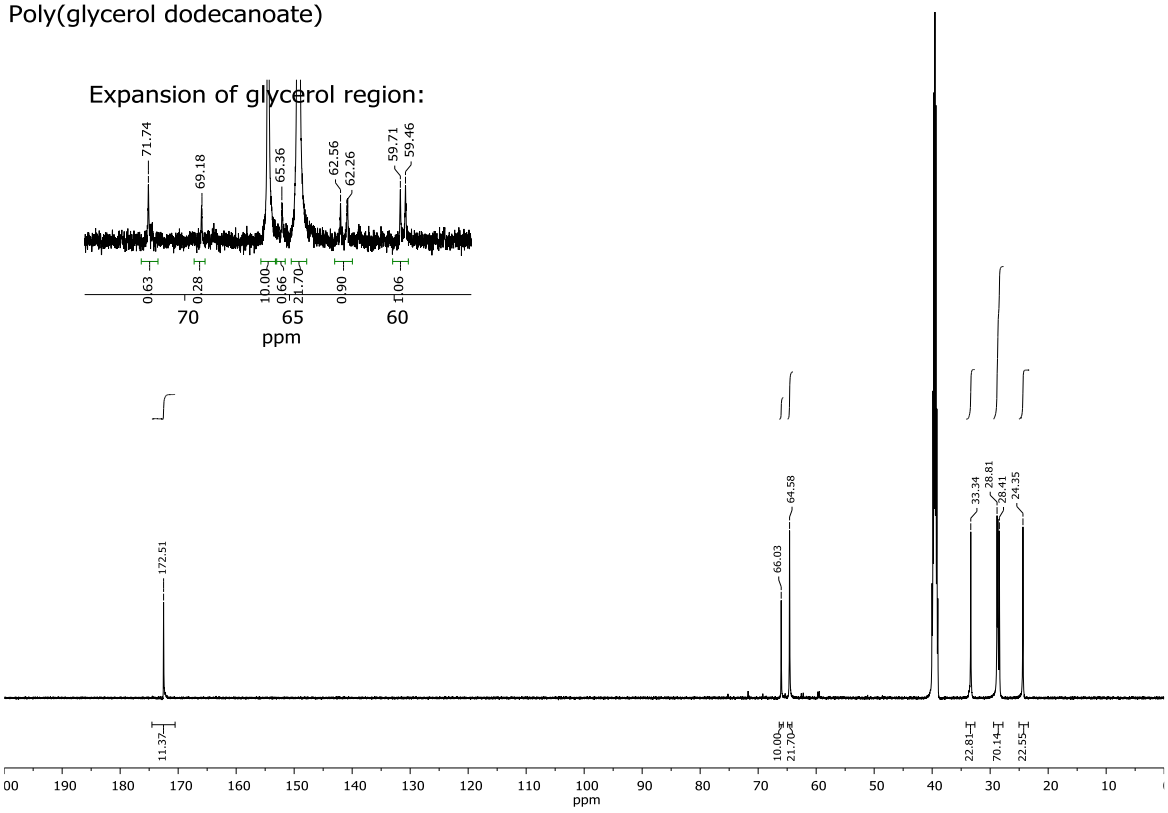

Poly(glycerol adipate)

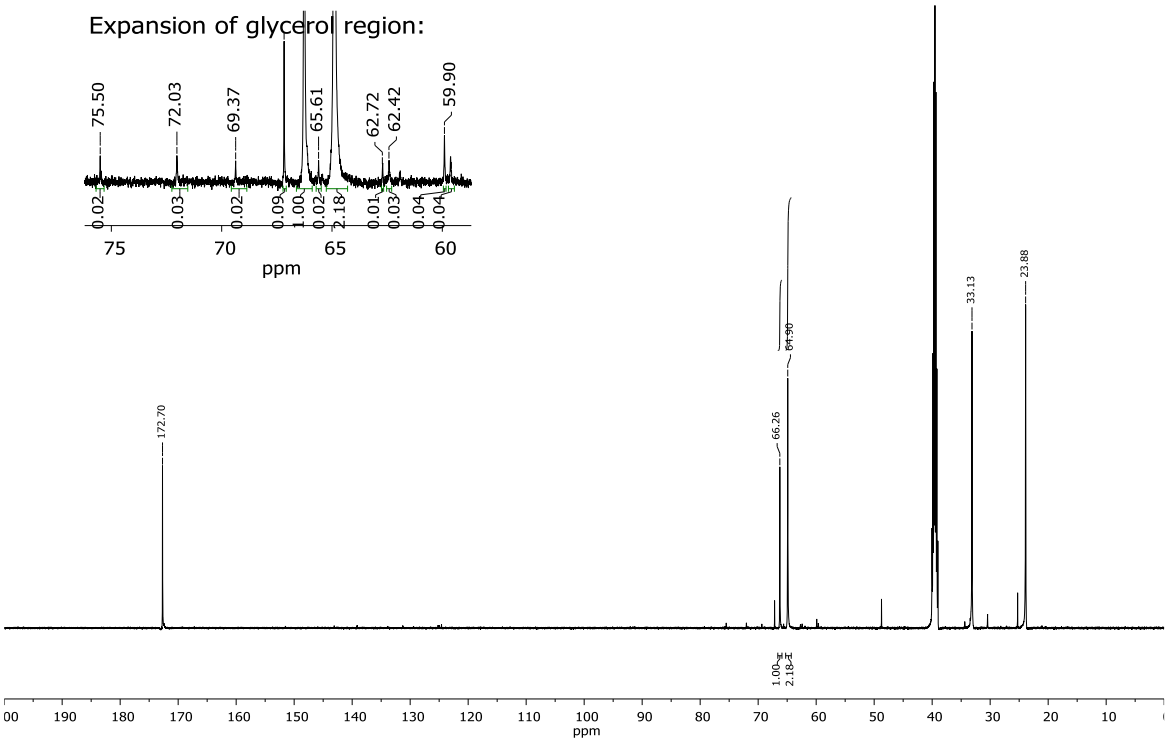

Poly(glycerol isophthalate)

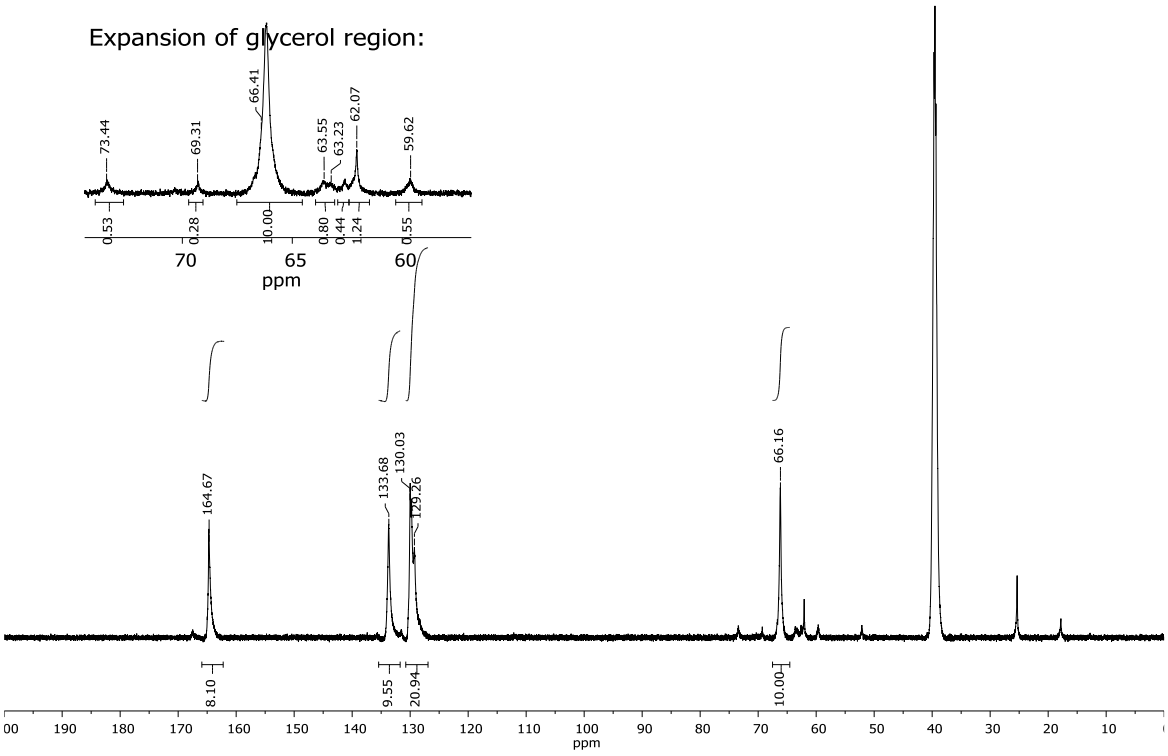

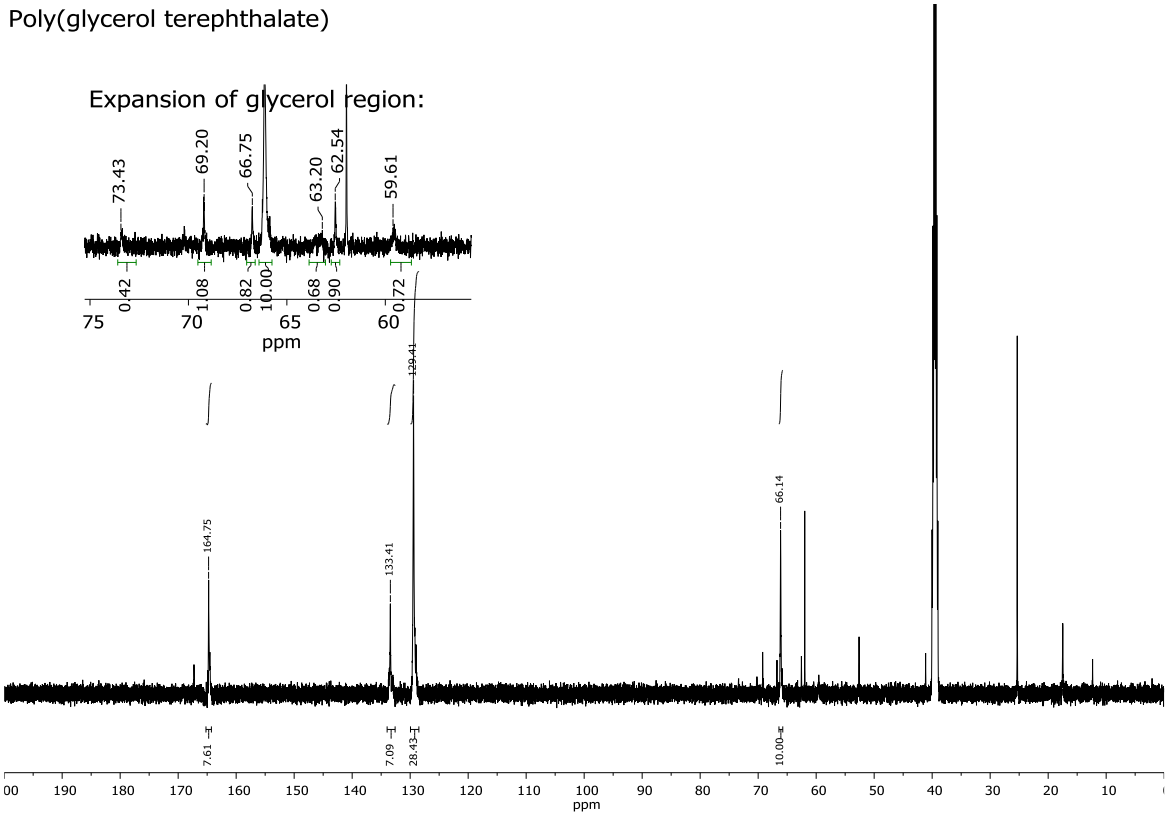
Poly(glycerol terephthalate)
Expansion of glycerol region:
73.43
69.20
66.75
63.20
62.54
59.61
0.42
1.08
0.82
10.00
0.68
0.90
0.72
75
70
65
60
ppm
129.41
164.75
133.41
66.14
7.61
7.09
28.43
10.00
ppm

1.2 Chapter 3

^{1}H NMR (500 MHz, $CDCl_3$) Ethyl 2,3,4,6 tetra-*O*-acetyl α-D-mannopyranoside

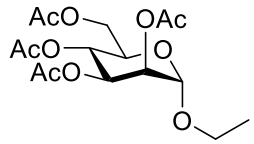

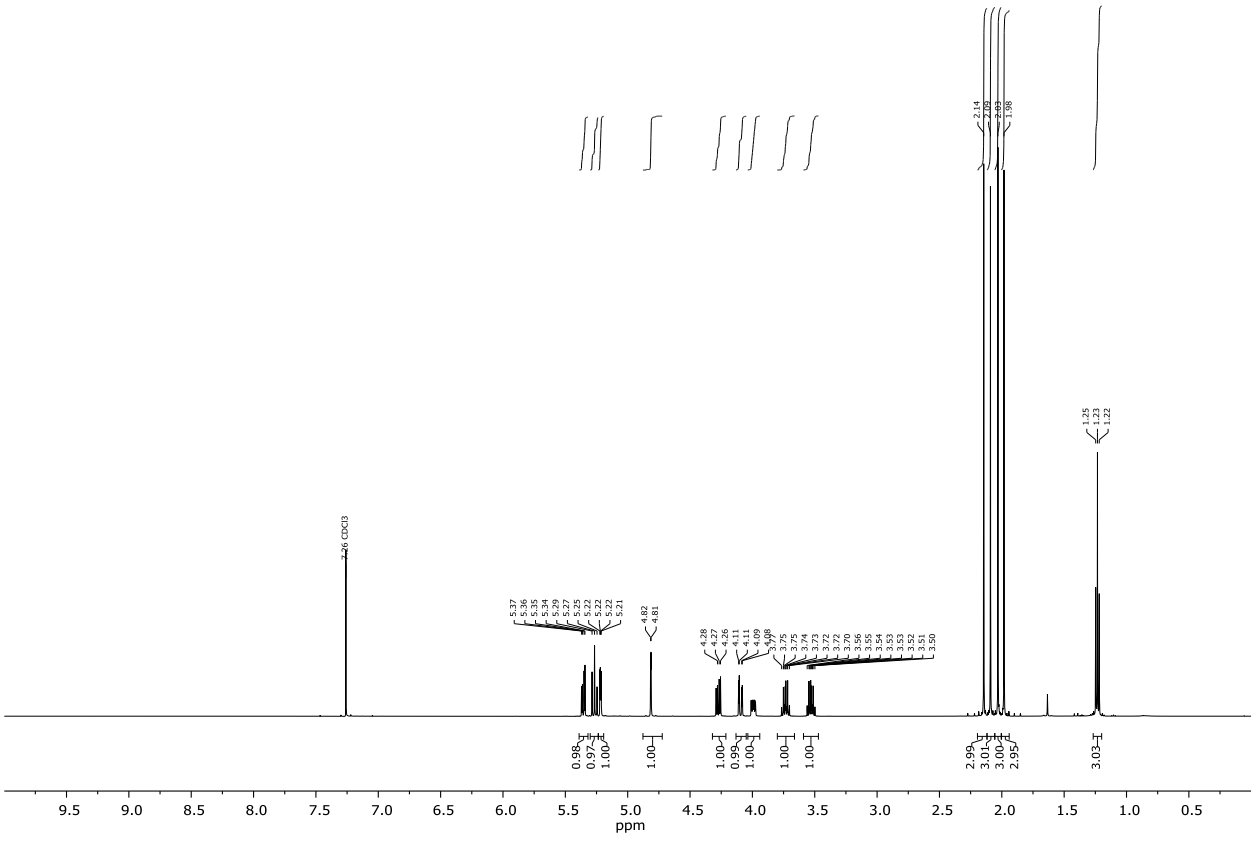

^{13}C NMR (126 MHz, $CDCl_3$) Ethyl 2,3,4,6-tetra-*O*-acetyl α-D-mannopyranoside

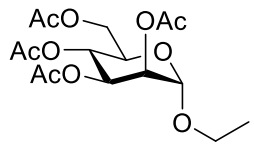

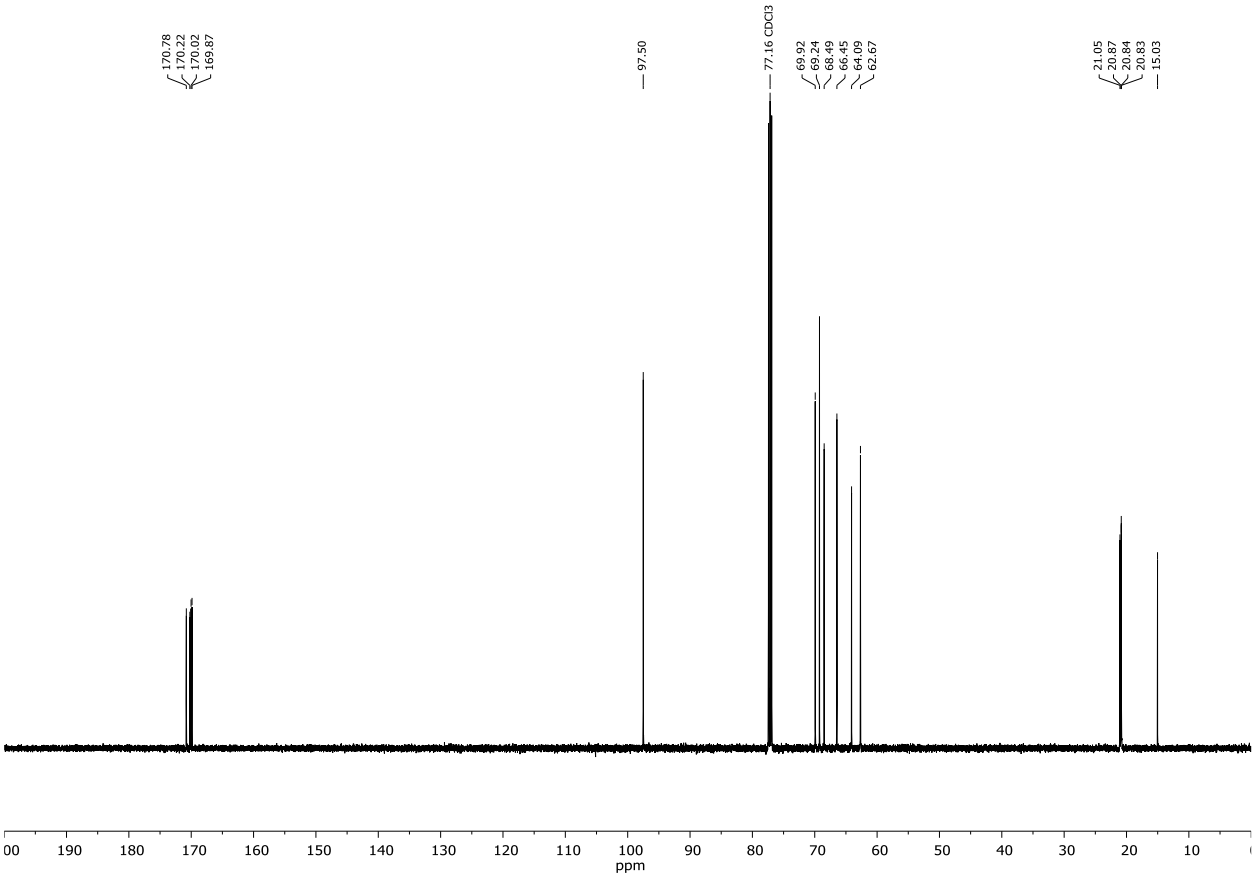

^{1}H-^{1}H COSY NMR (500 MHz, $CDCl_3$) Ethyl 2,3,4,6-tetra-*O*-acetyl α-D-mannopyranoside

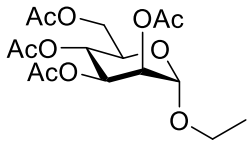

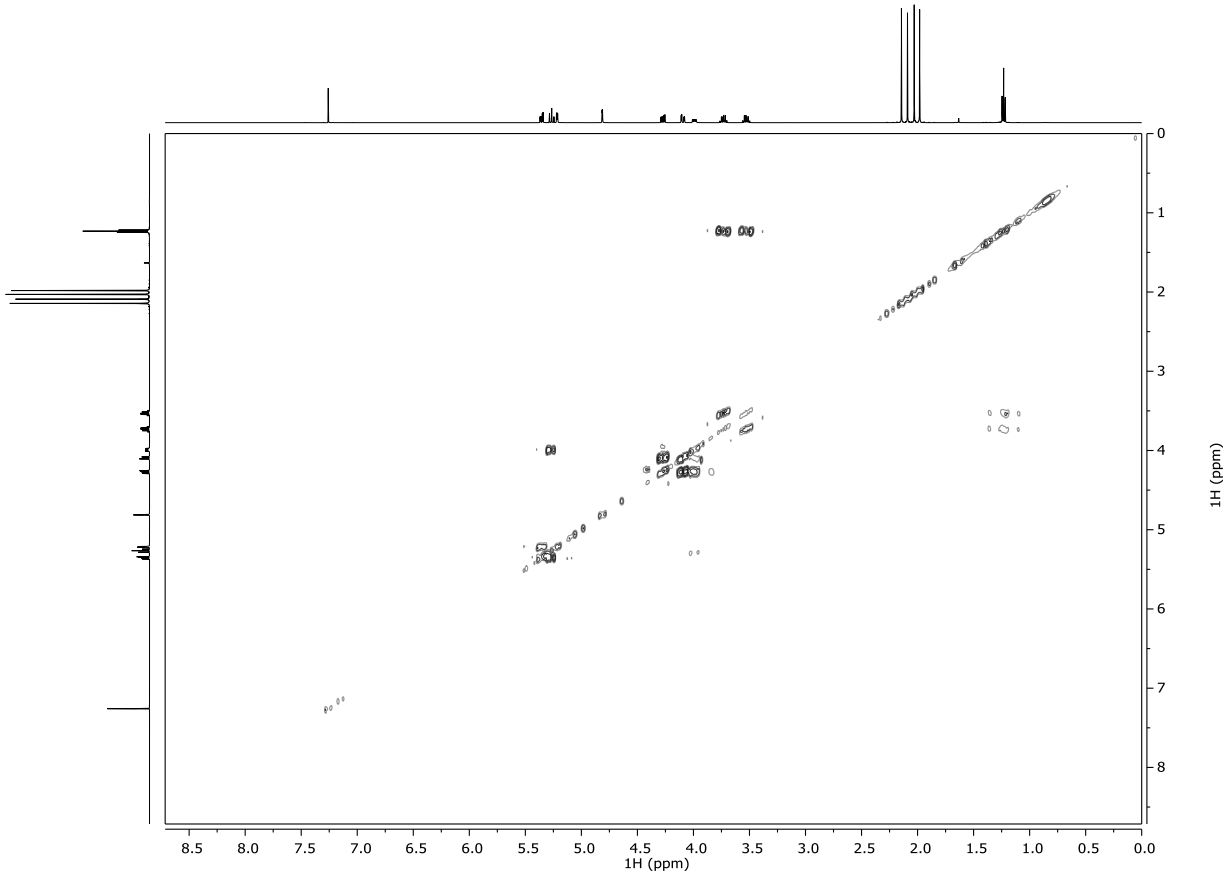

^{1}H-^{13}C HSQC NMR (500 MHz, $CDCl_3$) Ethyl 2,3,4,6-tetra-*O*-acetyl α-D-mannopyranoside

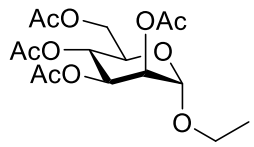

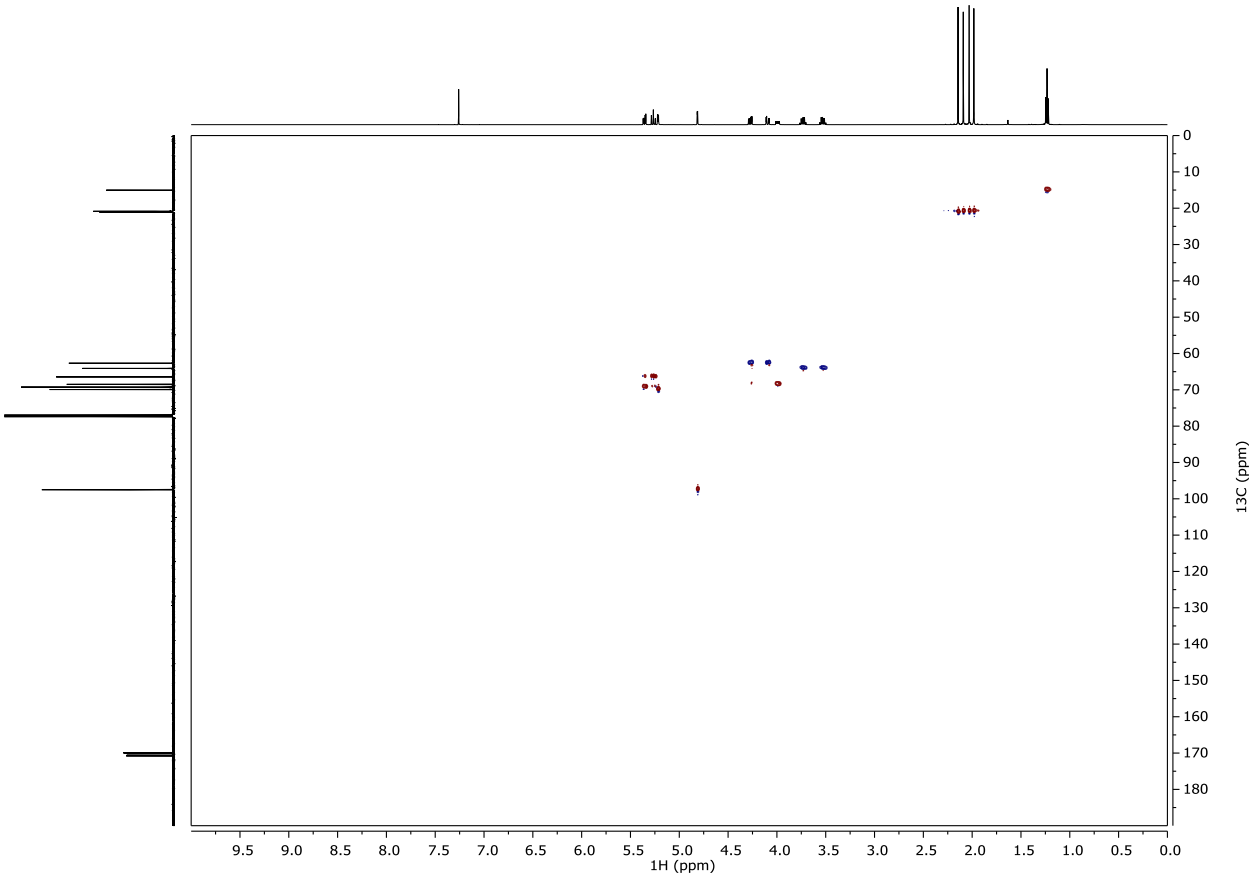

^{1}H-^{13}C HMBC NMR (500 MHz, $CDCl_3$) Ethyl 2,3,4,6-tetra-*O*-acetyl α-D-mannopyranoside

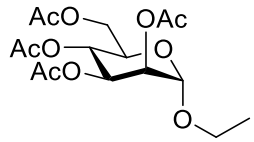

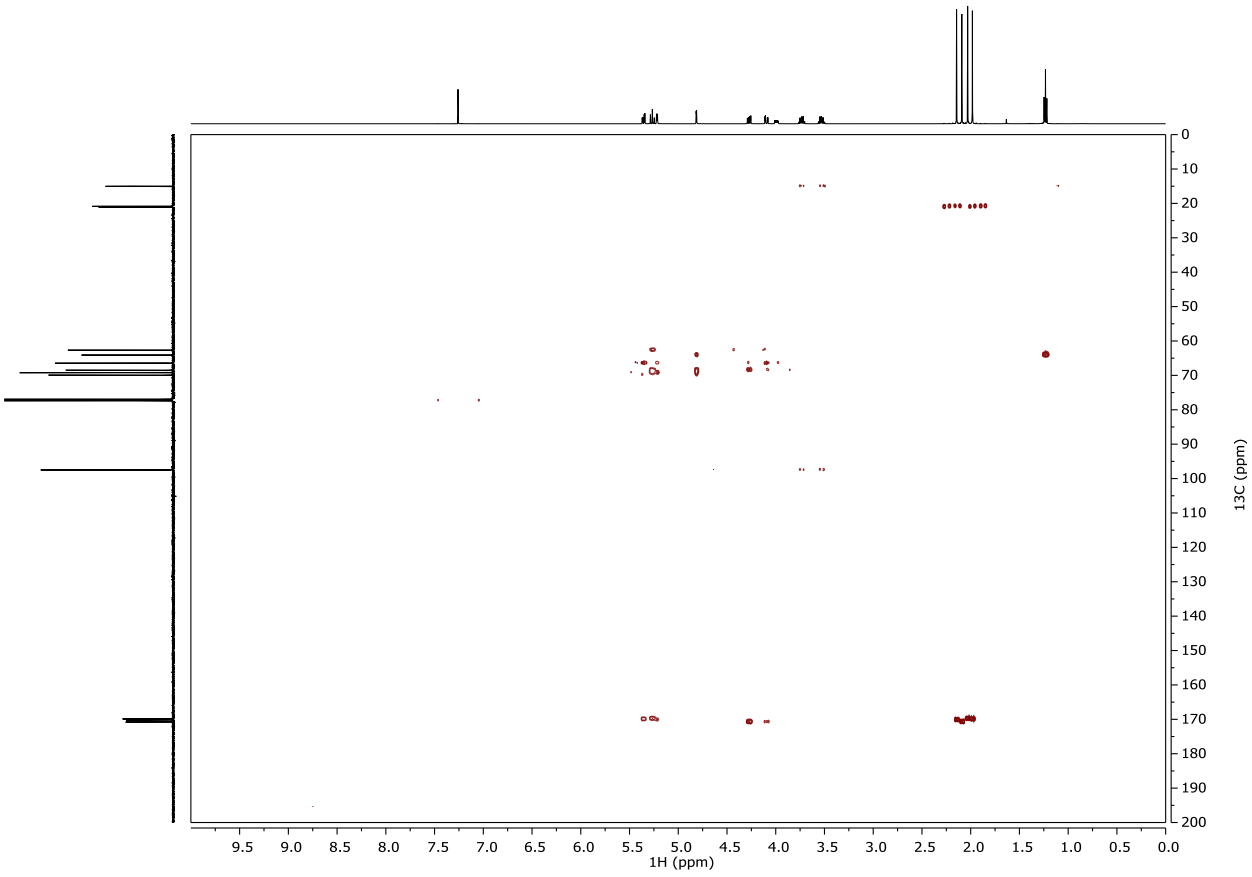

^{1}H NMR (500 MHz, DMSO-d_6) Ethyl α-D-mannopyranoside

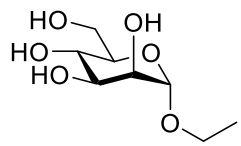

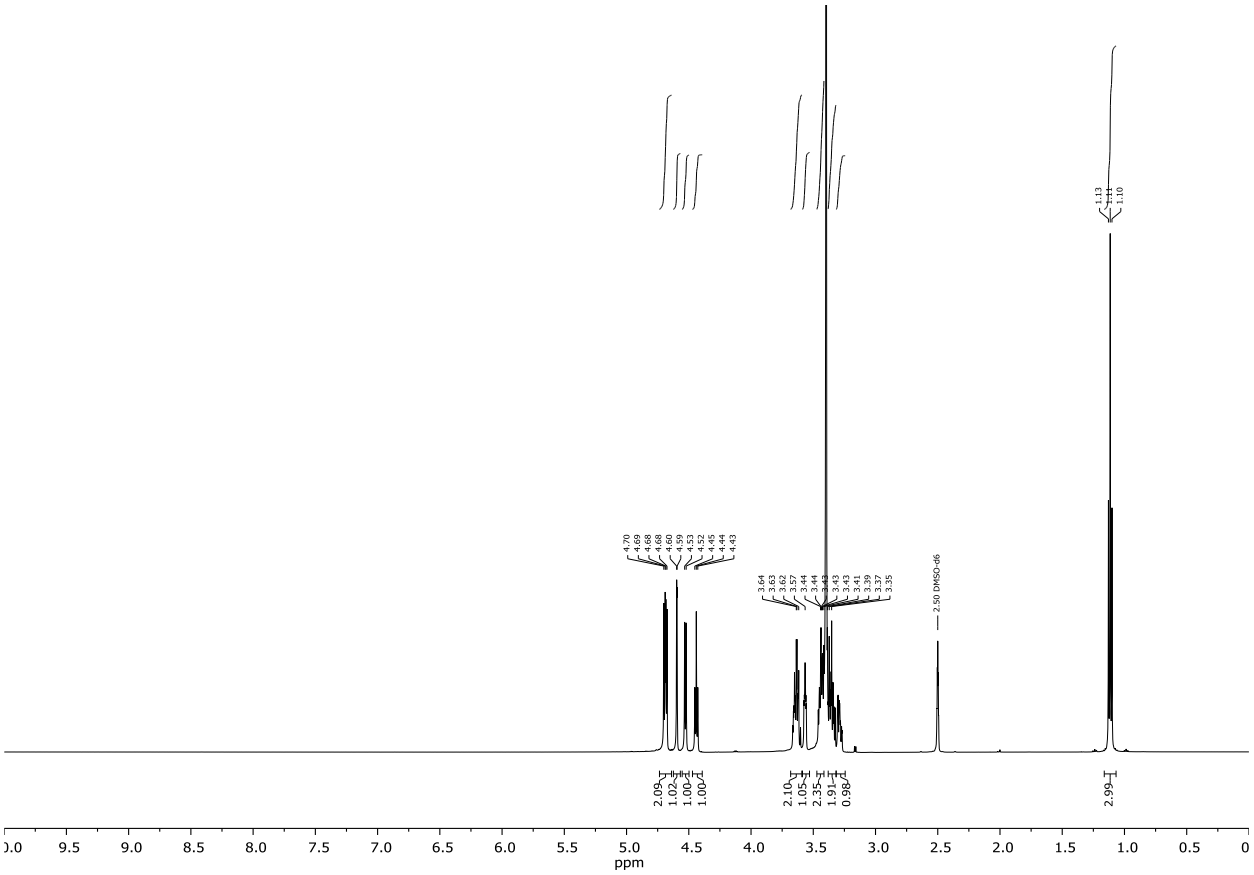

^{13}C NMR (126 MHz, DMSO-d_6) Ethyl α-D-mannopyranoside

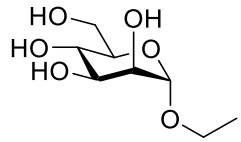

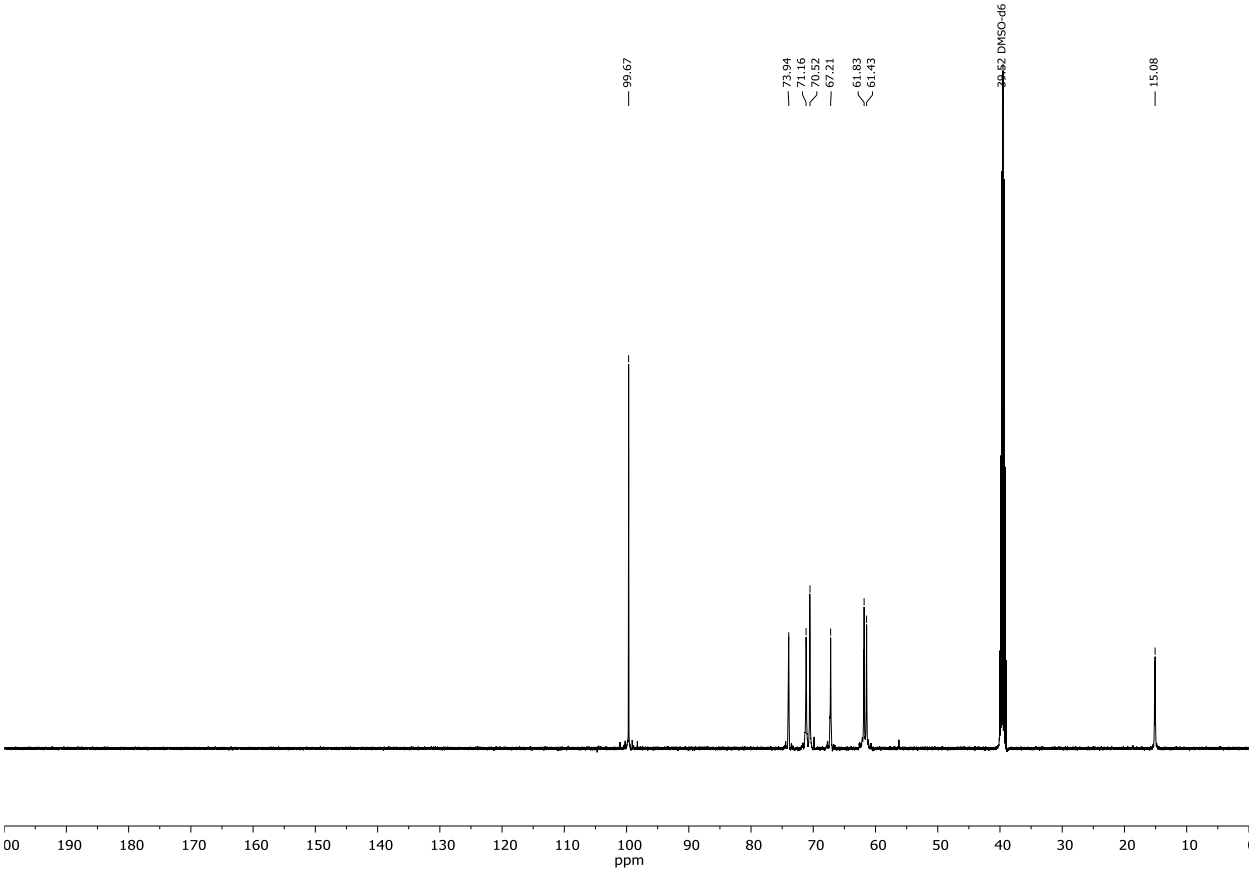

^{1}H-^{1}H COSY NMR (500 MHz, DMSO-d_6) Ethyl α-D-mannopyranoside

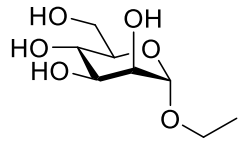

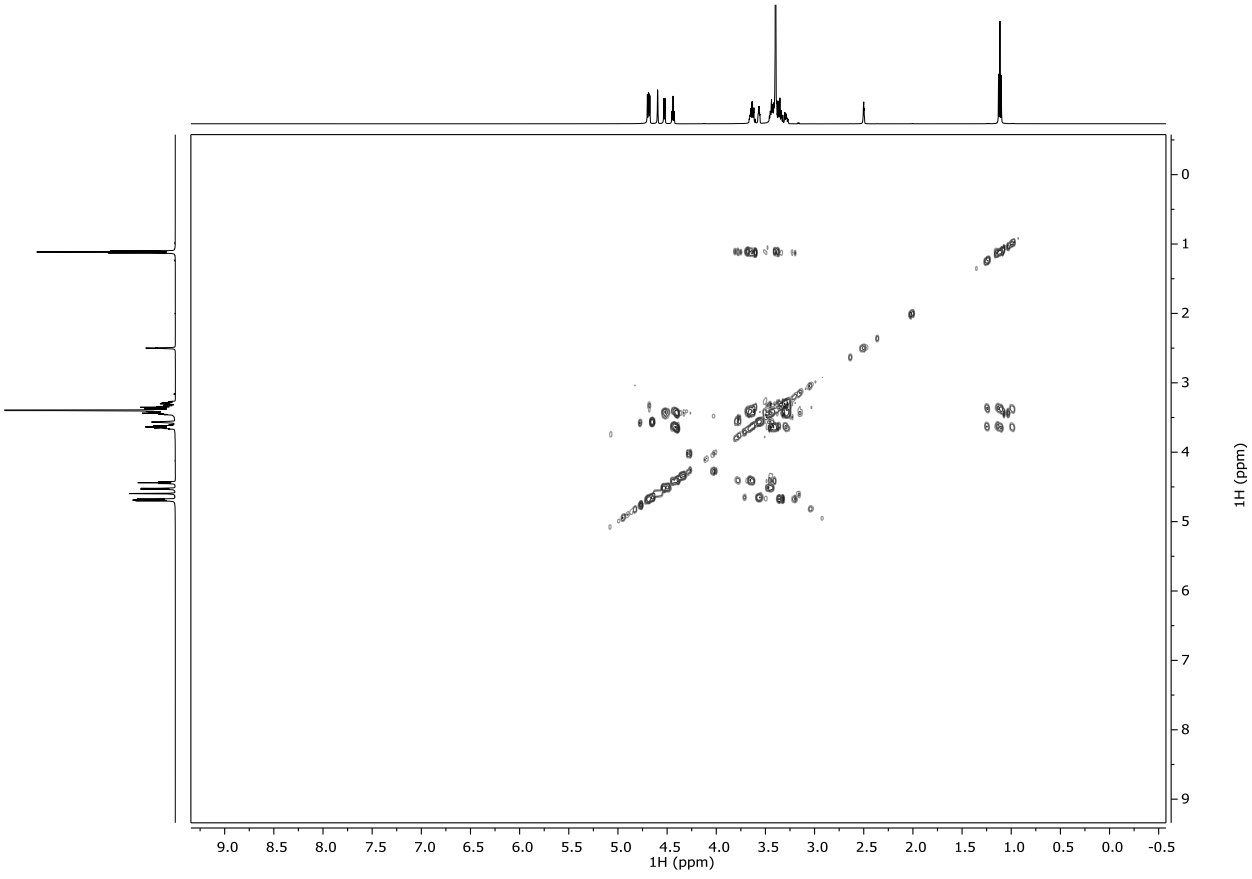

^{1}H-^{13}C HSQC NMR (500 MHz, DMSO-d_6) Ethyl α-D-mannopyranoside

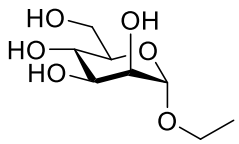

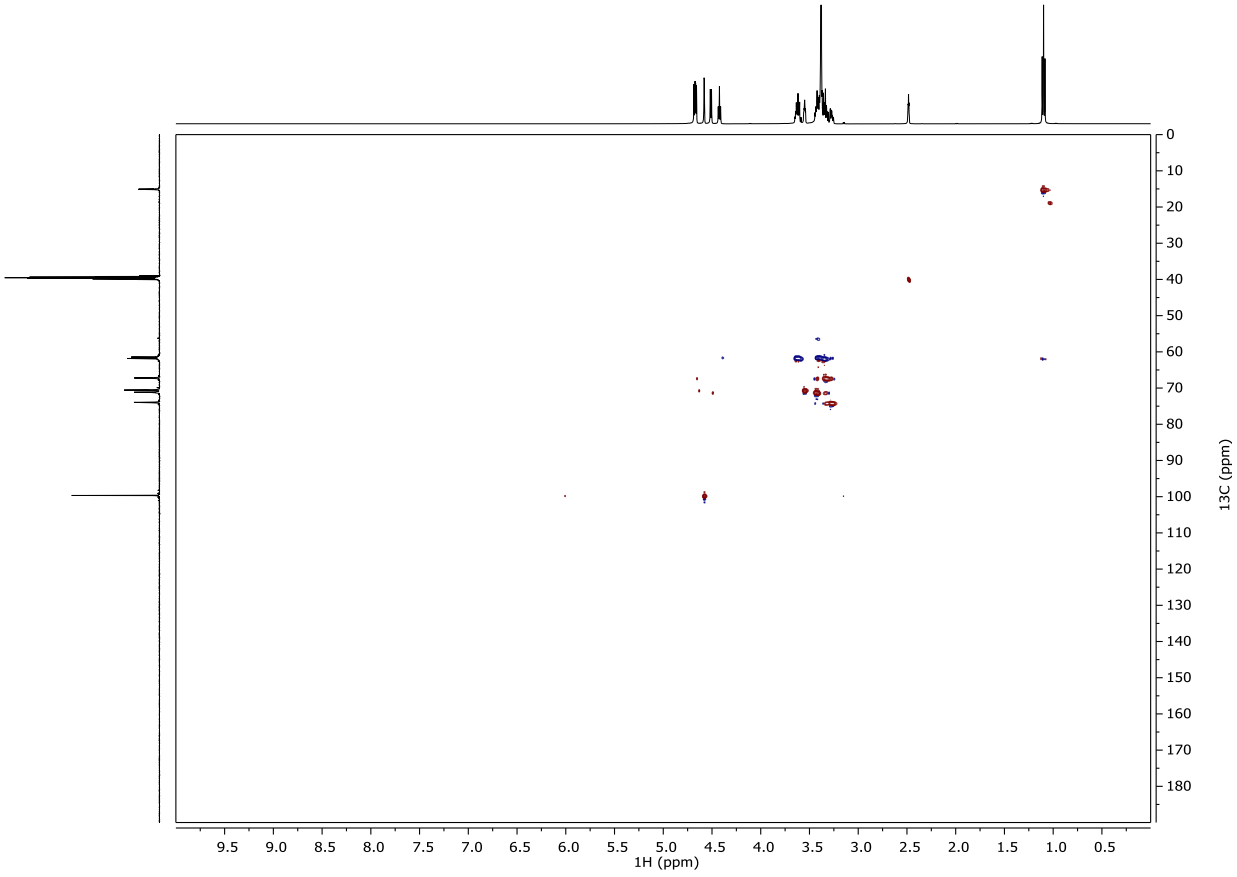

^{1}H-^{13}C HMBC NMR (500 MHz, DMSO-d_6) Ethyl α-D-mannopyranoside

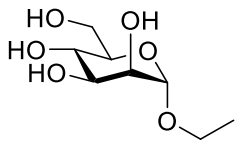

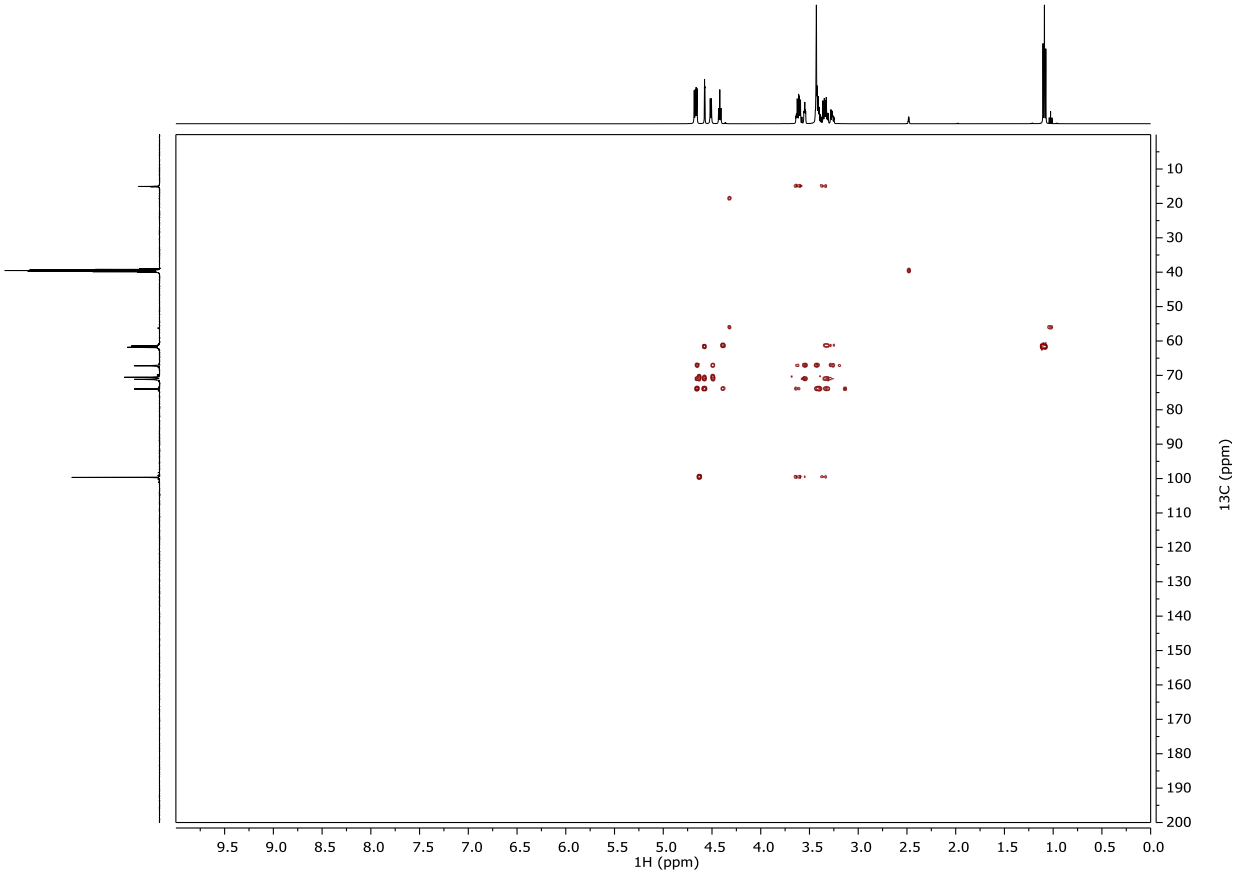

^{1}H NMR (500 MHz, DMSO-d_6) 2-Ethylhexyl 2,3,5,6-tetra-*O*-acetyl α-D-galactopyranoside

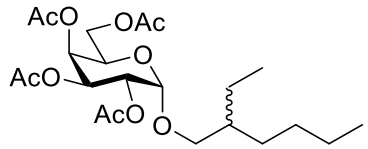

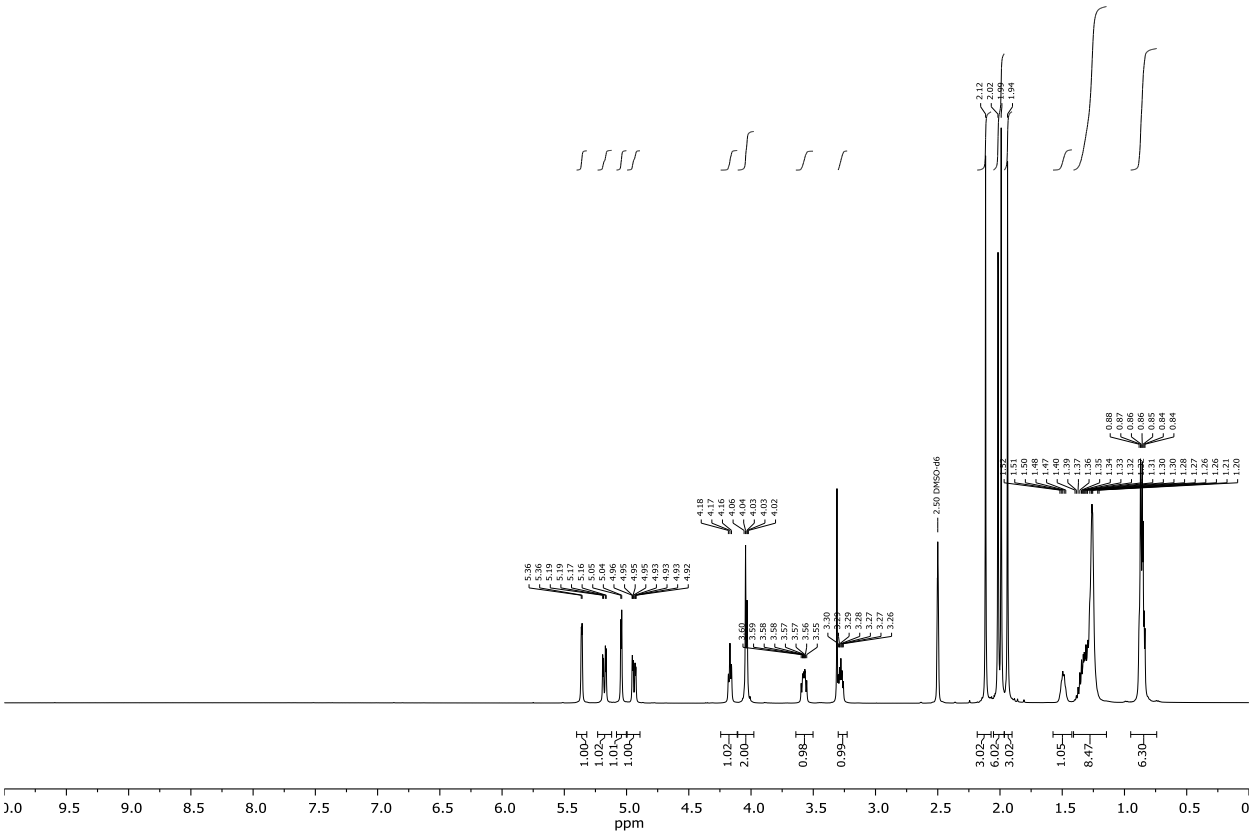

^{13}C NMR (126 MHz, DMSO-d_6) 2-Ethylhexyl 2,3,5,6-tetra-*O*-acetyl α-D-galactopyranoside

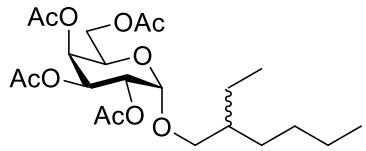

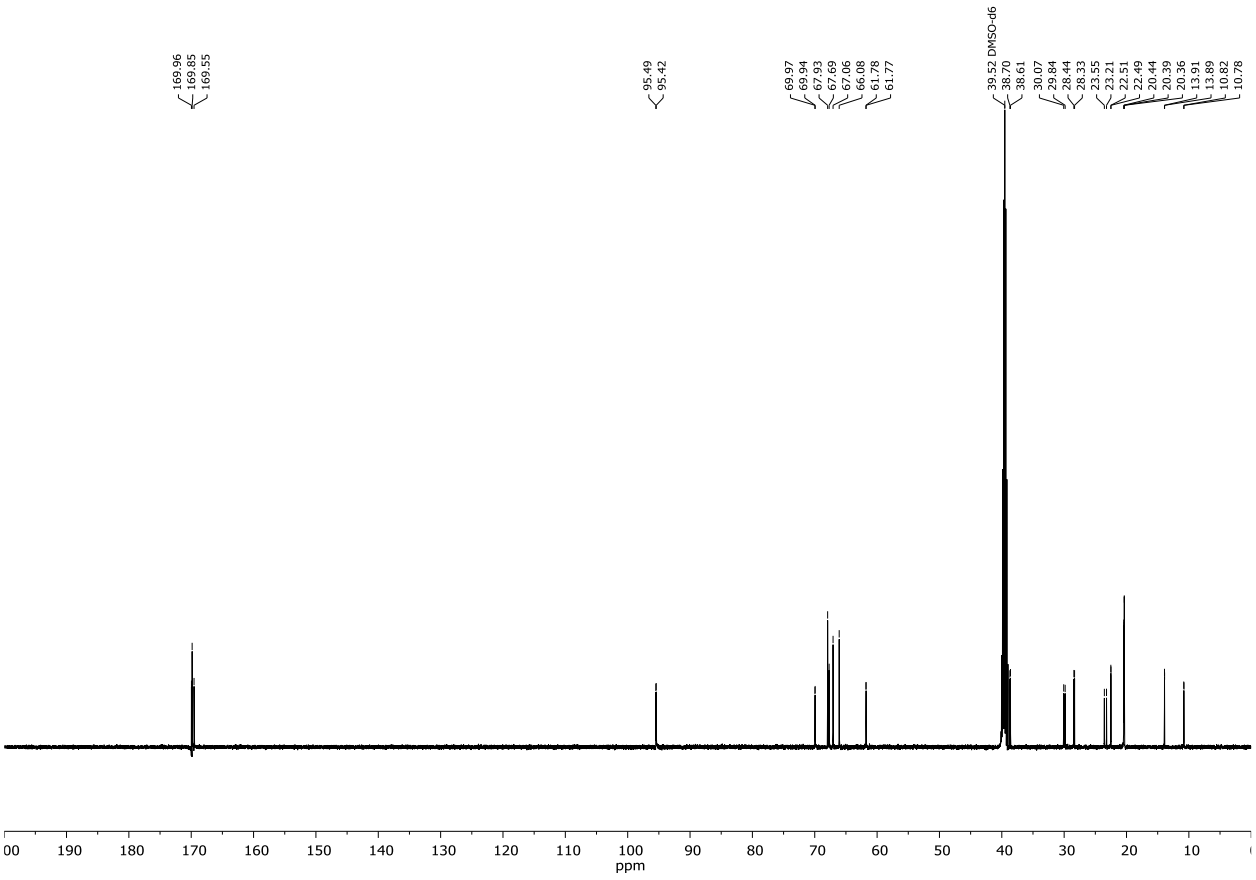

^{1}H-^{1}H COSY NMR (500 MHz, DMSO-d_6) 2-Ethylhexyl 2,3,5,6-tetra-*O*-acetyl α-D-galactopyranoside

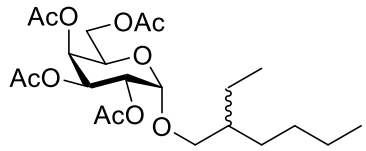

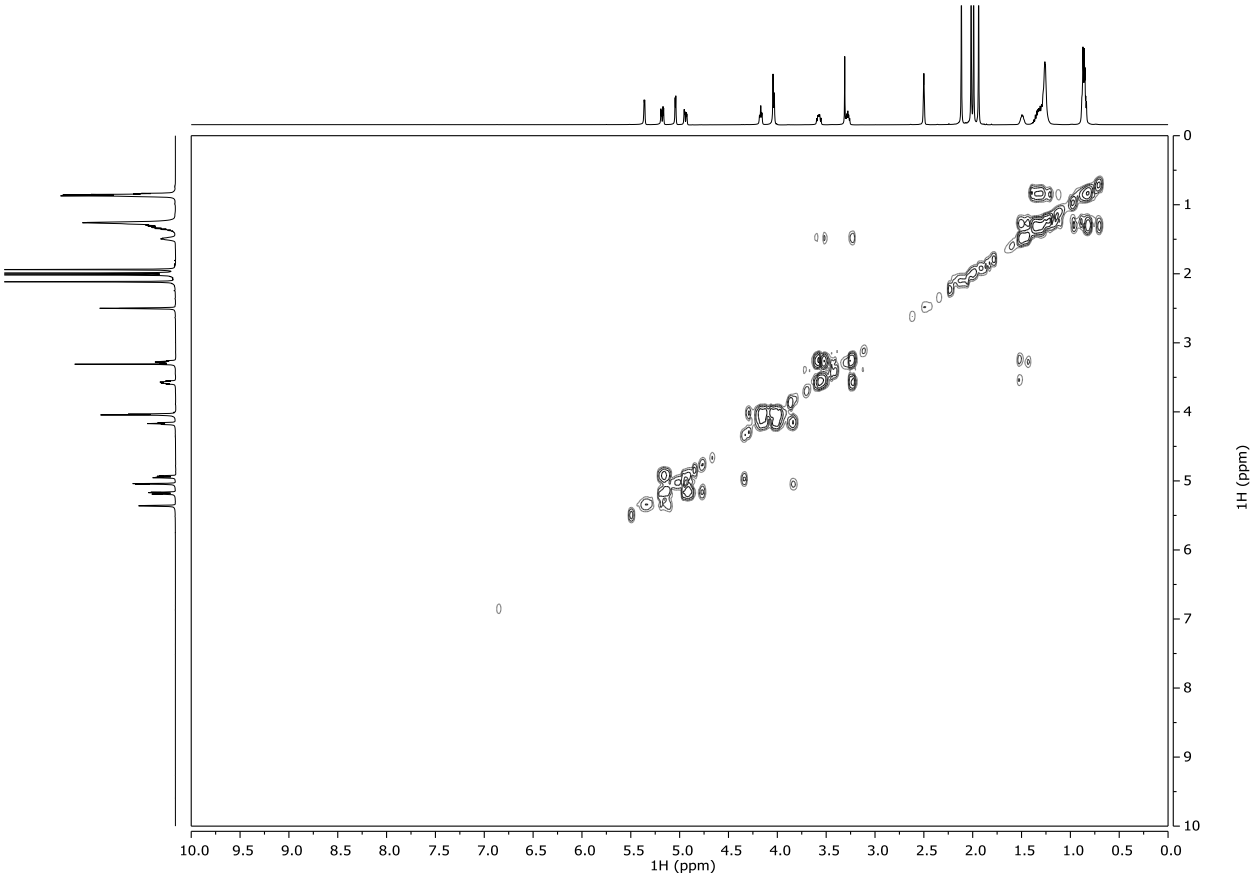

^{1}H-^{13}C HSQC NMR (500 MHz, DMSO-d_6) 2-Ethylhexyl 2,3,5,6-tetra-*O*-acetyl α-D-galactopyranoside

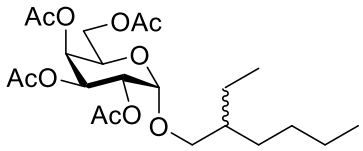

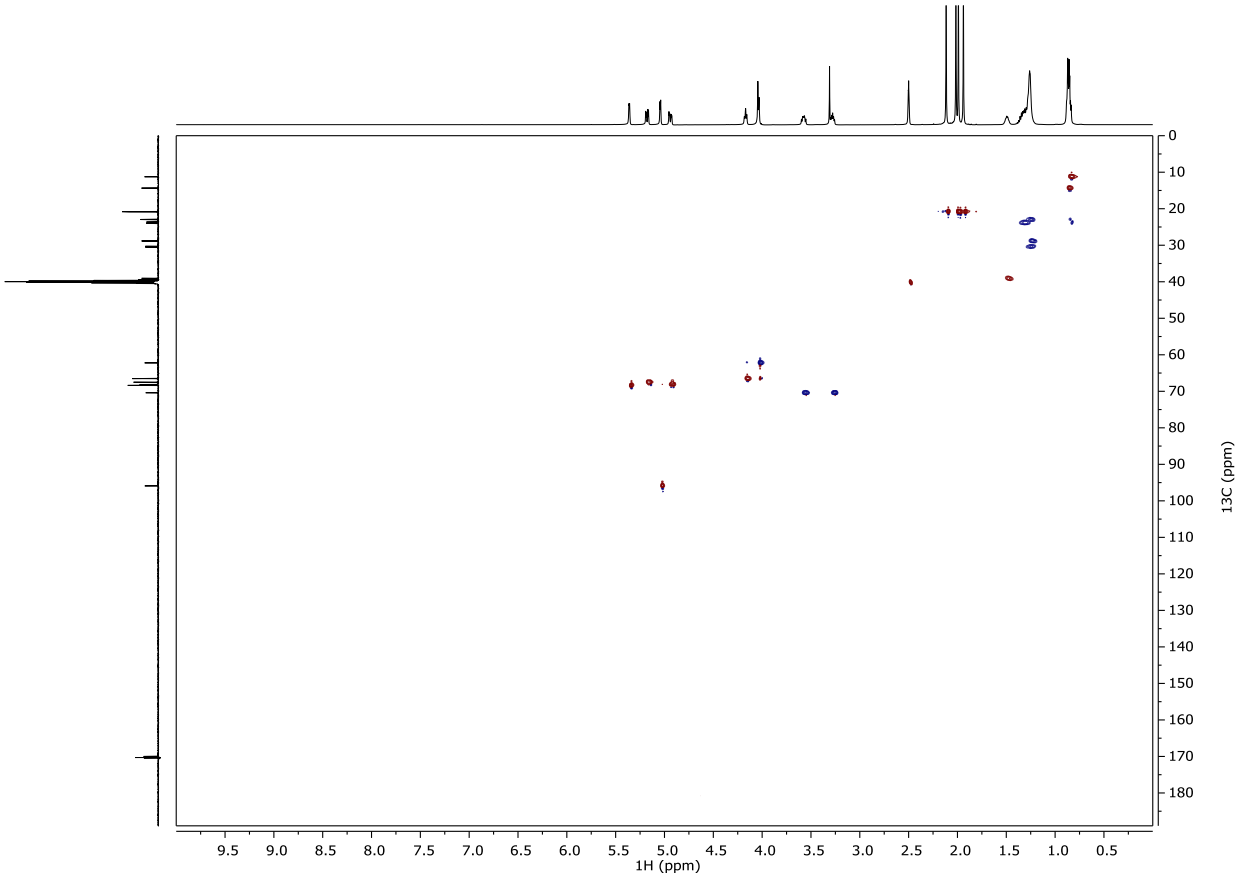

^{1}H-^{13}C HMBC NMR (500 MHz, DMSO-d_6) 2-Ethylhexyl 2,3,5,6-tetra-*O*-acetyl α-D-galactopyranoside

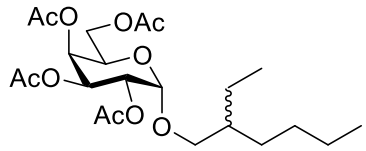

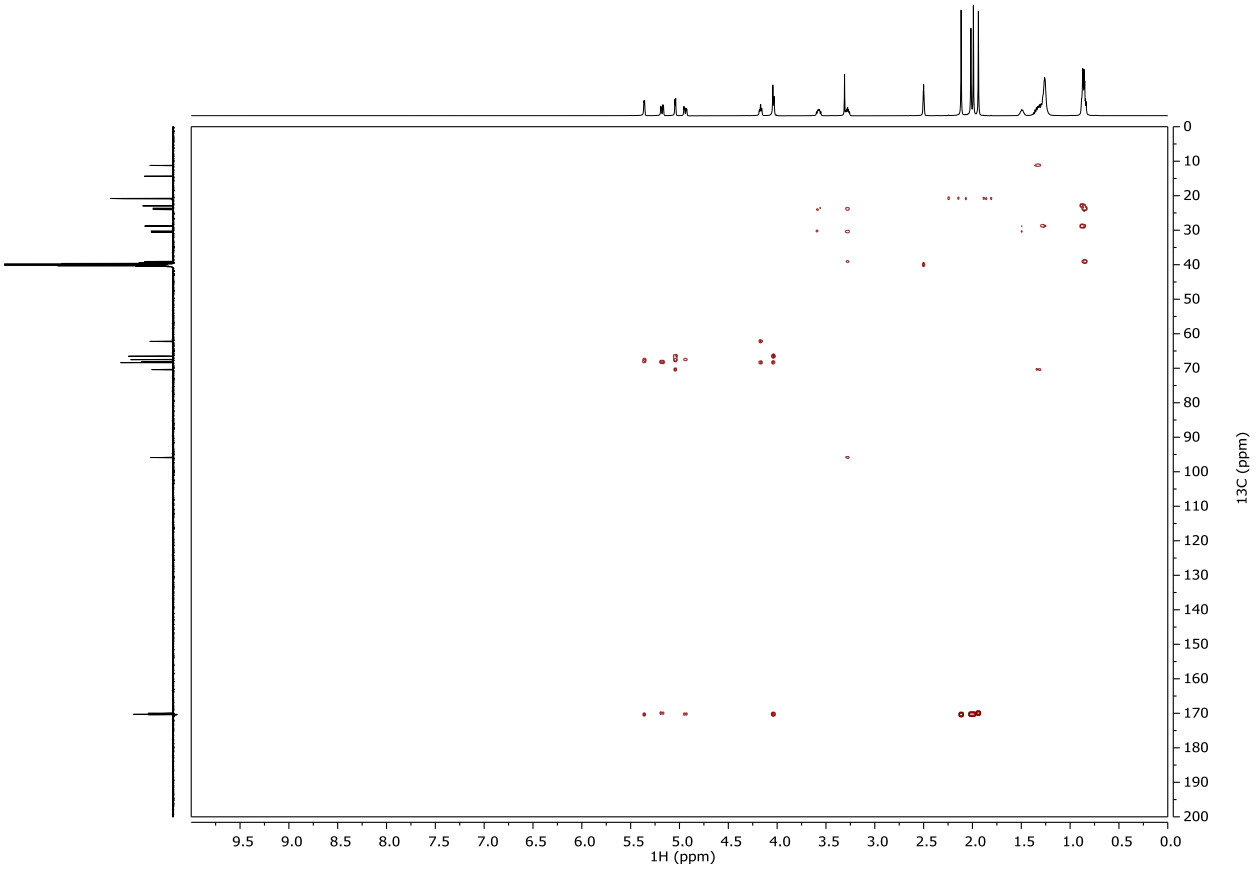

^{1}H NMR (500 MHz, DMSO-d_6) 2-Ethylhexyl α-D-galactopyranoside

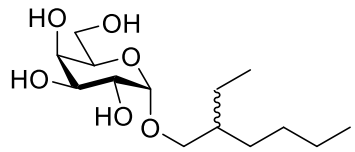

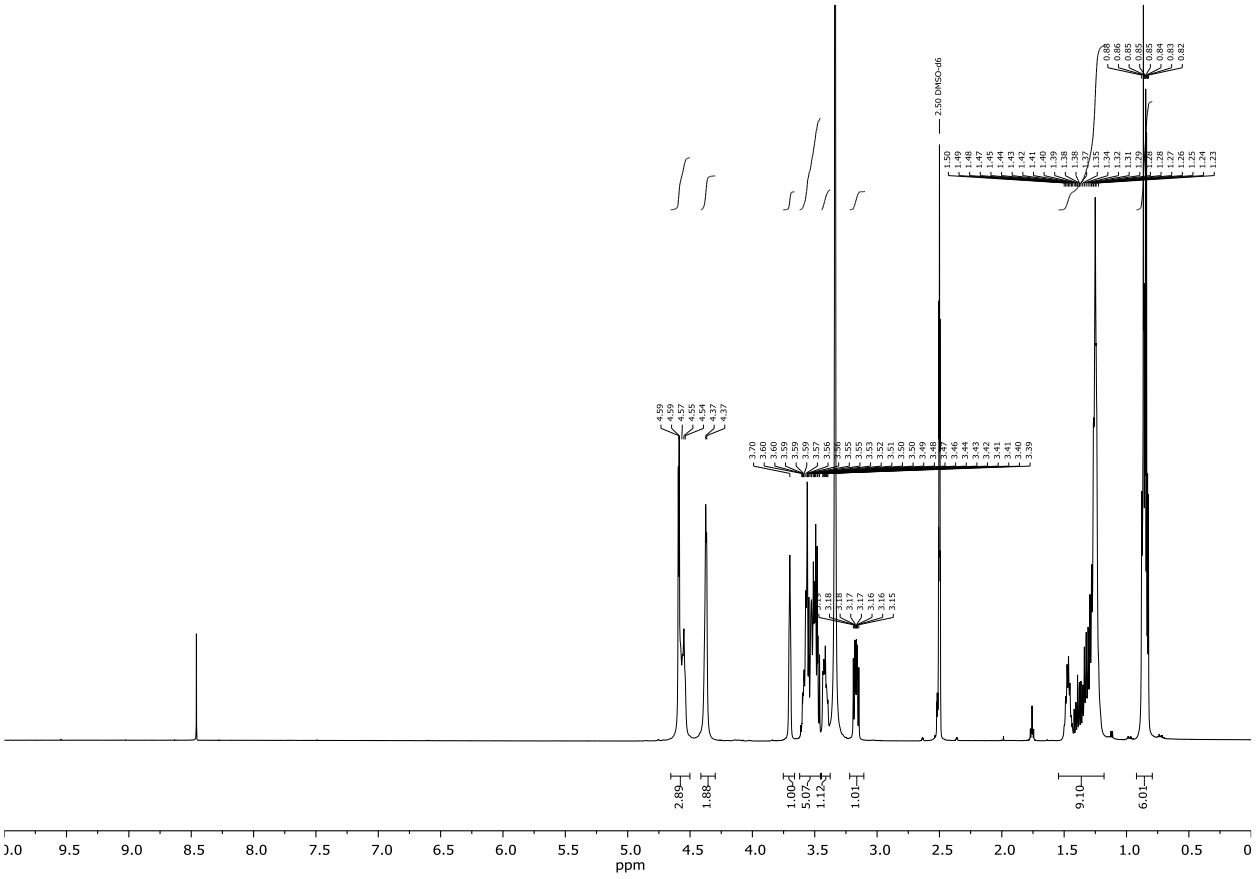

^{13}C NMR (126 MHz, DMSO-d_6) 2-Ethylhexyl α-D-galactopyranoside

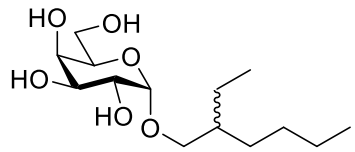

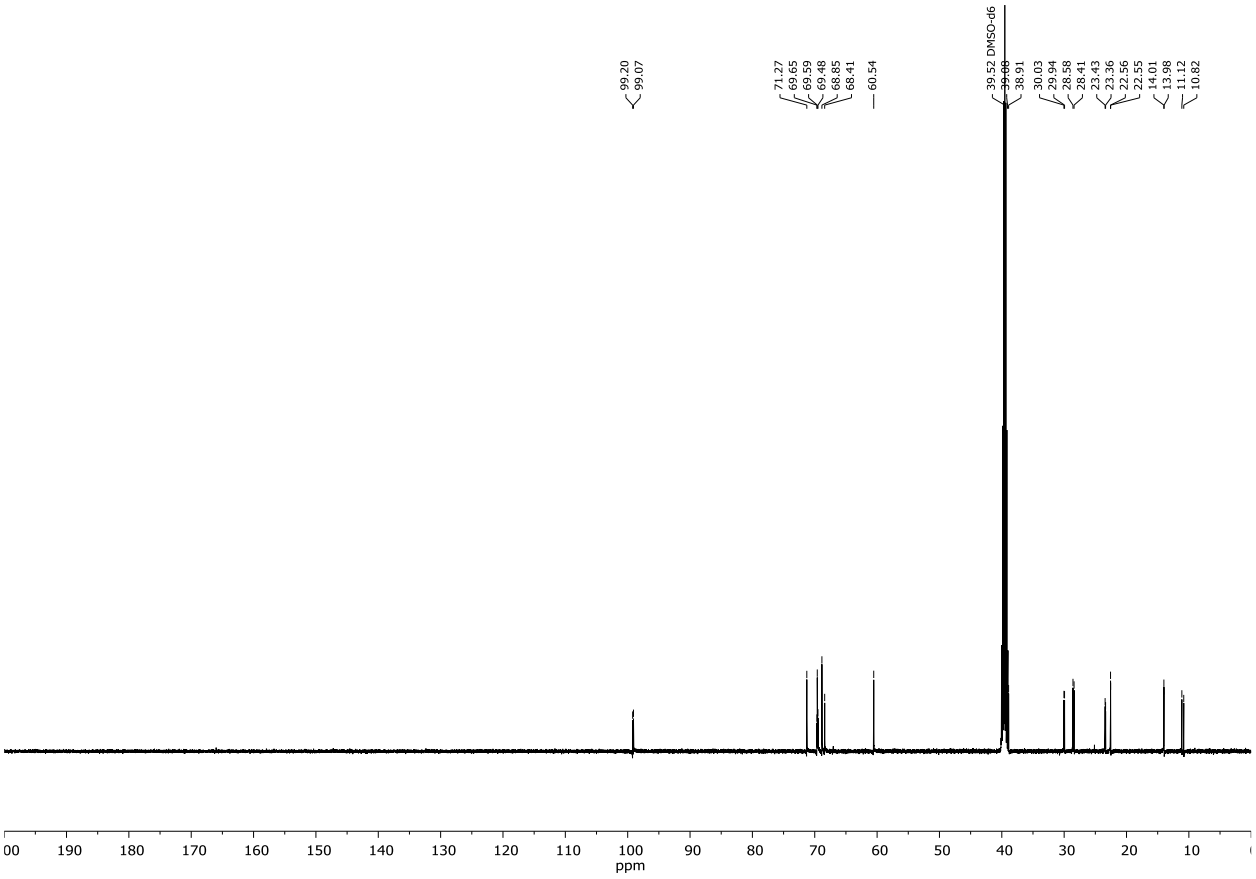

^{1}H-^{1}H COSY NMR (500 MHz, DMSO-d_6) 2-Ethylhexyl α-D-galactopyranoside

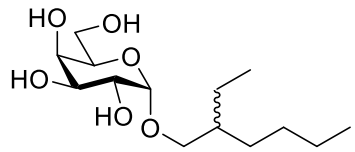

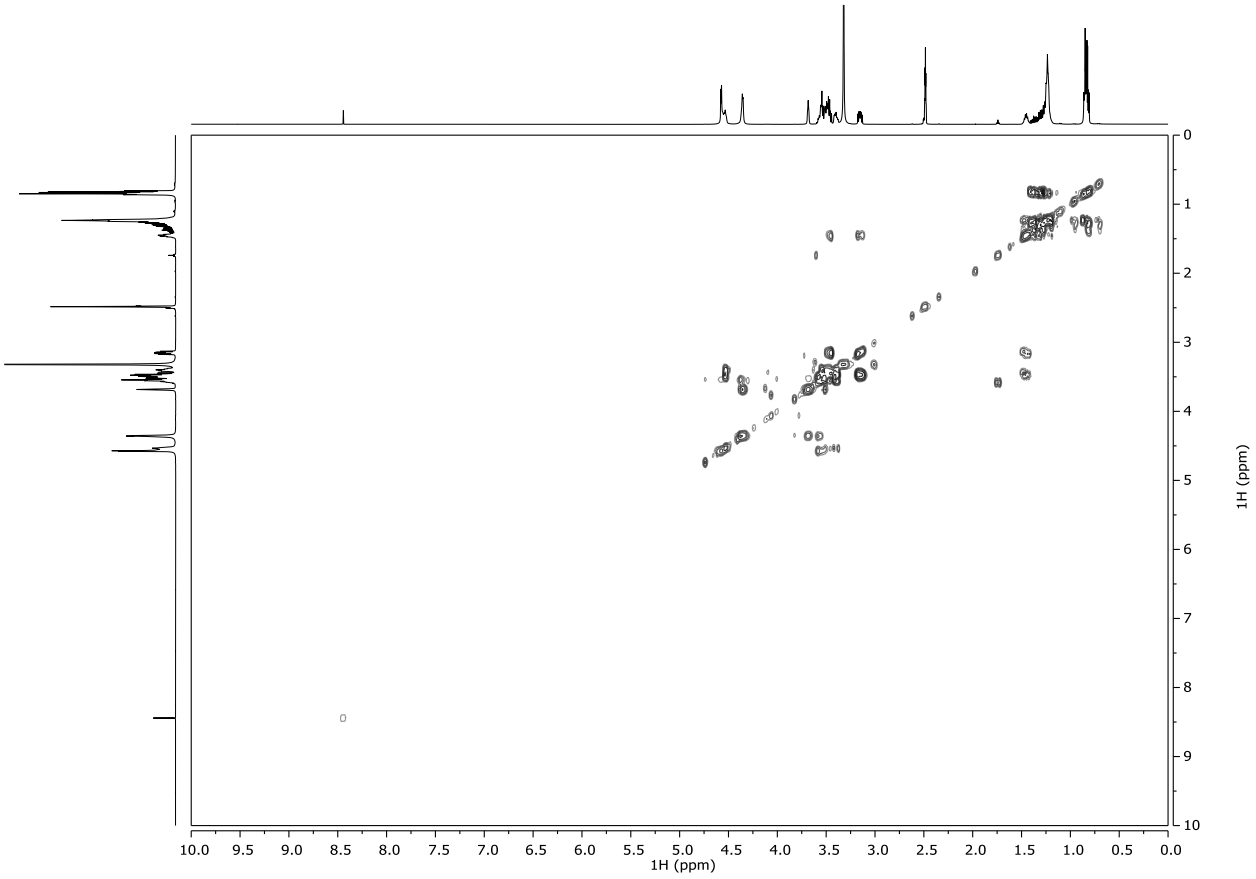

^{1}H-^{13}C HSQC NMR (500 MHz, DMSO-d_6) 2-Ethylhexyl α-D-galactopyranoside

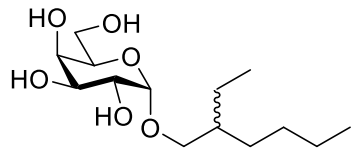

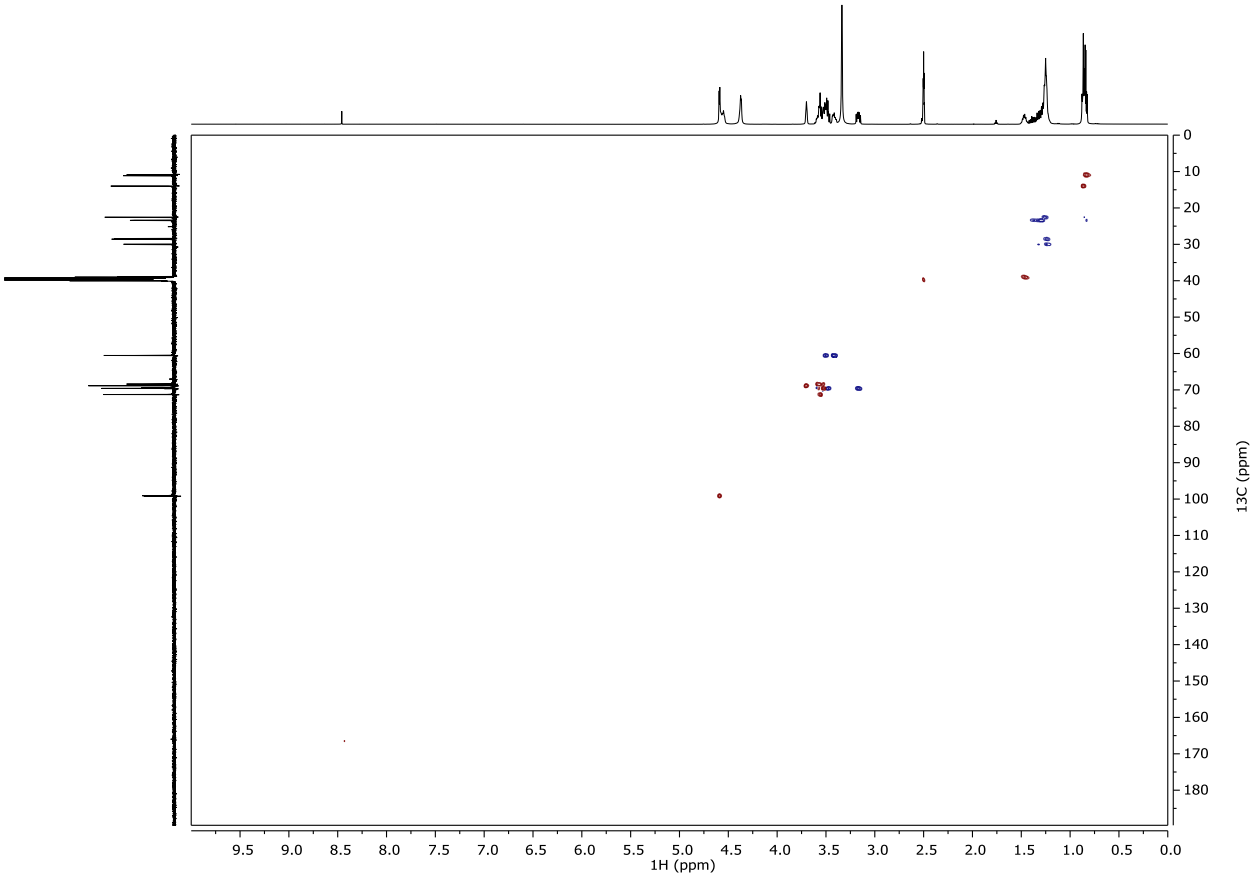

^{1}H-^{13}C HMBC NMR (500 MHz, DMSO-d_6) 2-Ethylhexyl α-D-galactopyranoside

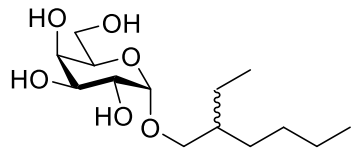

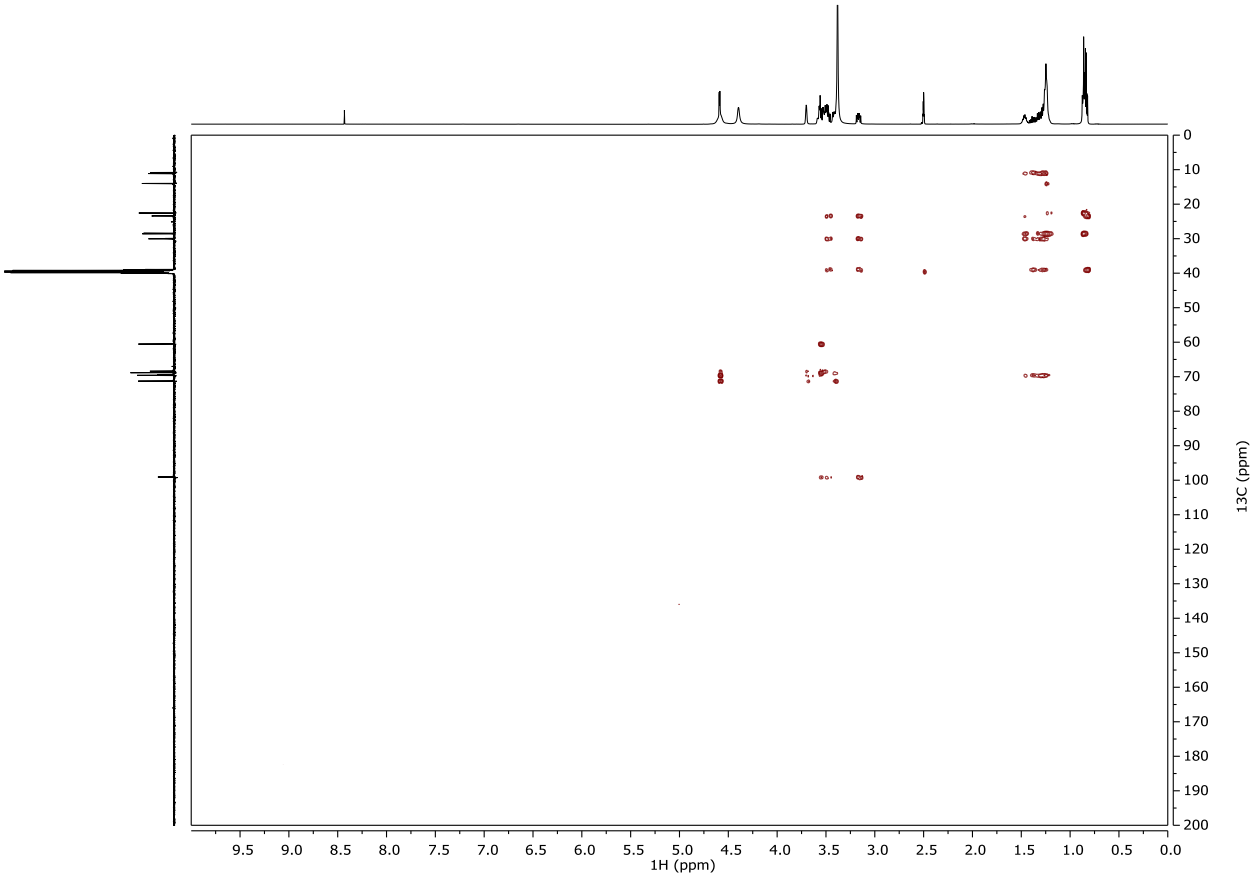

^{1}H NMR (500 MHz, DMSO-d_6) 2-Ethylhexyl 2,3,5,6-tetra-*O*-acetyl β-D-galactopyranoside

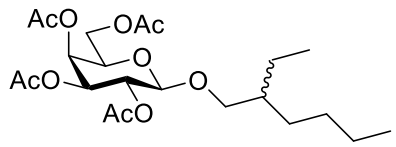

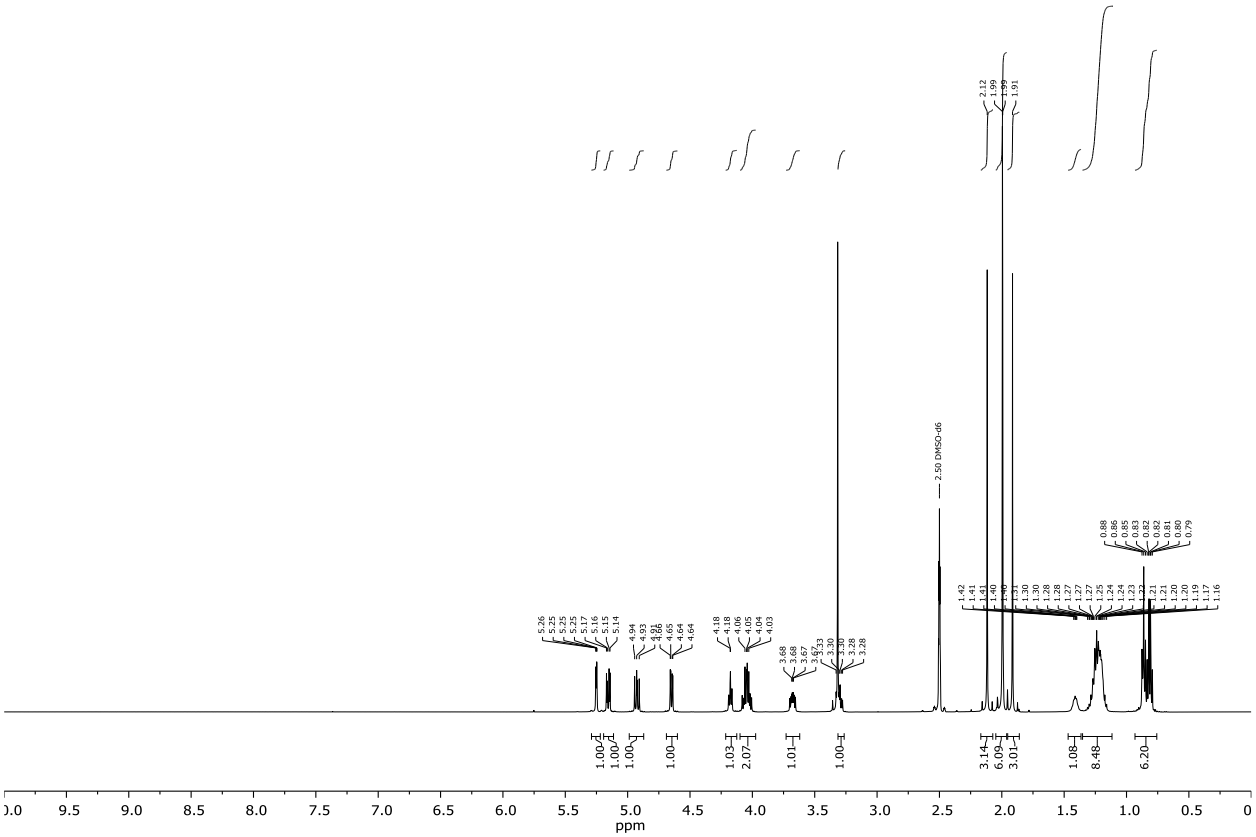

^{13}C NMR (126 MHz, DMSO-d_6) 2-Ethylhexyl 2,3,5,6-tetra-*O*-acetyl β-D-galactopyranoside

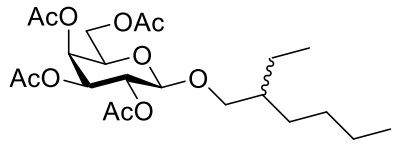

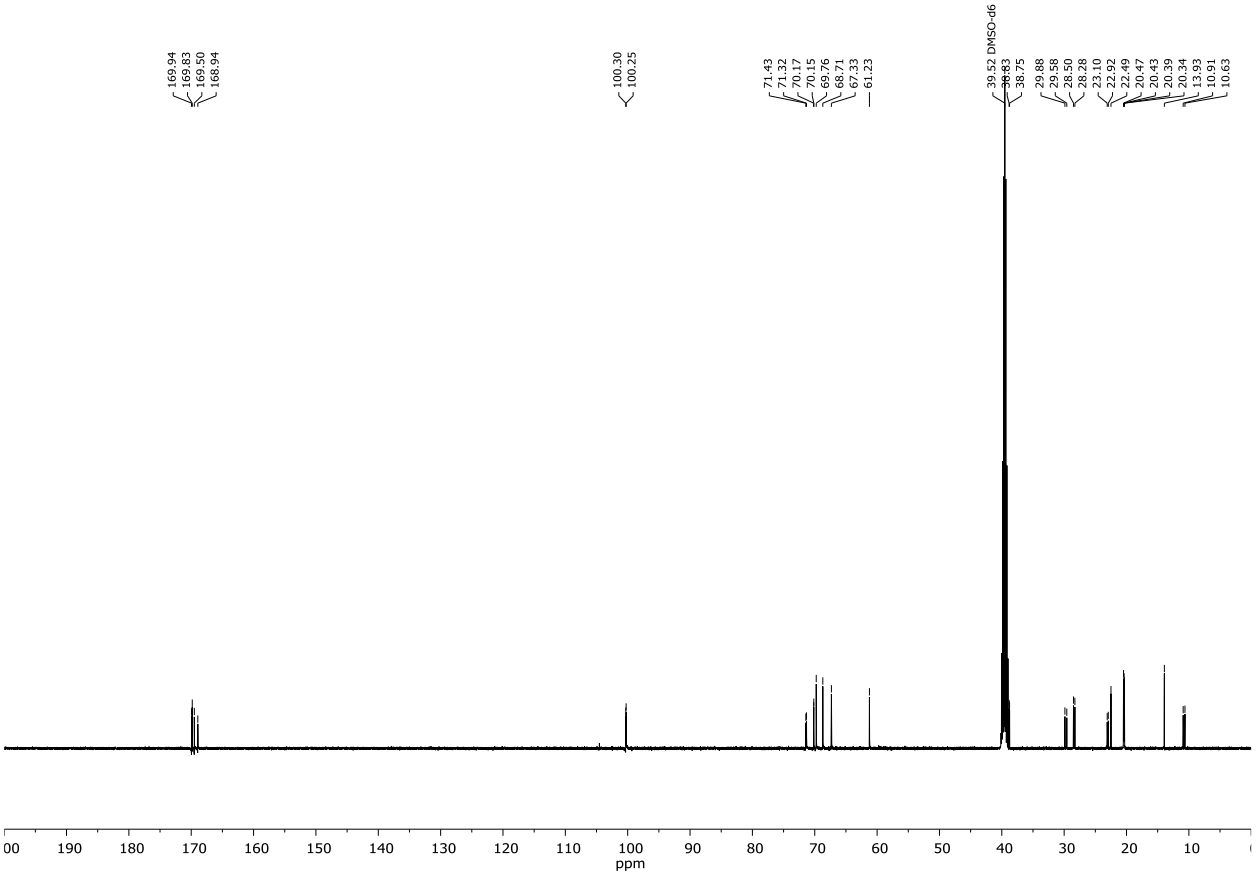

^{1}H-^{1}H COSY NMR (500 MHz, DMSO-d_6) 2-Ethylhexyl 2,3,5,6-tetra-*O*-acetyl β-D-galactopyranoside

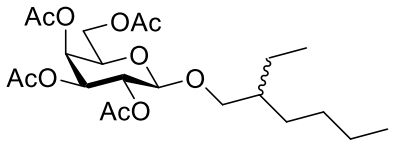

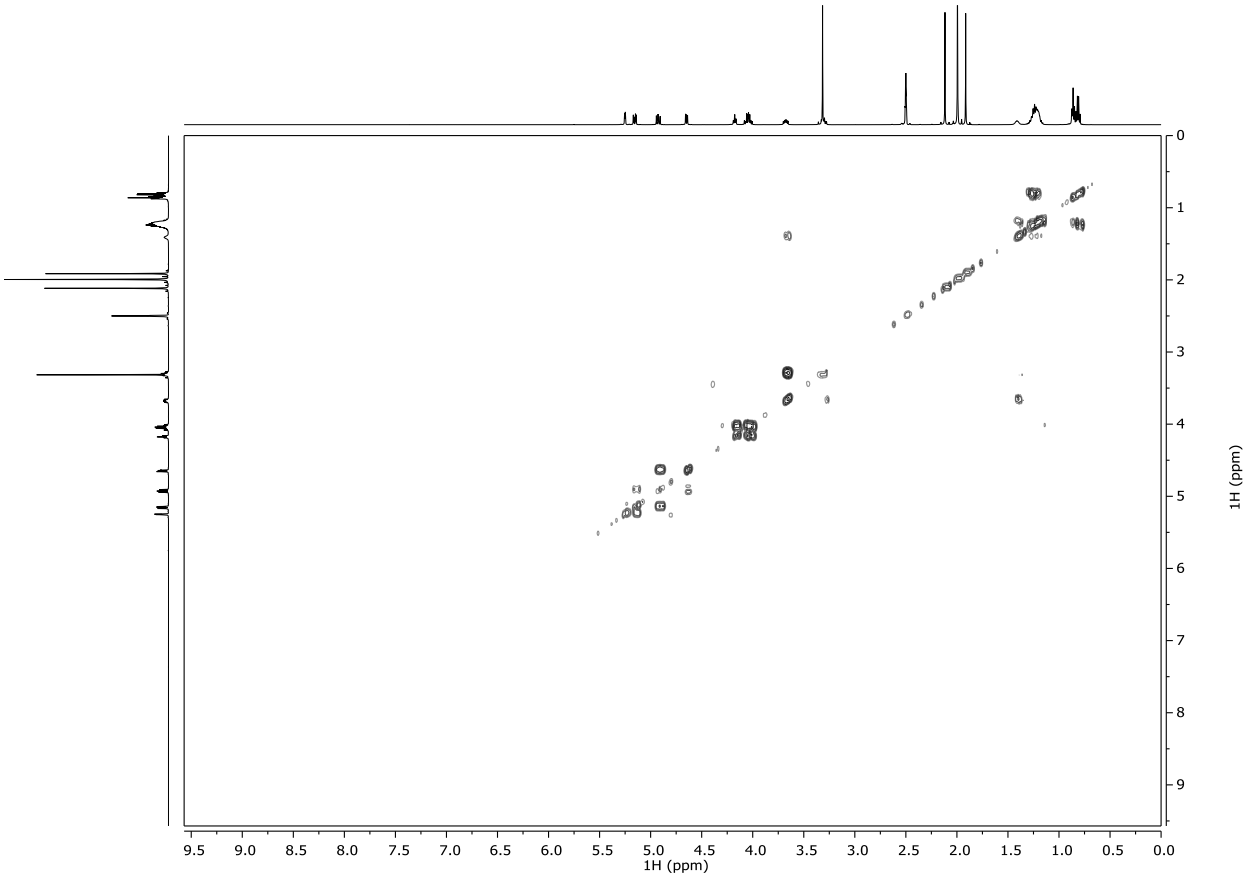

^{1}H-^{13}C HSQC NMR (500 MHz, DMSO-d_6) 2-Ethylhexyl 2,3,5,6-tetra-*O*-acetyl β-D-galactopyranoside

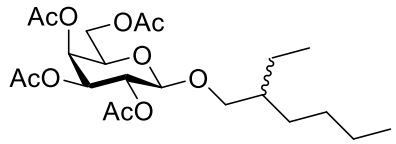

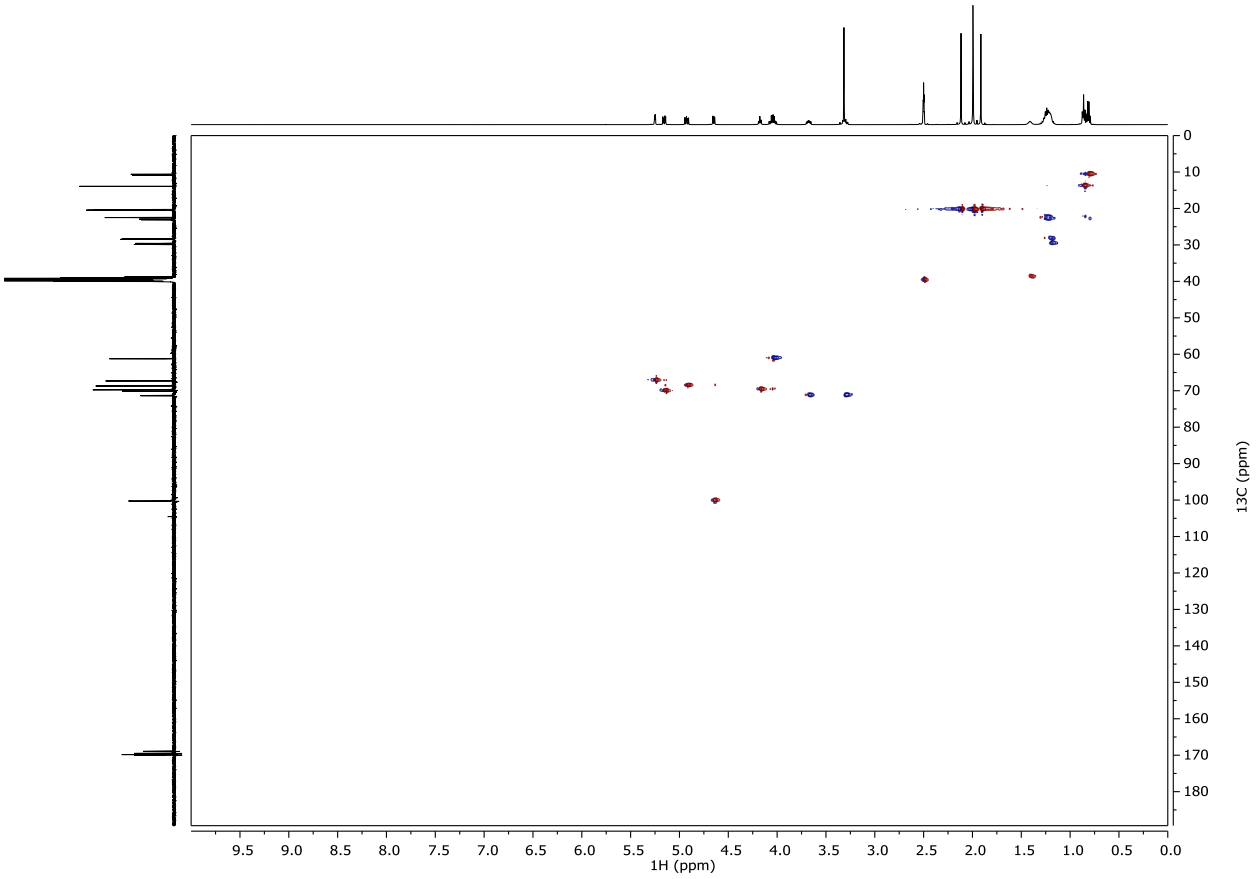

^{1}H-^{13}C HMBC NMR (500 MHz, DMSO-d_6) 2-Ethylhexyl 2,3,5,6-tetra-*O*-acetyl β-D-galactopyranoside

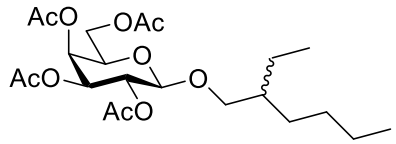

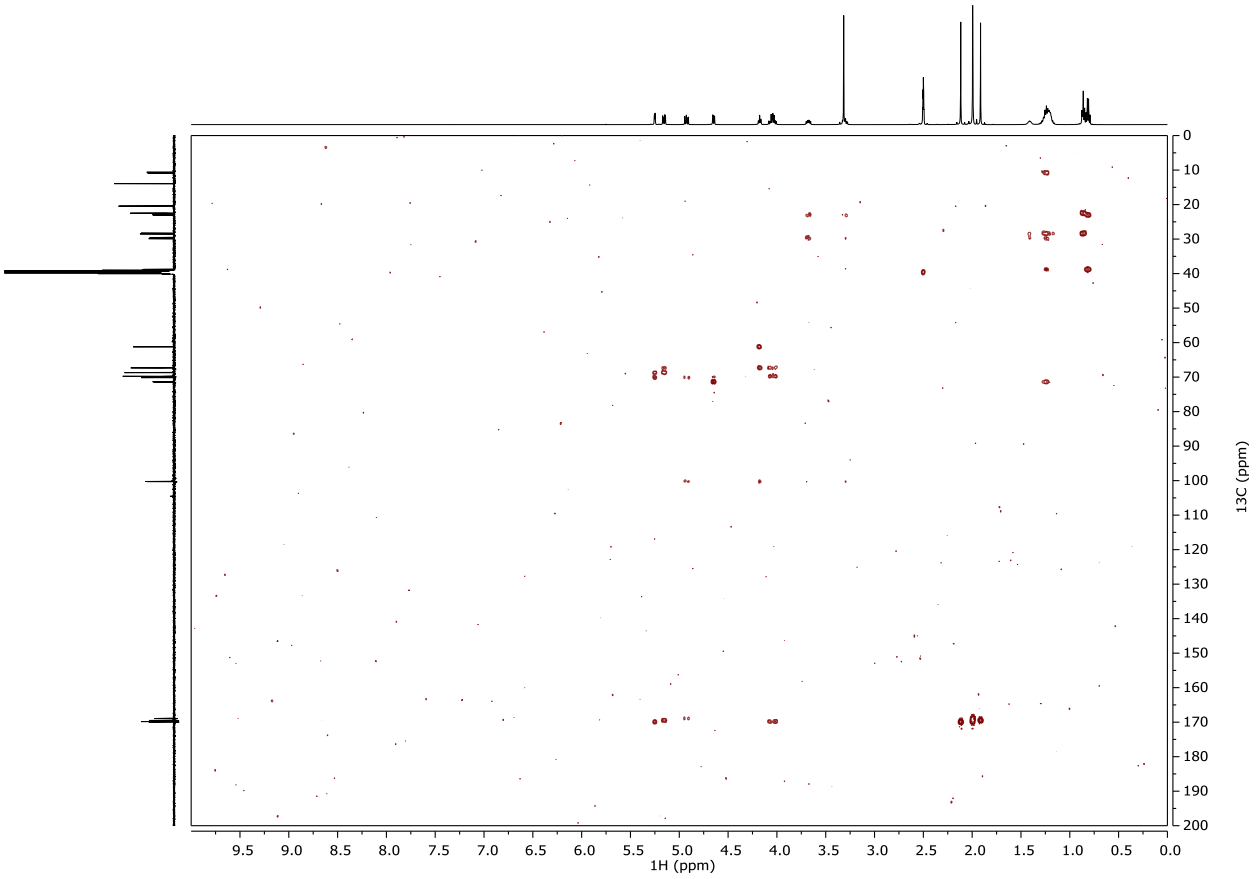

^{1}H NMR (500 MHz, DMSO-d_6) 2-Ethylhexyl β-D-galactopyranoside

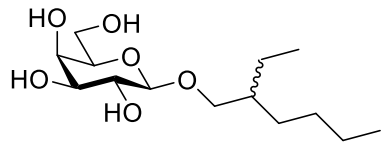

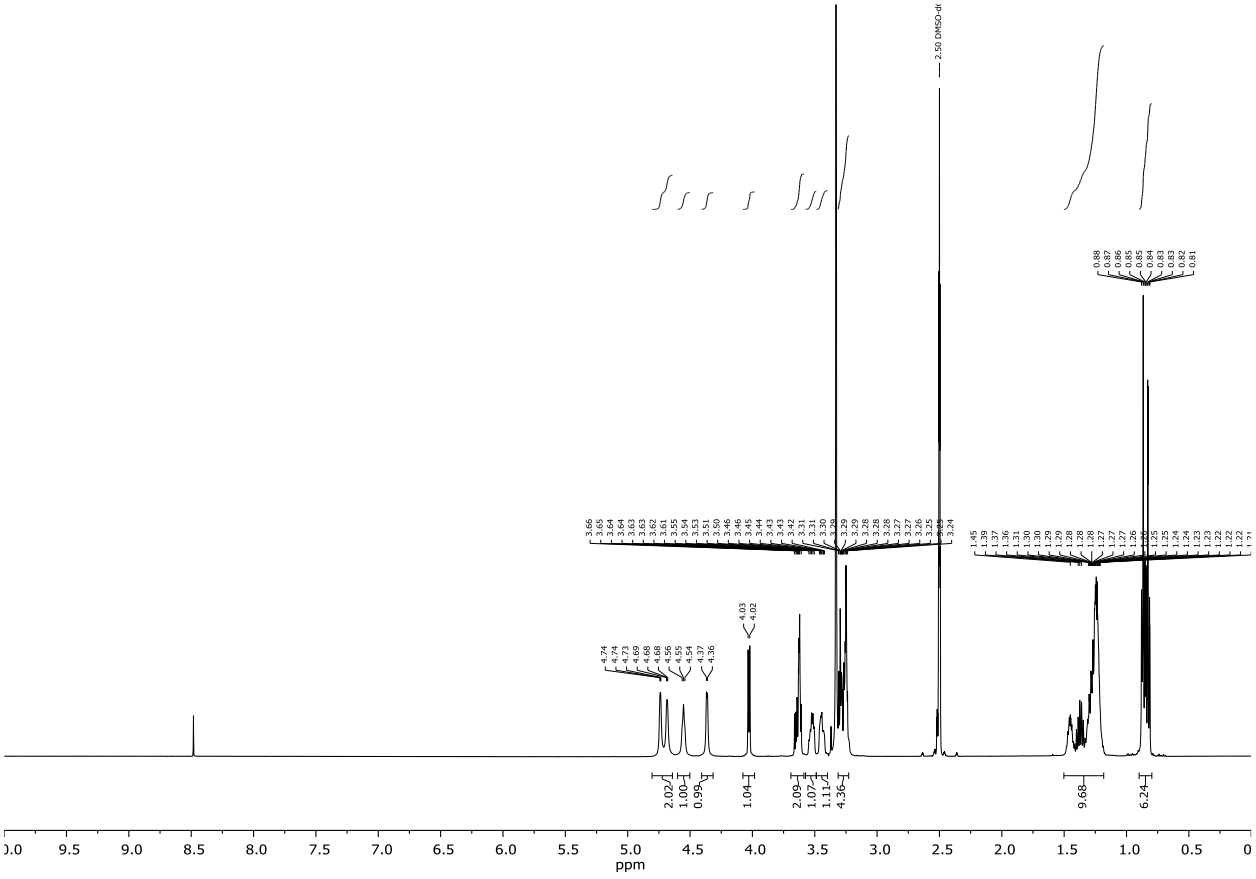

^{13}C NMR (126 MHz, DMSO-d_6) 2-Ethylhexyl β-D-galactopyranoside

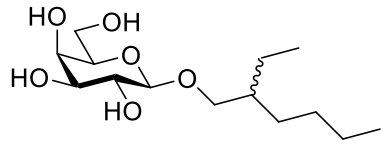

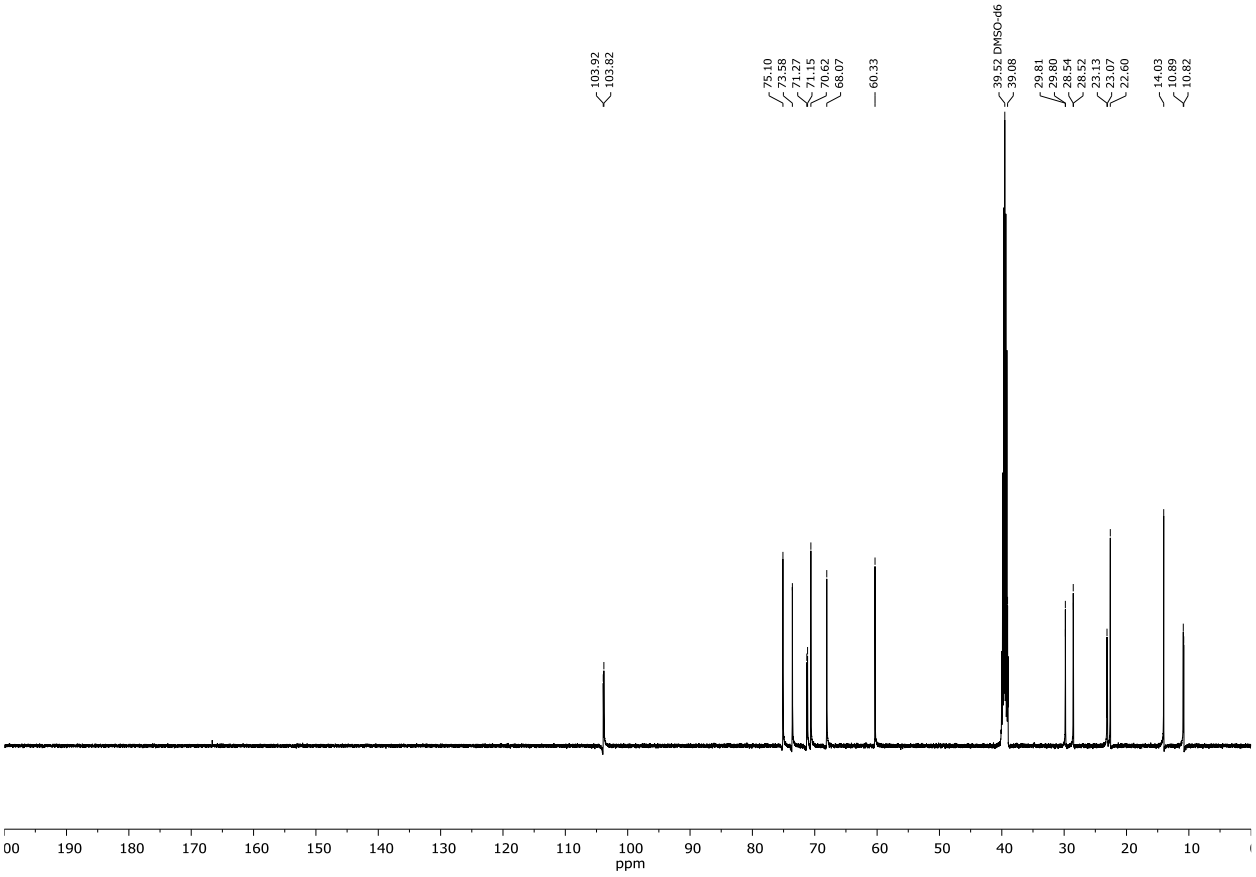

^{1}H-^{1}H COSY NMR (500 MHz, DMSO-d_6) 2-Ethylhexyl β-D-galactopyranoside

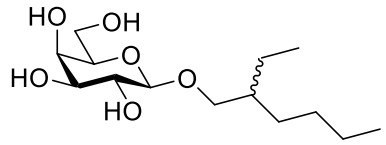

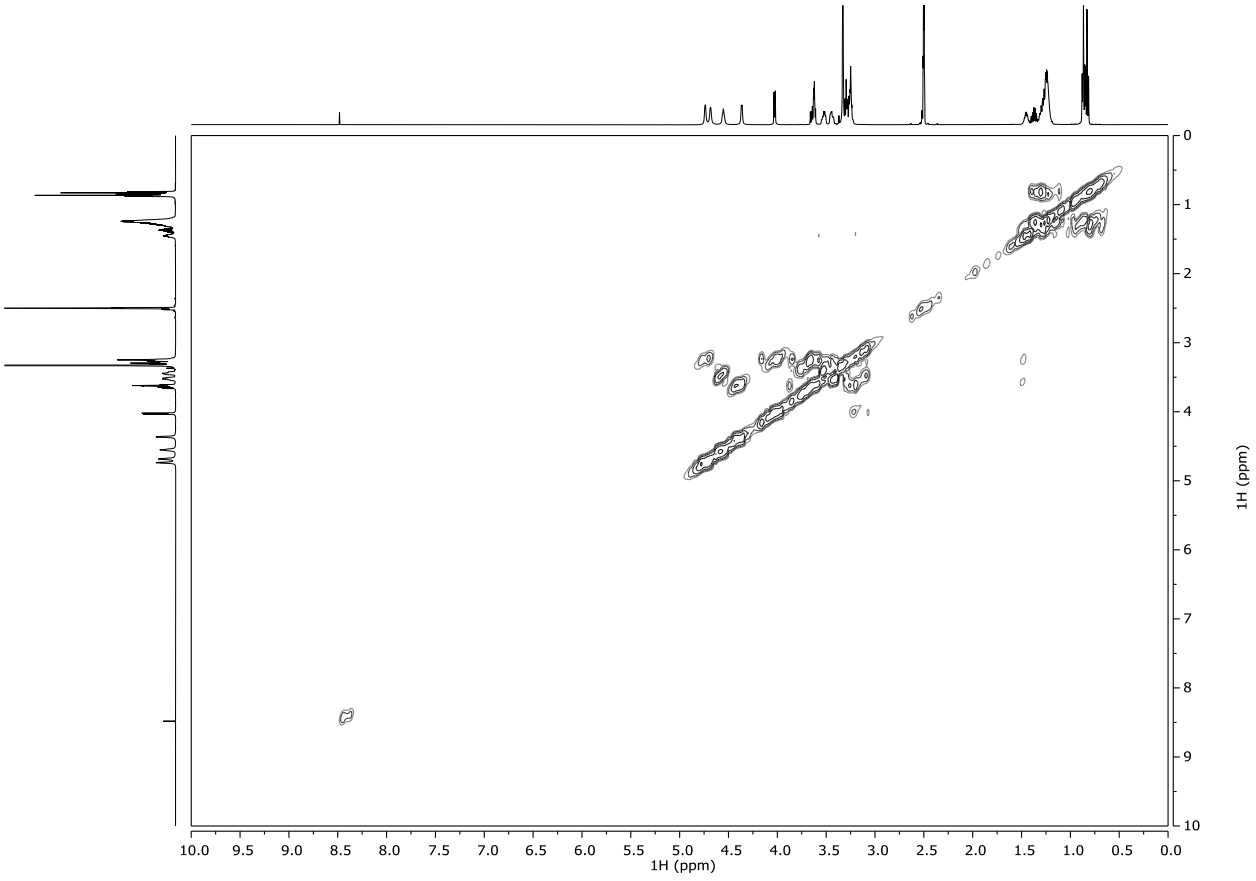

^{1}H-^{13}C HSQC NMR (500 MHz, DMSO-d_6) 2-Ethylhexyl β-D-galactopyranoside

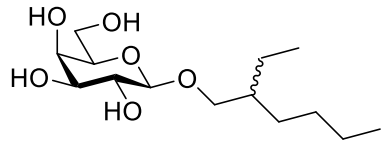

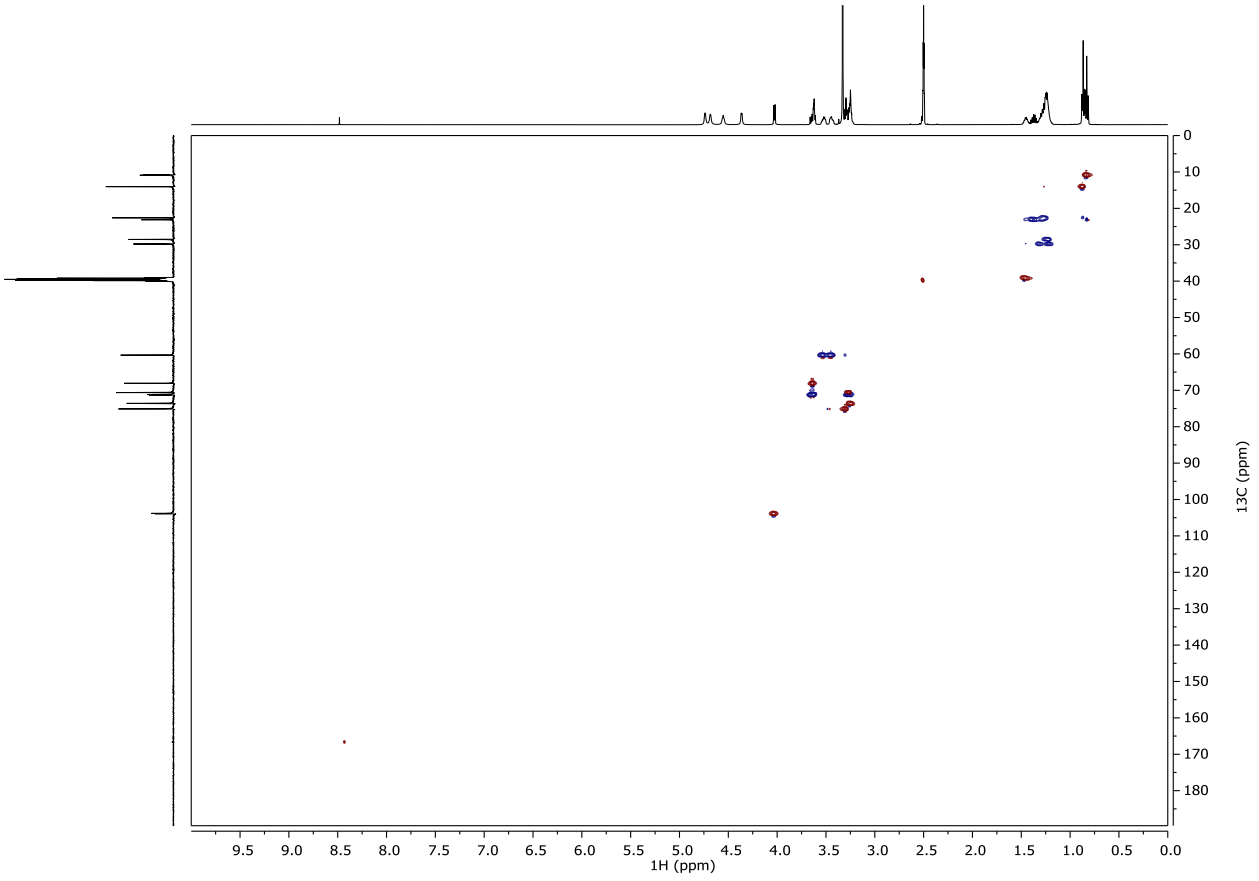

^{1}H-^{13}C HMBC NMR (500 MHz, DMSO-d_6) 2-Ethylhexyl β-D-galactopyranoside

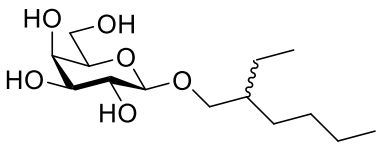

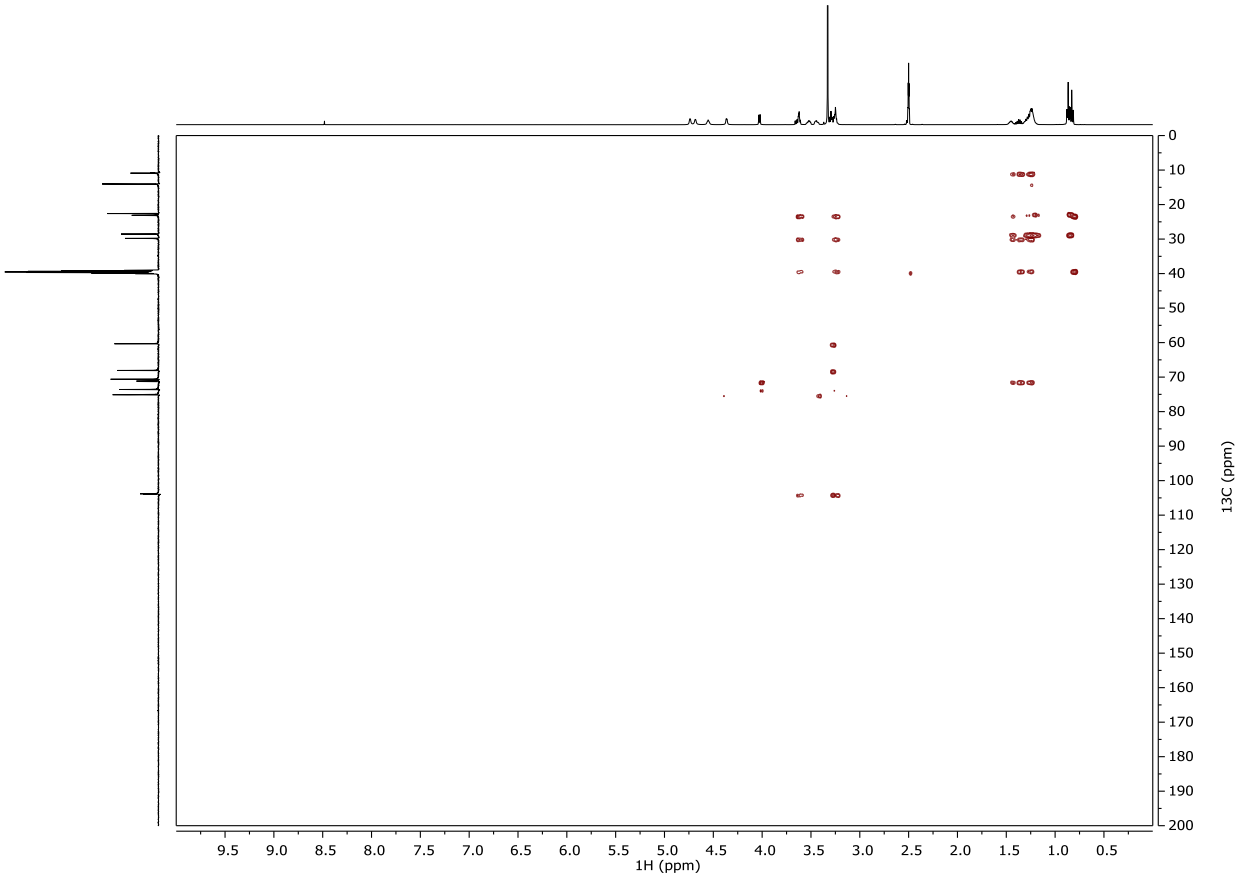

^{1}H NMR (500 MHz, $CDCl_3$) 2-Ethylhexyl 2,3,5,6-tetra-*O*-acetyl α-D-mannopyranoside

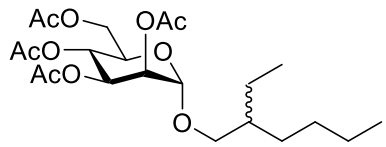

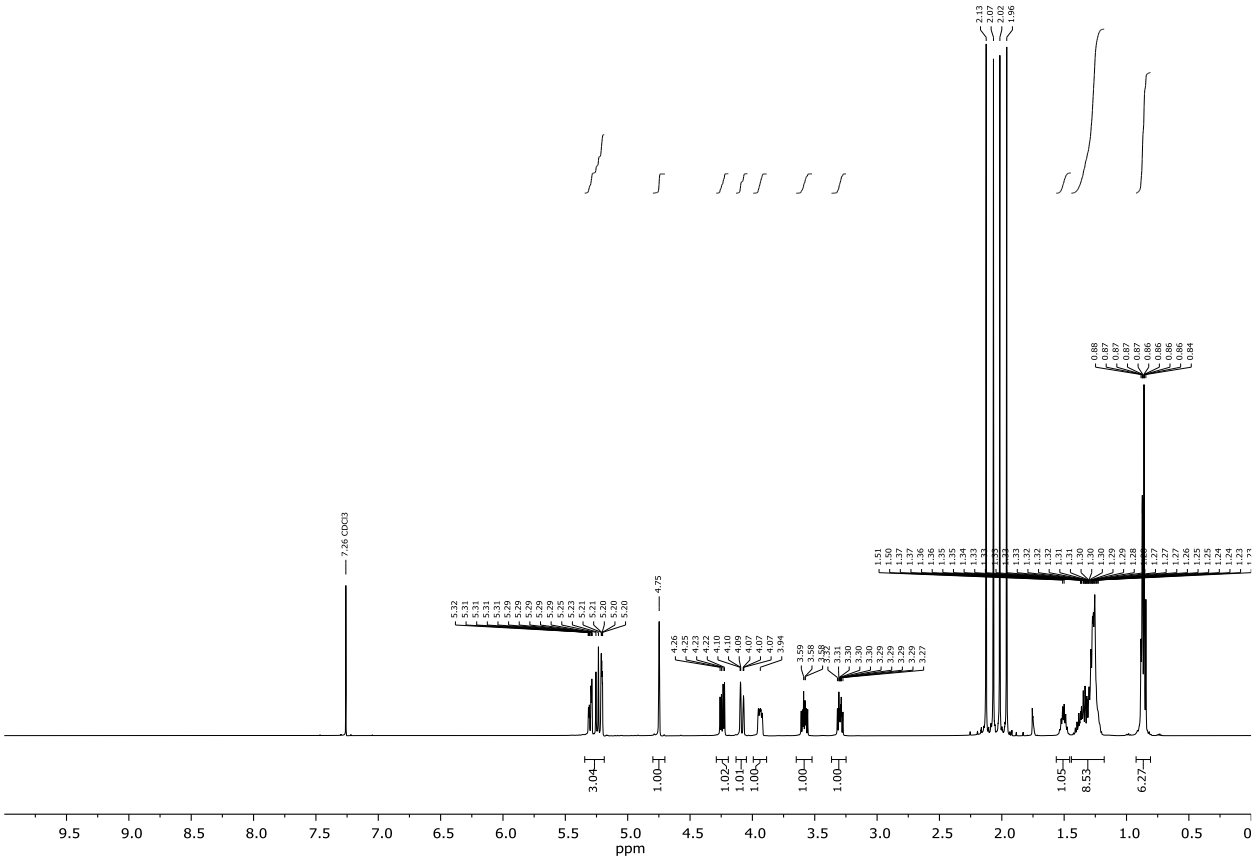

^{13}C NMR (126 MHz, $CDCl_3$) 2-Ethylhexyl 2,3,5,6-tetra-*O*-acetyl α-D-mannopyranoside

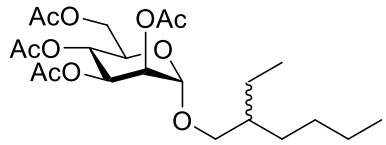

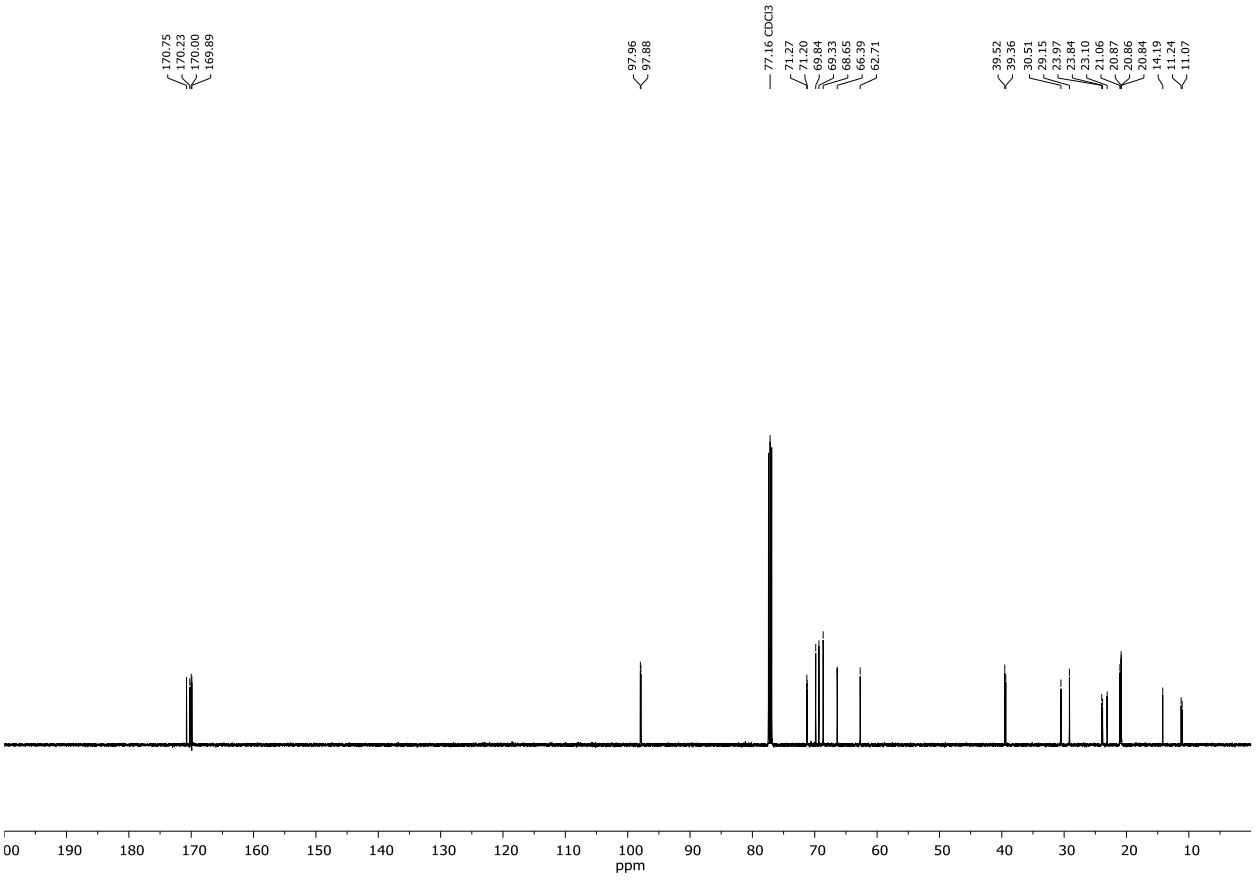

^{1}H-^{1}H COSY NMR (500 MHz, $CDCl_3$) 2-Ethylhexyl 2,3,5,6-tetra-*O*-acetyl α-D-mannopyranoside

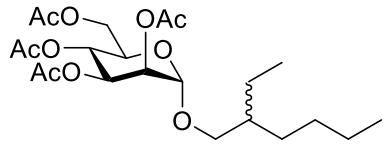

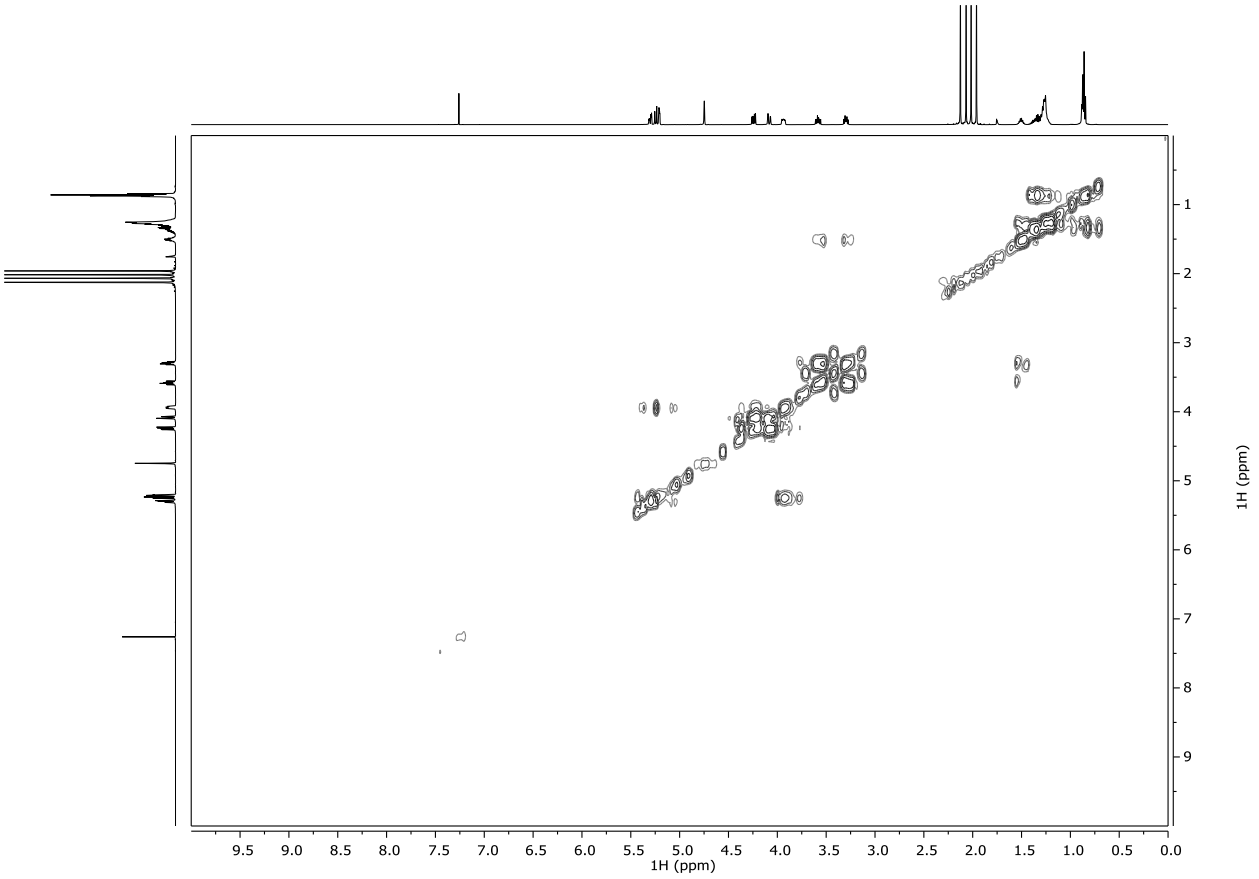

^{1}H-^{13}C HSQC NMR (500 MHz, $CDCl_3$) 2-Ethylhexyl 2,3,5,6-tetra-*O*-acetyl α-D-mannopyranoside

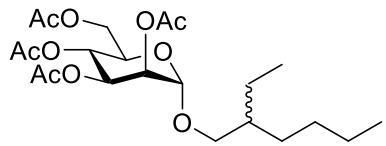

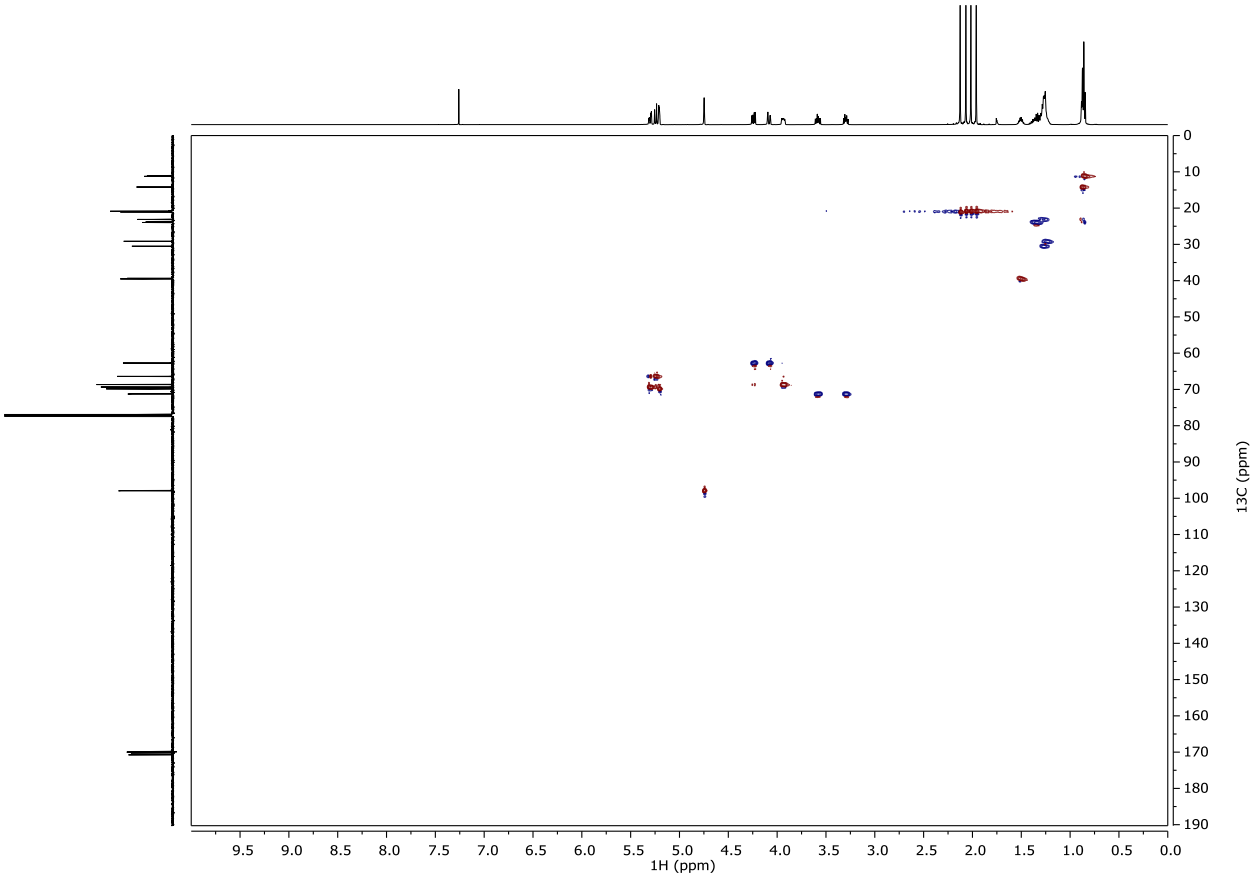

^{1}H-^{13}C HMBC NMR (500 MHz, $CDCl_3$) 2-Ethylhexyl 2,3,5,6-tetra-*O*-acetyl α-D-mannopyranoside

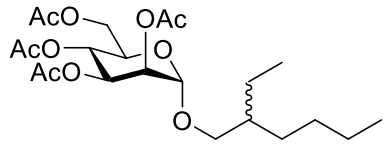

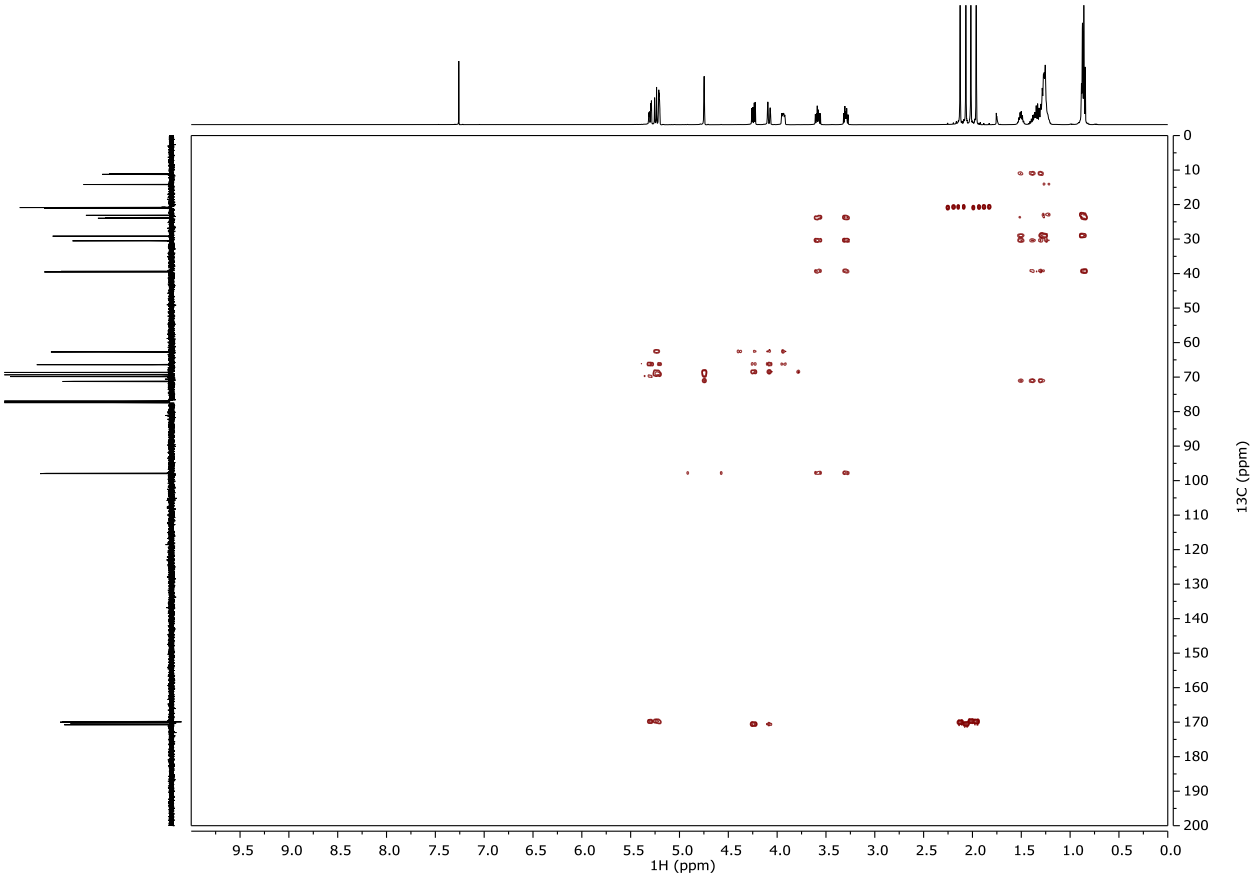

^{1}H NMR (500 MHz, DMSO-d_6) 2-Ethylhexyl-α-D-mannopyranoside

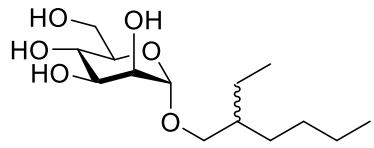

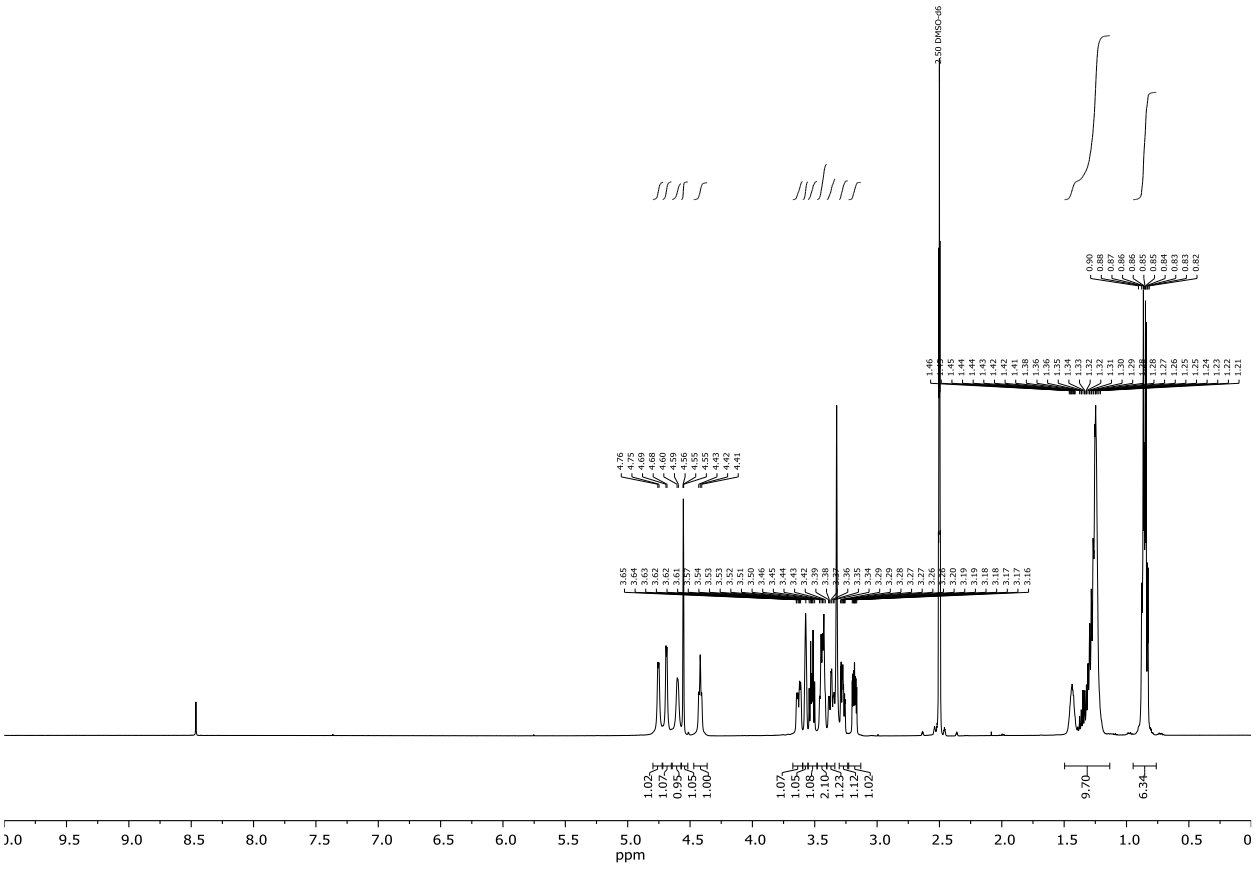

^{13}C NMR (126 MHz, DMSO-d_6) 2-Ethylhexyl-α-D-mannopyranoside

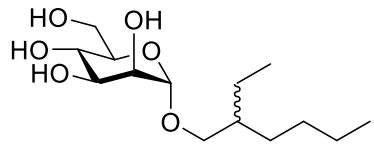

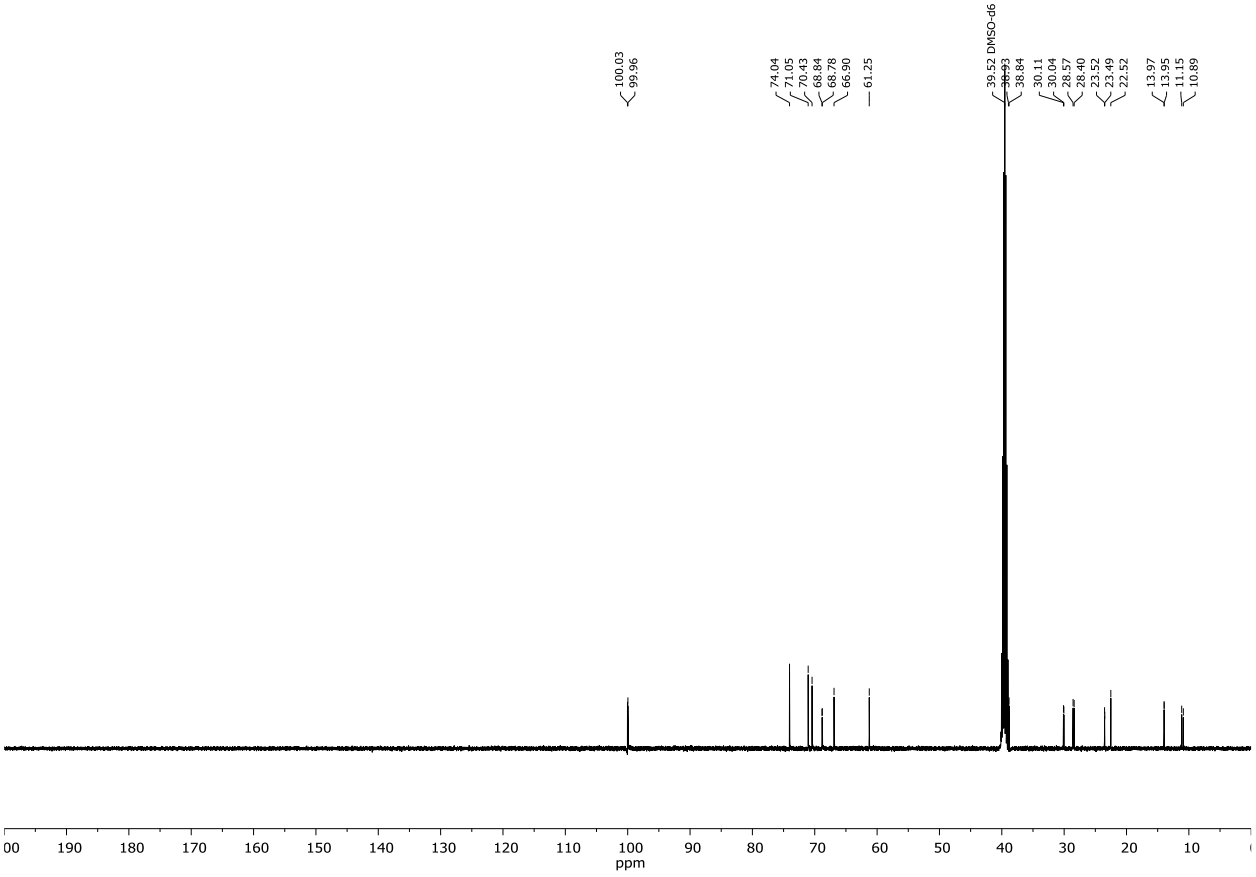

^{1}H-^{1}H COSY NMR (500 MHz, DMSO-d_6) 2-Ethylhexyl-α-D-mannopyranoside

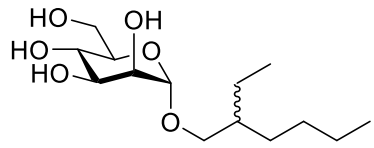

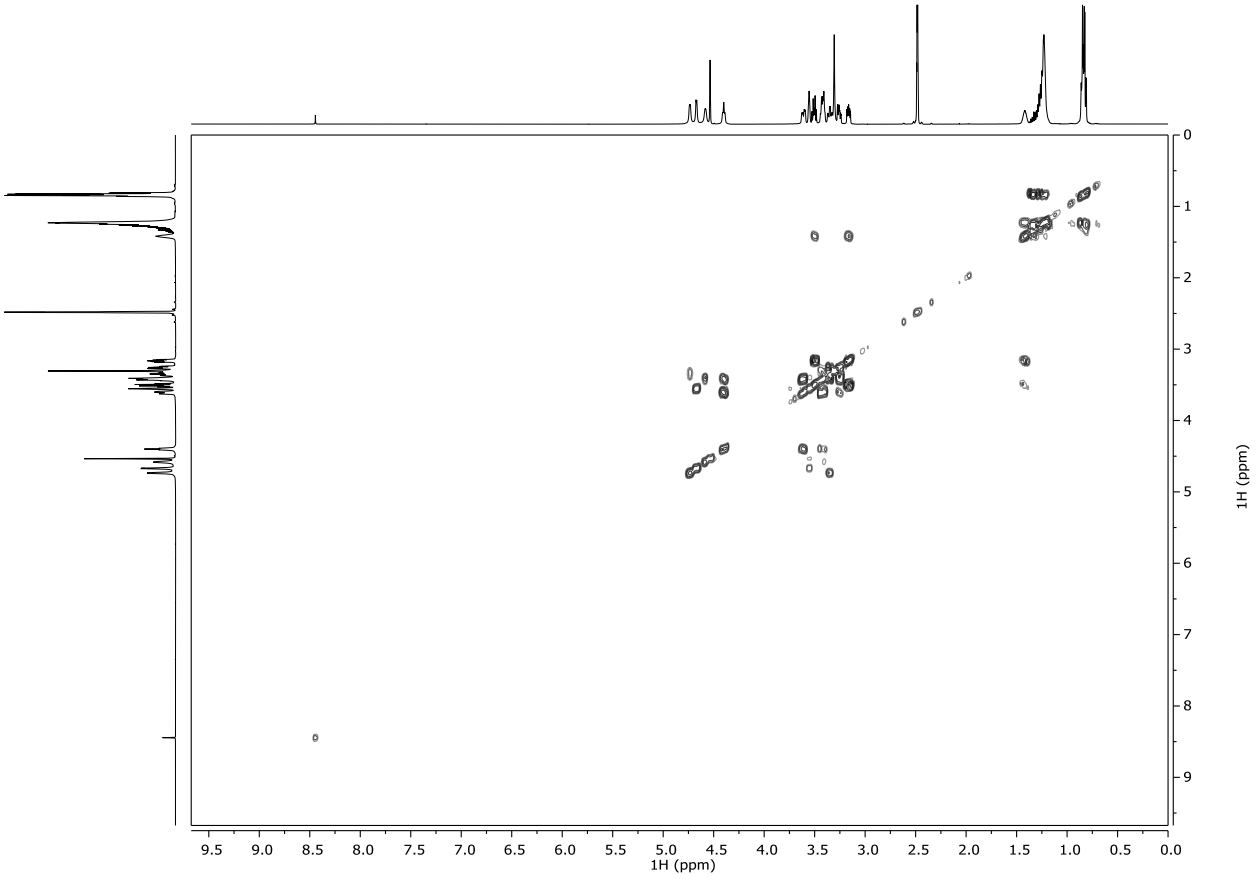

^{1}H-^{13}C HSQC NMR (500 MHz, DMSO-d_6) 2-Ethylhexyl-α-D-mannopyranoside

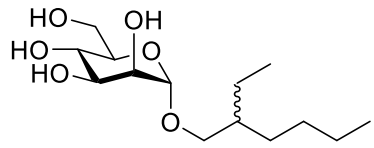

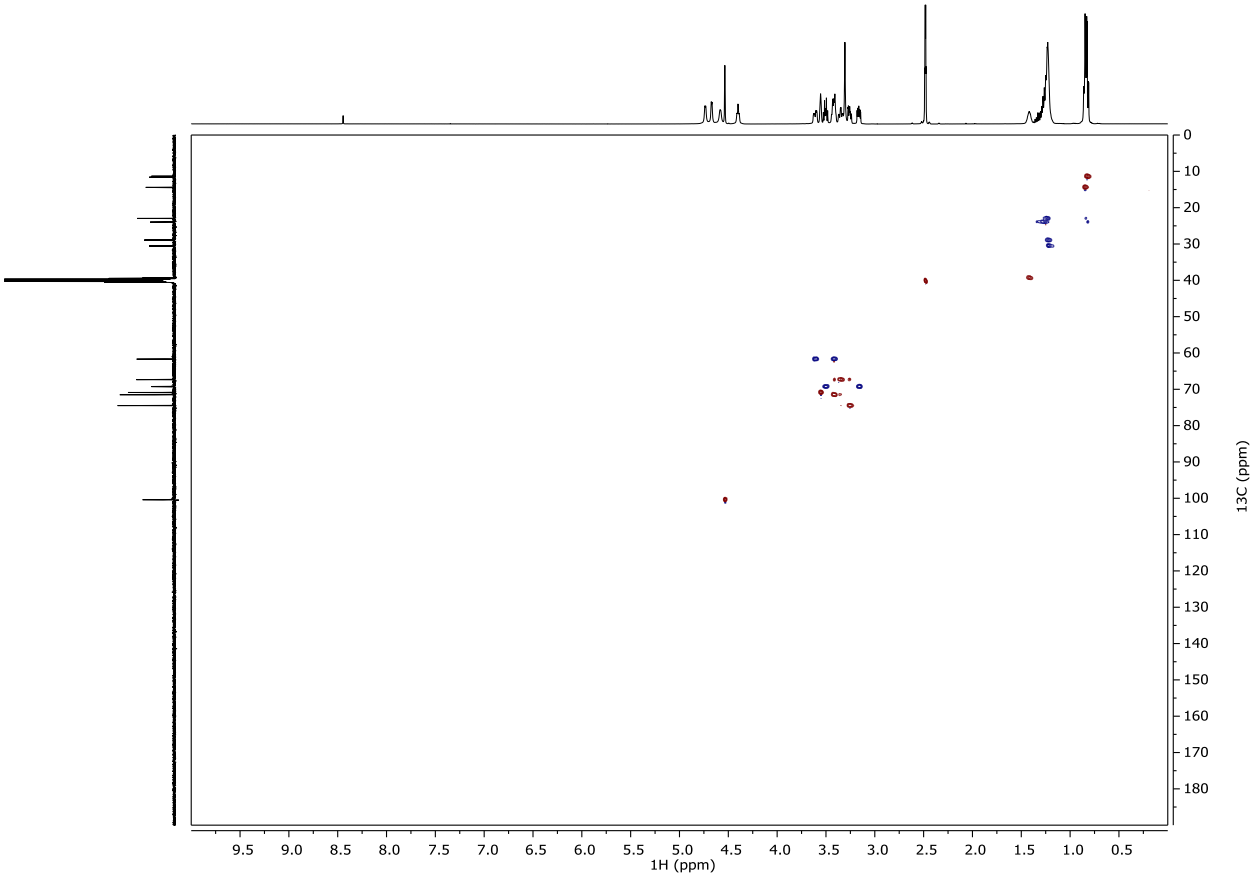

^{1}H-^{13}C HMBC NMR (500 MHz, DMSO-d_6) 2-Ethylhexyl-α-D-mannopyranoside

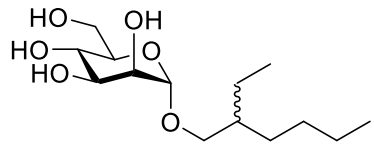

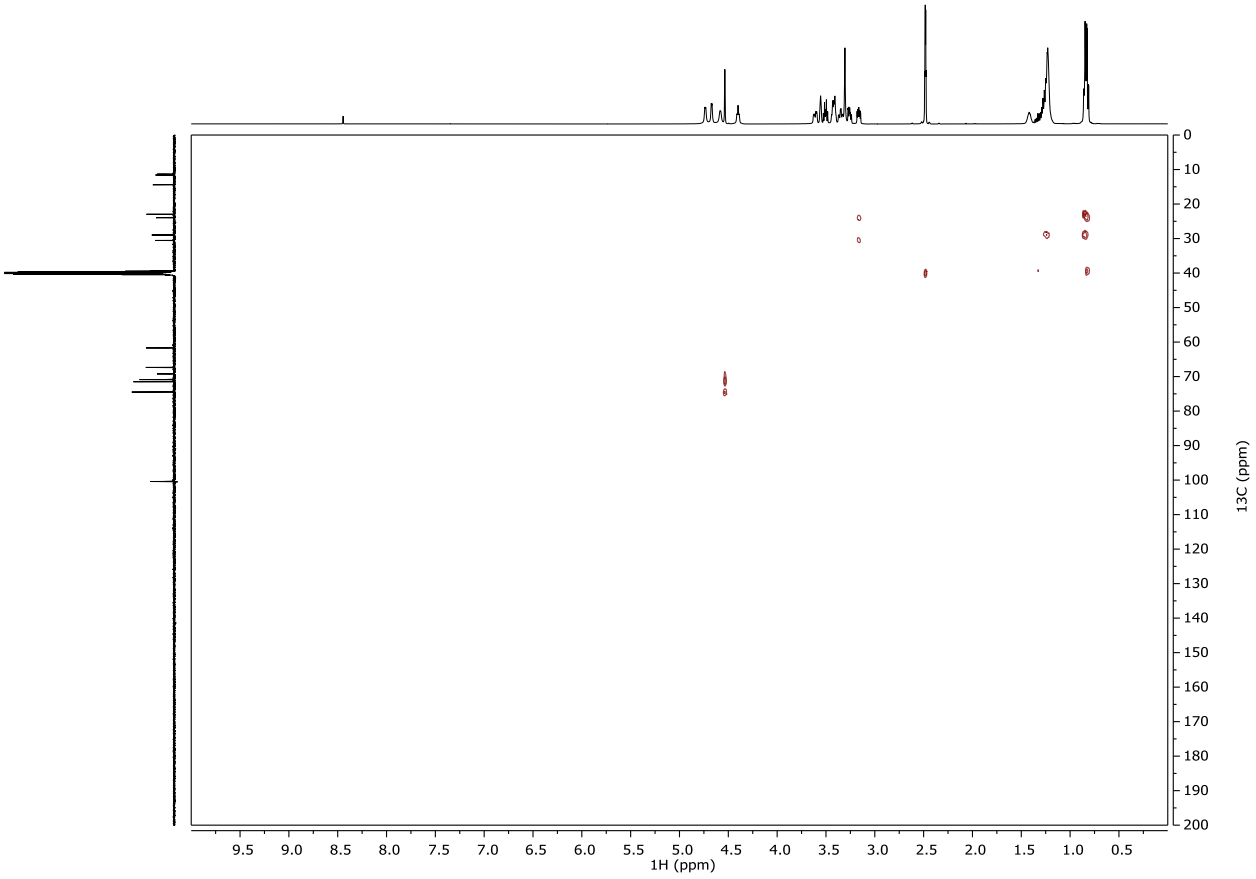

^{1}H NMR (500 MHz, DMSO-d_6) Poly(αOMegal sebacate)

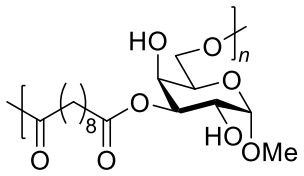

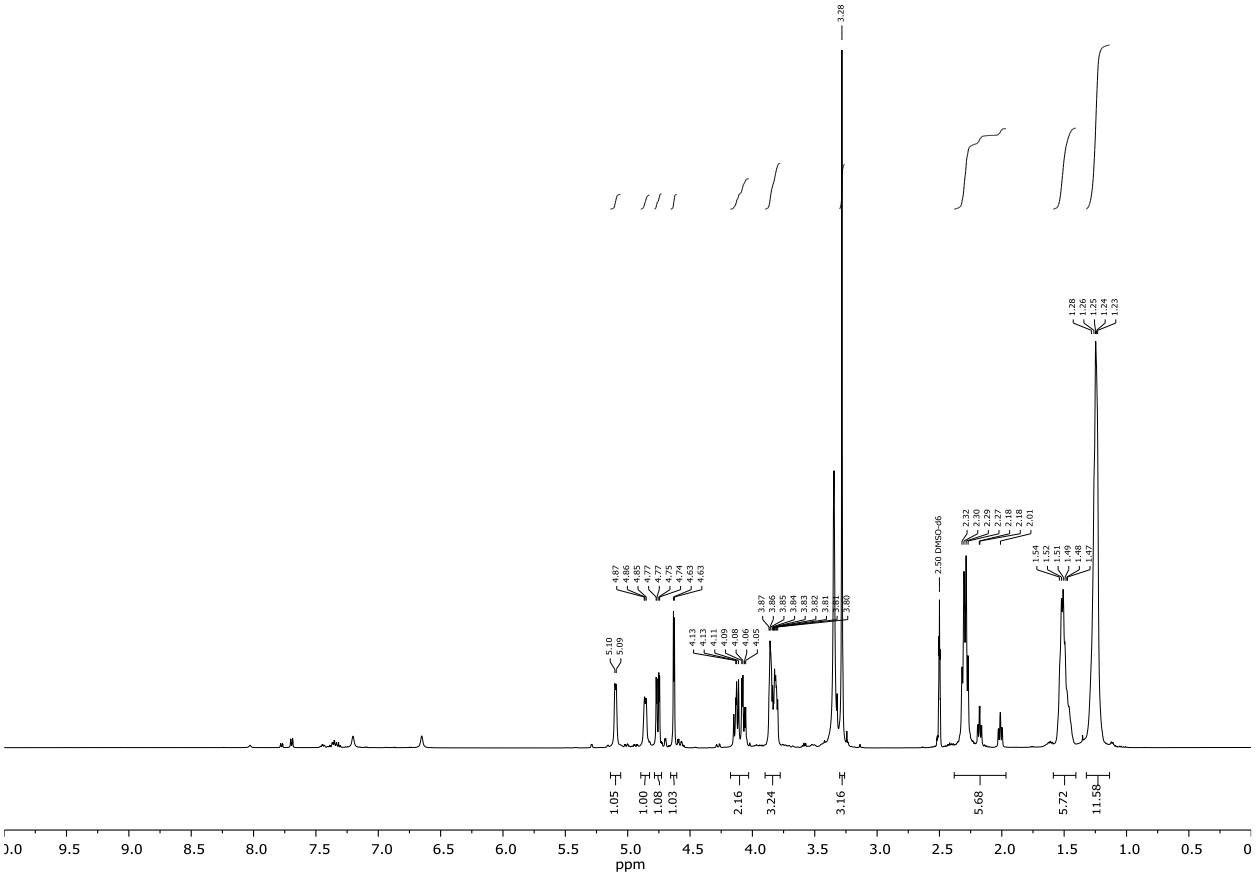

^{13}C NMR (126 MHz, DMSO-d_6) Poly(αOMegal sebacate)

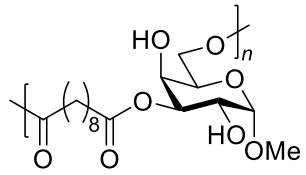

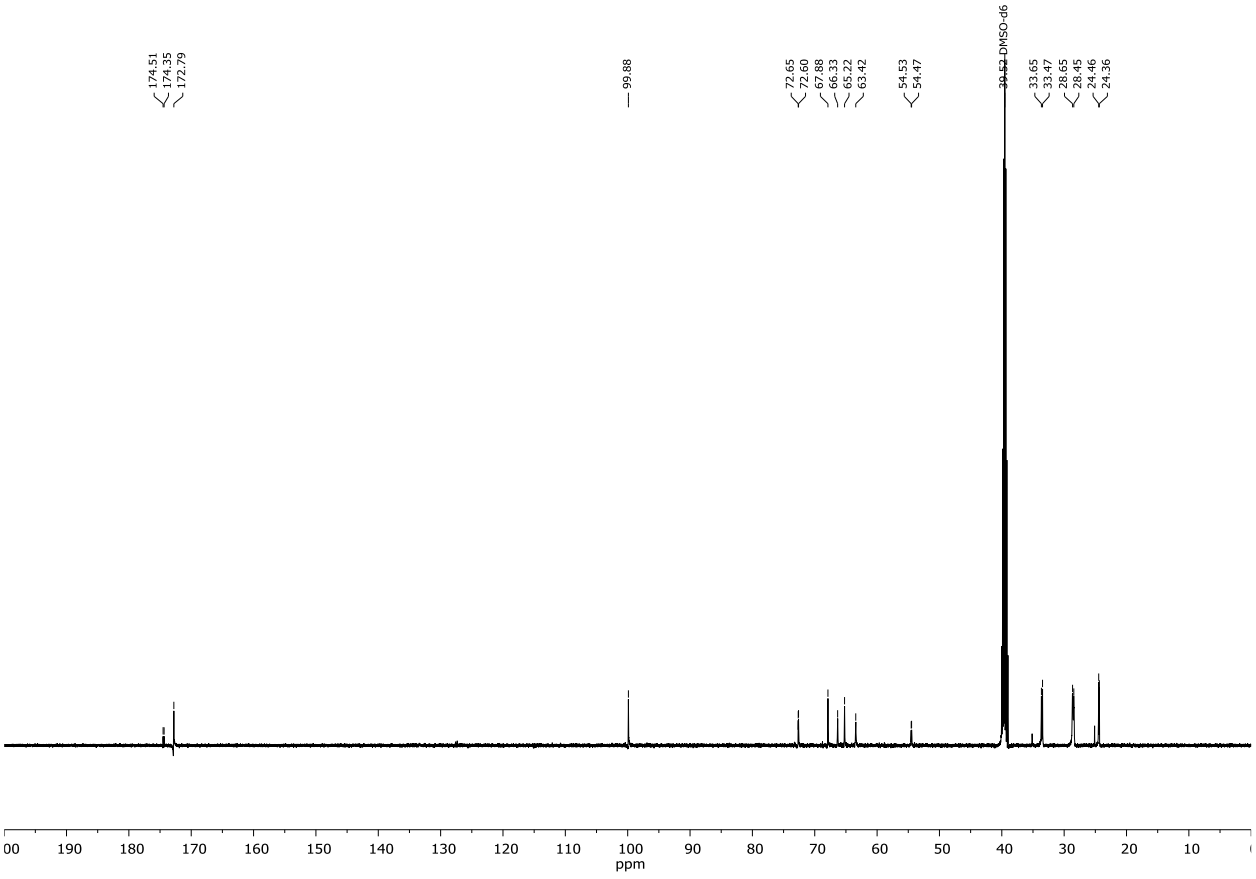

^{1}H-^{1}H COSY NMR (500 MHz, DMSO-d_6) Poly(αOMegal sebacate)

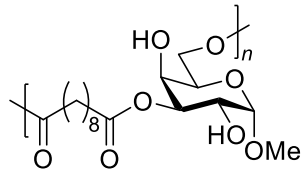

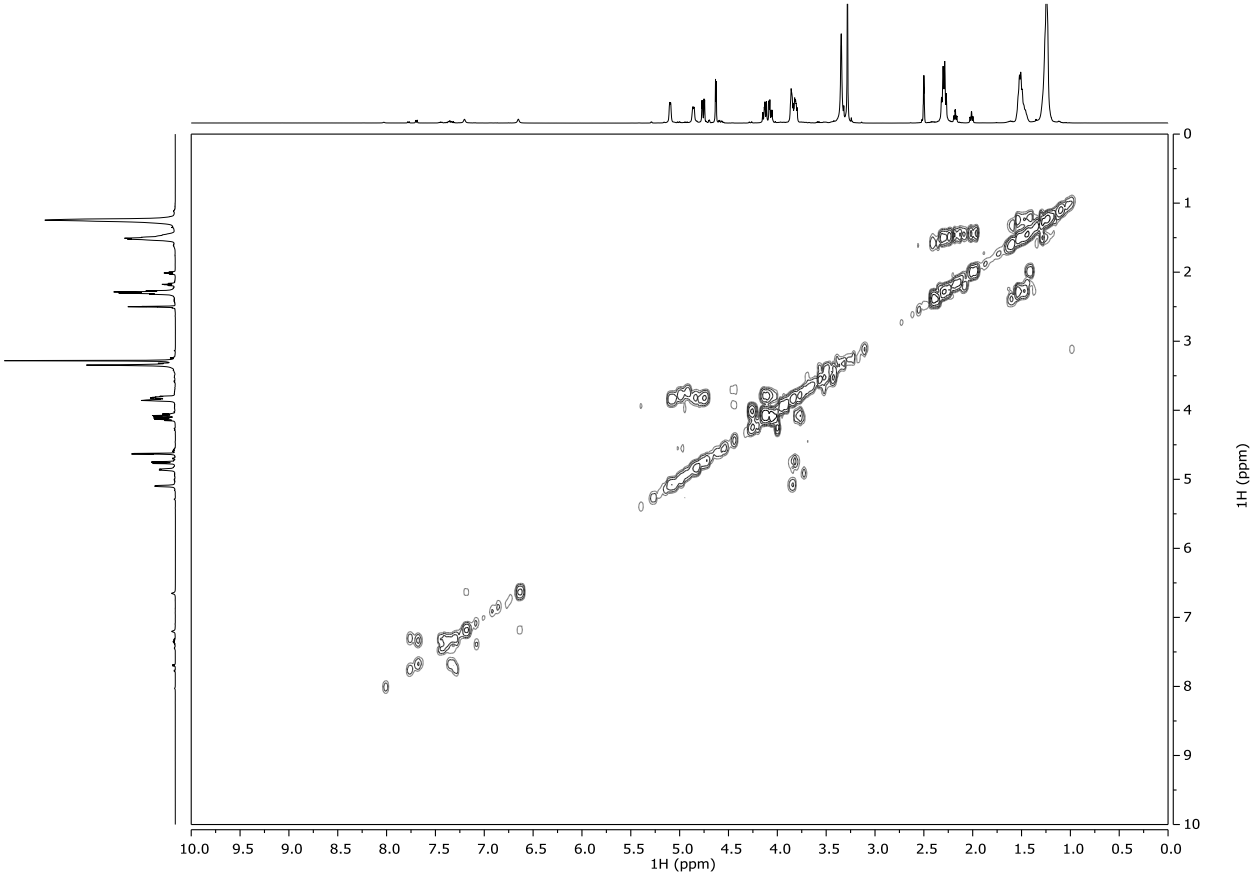

^{1}H NMR (500 MHz, DMSO-d_6) Poly(βOMegal sebacate)

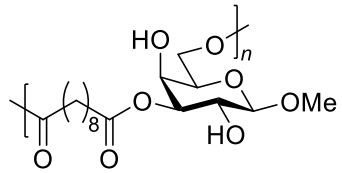

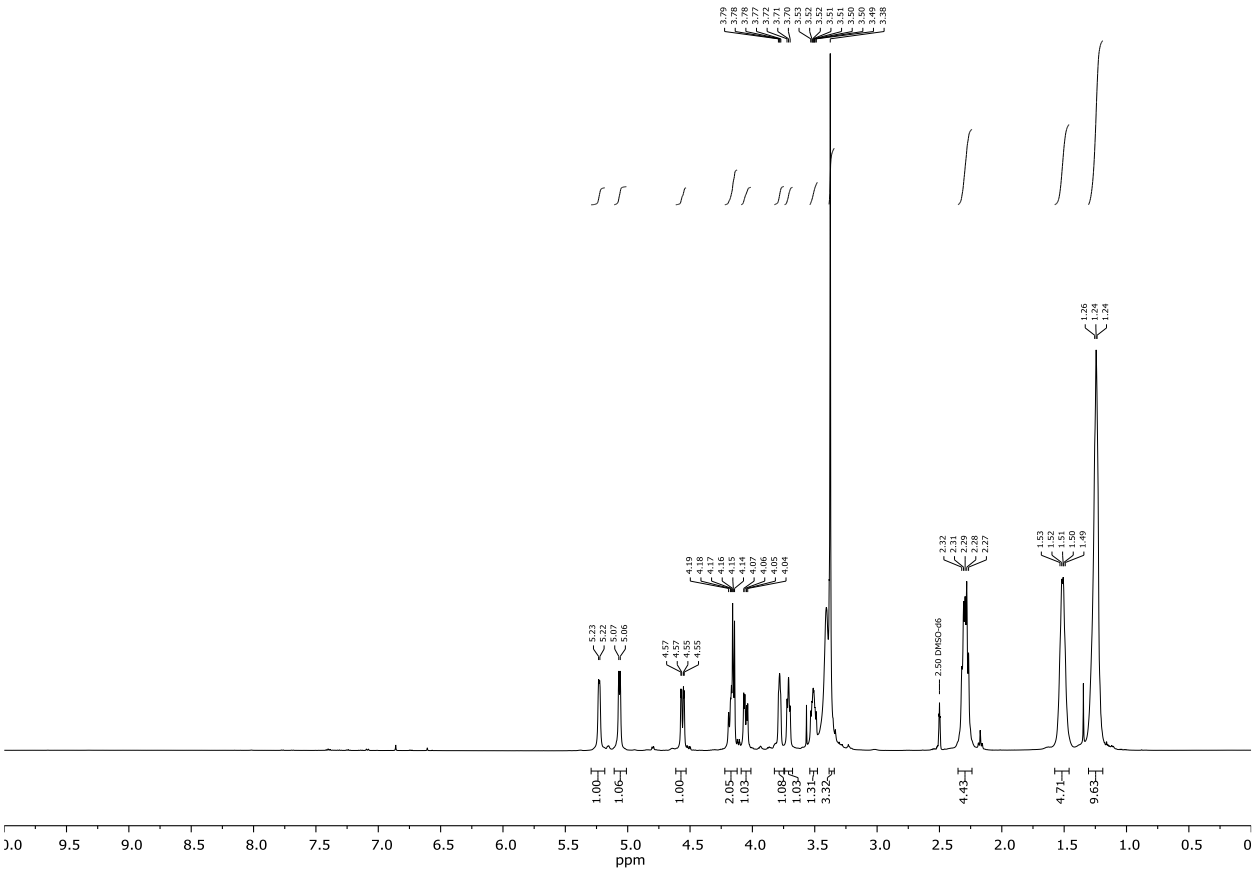

^{13}C NMR (126 MHz, DMSO-d_6) Poly(βOMegal sebacate)

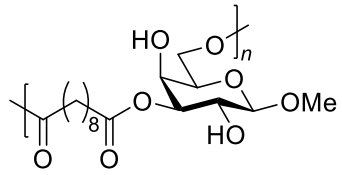

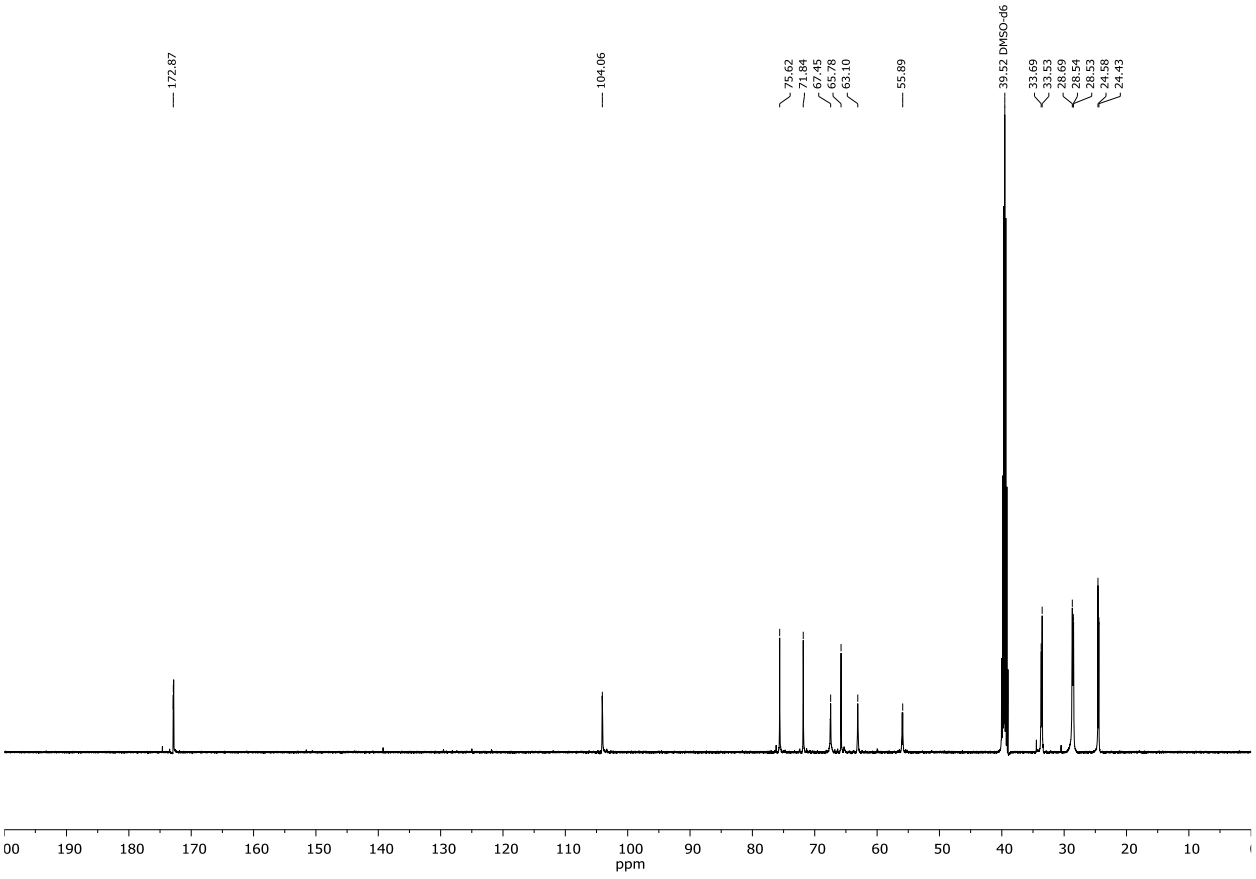

^{1}H-^{1}H COSY NMR (500 MHz, DMSO-d_6) Poly(βOMegal sebacate)

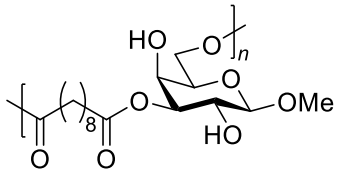

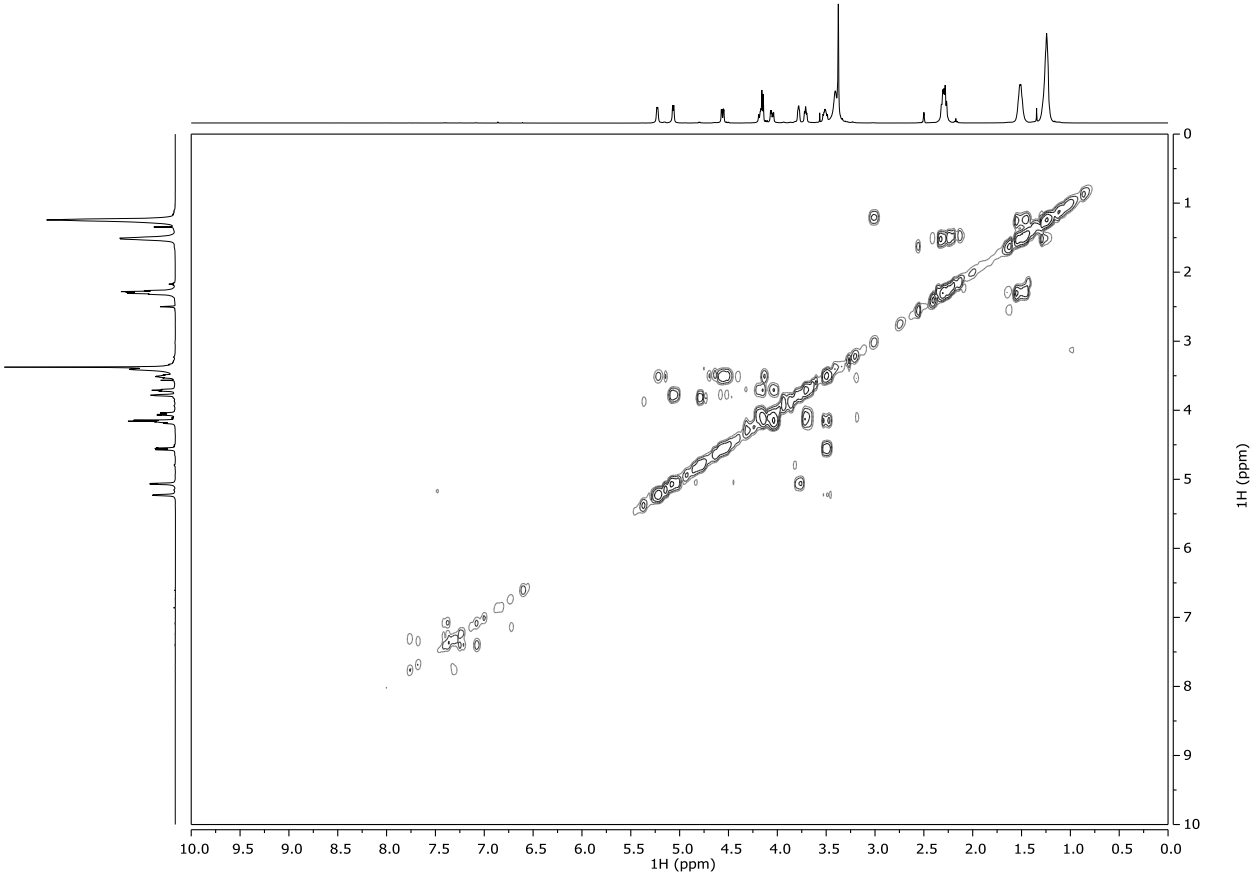

^{1}H NMR (500 MHz, DMSO-d_6) Poly(αOEtgal sebacate)

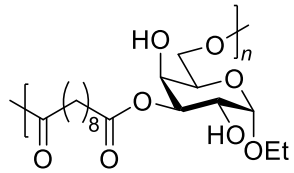

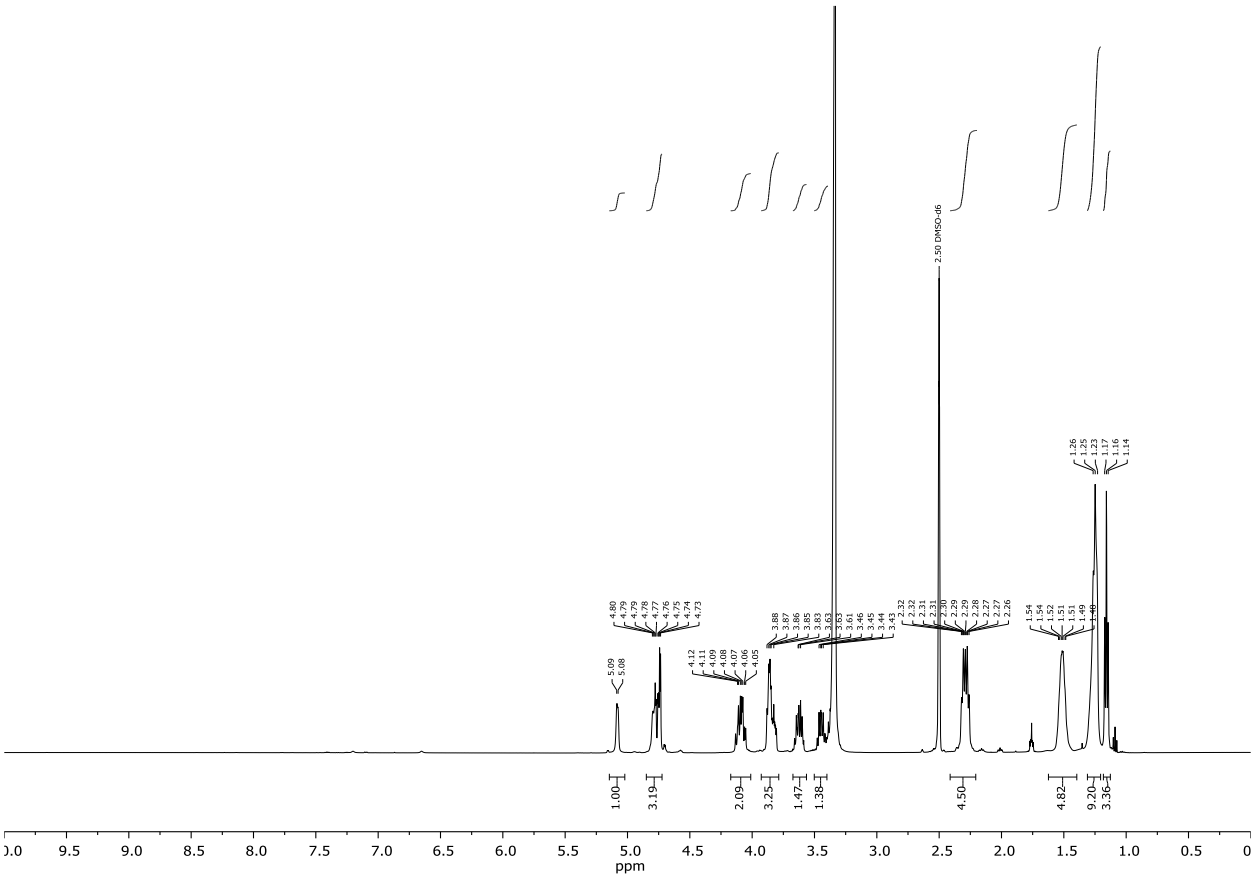

^{13}C NMR (126 MHz, DMSO-d_6) Poly(αOEtgal sebacate)

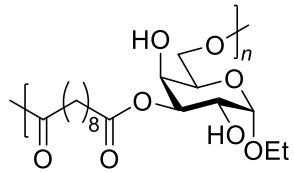

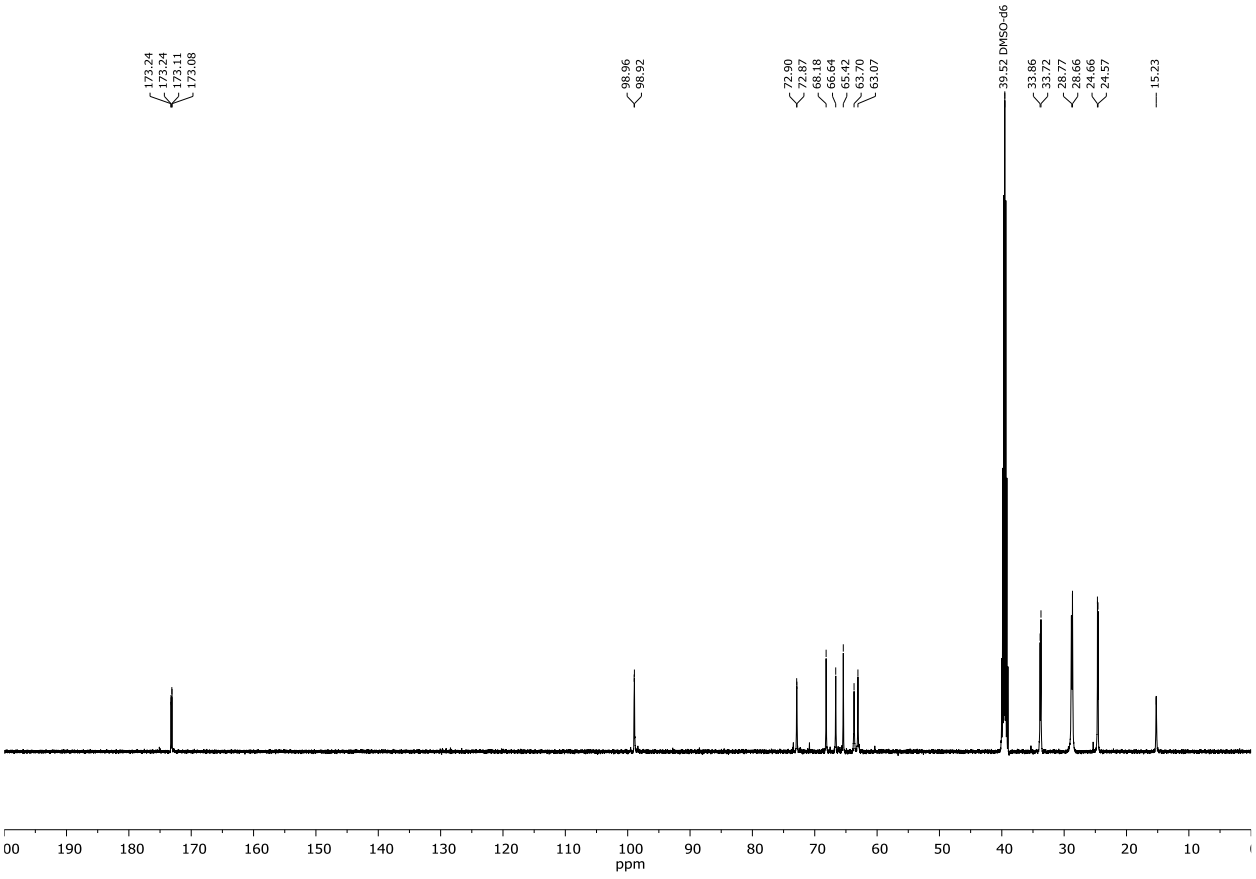

^{1}H-^{1}H COSY NMR (500 MHz, DMSO-d_6) Poly(αOEtgal sebacate)

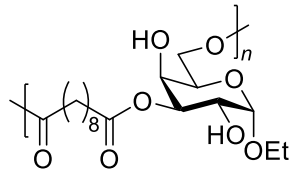

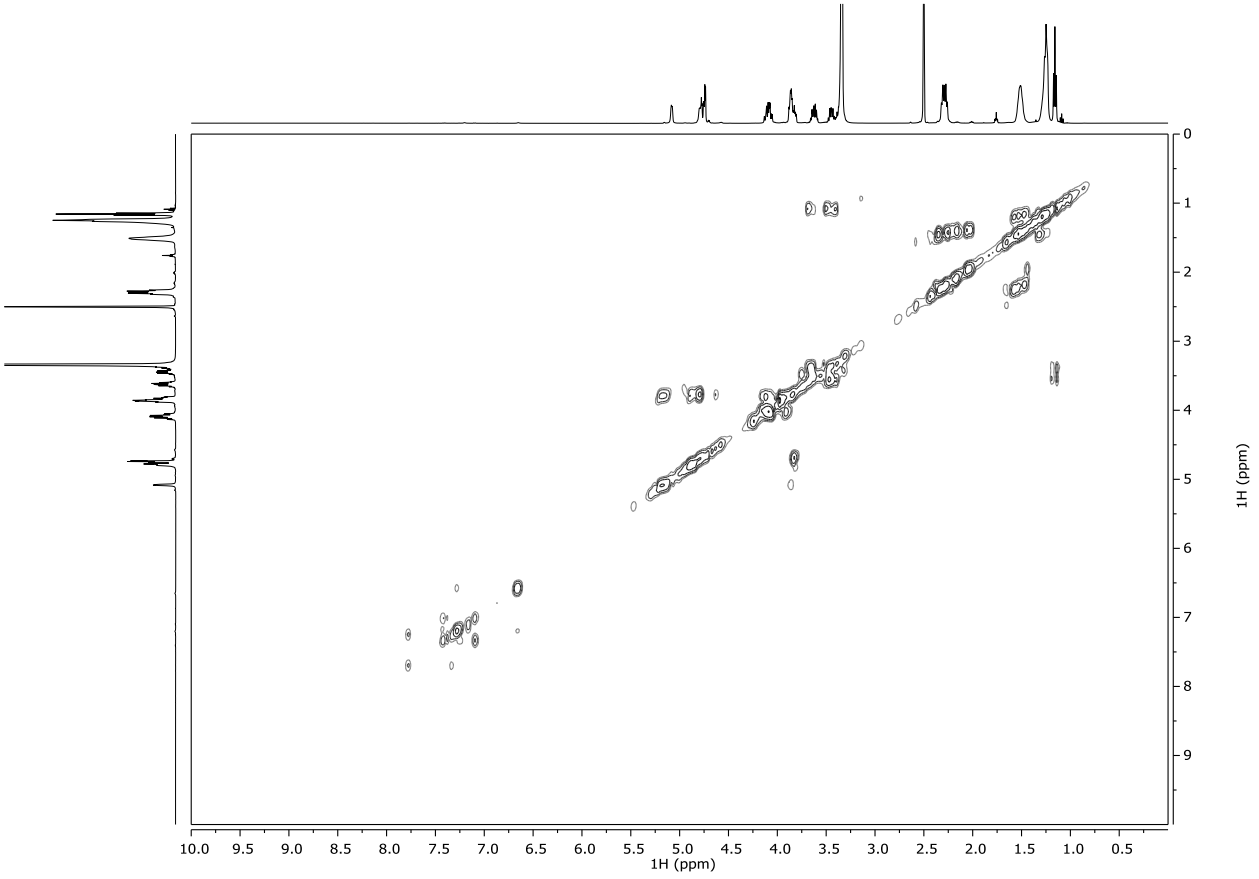

^{1}H NMR (500 MHz, DMSO-d_6) Poly(βOEtgal sebacate)

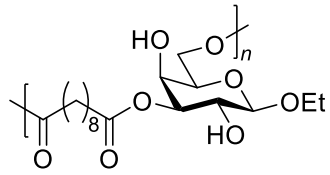

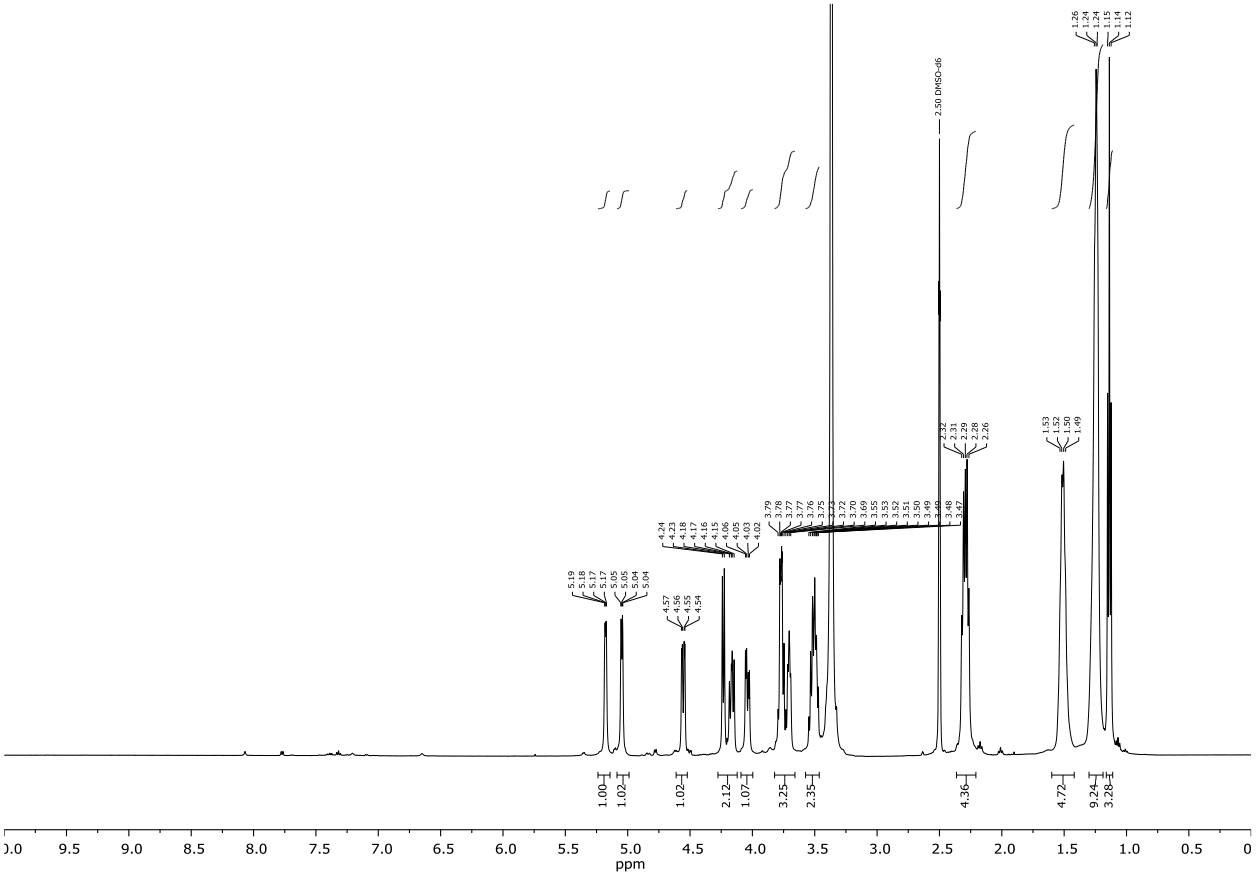

^{13}C NMR (126 MHz, DMSO-d_6) Poly(βOEtgal sebacate)

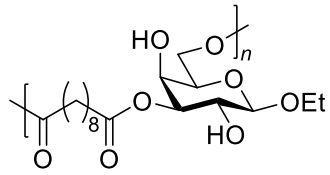

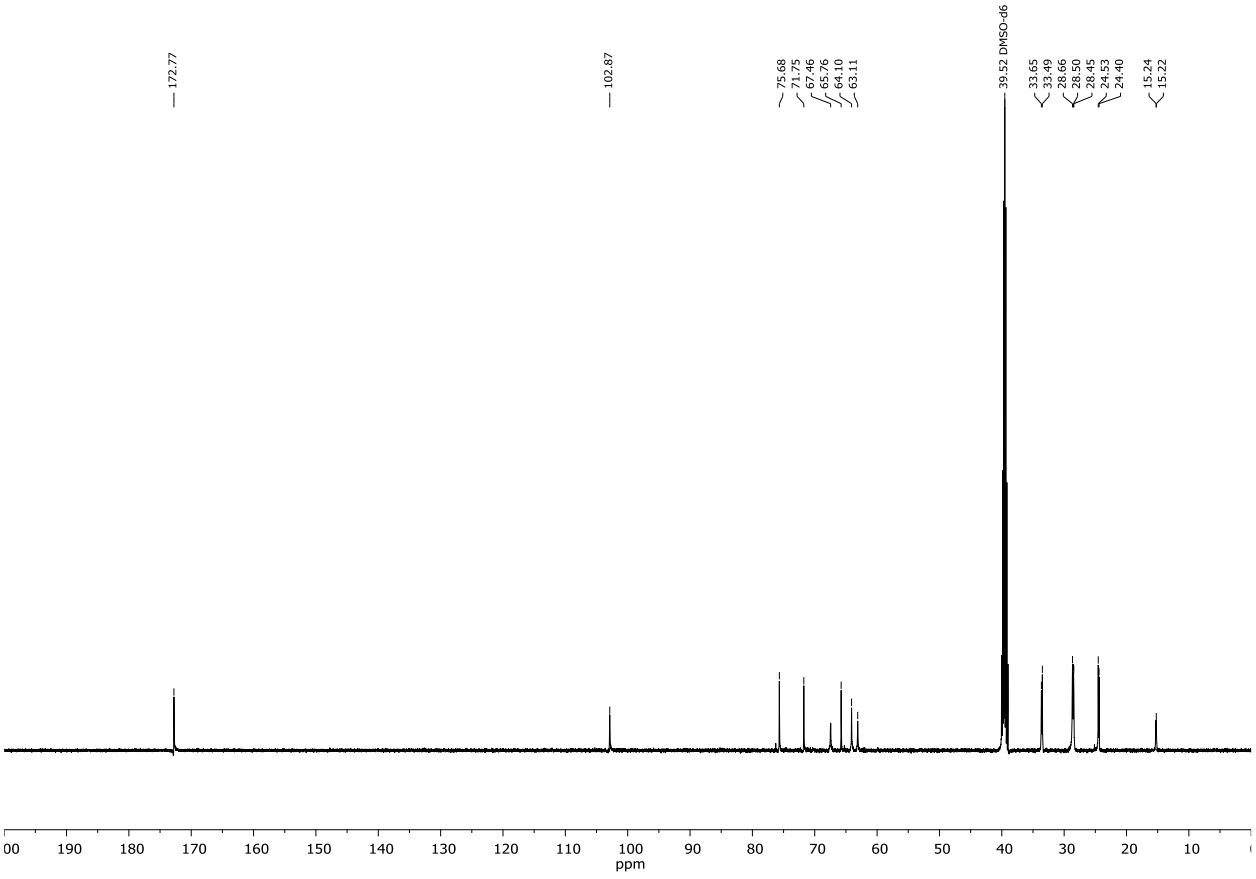

^{1}H-^{1}H COSY NMR (500 MHz, DMSO-d_6) Poly(βOEtgal sebacate)

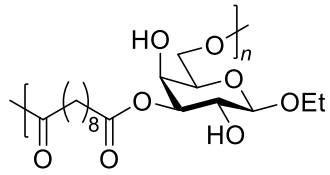

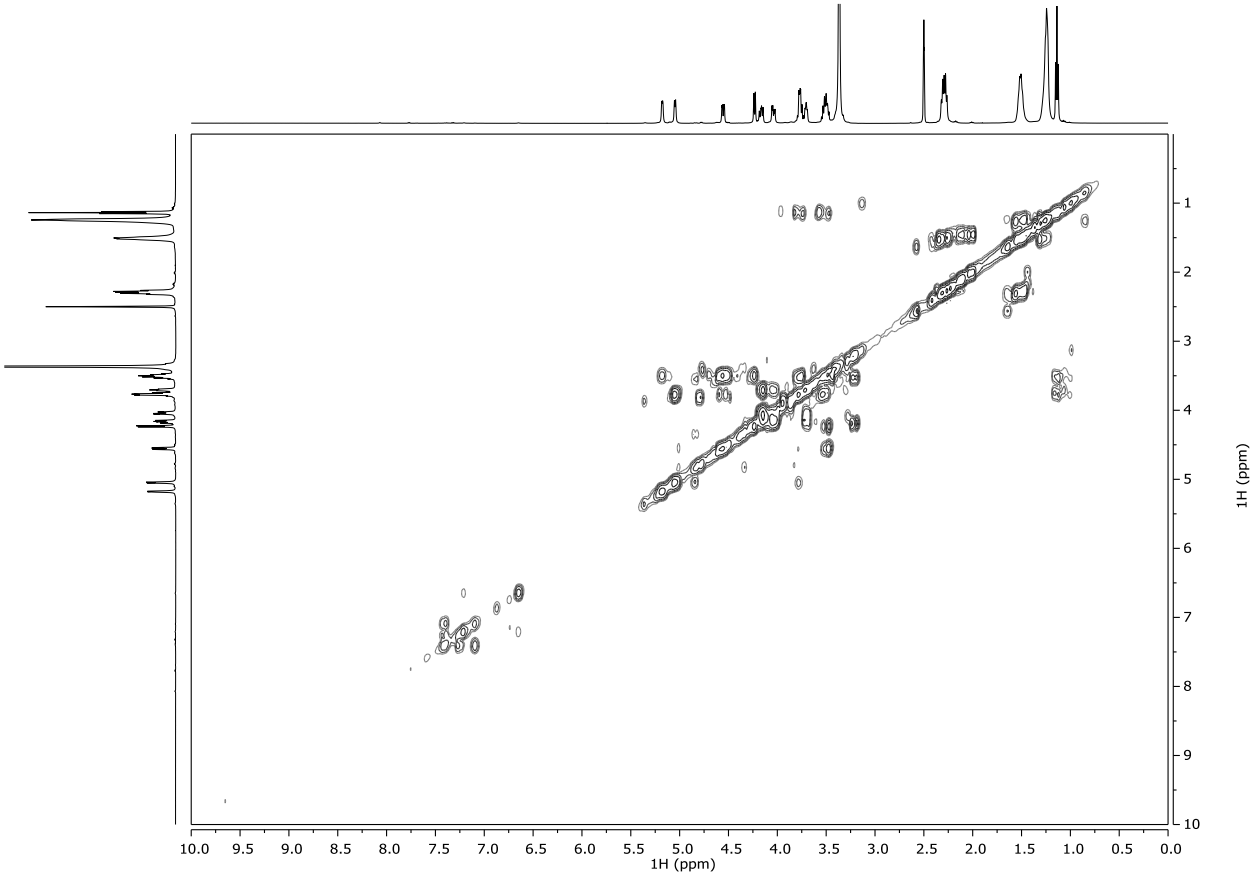

^{1}H NMR (500 MHz, DMSO-d_6) Poly(αO*n*-octgal sebacate)

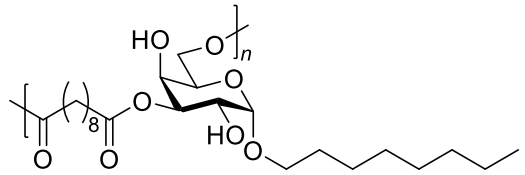

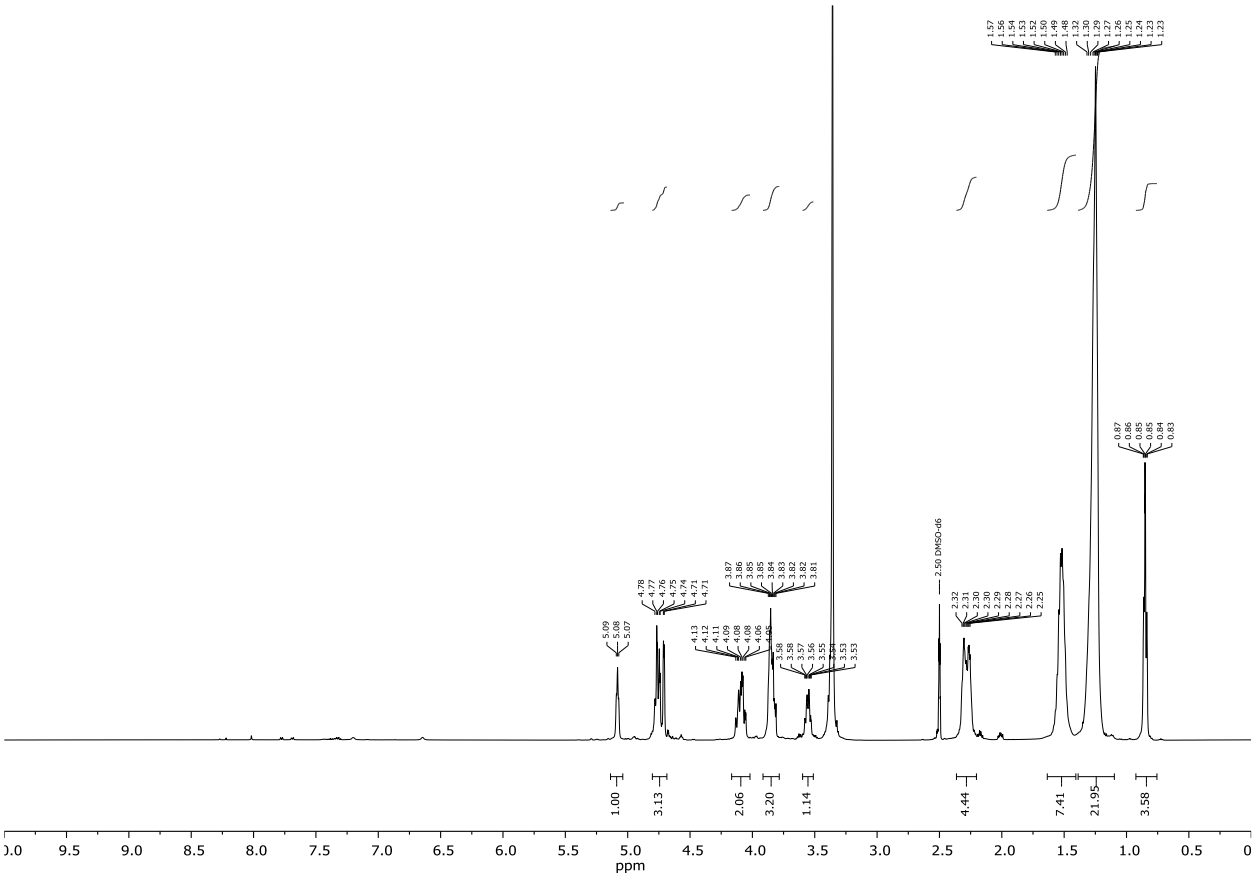

^{13}C NMR (126 MHz, DMSO-d_6) Poly(αO*n*-octgal sebacate)

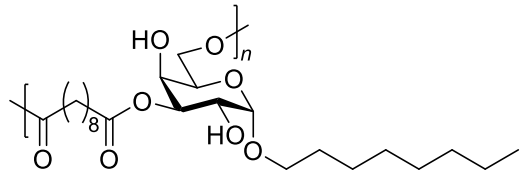

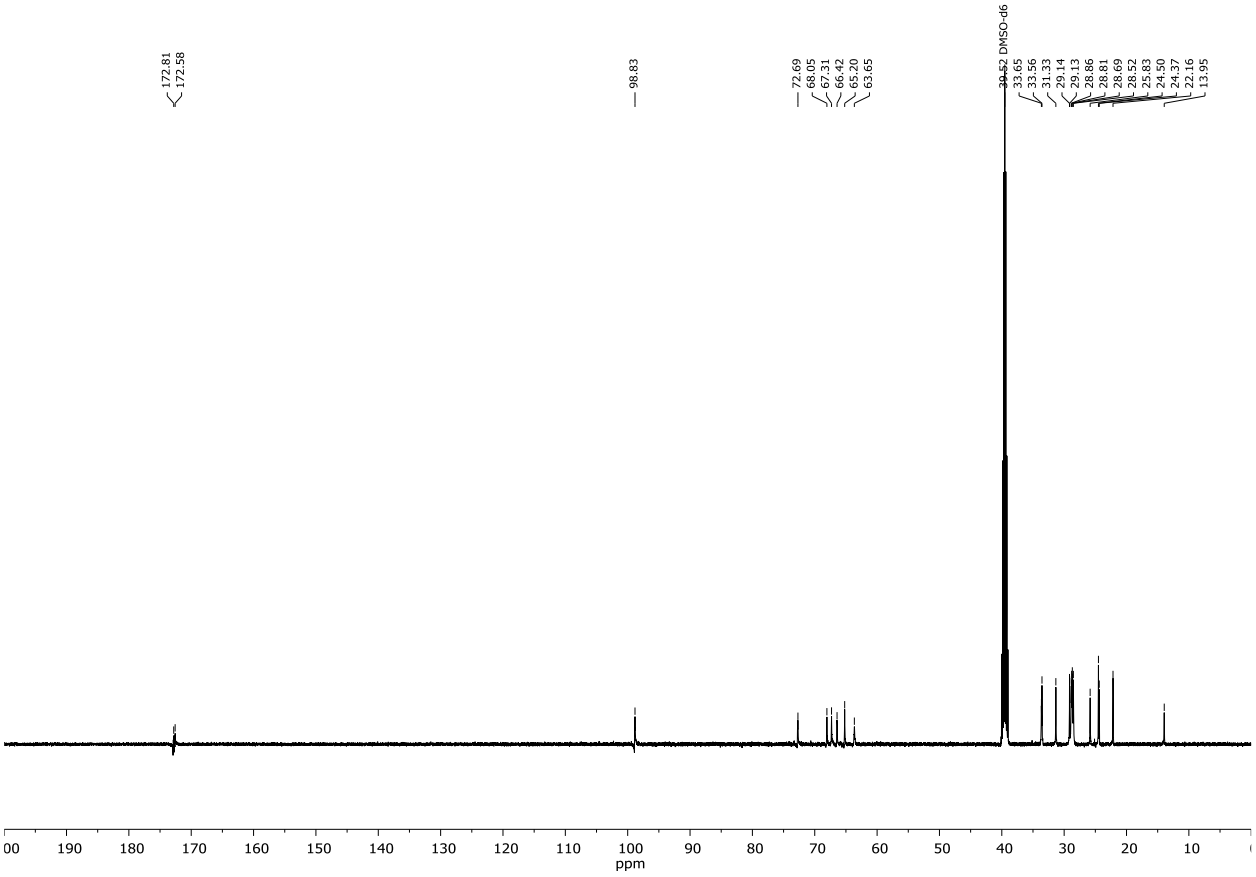

^{1}H-^{1}H COSY NMR (500 MHz, DMSO-d_6) Poly(αO*n*-octgal sebacate)

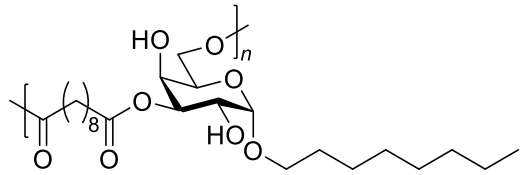

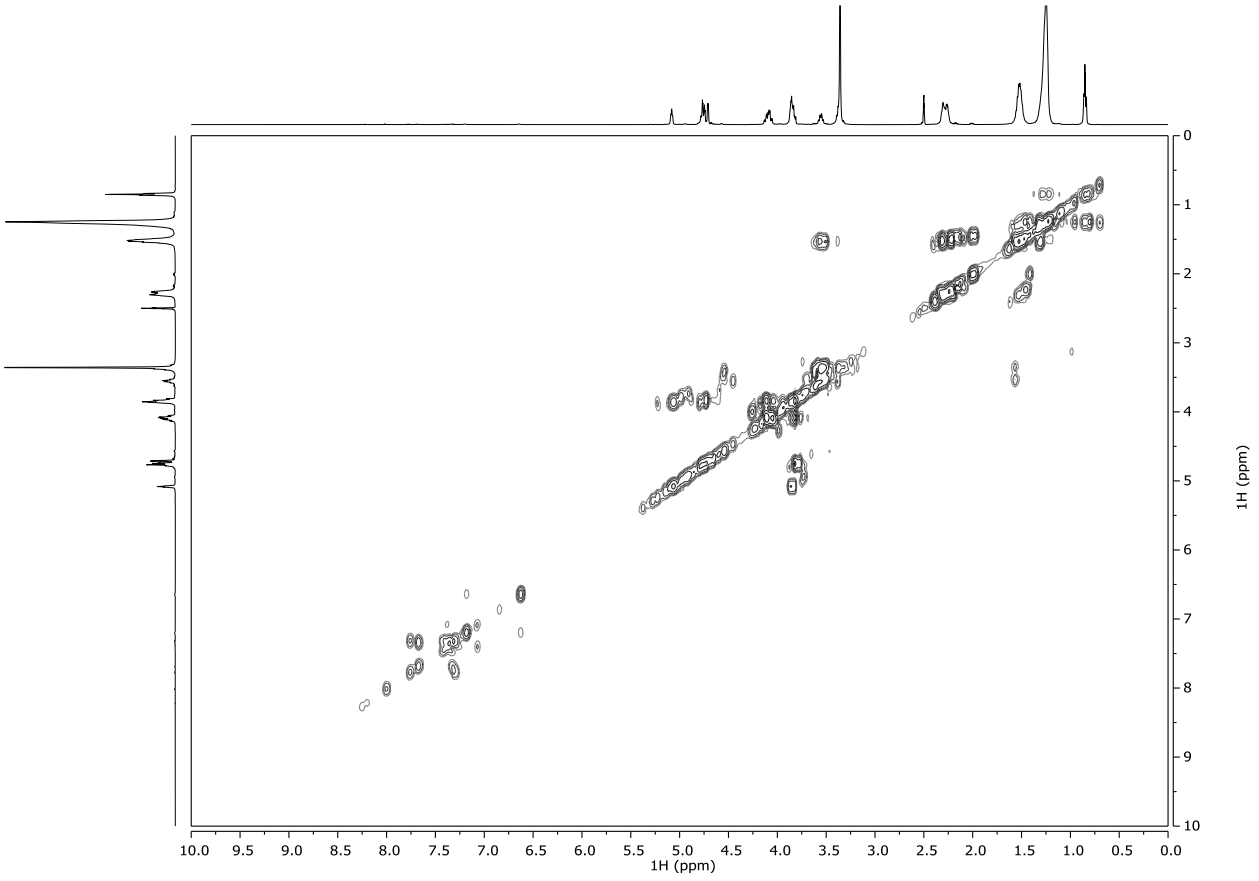

^{1}H NMR (500 MHz, DMSO-d_6) Poly(βO*n*-octgal sebacate)

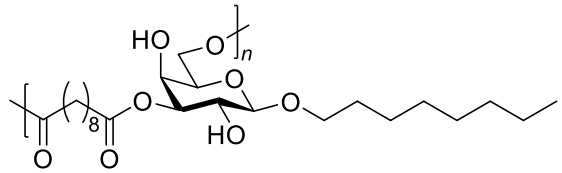

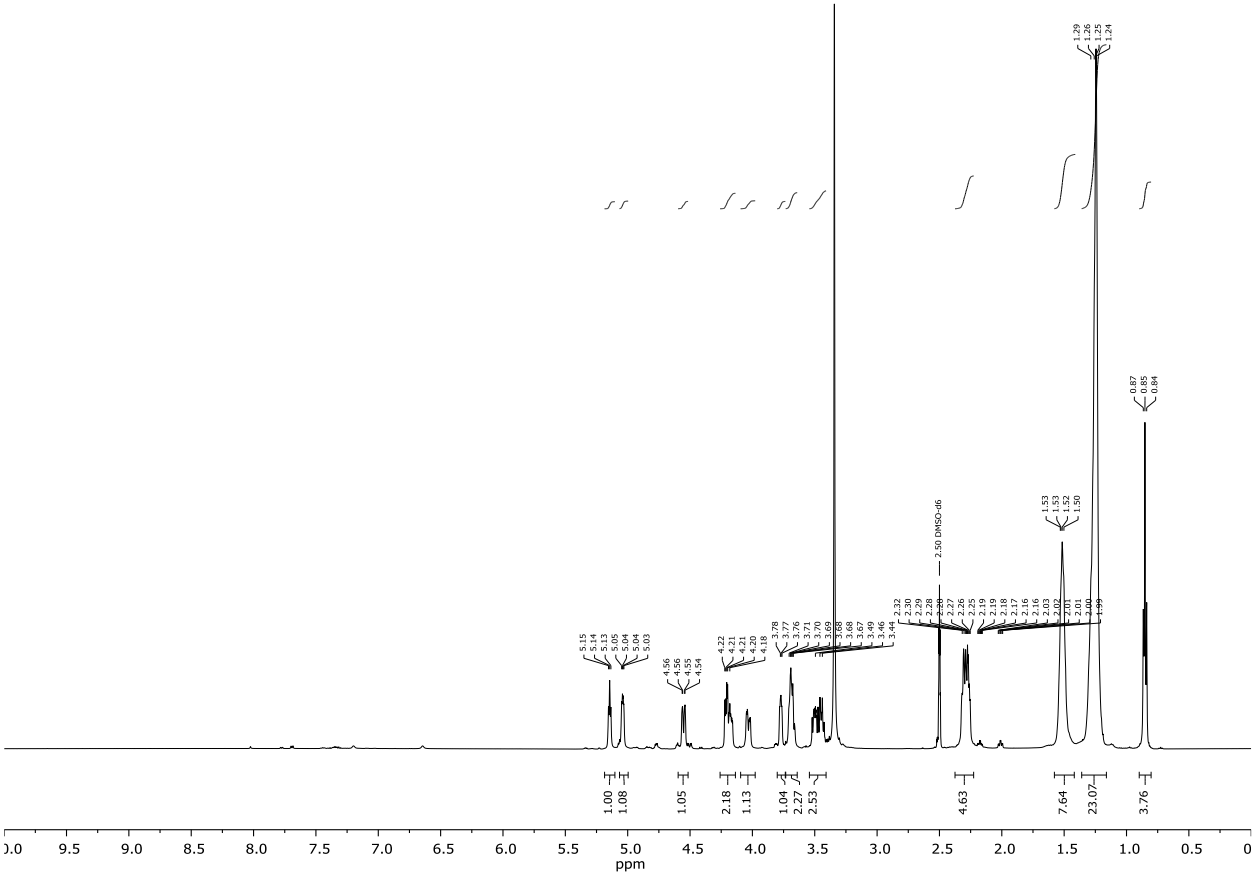

^{13}C NMR (126 MHz, DMSO-d_6) Poly(βO*n*-octgal sebacate)

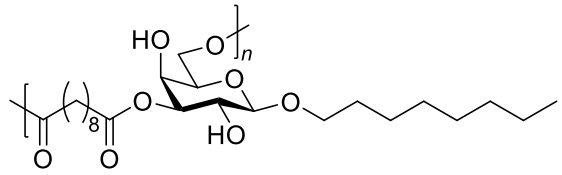

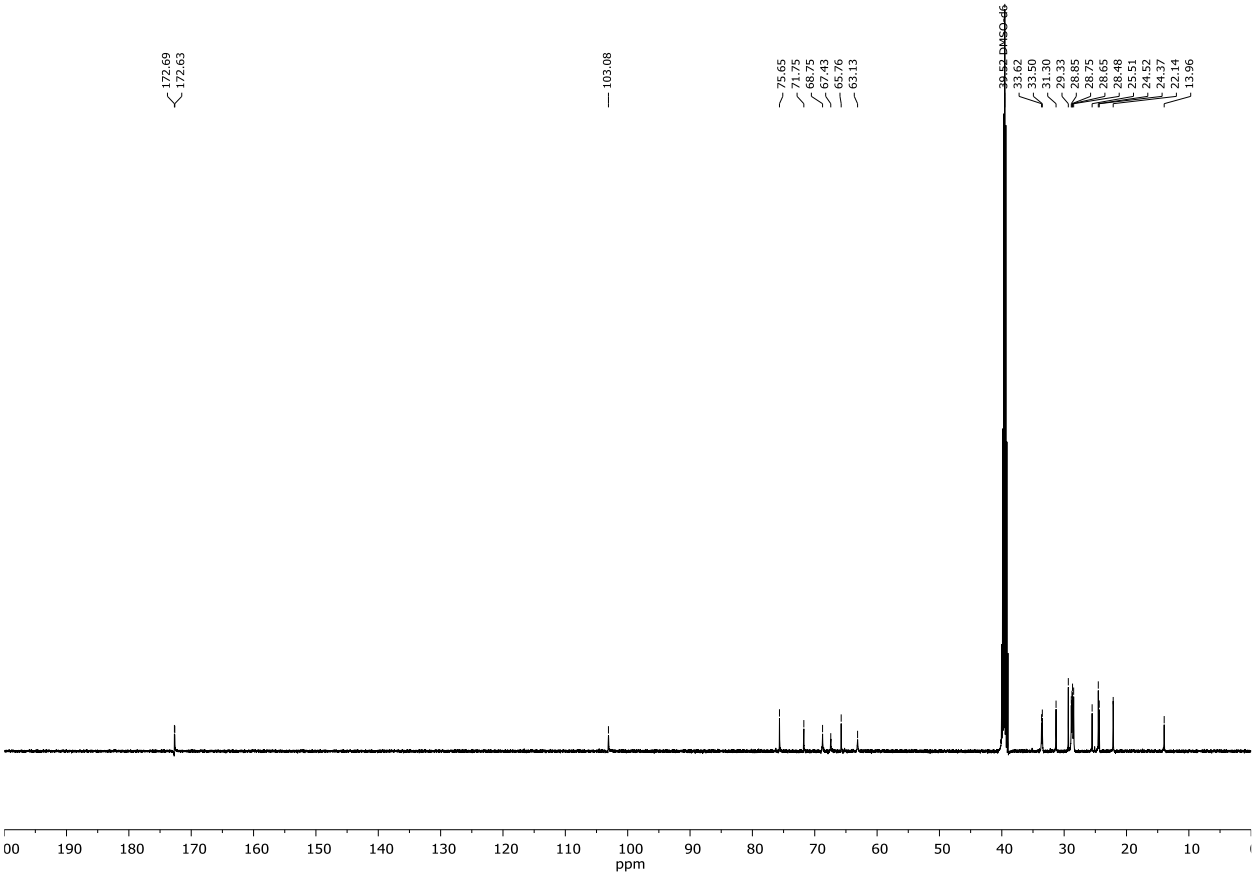

^{1}H-^{1}H COSY NMR (500 MHz, DMSO-d_6) Poly(βO*n*-octgal sebacate)

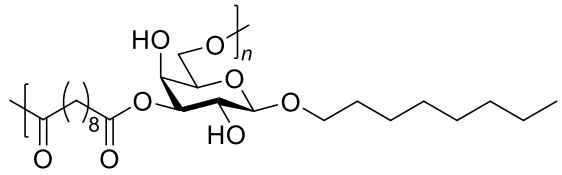

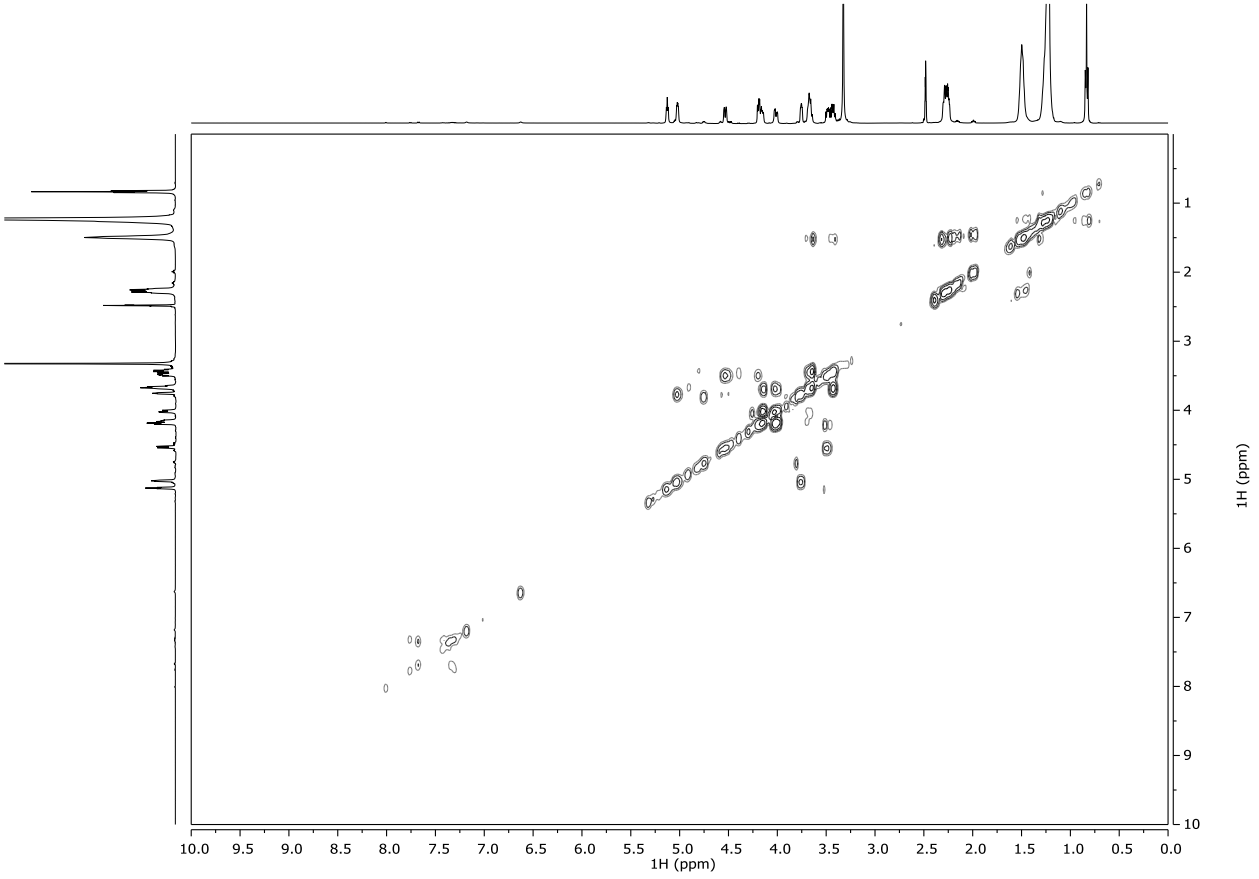

^{1}H NMR (500 MHz, DMSO-d_6) Poly(αO*i*-octgal sebacate)

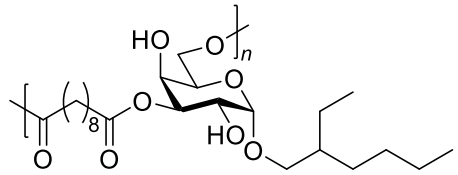

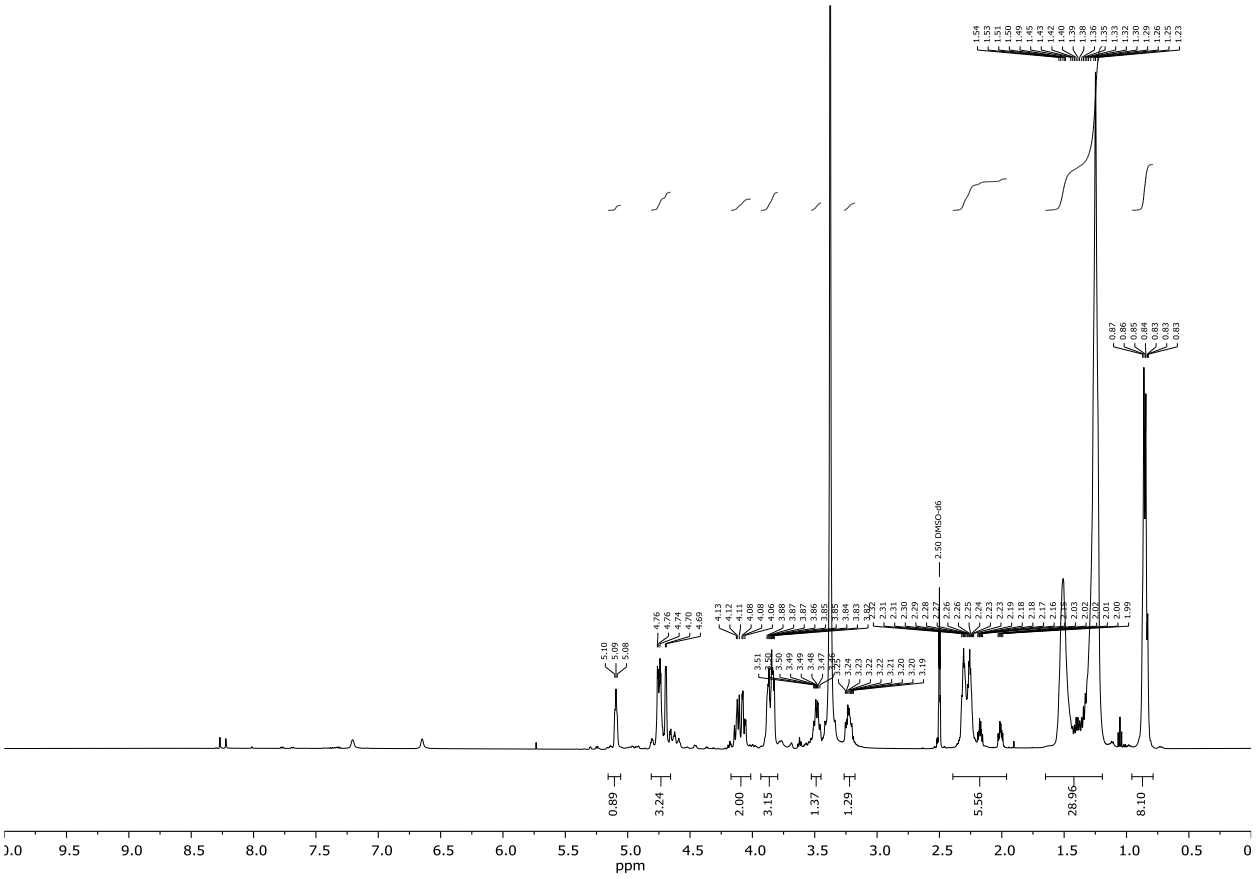

^{13}C NMR (126 MHz, DMSO-d_6) Poly(αO*i*-octgal sebacate)

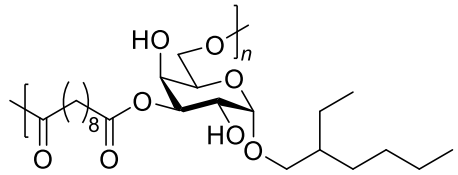

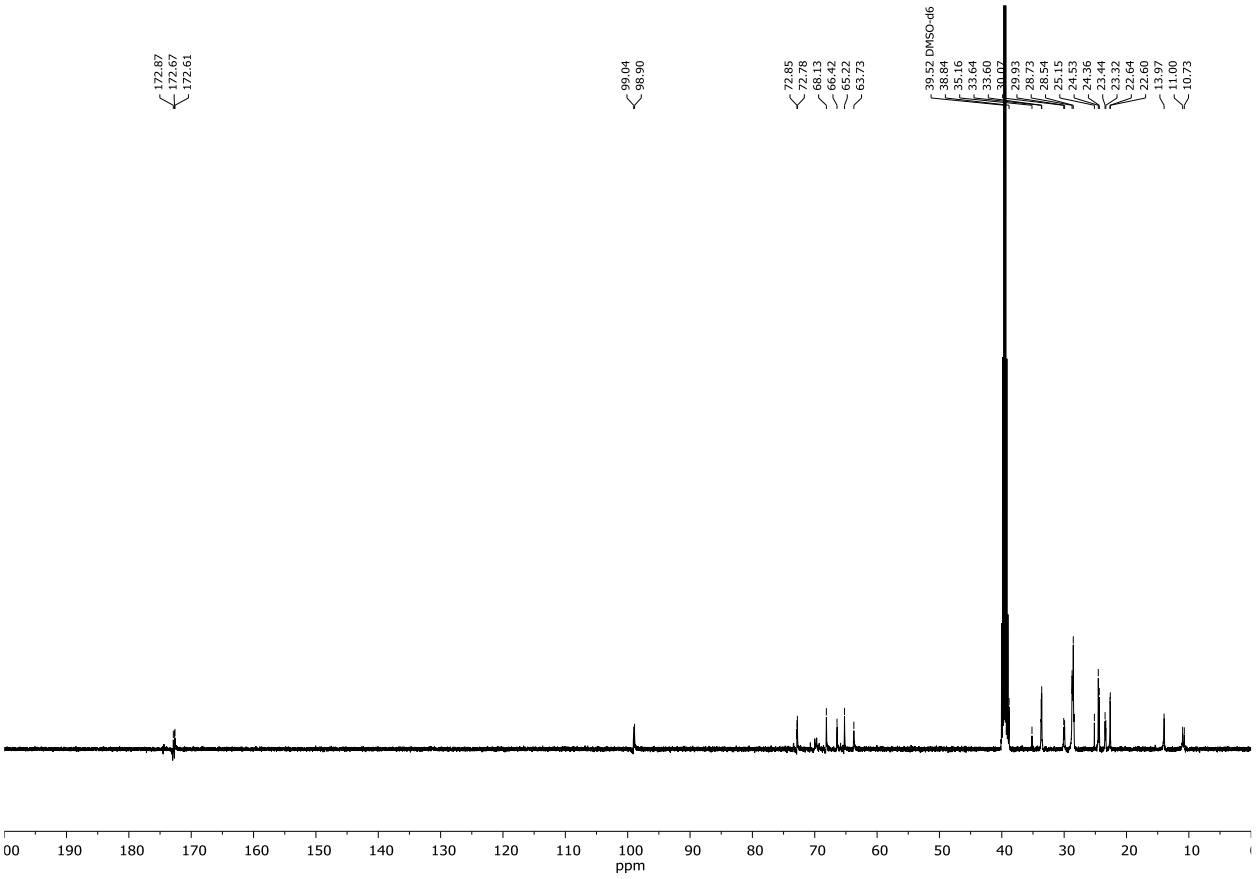

^{1}H-^{1}H COSY NMR (500 MHz, DMSO-d_6) Poly(αO*i*-octgal sebacate)

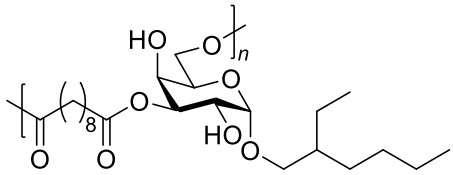

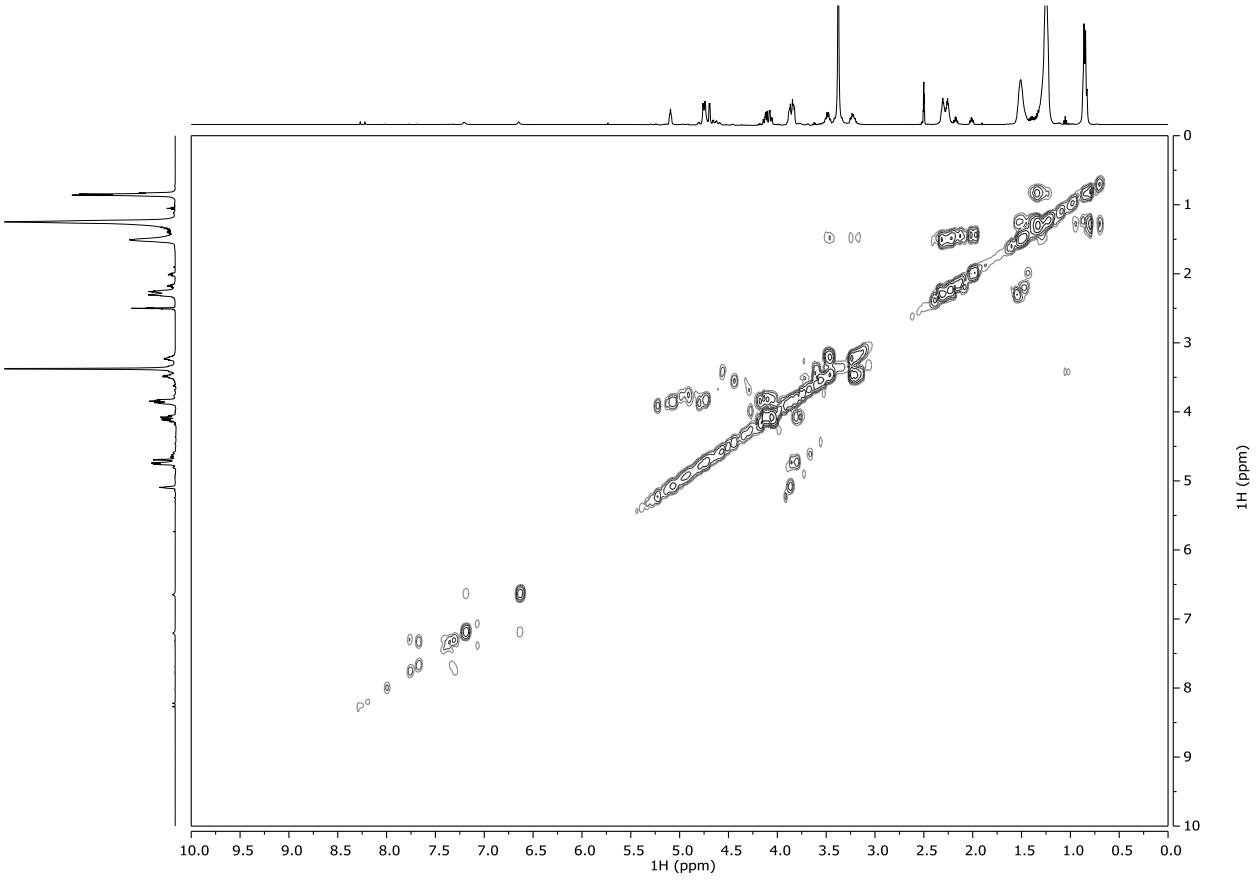

^{1}H NMR (500 MHz, DMSO-d_6) Poly(βO*i*-octgal sebacate)

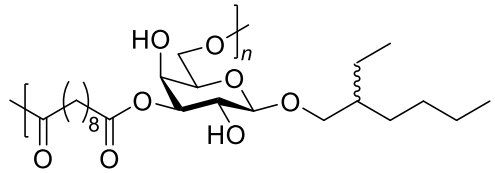

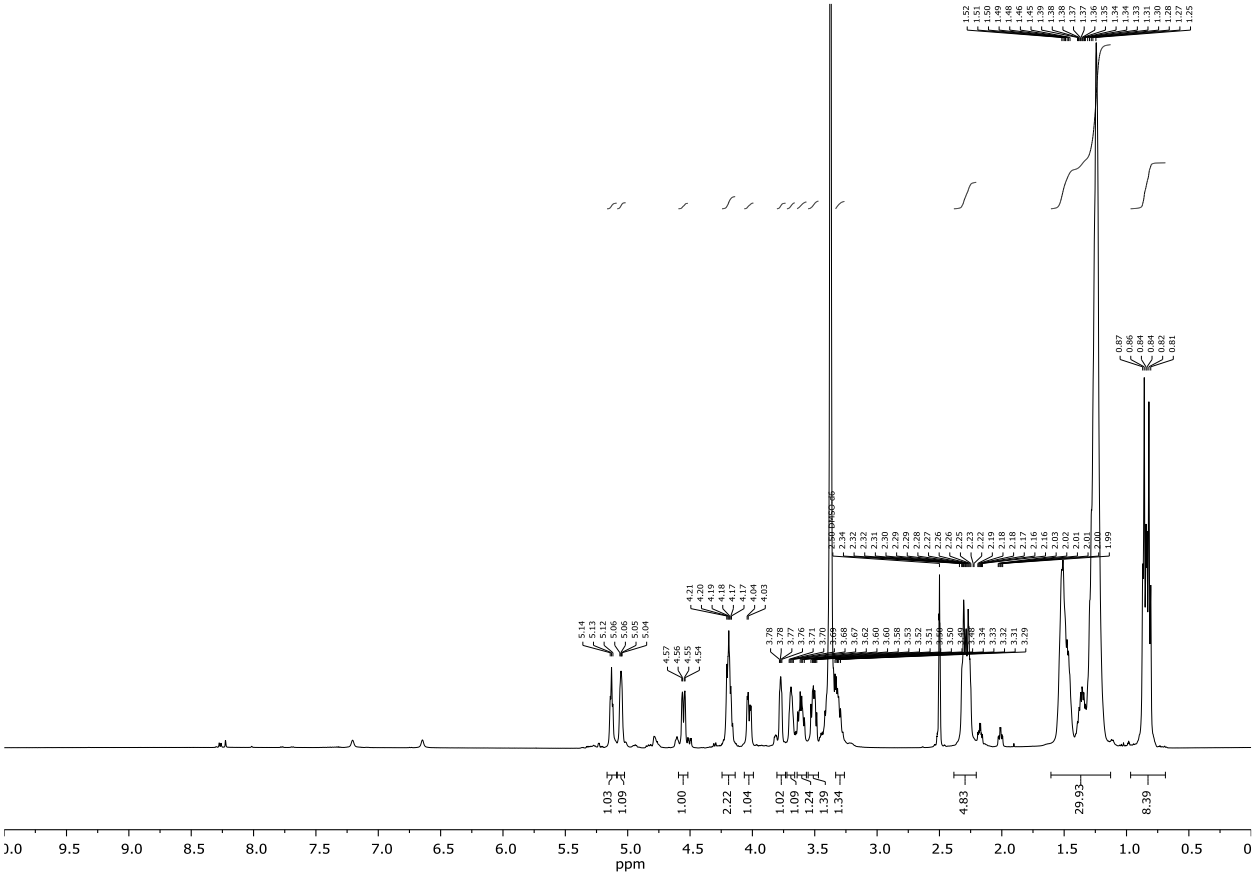

^{13}C NMR (126 MHz, DMSO-d_6) Poly(βO*i*-octgal sebacate)

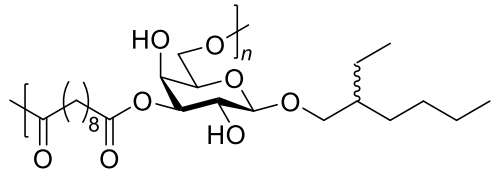

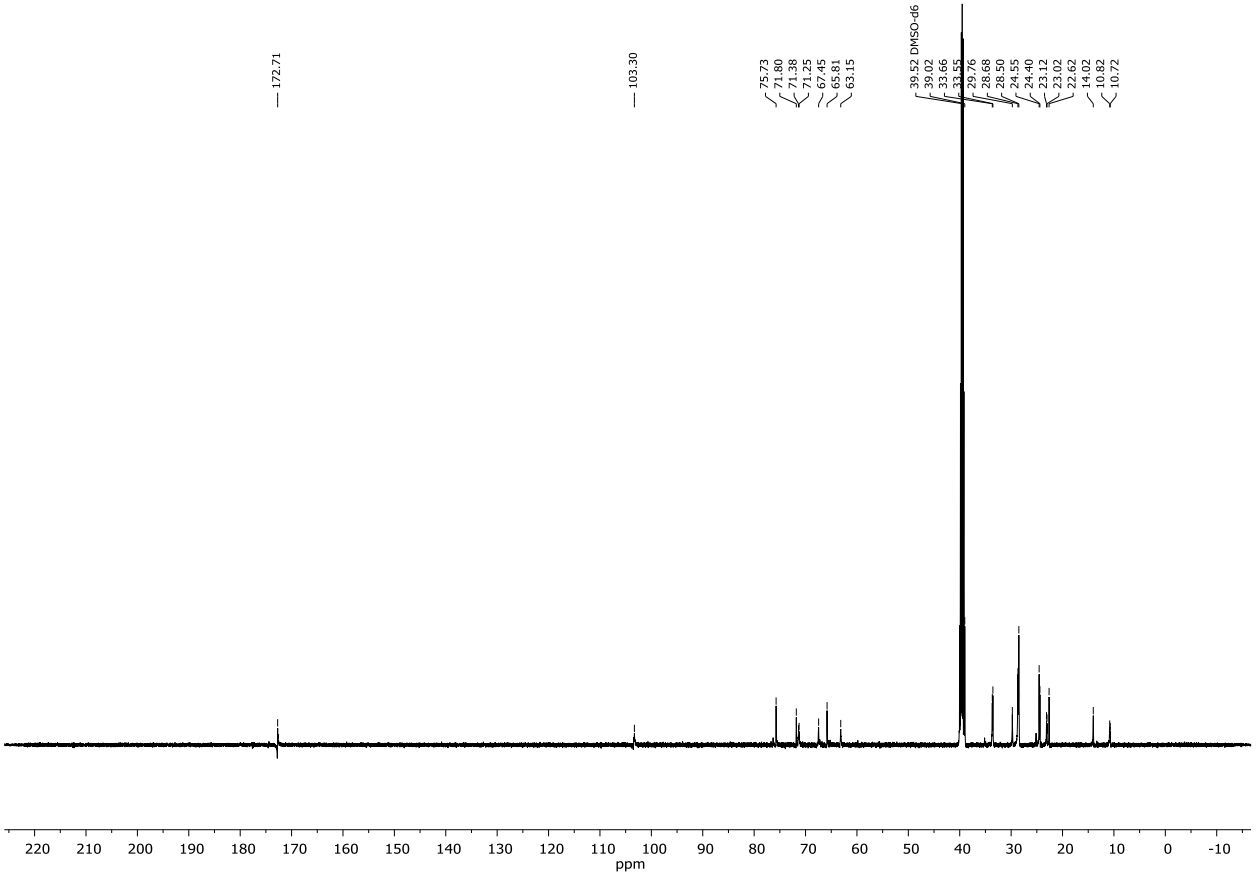

^{1}H-^{1}H COSY NMR (500 MHz, DMSO-d_6) Poly(βO*i*-octgal sebacate)

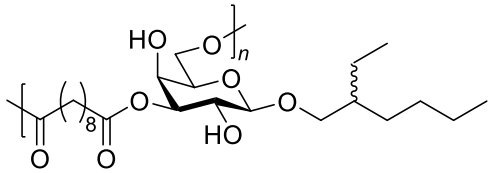

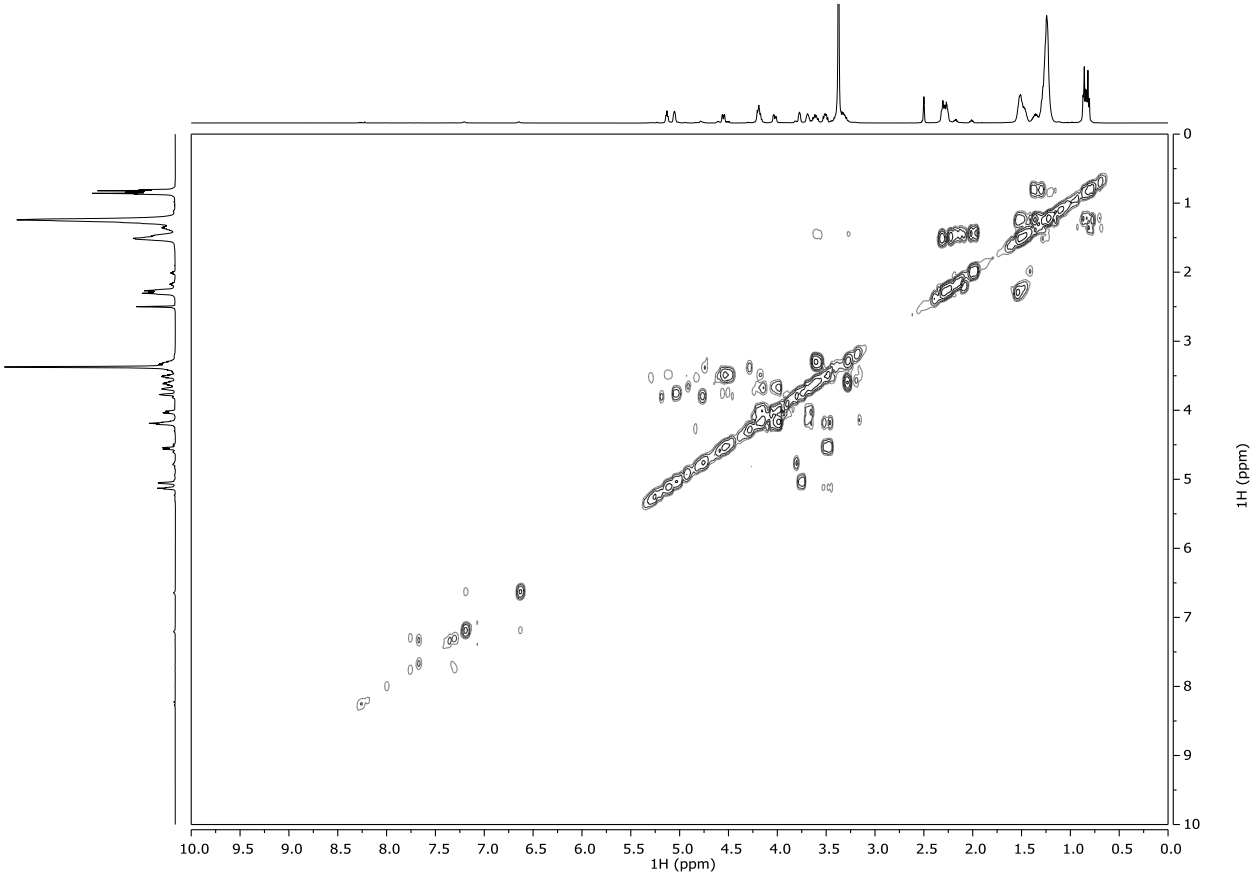

^{1}H NMR (500 MHz, DMSO-d_6) Poly(βOMegal dodecanoate)

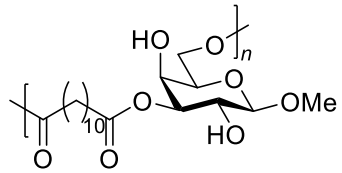

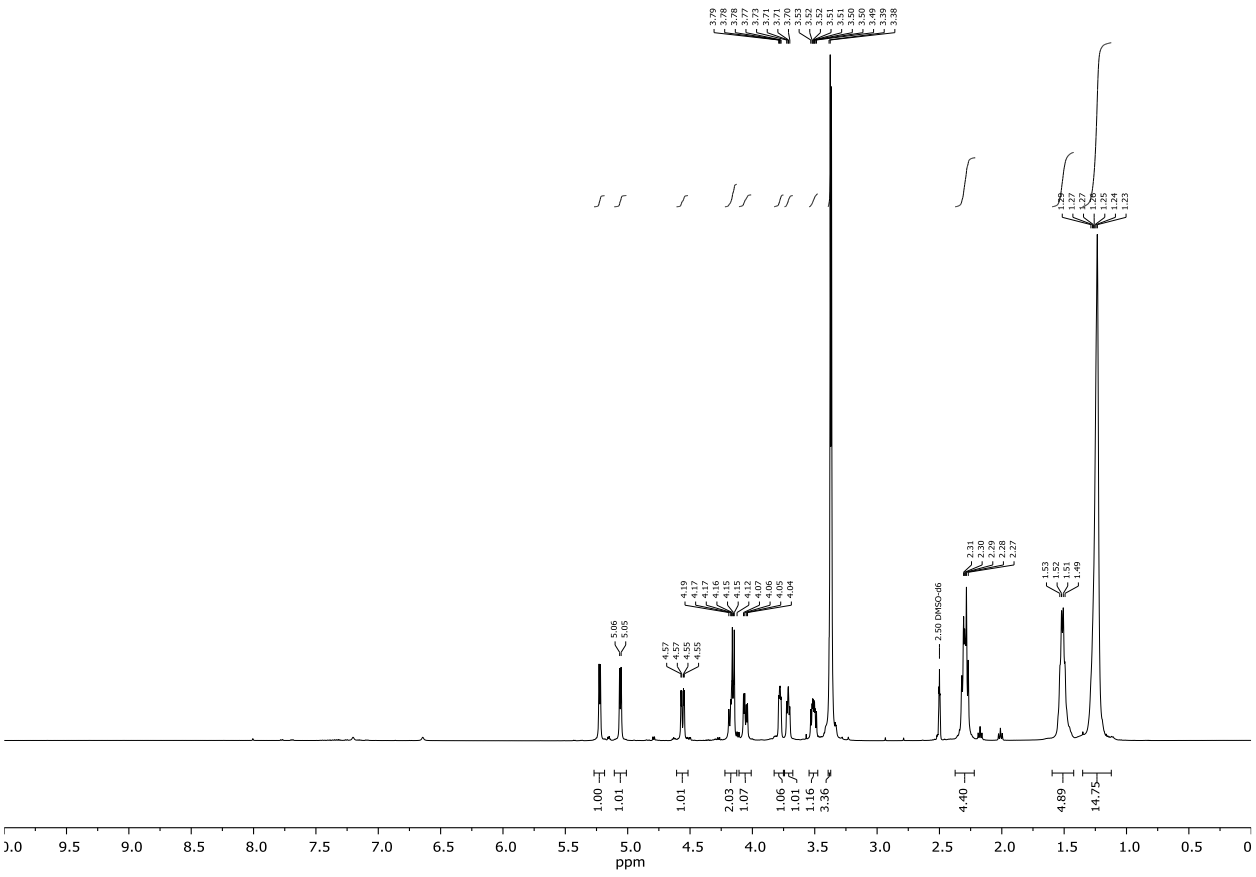

^{13}C NMR (126 MHz, DMSO-d_6) Poly(βOMegal dodecanoate)

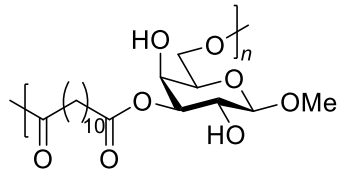

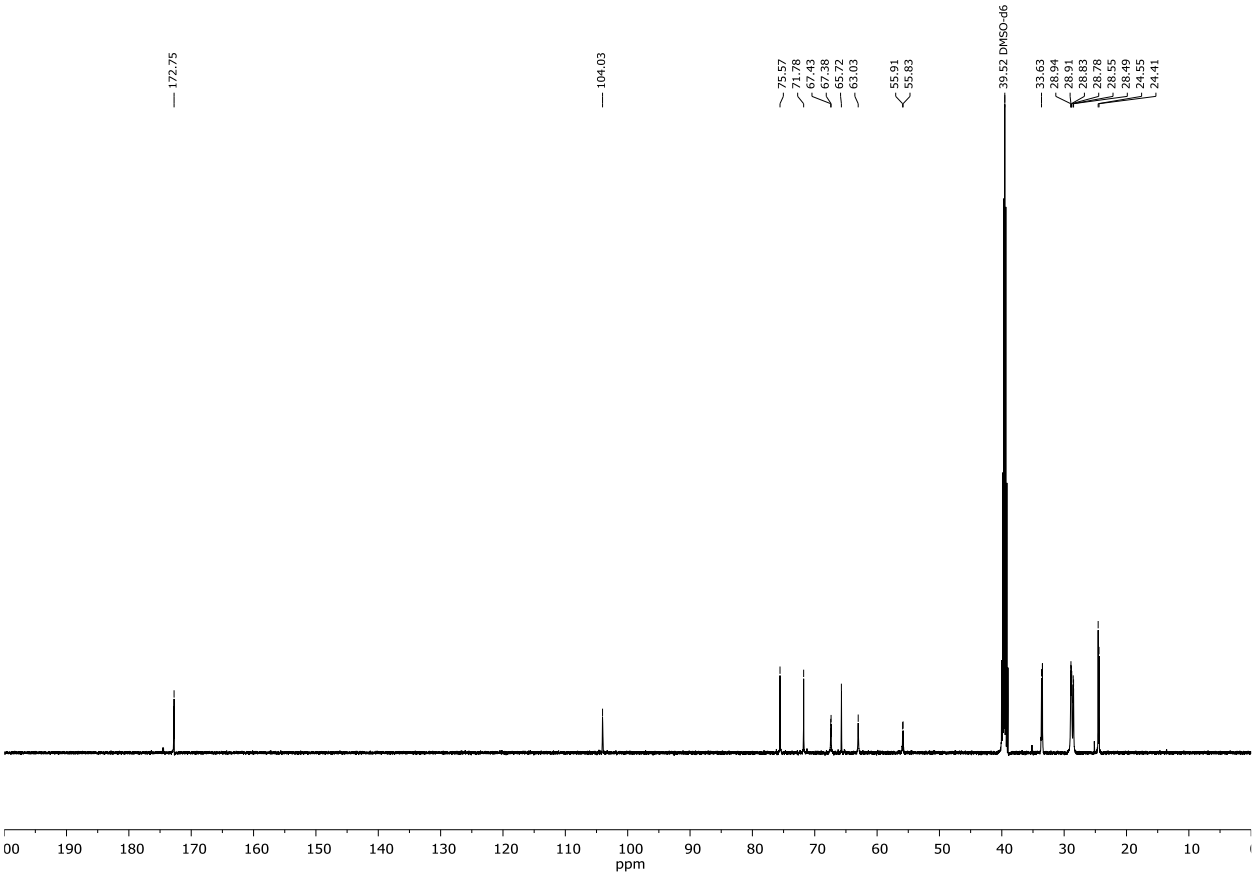

^{1}H-^{1}H COSY NMR (500 MHz, DMSO-d_6) Poly(βOMegal dodecanoate)

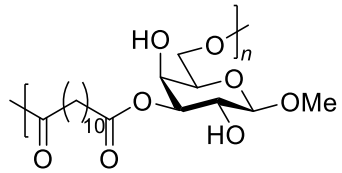

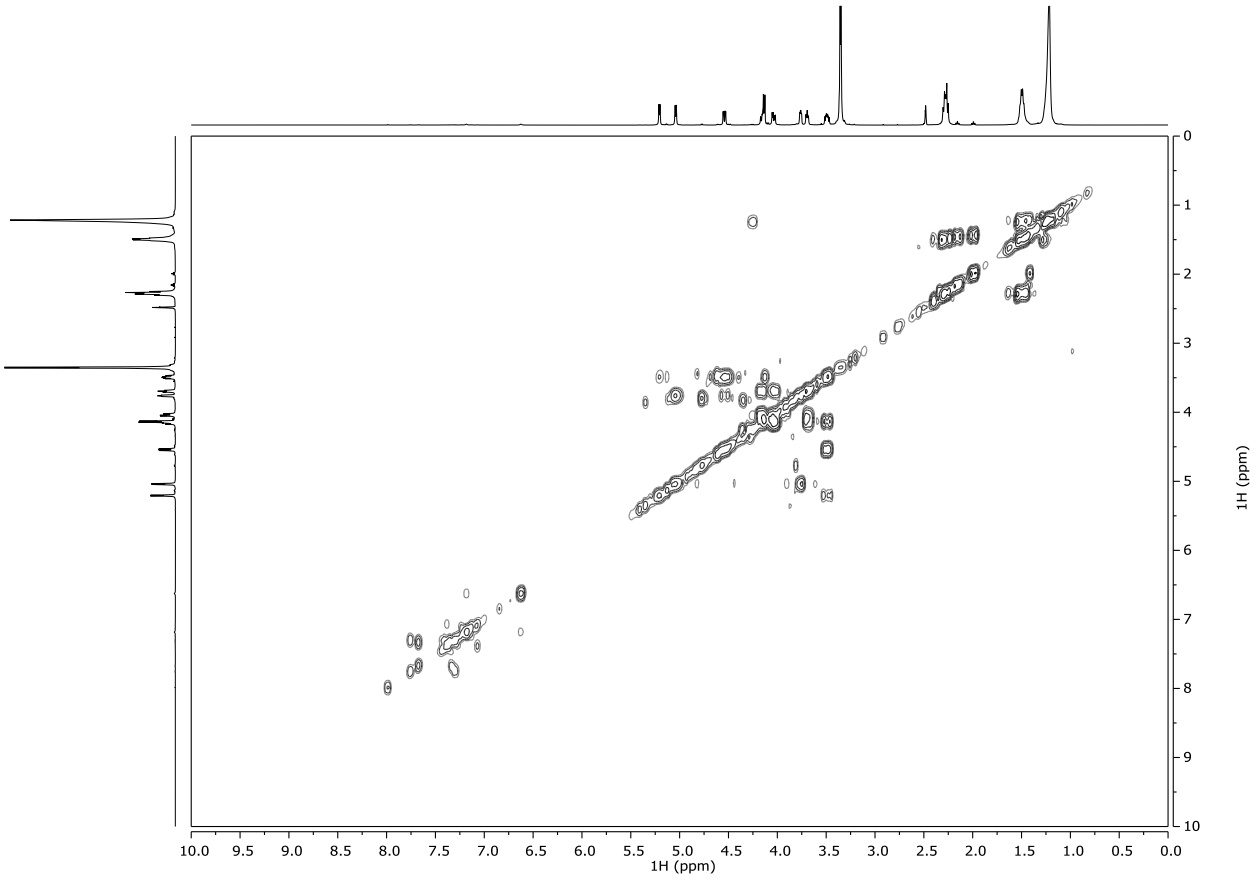

^{1}H NMR (500 MHz, DMSO-d_6) Poly(βOMegal adipate)

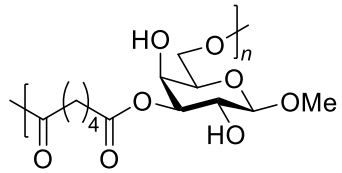

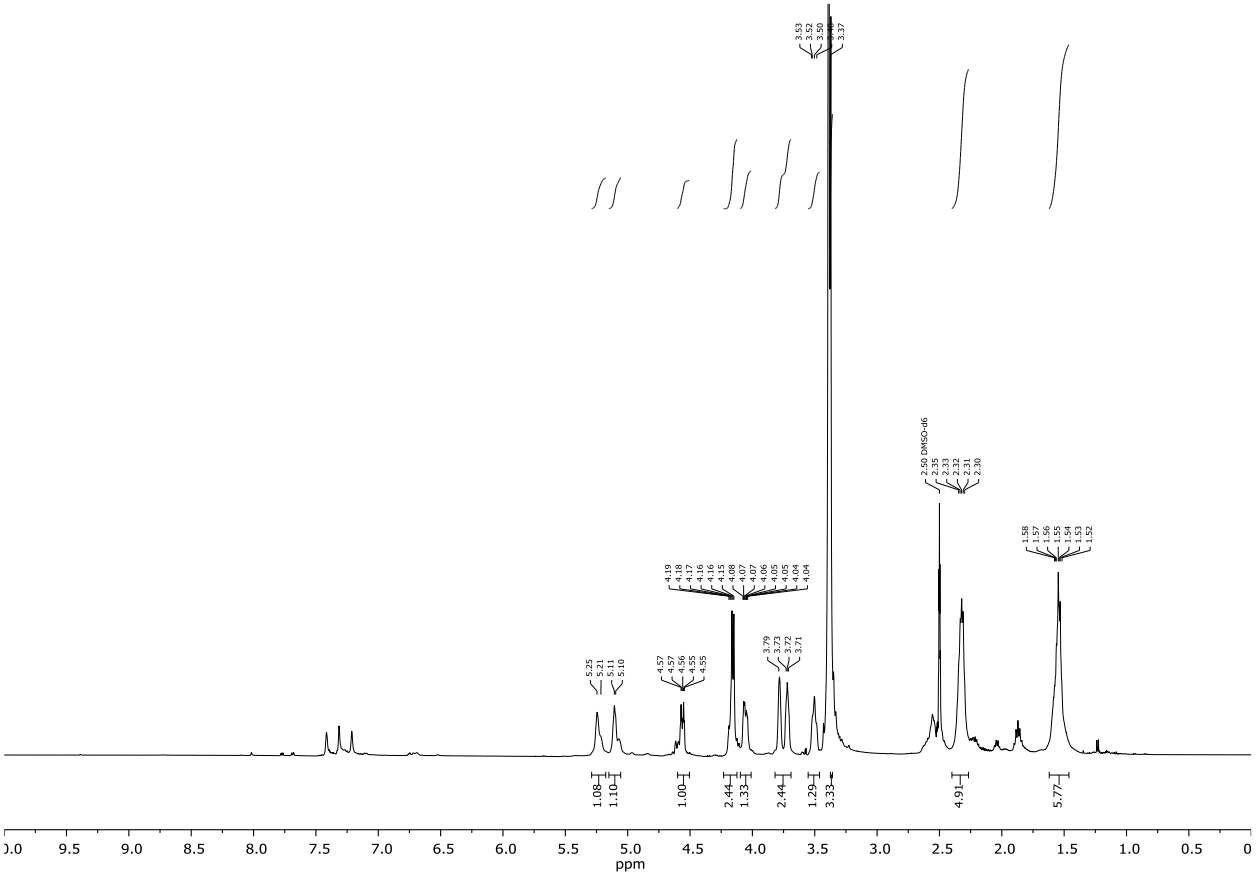

^{13}C NMR (126 MHz, DMSO-d_6) Poly(βOMegal adipate)

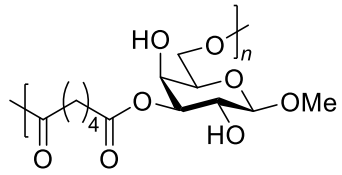

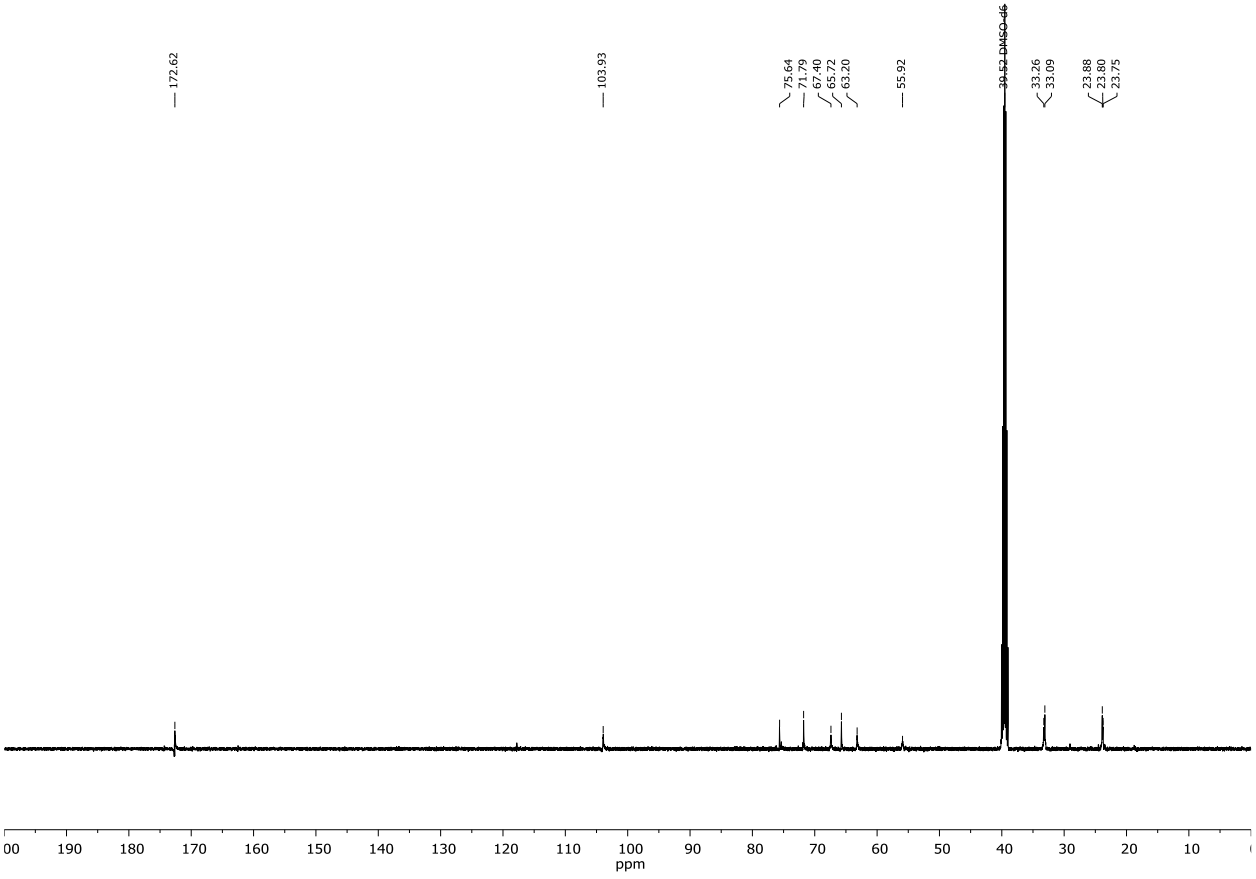

^{1}H-^{1}H COSY NMR (500 MHz, DMSO-d_6) Poly(βOMegal adipate)

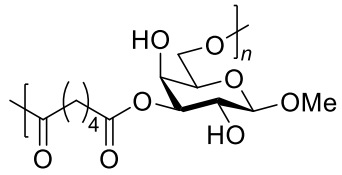

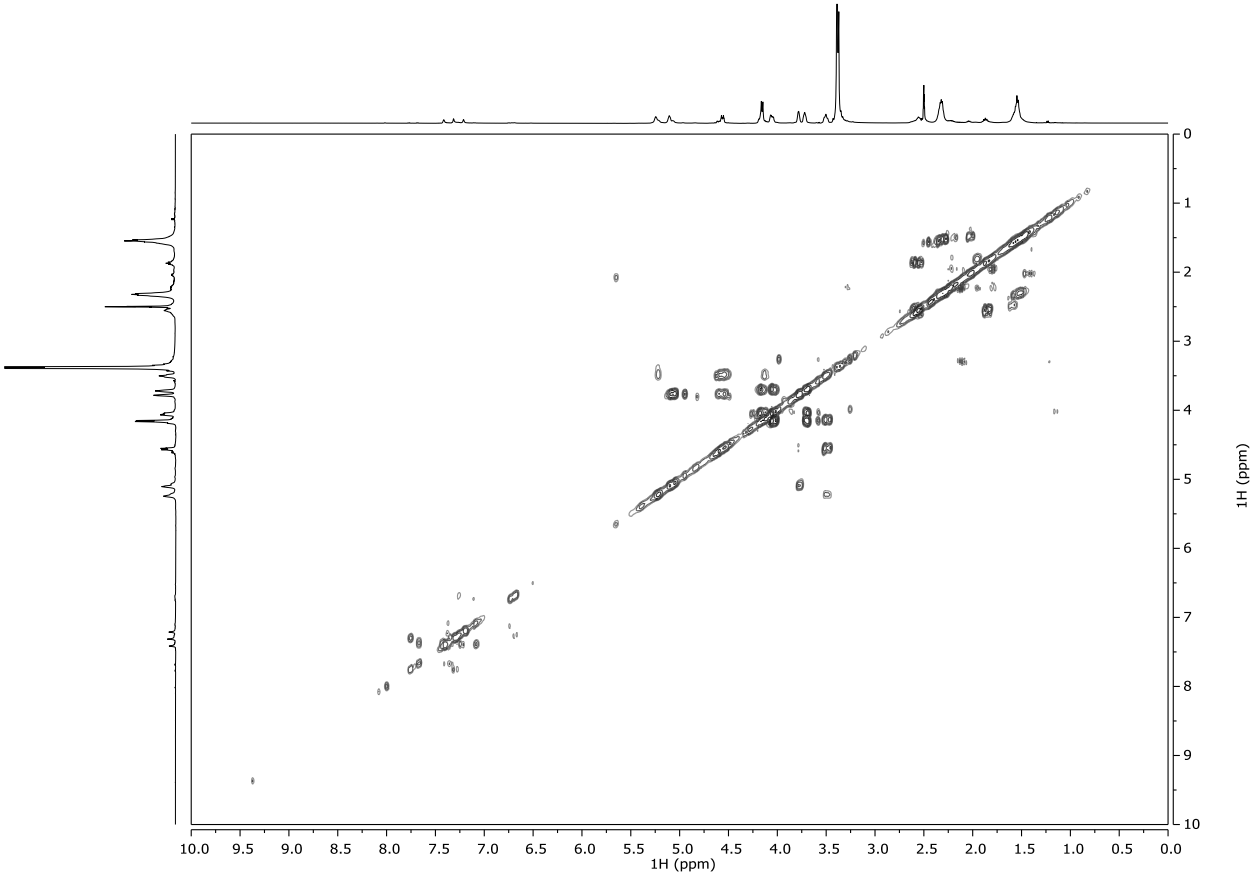

^{1}H NMR (500 MHz, DMSO-d_6) Poly(βOMegal isophthalate)

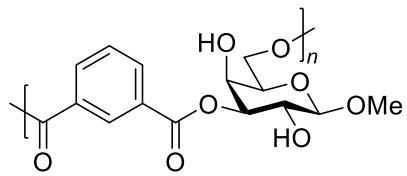

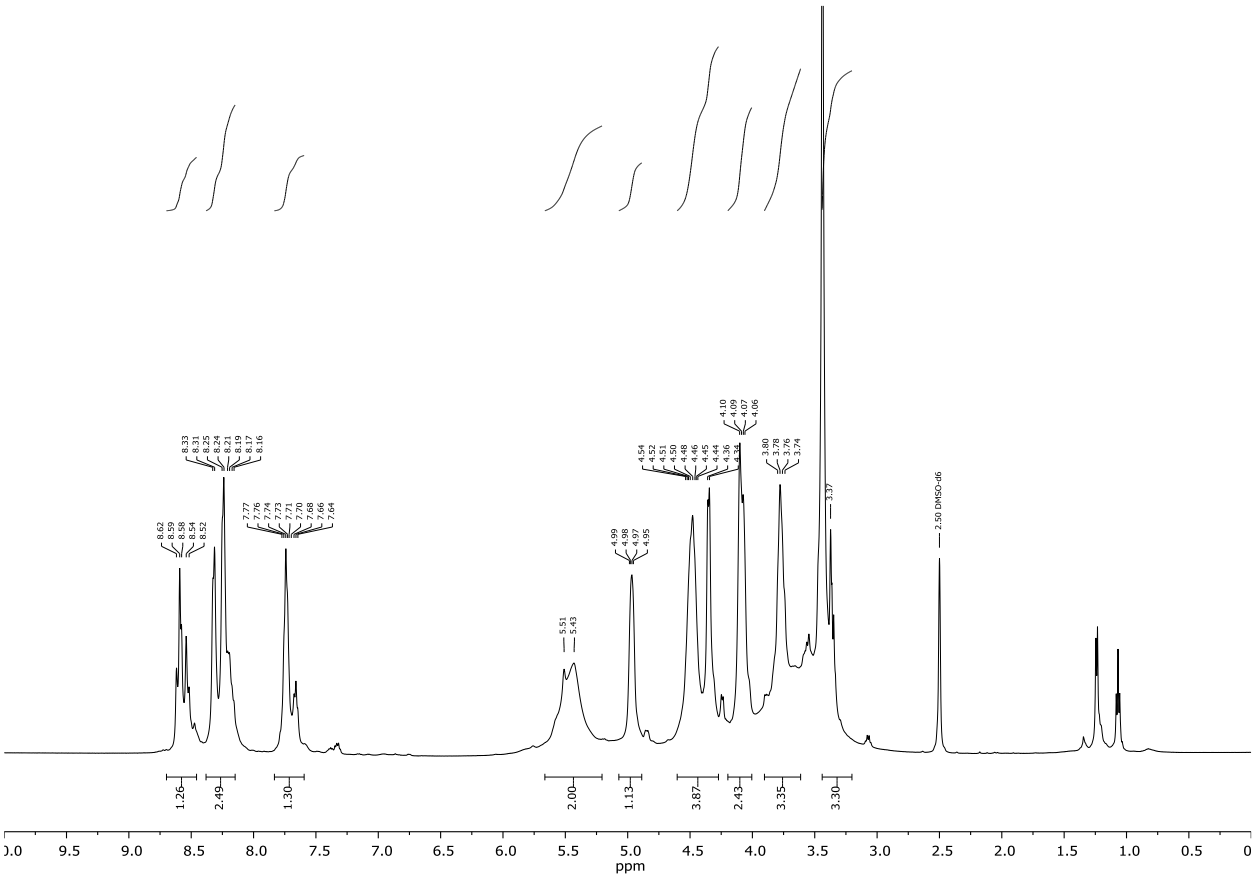

^{13}C NMR (126 MHz, DMSO-d_6) Poly(βOMegal isophthalate)

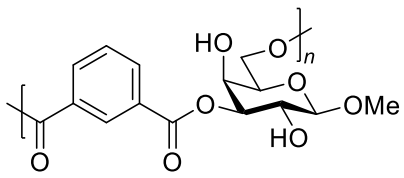

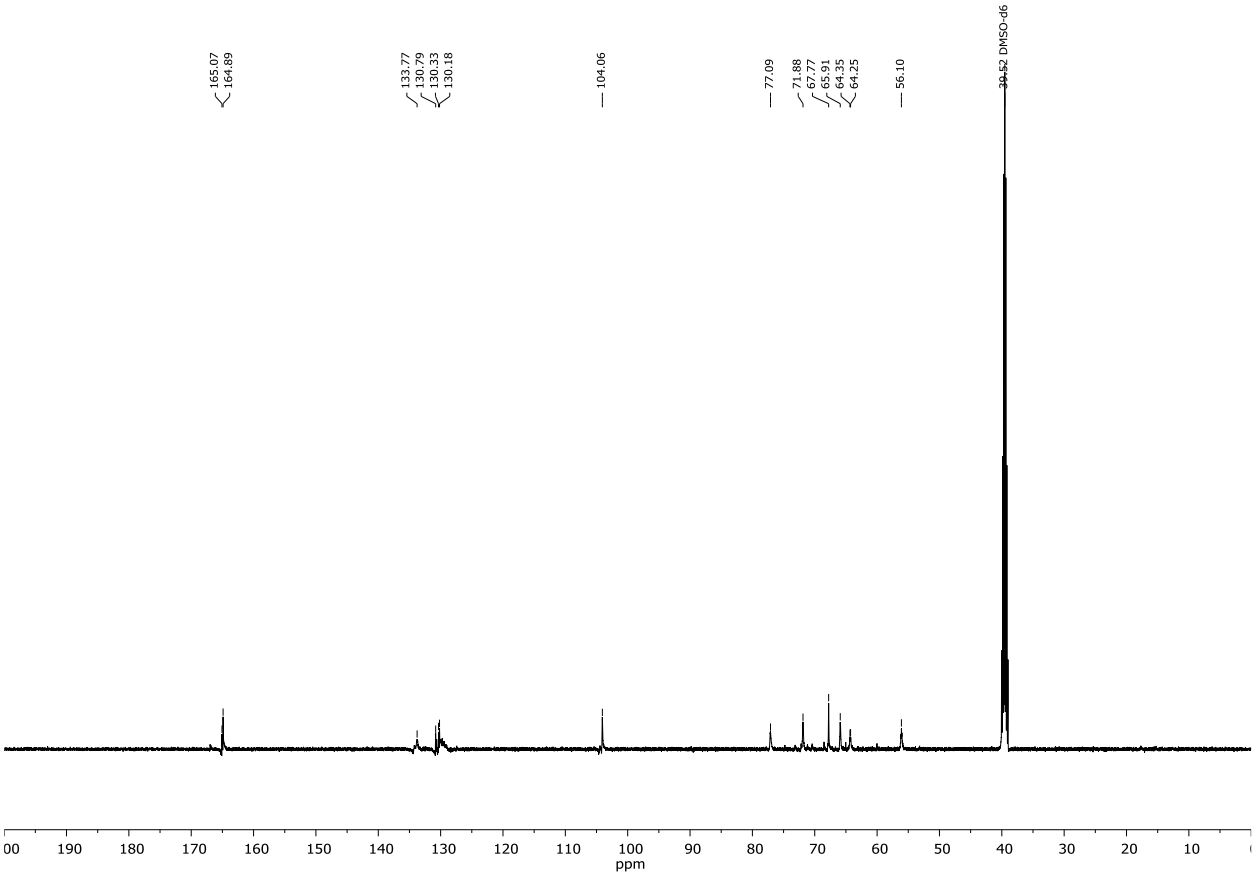

^{1}H-^{1}H COSY NMR (500 MHz, DMSO-d_6) Poly(βOMegal isophthalate)

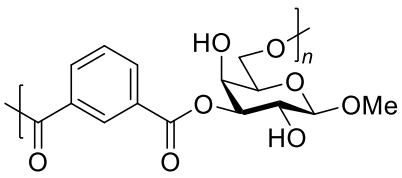

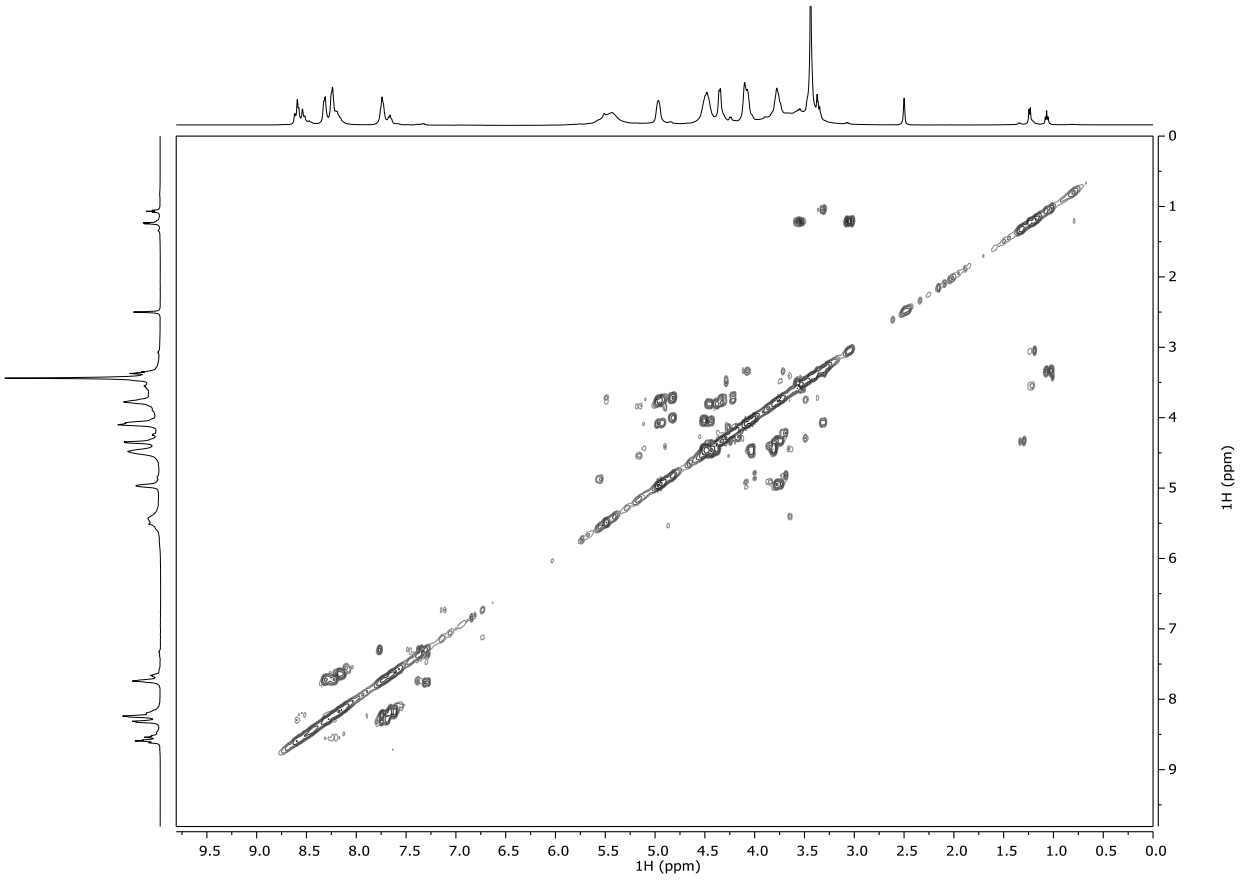

^{1}H NMR (500 MHz, DMSO-d_6) Poly(αOMeman sebacate)

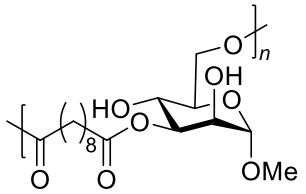

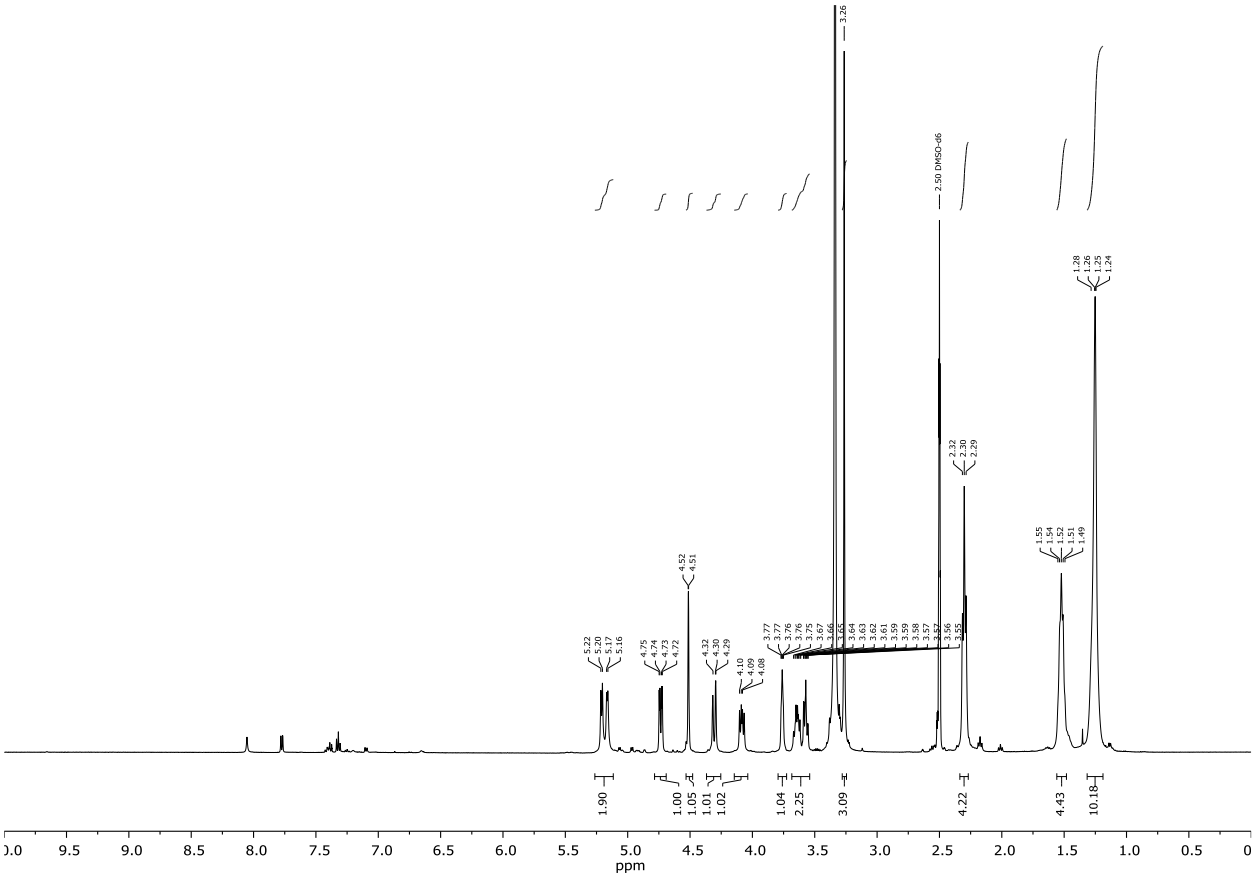

^{13}C NMR (126 MHz, DMSO-d_6) Poly(αOMeman sebacate)

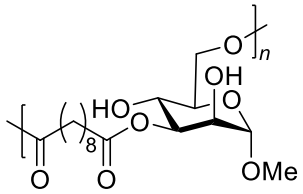

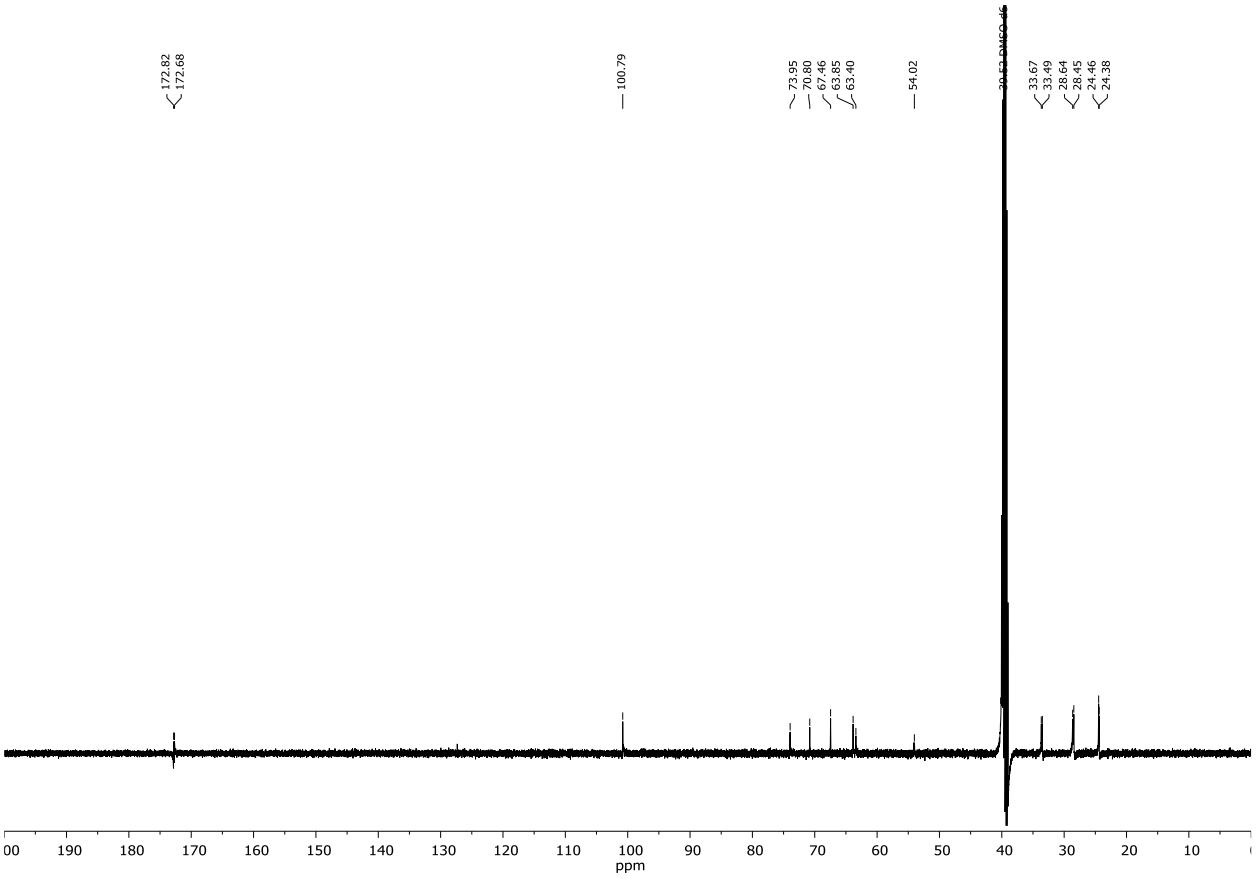

^{1}H-^{1}H COSY NMR (500 MHz, DMSO-d_6) Poly(αOMeman sebacate)

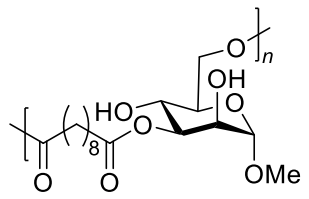

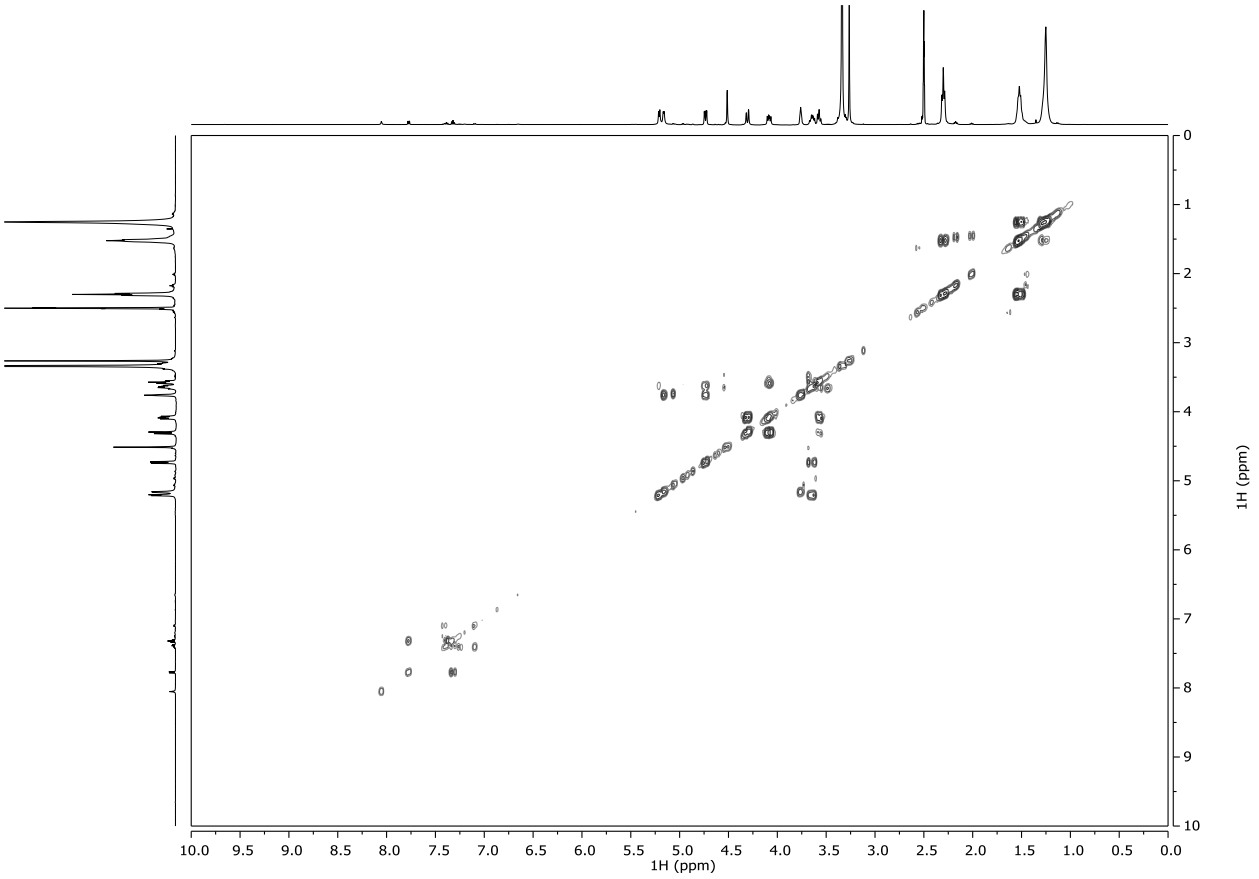

^{1}H NMR (500 MHz, DMSO-d_6) Poly(αOEtman sebacate)

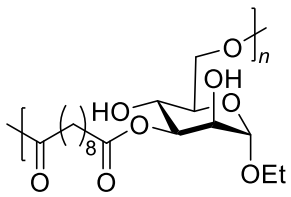

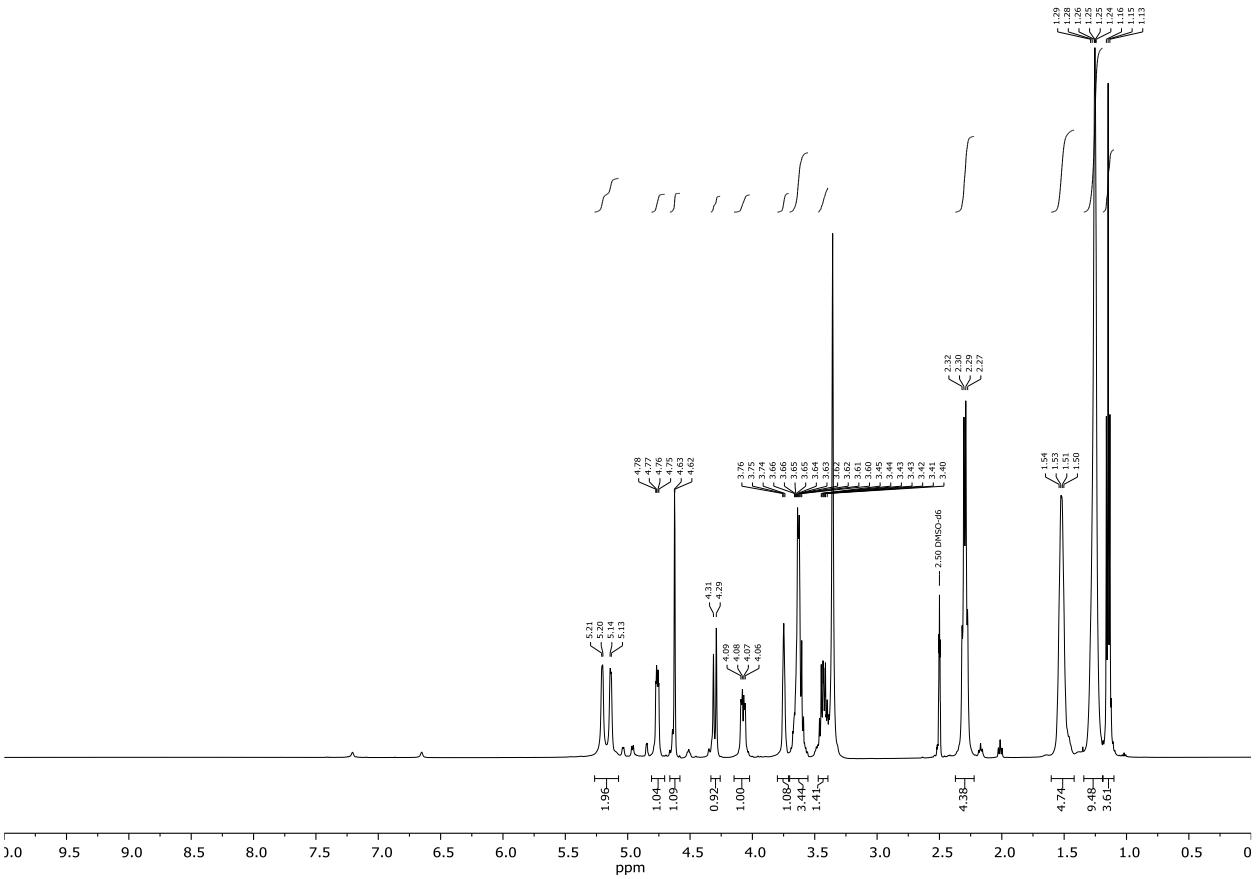

^{13}C NMR (126 MHz, DMSO-d_6) Poly(αOEtman sebacate)

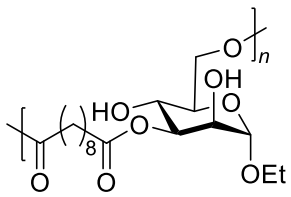

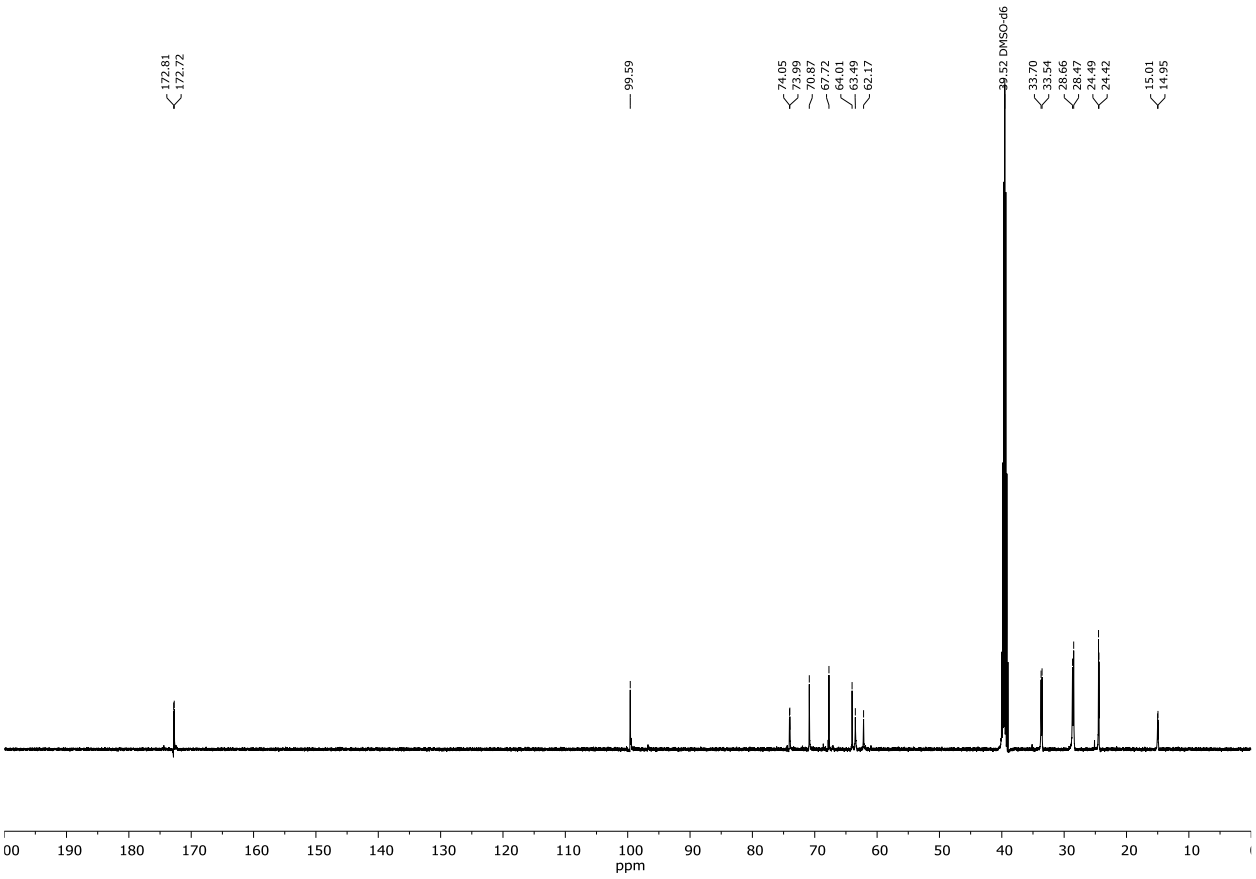

^{1}H-^{1}H COSY NMR (500 MHz, DMSO-d_6) Poly(αOEtman sebacate)

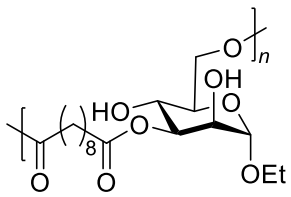

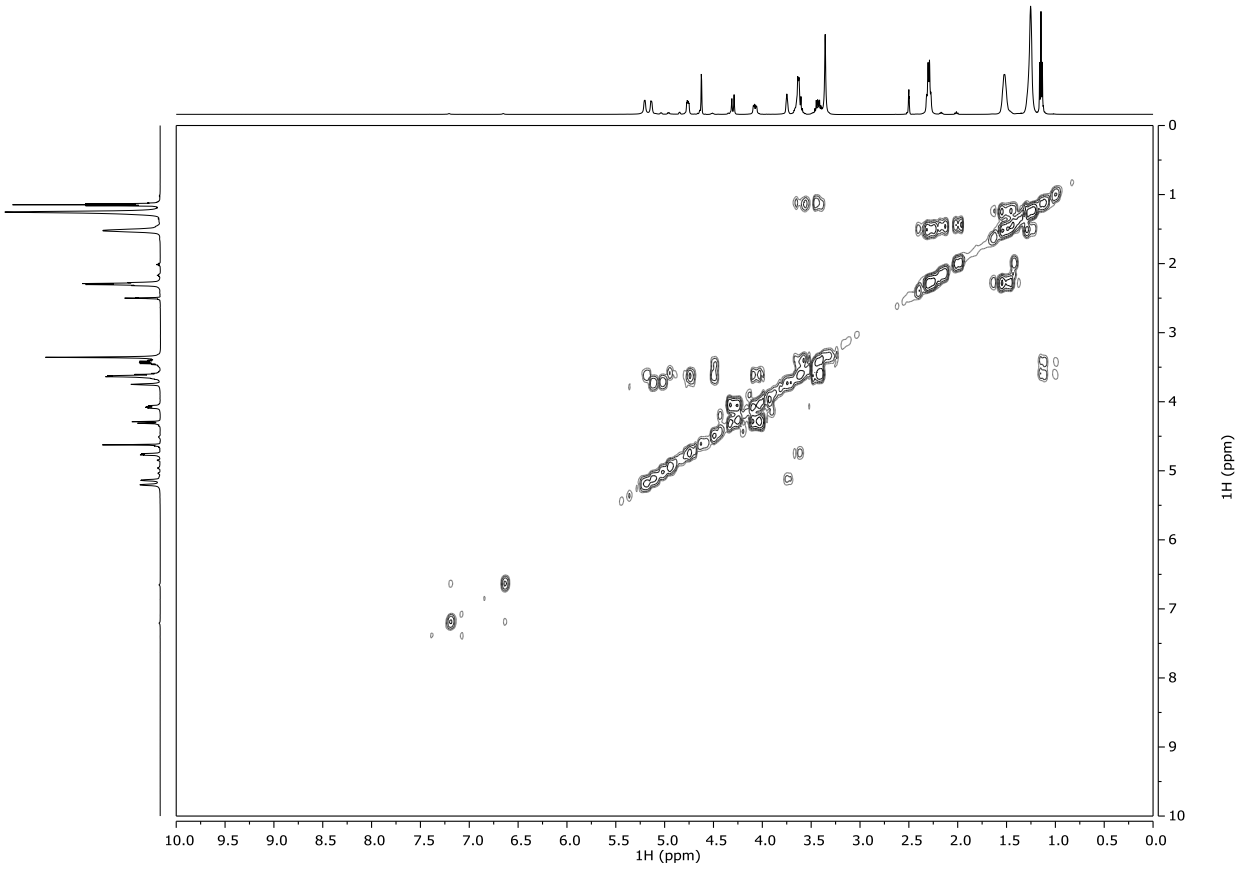

^{1}H NMR (500 MHz, DMSO-d_6) Poly(αO*n*-octman sebacate)

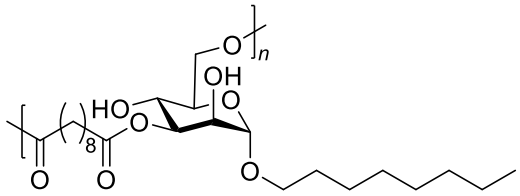

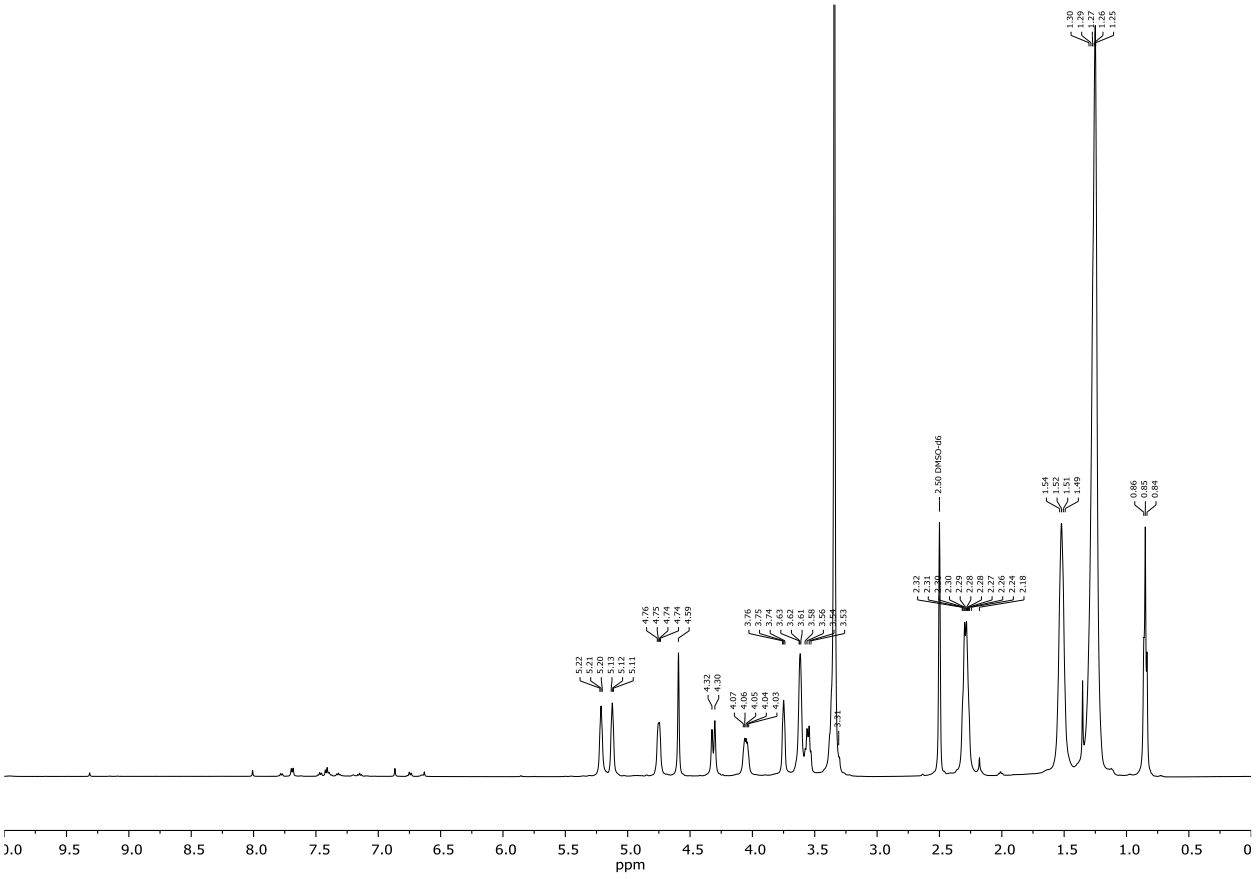

^{13}C NMR (126 MHz, DMSO-d_6) Poly(αO*n*-octman sebacate)

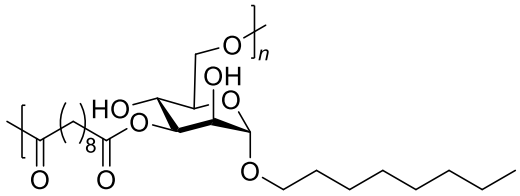

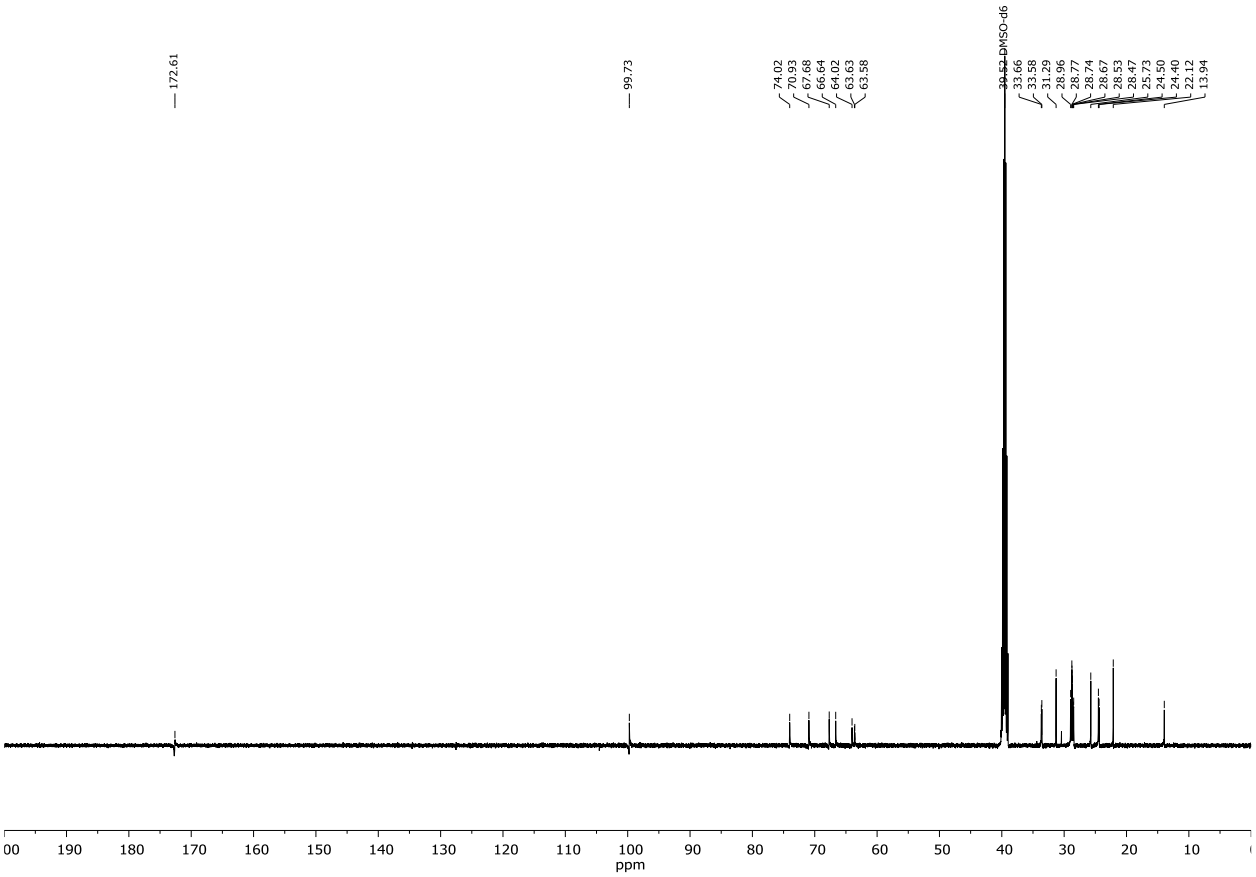

^{1}H-^{1}H COSY NMR (500 MHz, DMSO-d_6) Poly(αO*n*-octman sebacate)

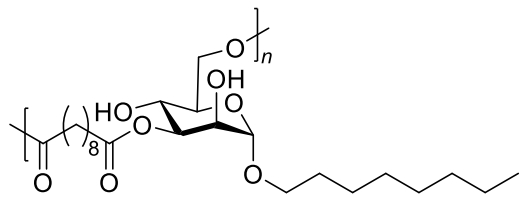

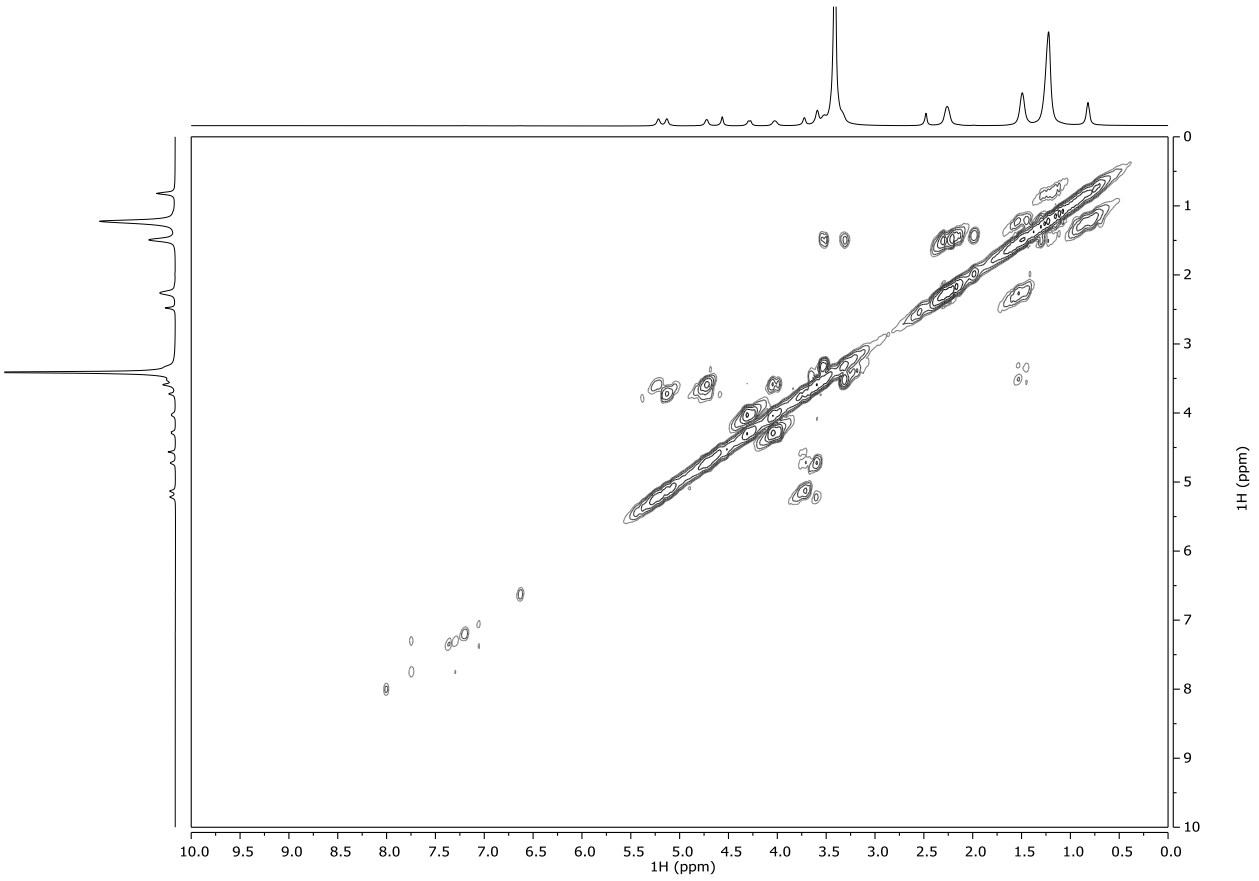

^{1}H NMR (500 MHz, DMSO-d_6) Poly(αO*i*-octman sebacate)

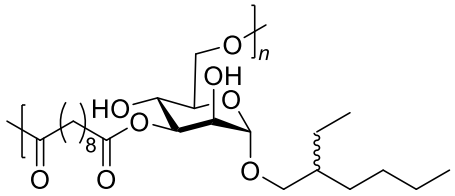

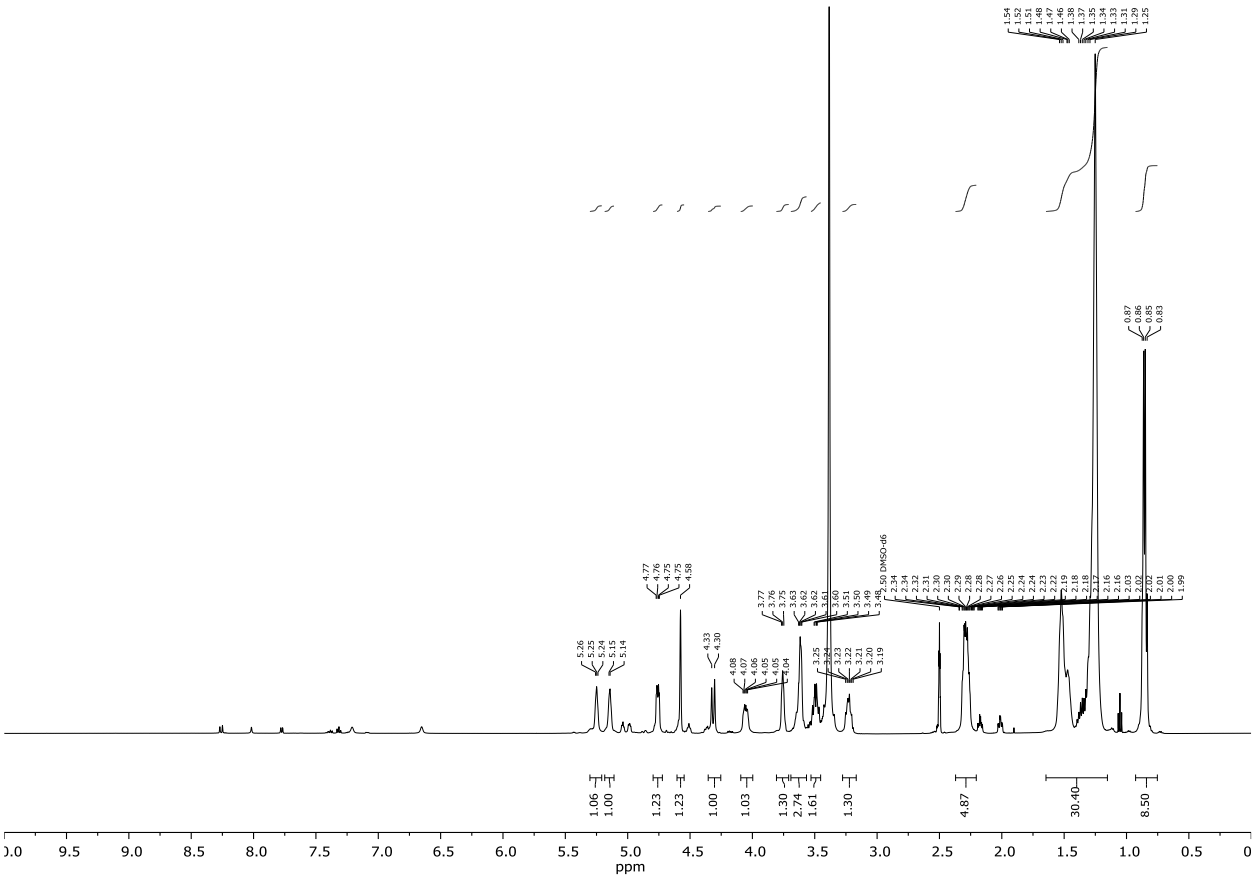

^{13}C NMR (126 MHz, DMSO-d_6) Poly(αO*i*-octman sebacate)

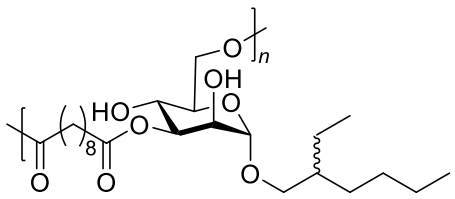

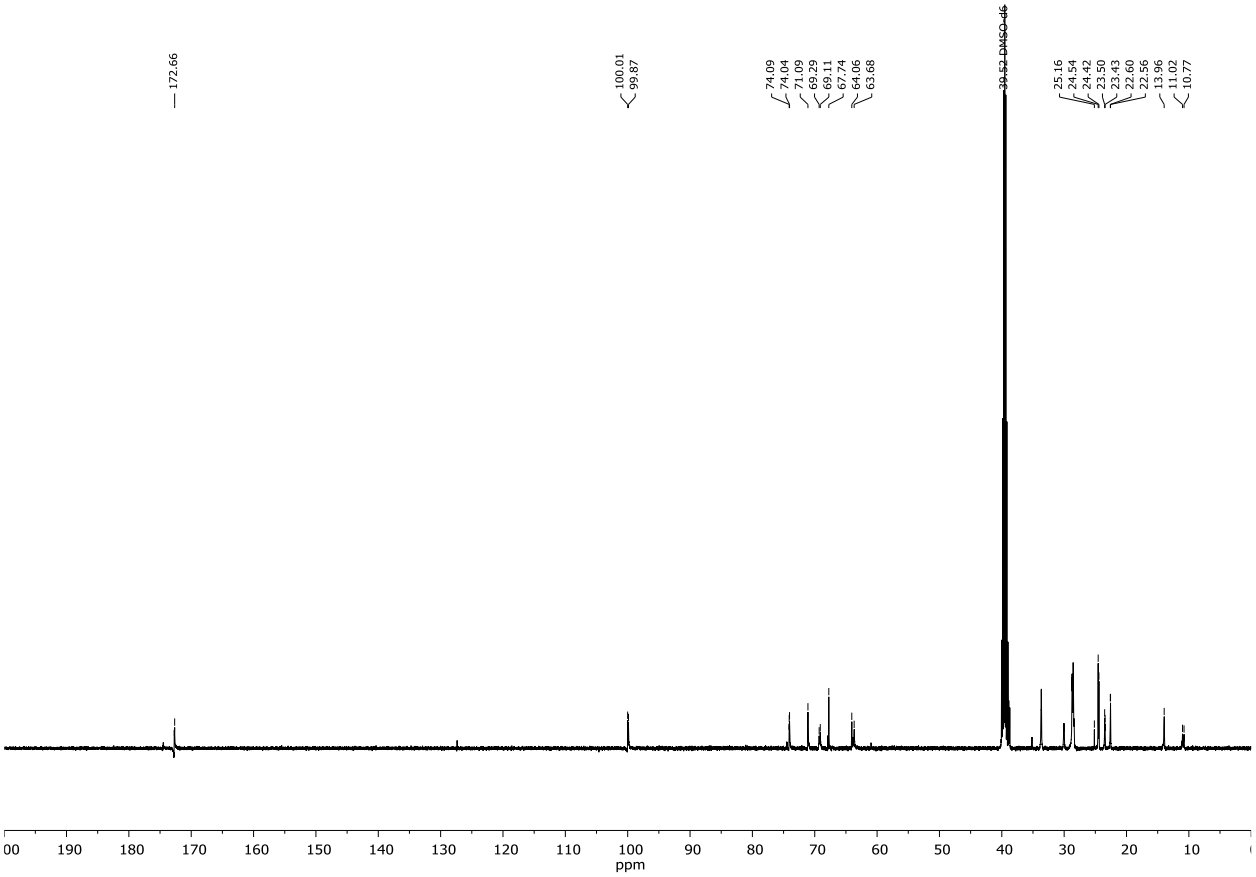

^{1}H-^{1}H COSY NMR (500 MHz, DMSO-d_6) Poly(αO*i*-octman sebacate)

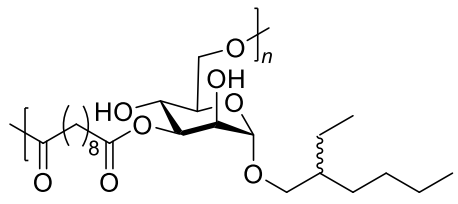

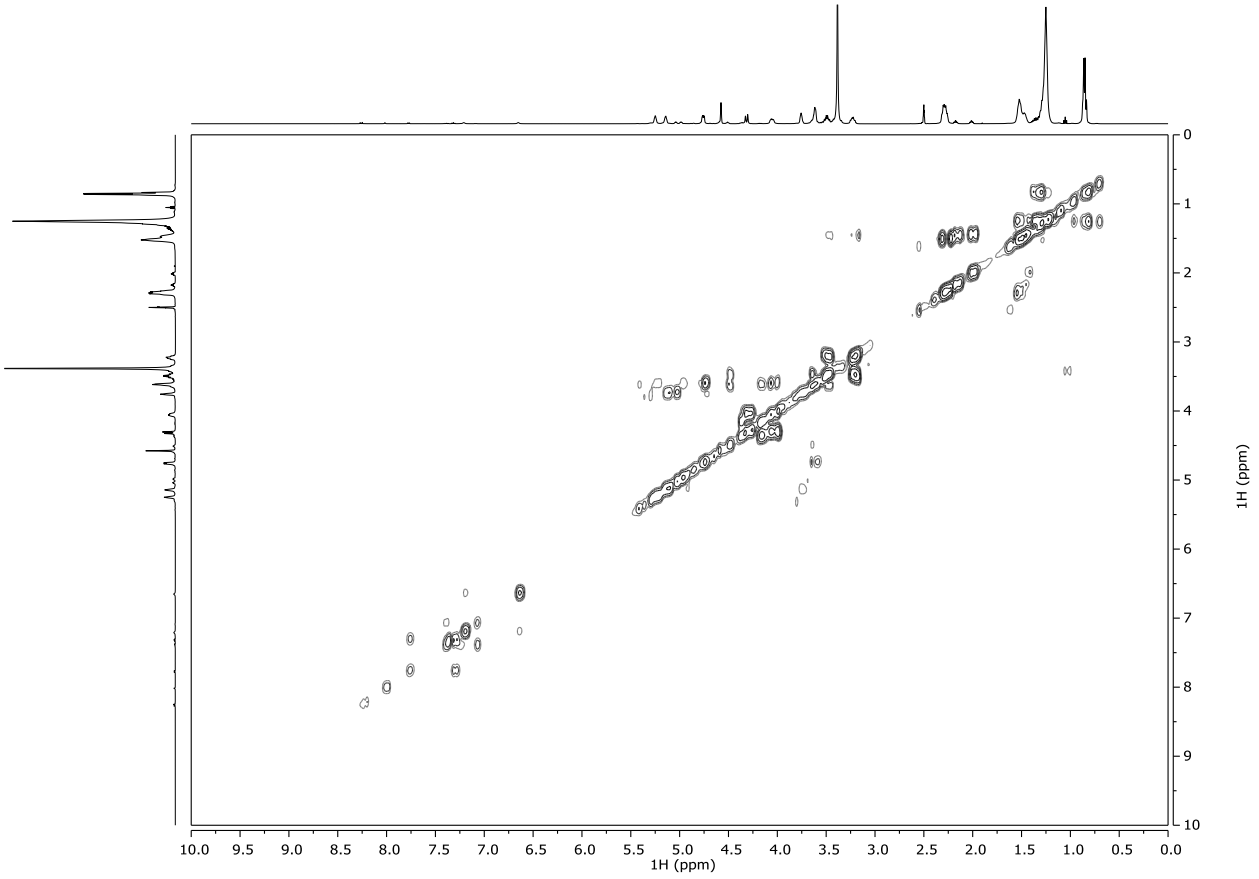

^{1}H NMR (500 MHz, DMSO-d_6) 3-*O*-butanoyl methyl α-D-galactopyranoside (3.XX)

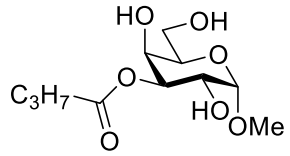

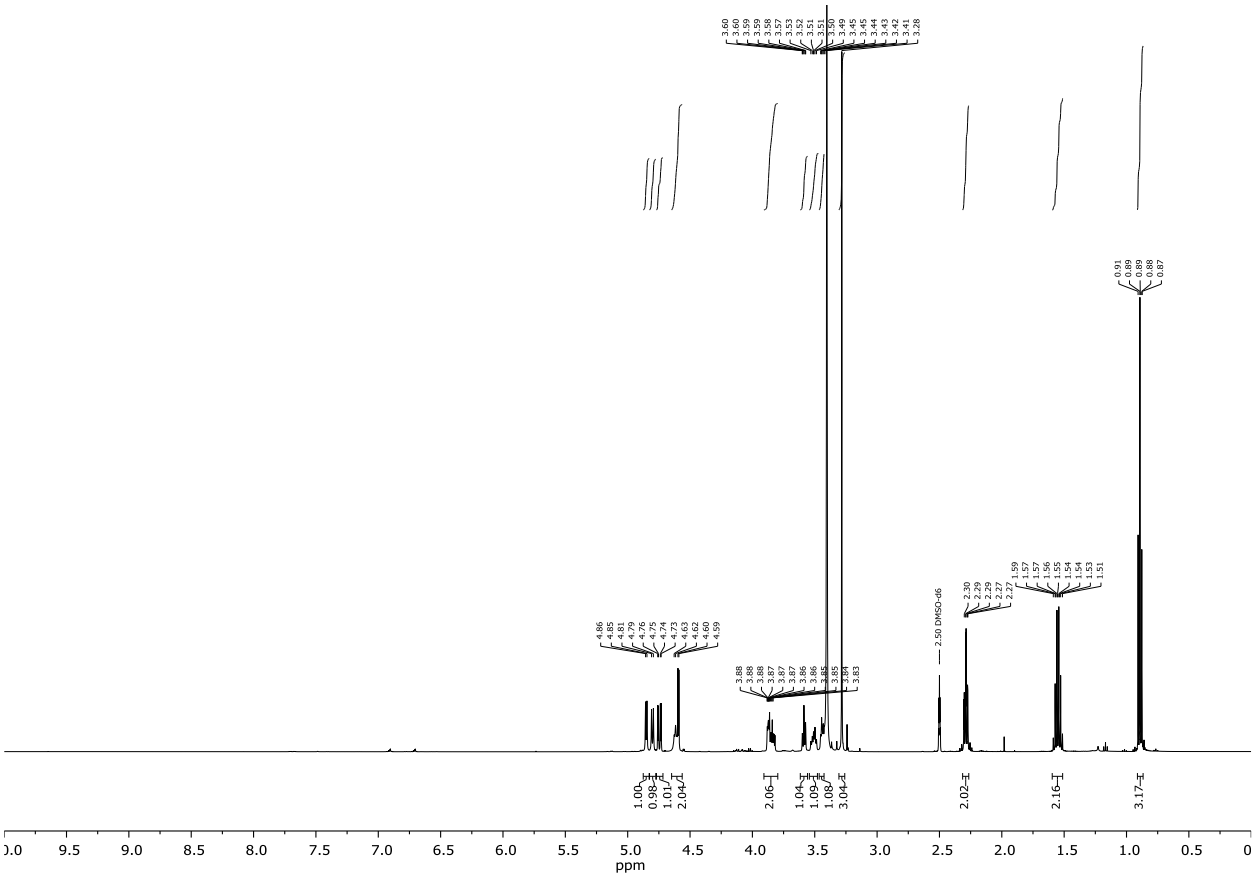

^{13}C NMR (126 MHz, DMSO-d_6) 3-*O*-butanoyl methyl α-D-galactopyranoside (3.XX)

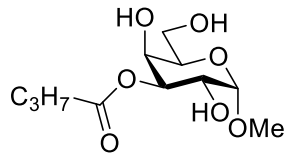

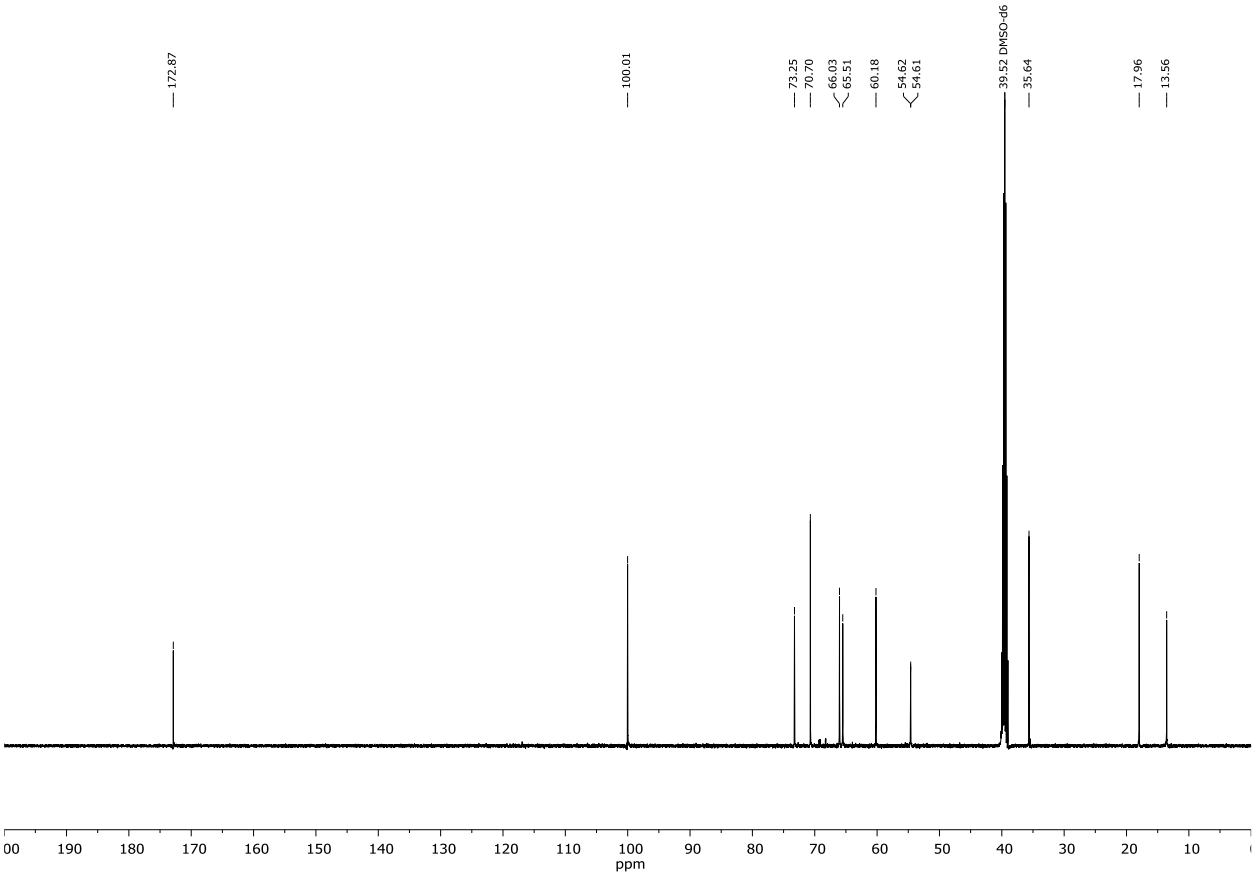

^{1}H-^{1}H COSY NMR (500 MHz, DMSO-d_6) 3-*O*-butanoyl methyl α-D-galactopyranoside (3.XX)

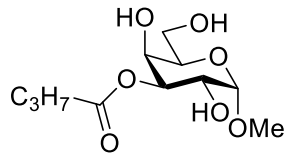

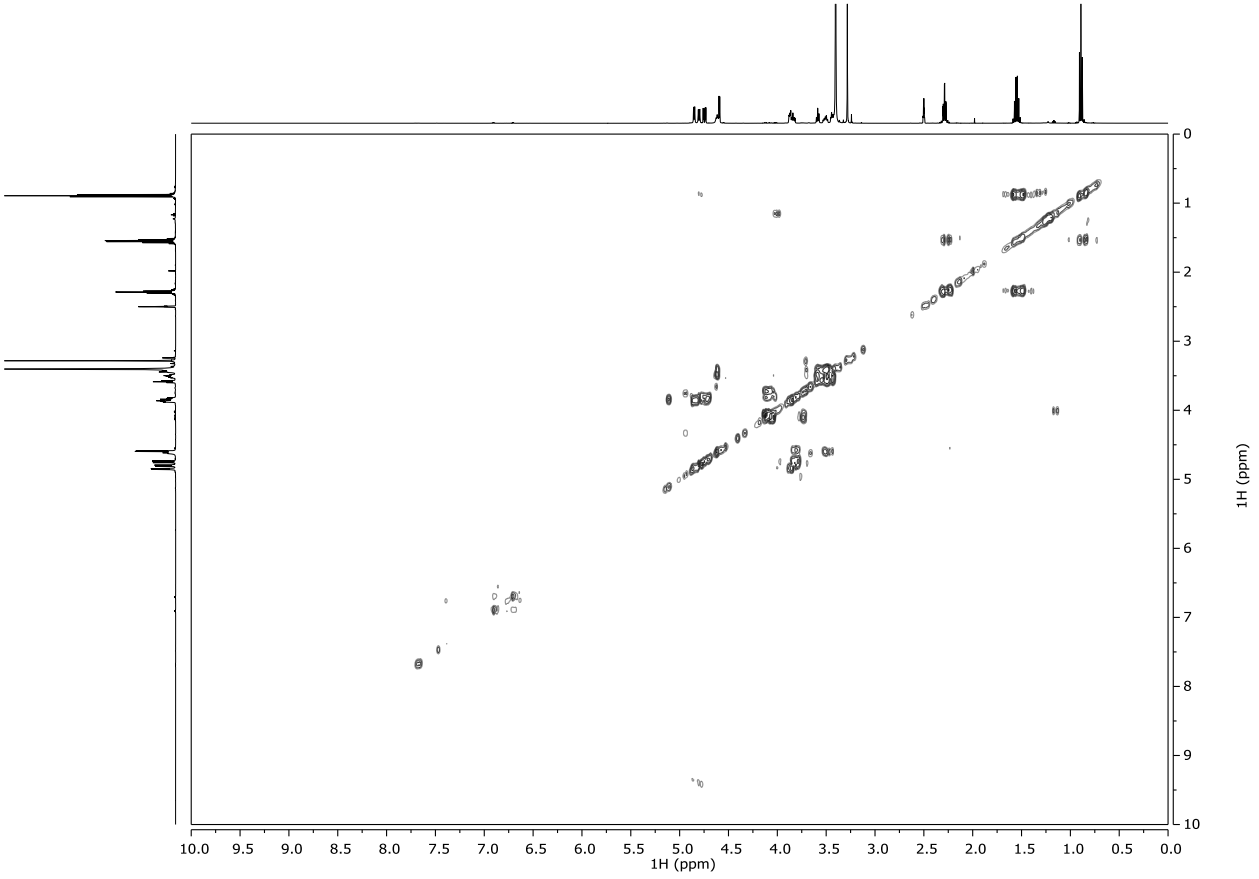

^{1}H NMR (500 MHz, DMSO-d_6) 3-*O*-butanoyl methyl β-D-galactopyranoside (**3.01**)

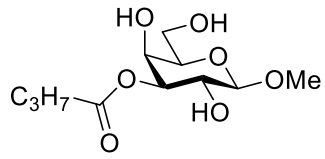

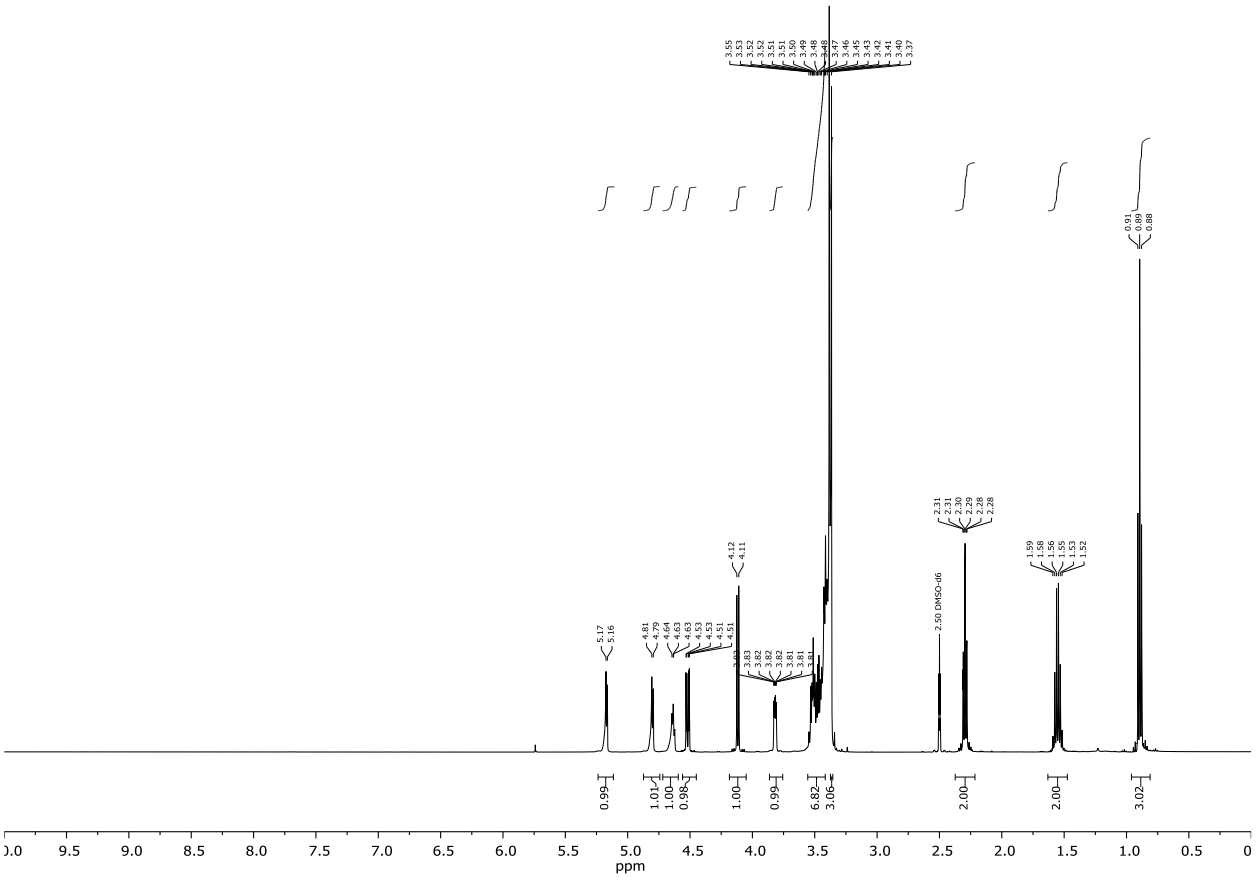

^{13}C NMR (126 MHz, DMSO-d_6) 3-*O*-butanoyl methyl β-D-galactopyranoside (**3.01**)

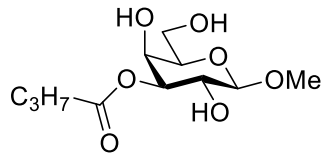

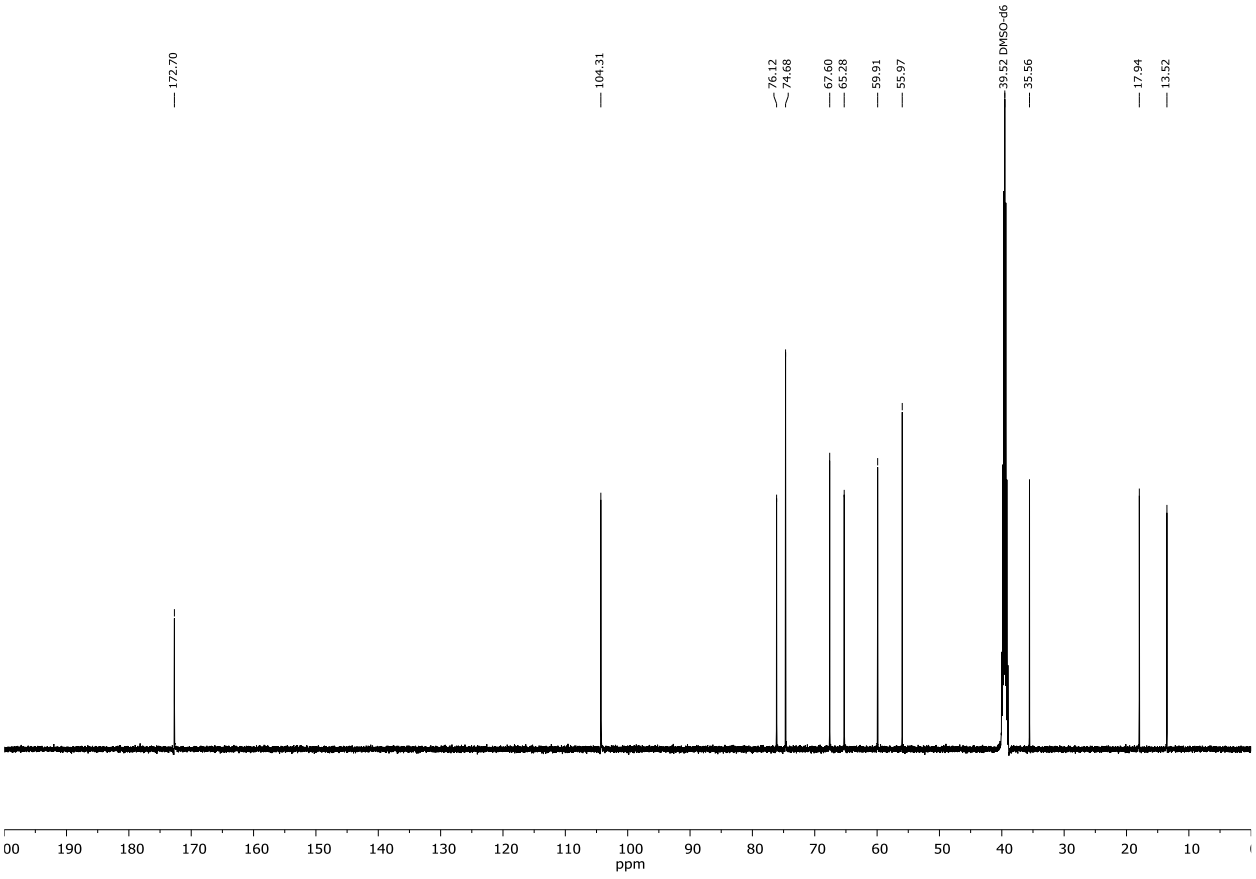

^{1}H-^{1}H COSY NMR (500 MHz, DMSO-d_6) 3-*O*-butanoyl methyl β-D-galactopyranoside (**3.01**)

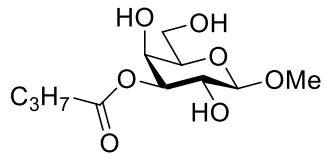

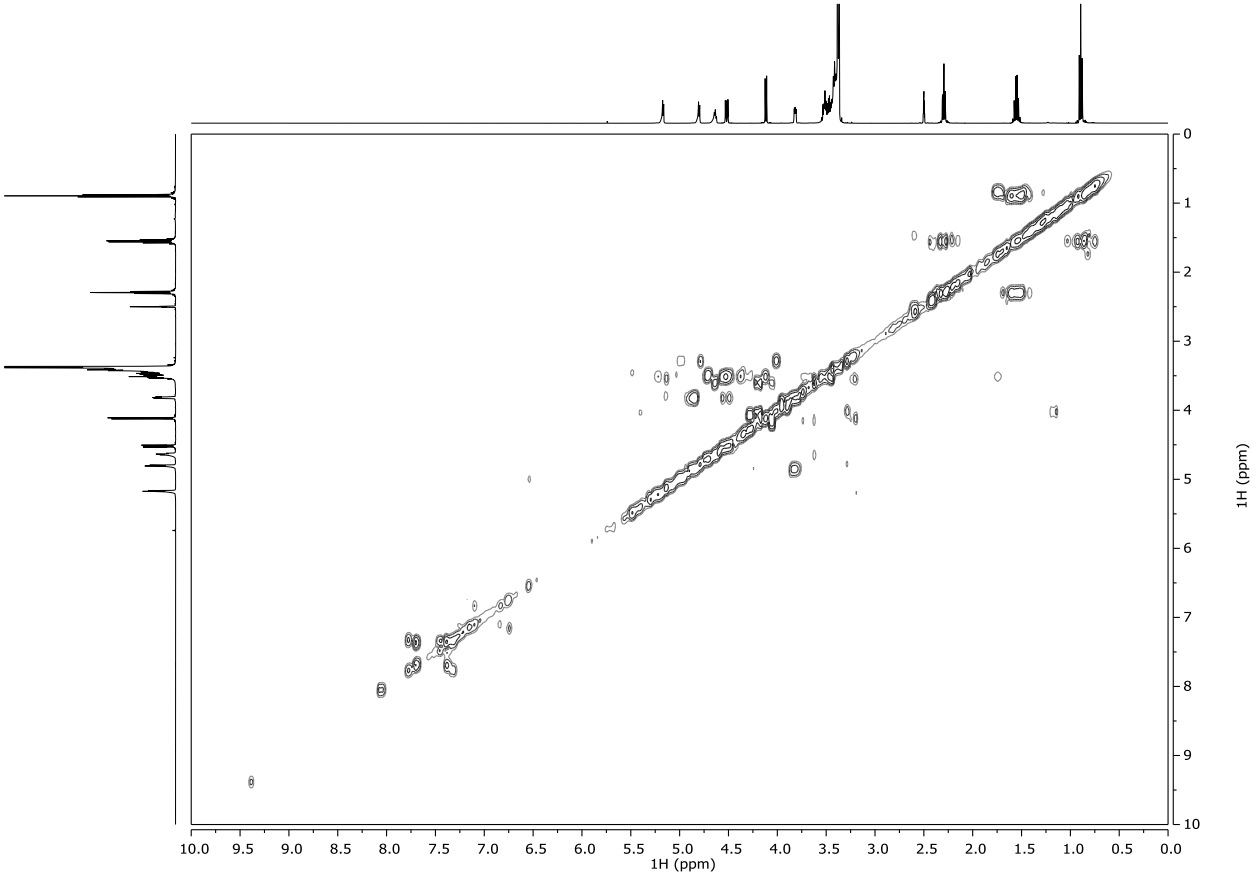

^{1}H NMR (500 MHz, DMSO-d_6) 3-*O*-butanoyl methyl α-D-mannopyranoside (3.XX)

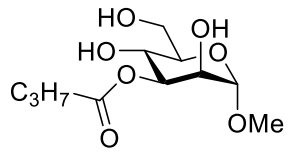

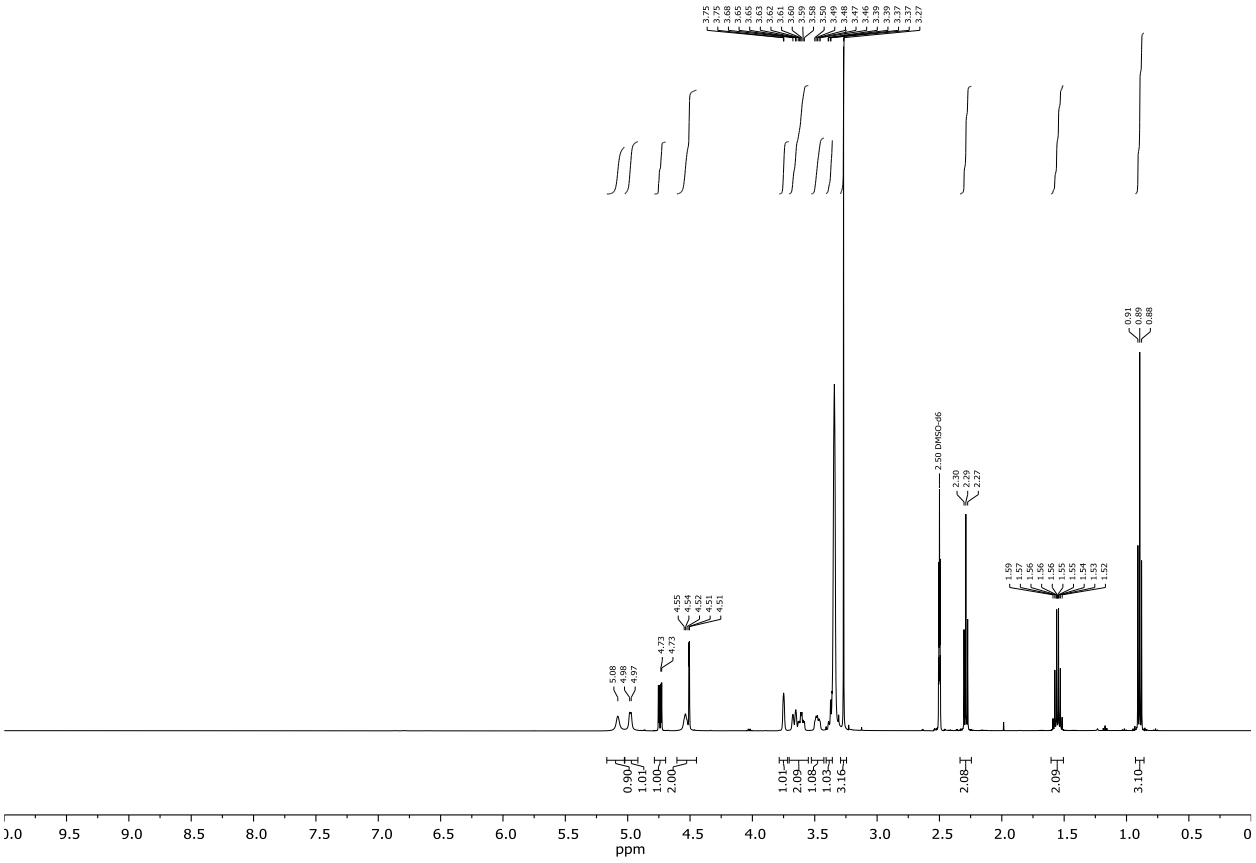

^{13}C NMR (126 MHz, DMSO-d_6) 3-*O*-butanoyl methyl α-D-mannopyranoside (3.XX)

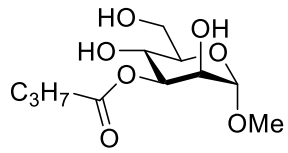

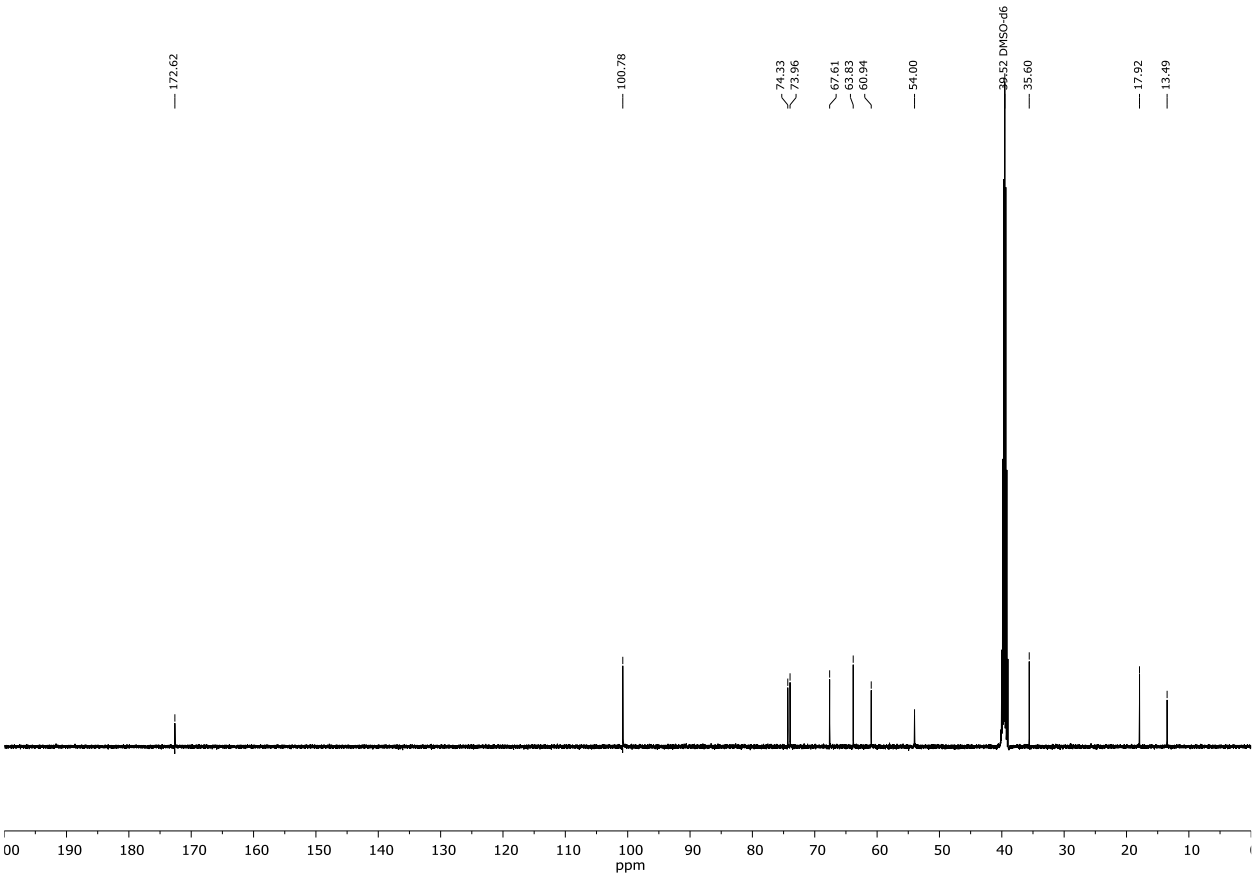

^{1}H-^{1}H COSY NMR (500 MHz, DMSO-d_6) 3-*O*-butanoyl methyl α-D-mannopyranoside (3.XX)

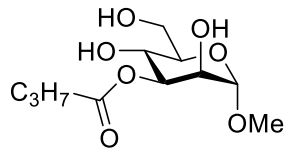

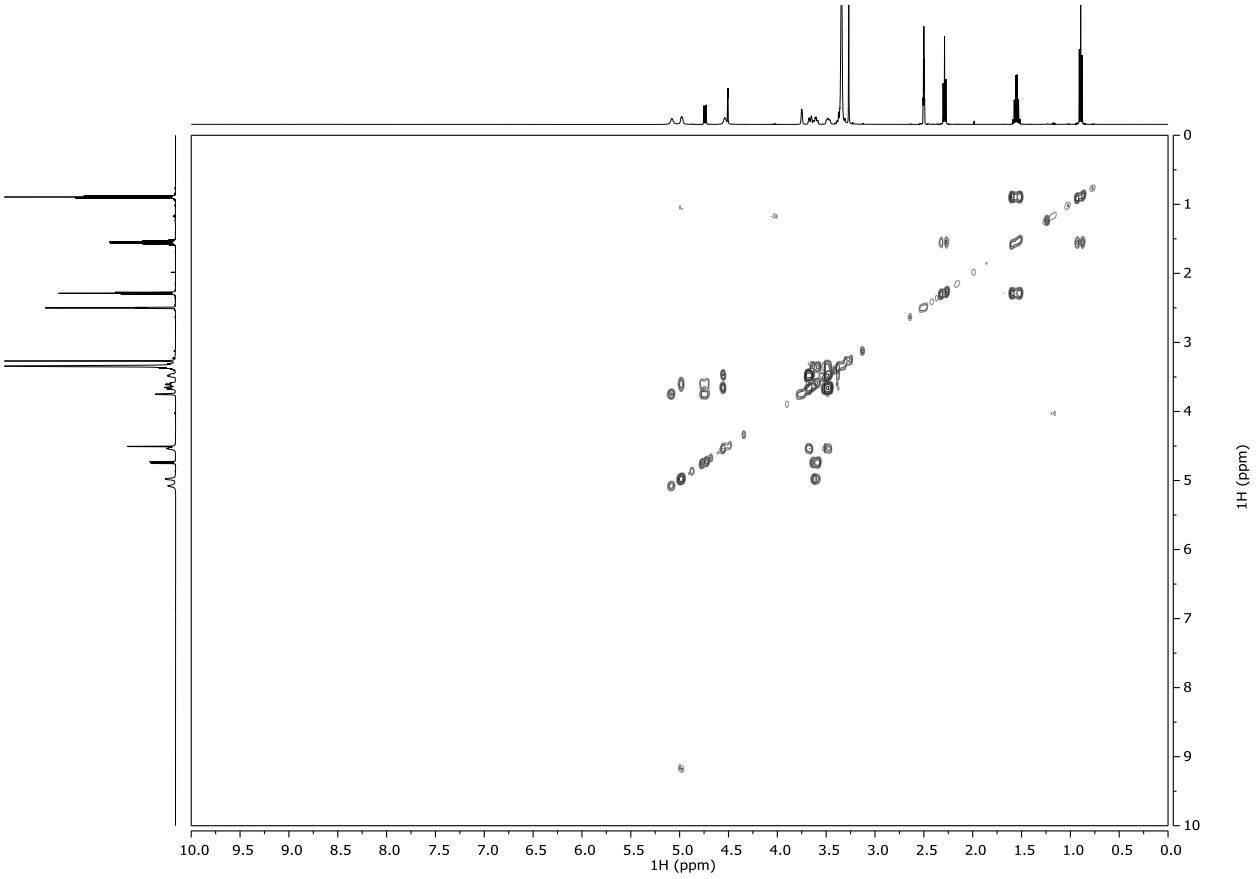

2 FTIR Spectra of Cross-linked PGS

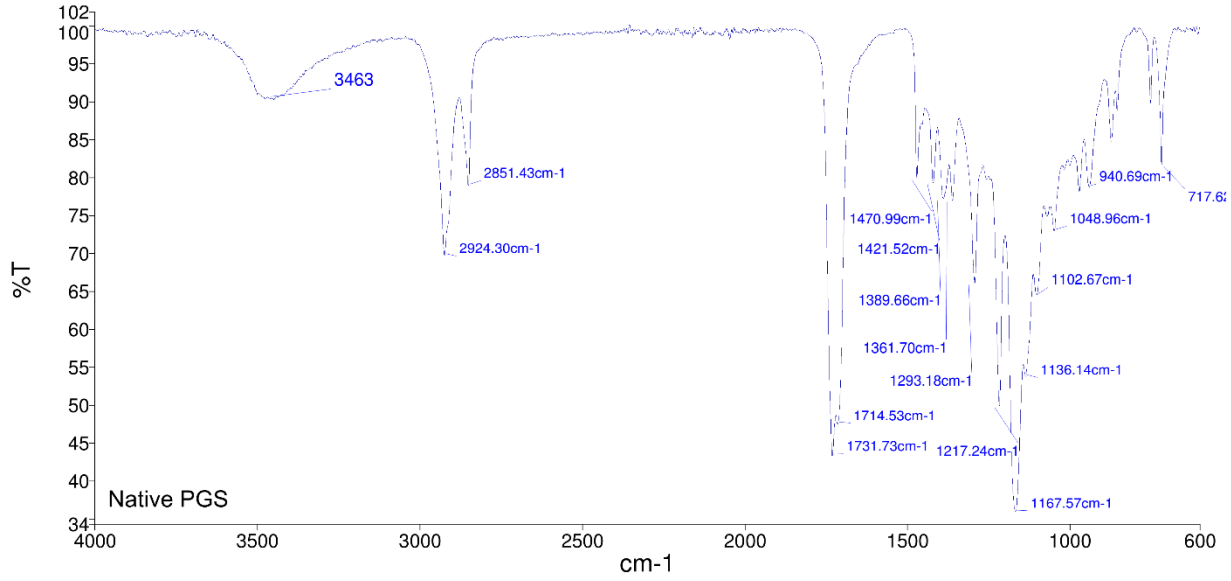

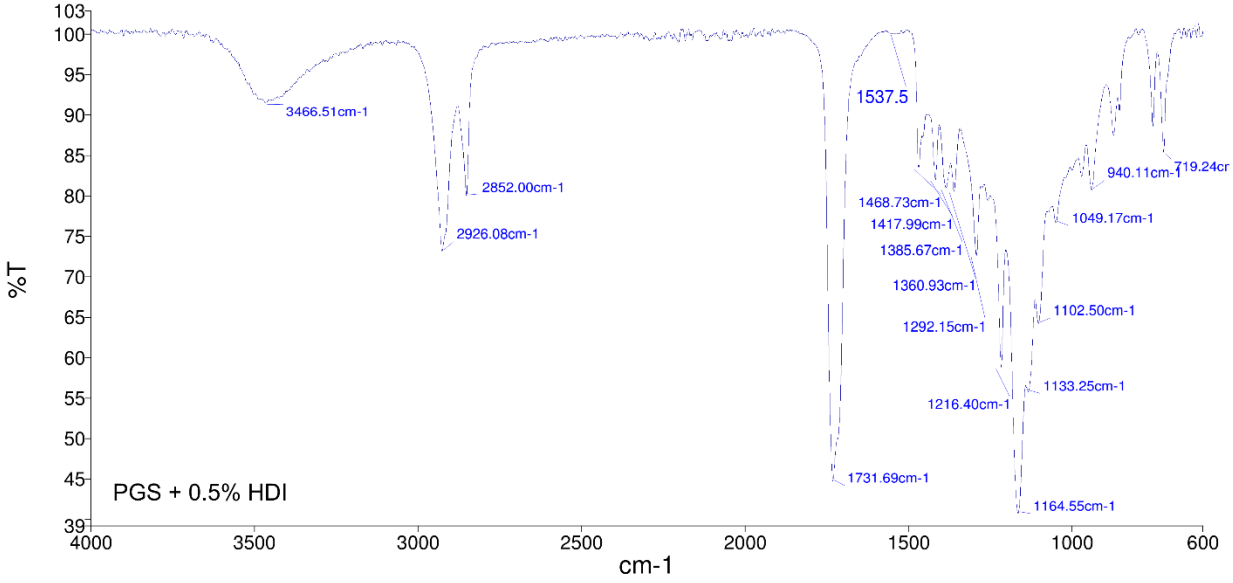

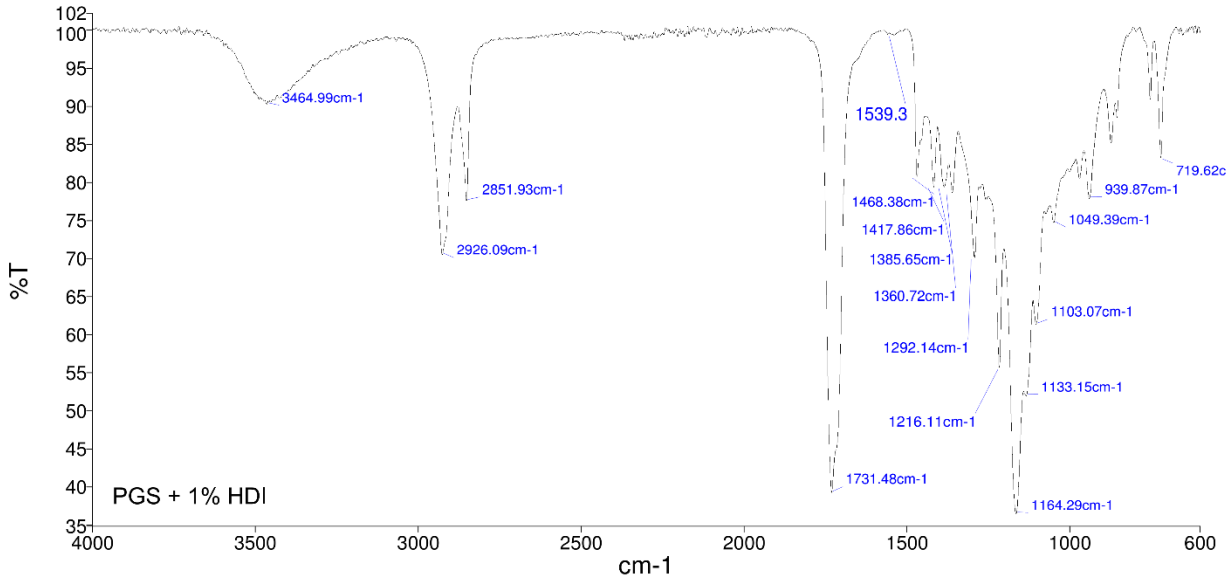
%T
cm-1
PGS + 1% HDI
3464.99cm-1
2851.93cm-1
2926.09cm-1
1539.3
1468.38cm-1
1417.86cm-1
1385.65cm-1
1360.72cm-1
1292.14cm-1
1216.11cm-1
1731.48cm-1
1164.29cm-1
1133.15cm-1
1103.07cm-1
1049.39cm-1
939.87cm-1
719.62c

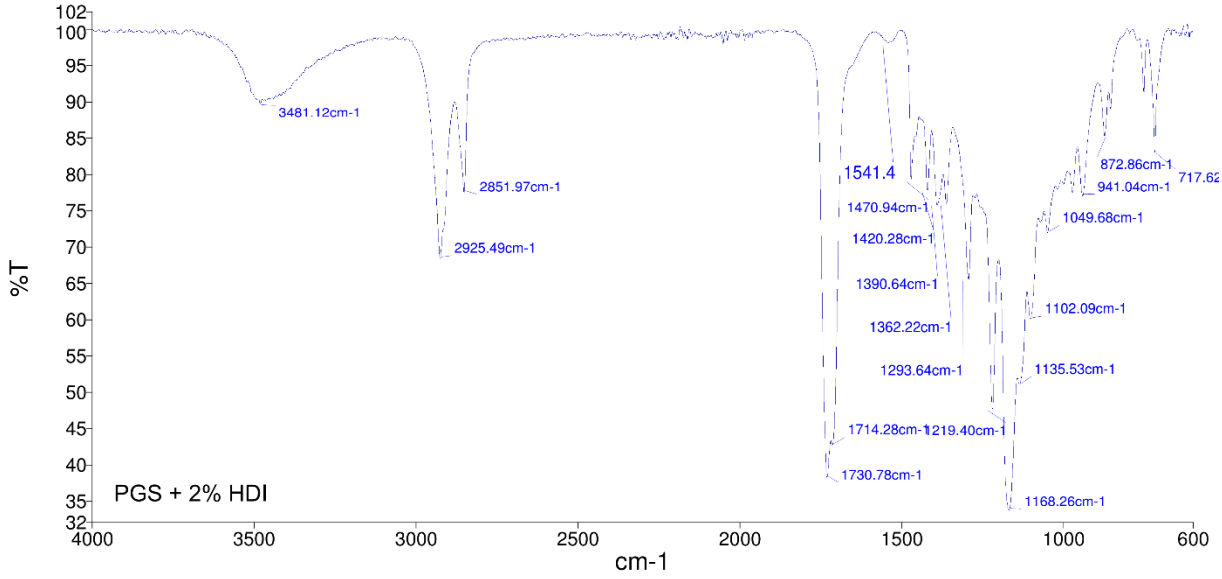
%T
cm-1
PGS + 2% HDI
3481.12cm-1
2851.97cm-1
2925.49cm-1
1541.4
1470.94cm-1
1420.28cm-1
1390.64cm-1
1362.22cm-1
1293.64cm-1
1714.28cm-1
1730.78cm-1
1219.40cm-1
1168.26cm-1
1135.53cm-1
1102.09cm-1
1049.68cm-1
941.04cm-1
872.86cm-1
717.62

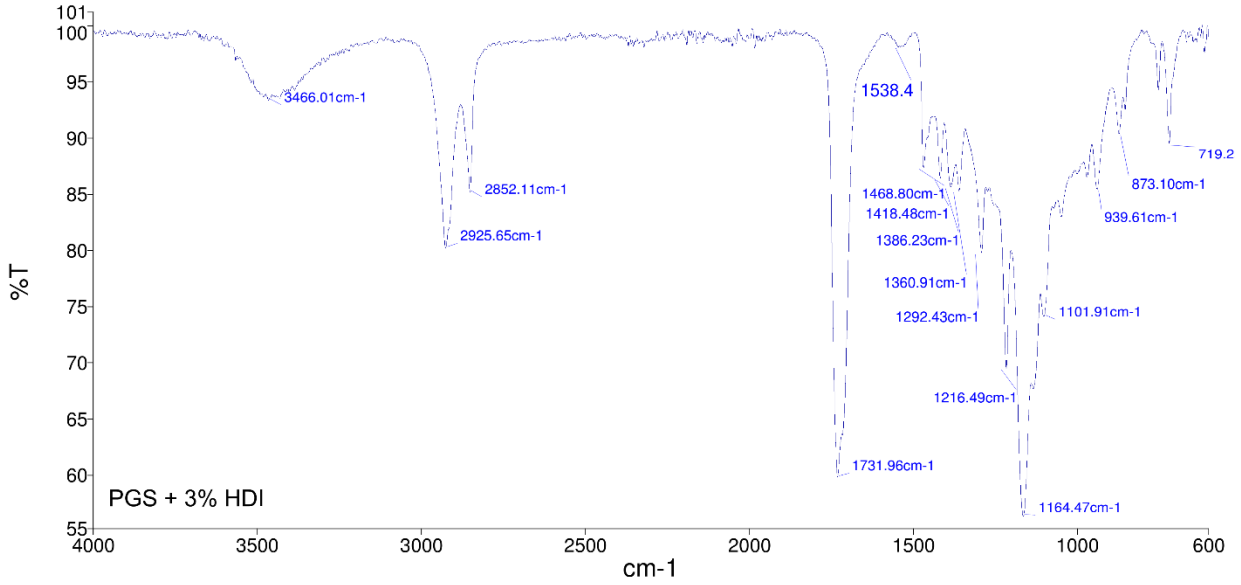
%T
cm-1
PGS + 3% HDI
3466.01cm-1
2852.11cm-1
2925.65cm-1
1538.4
1468.80cm-1
1418.48cm-1
1386.23cm-1
1360.91cm-1
1292.43cm-1
1216.49cm-1
1731.96cm-1
1164.47cm-1
1101.91cm-1
939.61cm-1
873.10cm-1
719.2

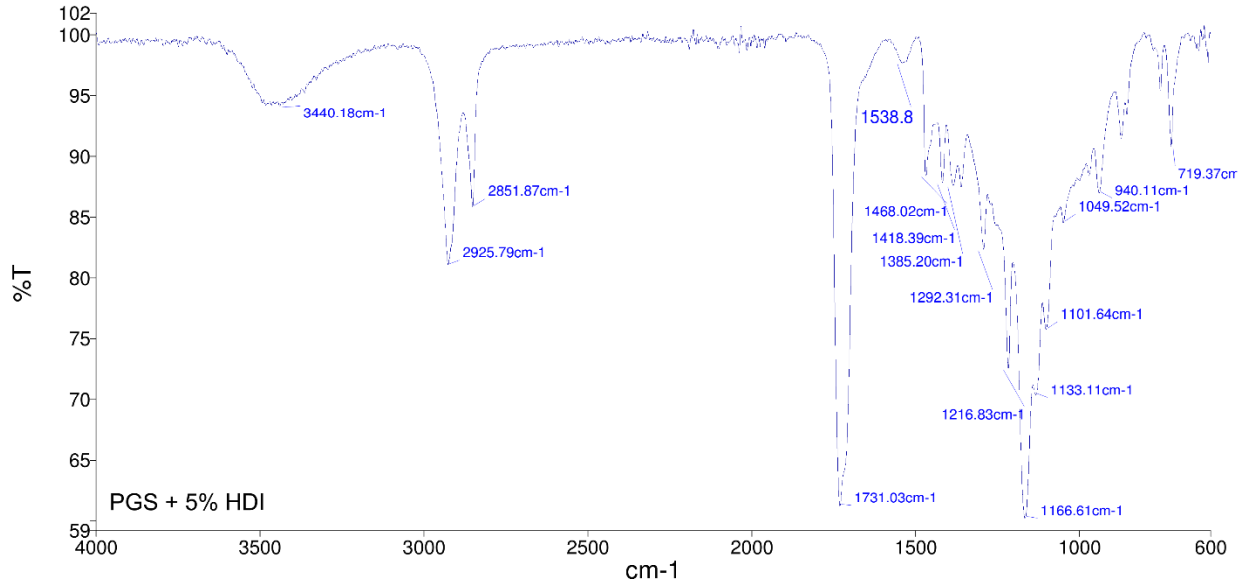
%T
cm-1
PGS + 5% HDI
3440.18cm-1
2851.87cm-1
2925.79cm-1
1538.8
1468.02cm-1
1418.39cm-1
1385.20cm-1
1292.31cm-1
1216.83cm-1
1731.03cm-1
1166.61cm-1
1133.11cm-1
1101.64cm-1
1049.52cm-1
940.11cm-1
719.37cm

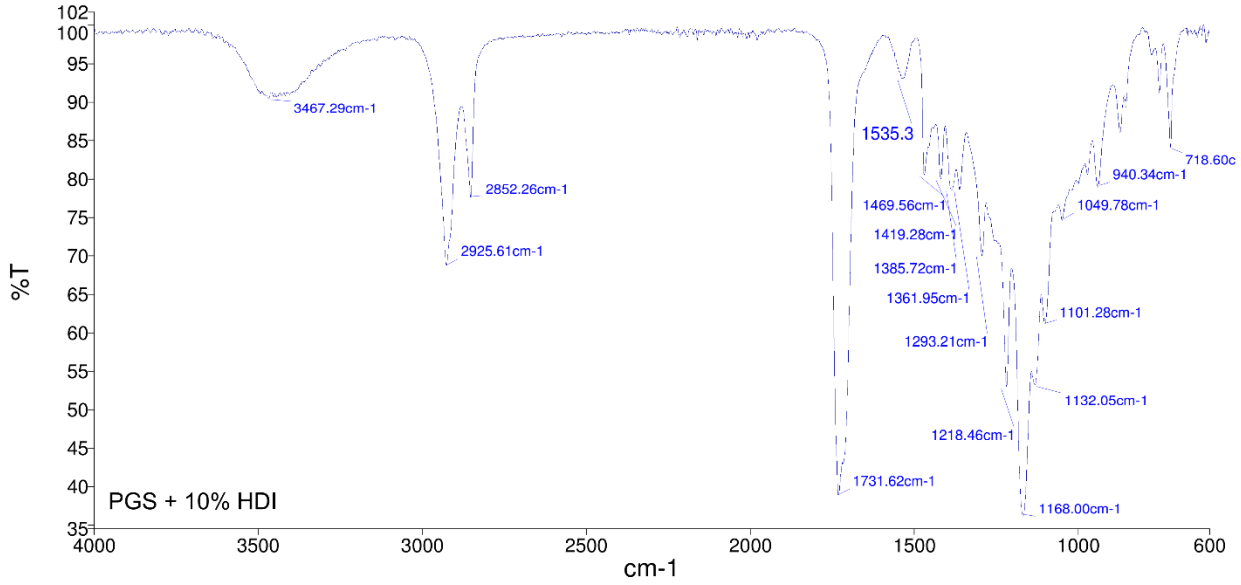
%T
cm-1
PGS + 10% HDI
3467.29cm-1
2852.26cm-1
2925.61cm-1
1535.3
1469.56cm-1
1419.28cm-1
1385.72cm-1
1361.95cm-1
1293.21cm-1
1218.46cm-1
1731.62cm-1
1168.00cm-1
1132.05cm-1
1101.28cm-1
1049.78cm-1
940.34cm-1
718.60c

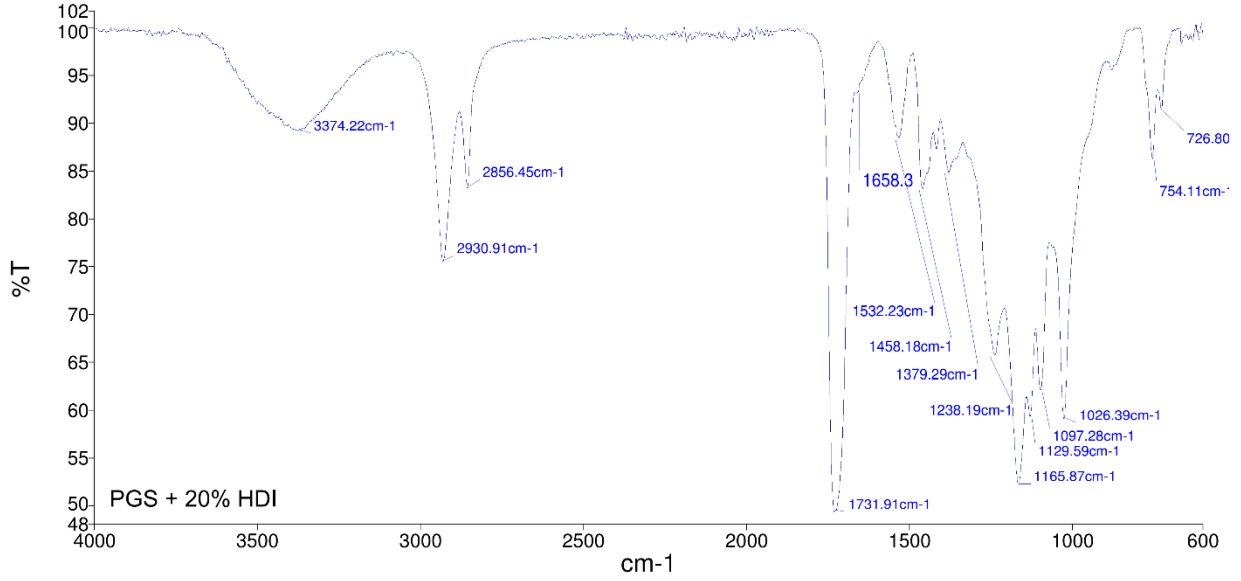
%T
cm-1
PGS + 20% HDI
3374.22cm-1
2856.45cm-1
2930.91cm-1
1658.3
1532.23cm-1
1458.18cm-1
1379.29cm-1
1238.19cm-1
1731.91cm-1
1165.87cm-1
1129.59cm-1
1097.28cm-1
1026.39cm-1
754.11cm-
726.80

3 GPC Traces

3.1 Chapter 2

Poly(glycerol sebacate)

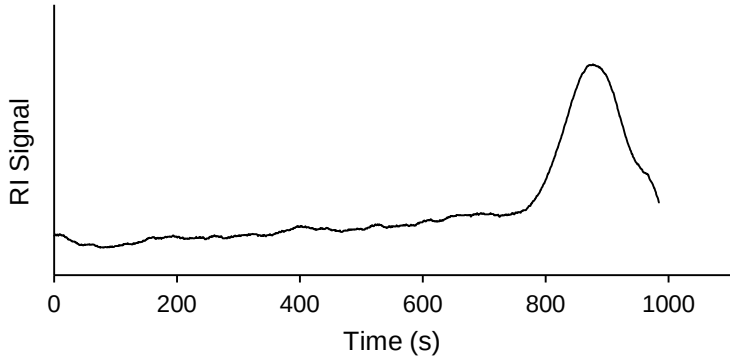

Poly(glycerol dodecanoate)

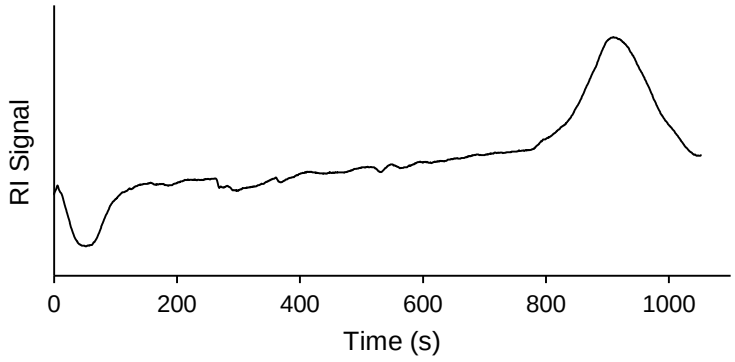

Poly(glycerol adipate)

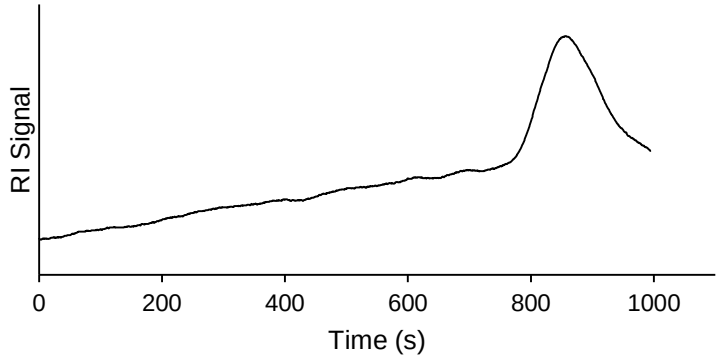

Poly(glycerol isophthalate)

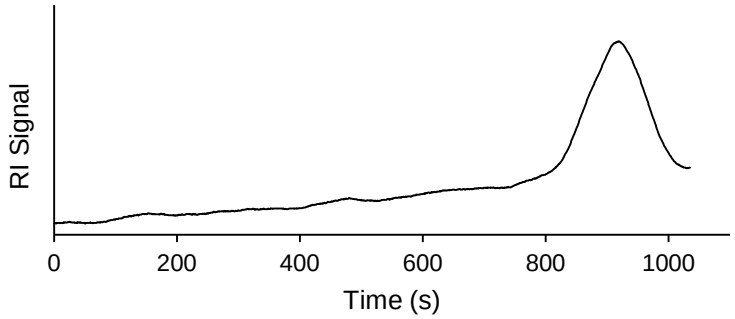

Poly(glycerol terephthalate)

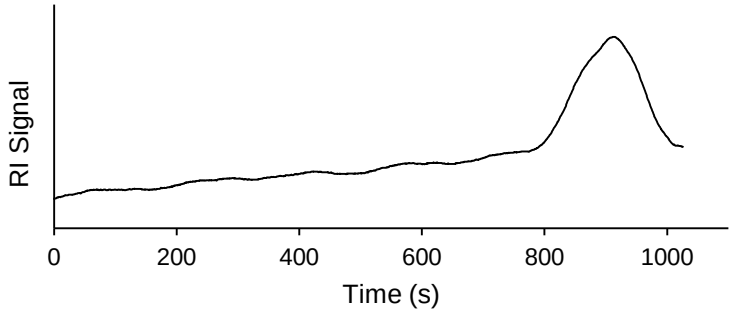

3.2 Chapter 3

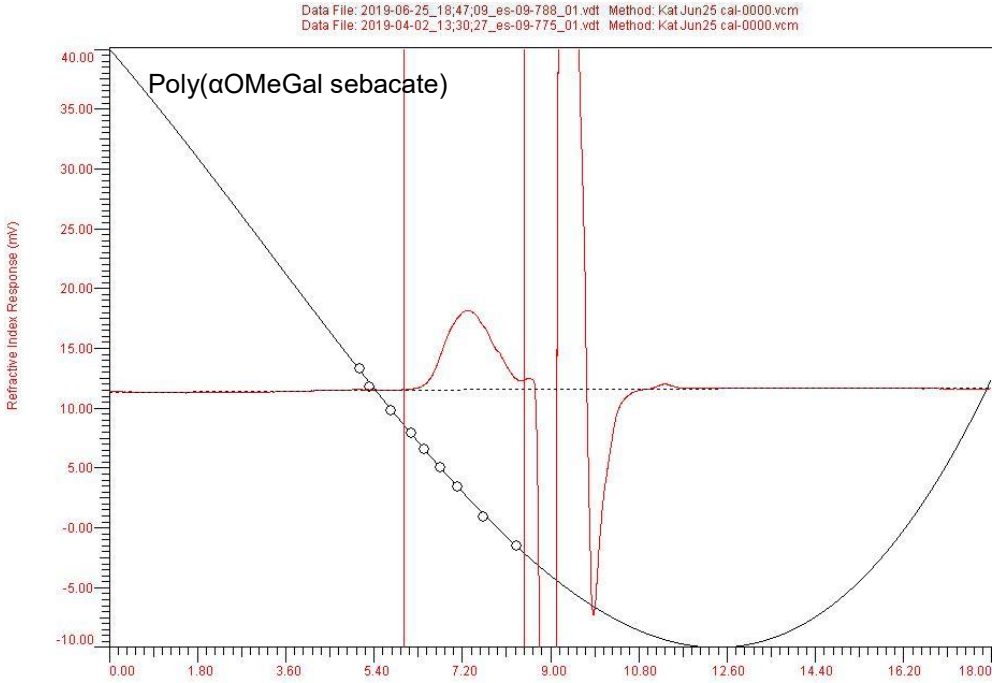
Data File: 2019-06-25_18;47;09_es-09-788_01.vdt Method: Kat Jun25 cal-0000.vcm
Data File: 2019-04-02_13;30;27_es-09-775_01.vdt Method: Kat Jun25 cal-0000.vcm
Poly(αOMeGal sebacate)
Refractive Index Response (mV)
40.00
35.00
30.00
25.00
20.00
15.00
10.00
5.00
-0.00
-5.00
-10.00
0.00
1.80
3.60
5.40
7.20
9.00
10.80
12.60
14.40
16.20
18.00

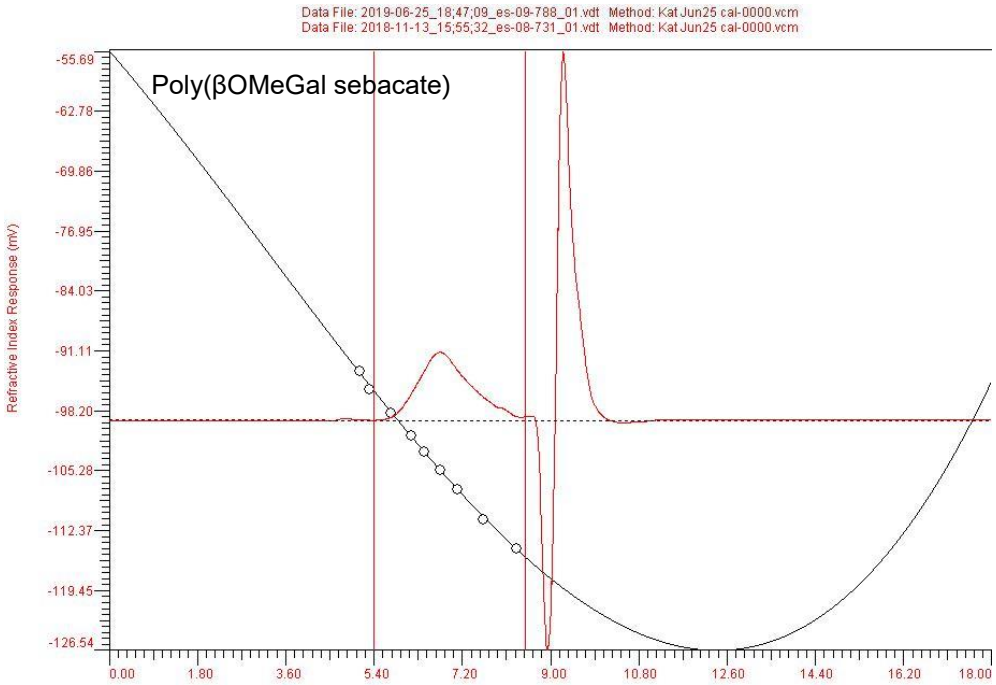
Data File: 2019-06-25_18;47;09_es-09-788_01.vdt Method: Kat Jun25 cal-0000.vcm
Data File: 2018-11-13_15;55;32_es-08-731_01.vdt Method: Kat Jun25 cal-0000.vcm
Poly(βOMeGal sebacate)
Refractive Index Response (mV)
-55.69
-62.78
-69.86
-76.95
-84.03
-91.11
-98.20
-105.28
-112.37
-119.45
-126.54
0.00
1.80
3.60
5.40
7.20
9.00
10.80
12.60
14.40
16.20
18.00

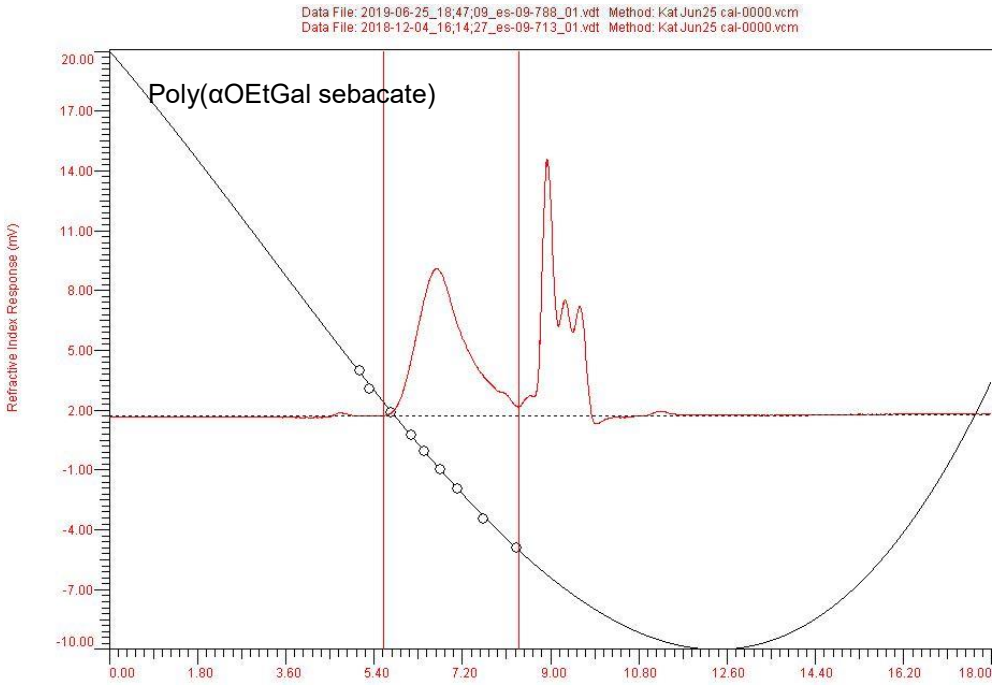
Data File: 2019-06-25_18;47;09_es-09-788_01.vdt Method: Kat Jun25 cal-0000.vcm
Data File: 2018-12-04_16;14;27_es-09-713_01.vdt Method: Kat Jun25 cal-0000.vcm
Poly(αOEtGal sebacate)
Refractive Index Response (mV)
20.00
17.00
14.00
11.00
8.00
5.00
2.00
-1.00
-4.00
-7.00
-10.00
0.00
1.80
3.60
5.40
7.20
9.00
10.80
12.60
14.40
16.20
18.00

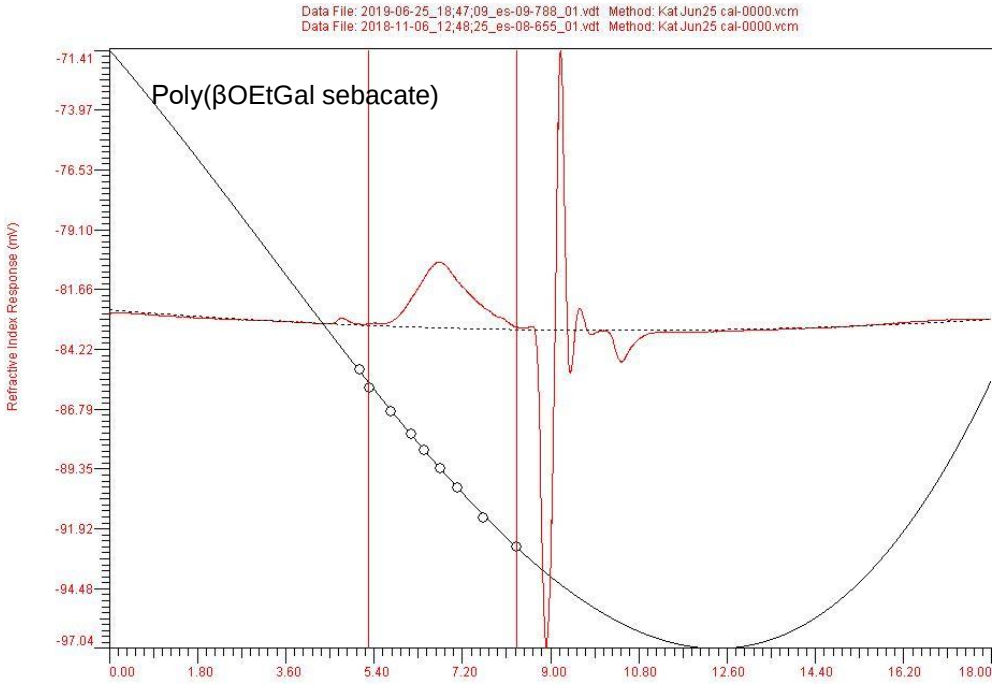
Data File: 2019-06-25_18;47;09_es-09-788_01.vdt Method: Kat Jun25 cal-0000.vcm
Data File: 2018-11-06_12;48;25_es-08-655_01.vdt Method: Kat Jun25 cal-0000.vcm
Poly(βOEtGal sebacate)
Refractive Index Response (mV)
-71.41
-73.97
-76.53
-79.10
-81.66
-84.22
-86.79
-89.35
-91.92
-94.48
-97.04
0.00
1.80
3.60
5.40
7.20
9.00
10.80
12.60
14.40
16.20
18.00

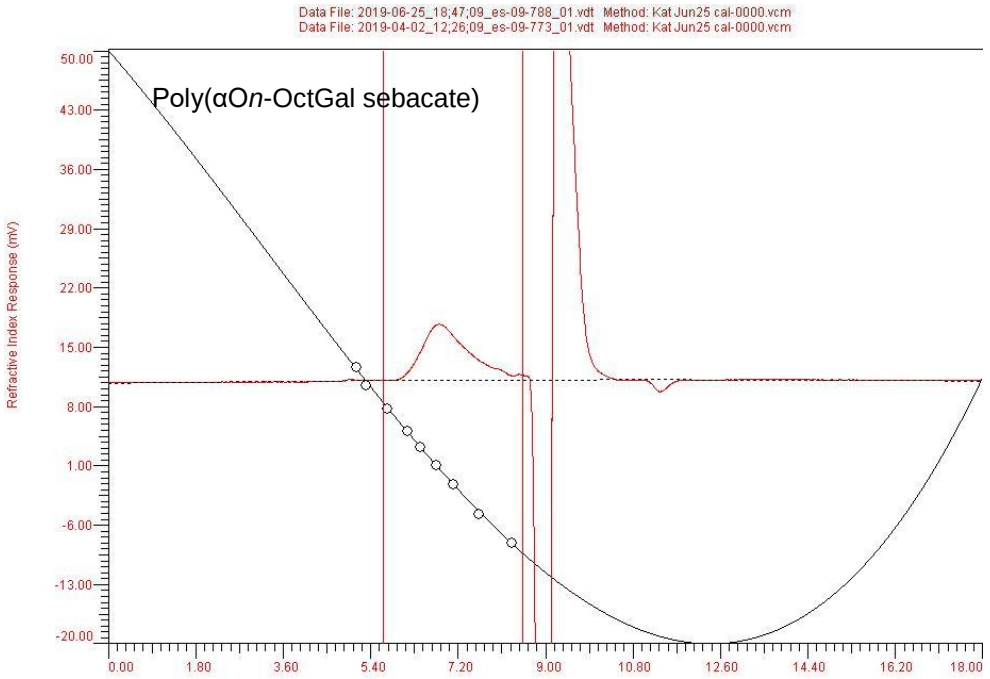
Data File: 2019-06-25_18;47;09_es-09-788_01.vdt Method: Kat Jun25 cal-0000.vcm
Data File: 2019-04-02_12;26;09_es-09-773_01.vdt Method: Kat Jun25 cal-0000.vcm
Poly(αO*n*-OctGal sebacate)
Refractive Index Response (mV)
50.00
43.00
36.00
29.00
22.00
15.00
8.00
1.00
-6.00
-13.00
-20.00
0.00
1.80
3.60
5.40
7.20
9.00
10.80
12.60
14.40
16.20
18.00

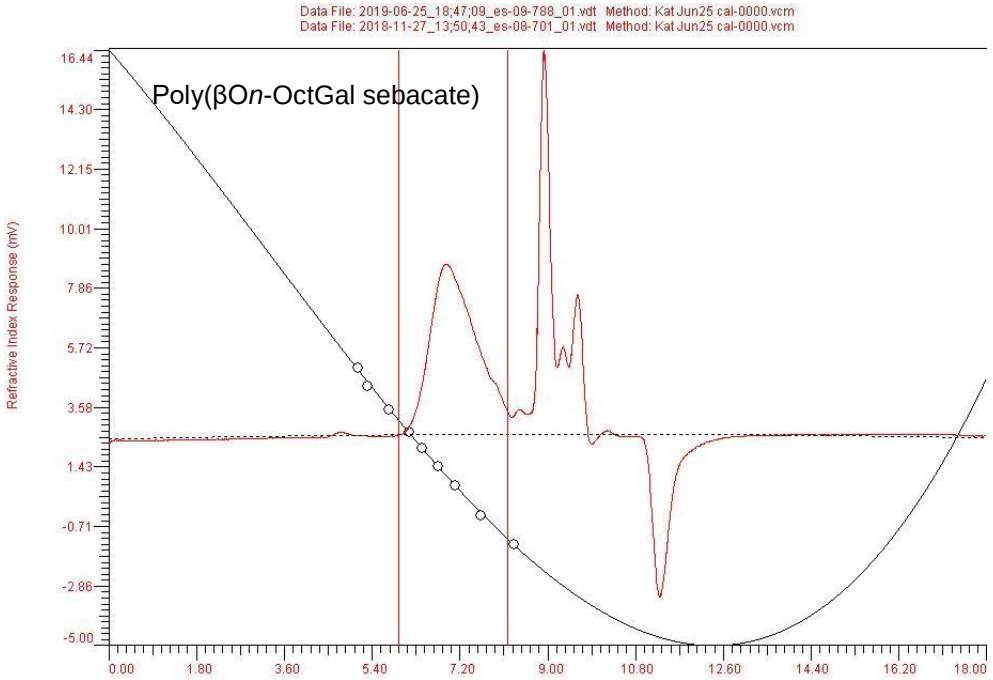
Data File: 2019-06-25_18;47;09_es-09-788_01.vdt Method: Kat Jun25 cal-0000.vcm
Data File: 2018-11-27_13;50;43_es-08-701_01.vdt Method: Kat Jun25 cal-0000.vcm
Poly(βO*n*-OctGal sebacate)
Refractive Index Response (mV)
16.44
14.30
12.15
10.01
7.86
5.72
3.58
1.43
-0.71
-2.86
-5.00
0.00
1.80
3.60
5.40
7.20
9.00
10.80
12.60
14.40
16.20
18.00

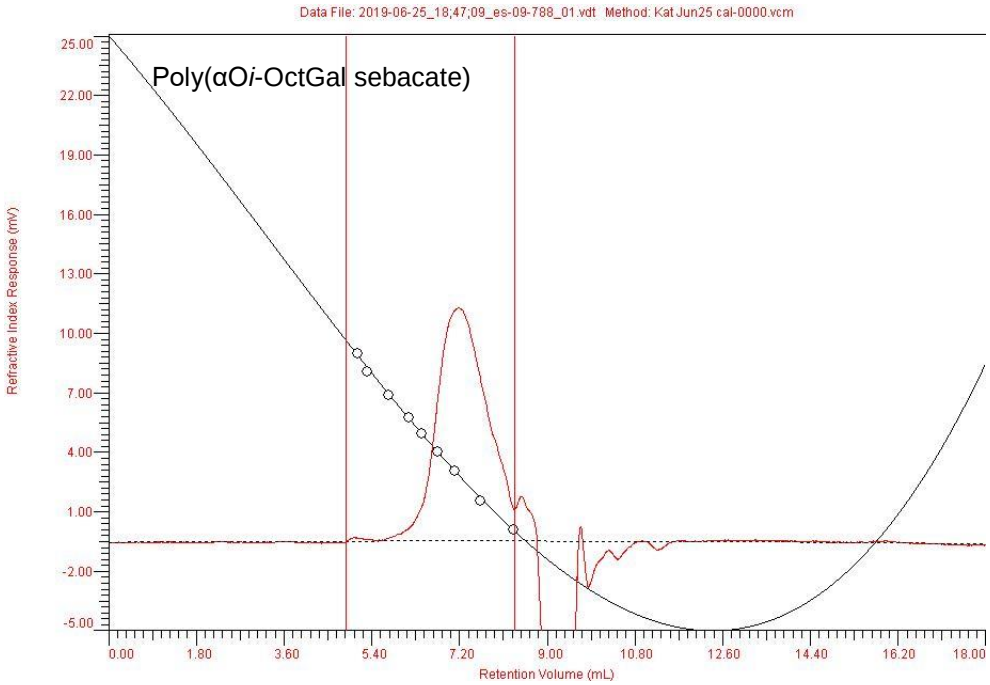
Data File: 2019-06-25_18;47;09_es-09-788_01.vdt Method: Kat Jun25 cal-0000.vcm
Poly(αO*i*-OctGal sebacate)
Refractive Index Response (mV)
Retention Volume (mL)

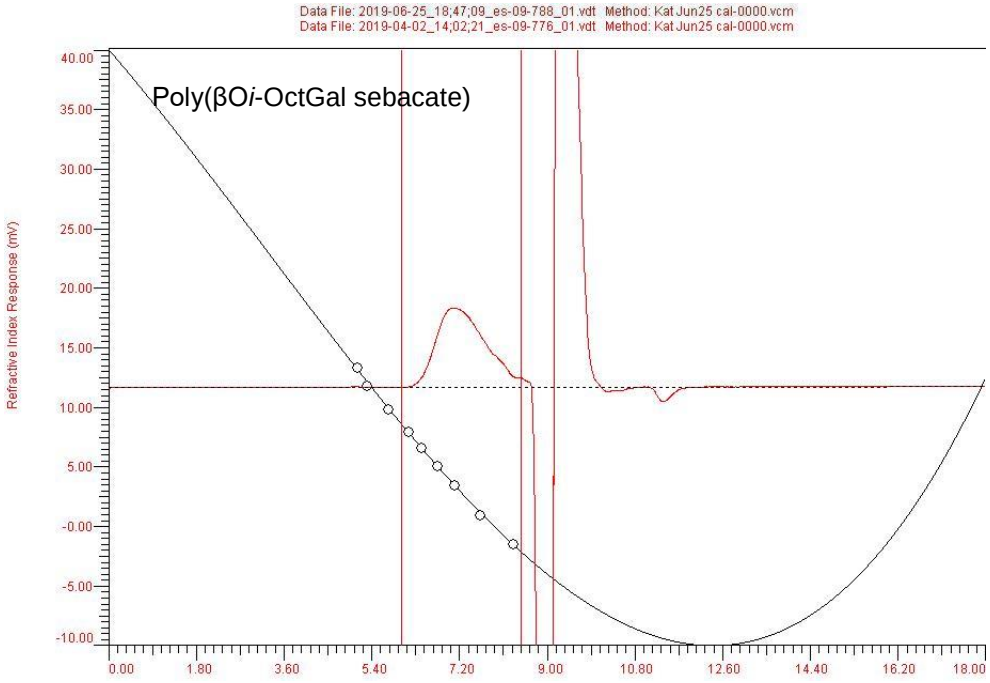
Data File: 2019-06-25_18;47;09_es-09-788_01.vdt Method: Kat Jun25 cal-0000.vcm
Data File: 2019-04-02_14;02;21_es-09-776_01.vdt Method: Kat Jun25 cal-0000.vcm
Poly(βO*i*-OctGal sebacate)
Refractive Index Response (mV)

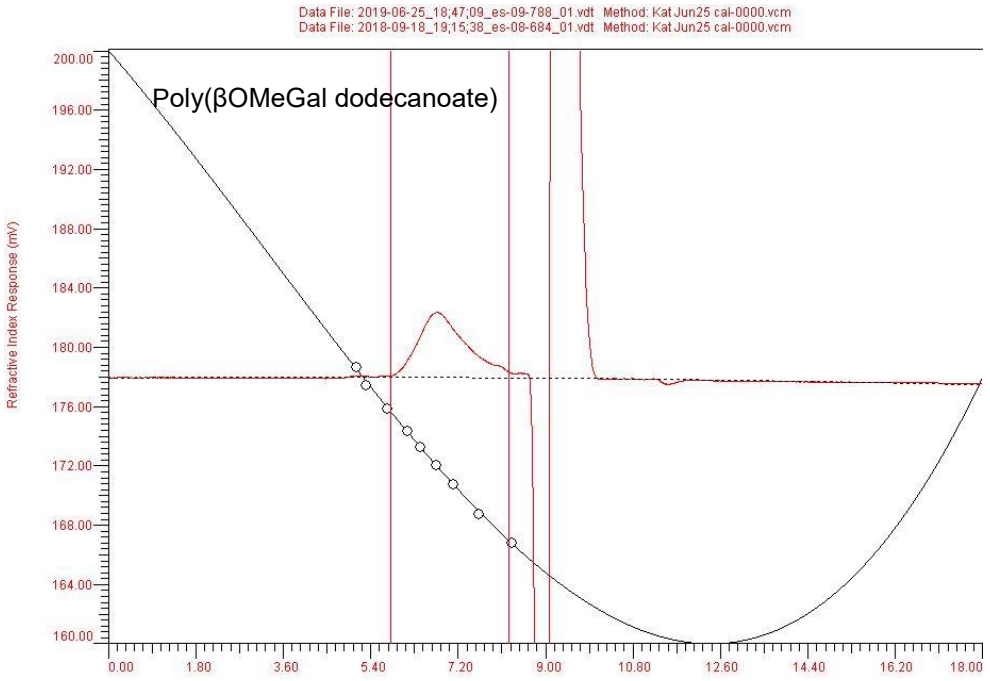
Data File: 2019-06-25_18;47;09_es-09-788_01.vdt Method: Kat Jun25 cal-0000.vcm
Data File: 2018-09-18_19;15;38_es-08-684_01.vdt Method: Kat Jun25 cal-0000.vcm
Poly(βOMeGal dodecanoate)
Refractive Index Response (mV)
200.00
196.00
192.00
188.00
184.00
180.00
176.00
172.00
168.00
164.00
160.00
0.00
1.80
3.60
5.40
7.20
9.00
10.80
12.60
14.40
16.20
18.00

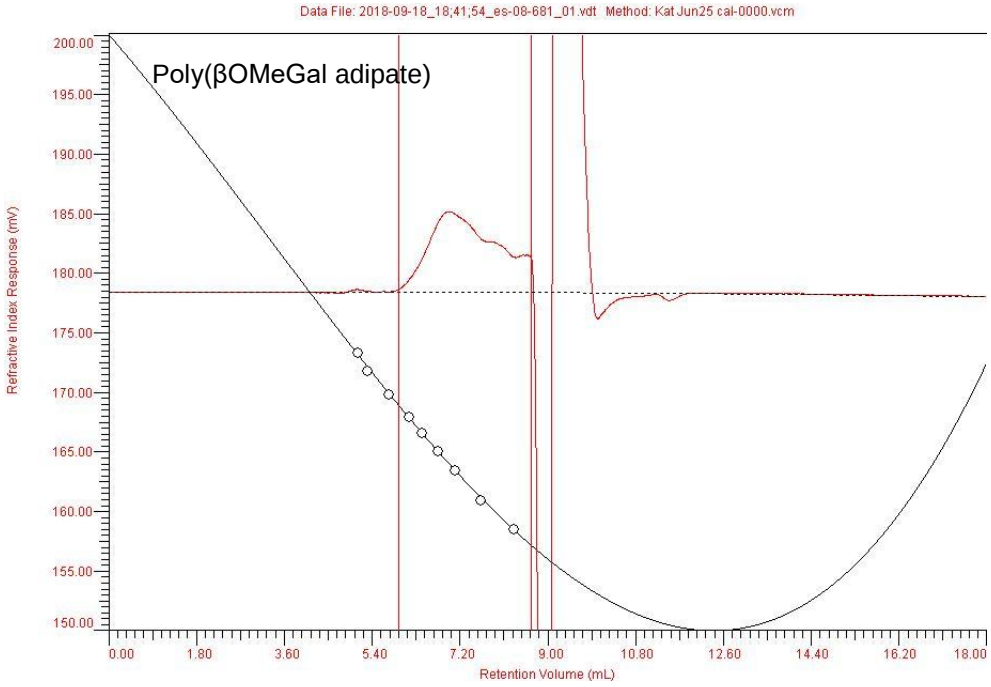
Data File: 2018-09-18_18;41;54_es-08-681_01.vdt Method: Kat Jun25 cal-0000.vcm
Poly(βOMeGal adipate)
Refractive Index Response (mV)
200.00
195.00
190.00
185.00
180.00
175.00
170.00
165.00
160.00
155.00
150.00
0.00
1.80
3.60
5.40
7.20
9.00
10.80
12.60
14.40
16.20
18.00
Retention Volume (mL)

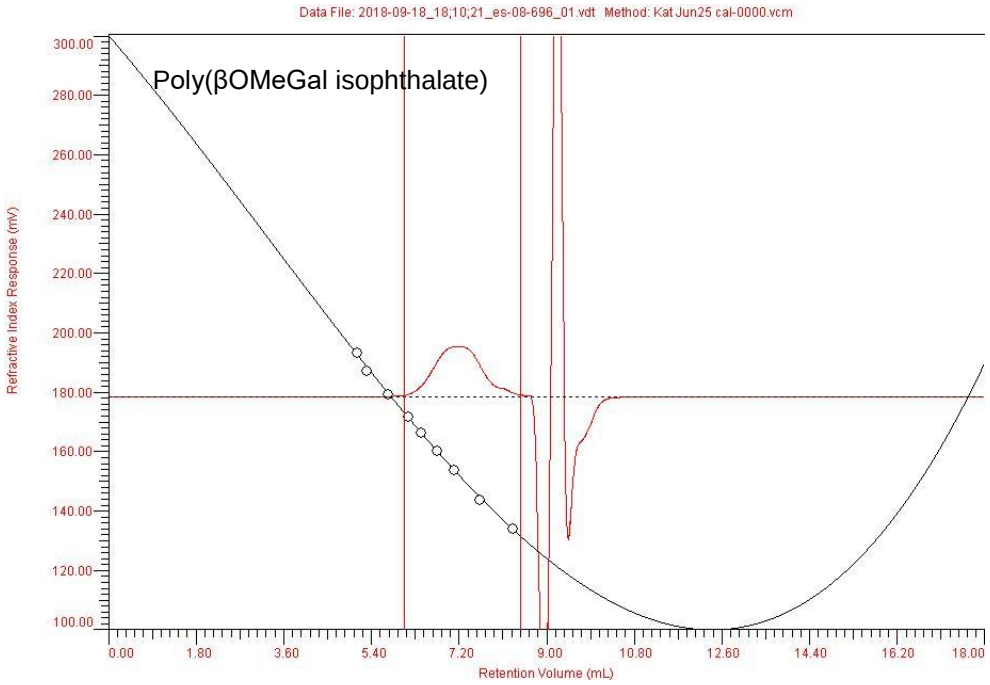
Data File: 2018-09-18_18;10;21_es-08-696_01.vdt Method: Kat Jun25 cal-0000.vcm
Poly(βOMeGal isophthalate)
Refractive Index Response (mV)
300.00
280.00
260.00
240.00
220.00
200.00
180.00
160.00
140.00
120.00
100.00
0.00
1.80
3.60
5.40
7.20
9.00
10.80
12.60
14.40
16.20
18.00
Retention Volume (mL)

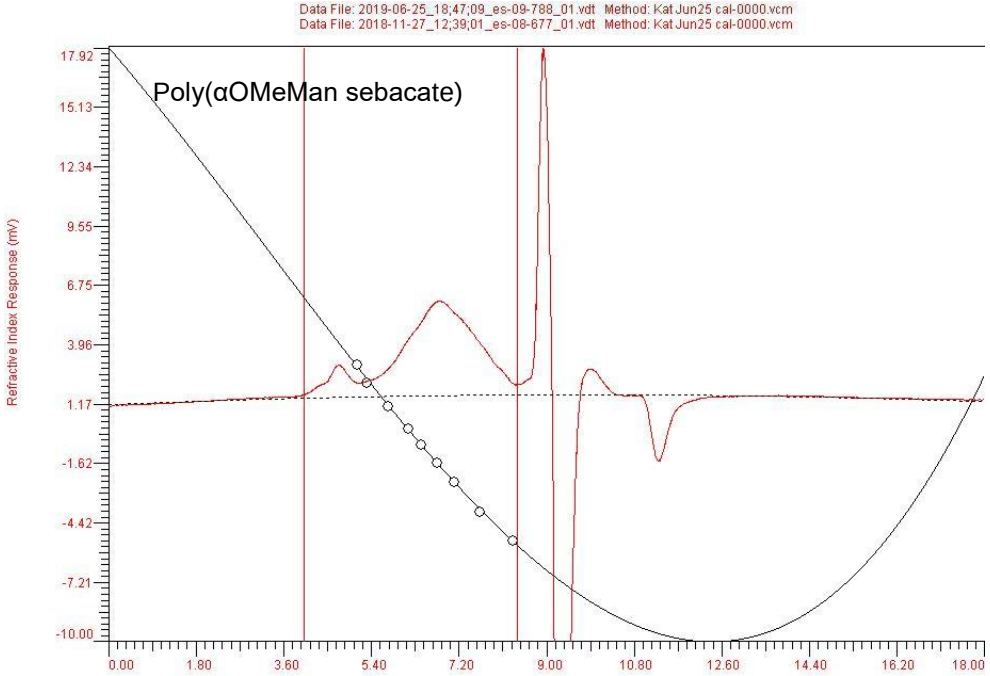
Data File: 2019-06-25_18;47;09_es-09-788_01.vdt Method: Kat Jun25 cal-0000.vcm
Data File: 2018-11-27_12;39;01_es-08-677_01.vdt Method: Kat Jun25 cal-0000.vcm
Poly(αOMeMan sebacate)
Refractive Index Response (mV)
17.92
15.13
12.34
9.55
6.75
3.96
1.17
-1.62
-4.42
-7.21
-10.00
0.00
1.80
3.60
5.40
7.20
9.00
10.80
12.60
14.40
16.20
18.00

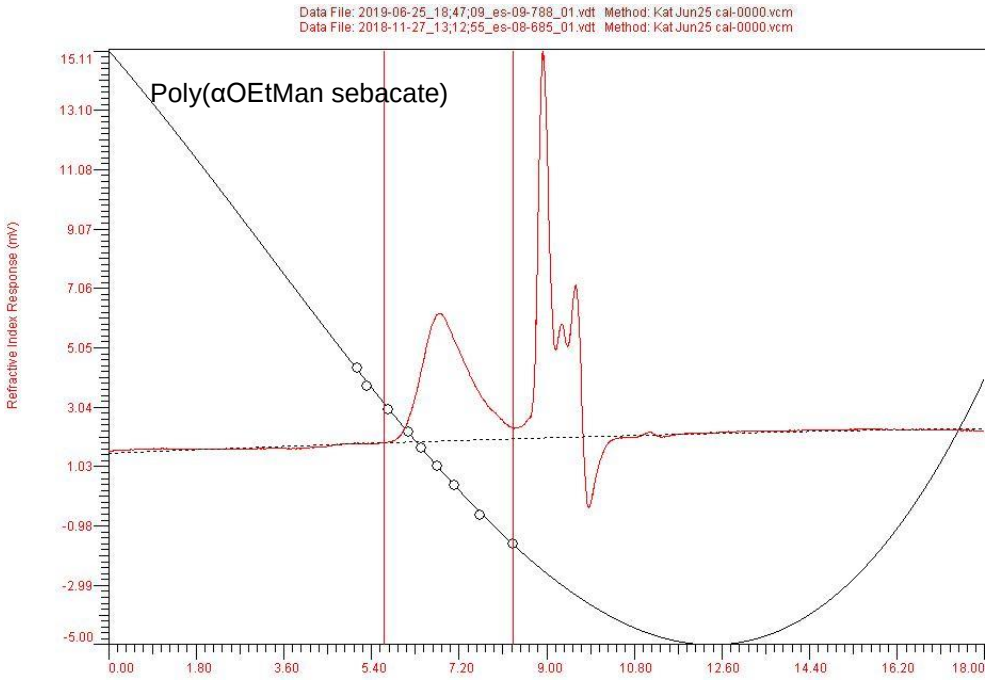
Data File: 2019-06-25_18;47;09_es-09-788_01.vdt Method: Kat Jun25 cal-0000.vcm
Data File: 2018-11-27_13;12;55_es-08-685_01.vdt Method: Kat Jun25 cal-0000.vcm
Poly(αOEtMan sebacate)
Refractive Index Response (mV)
15.11
13.10
11.08
9.07
7.06
5.05
3.04
1.03
-0.98
-2.99
-5.00
0.00
1.80
3.60
5.40
7.20
9.00
10.80
12.60
14.40
16.20
18.00

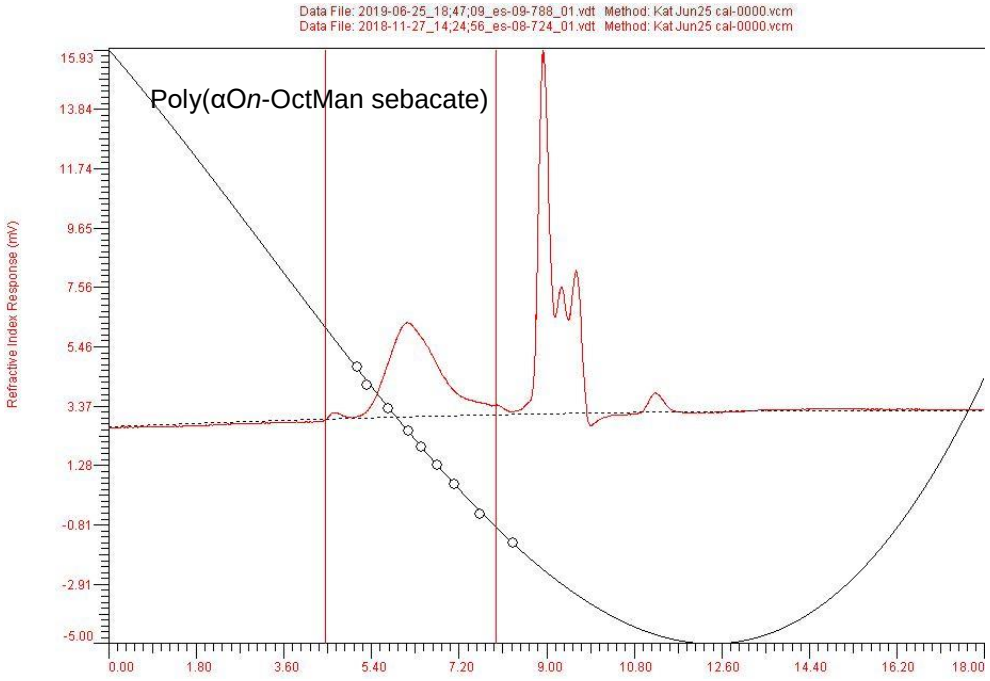
Data File: 2019-06-25_18;47;09_es-09-788_01.vdt Method: Kat Jun25 cal-0000.vcm
Data File: 2018-11-27_14;24;56_es-08-724_01.vdt Method: Kat Jun25 cal-0000.vcm
Poly(αO*n*-OctMan sebacate)
Refractive Index Response (mV)
15.93
13.84
11.74
9.65
7.56
5.46
3.37
1.28
-0.81
-2.91
-5.00
0.00
1.80
3.60
5.40
7.20
9.00
10.80
12.60
14.40
16.20
18.00

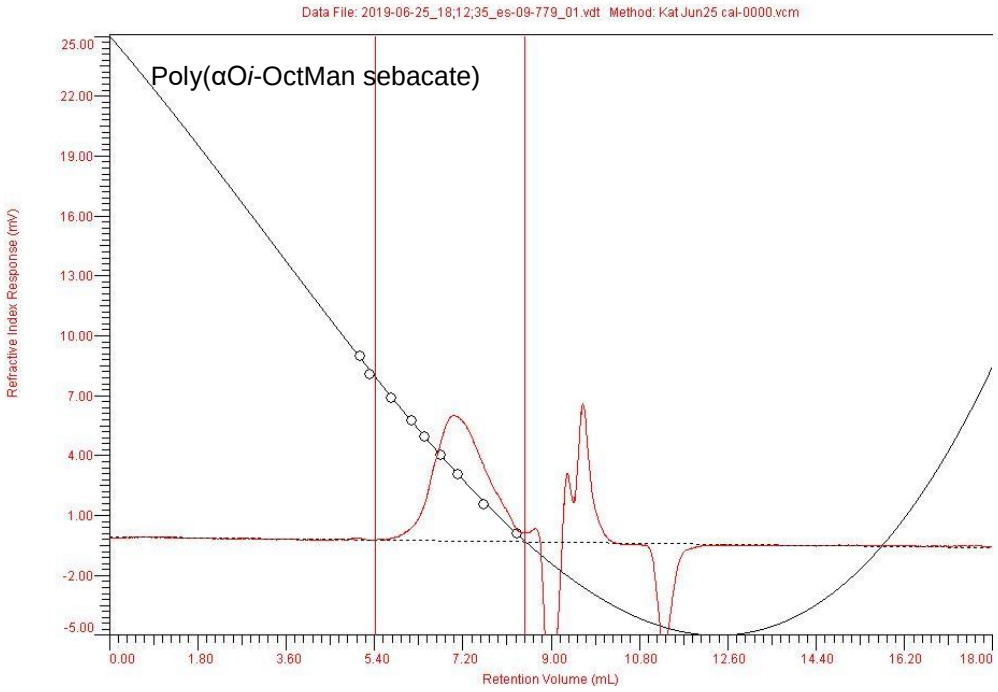

4 DSC Thermograms

4.1 Chapter 2

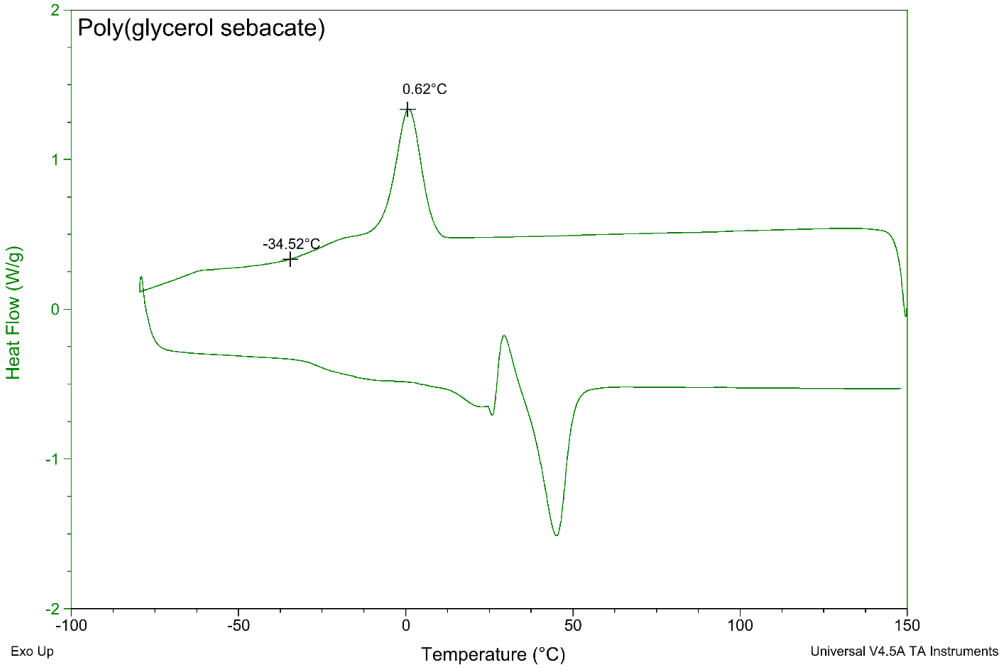

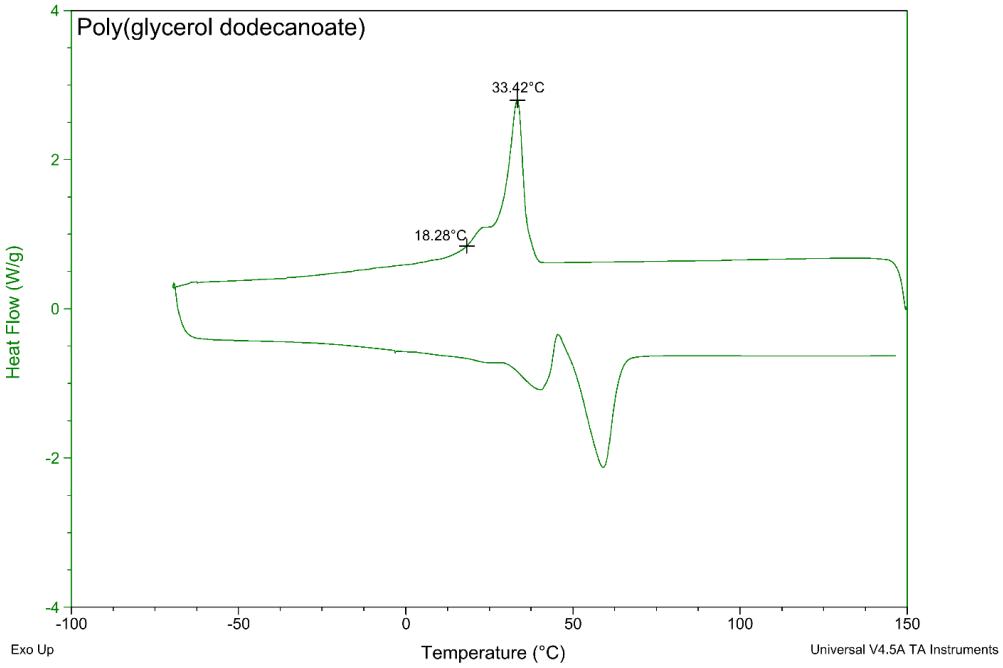
Poly(glycerol dodecanoate)
33.42°C
18.28°C
Heat Flow (W/g)
4
2
0
-2
-4
-100
-50
0
50
100
150
Exo Up
Temperature (°C)
Universal V4.5A TA Instruments

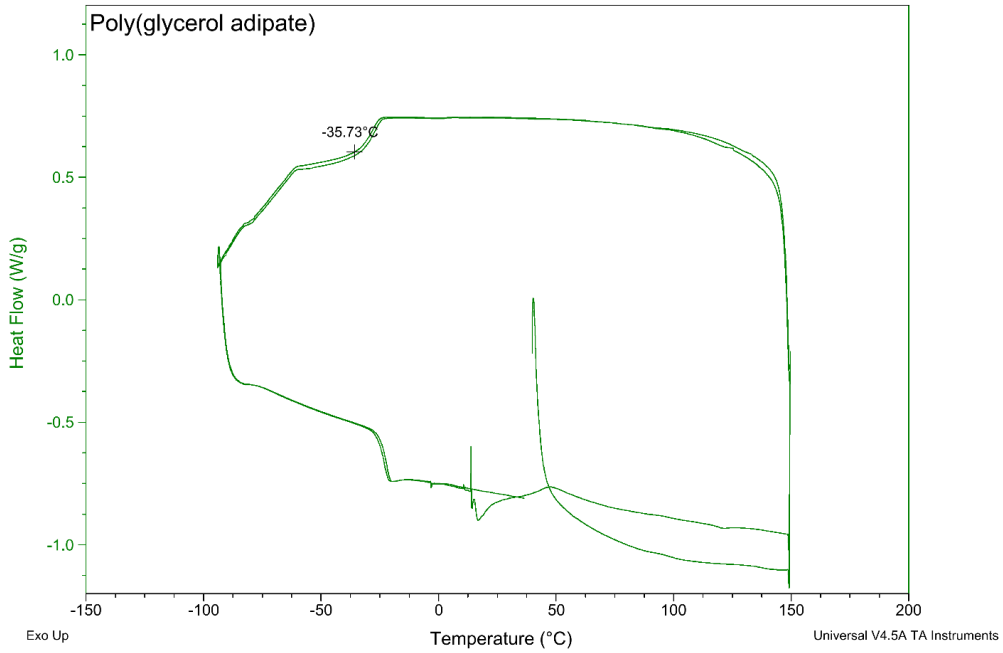
Poly(glycerol adipate)
-35.73°C
Heat Flow (W/g)
1.0
0.5
0.0
-0.5
-1.0
-150
-100
-50
0
50
100
150
200
Exo Up
Temperature (°C)
Universal V4.5A TA Instruments

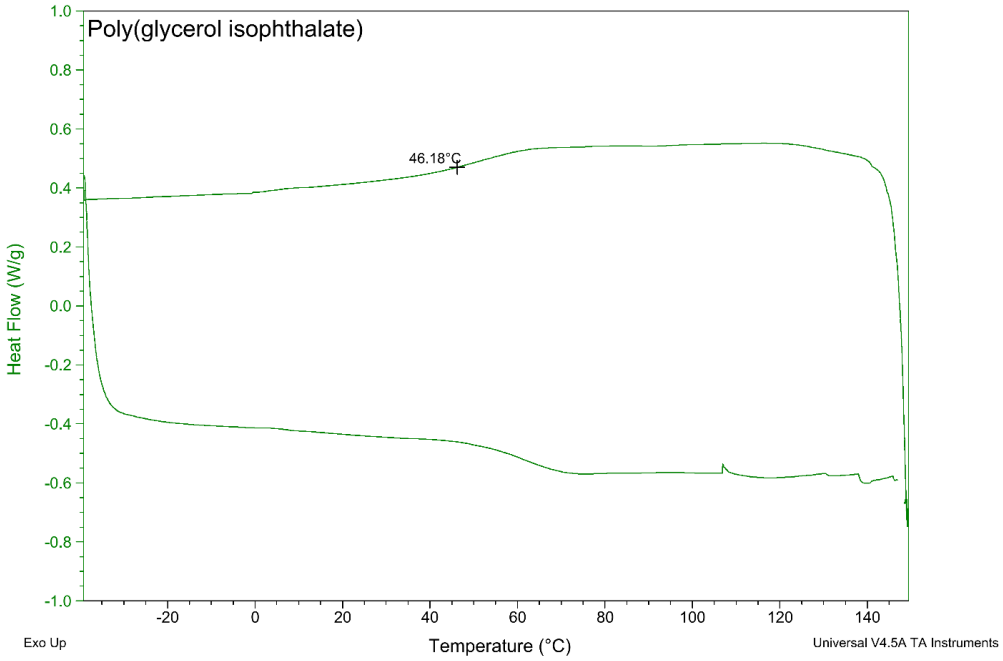
Poly(glycerol isophthalate)
46.18°C
Heat Flow (W/g)
Temperature (°C)
Exo Up
Universal V4.5A TA Instruments

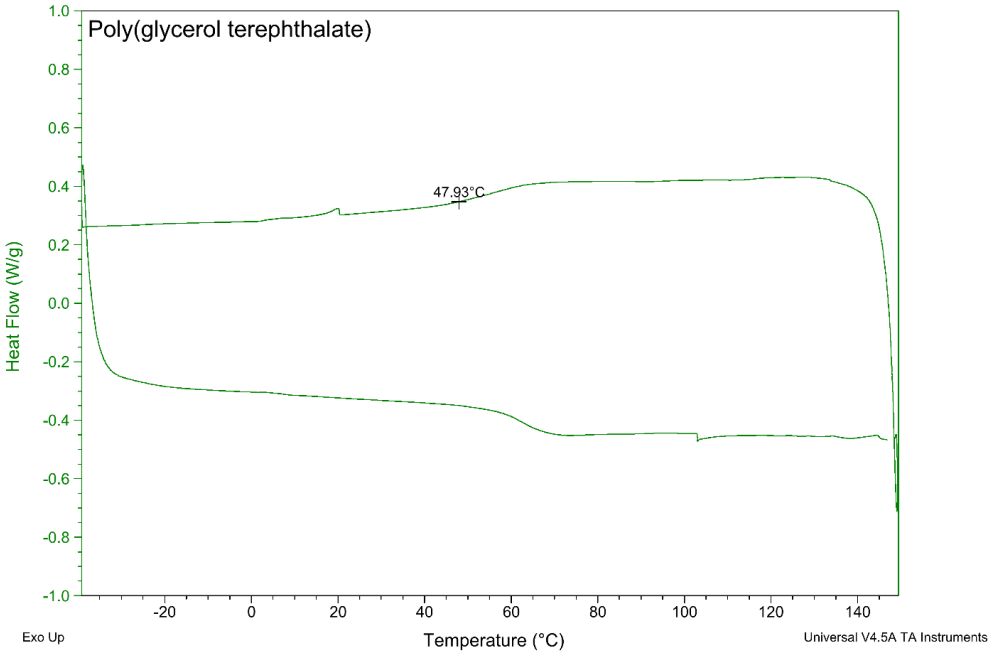
Poly(glycerol terephthalate)
47.93°C
Heat Flow (W/g)
Temperature (°C)
Exo Up
Universal V4.5A TA Instruments

4.2 Chapter 4

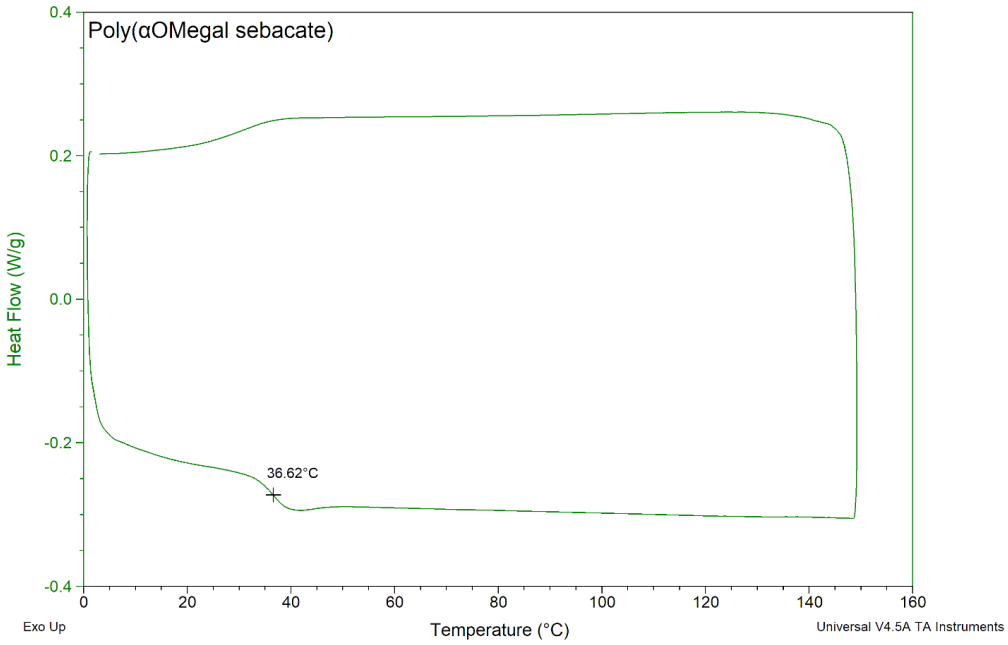
Poly(αOMegal sebacate)
Heat Flow (W/g)
0.4
0.2
0.0
-0.2
-0.4
36.62°C
0
20
40
60
80
100
120
140
160
Exo Up
Temperature (°C)
Universal V4.5A TA Instruments

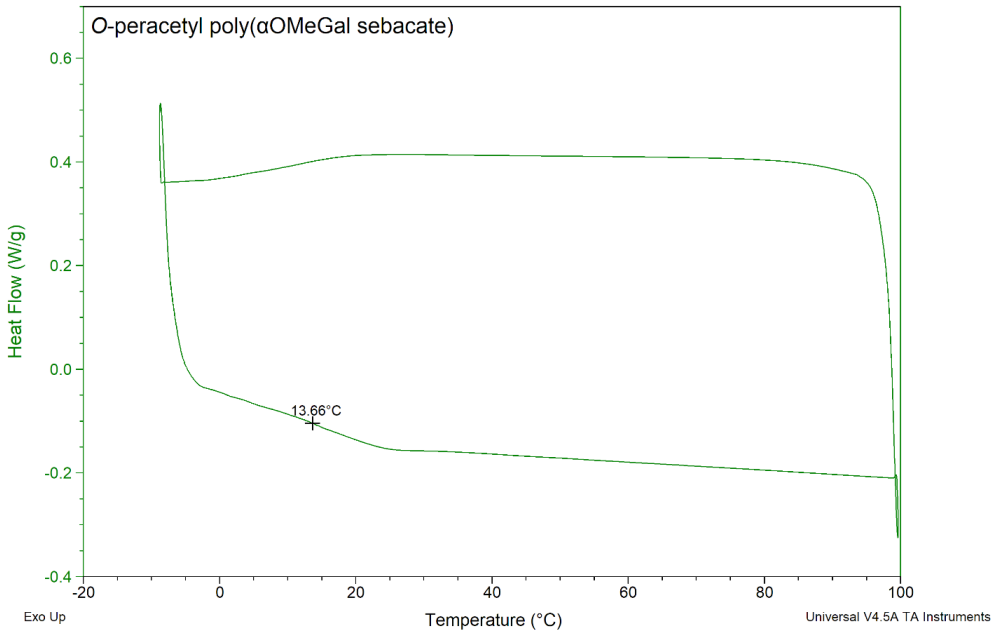
O-peracetyl poly(αOMeGal sebacate)
Heat Flow (W/g)
0.6
0.4
0.2
0.0
-0.2
-0.4
13.66°C
-20
0
20
40
60
80
100
Exo Up
Temperature (°C)
Universal V4.5A TA Instruments

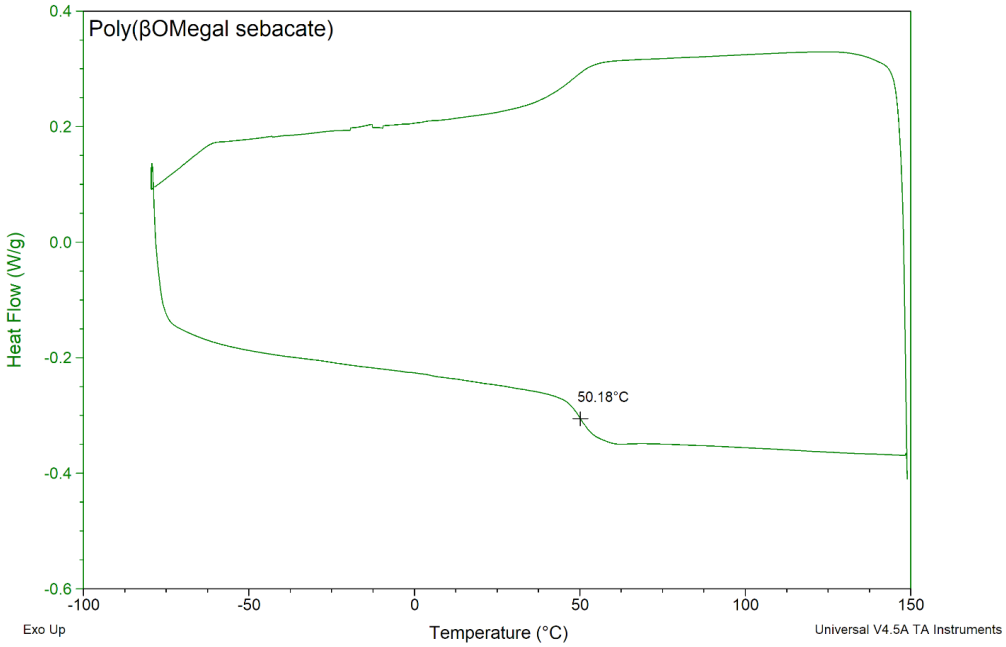
Poly(βOMegal sebacate)
Heat Flow (W/g)
0.4
0.2
0.0
-0.2
-0.4
-0.6
50.18°C
-100
-50
0
50
100
150
Exo Up
Temperature (°C)
Universal V4.5A TA Instruments

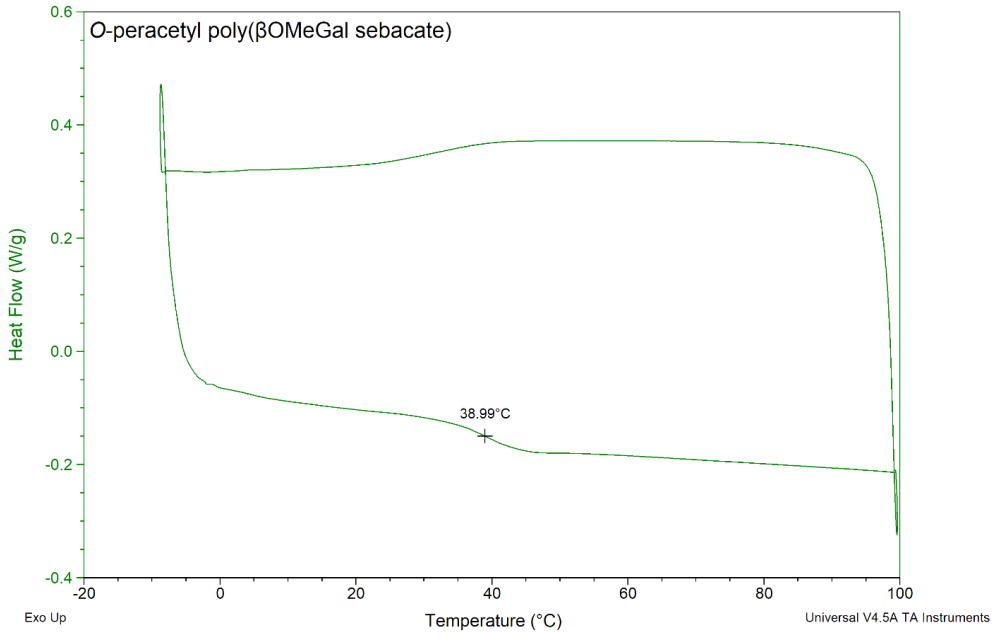
O-peracetyl poly(βOMeGal sebacate)
Heat Flow (W/g)
0.6
0.4
0.2
0.0
-0.2
-0.4
38.99°C
-20
0
20
40
60
80
100
Exo Up
Temperature (°C)
Universal V4.5A TA Instruments

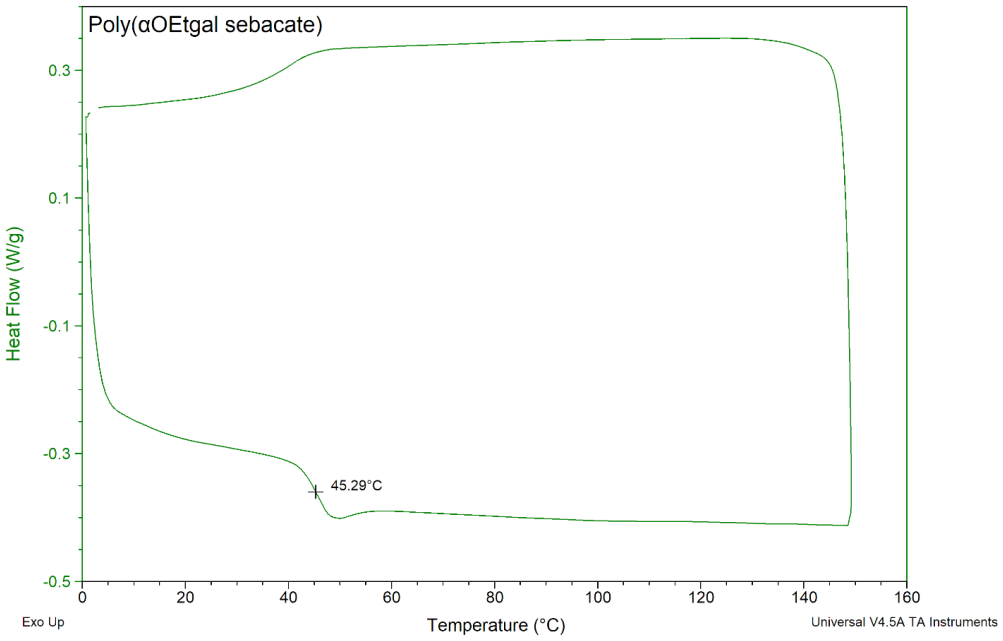
Poly(αOEtgal sebacate)
Heat Flow (W/g)
0.3
0.1
-0.1
-0.3
-0.5
45.29°C
0
20
40
60
80
100
120
140
160
Exo Up
Temperature (°C)
Universal V4.5A TA Instruments

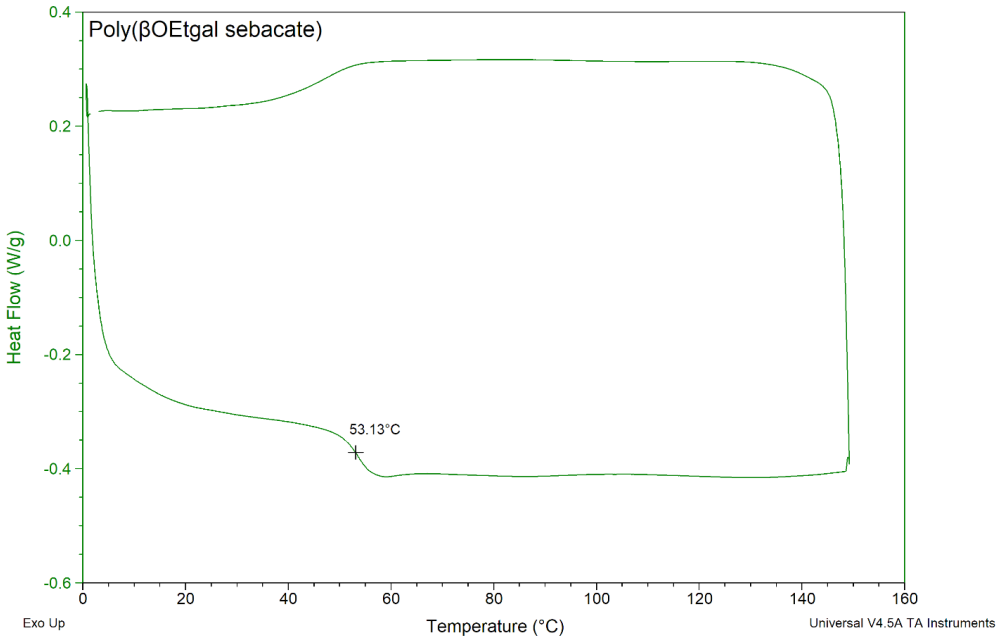
Poly(βOEtgal sebacate)
Heat Flow (W/g)
0.4
0.2
0.0
-0.2
-0.4
-0.6
53.13°C
0
20
40
60
80
100
120
140
160
Exo Up
Temperature (°C)
Universal V4.5A TA Instruments

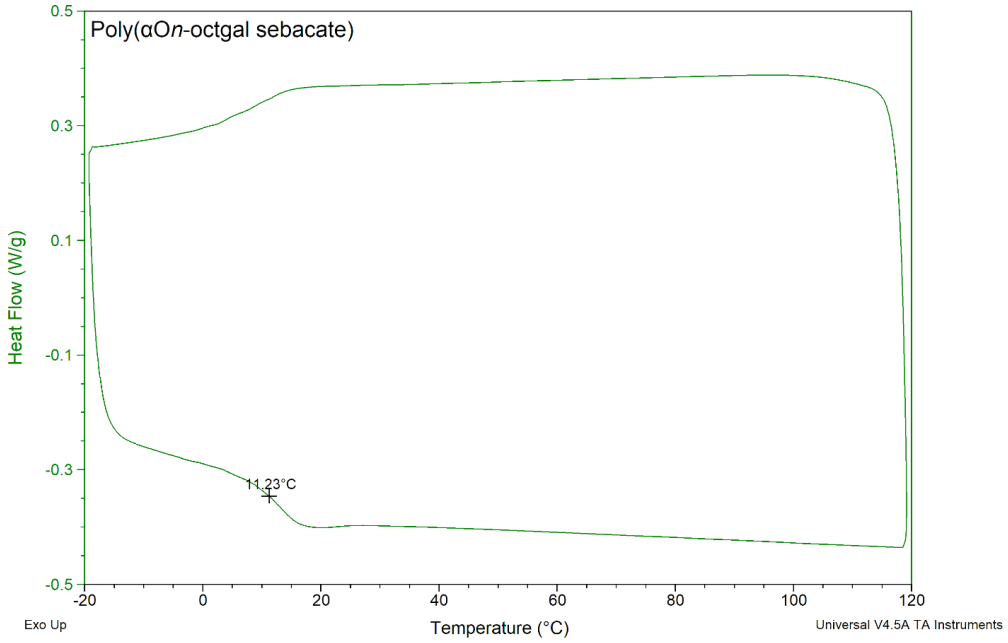
Poly(αO*n*-octgal sebacate)
Heat Flow (W/g)
0.5
0.3
0.1
-0.1
-0.3
-0.5
11.23°C
-20
0
20
40
60
80
100
120
Exo Up
Temperature (°C)
Universal V4.5A TA Instruments

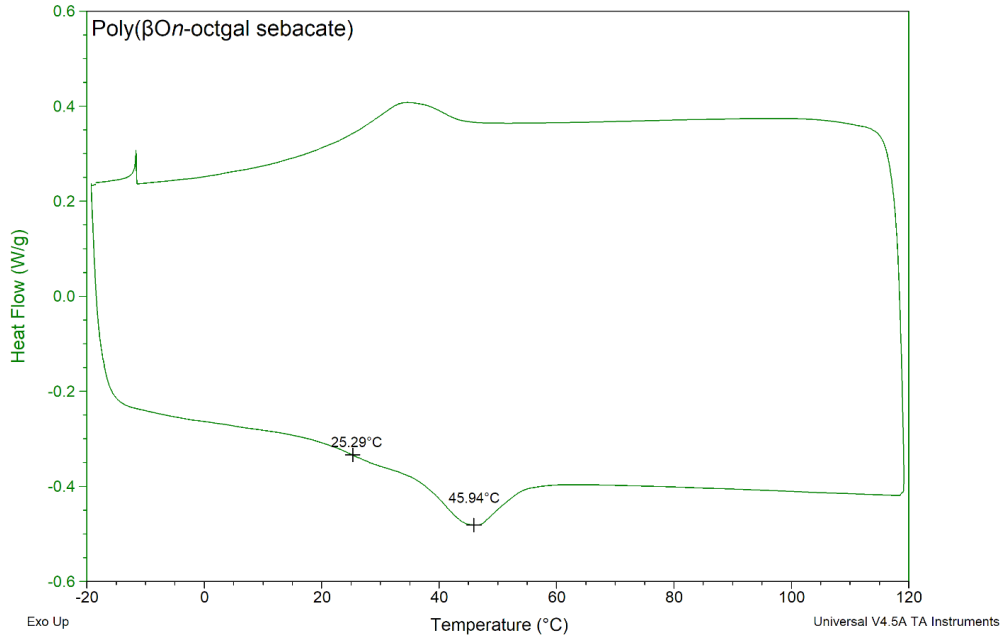
Poly(βO*n*-octgal sebacate)
Heat Flow (W/g)
0.6
0.4
0.2
0.0
-0.2
-0.4
-0.6
25.29°C
45.94°C
-20
0
20
40
60
80
100
120
Exo Up
Temperature (°C)
Universal V4.5A TA Instruments

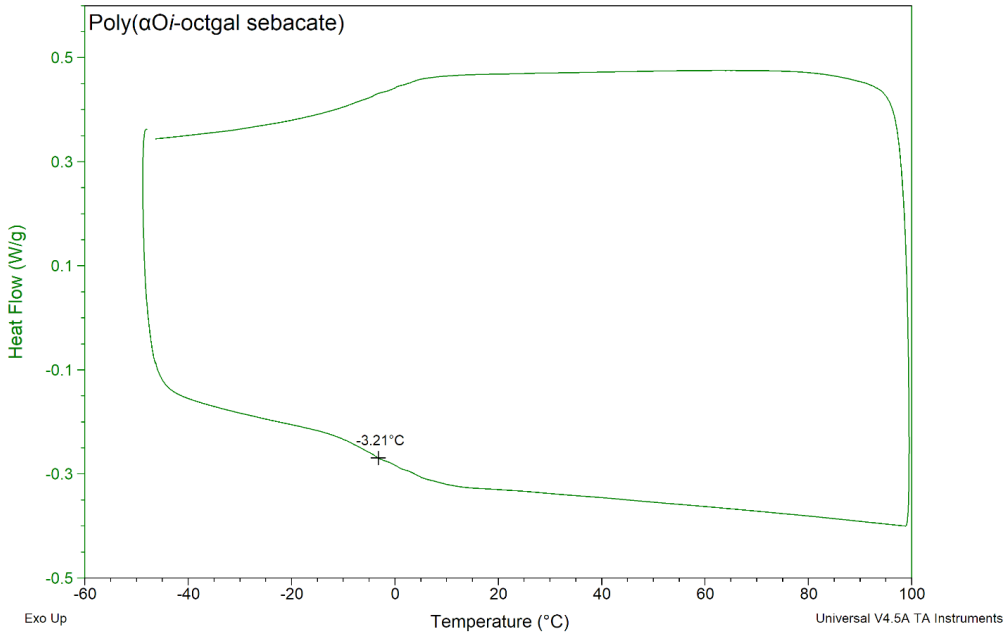
Poly(αO*i*-octgal sebacate)
Heat Flow (W/g)
0.5
0.3
0.1
-0.1
-0.3
-0.5
-3.21°C
-60
-40
-20
0
20
40
60
80
100
Exo Up
Temperature (°C)
Universal V4.5A TA Instruments

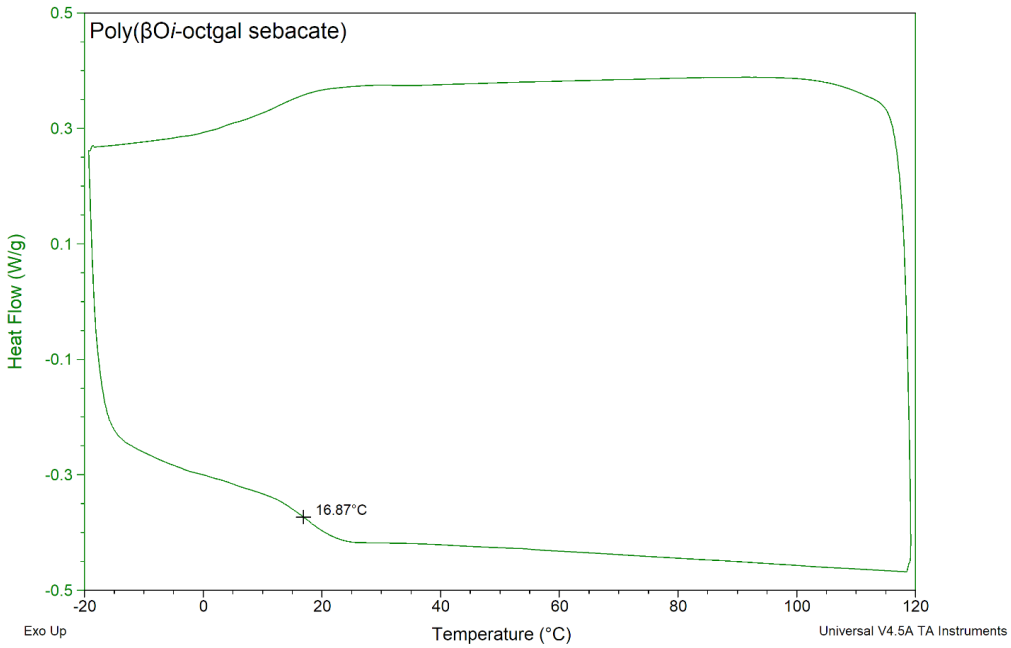
Poly(βO*i*-octgal sebacate)
Heat Flow (W/g)
0.5
0.3
0.1
-0.1
-0.3
-0.5
16.87°C
-20
0
20
40
60
80
100
120
Exo Up
Temperature (°C)
Universal V4.5A TA Instruments

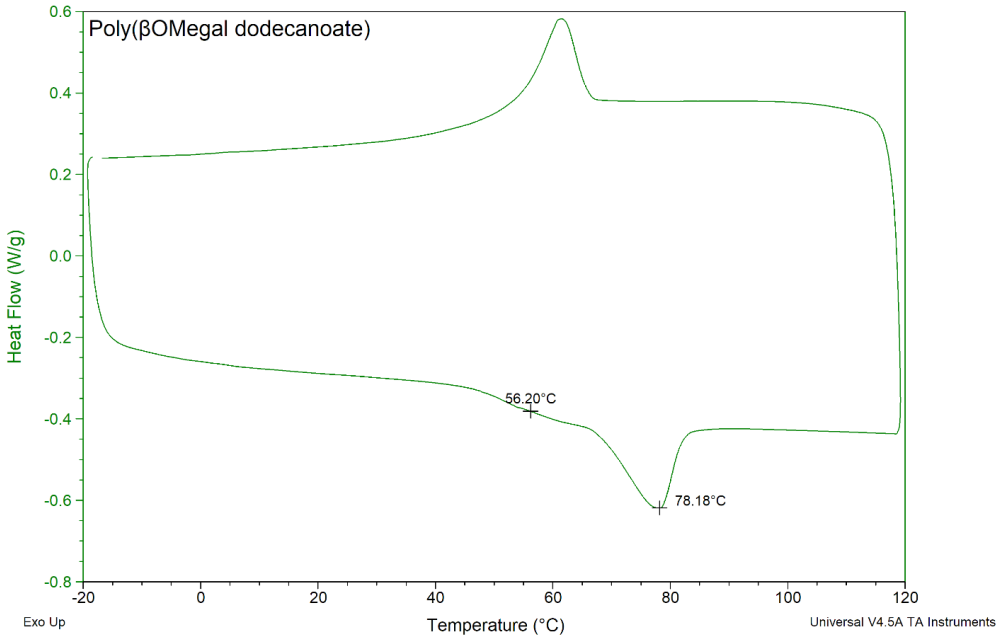
Poly(βOMegal dodecanoate)
Heat Flow (W/g)
0.6
0.4
0.2
0.0
-0.2
-0.4
-0.6
-0.8
56.20°C
78.18°C
-20
0
20
40
60
80
100
120
Exo Up
Temperature (°C)
Universal V4.5A TA Instruments

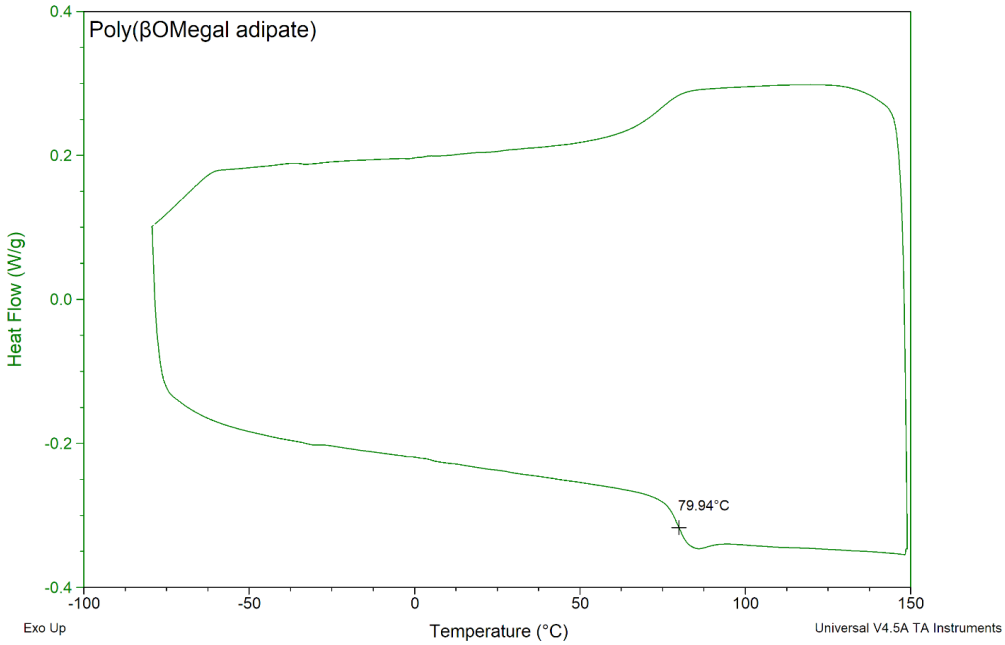
Poly(βOMegal adipate)
Heat Flow (W/g)
0.4
0.2
0.0
-0.2
-0.4
79.94°C
-100
-50
0
50
100
150
Exo Up
Temperature (°C)
Universal V4.5A TA Instruments

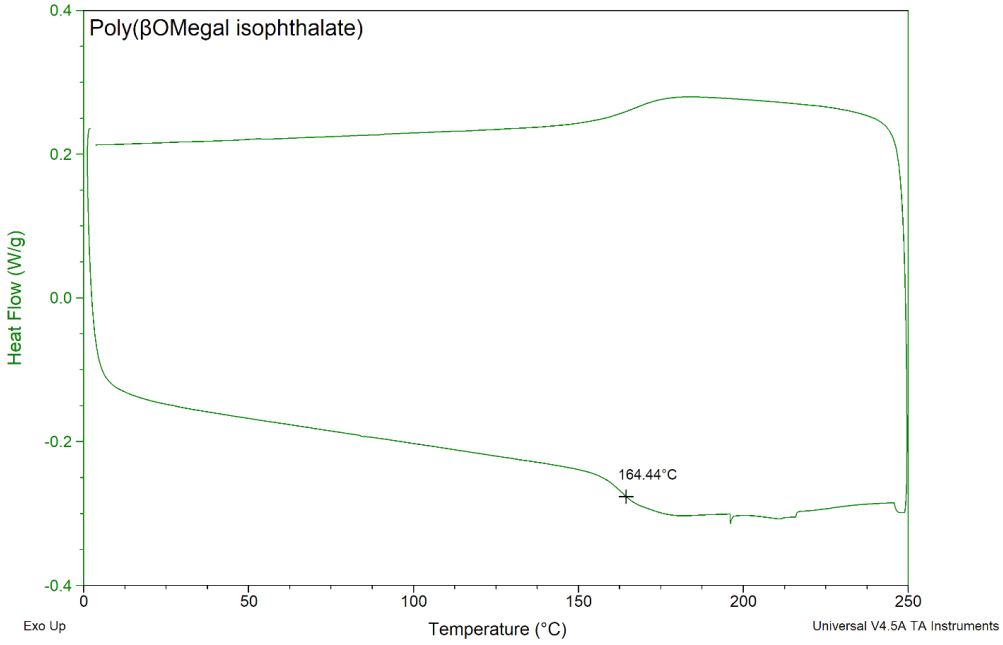
Poly(βOMegal isophthalate)
Heat Flow (W/g)
0.4
0.2
0.0
-0.2
-0.4
164.44°C
0
50
100
150
200
250
Exo Up
Temperature (°C)
Universal V4.5A TA Instruments

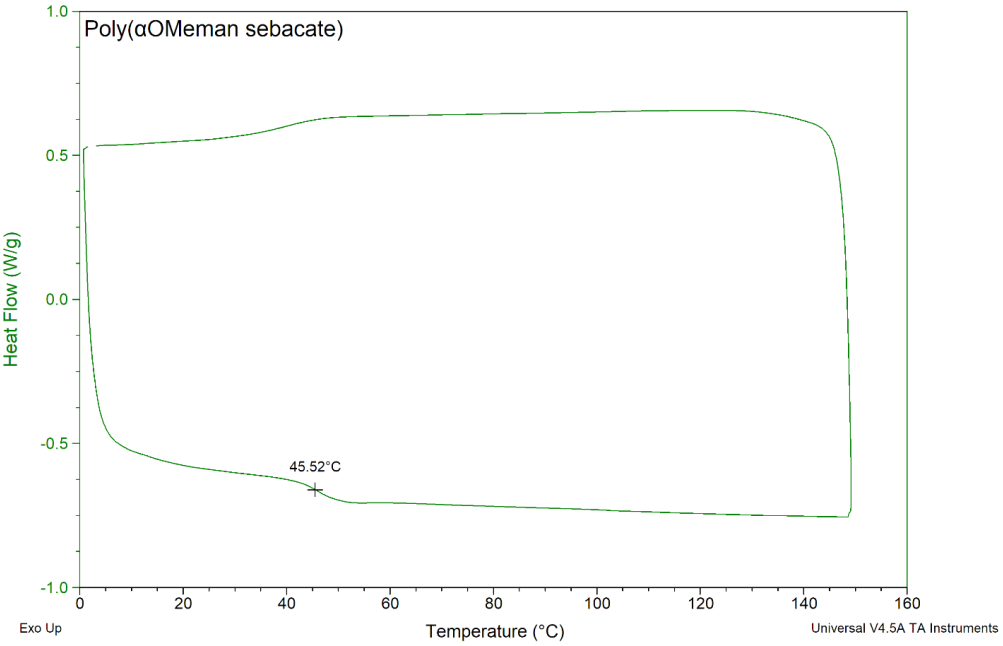
Poly(αOMeman sebacate)
Heat Flow (W/g)
1.0
0.5
0.0
-0.5
-1.0
45.52°C
0
20
40
60
80
100
120
140
160
Exo Up
Temperature (°C)
Universal V4.5A TA Instruments

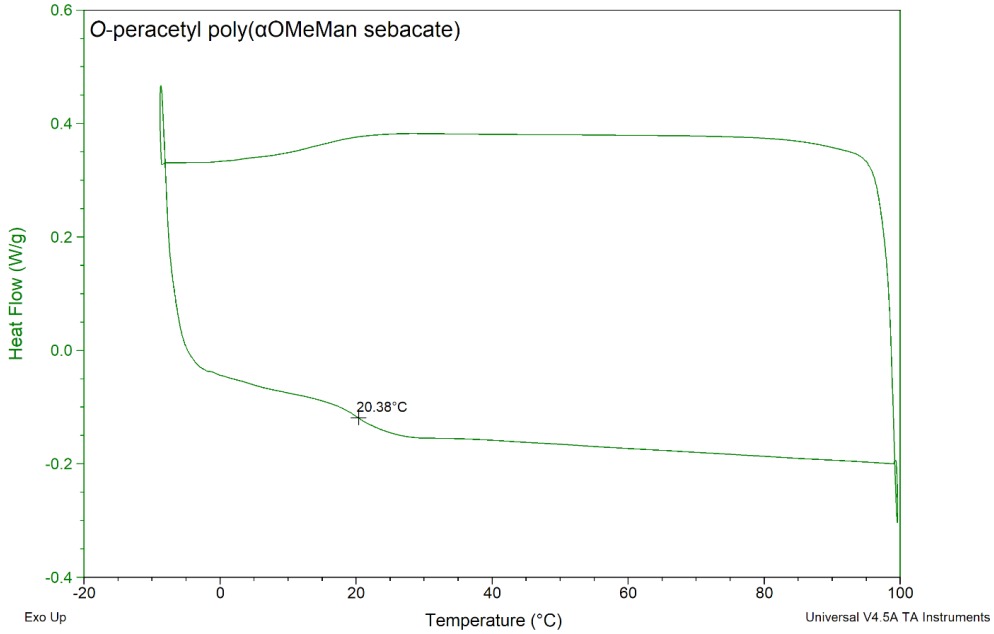
O-peracetyl poly(αOMeMan sebacate)
Heat Flow (W/g)
0.6
0.4
0.2
0.0
-0.2
-0.4
20.38°C
-20
0
20
40
60
80
100
Exo Up
Temperature (°C)
Universal V4.5A TA Instruments

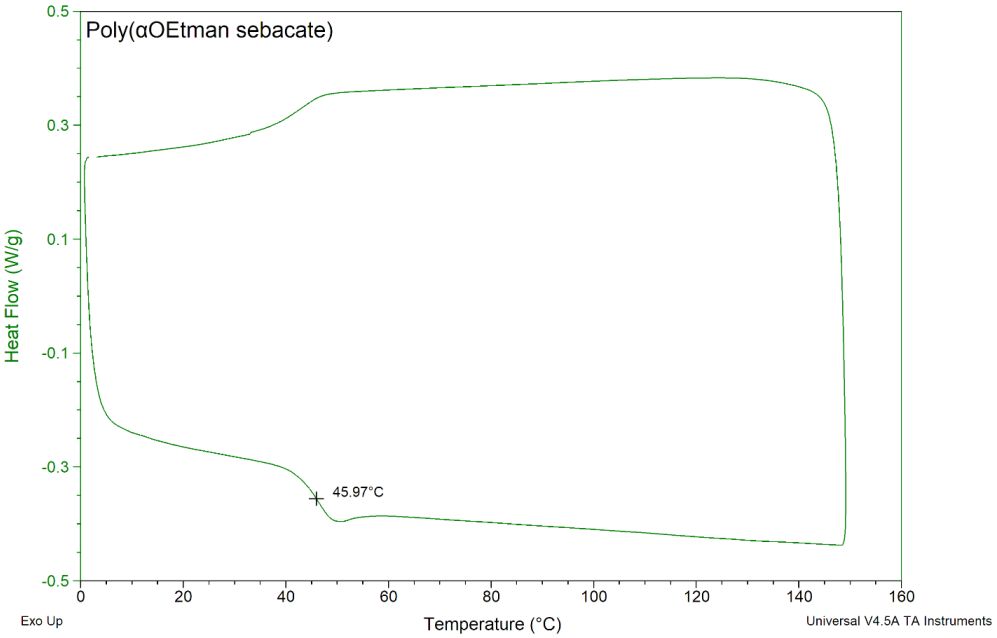
Poly(αOEtman sebacate)
Heat Flow (W/g)
0.5
0.3
0.1
-0.1
-0.3
-0.5
45.97°C
0
20
40
60
80
100
120
140
160
Exo Up
Temperature (°C)
Universal V4.5A TA Instruments

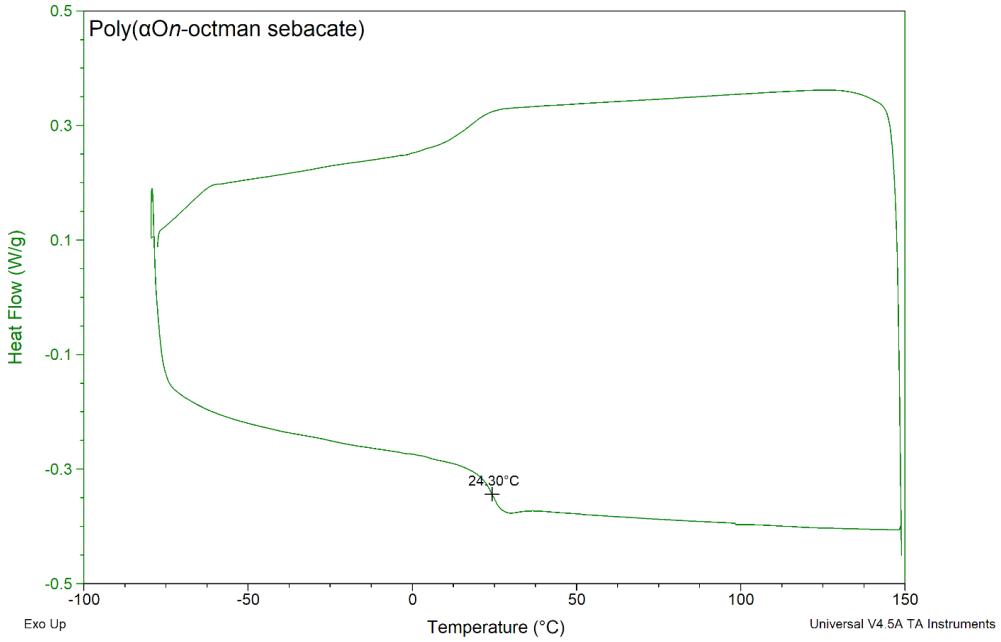
Poly(αO*n*-octman sebacate)
Heat Flow (W/g)
0.5
0.3
0.1
-0.1
-0.3
-0.5
24.30°C
-100
-50
0
50
100
150
Exo Up
Temperature (°C)
Universal V4.5A TA Instruments

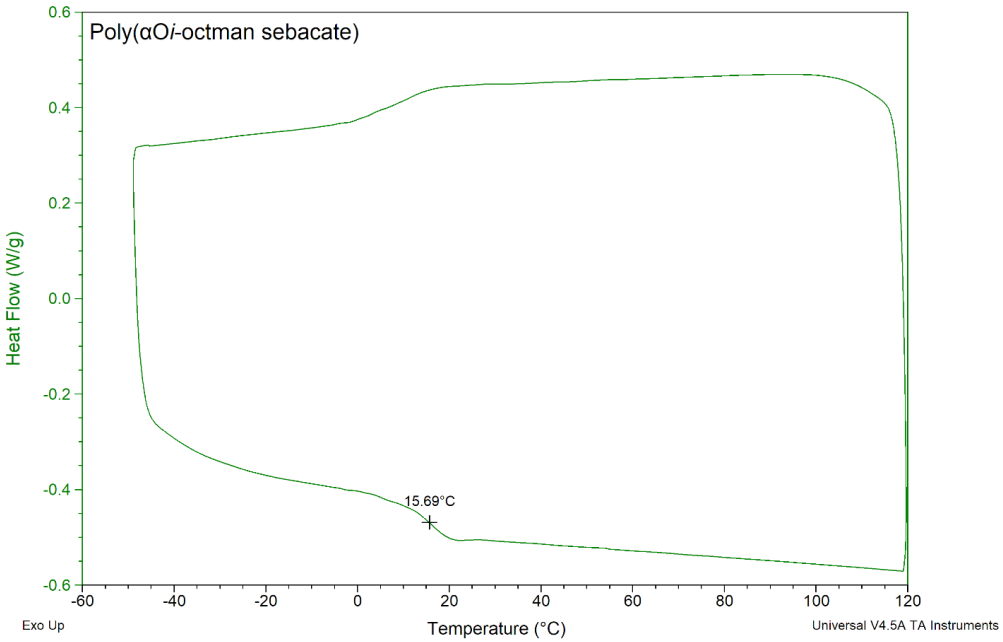
Poly(αO*i*-octman sebacate)
Heat Flow (W/g)
0.6
0.4
0.2
0.0
-0.2
-0.4
-0.6
15.69°C
-60
-40
-20
0
20
40
60
80
100
120
Exo Up
Temperature (°C)
Universal V4.5A TA Instruments

5 DMA Traces

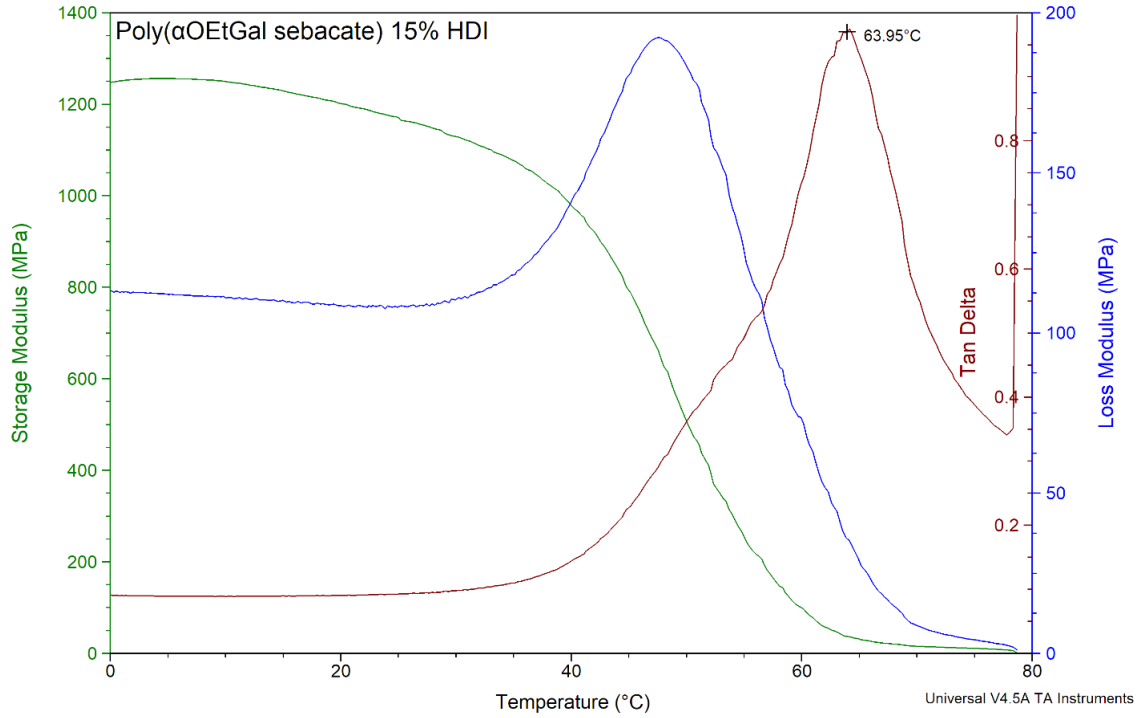
Poly(αOEtGal sebacate) 15% HDI
63.95°C
Storage Modulus (MPa)
Tan Delta
Loss Modulus (MPa)
Temperature (°C)
Universal V4.5A TA Instruments

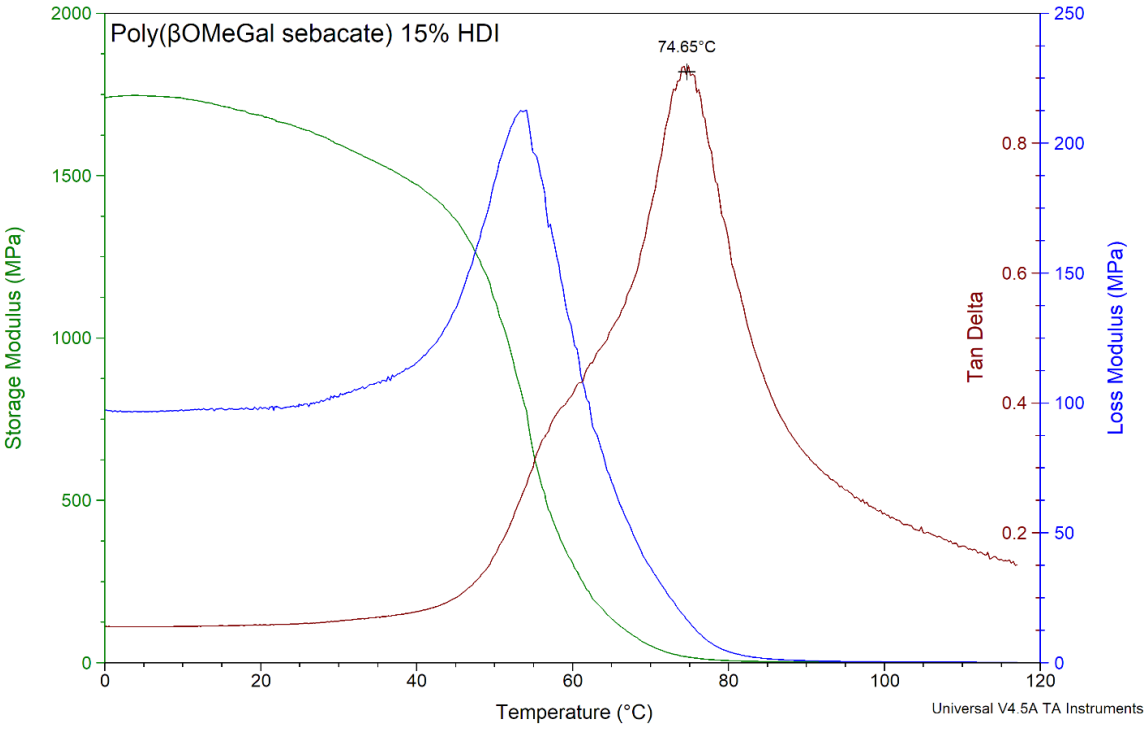
Poly(βOMeGal sebacate) 15% HDI
74.65°C
Storage Modulus (MPa)
Tan Delta
Loss Modulus (MPa)
Temperature (°C)
Universal V4.5A TA Instruments

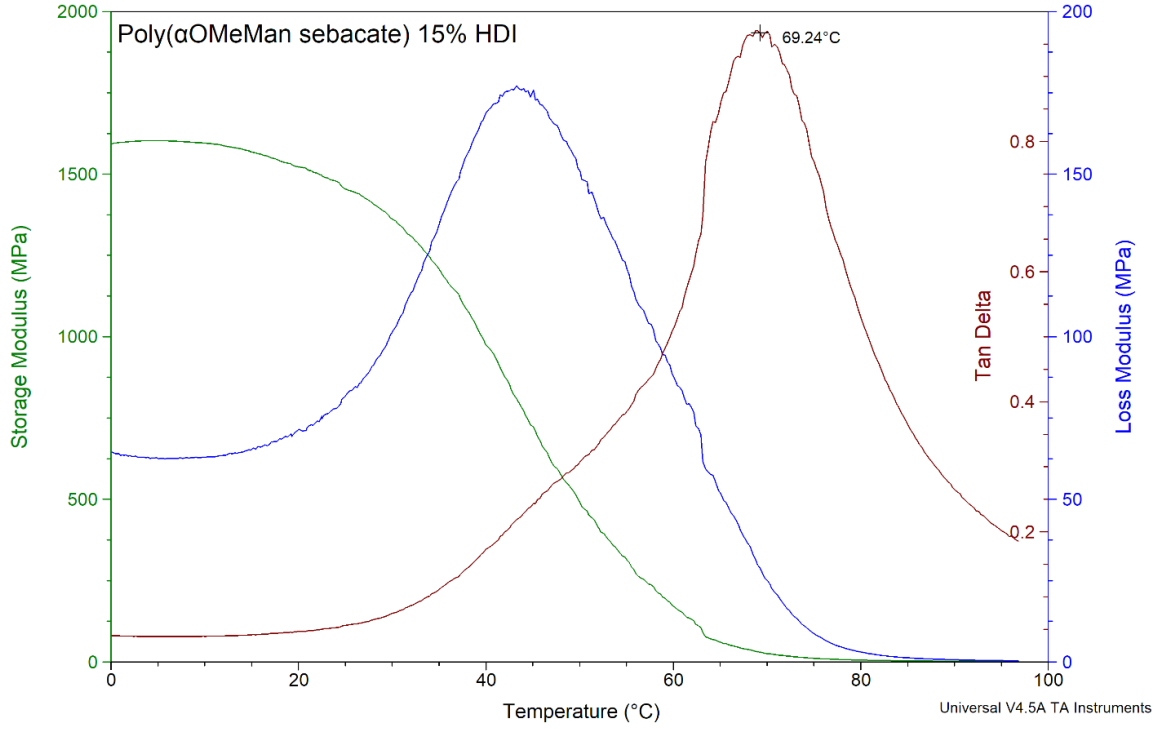
Poly(αOMeMan sebacate) 15% HDI
69.24°C
Storage Modulus (MPa)
Tan Delta
Loss Modulus (MPa)
Temperature (°C)
Universal V4.5A TA Instruments

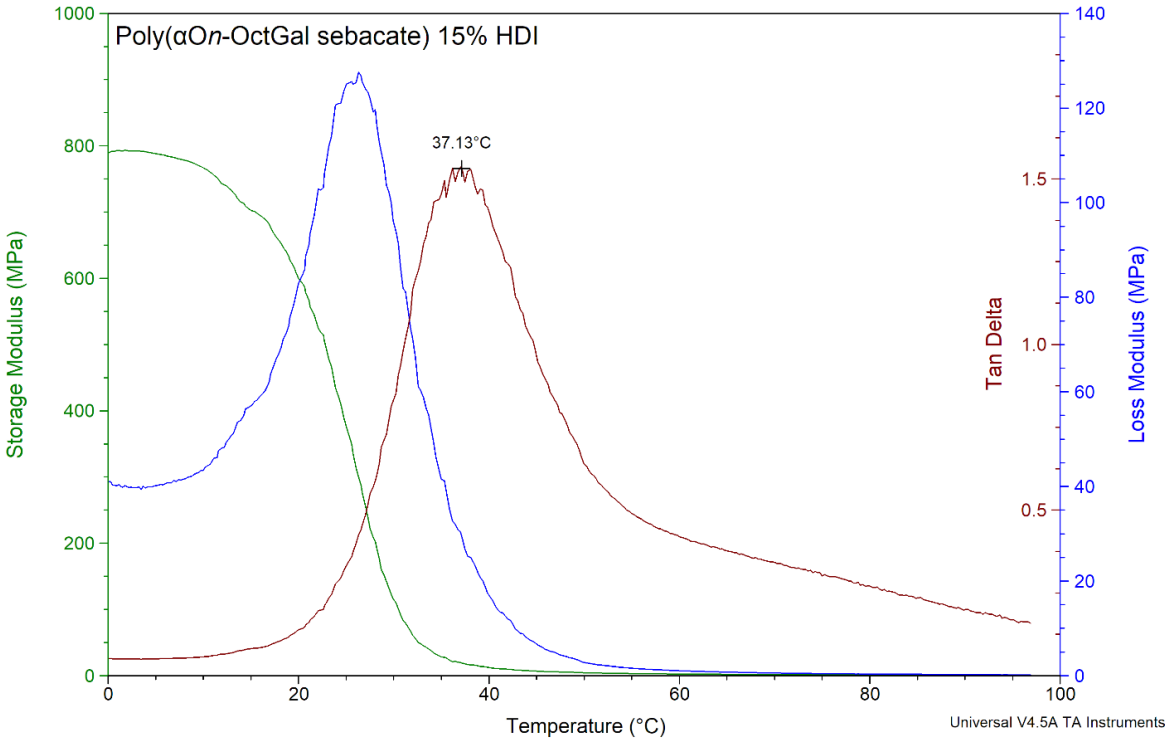
Poly(αO*n*-OctGal sebacate) 15% HDI
37.13°C
Storage Modulus (MPa)
Tan Delta
Loss Modulus (MPa)
Temperature (°C)
Universal V4.5A TA Instruments

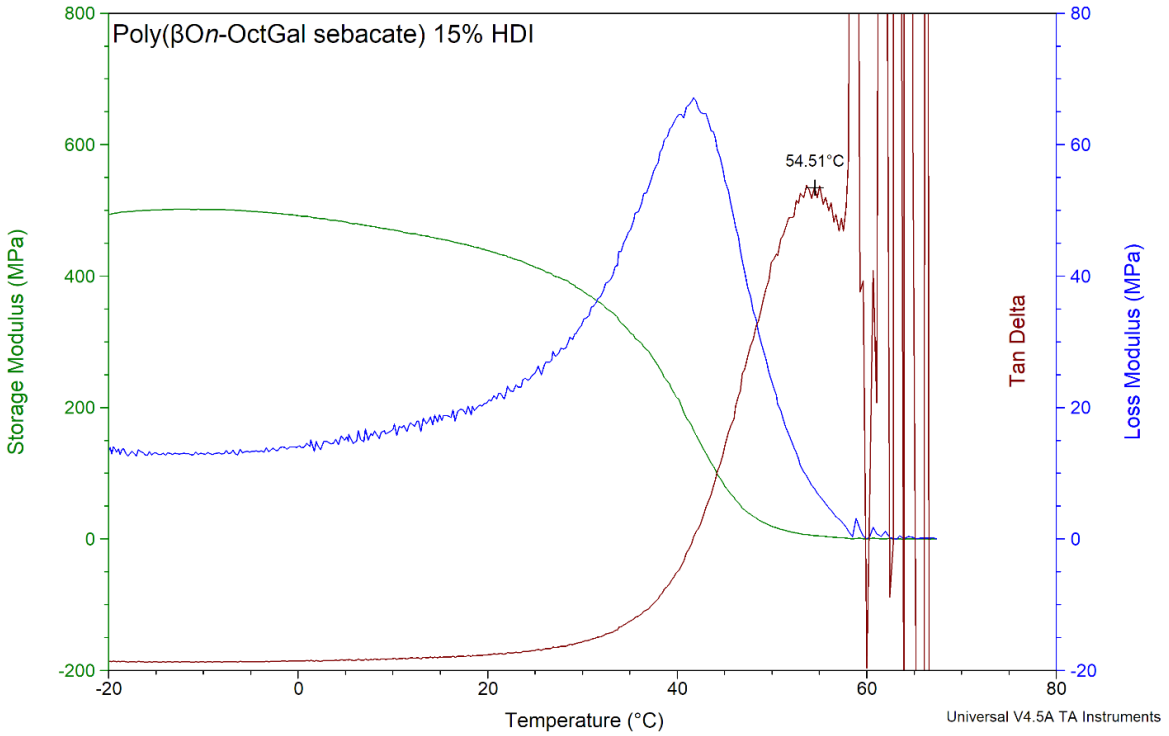
Poly(βO*n*-OctGal sebacate) 15% HDI
54.51°C
Storage Modulus (MPa)
Tan Delta
Loss Modulus (MPa)
Temperature (°C)
Universal V4.5A TA Instruments

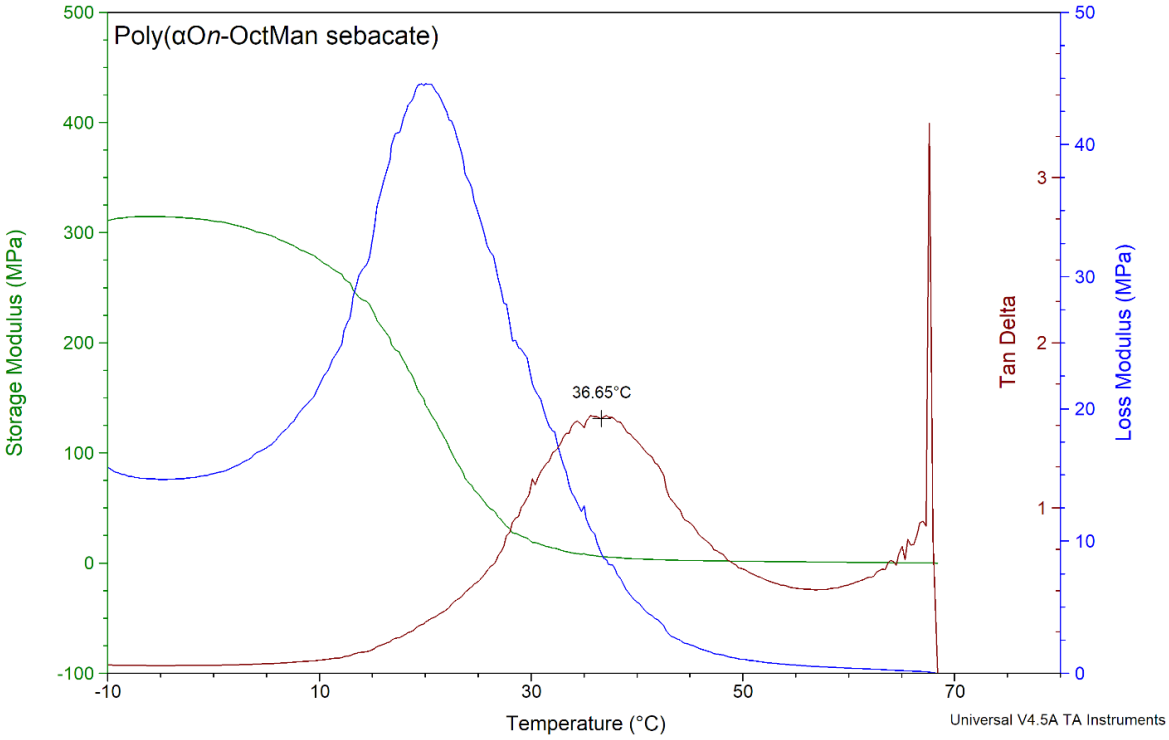
Poly(αO*n*-OctMan sebacate)
36.65°C
Storage Modulus (MPa)
Tan Delta
Loss Modulus (MPa)
Temperature (°C)
Universal V4.5A TA Instruments

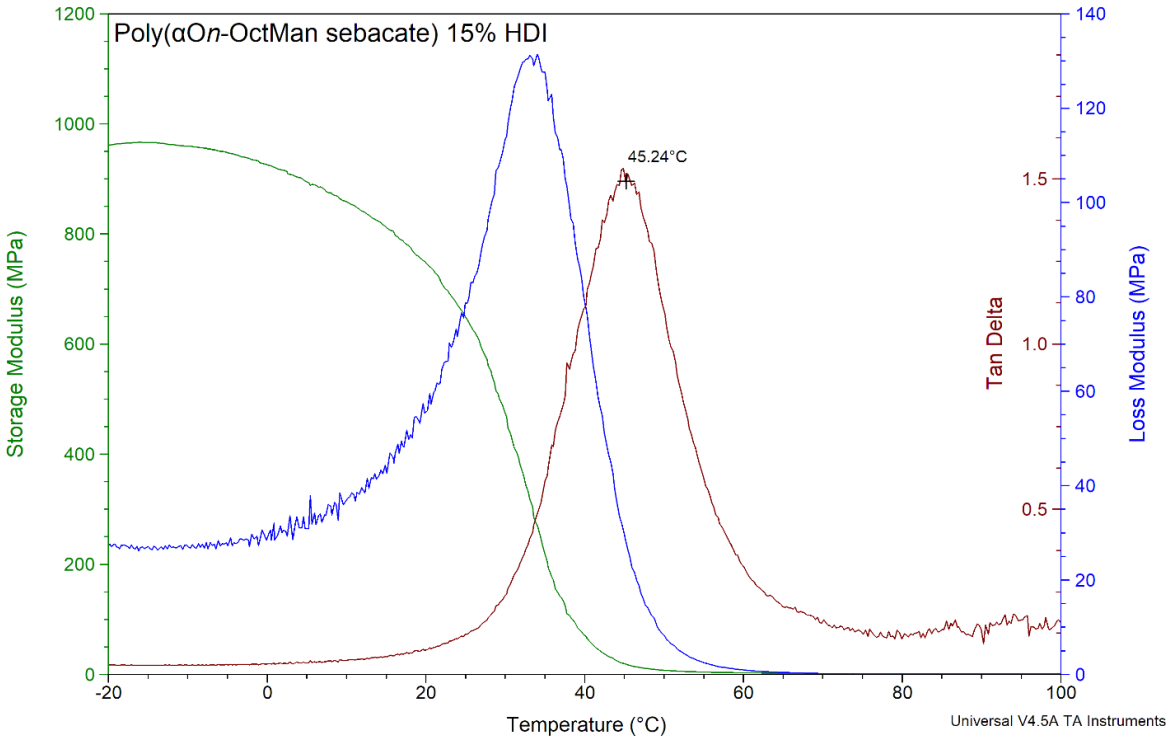
Poly(αO*n*-OctMan sebacate) 15% HDI
45.24°C
Storage Modulus (MPa)
Tan Delta
Loss Modulus (MPa)
Temperature (°C)
Universal V4.5A TA Instruments
1200
1000
800
600
400
200
0
140
120
100
80
60
40
20
0
1.5
1.0
0.5
-20
0
20
40
60
80
100